

Appendix A

National Ecosystem Restoration Benefits Evaluation

FINAL
NATIONAL ECOSYSTEM RESTORATION BENEFITS EVALUATION

AN ASSESSMENT OF THE ECOLOGICAL UPLIFT ASSOCIATED
WITH THE RESTORATION OF THE CAÑO MARTÍN PEÑA
FOCUSING ON BENEFITS TO THE STUDY AREA

Prepared for:



Corporación del Proyecto ENLACE del Caño Martín Peña
Apartado Postal 41308
San Juan, Puerto Rico 00940-1308

February 2016

Contents

	Page
List of Figures	iv
List of Tables	iv
Acronyms and Abbreviations	v
Executive Summary	vii
1.0 INTRODUCTION.....	1-1
1.1 BACKGROUND	1-1
1.2 PURPOSE OF THIS APPENDIX.....	1-2
1.3 ECOLOGICAL HEALTH OF SAN JOSÉ LAGOON.....	1-2
1.4 EXPECTATIONS OF ECOSYSTEM RESPONSES WITH PROJECT IMPLEMENTATION – PRIOR DETERMINATIONS OF PROBABLE BENEFITS.....	1-3
1.5 SEASCAPES AND THE INTER-CONNECTEDNESS OF FISH HABITATS IN TROPICAL MARINE ECOSYSTEMS.....	1-4
1.6 ANTICIPATED BENEFITS TO FISH HABITATS OF A RESTORED CAÑO MARTÍN PEÑA	1-5
2.0 PERFORMANCE METRIC DEVELOPMENT.....	2-1
2.1 OVERVIEW OF MODELS AND EXISTING DATA SETS	2-1
2.1.1 Hydrodynamic Model	2-2
2.1.1.1 Model Features and Calibration.....	2-2
2.1.2 Benthic Index.....	2-3
2.1.2.1 Benthic Index Model Features and Quantification of Anticipated Benefits	2-5
2.1.3 Scientific Basis for Habitat Models	2-8
2.1.3.1 Fish Habitat Model Features and Quantification of Anticipated Benefits	2-10
2.1.3.2 Mangrove Habitat Model Features and Quantification of Anticipated Benefits.....	2-13
2.2 RESULTS.....	2-16
2.2.1 Quantification of Benefits Based on the Benthic Index Model	2-16
2.2.2 Quantification of Benefits Based on the Fish Habitat Model	2-17
2.2.3 Quantification of Benefits Based on the Mangrove Habitat Model.....	2-20
2.3 TIMELINE OF EXPECTED ECOSYSTEM RECOVERY	2-22
3.0 BENEFITS EVALUATION	3-1
4.0 LITERATURE CITED.....	4-1
Appendixes:	
A1 San Juan Bay Estuary (SJBE) Conceptual Ecological Model	
A2 Hydrodynamic and Water Quality Model Study of San Juan Bay Estuary (Bunch et al. 2000)	
A3 Development of the Benthic Index for the San Juan Bay Estuary System (PBS&J 2009a)	
A4 Mapped Habitat and Caño Martín Peña Channel Configurations	

Figures

	Page
1	Locations and Benthic Index Scores for Stations located in San José Lagoon Values are color-coded as to their Benthic Index Scores 2-4
2	Relationship between residence time (days) and benthic index scores for shallow (<2 m) locations throughout the San Juan Bay Estuary 2-6
3	Open water habitat within the San Juan Bay Estuary System..... 2-11
4	GIS-based estimates of reef habitat in waters adjacent to the San Juan Bay Estuary 2-12
5	GIS-based estimates of mangrove cover throughout the San Juan Bay Estuary 2-13
6	Example photographs of mangrove prop roots in various portions of the San Juan Bay Estuary 2-14
7	Relationship of the number of crabs and the distance from the Caño Martín Peña 2-15
8	Spatial extent of water depth areas within San José Lagoon 2-18
9	Average Annual Habitat Unit lift for the combined models for each project alternative based upon an estimated recovery time for the habitats of 3 years and a 50-year project period..... 3-6

Tables

1	Comparison of water quality data and fish species richness in San José and Piñones Lagoons..... 1-3
2	Quantification of Open Water/Seagrass and Reef Habitat Unit Benefits with Project Implementation 2-19
3	Quantification of Open Water Habitat Unit Benefits for the No Action and Project Alternatives within the Caño Martín Peña 2-19
4	Quantification of Mangrove Habitat Unit Benefits with Project Implementation..... 2-21
5	Quantification of Mangrove Habitat Unit Benefits for the No Action and Project Alternatives within the Caño Martín Peña 2-21
6	Summary of Ecosystem Response Timelines for Completed Restoration Projects 2-23
7	Average Annual Habitat Unit lift for the project alternatives 3-4
8	Summary of Net Average Annual Habitat Units for the Models..... 3-5

Acronyms and Abbreviations

ADCP	Acoustic Doppler Current Profilers
CFU	Fecal coliform bacteria units
CH3D-WES	Curvilinear Hydrodynamics in 3 Dimensions, WES version
CMP-ERP	Caño Martín Peña Ecosystem Restoration Project
ECO-PCX	Ecosystem Restoration Planning Center of Expertise
GIS	Geographic Information System
HU	habitat units
m	meter
mg/L	milligrams per liter
ml	milliliters
NER	National Ecosystem Restoration
NOAA	National Oceanic and Atmospheric Administration
ppt	parts per thousand
SJB	San Juan Bay
SJBE	San Juan Bay Estuary
SJBEP	San Juan Bay Estuary Program
µg	micrograms
USACE	U.S. Army Corps of Engineers
USDA	U.S. Department of Agriculture
USEPA	U.S. Environmental Protection Agency
WRDA	Water Resources Development Act

This page intentionally left blank.

Executive Summary

An assessment of the expected ecological uplift associated with the restoration of the Caño Martín Peña was completed, focusing on the benefits to benthic, mangrove, and fish habitat throughout the San Juan Bay Estuary system. General conclusions include the following:

Existing Conditions

- The closure of the historical connection between San Juan Bay and San José Lagoon has resulted in reduced tidal exchange into San José Lagoon via the Caño Martín Peña.
- The current configuration of the San Juan Bay Estuary is one where the fish habitat resources of San Juan Bay and Condado Lagoon are separated from the habitats of San José Lagoon, Suárez Canal, and the La Torrecilla and Piñones Lagoons.
- Reduced tidal exchange has resulted in a condition wherein the waters of San José Lagoon exhibit strong salinity stratification, with a surface layer of brackish, oxygenated waters overlying more saline and hypoxic to anoxic bottom waters.
- Biological surveys of the San José Lagoon have found that the hypoxic to anoxic bottom waters appear to be a regular feature, rather than a temporary condition.
- Implementation of pollution controls since the 1970s have resulted in a trend of improving water quality in the San Juan Bay Estuary.

Restoration Potential and the “Seascape”

- For at least the past 30 years, marine resource managers have documented the importance of the inter-connectedness of habitats such as mangroves, seagrass meadows, open water features, and coral reefs. These habitats function together as a series of linked features referred to as the “seascape.”
- Reestablishment of the tidal connection between San Juan Bay and the San José Lagoon would recreate the historical inter-connectedness of the San Juan Bay Estuary, from La Torrecilla and Piñones Lagoons in the east to San Juan Bay in the west, as well as the historical inter-connectedness of the seascape features of the San Juan Bay Estuary system.
- Reestablishment of the tidal connection is anticipated to benefit not only those species that only utilize the estuarine portions of the San Juan Bay Estuary, but also those species that use mangroves, seagrass beds, and estuarine waters for only a portion of their life cycle.
- Species that use estuarine seascape features for a portion of their life cycle, while also using nearshore reef environments for (typically) adult stages, include a number of recreationally and commercially important species of fish in Puerto Rico.
- Reestablishment of the historical tidal connection between San Juan Bay and the San José Lagoon would not only benefit the health of benthic communities, and the open water and mangrove habitats of San José Lagoon, but it would also benefit those systems that would be newly connected through San José Lagoon (e.g. San Juan Bay and Condado Lagoon) as well as

those waterbodies that would be connected through a healthier San José Lagoon (e.g., Suárez Canal, La Torrecilla Lagoon, Piñones Lagoon).

Calculating Ecological Uplift in the San Juan Bay Estuary

- Calculating restoration benefits (ecological uplift) for the benthic community involved the use of a Benthic Index Model, which integrated data from a benthic index for the San Juan Bay Estuary and a hydrodynamic model for the San Juan Bay Estuary.
- An approach was developed to scale benefits to both nearby and more distant habitats when quantifying the amount of seascape features (seagrass meadows, open waters, mangroves, coral reefs) that would benefit from reestablishment of the historical inter-connectedness of the San Juan Bay Estuary.

The Benthic Index Model

- A benthic index was previously developed for the San Juan Bay Estuary. The benthic index is a mathematical technique used to quantify the species diversity and relative pollution tolerance of benthic communities. Benthic index scores were based on two equations: the derivation of a species diversity index, and then the modification of that index score as a function of the relative amount of pollution tolerant or pollution sensitive taxa. There are no confidence intervals or validation steps involved in the calculation of benthic index scores; it is a two-step univariate analysis.
- Use of the benthic index found that scores (which reflect species diversity of benthic communities) were inversely correlated with distance from the Atlantic Ocean, suggesting that tidal exchange has a positive influence on species diversity of benthic communities.
- After reproducing a previously developed hydrodynamic model for San Juan Bay, it was found that residence time was inversely correlated with benthic index scores across San Juan Bay; areas with longer residence times (reduced tidal exchange) were typically characterized by lower benthic index scores.
- Model output from the hydrodynamic model concluded that restoring the historical connection between San Juan Bay and San José Lagoon would significantly reduce residence time estimates for San José Lagoon.
- Based on the previously derived correlation between residence time and benthic index scores, the anticipated increased tidal exchange in San José Lagoon is expected to result in a substantial increase in benthic index scores throughout the lagoon. This relationship was used to develop a Benthic Index Model to estimate current condition and future project benefits from restoring the Caño Martín Peña.
- The Benthic Index Model is properly associated with the residence time within San José Lagoon because the Benthic Index improvement in San José Lagoon depends upon the water with the Lagoon turning over with the reduced residence time and increased dissolved oxygen levels are anticipated in bottom waters of San José Lagoon as a function of decreased salinity stratification, brought about through increasing the exchange of more saline surface waters.

The Fish Habitat and Mangrove Habitat Models

- For the seascape features of open water habitat, seagrass meadows and coral reefs, a scaling technique was applied wherein anticipated benefits were first quantified as acres of habitat (based on Geographic Information System [GIS]) and then habitat quantities were scaled based on how directly connected those areas were to the Caño Martín Peña and San José Lagoon. Seascape features that were less directly connected (e.g., coral reefs) were assigned a lower per acre score than features with a more direct connection (e.g., open waters of Suárez Canal). A Fish Habitat Model was the result of this effort and the model was used to predict current conditions and future project benefits from restoring the Caño Martín Peña.
- For the seascape feature of mangrove forests, a scaling technique was applied wherein anticipated benefits were first quantified as acres of mangrove habitat (based on GIS) and then scaled based on the degree of inter-connectedness based on the current variability in tide phase and the anticipated moderation of that variability through restoration. Mangrove habitats in areas with similar timing of tidal phases were assigned a higher per acre score than areas that had more dissimilar timing of tidal phases. A Mangrove Habitat Model was the result of this effort and the model was used to predict current conditions and future project benefits from restoring the Caño Martín Peña.
- The two approaches to quantifying anticipated benefits of inter-connectedness of seascape features were thus conservative estimates, such that habitats farther away or less directly connected to the Caño Martín Peña and San José Lagoon were given lower per acre scores than habitats that are closer and more directly connected.
- Flux or surface tide level equalization within the estuary system is the appropriate relationship for the Fish Habitat and Mangrove Habitat Models because these models depend upon surface waters moving throughout the system and distributing fish and invertebrate larvae and juveniles to these habitats along with the redistribution of vegetation seeds.

Alternatives

- The four project alternatives — no action, the 75-foot-wide by 10-foot-deep alternative, the 100-foot-wide by 10-foot-deep alternative, and the 125-foot-wide by 10-foot-deep alternative with a weir on the western end of the project — were evaluated using the ecological models.
- The presence of a weir associated with the 100-foot-wide and 125-foot-wide channel would replicate the cross sectional area of the 75-foot-wide channel alternative, thereby restricting water flow of the 100-foot-wide and 125-foot-wide alternatives to equal that of the 75-foot-wide alternative. As a result, the hydrodynamics of the two alternatives would be equal, which, in turn, would result in equal ecological benefits.

National Ecosystem Restoration (NER) Benefit Results

- The Benthic Index Model was used to calculate the Benthic Index of each alternative based upon the modeled residence time. The performance of the alternative was developed using an estimated maximum Benthic Index value of 3.0. Based upon project performance the no action, 75-foot-wide alternative, 100-foot-wide alternative with a weir, and 125-foot-wide

alternative with a weir have total habitat units of 363.0, 663.8, 663.8, and 663.8, respectively. Using the projected 3-year recovery over the 50-year project period, the three constructed project alternatives would have net average annual habitat units of 294.5.

- The Fish Habitat Model was used to calculate the habitat unit scores for each of the alternatives based upon the scaling factors. Based upon project performance the 75-foot-wide alternative with a weir, and 100-foot-wide alternative with a weir have net habitat units of 5,154.0; 5,159.2; and 5,164.6, respectively. Using the projected 3-year recovery over the 50-year project period, the three constructed project alternatives would have net average annual habitat units of 5,050.9, 5,056.0, and 5,061.3, respectively.
- The Mangrove Habitat Model was used to calculate the net habitat units for each of the alternatives based upon the scaling factors. Based upon project performance the 75-foot-wide alternative, 100-foot-wide alternative with a weir, and 125-foot-wide alternative with weir have net habitat units of 803.8; 798.6; and 793.2, respectively. Using the projected 3-year recovery over the 50-year project period, the three constructed project alternatives would have net average annual habitat units of 787.7, 782.7, and 777.4.
- The total net average annual habitat units for the three constructed project alternatives are estimated to be 6,133.
- Prior research on other estuarine restoration efforts, including those with hydrologic restoration features, suggests measurable improvements in water quality, benthic community health and fish and fish habitat would be expected to occur within 1 to 3 years after project completion. A 3-year linear increase in benefits was used to calculate the average annual habitat unit lift provided by the models.
- Existing water quality (e.g. pollutants) in the San Juan Bay Estuary can sustain restoration benefits achieved by the CMP.

1.0 INTRODUCTION

1.1 BACKGROUND

The Caño Martín Peña is a waterway approximately 4 miles long, connecting San Juan Bay and San José Lagoon, in metropolitan San Juan, Puerto Rico. It is part of the San Juan Bay Estuary (SJBE) system, the only tropical estuary that is included in the U.S. Environmental Protection Agency (USEPA) National Estuary Program. The total drainage area of the Caño Martín Peña is about 4 square miles (2,500 acres). The eastern 2.2-mile-long segment of the Caño Martín Peña and adjacent areas, including the San José Lagoon, are the primary focus of the restoration project; however restoration benefits are envisioned to occur throughout the SJBE system.

Historical problems with the Caño Martín Peña are described in the Reconnaissance Report developed by the U.S. Army Corps of Engineers (U.S. Army Corps of Engineers [USACE] 2004). Originally, the Caño Martín Peña had an average width of approximately 200 feet, with an unknown depth, and it was surrounded by extensive wetlands. The canal was an important ecological resource and acted as a transportation conduit between the cities of San Juan and Carolina. The wetlands surrounding the Caño Martín Peña have been used as a dredged material disposal area for port and channel projects. Urban development has encroached upon the Caño Martín Peña to the point where the canal is blocked as a result of sediment and debris accumulation, and structure encroachment along the eastern portion. At present, there is very little tidal exchange between San José Lagoon and San Juan Bay, resulting in reduced flushing and poor water quality (salinity stratifications and hypoxic conditions) in San José Lagoon. The lack of adequate infrastructure including a combined sewer system (stormwater and wastewater) has exacerbated the degradation of water quality caused by leachate from direct discharges of untreated sewage into the Caño Martín Peña. Encroachment along the eastern half of Caño Martín Peña has increased the intensity and frequency of flooding, affecting nearby communities with a combination of storm and untreated sanitary waters. Wildlife habitat loss has occurred within the system as a result of direct (e.g., construction, dredging, filling) and indirect impacts. Mangrove and other native flora and associated fauna have significantly diminished in the Caño Martín Peña and adjacent areas.

The ENLACE Caño Martín Peña restoration project is the latest of several attempts to bring about an improvement in the quality of life for residents living along the Caño Martín Peña and to restore and/or improve water quality and habitat values in both the Caño Martín Peña and the San Juan Bay Estuary system. The relocation and resettlement of residents from areas adjacent to the eastern segment of the Caño Martín Peña began in 1998. These initial efforts were carried out with the anticipation that such actions would be followed by the initiation of an Ecosystem Restoration Project (the CMP-ERP) that was presented to the U.S. Congress in 2002 (USACE 2004).

The CMP-ERP proposes to dredge the eastern segment of the canal to restore the Caño Martín Peña and adjacent areas and increase tidal flushing within the San Juan Bay Estuary system, in order to achieve environmental restoration. Ancillary benefits would include the reduction of flooding, allowing for the potential for environmentally sound waterway transportation, and the promotion of recreation and tourism. Previous studies (USACE 2004) suggest that the environmental restoration of the Caño Martín Peña can be achieved by dredging the canal and constructing a vertical steel sheet pile and concrete bulkhead system, with a transitional section towards the opening to the San José Lagoon. A major function of the dredging is to provide restoration of tidal exchange between the San José Lagoon and the San Juan Bay, i.e. the east and west sides of the San Juan Bay Estuary system; this increased flushing would provide an ecological lift for both the Caño Martín Peña and the entire estuary system. The proposed construction would be designed to allow tidal inundation and thus, preservation and/or improvement of the mangrove community between the open water and upland areas. Existing water quality in the San Juan Bay Estuary would be able to sustain restoration benefits achieved through implementation of the CMP-ERP.

1.2 PURPOSE OF THIS APPENDIX

The purpose of this Appendix is to describe the methodology used to calculate National Ecosystem Restoration (NER) benefits anticipated to occur from the construction of the CMP-ERP within the San Juan Bay Estuary, including anticipated benefits to fish habitat in the nearshore reefs. The anticipated benefits from the project include:

- 1) improved benthic habitats of San José and Los Corozos Lagoons,
- 2) increased health of the fish habitats of the open waters of the San Juan Bay Estuary and the nearshore reefs, associated with increased inter-connectedness of the San Juan Bay Estuary to a restored Caño Martín Peña and San José Lagoon, and
- 3) improved mangrove habitat through increased inter-connectedness throughout the San Juan Bay Estuary.

1.3 ECOLOGICAL HEALTH OF SAN JOSÉ LAGOON

Several prior studies have focused on the water quality characteristics of the San José Lagoon, including Kennedy et al. (1996), Cerco et al. (2003) and Atkins (2011a, 2011b). The most comprehensive assessments of the ecological health, not just water quality, of San José Lagoon are those compiled within the San Juan Bay Estuary Program's Comprehensive Conservation and Management Plan (2000). In 2007, the U.S. Environmental Protection Agency summarized prior assessments of the environmental conditions within the San Juan Bay Estuary system as being "poor" based on a series of metrics. Within the categories of water quality, sediment quality, and the health of benthic communities, San José Lagoon was consistently found to be the unhealthiest portion of the San Juan Bay Estuary (EPA 2007). Recently completed reports on the water quality (Atkins 2011a,

2011b) and benthic communities of San José Lagoon (PBS&J 2009a) support the conclusions of these earlier assessments that the ecological health of San José Lagoon is severely compromised.

The water quality index compiled by the San Juan Bay Estuary Program (Bauza 2013) gave a score of “D” to San José Lagoon, lower than any other portion of the San Juan Bay Estuary other than the Caño Martín Peña. The Benthic Index report produced for the San Juan Bay Estuary Program showed that in terms of species diversity and the proportion of taxa in pollution-tolerant families, the benthic communities of San José Lagoon were fairly healthy in waters shallower than 4 feet, but the health of the benthic communities was much lower in those areas with water depths greater than 4 feet (PBS&J 2009a). While the mangrove-lined San José Lagoon would not be expected to have water quality similar to that of the better-flushed San Juan Bay or Condado Lagoon, even in an undisturbed condition, it has a lower number of species of fish and much worse water quality than the similarly mangrove-lined waterbody of Piñones Lagoon (Table 1).

Table 1
Comparison of water quality data and fish species richness in San José and Piñones Lagoons.
Water quality data are mean values from 2002 to 2005 (SJBEP 2008).
Fish species data from SJBEP (1996).

Parameter	San José Lagoon	Piñones Lagoon
Salinity (ppt)	11.9	27.5
Dissolved oxygen (mg / liter)	4.55	5.90
Ammonium (mg / liter)	0.38	0.05
Phosphorus (mg / liter)	0.25	0.07
Fecal coliform bacteria (cfu / 100 ml)	1,032	7
Fish species recorded	14	17

1.4 EXPECTATIONS OF ECOSYSTEM RESPONSES WITH PROJECT IMPLEMENTATION – PRIOR DETERMINATIONS OF PROBABLE BENEFITS

The low surface salinities of San José Lagoon, compared to Piñones Lagoon (Table 1), give rise to salinity stratification in those portions of San José Lagoon deeper than 4 feet (Atkins 2011a). This salinity stratification then gives rise to the widespread distribution of hypoxic to anoxic water within the bottom waters of San José Lagoon, which in turn appears to explain the reduced quality of the benthic communities documented in both EPA (2007) and PBS&J (2009a) (Figure 1). It has been shown that reestablishing the historical hydrologic connection between San Juan Bay and San José Lagoon would act to decrease salinity stratification and thus improve the ecological health of San José Lagoon (Atkins 2011a), a conclusion similar to those reached by prior assessments of the likely benefits of hydrologic restoration of the Caño Martín Peña (e.g., Bunch et al. 2000, Cerco et al. 2003).

In consideration of the entirety of reports and data available, the San Juan Bay Estuary Program has committed itself to working with ENLACE to complete the Caño Martín Peña project as part of its efforts to bring about a holistic ecosystem restoration of the San Juan Bay Estuary system (EPA 2007). A “high priority” action within the San Juan Bay Estuary Program’s Comprehensive Conservation and Management Plan (2000) is to restore the historical tidal flow regime in the Caño Martín Peña.

1.5 SEASCAPES AND THE INTER-CONNECTEDNESS OF FISH HABITATS IN TROPICAL MARINE ECOSYSTEMS

As noted by many researchers, and summarized by the National Marine Fisheries Service (<http://www.habitat.noaa.gov/pdf/fisherieshabitatcriticalhabitatcomparison.pdf>), fish habitat can be defined as “. . . habitat necessary for managed fish to complete their life cycle . . .” Important in this definition is the term “life cycle,” which denotes that different types of fish habitat may be important for only a portion of an organism’s lifespan.

More than thirty years ago, marine biologists referred to the combination of mangrove forests, seagrass meadows, and coral reefs as the “seascape” that supports fisheries in sub-tropical and tropical regions (Ogden and Gladfelter 1983, Birkeland 1985). These early researchers noted the dependence of various species of fish on the combination of these inter-connected seascape components.

More recently, Moberg and Rönnbäck (2003) summarized the state of knowledge related to the inter-connectedness of mangroves, open water, seagrass beds and coral reefs. In their review of numerous studies conducted over the past several decades, the authors concluded that “mangroves, seagrass beds and coral reef ecosystems are not autonomous units, but rather integral parts of a ‘seascape’ interlinked by ecological and hydrodynamic processes.” In South Florida, for example, Porter and Porter (2001) contains numerous examples of the ecological linkages that tie together South Florida ecosystems as far removed from each other as the freshwater marshes of the Everglades, the seagrass meadows and patch reefs of Florida Bay, and the offshore coral reef.

The concept that improvements to the health of the benthos and water column of the Caño Martín Peña and San José Lagoon would benefit the ecological health of the wider San Juan Bay Estuary is one that is supported by prior efforts conducted in San Juan Bay (e.g., Bunch et al. 2000, Cerco et al. 2003). The notion that the offshore reefs would also benefit from the CMP-ERP, via enhanced probabilities that recreationally and commercially important fish species would be able to successfully complete their life cycles, is also supported by decades of research into the concept of the interconnectedness of mangrove, seagrass, and reef habitats in a wider seascape in tropical marine ecosystems.

1.6 ANTICIPATED BENEFITS TO FISH HABITATS OF A RESTORED CAÑO MARTÍN PEÑA

The objective of this Appendix is to summarize the techniques, results, and interpretation of results used to quantify the expected benefits to benthic, fish, and mangrove habitat associated with the restoration of the historical tidal connection between San Juan Bay and the San José Lagoon. Expected benefits are then quantified in terms of three main responses: 1) improved health of the benthic habitat of San José and Los Corozos Lagoons, 2) enhanced value of fish habitat associated with the increased health and inter-connectedness of the open waters, seagrass meadows, and offshore reefs in and adjacent to the San Juan Bay Estuary, and 3) enhanced value of mangrove habitat associated with the increased health and inter-connectedness of that habitat within the San Juan Bay Estuary system.

The results of these benefit quantifications are scaled so that benefits to ecosystem components such as offshore reefs, while anticipated, are given a lower “score” than habitats closer to the project site, such as mangroves in San José Lagoon. The scaling technique allows for the inclusion of anticipated benefits that would extend to the entirety of seascape features, without exaggerating such benefits. Finally, an expected timeline of system responses is proposed, based on prior and similar habitat restoration projects.

Currently, fish within San Juan Bay cannot directly access the mangroves, seagrass meadows, and open water habitats of San José Lagoon, the Suárez Canal, La Torrecilla Lagoon and Piñones Lagoon, just as fish within those waterbodies cannot directly access the habitats afforded by San Juan Bay (located to the west of the western end of the Caño Martín Peña). Due to the current condition of the Caño Martín Peña, there is essentially no tidal exchange between San Juan Bay and the San José Lagoon, i.e., the eastern and western sides of San Juan Bay Estuary system, creating essentially two estuary systems connected independently to the ocean waters by inlets. Because there is low or no exchange of water on a normal tidal cycle, the water quality within the Caño Martín Peña and San José Lagoon has been repeatedly shown to be very poor (i.e., Kennedy et al. 1996, Webb and Gomez-Gomez 1998, San Juan Bay Estuary Program 2000) with multiple exceedances of relevant water quality standards (i.e., Puerto Rico Environmental Quality Board 2010).

The restoration of the Caño Martín Peña is not only expected to benefit water quality and fish habitat within the Caño Martín Peña, San José Lagoon, and Los Corozos Lagoon (i.e., Atkins 2011a); it would benefit fisheries outside of these water bodies by allowing easier access to the variety of fish habitat (i.e., open water, seagrass meadows, hard bottom, mangrove fringes) found throughout the newly inter-connected waters of San Juan Bay, San José Lagoon, the Suárez Canal, La Torrecilla Lagoon and Piñones Lagoon (i.e., the entire San Juan Bay Estuary system).

The Sport Fisheries Study (Atkins 2011b) includes an assessment of the red mangrove prop root community within the Caño Martín Peña and within zones in designated distances away from the

Caño Martín Peña. It was found that the numbers and diversity of the attached (e.g., mussels and oysters) and mobile (e.g., crabs) organisms found on the roots increased from the Caño Martín Peña and western San José Lagoon out to La Torrecilla Lagoon, thus providing an indicator of water quality improvement that would likely respond to the improvements provided by the opening of the Caño Martín Peña. Through this preliminary study, a significant relationship was found between the number of crabs found on mangrove prop roots and distance from the Caño Martín Peña (Section 2.1.3.2).

2.0 PERFORMANCE METRIC DEVELOPMENT

A key component of environmental benefits analyses is the development of metrics to evaluate achievement of restoration objectives (McKay et al. 2010). USACE policy requires restoration projects use metrics that are “expressed quantitatively” [Engineering Report 1105-2-100A (USACE 2000)]. A conceptual ecological model was developed for the Caño Martín Peña and included as Appendix A1 of this document. This model was used to develop hypotheses about relationships within the system and to assist in understanding changes brought about by planned project elements. The planning objectives for the Caño Martín Peña Feasibility Study include:

1. Improve fish habitat in the San Juan Bay Estuary (SJBE) system by increasing connectivity and tidal access to estuarine areas;
2. Restore benthic habitat in San José Lagoon by increasing dissolved oxygen in bottom waters and improving the salinity regime to levels that support native estuarine benthic species; and
3. Increase the distribution and population density and diversity of native fish and aquatic invertebrates in the mangrove community by improving hydrologic conditions in the SJBE system.

The opening of the Caño Martín Peña will result in changes in the stressors affecting the San Juan Bay Estuary, thereby, resulting in changes in the attributes of the estuary system. These attributes include sediment and water quality, organisms, and habitats within the system. The performance metrics or measures are used to evaluate those changes. Several hypotheses are evident in the planning objectives described above. Improved water flow and circulation will:

- improve water quality within the system;
- improve mangrove habitat and functionality within the system;
- enhance the ability of fish species and life history stages of fish species to move throughout the estuary system; and
- improve conditions for benthic communities within the system.

All of these relationships and hypotheses were considered for performance metric development. The previous discussion has described where benefits are expected to occur within the system; the following discussion will develop the quantification of those benefits which will become performance metrics in the CMP-ERP Monitoring Plan.

2.1 OVERVIEW OF MODELS AND EXISTING DATA SETS

An existing hydrodynamic model originally produced for San Juan Bay by Bunch et al. (2000; Appendix A2) was used as the basis for the development of all of the ecological models developed for the NER benefits evaluation. A previously developed benthic index (PBS&J 2009a) was used in the

development of the Benthic Index Model. These two “base” models and equations are initially described below and the documents further describing these models are attached as Appendix A2 (hydrodynamic model) and C (benthic index). The three ecological models used in the NER benefits evaluation—Benthic Index Model, Fish Habitat Model, and Mangrove Habitat Model—are described after the descriptions of the hydrodynamic model and benthic index. The hydrodynamic model is an approved model by USACE Headquarters, and the habitat models have been evaluated by the USACE Ecosystem Restoration Planning Center of Expertise (ECO-PCX) and approved for single-use by the Model Certification Team, USACE HQ.

2.1.1 Hydrodynamic Model

The quantification of anticipated benefits summarized here is mostly based on assessments developed from existing efforts. These prior efforts include a hydrodynamic model originally produced for San Juan Bay by Bunch et al. (2000; Appendix A2), which was recreated with various potential tidal reestablishment scenarios by Atkins (2011a). The hydrodynamic model used was the Curvilinear-grid Hydrodynamics model in 3-Dimensions, developed by USACE researchers from the Waterways Experimental Station model (i.e., **Curvilinear Hydrodynamics in 3 Dimensions**, WES version = CH3D-WES). The physical boundaries of the hydrodynamic model (Bunch et al. 2000) are consistent with the physical boundaries of the estuary and nearshore waters used by the San Juan Bay Estuary Program in developing its various resource management programs. The data sources used for model calibration and verification, as well as details of model output from various project scenario runs, are summarized in Section 2.1.1.1. Additional detail can be found in Atkins (2011a).

2.1.1.1 Model Features and Calibration

The hydrodynamic model originally developed by USACE researchers (Bunch et al. 2000) was calibrated based on data that was collected to characterize both boundary conditions and conditions within the San Juan Bay Estuary. Model output was compared to actual field data collected over a 3-month period as summarized by Fagerburg (1998). The model variables used for the hydrodynamic modeling efforts are water level elevations, water velocities, and salinity. The data sets used for model calibration are described below. The model outputs of greatest interest was residence time and tidal exchange, which was a derived based on inflow from the landscape and inter-basin flows.

Field data used for calibration purposes included water-surface elevations, salinity and water velocities. Data were collected at several locations throughout the San Juan Bay Estuary during June to August 1995. Acoustic Doppler Current Profilers (ADCP) were used to quantify velocities at canal locations that connected the various waterbodies of the San Juan Bay Estuary, as shown in Bunch et al. (2000). Due to issues associated with fouling of sensors, flow data were mostly restricted to short-term measurements (Fagerburg 1998). Salinity data were collected and summarized by Kennedy et al. (1996).

At six locations, model output on tidal elevations were compared to measured data, with results originally shown in Bunch et al. (2000). Re-created model output was then compared to the original calibration efforts in Atkins (2011a). Both the original model and the recreated model results for the three month modeling period (June through August 1995) were very close for tidal stage throughout the estuary and flux (water exchange) in the Caño Martín Peña.

At those same six locations, model output was compared to measured salinity data collected from both surface and bottom waters, with results originally shown in Bunch et al. (2000). Re-created model output was then compared to the original calibration efforts in Atkins (2011a). Salinity results, for the three month modeling period, agreed in pattern but were not precisely the same.

For reasons stated above, the model was most useful for tide stage and tidal exchange (flux) in understanding the changes in the estuary from the restoration project alternatives. These attributes of the hydrodynamic model were used in the further development of the ecological models. Model output on flow rates were compared to measured flows at the following locations: 1) Caño Martín Peña (between San Juan Bay and San José Lagoon), 2) Suárez Canal (between San José Lagoon and La Torrecilla Lagoon), and 3) La Torrecilla-Piñones Canal (between La Torrecilla and Piñones Lagoons). Model results were compared to measured flow data over the modeling period in Bunch et al. (2000) and then recreated model output was compared to the original calibration efforts in Atkins (2011a).

2.1.2 Benthic Index

The benthic index is a mathematical technique with a purpose to be used to quantify the species diversity and relative pollution tolerance of benthic communities. The objective was to refine the diversity index typically used for evaluating benthic communities to be more useful in interpreting benthic community data in the San Juan Bay estuary. Benthic index scores are based on two equations: the derivation of a species diversity index, and then the modification of that index score as a function of the relative amount of pollution tolerant or pollution sensitive taxa. There are no confidence intervals or validation steps involved in the calculation of benthic index scores; it is a two-step univariate analysis.

A prior report for the San Juan Bay Estuary Program was conducted to meet U.S. EPA guidance for the development of an index of health of benthic communities throughout the San Juan Bay Estuary. That report (PBS&J 2009a; Appendix A3) used an extensive data base on the species composition prepared by Rivera (2005) (example station locations from San José Lagoon, Figure 1). The benthic index was produced in an iterative manner. The first step involved the calculation of the Shannon Diversity Index:



Figure 1. Locations and Benthic Index Scores for Stations located in San José Lagoon Values are color-coded as to their Benthic Index Scores (PBS&J 2009a).

$$H = -\sum_{i=1}^S (P_i * \ln P_i)$$

Where:

- H= Shannon Diversity Index score,
- P_i= Proportion of sample comprised of family i,
- Ln = natural log, and
- S = Number of families in the sample

The Shannon Diversity Index score was then further modified, as per guidance from existing literature, so that scores would increase due to the presence of members of the families Aoridae and Ampeliscidae, which represent pollution-sensitive organisms (Lee et al 2005, Weston 1996, Traunspurger and Drews 1996). Scores would also decrease due to the presence of members of the families Capitellidae and Tubificidae, which are regarded as pollution-tolerant and/or tolerant of disturbed benthic habitats (Paul et al. 2001, Pinto et al. 2009).

Combined, the final benthic index score is calculated as:

$$B = H - P_{\text{Cap}}^2 - P_{\text{Tub}}^2 + P_{\text{Aor}}^{0.5} + P_{\text{Amp}}^{0.5}$$

Where:

B = Benthic Index Score,

H = Shannon Diversity Score,

P_{Cap} = Proportion of the sample in the family Capitellidae,

P_{Tub} = Proportion of the sample in the family Tubificidae,

P_{Aor} = Proportion of the sample in the family Aoridae, and

P_{Amp} = Proportion of the sample in the family Ampeliscidae.

In the original report prepared for the San Juan Bay Estuary Program (Appendix A3), the authors determined that benthic index scores were lowest in the Caño Martín Peña, followed by the San José Lagoon. It was also determined that distance from the Atlantic Ocean, used as a surrogate for tidal influence, was a better predictor of benthic index scores than water depth.

2.1.2.1 Benthic Index Model Features and Quantification of Anticipated Benefits

The Benthic Index Model refers to the statistically significant bivariate model derived between residence time (as an independent model variable) and benthic index scores (as potentially statistically significant dependent model variables). Because residence time is a variable that the hydrodynamic model predicts well, the purpose of the Benthic Index Model is to develop this relationship between residence time and benthic index scores for the objective of using the model to evaluate the differences between the modeled project alternatives. The mathematical relationship between these two model variables does allow for the quantification of confidence intervals for the derived relationship, and a comparison between measured and modeled values allows for some measure of model validation, at least for existing conditions.

The scientific basis of the Benthic Index Model is developed in the report produced by Atkins (2011a) and summarized here. Output from the hydrodynamic model was used to determine whether the previously derived correlation between benthic index scores and distance from the Atlantic Ocean, as a surrogate for tidal influence (PBS&J 2009a), could be replicated with residence time. If a statistically significant relationship could be found, then the hydrodynamic model could be used to predict changes in residence time with different scenarios for restoring the tidal connection between San Juan Bay and San José Lagoon, and anticipated changes in benthic index scores could be calculated. The model variables used for the linked hydrodynamic-Benthic Index Model are the hydrodynamic model output of residence time (as an independent variable) and benthic index scores

(as a potentially statistically significant independent response variable). The model assumptions are that residence time affects benthic index scores, and the derived mathematical equation reveals the direction of the relationship, the variability associated with the derived relationship, and the statistical significance of the relationship. The Benthic Index Model is properly associated with the residence time within San José Lagoon because the benthic index improvement in San José Lagoon depends upon the water within the Lagoon turning over with the reduced residence time and increased dissolved oxygen levels are anticipated in bottom waters of San José Lagoon as a function of decreased salinity stratification, brought about through increasing the exchange of more saline surface waters (further discussion in 2.2.1). Larger, deeper waterbodies like San Juan Bay proper will not experience a significant reduction in residence time with the opening of the Caño Martín Peña; whereas, smaller, fairly shallow waterbodies like San José Lagoon will experience significant reductions in residence time.

Figure 2 (reproduced from Figure 19 in Atkins 2011a) illustrates the statistically significant relationship between benthic index scores and residence time in the San Juan Bay Estuary.

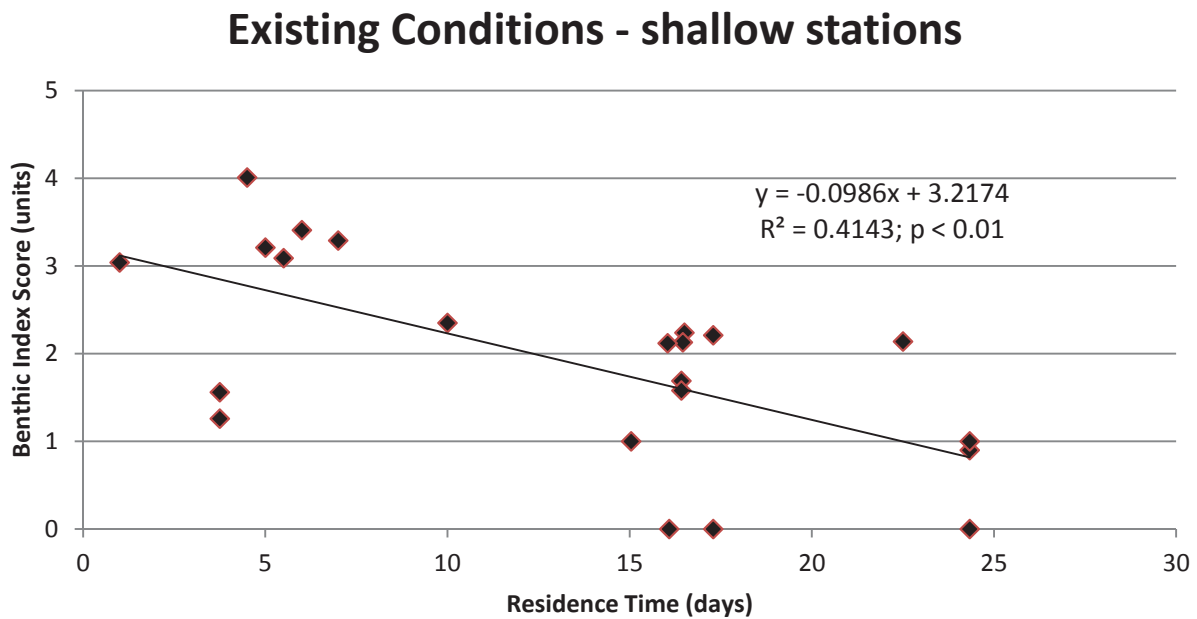


Figure 2. Relationship between residence time (days) and benthic index scores for shallow (<2 m) locations throughout the San Juan Bay Estuary.

The derived and statistically significant relationship (=Benthic Index Model) between residence time and benthic index scores is:

$$BI = - 0.0986 (RT) + 3.2174 (r^2 = 0.4143; p < 0.01)$$

Where:

- BI = benthic index score
- RT = residence time, and
- 0.0986 and 3.2174 are constants

The relationship between benthic index scores and residence time is empirically-based. A limitation of the model is that the exact mechanism through which residence time influences benthic index scores is not determined. The thought is that tidal mixing will decrease salinity stratification and increase oxygen level, thereby increasing benthic index scores (Section 2.2.1 for further discussion). Since the relationship between residence time and benthic index scores is mathematically derived, there are no assumed or literature-derived variables other than those in the calibrated hydrodynamic model. The r-squared value of 0.4143 indicates that approximately 41 percent of the variability in benthic index scores can be attributed to variability in residence time.

The hydrodynamic model was then used to calculate changes in residence time for San José Lagoon with various project channel width configurations (Atkins 2011a). Based on a number of different constraints related to costs of debris removal, issues with bank stabilization and scouring from tidal currents, etc., a channel configuration with a weir-restricted cross-section width of 75 feet became the preferred alternative project scenario. The remainder of the project length would have a 100-foot width; however, the hydrodynamics of the system are determined by the 75-foot constriction.

The residence time in San José Lagoon was also determined by the standard definition of the volume of water divided by the average inflow rate. The volume was computed to be the area of the lagoon (the area of the cells within the hydrodynamic model within the lagoon) times an assumed depth of 6 feet. This depth was assumed to be 6 feet because field data indicated stratification at around 6 feet of water depth in the San José Lagoon (see Section 2.2.1 for further discussion) (Atkins 2011b). Above this depth the salinity is relatively low and the water has relatively high dissolved oxygen levels. Below 6 feet of depth, the water has a relatively high salinity and little to no dissolved oxygen. This indicates that the water below 6 feet of depth is not involved in typical tidal circulation.

The inflow rates in both the Caño Martín Peña and the Suárez Canal were determined by analyzing the hourly flow rates over the three month modeling period (June through August 1995, see Section 2.1.1.1 and Bunch et al. 2000). The absolute values of the hourly flows were averaged and then divided by two; the assumption being that the flow in equals the flow out. The residence time computed for the existing condition for the San José Lagoon using this method is 16.9 days.

The above method was considered the best method using the model. The following describes a second method used to verify the volume exchange method. There were eleven data output locations (grids) selected in San José Lagoon. The residence time as determined by the time required for the salinity at a location to increase from zero to 90 percent of the boundary inflow salinity. The average residence time at the data output locations was 16.57 days with a standard deviation of 0.41 days. The residence time values ranged from 16.04 to 17.29 days, within the range computed by volume exchange.

Upon restoration of the historical tidal connection between San Juan Bay and San José Lagoon, with a controlling channel width of 75 feet and with a modeled channel depth of 9 feet (model depths are in 3-foot increments; project construction depth is 10 feet), the average modeled residence time for San José Lagoon decreases to approximately 3.9 days (Atkins 2011a).

Based on the empirically-derived relationship between residence time and benthic index scores, average benthic index scores are estimated at 1.55 and 2.84 for existing conditions and with a 75-foot controlling channel width, respectively, based on the equation shown above. The average benthic index score for shallow stations in San José Lagoon is 1.33, vs. the predicted value of 1.55 based on the derived equation, a difference of 17 percent. The 17 percent difference between model output and measured data found here is much less than the average difference between modeled vs. measured phytoplankton abundance (quantified as μg chlorophyll-*a* / liter) found by Cerco and Noel (2004) in their report on water quality modeling efforts in the Chesapeake Bay, illustrating the value of this metric as a measure of project success.

2.1.3 Scientific Basis for Habitat Models

The following outlines the scientific basis for the two habitat models — the Fish Habitat Model and the Mangrove Habitat Model.

The availability of mangrove nursery habitat has a striking impact on the community structure and biomass of fish inhabiting reef habitats as adults, as the biomass of several species more than doubled when mangrove habitats were available to reef-dwelling species (Mumby 2006). In the Gulf of California, Aburto-Oropeza et al. (2008) showed that fisheries landings in offshore waters were positively correlated with the local abundance of mangroves. In addition, the presence of mangroves significantly increases species richness and the abundance of shrimp in seagrass beds, relative to seagrass beds without adjacent mangroves (Skilleter et al. 2005). In research focused on the Caribbean, including Puerto Rico, Nagelkerken, et al. (2001, 2002) concluded that for some of the fish species they investigated, adult densities on coral reefs appear to be a function of the presence of nearby mangroves and seagrass beds, which function as nurseries for the juveniles.

These conclusions imply that documented declines in fishery landings in Puerto Rico (Matos-Caraballo 2008) can be attributed at least in part to the decline in the quantity and quality of accessible nearshore habitats. These conclusions also imply that restoring the historical inter-

connectedness between the seascape features of San Juan Bay and the nearshore reefs will benefit the long-term health of both inshore and nearshore marine ecosystems, which should improve both fisheries and fishing-related tourism. The San Juan Bay Estuary system is unique in that it is one of the only combined reef and estuary systems on the north coast of Puerto Rico making it significant in the relationships described above.

Within the San Juan Bay Estuary, there are at least seven species of fish that occupy a combination of mangroves, seagrass meadows and coral reefs at various life-history stages (SJBEP 1996, Nagelkerken et al. 2001, 2002). Those species include doctor fish (*Acanthurus chirugus*), yellowfin mojarra (*Gerres cinereus*), schoolmaster (*Lutjanus apodus*), gray snapper (*L. griseus*), yellowtail snapper (*Ocyurus chrysurus*), blue parrotfish (*Scarus coeruleus*), and great barracuda (*Sphyraena barracuda*). In addition, the spiny lobster (*Panulirus argus*) is presently found in Condado Lagoon (Jorge Bauza, personal communication) and this species has been documented to use mangrove habitats as well as seagrass meadows and coral ledges during portions of their life history (Acosta and Butler 1997).

Of particular local interest, mutton snapper (*L. analis*) is an important commercial fishery in Puerto Rico, but one that is in decline (Cummings 2007, Sais et al. 2008). Although the commercial fishery for this species targets adults in both open waters and reef environments, this species uses mangrove habitat during post-larval, juvenile and adult phases (Sais et al. 2008). While fishing pressure undoubtedly plays an important role in the health of the fishery, direct and indirect impacts to nearshore fish habitats are thought to be an additional reason for the decline in the health of this fishery (Sais et al. 2008).

The inter-dependence of the fish habitats of mangroves, seagrass meadows, open water, and nearby coral reefs as inter-connected “seascape” features that support fish and fisheries is discussed in Sections 1.4 through 1.6. More locally, Sais et al. (2008) warned that impacts to nearshore mangrove and seagrass habitats would have repercussions beyond these estuarine locations alone. As related to mangrove, seagrass meadows and the open water features of Puerto Rico’s various estuarine environments, Sais et al. (2008) concluded that, “impacts to these important habitats also lead to effects in coral reefs due to the loss of juvenile habitat for reef species such as spiny lobster, snappers, and groupers.” The reverse is equally true, habitat restoration focused on Puerto Rico’s estuarine waters, seagrass meadows and mangroves should benefit reef fish populations, and thus the reefs themselves.

Prior researchers have also concluded that restoration of the historical tidal connection between San Juan Bay and the San José Lagoon would benefit the ecological health of the wider San Juan Bay Estuary (e.g. Bunch et al. 2000, Cerco et al. 2003). The concept that the offshore reefs would also benefit from the restoration of the Caño Martín Peña is based on enhanced probabilities that recreationally and commercially important fish species would be able to successfully complete their life cycles if San José Lagoon became a healthier waterbody, and if more fish habitats in the San Juan

Bay Estuary complex would be more fully inter-connected. This concept is fully consistent with a determination that increased inter-connectedness of the seascape features of mangroves, open water, seagrass meadows and reefs would benefit all of these seascape features, not simply the one(s) being actively restored (Moberg and Rönnbäck 2003).

Flux or surface tide level equalization within the estuary system is the appropriate relationship for the Fish Habitat and Mangrove Habitat Models because these models depend upon surface waters moving efficiently throughout the estuary system and distributing fish and invertebrate larvae and juveniles to these habitats along with the redistribution of mangrove seeds to appropriate locations. Surface tide level will become more equal throughout the San Juan Bay Estuary system with the opening of the Caño Martín Peña.

2.1.3.1 Fish Habitat Model Features and Quantification of Anticipated Benefits

The purpose of the Fish Habitat Model is to develop a GIS-based assessment of the anticipated benefits to the seascape features of open water, seagrass meadows, and coral reefs associated with the restoration of the historical tidal connection between San Juan Bay and San José Lagoon for use in evaluating the differences between the project alternatives. The variables used for the Fish Habitat Model are GIS-derived acreage estimates of the fish habitats of open water/seagrass meadows and reefs, as modified by scaling factors that were used to decrease habitat benefit calculations with greater distance from the restored tidal connection between San Juan Bay and San José Lagoon. The model assumptions are that increasing the inter-connectedness of the various fish habitats of the San Juan Bay Estuary system and adjacent coastal waters will increase the habitat value of these newly inter-connected habitats, but that that degree of benefit will be most strongly expressed in areas closest to the restored tidal connection. A limitation of the fish habitat model is that the exact mechanism through which the inter-connectedness influences fish habitat has not been determined; therefore, the level of influence has associated uncertainty.

The quantification of benefits to the fish habitats that constitute the seascape features of the San Juan Bay Estuary is based on a two-step process. The first step involves the use of existing GIS maps to quantify acreage associated with the habitats of open water, seagrass meadows, and nearby coral reefs. Model boundaries were those previously delimited by the San Juan Bay Estuary Program. For the habitats of open waters, seagrass meadows and adjacent coral reefs the GIS layers summarized in the report “Methods Used to Map the Benthic Habitats of Puerto Rico and the U.S. Virgin Islands” (NOAA 2011) were accessed and clipped to meet bay segment boundaries that were reviewed and approved by local researchers in February 2013. For the Caño Martín Peña, the actual mapped habitats and channel configurations (Appendix A4) were used to quantify the acres for the proposed channel alternatives.

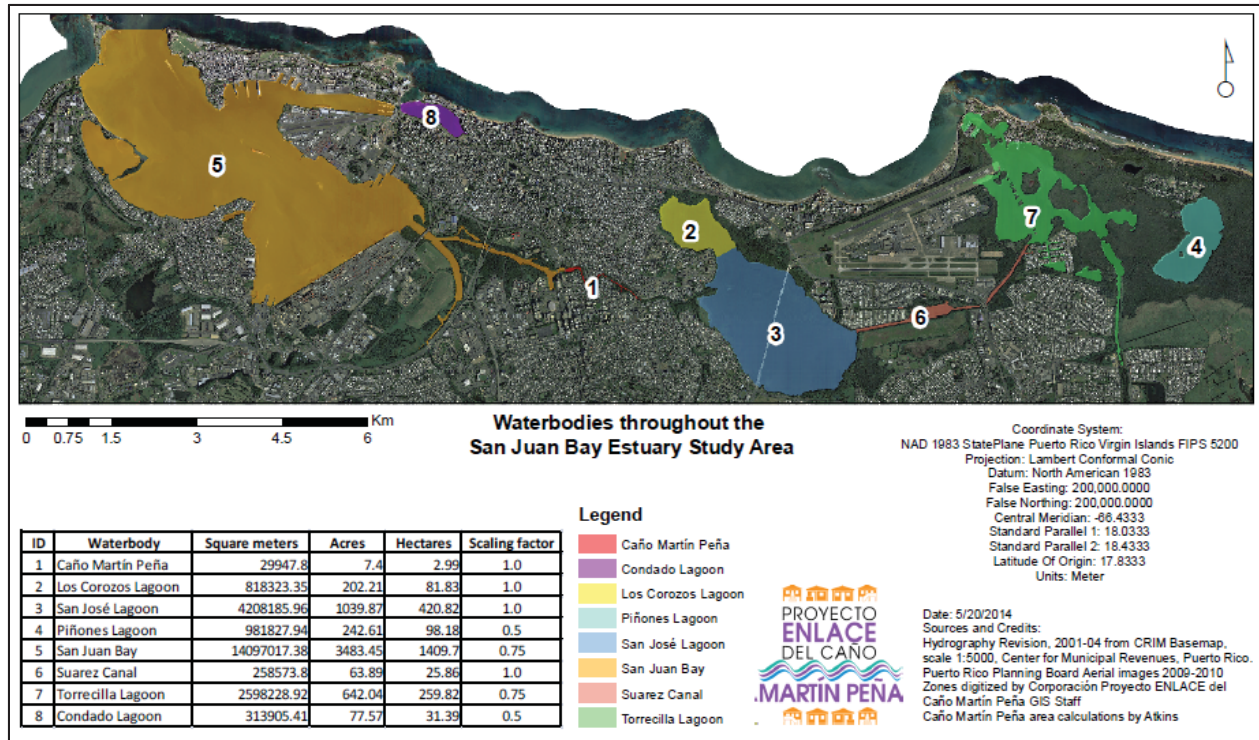


Figure 3. Open water habitat within the San Juan Bay Estuary System.

The GIS layers of both open water within the San Juan Bay Estuary system and seagrass were combined, as seagrass coverage in San Juan Bay is sparse, and mostly restricted to Condado and La Torrecilla Lagoons. Seagrass coverage estimates for the San Juan Bay Estuary vary substantially, but little coverage has been recorded in San Juan Bay, San José Lagoon and Piñones Lagoon. Consequently, seagrass cover estimates are contained within the acreage estimates for the category of “open water” for the various segments of San Juan Bay (Figure 3). The eastern and western boundaries shown for the reef tract are based on well-defined geographic borders in the GIS data set from the National Oceanic and Atmospheric Administration, NOAA (2011). The delineation of the area termed the “Central Reef Tract” is also based on natural borders in the NOAA (2011) data set. The “open water” over the reef tract is included in the reef category.

The acreage estimates for the combined areas of open water and seagrass habitat were quantified using GIS for each of the following waterbodies: 1) Caño Martín Peña (from the existing condition and project alternatives), 2) Los Corozos Lagoon, 3) San José Lagoon, 4) Piñones Lagoon, 5) San Juan Bay, 6) Suárez Canal, 7) La Torrecilla Lagoon, and 8) Condado Lagoon (Figure 3). For the reef tract, GIS coverage was divided between West Near Inlet, East Near Inlet, and Central Reef Tract portions (Figure 4).

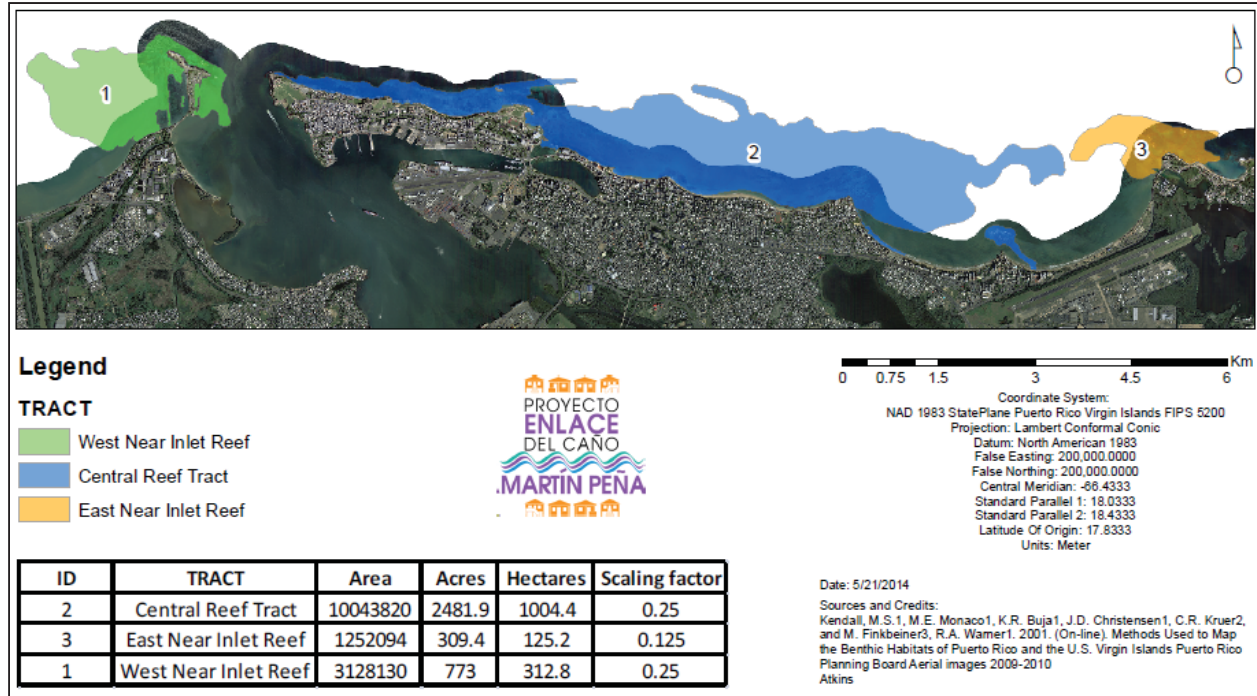


Figure 4. GIS-based estimates of reef habitat in waters adjacent to the San Juan Bay Estuary.

The fish habitats associated with open waters and seagrass meadows (if present) in Caño Martín Peña, San José Lagoon, the Suárez Canal, and Los Corozos Lagoon would directly benefit from the restoration of the historical tidal connection between San Juan Bay and San José Lagoon, and therefore the anticipated ecological uplift with project implementation is calculated by multiplying acres of open water habitat by a scaling factor of 1.0. For areas other than San José Lagoon, an approach was used whereby the relative degree of connectivity between a given location and San José Lagoon would be the basis for scaling habitat uplift estimates. The scaling factor decreased in increments of 0.25 for every intervening waterbody between a location and San José Lagoon, until reaching the farthest locations for any reasonable expectations of environmental benefit. Thus, the fish habitat benefits associated with open waters and seagrass meadows (if present) in San Juan Bay and La Torrecilla Lagoon are less direct than in San José Lagoon, and the anticipated ecological uplift is calculated by multiplying their acres of habitat by the scaling factor of 0.75. For Condado and Piñones Lagoons, the fish habitat uplift associated with open waters and seagrass meadows (if present) are less direct still, and the anticipated ecological uplift with project implementation is calculated by multiplying habitat acres by a scaling factor of 0.50.

Although it is anticipated that reef habitats will benefit from the restored water quality that would occur in San José Lagoon and the Caño Martín Peña, and that both local research (Sais et al. 2008) and a more global understanding of marine ecosystem management (e.g., Moberg and Rönnbäck 2003) support such a contention, a conservative approach to quantifying anticipated ecological uplift is appropriate. Consequently, the fish habitat uplift associated with the reef tract upon project

implementation is calculated by multiplying reef acreage estimates in the eastern near inlet and western near inlet regions by a scaling factor of 0.25. For the Central Reef Tract, a scaling factor of 0.125 is used.

2.1.3.2 Mangrove Habitat Model Features and Quantification of Anticipated Benefits

For mangroves, the GIS data layers summarized in the report “The Puerto Rico Gap Analysis Project” (USDA 2008) were accessed and clipped to meet model boundaries that were reviewed and approved by local researchers in February 2013. The boundaries for mangrove habitat shown in Figure 5 are based on the geographic boundaries for the San Juan Bay Estuary program. The mangrove habitat data layer does not overlap with the data layers described above for the Fish Habitat Model avoiding “double counting” of acreage between the two habitat models. Note that the mangroves associated with Piñones Lagoon stops at a boundary considered to be the eastern edge of that lagoon and does not extend further to include the mangrove system that continues to the east. For the Caño Martín Peña, the actual mapped proposed mangrove habitat and channel configurations (Appendix A4) were used to quantify the acres for the proposed channel alternatives.

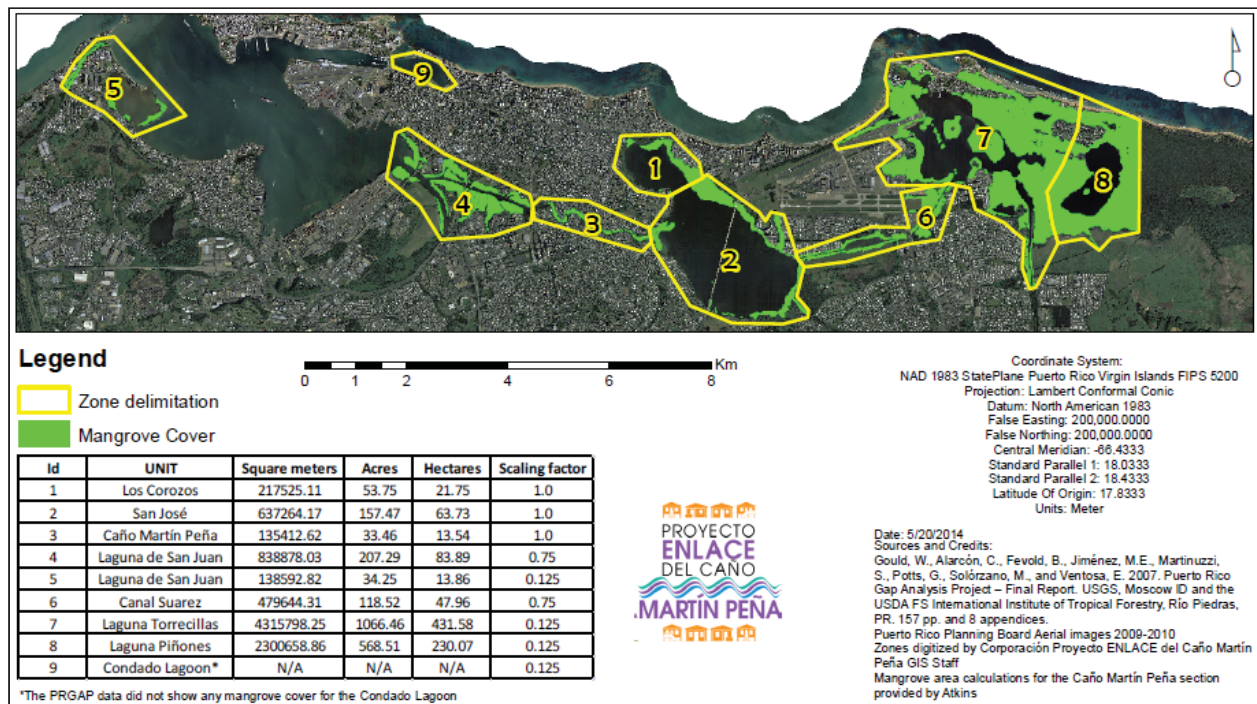


Figure 5. GIS-based estimates of mangrove cover throughout the San Juan Bay Estuary.

The purpose of the Mangrove Habitat Model is to develop a GIS-based assessment of the anticipated benefits to the seascape feature of mangroves that are anticipated to occur with the restoration of the historical tidal connection between San Juan Bay and San José Lagoon for use in evaluating the differences between the project alternatives. For mangroves, no habitats exist along the exposed

shoreline where the reef habitat is found. The variables used for the mangrove model are GIS-derived acreage estimates of mangrove habitat, as modified by scaling factors that were used to decrease habitat benefit calculations with greater distance from the restored tidal connection between San Juan Bay and San José Lagoon. The model assumptions are that restoring the historical tidal connection between San Juan Bay and San José Lagoon will increase the mangrove habitat value, based on a mathematically derived relationship that was developed between distance from the Caño Martín Peña and the abundance of fish life history stages within the mangroves and invertebrates found on and around the mangrove prop roots, but that that degree of benefit will be most strongly expressed in areas closest to the restored tidal connection.

In the Sports Fishery Study (Appendix A4; Atkins 2011b), a relationship was found between distance from the Caño Martín Peña and the abundance of invertebrates associated with the mangrove community, as illustrated in Figure 6.

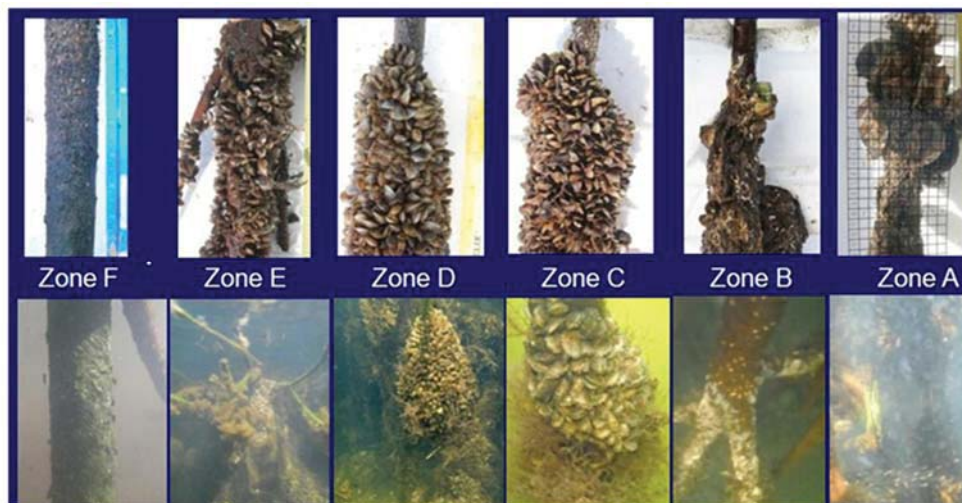


Figure 6. Example photographs of mangrove prop roots in various portions of the San Juan Bay Estuary. Zone A = northern La Torrecilla Lagoon close to the inlet, Zone B = southern La Torrecilla Lagoon, Zone C – Suárez Canal, Zone D = eastern San José Lagoon, Zone E – western San José Lagoon, and Zone F = Caño Martín Peña (Atkins 2011b).

In that study (Atkins 2011b), the number of aquatic invertebrates found on submerged portions of red mangrove prop roots increased with increasing distance from the poorly flushed waters of the Caño Martín Peña and western San José Lagoon, indicating that the fish habitat value of mangroves would be expected to increase with the restoration of the historical tidal connection between San Juan Bay and San José Lagoon (Figure 7).

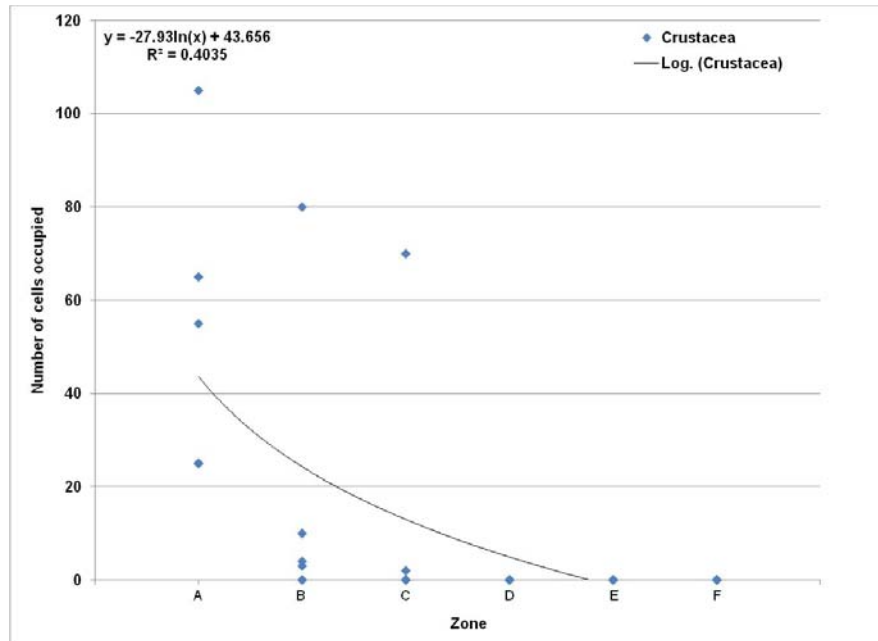


Figure 7. Relationship of the number of crabs and the distance from the Caño Martín Peña (Atkins 2011b).

The mangrove habitat (e.g., vegetation health and seed distribution) and the organisms (e.g., fish and invertebrate life stages) associated with that habitat in Caño Martín Peña and San José Lagoon would directly benefit from the restoration of the historical tidal connection between San Juan Bay and San José Lagoon. The mangrove habitat in eastern San Juan Bay and Suárez Lagoon is somewhat more distant, and the anticipated ecological uplift is less direct; benefits are calculated by multiplying acres of mangrove habitat by the scaling factor of 0.75. Mangrove uplift for La Torrecilla Lagoon is quantified as acreage multiplied by 0.25. For the more distant areas of western San Juan Bay, Condado Lagoon and Piñones Lagoon, anticipated ecological uplift of mangrove habitat is quantified by multiplying acres of mangroves by 0.125.

This scaling method for the Mangrove Habitat Model uses the differential in tide phase within San Juan Bay Estuary system reported by Fagerburg (1998) in the field data study for the hydrodynamic model calibration. In that study, Fagerburg (1998) reported finding a large tide differential (in hours) in the waterbodies immediately east of the Caño Martín Peña and a smaller differential tide phasing in waterbodies further east and west. This is because San José Lagoon is dependent on tidal waters entering through Suárez Canal and Boca de Cangrejos on the east side of the San Juan Bay Estuary system. The tide differential roughly correlates with residence time, i.e. the larger the differential in the tide phase the longer residence time of the water within the waterbody; however, as stated previously, the tide phase differential relates more to changes in surface waters, whereas, the residence time is related to the exchange of the volume of water within a waterbody. Opening the Caño Martín Peña will nearly equilibrate the tidal phase within the central portion of the San Juan Bay Estuary system as tidal waters are able to enter the central portion of the estuary system from

both the East and the West. The greatest benefits will occur within the Caño Martín Peña, San José Lagoon, and Los Corozos Lagoon. Suárez Canal and the western portion of the Caño Martín Peña will also benefit greatly, but less so, as evidenced by tidal phasing. The scaling factor decreased in increments of 0.125 based on the relative degree of similarity of tidal phases. This increase in flow and equalization will also increase the movement of fish and invertebrate eggs, larvae, and juvenile and plant seeds throughout the system. A level of uncertainty does exist with this scaling approach and further calibration or validation of the Mangrove Habitat Model cannot be done at this time. Validation will occur through the adaptive management and monitoring program.

2.2 RESULTS

2.2.1 Quantification of Benefits Based on the Benthic Index Model

The objective of the Benthic Index Model was to use the relationship of residence time and benthic index scores to evaluate the environmental benefits produced by the project alternatives within the San Juan Bay Estuary system. Based on the restoration of the historical tidal connection between San Juan Bay and San José Lagoon, the average modeled residence time (based on volume replacement) in San José Lagoon is anticipated to decrease from an average of 16.6 days down to 3.9 days (Section 2.1.2.1). Using the empirically-derived relationship between residence time and benthic index scores, benthic index scores would increase from a current value of 1.33 to an anticipated value of 2.84 with such a change in tidal exchange; however, not all of the waters of San José Lagoon would be expected to benefit from the change in tidal flushing. Some portions of the lagoon are shallow enough that salinity stratification and hypoxia do not occur, which is the most likely basis for the reduced benthic index scores in San José Lagoon (Atkins 2011a). Also, there are deep dredge pits in San José Lagoon; those areas are likely to continue to be problematic for water quality regardless of any potential changes in tidal mixing.

To estimate the spatial extent of benthic communities expected to benefit, with regard to the benthic index model, the water quality surveys conducted in the Hydrodynamic and Water Quality Modeling Effort (Atkins 2011a) were examined in greater detail. A close examination of the water column profiles contained in that report shows that salinity stratification and bottom water hypoxia/anoxia occurs at depths greater than about 4 feet. Waters shallower than 4 feet do not show evidence of salinity stratification. There are a number of deep dredge pits in the San José Lagoon, mostly in the southeastern portion of the lagoon. The deep waters of these dredge pits grade down to depths in excess of 20 feet from a more typical depth within the lagoon of approximately 6 feet. It was thus concluded that waters shallower than 4 feet would not likely benefit from enhanced tidal circulation, as they are too shallow to exhibit hypoxia/anoxia brought about by salinity stratification. Those bottom areas associated with deep dredge pits which will likely continue to be problematic in terms of hypoxia and anoxia.

Figure 8 displays those portions of San José Lagoon that are between 4 and 6 feet in depth. These areas represent the portions of San José Lagoon that are anticipated to have improved benthic index scores upon restoration of the historical tidal connection between San Juan Bay and San José Lagoon.

The amount of bay bottom anticipated to benefit from tidal restoration is quantified as those portions of San José Lagoon between 4 and 6 feet in depth (Figure 8). The benefit would be expected to arise due to reduced frequencies and/or duration of hypoxia/anoxia due to reduced salinity stratification. The benefit is expected to be expressed in terms of areas with increased diversity of benthic communities, which can be tracked over time as benthic index scores calculated as in PBS&J (2009a). The spatial extent of the bay bottom to benefit in this manner (Figure 8) is quantified at 702 acres.

2.2.2 Quantification of Benefits Based on the Fish Habitat Model

The objective of the Fish Habitat Model was to use the relationship of the level of inter-connectedness created by the project alternatives to evaluate the environmental benefits of that alternative within the San Juan Bay Estuary system. The GIS layers for the fish habitat features of open water/seagrass, and reefs were mapped and quantified as described in Section 2.1.3.1. The acres of fish habitats were then multiplied by the scaling factors described in Section 2.1.3.1, so that the ecological uplift associated with an acre of habitat would be greater for those waterbodies closest to the restored Caño Martín Peña and San José Lagoon, compared to areas that would also benefit, but indirectly. Indirect benefits are anticipated to occur as well, but the approach of scaling responses based on geographic proximity to the restored tidal connection is a conservative approach to the quantification of anticipated benefits.

Table 2 provides the location/habitat feature, existing acreage of habitat, scaling factor, and open water habitat units for the proposed, preferred channel alternative (the 100-foot-wide channel with the weir) within the Caño Martín Peña representing the “with” benefits improvement of that alternative. There are habitat units that exist within the system with the No Action Alternative (existing condition) represented by the net habitat units “without” benefits column in Table 2. Under the No Action Alternative, it is expected that the current conditions for open water/seagrass and reef habitat would remain the same and/or continue to degrade within the San Juan Bay Estuary system and the Caño Martín Peña.

To be clear, the acres of habitat within the San Juan Bay Estuary system only change for each project alternative within the Caño Martín Peña where that location/habitat feature is represented by real acres of existing and constructed acres of open water habitat. The real, constructed habitat represents the benefits within the Caño Martín Peña. Those changes between the project alternatives are represented in Table 3.

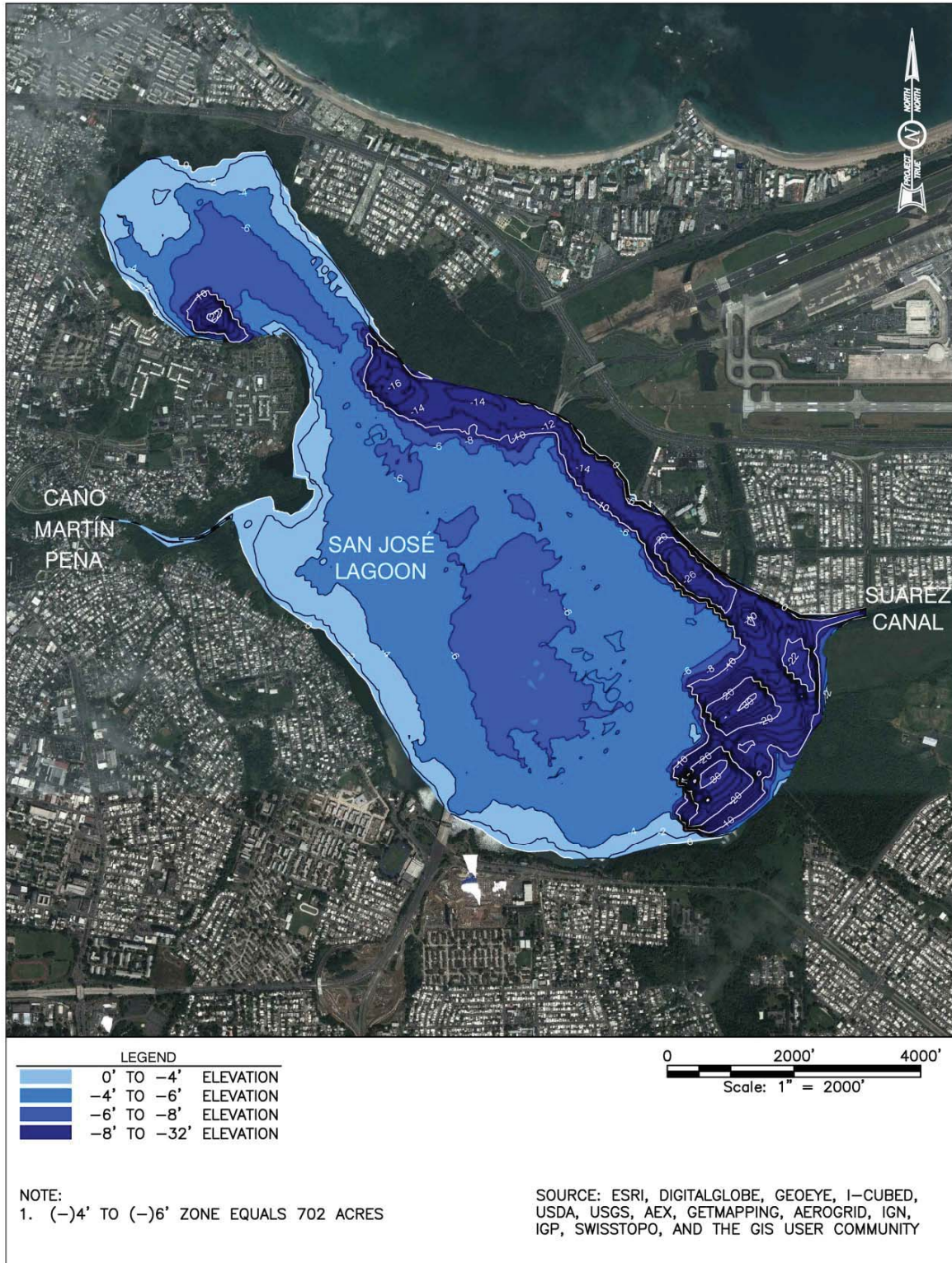


Figure 8. Spatial extent of water depth areas within San José Lagoon. Those depths with expectation of improvement in hypoxia/anoxia are the 702 acres located within the 4- to 6-foot elevation.

Table 2
Quantification of Open Water/Seagrass and Reef Habitat
Unit Benefits with Project Implementation.

Location / Habitat Feature	Acres of Habitat	Scaling Factor ¹	Net Habitat Units with Benefits	Net Habitat Units without Benefits
San Juan Bay	3,483.4	0.75	2,612.6	870.8
Condado Lagoon	77.6	0.50	38.8	38.8
San José Lagoon	1,039.9	1.00	1,039.9	0.0
La Torrecilla Lagoon	642.0	0.75	481.5	160.5
Piñones Lagoon	242.6	0.50	121.3	121.3
Suárez Canal	63.9	1.00	63.9	0.0
Caño Martín Peña	7.4	-	18.2	7.4 ²
Los Corozos Lagoon	202.2	1.00	202.2	0.0
Western near Inlet Reef	773.0	0.25	193.3	579.8
Eastern near Inlet Reef	309.4	0.25	77.4	232.0
Central Reef Tract	2,481.9	0.125	310.2	2,171.7
SUBTOTAL	9,323.3	-	5,159.2³	4,182.3³

¹ For the CMP, instead of a scaling factor, Net Habitat Unit Benefits were calculated by comparing the existing habitat units of the CMP (No Action Alternative) versus the projected habitat units of the CMP under the NER Plan (see Table 3).

² For the CMP, the existing 7.4 acres/habitat units are not included as part of, or added to, NER benefit calculations.

³ Under the NER Plan, the amount of open water within the CMP would increase from the existing 7.4 acres/habitat units to 25.6 acres/habitat units, thus increasing the overall total open water habitat from 9,323.3 acres/habitat units to 9,341.6 acres/habitat units.

Table 3
Quantification of Open Water Habitat Unit Benefits for the
No Action and Project Alternatives within the Caño Martín Peña.

Project Alternative	Existing Acres in CMP	Net Increase of Habitat Units in CMP	Total Net Habitat Units with Benefits
No Action	7.4	0.0	0.0
75-foot-wide	20.4	13.0	5,154.0 ¹
100-foot-wide with weir (NER Plan)	25.6	18.2	5,159.2
125-foot-wide with weir	31.0	23.6	5,164.6 ²

¹ For the 75-foot-wide alternative, the total net habitat units with benefits includes the increase of 13 HUs within the CMP and the 5,141 HUs for all other SJBE features identified in Table 2 (Net Habitat Units with Benefits).

² For the 125-foot-wide alternative, the total net habitat units with benefits includes the increase of 23.6 HUs within the CMP and the 5,141 HUs for all other SJBE features identified in Table 2 (Net Habitat Units with Benefits)..

2.2.3 Quantification of Benefits Based on the Mangrove Habitat Model

The objective of the Mangrove Habitat Model was to use the relationship of the level of tidal equalization (a measure of inter-connectedness) created by the project alternatives to evaluate the environmental benefits of that alternative within the San Juan Bay Estuary system. The GIS layers for the fish habitat feature of mangroves was mapped and quantified as described in Section 2.1.3.2. The acres of mangrove habitats were then multiplied by the scaling factors described in Section 2.1.3.2, so that the ecological uplift associated with an acre of mangroves would be greater for those waterbodies closest to the restored Caño Martín Peña and San José Lagoon, compared to areas that would also benefit, but indirectly. Indirect benefits are anticipated to occur as well, but the approach of scaling responses based on geographic proximity to the restored tidal connection is a conservative approach to the quantification of anticipated benefits.

Table 4 displays the location, existing acreage of mangrove habitat, scaling factor, and resulting habitat units for the mangrove habitat model. The net habitat units “with” benefits, as with the fish model, represents the benefits of the preferred alternative (100 foot-wide channel with the weir). Again, as with the fish model, there are mangrove habitats units within the San Juan Bay Estuary system in the no action alternative (existing condition) represented by the “without” benefits column. Under the no action alternative, it is expect that current conditions for mangrove habitat would remain the same and/or continue to degrade within the San Juan Bay Estuary system and Caño Martín Peña.

The net habitat units for each alternative only changes with the additional acres of mangrove habitat added to the Caño Martín Peña with channel construction. Table 5 provides the mangrove habitat units for the existing condition and proposed channel alternatives within the Caño Martín Peña. The 125-foot alternative with a weir does indicate a net loss of 4.4 Habitat Units within the Caño Martín Peña.

Table 4
Quantification of Mangrove Habitat Unit Benefits with Project Implementation.

Location	Existing Acres of Habitat	Scaling Factor ¹	Net Habitat Units with Benefits	Net Habitat Units without Benefits
Western San Juan Bay	34.2	0.125	4.3	29.9
Eastern San Juan Bay	207.3	0.75	155.5	51.8
Condado Lagoon	NM ²	0.125	NM	NM
San José Lagoon	157.5	1.00	157.5	0.0
La Torrecilla Lagoon	1,066.5	0.25	266.6	799.9
Piñones Lagoon	568.5	0.125	71.1	497.4
Suárez Canal	118.5	0.75	88.9	29.6
Caño Martín Peña	33.5	-	1.0	33.5 ³
Los Corozos Lagoon	53.8	1.00	53.8	0.0
SUB-TOTAL	2,241.8	-	798.6⁴	1442.2⁴

¹ For the CMP, instead of a scaling factor, Net Habitat Unit Benefits were calculated by comparing the existing habitat units of the CMP (No Action Alternative) versus the projected habitat units of the CMP under the NER Plan (see Table 5).

² NM = none mapped / not shown in GIS data files

³ For the CMP, the existing 33.5 acres/habitat units of mangroves are not included as part of, or added to, NER benefit calculations.

⁴ Under the NER Plan, the amount of mangrove habitat within the CMP would increase from the existing 33.5 acres/habitat units to 36.5 acres/habitat units, thus increasing the overall total mangrove habitat from 2,239.8 acres/habitat units to 2,240.8 acres/habitat units.

Table 5
Quantification of Mangrove Habitat Unit Benefits for the No Action and Project Alternatives within the Caño Martín Peña.

Project Alternative	Existing Acres in CMP	Net Increase of Habitat Units in CMP	Total Net Habitat Units with Benefits
No Action	33.5	0.0	0.0
75-foot-wide	39.6	6.2	803.8 ¹
100-foot-wide with weir (NER Plan)	34.5	1.0	798.6
125-foot-wide with weir	29.1	-4.4	793.2 ²

¹ For the 75-foot-wide alternative, the total net habitat units with benefits includes the increase of 6.2 HUs within the CMP and the 797.6 HUs for all other SJBE features identified in Table 4 (Net Habitat Units with Benefits)..

² For the 125-foot-wide alternative, the total net habitat units with benefits includes the increase of -4.4 HUs within the CMP and the 797.6 HUs for all other SJBE features identified in Table 4 (Net Habitat Units with Benefits).

2.3 TIMELINE OF EXPECTED ECOSYSTEM RECOVERY

A literature search was completed to determine the probable timelines required for ecological restoration such as that envisioned for the Caño Martín Peña project. Restoration projects, where the focus of activities was the reestablishment of historical hydrologic connections, were included, as well as restoration that occurred via the reduction in external pollutant loads. These projects typically experience hydrologic changes (e.g., tide, water velocity, residence time) quickly after restoration. Water quality changes are experienced with greater water movement and flushing. Finally, overtime, the organism response will follow with the improved water quality. This same timeline for change is anticipated for the Caño Martín Peña project; however, there is uncertainty in the amount of time that it will take the habitats and organisms in the habitats to respond to the hydrologic and water quality changes. The results of this literature review are summarized in Table 6.

Based on restoration projects completed in both temperate and sub-tropical estuarine environments, positive responses of water quality and benthic communities would be expected to occur within the first 3 years of implementing a project such as the restoration of the tidal connection between San Juan Bay and the San José Lagoon. For those projects that included a fish habitat component, there is no discernible difference between the timeline of recovery of fisheries resources and the timeline for recovery of either benthic communities or water quality. Quantification of fisheries responses seems to be less often pursued than is the case for water quality monitoring and/or benthic community responses, yet the existing information suggests a similar timeline is expected. For ecosystem restoration projects as a whole, ecosystem recovery would be expected to be substantial and documentable within a few years. For those projects where activities focused on the restoration of historical tidal connections, all seven examples shown in Table 4 had initial recovery within a 1-year period. Of these seven studies, three of them showed evidence of substantial recovery of benthic communities within the first year after restoration of tidal connections, three had documentation of substantial recovery within a 2-year period, and the remaining study documented substantial recovery within a 3-year period. All seven examples used words such as “substantial” or “significant” or “noticeable” to portray the level of ecosystem response to the restoration of historical tidal connections. As such, a trajectory of fish habitat responses over time would indicate relatively rapid recovery is expected in a restored San Juan Bay Estuary.

Table 6
Summary of Ecosystem Response Timelines for Completed Restoration Projects.

Study	Location	Type of Restoration	Highlights of System Response	Timeline for Initial Response	Timeline for Substantial Recovery
Dean and Haskin 1964	Raritan Bay, New Jersey	Removal of point source pollution	Benthic community recovery	Within 1 year	Within 3 years
Rosenberg 1973	Sweden	Removal of point source pollution	Benthic community recovery	Within 1 year	Within 6 years
Rosenberg 1976	Sweden	Removal of point source pollution	Benthic community recovery	Within 1 year	Within 8 years
Wu 1982	Hong Kong	Removal of point source pollution	Water quality and benthic community recovery	Within 1 year	Within 1 year
Karakassis et al. 1999	Greece	Removal of fish farm influences	Benthic community recovery	Within 1 year	Within 2 years
Vose and Bell 1994	Tampa Bay, Florida	Restoration of historical tidal exchange	Water and sediment quality, benthic community and fish abundance recovery	Within 1 year	Within 2 years
Zajac and Whitlatch 2001	Alewife Cove, Connecticut	Restoration of historical tidal exchange	Sediment quality, benthic community recovery	Within 1 year	Within 3 years
Raposa 2002	Narragansett Bay, Rhode Island	Restoration of historical tidal exchange	Water quality and benthic community recovery	Within 1 year	Within 2 years
Roman et al. 2002	Narragansett Bay, Rhode Island	Restoration of historical tidal exchange	Water quality, benthic community and fish abundance recovery	Within 1 year	Within 1 year
Thelen and Thiet 2008	East Bay, Rhode Island	Restoration of historical tidal exchange	Water quality, benthic community and fish abundance recovery	Within 1 year	Within 1 year
PBS&J 2009b	Key Largo, Florida	Restoration of historical tidal exchange	Water quality	Within 1 year	Within 1 year
Marcus 2010	Key Largo, Florida	Restoration of historical tidal exchange	Benthic community recovery	Within 1 year	Within 2 years

This page intentionally left blank.

3.0 BENEFITS EVALUATION

The commercial and recreational benefits derived from the ecological uplift anticipated to occur with the proposed Caño Martín Peña Ecosystem Restoration Project could be substantial. Matos-Caraballo (2008) estimates that between 1.2 to 1.8 million pounds of fish and shellfish are landed in Puerto Rico annually by commercial fisheries, valued at between \$2.8 and \$4.2 million. This represents economic benefits for the 809 part- or full-time commercial fishermen in the Island, and for the countless businesses that rely upon this harvest. The “north” region, which includes the San Juan Bay Estuary area, is responsible for approximately 5 percent of this amount (Matos-Caraballo, 2007). In contrast, the marine recreational fishery in Puerto Rico is over 15 times more valuable than the commercial fishery (Lilyestrom, personal communication, 2013). While there were 809 commercial fishermen in 2008, there were approximately 30,000 non-resident and 192,128 resident recreational anglers in Puerto Rico (LeGore 2007). The additional habitat, habitat-connectivity, and habitat-suitability that the Caño Martín Peña Ecosystem Restoration Project will provide are sure to add stability to this important component of Puerto Rico’s tourism-related economy.

The large-scale and inter-twined ecosystem recovery envisioned as a project outcome is consistent with the Conceptual Ecosystem Model developed for the Caño Martín Peña restoration project (Appendix A1). The techniques used to develop the estimated ecosystem response quantified here involved logic, techniques, and peer-review processes that were carried out in a manner consistent with guidance outlined in Fischenich (2008 and 2010).

The purpose of the benefits evaluation is to use the information developed further in the previous sections of the Appendix with the objective to determine the anticipated Habitat Units obtained from each project alternative and the anticipated average annual Habitat Units achieved over the project period (50 years). Four project alternatives - the existing condition, the 75-foot-wide by 10-foot-deep alternative, the 100-foot-wide by 10-foot-deep alternative with a weir on the western end of the project, and the 125-foot-wide by 10-foot-deep alternative with a weir on the western end of the project - were evaluated using the ecological models. The weir is included in the larger project widths to prevent potential scouring from tidal current on the western end of the project. Although the western and eastern segments of the Project Channel have different cross-sectional areas and bottom elevations for the 100- and 125-foot alternatives with the weir, water flow through a tidal system such as the CMP is, and would continue to be, restricted by the smallest cross-sectional area. Accordingly, once the weir is included in the larger channel configurations, there is no further benefit to residence time in San José Lagoon with channel widths wider than 75 feet, and thus no additional national ecosystem restoration benefits. Therefore, the NER benefits related to ecological uplift for all alternatives would be the same as the 75-foot channel alternative. Open water and mangrove habitat restoration within the Project Channel are included in the calculation of NER benefits for the alternatives; however, there would be a minor variation in habitat scores as it related to open water and mangrove habitat within the Project Channel between the alternatives, and as such, the benefits

are assumed to be equal among the alternatives. The results of the benefits evaluation are presented in Table 7.

The following is an explanation of the inputs to the benefits evaluation, for each of the project alternatives, proceeding across the headings presented in Table 7.

- **Residence time** – the average residence time in San José Lagoon calculated from the hydrodynamic model.
- **Benthic Index** – the benthic index score calculated from the residence time using the Benthic Index Model.
- **Benthic Index Project Performance** – the performance of the project alternative based upon the maximum benthic index score of 3.0 estimated using the model and a 200-foot-wide by 10-foot-deep alternative. This would approximately match the maximum predicted value for the Benthic Index in San José Lagoon after restoring the Caño Martín Peña to its original width and depth.
- **Benthic Index Habitat Units** – the Habitat Units based upon the project performance with the maximum area of benefit of 702 acres.
- **Benthic Index Net Habitat Units** – the Habitat Units provided by the project above no action.
- **Net Benthic Habitat Net Average Annual Habitat Units** – net average annual Habitat Units considering the Benthic Index Model is based upon the recovery of the area in San José Lagoon to the predicted Benthic Index value with the expected linear time of recovery of 3 years to full benefit from the existing condition and the project period of 50 years.
- **Fish Habitat Model Net Habitat Units** – the Habitat Unit score based upon the percentage lift from the existing condition depending on the location of the habitat.
- **Fish Habitat Model Net Average Annual Habitat Units** - The average annual Habitat Units for the Fish Habitat Model is based upon the linear recovery time of 3 years to full benefit from the existing condition and a project period of 50 years.
- **Mangrove Habitat Model Net Habitat Units** – the Habitat Unit score based upon the percentage lift from the existing condition depending on the location of the habitat.
- **Mangrove Habitat Model Net Average Annual Habitat Units** - The average annual Habitat Units for the Mangrove Habitat Model is based upon the linear recovery time of 3 years to full benefit from the existing condition and a project period of 50 years.
- **Total Net Average Annual Habitat Units** - The total average annual Habitat Units is the combination of the average annual Habitat Units for the Benthic Index Model, the Fish Habitat Model, and the Mangrove Habitat Model.

The calculation of the Benthic Index and the development of the Benthic Index Model are explained Sections 2.1.2 and 2.1.2.1, respectively. The performance of the Benthic Index Model is based on achieving a Benthic Index value of 3.0, which would be approximately the maximum predicted value for the Benthic Index in San José Lagoon after restoring the Caño Martín Peña to its original width

and depth of an estimated 200 feet by 10 feet (Section 1.1). The Habitat Units, as explained in Section 2.2.1, are based upon the project performance and the maximum spatial extent of the area of San José Lagoon that would benefit from the opening of the Caño Martín Peña (702 acres). The net average annual Habitat Units (294.54 Habitat Units) for the Benthic Index Model is based upon the recovery of the area in San José Lagoon to the predicted, modeled Benthic Index Habitat Units (663.81 Habitat Units) starting from no action (362.95 Habitat Units) with the expected time of recovery of 3 years (linearly from the existing condition to the predicted, modeled score) and the project period of 50 years (Section 2.3).

The quantification of the Fish Habitat Model is explained in Section 2.1.3.1. The total acreage of open water and reef habitat were calculated from available GIS data. The construction of the CMP-ERP would result in the eventual benefit to open water and reef habitat of additional net habitat units based upon the scaling factors and the proposed Caño Martín Peña channel alternatives (5,154.01 Habitat Units for the 75-foot Alternative; 5,159.16 Habitat Units for the 100-foot Alternative with weir; and 5,164.56 Habitat Units for the 125-foot Alternative with weir), as explained in Sections 2.2.2 and 3.2. The net average annual Habitat Units for the Fish Habitat Model varies between the proposed Caño Martín Peña channel alternatives (5,050.93 Habitat Units for the 75-foot Alternative; 5,055.98 Habitat Units for the 100-foot Alternative with weir; and 5,061.27 Habitat Units for the 125-foot Alternative with weir) and is based upon the recovery time of 3 years (linearly from the existing condition to the predicted, modeled score) and a project period of 50 years (Section 2.3).

The Mangrove Habitat Model is also quantified based on a scaling factor and the total mangrove habitat acres within the San Juan Bay Estuary system from available GIS data (Section 2.1.3.2 and 2.2.3). The net Habitat Units would be those Habitat Units (803.77 Habitat Units for the 75-foot Alternative; 798.63 Habitat Units for the 100-foot Alternative with weir; and 793.23 Habitat Units for the 125-foot Alternative with weir) gained with each project alternative above the no action alternative (Section 3.2). The net average annual Habitat Units for the Mangrove Habitat Model (787.69 Habitat Units for the 75-foot Alternative; 782.66 Habitat Units for the 100-foot Alternative with weir; and 777.37 Habitat Units for the 125-foot Alternative with weir) is based upon the recovery time of 3 years (linearly from the existing condition to the predicted, modeled score) and a project period of 50 years (Section 2.3).

Table 7
Average Annual Habitat Unit lift for the project alternatives

Project Condition	Residence Time (days)	Benthic Index ¹	Benthic Index Project Performance	Benthic Index Habitat Units (HU) ²	Benthic Index Net HU	Net Benthic Index Net Average Annual HU ³	Fish Habitat Model Net HU ⁴	Fish Habitat Model Net Average Annual HU ³	Mangrove Habitat Model Net HU ⁴	Mangrove Habitat Model Net Average Annual HU ³	Total Net Habitat Units	Total Net Average Annual HU ⁵
No Action	16.9	1.55	51.70%	362.95	0	0	0	0	0	0	0	0
75-ft-wide Alternative	3.9	2.84	94.56%	663.81	300.86	294.54	5,154.01	5,050.93	803.77	787.69	6,258.64	6,133.16
100-ft-wide Alternative with weir (NER Plan)	3.9	2.84	94.56%	663.81	300.86	294.54	5,159.16	5,055.98	798.63	782.66	6,258.65	6,133.17
125-ft-wide Alternative with weir	3.9	2.84	94.56%	663.81	300.86	294.54	5,164.56	5,061.27	793.23	777.37	6,258.65	6,133.17

¹ Based upon a maximum Benthic Index Score of 3.0 (see text for further explanation).

² Based upon an expected area to benefit = those regions between -4 and -6 feet in water depth within San José Lagoon (= 702 acres maximum).

³ Average annual habitat unit lift from existing condition based upon a 3-year recovery time after project construction.

⁴ See text for explanation.

⁵ Combined Benthic Index Average Annual HU lift, Fish Habitat Model Average Annual HU lift and Mangrove Habitat Model HU lift based upon a 3-year recovery time after project construction [Columns F + H + J = K].

Table 8
Summary of Net Average Annual Habitat Units for the Models

Project Condition	Benthic Index	Fish Habitat	Mangrove Habitat	Total
No Action	0	0	0	0
75-foot-wide Alternative	294.54	5,050.93	787.69	6,133.16
100-foot-wide Alternative with weir (NER Plan)	294.54	5,055.98	782.66	6,133.17
125-foot-wide Alternative with weir	294.54	5,061.27	777.37	6,133.17

The net total average annual Habitat Units (6,133.2 Habitat Units) is the combination of the net average annual Habitat Units for the Benthic Index Model, the Fish Habitat Model, and the Mangrove Habitat Model. The net average annual habitat units do not vary significantly between alternatives because, as the proposed channel configuration becomes wider, the open water habitat increases and the proposed mangrove habitat decreases. Tables 3 and 5 show this shift with the project alternatives. Figure 9 shows the anticipated Habitat Units over the project period timeline accumulating linearly over the first 3 years of recovery and maintain the full habitat units over the 50-year project period. Because of the 75-foot constriction caused by the proposed weir, all of the proposed construction alternatives for the project have essentially the same estimated performance (i.e., Habitat Unit lift) over the 50-year project period.

Uncertainties and limitations exist with any model that attempts to predict an environmental parameter. As has been expressed in this Appendix and the supporting literature, changes in benthic, fish, and mangrove habitat are anticipated to occur with the restoration of the Caño Martín Peña. There are uncertainties and limitations that have been expressed as to the exact mechanisms behind the correlations with hydrologic and water quality changes and the anticipated organism and habitat changes. A limitation of the fish habitat model is that the exact mechanism through which the inter-connectedness influences fish habitat has not been determined; therefore, the level of influence has an associated uncertainty. While the timeline for ecosystem response is anticipated to be approximately 3 years for the Caño Martín Peña project, there is uncertainty in the amount of time that it will take the habitats and organisms in the habitats to respond to the hydrologic and water quality changes. Lastly, there is uncertainty associated with the scaling approach as it relates to the scaling factors identified for the various waterbodies and habitats associated with both the Fish Habitat and the Mangrove Habitat Models. The calculation of the fish and mangrove habitat scores is directly influenced by the assigned scaling factors, and the actual ecological benefit could be greater than, or lesser than, the projected benefits assigned for both habitat models. Much of the validation of the models and the performance of the models/metrics will be dependent upon the data collected using the Adaptive Management and Monitoring Program.

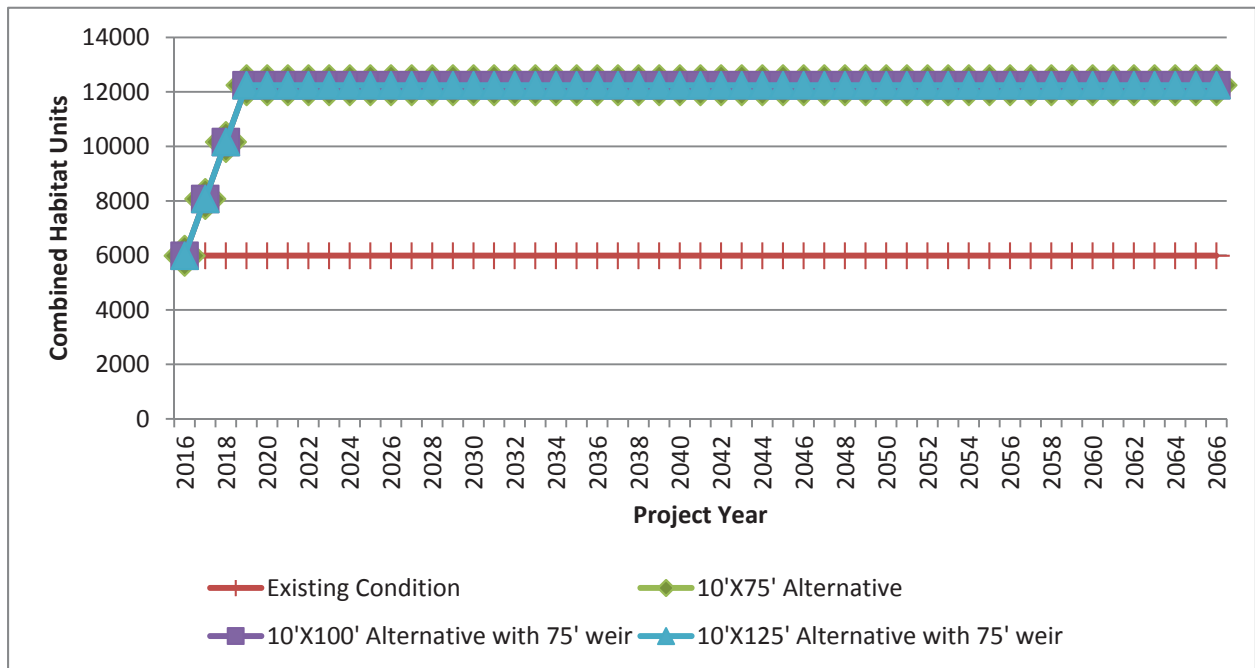


Figure 9. Average Annual Habitat Unit lift for the combined models for each project alternative based upon an estimated recovery time for the habitats of 3 years and a 50-year project period.

4.0 LITERATURE CITED

- Aburto-Oropeza, O., E. Ezcura, G. Danemann, V. Valdez, J. Murray, and E. Sala. 2008. Mangroves in the Gulf of California increase fishery yields. *Proceedings of the National Academy of Sciences* 105(30): 10456–10459.
- Acosta, C.A. and M.J. Butler. 1997. Role of mangrove habitat as a nursery for juvenile spiny lobster, *Panulirus argus*, in Belize. *Marine and Freshwater Research* 48:721–727.
- Atkins. 2011a. *Task 6.0 – Hydrodynamic and Water Quality Modeling Efforts*. Technical Memorandum for ENLACE – Caño Martín Peña Restoration Project. San Juan, Puerto Rico. 44 pp.
- . 2011b. Sport Fisheries Studies Technical Memorandum: Caño Martín Peña Ecosystem Restoration Project – San Juan, Puerto Rico Corporación del Proyecto ENLACE del Caño Martín Peña. 54 pp.
- Bauza, J. 2013. Tercer Informe de la condición ambiental del Estuario de la Bahía de San Juan (edición 2013).
- Birkeland C. 1985. Ecological interactions between tropical coastal ecosystems. *UNEP Regional Seas Reports and Studies* 73:1–26.
- Bunch, B.W., C.F. Cerco, M.S. Dortch, B.H. Johnson, and K.W. Kim. 2000. Hydrodynamic and Water Quality Model Study of San Juan Bay Estuary. ERDC TR-00-1, U.S. Army Engineer Research and Development Center, Vicksburg, Mississippi.
- Cerco, C., B. Bunch, M. Dortch, B. Johnson, and K. Kim. 2003. Eutrophication and pathogen abatement in the San Juan Bay Estuary. *Journal of Environmental Engineering* 129(4): 318–327.
- Cerco, C.F., and M.R. Noel. 2004. *The 2002 Chesapeake Bay Eutrophication Model*. Final report for the U.S. Environmental Protection Agency and the U.S. Army Corps of Engineers.
- Cummings, N.J. 2007. An Examination of the Mutton snapper, *Lutjanus analis*, commercial catch per unit of effort data in Puerto Rico from 1983-2005 available for use in developing estimates of abundance. Sustainable Fisheries Division Contribution No. SFD-2007-18. 44 pp.
- Dean, D., and H.H. Haskin. 1964. Benthic repopulation of the Raritan River estuary following pollution abatement. *Limnology and Oceanography* 9:551–563.
- Fagerburg, T.L. 1998. San Juan Bay Estuary study: hydrodynamic field data collection,. Miscellaneous Paper CHL-98-3, U.S. Army Engineer Waterways Experiment Station, Vicksburg, Mississippi.
- Faunce, C., J. Tunnell, M. Burton, K. Ferguson, J. O’Hop, R. Muller, M. Feeley, and L. Crabtree. 2007. Life history of *Lutjanus analis* inhabiting Florida waters. SEDAR15A-DW-15. 35 pp.

- Fischenich, C. 2008. The application of conceptual models to ecosystem restoration. EBA Technical Notes Collection. ERDC/EBA TN-08-1. Vicksburg, Mississippi: U.S. Army Engineer Research and Development Center. www.wes.army.mil/el/emrrp.
- Fischenrich, C. 2010. Environmental Benefits Analysis Research Program. Improving benefit assessments using scientifically-based metrics and peer-reviewed methods in support of Federal investment in ecosystem restoration. A presentation by the ERDC Environmental Lab.
- Garcia-Sais, J.G., Appeldoorn, R., Battista, T., Bauer, L., Bruckner, A., Caldow, C., Carrubba, L., Corredor, J., Diaz, E., Lilyestrom, C., Garcia-Moliner, G., Delgado, E., Menza, C., Morrell, J., Pait, A., Sabater, J., Weil, E., Williams, E., and S. Williams. 2008. State of Coral Reef Ecosystems of Puerto Rico. 42 pp.
- Karakassis, I., E. Hatziyanni, M. Tsapakis, and W. Plaiti. 1999. Benthic recovery following cessation of fish farming: a series of successes and catastrophes. *Marine Ecology Progress Series* 184:205–218.
- Kennedy, R.H., Hains, J.J., Boyd, W.A., Lemons, J., Herrmann, F., Honnell, D., Howell, P., Way, C., Fernandez, F. Miller-Way, T., and R.R. Twilley. 1996. “San Juan Bay and Estuary Study Water Quality Data Collection.” Miscellaneous Paper EL-96-9. USACE Waterways Experimental Station.
- McKay, S.K., B.A. Pruitt, M. Harberg, A.P. Covich, M.A. Kenney, and J.C. Fischenich. 2010. Metric development for environmental benefits analysis. EBA Technical Notes Collection. ERDC TN-EMRRP-EBA-4. Vicksburg, MS: U.S. Army Engineer Research and Development Center. <http://cw-environment.usace.army.mil/eba/>.
- National Oceanic and Atmospheric Administration (NOAA). 2001. (M.S., M.E. Monaco, K.R. Buja, J.D. Christensen, C.R. Kruer, M. Finkbeiner, and R.A. Warner). On-line. Methods Used to Map the Benthic Habitats of Puerto Rico and the U.S. Virgin Islands. National Ocean Service, National Centers for Coastal Ocean Science Biogeography Program.
- Lee J.S., K.T. Lee, and G.S. Park. 2005. Acute toxicity of heavy metals, tributyltin, ammonia, and polycyclic aromatic hydrocarbons to benthic amphipod *Grandidierella japonica*. *Ocean Science Journal* 40(2): 61–66.
- Marcus, J. 2010. Seagrass Recruitment 15 Months After the Removal of the Lake Surprise Causeway. Poster presentation at: Linking Science to Management: A Conference & Workshop on the Florida Keys Marine Ecosystem. Hawks Cay, Florida. October 2010.
- Matos-Caraballo, D. 2008. Lessons Learned from the Puerto Rico’s Commercial Fishery, 1988–2008. Commercial Fisheries Statistics Program, Puerto Rico’s DNER Fisheries Research Laboratory, P.O. Box 3665, Mayagüez, Puerto Rico.
- Moberg, F. and P. Rönnbäck. 2003. Ecosystem services of the tropical seascape: Interactions, substitutions and restoration. *Ocean and Coastal Management* 46:27–46.

- Mumby, P.J. 2006. Connectivity of reef fish between mangroves and coral reefs: Algorithms for the design of marine reserves at seascape scales. *Biological Conservation* 128:215–222.
- Nagelkerken, I., Roberts, C.M., van der Velde, G., Dorenbosch, M., van Riel, M.C., Cocheret, E., and P.H. Nienhuis. 2002. How important are mangroves and seagrass beds for coral-reef fish? The nursery hypothesis tested on an island scale. *Marine Ecology Progress Series* 244:299–305.
- Nagelkerken, I., S. Kleijnen, T. Klop, R.A. van den Brand, E.C. de la Moriniere, and G. van der Velde. 2001. Dependence of Caribbean reef fishes on mangroves and seagrass beds as nursery habitats: a comparison of fish faunas between bays with and without mangroves/ seagrass beds. *Marine Ecology Progress Series* 214:225–235.
- National Marine Fisheries Service. http://www.habitat.noaa.gov/pdf/fisheries_habitatcritical_habitatcomparison.pdf.
- Ogden JC, and E.H. Gladfelter. 1983. *Coral reefs, seagrass beds and mangroves: their interactions in the coastal zones of the Caribbean*. UNESCO Reports on Marine Science 23:133.
- Paul J.F., K.J. Scott, D.E. Campbell, J.E. Gentile, C.S. Strobel, R.M. Valente, S.B. Weisberg, A.F. Holland, and J.A. Ransinghe. 2001. Developing and applying a benthic index of estuarine condition for the Virginian Biogeographic Province. *Ecological Indicators* 1:83–99.
- PBS&J. 2009a. Development of the Benthic Index for the San Juan Bay Estuary System. Final Report to the San Juan Bay Estuary Program. 30 pp + appendices.
- . 2009b. Responses of Water Quality and Seagrass Coverage to the Removal of the Lake Surprise Causeway. Final Report to the Florida Department of Transportation. 34 pp.
- Pinto R., J. Patricio, A. Baeta, B.D. Fath, J.M. Neto, and J.C. Marques. 2009. Review and evaluation of estuarine biotic indices to assess benthic condition. *Ecological Indicators* 9:1–25.
- Porter, J.W., and K.G. Porter. 2001. *The Everglades, Florida Bay, and Coral Reefs of the Florida Keys: An Ecosystem Sourcebook*. CRC Press. Boca Raton, Florida.
- Puerto Rico Environmental Quality Board. 2010. “305(b) and 303(d) Integrated Report.”
- Raposa, K. 2002. Early responses of fishes and crustaceans to restoration of a tidally restricted New England salt marsh. *Restoration Ecology* 10:665–676.
- Rivera J.A. 2005. Finding of the Benthic Assessment of the San Juan Bay Estuary, Puerto Rico. Final Report. NOAA-EPA Interagency Agreement #DW 1394 1778-01. 83 pp.
- Roman, C.T., Raposa, K.B., Adamowicz, S.C., James-Pirri, M.J., and J.G. Catena. 2002. Quantifying vegetation and nekton response to tidal restoration of a New England salt marsh. *Restoration Ecology* 10:450–460.
- Rosenberg, R. 1973. Succession in benthic macrofauna in a Swedish fjord subsequent to the closure of a sulphite pulp mill. *Oikos* 24:244–258.

- San Juan Bay Estuary Program. 1996. Lista Sobre Flora y Fauna del Estuario de la Bahía de San Juan. San Juan Bay Estuary Program, San Juan, Puerto Rico. 79 pp.
- . 2000. Comprehensive Conservation and Management Plan. San Juan Bay Estuary Program, San Juan, Puerto Rico.
- . 2008. Quality Assurance Project Plan for the San Juan Bay Estuary Water Quality Volunteer Monitoring Program. San Juan Bay Estuary Program, San Juan, Puerto Rico.
- Skilleter, G.A., A. Olds, N.R. Loneragan, and Y. Zharikov. 2005. The value of patches of intertidal seagrass to prawns depends on their proximity to mangroves. *Marine Biology* 147(2): 353–365.
- Thelen, B.A., and R.K. Thiet. 2008. Molluscan community recovery following partial tidal restoration of a New England estuary, USA. *Restoration Ecology* 17:695-703.
- Traunspurger W., C. Drews. 1996. Toxicity analysis of freshwater and marine sediments with meio- and macrobenthic organisms: a review. *Hydrobiologia* 328, 215-261.
- U.S. Army Corps of Engineers (USACE). 2000. United States Army Corps of Engineers, Engineering Report 1105-2-100, Planning Guidance Notebook.
- , Jacksonville District. June 2004. Reconnaissance Report, Section 905(b) (WRDA 86) Analysis, Caño Martín Peña, Puerto Rico, Ecosystem Restoration. 22 pp.
- . 2010. Environmental Benefits Analysis Research Program. Improving benefit assessments using scientifically-based metrics and peer-reviewed methods in support of Federal investment in ecosystem restoration. A presentation by the ERDC Environmental Lab.
- U.S. Department of Agriculture (USDA) 2005. (Gould, W.A., Alarcón, C., Fevold, B., Jiménez, M.E., Martinuzzi, S., Potts, G. Quiñones, M., Solórzano, M., and E. Ventosa). The Puerto Rico Gap Analysis Project. Volume I: Land Cover, Vertebrate Species Distributions, and Land Stewardship. U.S. Department of Agriculture.
- U.S. Environmental Protection Agency (EPA). 2007. National Estuary Program Coastal Condition Report. Chapter 7 – Puerto Rico: San Juan Bay Estuary Partnership Coastal Condition. U.S. EPA. 17 pp. <http://www.epa.gov/owow/oceans/nepccr/index.html>.
- EPA. 2008. Indicator Development for Estuaries. United States Environmental Protection Agency. Washington, D.C. 138 pp.
- Vose, F.E., and S.S. Bell. 1994. Resident fishes and macrobenthos in mangrove-rimmed habitats: evaluation of habitat restoration by hydrologic modification. *Estuaries* 17:585–596.
- Webb, R., and F. Gomez-Gomez. 1998. “Synoptic Survey of water quality and bottom sediments, San Juan Bay Estuary System, Puerto Rico, December 1994–July 1995.” USGS Water-Resources Investigation Report 97-4144.

Weston D.P. 1996. Further development of a chronic *Ampelisca abdita* bioassay as an indicator of sediment toxicity. A special study of the San Francisco Estuary Regional Monitoring Program.

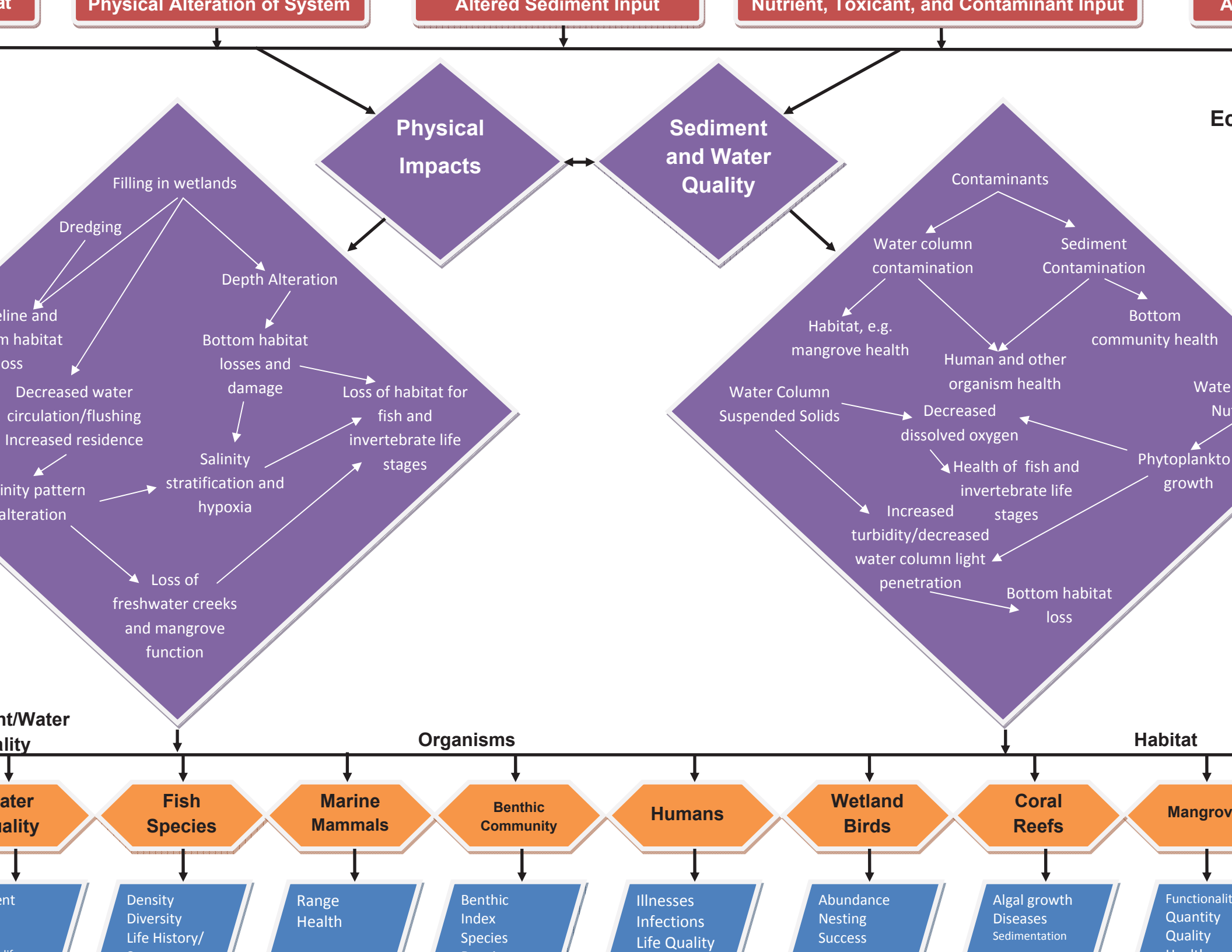
Yoshiura, L.M., and C. Lilyestrom. 1999. San José and La Torrecilla Lagoons Creel Survey. Report from Department of Natural and Environmental Resources, Marine Resources Division. 16 pp.

Zajac, R.N., and R.B. Whitlatch. 2001. Response of macrobenthic communities to restoration efforts in a New England estuary. *Estuaries* 24:167–183.

This page intentionally left blank.

Appendix A1

San Juan Bay Estuary Conceptual Ecological Model



Appendix A2

Hydrodynamic and Water Quality Model Study of San Juan Bay Estuary (Bunch et al. 2000)

ERDC TR-00-1

Engineer Research and
Development Center



US Army Corps
of Engineers®

Hydrodynamic and Water Quality Model Study of San Juan Bay Estuary

Barry W. Bunch, Carl F. Cerco, Mark S. Dortch,
Billy H. Johnson, Keu W. Kim

April 2000

The contents of this report are not to be used for advertising, publication, or promotional purposes. Citation of trade names does not constitute an official endorsement or approval of the use of such commercial products.

The findings of this report are not to be construed as an official Department of the Army position, unless so designated by other authorized documents.



PRINTED ON RECYCLED PAPER

Hydrodynamic and Water Quality Model Study of San Juan Bay Estuary

by Barry W. Bunch, Carl F. Cerco, Mark S. Dortch

Environmental Laboratory
U.S. Army Engineer Research and Development Center
3909 Halls Ferry Road
Vicksburg, MS 39180-6199

Billy H. Johnson, Keu W. Kim

Coastal and Hydraulics Laboratory
U.S. Army Engineer Research and Development Center
3909 Halls Ferry Road
Vicksburg, MS 39180-6199

Final report

Approved for public release; distribution is unlimited

Prepared for U.S. Army Engineer District, Jacksonville
Jacksonville, FL 32232-0019

Engineer Research and Development Center Cataloging-in-Publication Data

Hydrodynamic and water quality model study of San Juan Bay estuary / by Barry W. Bunch ... [et al.] ; prepared for U.S. Army Engineer District, Jacksonville.

298 p. : ill. ; 28 cm. — (ERDC ; TR-00-1)

Includes bibliographic references.

1. Hydrodynamics — Mathematical models. 2. Estuaries — Puerto Rico — San Juan Bay — Mathematical models. 3. San Juan Bay (P.R.) 4. Water quality — Puerto Rico — San Juan Bay — Testing. I. Bunch, Barry W. II. United States. Army. Corps of Engineers. Jacksonville District. III. Engineer Research and Development Center (U.S.) IV. Series: ERDC TR ; 00-1.

TA7 E8 no.ERDC TR-00-1

Contents

Preface	xi
1—Introduction	1
Background and Site Description	1
Objective and Scope	3
2—Approach	5
3—The Hydrodynamic Model	10
General	10
CH3D-WES Description	11
Boundary Conditions	24
Initial Conditions	34
Numerical Grid	36
4—Water Quality Model Formulation.	37
Introduction	37
Conservation of Mass Equation	39
Algae	40
Organic Carbon	54
Phosphorus.	58
Nitrogen	64
Chemical Oxygen Demand	70
Dissolved Oxygen.	70
Salinity	72
Temperature	72
Fecal Coliform.	73
Glossary	73
Predictive Sediment Submodel	78
5—Water Quality Model Input.	85
Hydrodynamics	85
Meteorological Data	86
Initial Conditions	87
Boundary Concentrations and Loading Estimates	88

6—Hydrodynamic Model Adjustment and Skill Assessment	102
Tide Reproduction	103
Salinity Reproduction.	106
Reproduction of the Exchange Between Canals	113
Model Coefficients	115
Conclusions	121
7—Water Quality Model Calibration and Skill Assessment	122
Scatter Plots	125
Longitudinal Transect Comparisons.	130
Time Series Comparisons	148
Calibration Conclusions	164
8—Management Scenarios	166
Methods	166
Scenario Descriptions.	167
Hydrodynamic Model Results	171
Water Quality Model Results	206
9—Conclusions and Recommendations	271
10—References	274
Appendix A: Transformed Horizontal Momentum Diffusion Terms . .	A1
Appendix B: Scenario Average Concentrations and Percent Change from Base Condition.	B1
SF 298	

List of Figures

Figure 1-1. The San Juan Bay and Estuary system, San Juan, PR . .	2
Figure 2-1. Water quality stations, San Juan Bay Estuary, summer 1995	8
Figure 2-2. Locations of management alternatives (scenarios) in the San Juan Bay Estuary system.	9
Figure 3-1. Numerical grid of San Juan estuarine system	17
Figure 3-2. San Juan Airport wind data	26
Figure 3-3. Freshwater inflows.	27
Figure 3-4. ADCIRC numerical grid	34
Figure 3-5. ADCIRC grid near Puerto Rico.	35

Figure 3-6. Tide computed by ADCIRC and applied on ocean boundary	35
Figure 4-1. The Monod formulation for nutrient-limited growth. . .	42
Figure 4-2. Effect of temperature on algal production.	44
Figure 4-3. Exponential temperature function	45
Figure 4-4. The ammonium preference function	49
Figure 4-5. Carbon-to-nitrogen ratio (mean and standard error) of seston in upper Chesapeake Bay	52
Figure 4-6. Carbon-to-phosphorus ratio (mean and standard error) of seston in upper Chesapeake Bay	52
Figure 4-7. Model algal phosphorus-to-carbon ratio.	53
Figure 4-8. Model carbon cycle	55
Figure 4-9. Effect of nitrate and dissolved oxygen on denitrification rate	57
Figure 4-10. Model phosphorus cycle	59
Figure 4-11. Effect of algal biomass and nutrient concentration on hydrolysis and mineralization	61
Figure 4-12. Chemostat simulation with and without variable phosphorus stoichiometry.	63
Figure 4-13. Model nitrogen cycle	65
Figure 4-14. Effect of dissolved oxygen and ammonium concentration on nitrification rate	68
Figure 4-15. Model dissolved oxygen cycle	71
Figure 4-16. Sediment model schematic	79
Figure 4-17. Sediment model layers and definitions	81
Figure 5-1. Water quality model grid, reduced from hydrodynamic model grid	87
Figure 5-2. Flows observed at Hato Rey, Rio Piedras, June-September 1995	91
Figure 5-3. Flows for Baldorioty de Castro Pump Station computed from pumping records for June-September 1995	93
Figure 5-4. Model sub-basins of the San Juan Bay Estuary System with model locations of freshwater inflows indicated by the arrows	93
Figure 5-5. Observed flows for Rio Piedras at Hato Rey versus observed rainfall plotted with the best-fit regression line	96

Figure 5-6. Computed flows based on pumping records for Baldorioty de Castro Pump Station versus observed rainfall plotted with the best-fit regression line	96
Figure 6-1. Location of data stations	102
Figure 6-2. Comparison of computed and observed tide at S3	103
Figure 6-3. Comparison of computed and observed tide at S4	104
Figure 6-4. Comparison of computed and observed tide at S8	104
Figure 6-5. Comparison of computed and observed tide at S9	105
Figure 6-6. Comparison of computed and observed tide at S10	105
Figure 6-7. Comparison of computed and observed tide at S6	106
Figure 6-8. Comparison of computed and observed salinity at SJB-3	108
Figure 6-9. Comparison of computed and observed salinity at SJB-5	109
Figure 6-10. Comparison of computed and observed salinity at PN-1.	110
Figure 6-11. Comparison of computed and observed salinity at S4	111
Figure 6-12. Comparison of computed and observed salinity at S5	112
Figure 6-13. Comparison of computed and observed salinity at S6	113
Figure 6-14. Comparison of computed and observed salinity at SC-1.	114
Figure 6-15. Comparison of near surface computed and observed salinity at S8	115
Figure 6-16. Comparison of computed and observed salinity at TL-1.	116
Figure 6-17. Comparison of near surface computed and observed salinity at TL-3.	117
Figure 6-18. Comparison of near surface computed and observed salinity at PL-1.	117
Figure 6-19. Comparison of near surface computed and observed salinity at PL-2.	118
Figure 6-20. Computed flux through Martin Pena Canal compared with USGS data	118
Figure 6-21. Computed flux through Suarez Canal compared with USGS data	119
Figure 6-22. Computed flux through Torrecilla-Pinones Canal compared with USGS data	119
Figure 6-23. Comparison of computed flux at Range 2 with flux determined from ADCP data	120

Figure 6-24. Comparison of computed flux at Range 4 with flux determined from ADCP data	120
Figure 6-25. Comparison of computed flux at Range 6 with flux determined from ADCP data	121
Figure 7-1. Calibration period scatter plots.	126
Figure 7-2. Longitudinal transect and observation stations used for preparing calibration-period average transect plots . . .	131
Figure 7-3. Calibration-period average, longitudinal transect plot of computed and observed water quality variables resulting from model calibration for summer 1995	132
Figure 7-4. Location of clams in the WQM.	139
Figure 7-5. Longitudinal transect calibration period average benthic algae	145
Figure 7-6. Longitudinal transect calibration period average sediment fluxes.	146
Figure 7-7. Laguna Los Corozos (Northern Laguna San José) calibration period time series.	149
Figure 7-8. Cano Martin Pena station MP-2 calibration period time series	152
Figure 7-9. Laguna Condado station LC-1 calibration period time series	156
Figure 7-10. Cano San Antonio station SA-1 calibration period time series	159
Figure 7-11. Computed and observed water quality variables at stations PL1 and PL2 (Laguna de Pinones) resulting from model calibration for summer 1995	161
Figure 8-1. Comparison of flux through Martin Pena Canal between Scenarios 1a and 1b	172
Figure 8-2. Comparison of flux through Suarez Canal between Scenarios 1a and 1b	173
Figure 8-3. Comparison of tide at S6 between Scenarios 1a and 1b .	174
Figure 8-4. Comparison of salinity at S4 between Scenarios 1a and 1b.	175
Figure 8-5. Comparison of salinity at S8 between Scenarios 1a and 1b.	176
Figure 8-6. Comparison of salinity at S6 between Scenarios 1a and 1b.	177

Figure 8-7. Comparison of tide at S6 between Scenarios 1a and 1c	177
Figure 8-8. Comparison of flux at Range 2 between Scenarios 1a and 1c	178
Figure 8-9. Comparison of flux at Range 4 between Scenarios 1a and 1c	179
Figure 8-10. Comparison of salinity at S4 between Scenarios 1a and 1c	180
Figure 8-11. Comparison of salinity at S6 between Scenarios 1a and 1c	181
Figure 8-12. Comparison of salinity at S8 between Scenarios 1a and 1c	182
Figure 8-13. Comparison of flux at Range 2 between Scenarios 1a and 2	183
Figure 8-14. Comparison of flux at Range 4 between Scenarios 1a and 2	184
Figure 8-15. Comparison of tide at S6 between Scenarios 1a and 2	185
Figure 8-16. Comparison of salinity at S4 between Scenarios 1a and 2	186
Figure 8-17. Comparison of salinity at S6 between Scenarios 1a and 2	187
Figure 8-18. Comparison of salinity at S8 between Scenarios 1a and 2	188
Figure 8-19. Comparison of tide at S6 between Scenarios 1a and 3	189
Figure 8-20. Comparison of flux at Range 4 between Scenarios 1a and 3	190
Figure 8-21. Comparison of flux at Range 2 between Scenarios 1a and 3	191
Figure 8-22. Comparison of salinity at S4 between Scenarios 1a and 3	192
Figure 8-23. Comparison of salinity at S6 between Scenarios 1a and 3	193
Figure 8-24. Comparison of salinity at S8 between Scenarios 1a and 3	194
Figure 8-25. Comparison of flux at Range 4 between Scenarios 1a and 4	195
Figure 8-26. Comparison of tide at S6 between Scenarios 1a and 4	196

Figure 8-27. Comparison of flux at Range 2 between Scenarios 1a and 4	197
Figure 8-28. Comparison of salinity at S4 between Scenarios 1a and 4	198
Figure 8-29. Comparison of salinity at S6 between Scenarios 1a and 4	199
Figure 8-30. comparison of salinity at S8 between Scenarios 1a and 4	200
Figure 8-31. Comparison of tide at S6 between Scenarios 1a and 6b .	201
Figure 8-32. Comparison of flux at Range 2 between Scenarios 1a and 6b	202
Figure 8-33. Comparison of flux at Range 4 between Scenarios 1a and 6b	203
Figure 8-34. Comparison of salinity at S4 between Scenarios 1a and 6b	204
Figure 8-35. Comparison of salinity at S6 between Scenarios 1a and 6b	205
Figure 8-36. Comparison of salinity at S8 between Scenarios 1a and 6b	206
Figure 8-37. Simulation averaged transect plots and sediment flux plots comparing Scenario 1b with Scenario 1a	209
Figure 8-38. Simulation averaged transect plots comparing Scenario 1c with Scenario 1a	217
Figure 8-39. Simulation averaged transect plots comparing Scenario 2 with Scenario 1a	224
Figure 8-40. Simulation averaged transect plots comparing Scenario 3 with Scenario 1a	231
Figure 8-41. Simulation averaged transect plots comparing Scenario 4 with Scenario 1a	238
Figure 8-42. Simulation averaged transect plots comparing Scenario 5a with Scenario 1a	245
Figure 8-43. Simulation averaged transect plots comparing Scenario 5b with Scenario 1a	251
Figure 8-44. Simulation averaged transect plots comparing Scenario 6a with Scenario 1a	258
Figure 8-45. Simulation averaged transect plots comparing Scenario 6b with Scenario 1a	265

List of Tables

Table 4-1.	Water Quality Model State Variables	37
Table 4-2.	Terms in Kinetics Equations	74
Table 4-3.	Sediment Model State Variables and Fluxes	80
Table 5-1.	Ocean Boundary Concentrations	89
Table 5-2.	SJBE Sub-Basins and Areas	94
Table 5-3.	SJBE Sub-Basin Curve Numbers.	97
Table 5-4.	SJBE Sub-Basin Flow Estimation Methods	98
Table 5-5.	Uniform Runoff Concentrations	99
Table 5-6.	Modified Runoff Concentrations.	100
Table 6-1.	Comparison of Harmonic Constituents of Tide Relative to San Juan Bay Tide	106
Table 7-1.	Parameter Values	122
Table 8-1.	Scenario Meteorological Conditions.	167
Table 8-2.	Management Water Quality Scenarios.	168
Table 8-3.	ICM Grid for Each Scenario	168
Table 8-4.	Scenarios Uniform Initial Conditions for Water Column	207
Table 9-1.	Summary of Impacts for Each Management Scenario . .	272

Preface

A hydrodynamic and water quality model study of San Juan Bay Estuary, Puerto Rico, was conducted from January 1996 through May 1999. This study was part of the United States Environmental Protection Agency's (USEPA) National Estuary Program. It was managed by the U.S. Army Engineer District, Jacksonville (CESAJ), and was sponsored by the USEPA Region II through the San Juan Bay Estuary Program (SJBEP), San Juan, Puerto Rico, and by the Caribbean Environment and Development Institute of San Juan, Puerto Rico, through a Cooperative Research and Development Agreement with the U.S. Army Engineer Research and Development Center (ERDC). Messrs. A. J. Salem, G. M. Strain, and James Duck were Chief, Acting Chief, and Chief, respectively, Planning Division, CESAJ, and Ms. Teré Rodríguez and Ms. Edna Villanueva were Directors, SJBEP. Mr. Mitch Granat of Planning Division, CESAJ, Mr. Jorge Tous of the Jacksonville District's Antilles Office, and Messrs. Héctor Abreu-Cintrón and Luis Jorge Rivera-Herrera of the SJBEP were the technical points of contact for this study.

Dr. Mark S. Dortch, Chief, Water Quality and Contaminant Modeling Branch (WQCMB), Environmental Processes and Effects Division (EPED), Environmental Laboratory (EL), ERDC, was the study manager and ERDC technical point of contact. The hydrodynamic modeling portion of this study was conducted by Drs. Billy H. Johnson and Keu W. Kim of the Waterways and Estuaries Division (WED), of the ERDC Coastal and Hydraulics Laboratory (CHL), under the general supervision of Dr. William H. McAnally, Chief, WED. The water quality modeling portion of this study was conducted by Drs. Carl F. Cerco and Barry W. Bunch of the WQCMB, EL, under the direct supervision of Dr. Dortch and the general supervision of Dr. Richard E. Price, Chief, EPED. Drs. Bunch and Kim conducted most of the day-to-day modeling tasks.

Dr. Jorge Capella, Mr. Aurelio Mercado, and Dr. Jorge Corredor from the University of Puerto Rico Marine Sciences Department, and Dr. Richard Signell from the U.S. Geological Survey in Woods Hole, MA, were members of the SJBEP Modeling Evaluation Group, which provided very valuable assistance for the study's model adjustment and skill assessment tasks. The SJBEP Management Committee and the Scientific and Technical Advisory Committee selected the management scenarios modeled and evaluated in the study.

This report was prepared by Drs. Bunch, Cerco, Dortch, Johnson, and Kim. The order of the authors is alphabetical and does not represent the amount of contribution provided by each to this study. Each author provided significant contributions to this study. However, Drs. Bunch and Johnson did provide the greatest amount of written contributions to the report.

At the time of publication of this report, Director of CHL was Dr. James R. Houston, Acting Director of EL was Dr. John W Keeley, and Acting Director of ERDC was Dr. Lewis E. Link. Commander of ERDC was COL Robin R. Cababa, EN.

This report should be cited as follows:

Bunch, B. W., Cerco, C. F., Dortch, M. S., Johnson, B. H., and Kim, K. W. (2000). "Hydrodynamic and Water Quality Model Study of San Juan Bay Estuary," ERDC TR-00-1, U.S. Army Engineer Research and Development Center, Vicksburg, MS.

The contents of this report are not to be used for advertising, publication, or promotional purposes. Citation of trade names does not constitute an official endorsement or approval of the use of such commercial products.

1 Introduction

Background and Site Description

Urbanization and anthropogenic influences from metropolitan areas of San Juan, Puerto Rico, have significantly impacted the water quality of the San Juan Bay Estuary (SJBE) system. Water quality impacts consist of eutrophication (i.e., nutrient enrichment), depressed dissolved oxygen (DO) concentrations, high concentrations of fecal coliform bacteria (FCB), an indicator of pathogens, and the presence of toxic substances. Portions of the SJBE system may have less than adequate flushing characteristics to assimilate pollutant loadings.

The San Juan Metropolitan area includes thirteen municipalities located on the north coast of Puerto Rico. Within this region, the municipalities of Toa Baja, Cataño, Guaynabo, Bayamón, San Juan, Trujillo Alto, Carolina, and Loiza share part of their territories with the SJBE or its watershed. Over 700,000 people live in the 240-km² SJBE drainage basin, of which 215 km² is land and 25 km² is covered with water.

The SJBE consists of five embayments (see Figure 1-1). From west to east these include: Bahía de San Juan, Laguna del Condado, Laguna San José (including Laguna Los Corozos), Laguna La Torrecilla, and Laguna de Piñones. San Juan Bay (ca. 7 km²) contains navigation channels, and the shoreline is highly developed. Laguna del Condado is a relatively small lagoon adjacent to an ocean inlet which keeps it well flushed. Laguna San José (4.6 km²) is the innermost lagoon which is shallow (mean depth of 1.5 m) and has the least tidal fluctuation of 5-10 cm with the tidal range in San Juan Bay and Laguna La Torrecilla being about 60 cm. As a result Laguna San José experiences little tidal flushing. Laguna La Torrecilla (2.5 km²) is connected to the ocean by Boca De Cangrejos and is bordered mostly by mangrove trees. Laguna de Piñones is connected to Laguna La Torrecilla through a small tidal creek with a width and depth of less than 5 m and 1 m, respectively. As a result, as in Laguna San José, tidal flushing in Laguna de Piñones is also small. Laguna de Piñones is surrounded by a large mangrove forest which can influence water quality in that lagoon.

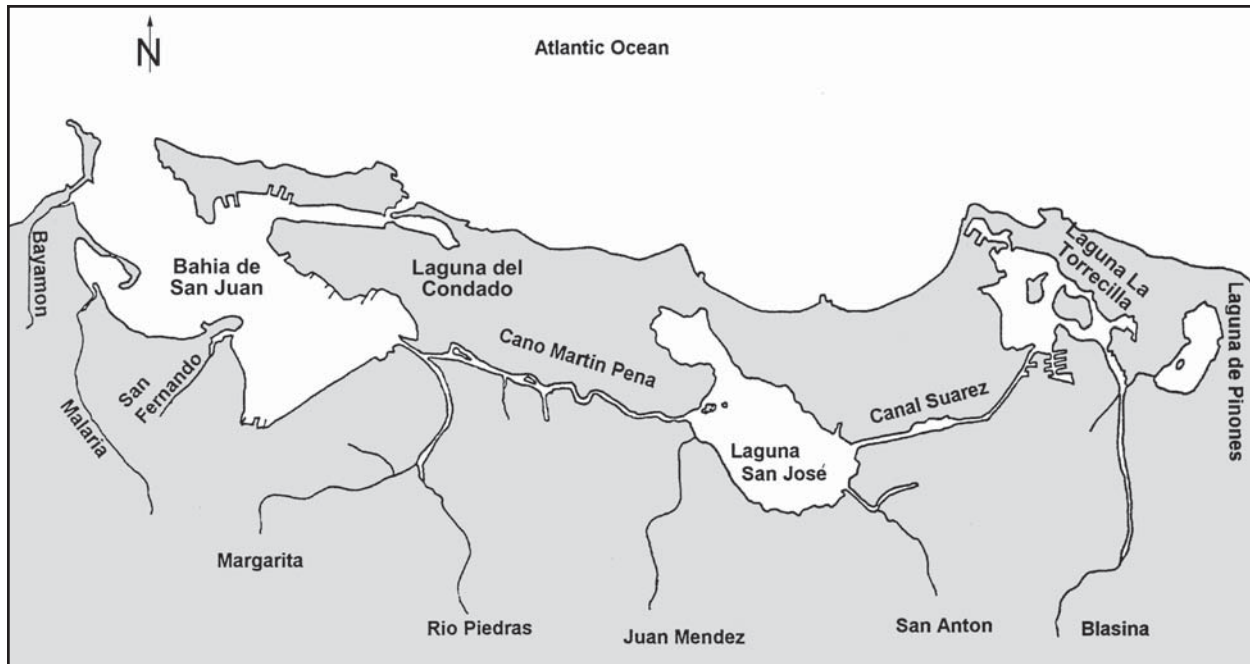


Figure 1-1. The San Juan Bay and Estuary system, San Juan, PR

The bay and lagoons are connected by narrow channels as shown in Figure 1-1. The two most distinct channels are Caño Martín Peña and Canal Suárez. Caño Martín Peña, which connects Laguna San José and San Juan Bay, is about 6 km long with a width that varies from a few meters at its eastern end to about 100 m at its western end with a dredged depth of 3.6 m. The average depth of the canal is about 1.2 m. The narrow, shallow constriction along the eastern end of Caño Martín Peña is due to sedimentation and debris and greatly impedes flushing of Laguna San José. As a result, the eastern portion of Caño Martín Peña and Laguna San José have the poorest water quality. Canal Suárez, which connects Laguna San José and Laguna La Torrecilla, is approximately 4 km long with widths ranging from greater than 30 m to less than 5 m where a major road crosses the canal. Depths of Canal Suárez range from as great as 10 m where dredging has taken place to less than 1 m at the narrow constriction. This constriction contributes to the reduced tidal range in Laguna San José. The SJBE system opens to the ocean at three locations, San Juan Bay, Laguna del Condado, and Laguna La Torrecilla.

Portions of the system have been altered due to dredging. An 11.9-m- (39-ft-) deep navigation channel traverses the interior and the perimeter of San Juan Bay. Borrow pits exist within Laguna del Condado, Laguna San José, and Laguna La Torrecilla where sand and fill mining occurred for the development of residential and service facilities, such as the Luis Muñoz Marín International Airport. The borrow pits are as deep as 10-18 m and are chemically stratified. Thus, the waters in the pits are low in DO and high in dissolved substances, including nutrients and chemical oxygen demand.

Treated municipal wastewater has been discharged off the coast since 1986. However, pollutants still enter the SJBE system from combined sewer overflows; runoff from residential, agricultural, and industrialized areas; faulty sewage lines; and un-sewered residential areas. Caño Martín Peña receives considerable untreated domestic wastes from adjacent residential areas. Storm water is collected and pumped directly into the SJBE or indirectly through its tributaries by a total of 12 pump stations that have a combined maximum capacity of over 900,000 gpm (56.8 m³/s). Pumped storm water is untreated and can contain pollutants. Additionally, pollutant loads can enter via freshwater inflow tributaries which enter the system through the Puerto Nuevo River, Malaria Channel, and three creeks, Juan Mèndez, San Antòn, and Blasina (see Figure 1-1). Freshwater flows are quite flashy as they are driven by local rainfall, and their water quality is dominated by local wash-off. There are no significant waste-water dischargers in the system, although there are two cooling water discharges from power plants.

Habitat loss has occurred within the system as a result of direct (e.g., construction, dredging, filling) and indirect impacts. Increased sediment runoff and eutrophication have increased water turbidity to the extent that benthic primary production is no longer possible in many locations. Water quality is poor in some areas of the system due to eutrophication and FCB contamination. Solid waste disposal is a problem within Caño Martín Peña as a result of inadequate waste collection from low income areas lining the canal.

Objective and Scope

San Juan Bay Estuary is one of the estuarine systems included in the U.S. Environmental Protection Agency's National Bay and Estuary Program (NEP; U.S. Environmental Protection Agency 1993). The NEP was started in 1987 as part of the Clean Water Act to protect and restore estuaries while supporting economic and recreational activities.

One of the goals of the San Juan Bay Estuary Program (SJBEP) and the Environmental Quality Board of Puerto Rico included the development of a hydrodynamic and a water quality model of the SJBE system for use in determining effective alternatives for water quality improvement and predicting the impacts of future development. The study reported herein was conducted to satisfy this goal. The objective of this study included development of such models and application of the models to evaluate the effectiveness of management alternatives on water quality improvement. Management alternatives considered included methods to increase system flushing and reduce pollutant loadings.

This study included four components: (1) bathymetric surveys; (2) hydrodynamic field data collection; (3) water quality data collection; and (4) hydrodynamic and water quality modeling. The first three

components were necessary to conduct the fourth. Recent bathymetric surveys were necessary for model input since considerable dredging, filling, and sedimentation had occurred since the last survey. Bathymetric data collection was conducted through contract by CESAJ. Recent data collection efforts did not contain the information required for hydrodynamic and water quality model calibration, thus, it was necessary to conduct components (2) and (3). These two efforts and the resulting data are documented by Kennedy et al. (1996) and Fagerburg (1998). Much of the data collected from components (2) and (3) are shown within this report where model results are compared against field observations to assess model accuracy.

There are many potential future uses for these models for evaluating the effects of changes in system hydrology, structural features, and/or pollutant loadings on circulation and water quality. These models can serve as valuable tools to help guide management and monitoring of the SJBE.

This report presents the approach, descriptions of the hydrodynamic and water quality models, including their input data, adjustment/calibration and skill assessment, methods used for and results of management scenario simulations, and conclusions and recommendations.

2 Approach

Depths within SJBES range from about 1 m to 20 m. Since the water column density and related water quality variables experience significant variation over the water depth in the deeper channels and borrow areas, a three-dimensional (3D) model was recommended. However, shallow areas were represented as vertically mixed (i.e., one layer), and the connecting channels were represented as laterally mixed (i.e., one segment wide) in some areas.

Numerical, 3D hydrodynamic and water quality models were used to simulate the effects of strategies to increase flushing and reduce pollutant loadings. The hydrodynamic model (HM) and the water quality model (WQM) were indirectly coupled without feedback. This means that the HM was executed and results were saved for subsequent use by the WQM to drive its transport terms. Hydrodynamic results were saved as hourly averages and used to provide hourly hydrodynamic updates to the WQM. Feedback from the WQM to the HM was not necessary since temperature and salinity, which affect water density and thus the hydrodynamics, were included in the HM simulations. Other water quality variables simulated by the WQM have an insignificant effect on water density. The models used the same computational grid but different time steps. The HM time step was one minute, whereas the WQM time step was variable and on the order of tens of minutes.

The 3D numerical hydrodynamic model, CH3D-WES (**C**urvilinear **H**ydrodynamics in **3** **D**imensions, WES version), was used for this study. The WES version of a former model (CH3D) was developed by Johnson et al. (1991 and 1993). Physical processes in the model include tides, wind, density effects, freshwater inflows, turbulence, and the effect of the earth's rotation. As its name implies, CH3D-WES makes hydrodynamic computations on a curvilinear or boundary-fitted planform grid. However, the vertical dimension is Cartesian which allows for modeling density stratification on relatively coarse grids. Shallow areas can be modeled with one layer which effectively treats such areas in a vertically averaged sense.

The CE-QUAL-ICM (referred to as ICM) multi-dimensional, water quality model (Cercio and Cole 1995) was used for this study. ICM uses the integrated compartment method (thus ICM) for numerical treatment, which

is the same as a finite volume approach. This model was originally developed during a study of Chesapeake Bay (Cercio and Cole 1993 and 1994, Cercio 1995a and 1995b) and has subsequently been applied to other systems, including lower Green Bay (Mark et al. 1993), Newark Bay (Cercio and Bunch 1997 and Cercio, Bunch, and Letter 1999), New York Bight (Hall and Dortch 1994), Indian River and Rehoboth Bay, Delaware (Cercio et al. 1994 and Cercio and Seitzinger 1997). This model can and has been linked to a variety of hydrodynamic models for transport. However, the most common linkage is to CH3D-WES. The WQM has multiple water quality state variables, including temperature, salinity, DO, various forms of nitrogen, phosphorus, silica, and carbon, suspended solids, and phytoplankton. The model also includes a benthic sediment diagenesis submodel (DiToro and Fitzpatrick 1993) that simulates the decay and mineralization of bottom organic matter (e.g., settled algae) and the resulting nutrient and DO fluxes between the sediments and water column. The sediment diagenesis submodel dynamically couples sediment-water column interactions. For example, pollutant loading changes eventually affect sediment oxygen demand, which affects water column DO. Thus, this approach extends the credibility of the model for predicting future water quality. For this study, the WQM included the following 16 state variables:

- temperature
- salinity
- dissolved oxygen
- phytoplankton (one group)
- dissolved organic carbon
- particulate organic carbon
- particulate organic nitrogen
- dissolved organic nitrogen
- nitrate+nitrite nitrogen
- ammonium nitrogen
- particulate organic phosphorus
- dissolved organic phosphorus
- total inorganic phosphorus (with partitioning to dissolved and particulate phases)
- chemical oxygen demand (released from sediments)
- total suspended solids
- fecal coliform bacteria

In previous applications, models would be calibrated with one data set, then run with another independent data set, without changing any model parameters to verify model accuracy and adequacy for making predictions. In practice, if the verification was considered insufficiently accurate by the modelers, the parameters would be adjusted, and both the calibration and verification data sets would be re-run to assess accuracy of each. This process would be repeated until the model demonstrated acceptable

accuracy for both the calibration and verification periods using the same coefficients. If the modelers were furnished a third data set, then all three periods would be used. In fact, modelers are data hungry and will use data whenever available to adjust/calibrate their models, with the hope of finding *universal* coefficients that are satisfactory for all periods. This procedure is basically the same as using all available data sets for model adjustment/calibration and assessing the accuracy, or *skill*, of the calibration. Therefore, the term “verification” has been recently dropped from the process and replaced with “skill assessment.” As an example, the Chesapeake Bay model (Cerco and Cole 1994) was calibrated and the skill assessed for a continuous three-year period, rather than calibrating for one or two years and verifying for another. This was a truly tough test of the model since it was run continuously for the three years where errors from one year were passed to the next. The model evaluation group for the Chesapeake Bay study knew that essentially the modelers would use all three years anyway to calibrate the model, so why not just calibrate all three years together? Thus, calibration/adjustment and skill assessment were conducted in the Chesapeake Bay study rather than calibration and verification, and this was the approach used in the present study.

The terms model adjustment and model calibration are used for the HM and WQM, respectively. The primary difference in these terms is that HM adjustment is limited to a few parameters, whereas WQM calibration can involve varying a host of parameters that affect water quality kinetic rates and transfers. Due to study funding constraints, it was possible to collect data from only one time period for use in model adjustment/calibration and skill assessment. Ideally, it is desirable to have data from multiple time periods, or to have data from a long period of time so that the model can be evaluated for a large range of conditions.

HM and WQM adjustment/calibration were accomplished with data collected over approximately two months during the summer of 1995. Summer conditions generally result in the most severe water quality conditions due to increased stratification and warmer water. The hydrodynamic data collection period extended from 22 June 1995 through 19 August 1995. The water quality data collection period extended from 26 June 1995 through 2 September 1995. Locations where surface water quality was sampled during this period are shown in Figure 2-1. Both models were applied for this approximately two-month period during model adjustment/calibration and skill assessment.

Each management scenario simulation was conducted using conditions from the summer of 1995 for boundary conditions for freshwater flows, tides, winds, meteorological, and water quality. However, it was necessary to run the WQM longer than the summer season in order to bring the system to a new state caused by altered circulation and/or loadings. Thus, for each simulation scenario, numerous runs of the WQM were made where each successive run used results from the previous run as initial conditions. This process was continued until water quality variables reached a new equilibrium condition, which required approximately eight months of

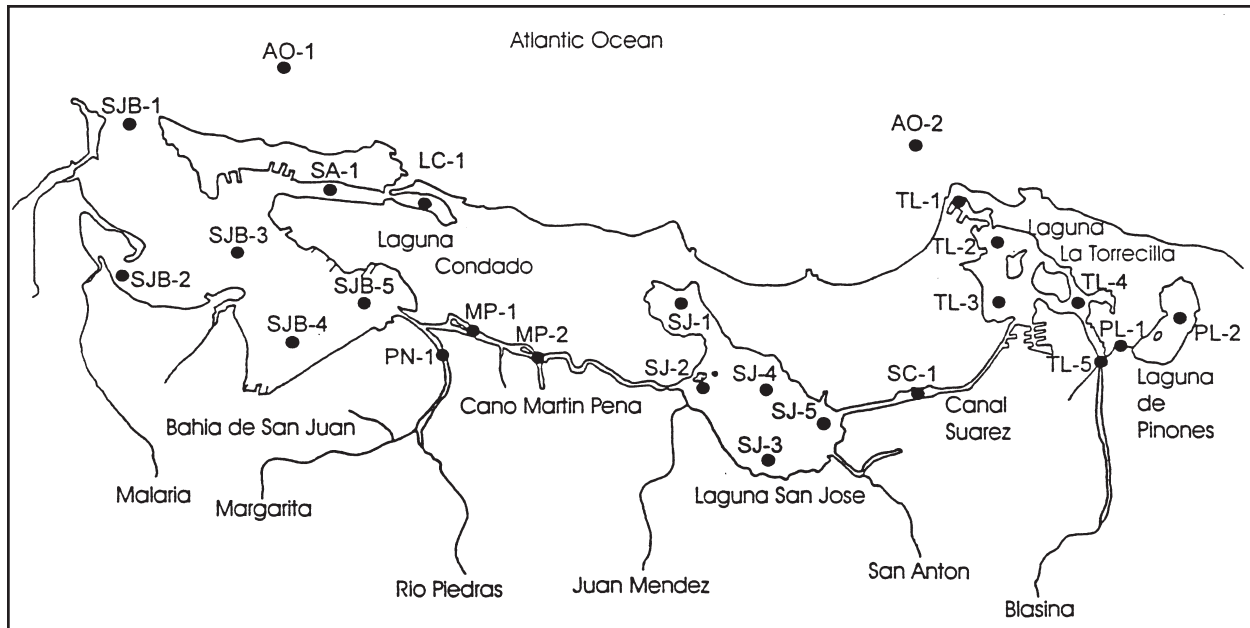


Figure 2-1. Water quality stations, San Juan Bay Estuary, summer 1995

water quality model simulation time. This procedure required using the HM output record repeatedly, or looping the hydrodynamics, to drive the WQM for longer periods. This approach approximated the long-term, steady-state response of the system to various management alternatives. The WQM required a relatively short time to reach equilibrium compared to other systems, which required on the order of several years. The part of the reason for this is believed to be due to the fact that relatively small changes in nutrient loadings to the system and/or system flushing characteristics were evaluated which required less time to reach equilibrium. Additionally, the model was repeatedly applied to warm-water conditions which accelerate reaction rates thus decreasing the time to reach equilibrium.

The results of each management scenario were then compared with results for a baseline scenario (Scenario 1a) which represented present conditions for circulation and loadings. The methods used in conducting scenario simulations are explained in more detail in Chapter 4. Looping the hydrodynamics to drive the water quality model to a long-term, steady-state, summer condition for scenario evaluations is considered a conservative approach, i.e., providing results that favor degraded rather than improved water quality, since summer conditions, which favor degraded water quality, do not persist repeatedly for long time frames. Management Scenarios 1b and 1c involved channel expansions in Caño Martín Peña. Scenario 2 involved filling dredged material borrow pits primarily in Laguna San José. Scenarios 3 and 4 evaluated channel expansion and a one-way tide gate in Canal Suárez, respectively. Scenarios 5a and 5b consisted of reductions of un-sewered loads to Caño Martín Peña and

removal of pump station loads at the Baldorioty de Castro outfall in northern Laguna San José, respectively. Scenarios 6a and 6b were limited combinations of the above scenarios. The location of each management alternative is shown on the map of Figure 2-2.

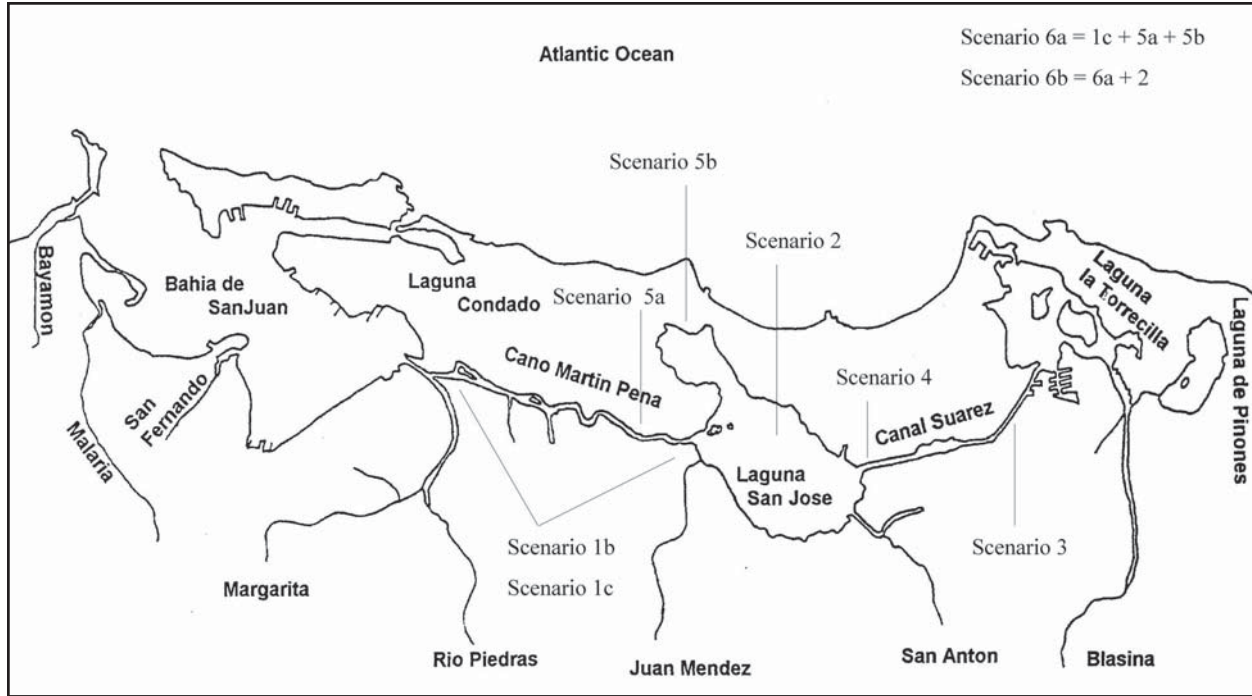


Figure 2-2. Locations of management alternatives (scenarios) in the San Juan Bay Estuary system

3 The Hydrodynamic Model

General

As noted, a 3D numerical hydrodynamic model of the San Juan Bay Estuary System has been developed to provide flow fields to the 3D water quality model of the system. As discussed in Chapter 2, to aid in model adjustment and skill assessment and to provide boundary conditions for production runs, a field data-collection effort was conducted during June-August 1995 (Fagerburg 1998). Water-surface elevations, salinity, and water-velocity data were collected at several locations. The short-term data were collected over 17-19 August 1995 when the crew went back to remove the long-term instruments. These data included Acoustic Doppler Current Profiler (ADCP) data collected over several ranges in an attempt to define the water flux through the connecting canals of the system. Model adjustment has primarily revolved around reproducing the observed tides throughout the system, reproducing the extreme stratification in salinity that often exists in the canals, and reproducing the net flux through the Martín Peña and Suárez Canals.

The verified numerical hydrodynamic model has been used to generate flow fields for various scenarios expected to improve the water quality of San José Lagoon. These include widening and deepening the Martín Peña Canal, removing a bridge from Suárez Canal that severely restricts the tidal flow, filling dredged holes throughout the system, and installing a tide gate in the Suárez Canal.

Discussions of the model adjustment and skill assessment effort and results from the scenario runs are presented in Chapters 6 and 8, respectively. In this chapter, theoretical details of the 3D numerical model are provided along with discussions of the computational grid and boundary forcings employed in its application to the San Juan Bay Estuary System.

CH3D-WES Description

The basic model (CH3D) was originally developed by Sheng (1986) for the U.S. Army Engineer Waterways Experiment Station (WES) but was extensively modified in its application to Chesapeake Bay. These modifications have consisted of different basic formulations as well as substantial recoding for more efficient computing. As its name implies, CH3D-WES makes hydrodynamic computations on a curvilinear or boundary-fitted planform grid. Physical processes impacting bay-wide circulation and vertical mixing that are modeled include tides, wind, density effects (salinity and temperature), freshwater inflows, turbulence, and the effect of the earth's rotation.

Adequately representing the vertical turbulence is crucial to a successful simulation of stratification/destratification. What is referred to as a $k-\epsilon$ turbulence model is employed. The boundary-fitted coordinates feature of the model provides enhancement to fit the irregular shoreline configuration of the San Juan Estuary system and permits adoption of an accurate and economical grid schematization. The solution algorithm employs an external mode consisting of vertically averaged equations to provide the solution for the free surface to the internal mode consisting of the full 3-D equations. Model details are discussed below.

Basic Equations

The basic equations for an incompressible fluid in a right-handed Cartesian coordinate system (x, y, z) are:

$$\frac{\partial u}{\partial x} + \frac{\partial v}{\partial y} + \frac{\partial w}{\partial z} = 0 \quad (3.1)$$

$$\begin{aligned} \frac{\partial u}{\partial t} + \frac{\partial u^2}{\partial x} + \frac{\partial uv}{\partial y} + \frac{\partial uw}{\partial z} &= fv - \frac{1}{\rho} \frac{\partial p}{\partial x} + \frac{\partial}{\partial x} \left(A_H \frac{\partial u}{\partial x} \right) \\ &+ \frac{\partial}{\partial y} \left(A_H \frac{\partial u}{\partial y} \right) + \frac{\partial}{\partial z} \left(A_v \frac{\partial u}{\partial z} \right) \end{aligned} \quad (3.2)$$

$$\begin{aligned} \frac{\partial v}{\partial t} + \frac{\partial uv}{\partial x} + \frac{\partial v^2}{\partial y} + \frac{\partial vw}{\partial z} &= -fu - \frac{1}{\rho} \frac{\partial p}{\partial y} + \frac{\partial}{\partial x} \left(A_H \frac{\partial v}{\partial x} \right) \\ &+ \frac{\partial}{\partial y} \left(A_H \frac{\partial v}{\partial y} \right) + \frac{\partial}{\partial z} \left(A_v \frac{\partial v}{\partial z} \right) \end{aligned} \quad (3.3)$$

$$\frac{\partial p}{\partial z} = -\rho g \quad (3.4)$$

$$\begin{aligned} & \frac{\partial T}{\partial t} + \frac{\partial uT}{\partial x} + \frac{\partial vT}{\partial y} + \frac{\partial wT}{\partial z} \\ &= \frac{\partial}{\partial x} \left(K_H \frac{\partial T}{\partial x} \right) + \frac{\partial}{\partial y} \left(K_H \frac{\partial T}{\partial y} \right) + \frac{\partial}{\partial z} \left(K_v \frac{\partial T}{\partial z} \right) \end{aligned} \quad (3.5)$$

$$\begin{aligned} & \frac{\partial S}{\partial t} + \frac{\partial uS}{\partial x} + \frac{\partial vS}{\partial y} + \frac{\partial wS}{\partial z} \\ &= \frac{\partial}{\partial x} \left(K_H \frac{\partial S}{\partial x} \right) + \frac{\partial}{\partial y} \left(K_H \frac{\partial S}{\partial y} \right) + \frac{\partial}{\partial z} \left(K_v \frac{\partial S}{\partial z} \right) \end{aligned} \quad (3.6)$$

$$\rho = \rho(T, S) \quad (3.7)$$

where

(u, v, w) = velocities in x-, y-, z-directions

t = time

f = Coriolis parameter defined as $2\Omega \sin \phi$ where Ω is the rotational speed of the earth and ϕ = latitude

ρ = density

p = pressure

A_H, K_H = horizontal turbulent eddy coefficients

A_v, K_v = vertical turbulent eddy coefficients

g = gravitational acceleration

T = temperature

S = salinity

Equation 3.4 implies that vertical accelerations are negligible. Thus, the pressure is hydrostatic.

Various forms of the equation of state can be used for Equation 3.7. In the present model, Equation 3.8 is used:

$$\rho = P / (\alpha + 0.698 P) \quad (3.8)$$

where

$$P = 5890 + 38T - 0.375T^2 + 3S$$

$$\alpha = 1779.5 + 11.25T - 0.0745T^2$$

and T is in degrees Celsius ($^{\circ}\text{C}$), S is in parts per thousand (ppt), and ρ is in g/cm^3 .

Working with the dimensionless form of the governing equations makes it easier to compare the relative magnitude of various terms in the equations. Therefore, the following dimensionless variables are used:

$$(u^*, v^*, w^*) = (u, v, wX_r / Z_r) / U_r$$

$$(x^*, y^*, z^*) = (x, y, zX_r / Z_r) / X_r$$

$$(\tau_x^*, \tau_y^*) = (\tau_x^w, \tau_y^w) / \rho_o f Z_r U_r$$

$$t^* = tf$$

$$\zeta^* = g\zeta / fU_r X_r = \zeta / S_r$$

$$\rho^* = (\rho - \rho_o) / (\rho_r - \rho_o)$$

$$T^* = (T - T_o) / (T_r - T_o)$$

$$A_H^* = A_H / A_{Hr}$$

$$A_v^* = A_v / A_{vr}$$

$$K_H^* = K_H / K_{Hr}$$

$$K_v^* = K_v / K_{vr}$$

where

$$(\tau_x^w, \tau_y^w) = \text{wind stress in x-, y-directions}$$

$$\zeta = \text{water-surface elevation}$$

$$\rho_o, T_o = \text{typical values for the water density and temperature}$$

and S_r , T_r , U_r , ρ_r , X_r , Z_r , A_{Hr} , A_{Vr} , K_{Hr} , and K_{Vr} are arbitrary reference values of the salinity, temperature, velocity, density, horizontal dimension, vertical dimension, horizontal viscosity, vertical viscosity, horizontal diffusion, and vertical diffusion, respectively. This then yields the following dimensionless parameters in the governing equations:

a. Vertical Ekman number:

$$E_v = A_{vr} / fZ_r^2$$

b. Lateral Ekman number:

$$E_H = A_{Hr} / fX_r^2$$

c. Vertical Prandtl (Schmidt) number:

$$Pr_v = A_{vr} / K_{vr}$$

d. Lateral Prandtl (Schmidt) number:

$$Pr_H = A_{Hr} / K_{Hr}$$

e. Froude number:

$$F_r = U_r / (gZ_r)^{1/2} \quad (6.26)$$

f. Rossby number:

$$R_o = U_r / fX_r$$

g. Densimetric Froude number:

$$Fr_D = F_r / \sqrt{\epsilon}$$

where

$$\epsilon = (\rho_r - \rho_0) / \rho_0$$

External-Internal Modes

The basic equations (Equations 3.1 through 3.8) can be integrated over the depth to yield a set of vertically integrated equations for the water surface, ζ , and unit flow rates U and V in the x - and y -directions. Using the dimensionless variables (asterisks have been dropped) and the parameters previously defined, the vertically integrated equations constituting the external mode are:

$$\frac{\partial \zeta}{\partial t} + \beta \left(\frac{\partial U}{\partial x} + \frac{\partial V}{\partial y} \right) = 0 \quad (3.9)$$

$$\frac{\partial U}{\partial t} = -H \frac{\partial \zeta}{\partial x} + \tau_{sx} - \tau_{bx} + V$$

$$\begin{aligned}
& -R_o \left[\frac{\partial}{\partial x} \left(\frac{UU}{H} \right) + \frac{\partial}{\partial y} \left(\frac{UV}{H} \right) \right] \\
& + E_H \left[\frac{\partial}{\partial X} \left(A_H \frac{\partial U}{\partial x} \right) + \frac{\partial}{\partial y} \left(A_H \frac{\partial U}{\partial y} \right) \right] \\
& - \frac{R_o}{Fr_D^2} \frac{H^2}{2} \frac{\partial \rho}{\partial x}
\end{aligned} \tag{3.10}$$

$$\begin{aligned}
\frac{\partial V}{\partial t} &= -H \frac{\partial \zeta}{\partial y} + \tau_{sy} - \tau_{by} - U \\
& - R_o \left[\frac{\partial}{\partial x} \left(\frac{UV}{H} \right) + \frac{\partial}{\partial y} \left(\frac{VV}{H} \right) \right] \\
& + E_H \left[\frac{\partial}{\partial x} \left(A_H \frac{\partial V}{\partial x} \right) + \frac{\partial}{\partial y} \left(A_H \frac{\partial V}{\partial y} \right) \right] \\
& - \frac{R_o}{Fr_D^2} \frac{H^2}{2} \frac{\partial \rho}{\partial y}
\end{aligned} \tag{3.11}$$

where

$$\beta = gZ_r / f^2 X_r^2 = (R_o / F_r)^2$$

H = total depth

τ_s, τ_b = surface and bottom shear stresses

As will be discussed later, the major purpose of the external mode is to provide the updated water-surface field.

The dimensionless form of the internal mode equations from which the 3-D velocity, salinity, and temperature fields are computed are:

$$\begin{aligned}
\frac{\partial hu}{\partial t} &= -h \frac{\partial \zeta}{\partial x} + E_v \frac{\partial}{\partial z} \left(A_v \frac{\partial hu}{\partial z} \right) + hv \\
& - R_o \left(\frac{\partial huu}{\partial x} + \frac{\partial huv}{\partial y} + \frac{\partial huw}{\partial z} \right)
\end{aligned}$$

$$\begin{aligned}
& + E_H \left[\frac{\partial}{\partial x} \left(A_H \frac{\partial hu}{\partial x} \right) + \frac{\partial}{\partial y} \left(A_H \frac{\partial hu}{\partial y} \right) \right] \\
& - \frac{R_o}{Fr_D^2} \left(\int_z^\zeta \frac{\partial p}{\partial x} dz \right)
\end{aligned} \tag{3.12}$$

$$\begin{aligned}
\frac{\partial hv}{\partial t} & = -h \frac{\partial \zeta}{\partial y} + E_v \frac{\partial}{\partial z} \left(A_v \frac{\partial hv}{\partial z} \right) - hu \\
& - R_o \left(\frac{\partial hvu}{\partial x} + \frac{\partial hvv}{\partial y} + \frac{\partial hvw}{\partial z} \right) \\
& + E_H \left[\frac{\partial}{\partial x} \left(A_H \frac{\partial hv}{\partial x} \right) + \frac{\partial}{\partial y} \left(A_H \frac{\partial hv}{\partial y} \right) \right] \\
& - \frac{R_o}{Fr_D^2} \left(\int_z^\zeta \frac{\partial p}{\partial y} dz \right)
\end{aligned} \tag{3.13}$$

$$w_{k+1/2} = w_{k-1/2} - \left(\frac{\partial uh}{\partial x} + \frac{\partial vh}{\partial y} \right) \tag{3.14}$$

$$\begin{aligned}
\frac{\partial hT}{\partial t} & = \frac{E_v}{Pr_v} \frac{\partial}{\partial z} \left(K_v \frac{\partial T}{\partial z} \right) - R_o \left(\frac{\partial huT}{\partial x} + \frac{\partial hvT}{\partial y} + \frac{\partial hwT}{\partial z} \right) \\
& + \frac{E_H}{Pr_H} \left[\frac{\partial}{\partial x} \left(K_H \frac{\partial hT}{\partial x} \right) + \frac{\partial}{\partial y} \left(K_H \frac{\partial hT}{\partial y} \right) \right]
\end{aligned} \tag{3.15}$$

$$\begin{aligned}
\frac{\partial hS}{\partial t} & = \frac{E_v}{Pr_v} \frac{\partial}{\partial z} \left(K_v \frac{\partial S}{\partial z} \right) - R_o \left(\frac{\partial huS}{\partial x} + \frac{\partial hvS}{\partial y} + \frac{\partial hwS}{\partial z} \right) \\
& + \frac{E_H}{Pr_H} \left[\frac{\partial}{\partial x} \left(K_H \frac{\partial hS}{\partial x} \right) + \frac{\partial}{\partial y} \left(K_H \frac{\partial hS}{\partial y} \right) \right]
\end{aligned} \tag{3.16}$$

In these equations h is the thickness of an internal layer, w is the vertical component of the velocity, and $k+1/2$ and $k-1/2$ represent the top and bottom, respectively, of the k^{th} vertical layer.

Boundary-Fitted Equations

To better resolve complex geometries in the horizontal directions, the CH3D-WES makes computations on the boundary-fitted or generalized curvilinear planform grid shown in Figure 3-1. This necessitates the transformation of the governing equations into boundary-fitted coordinates (ξ, η) . If only the x - and y -coordinates are transformed, a system of equations similar to those solved by Johnson (1980) for vertically averaged flow fields is obtained. However, in CH3D-WES not only are the x - and y -coordinates transformed into the (ξ, η) curvilinear system, but also the velocity is transformed such that its components are perpendicular to the (ξ, η) coordinate lines; i.e., contravariant components of the velocity are computed. This is accomplished by employing the following definitions for the components of the Cartesian velocity (u, v) in terms of contravariant components \bar{u} and \bar{v}

$$u = x_{\xi} \bar{u} + x_{\eta} \bar{v}$$

$$v = y_{\xi} \bar{u} + y_{\eta} \bar{v}$$

along with the following expressions for replacing Cartesian derivatives

$$f_x = \frac{1}{J} \left[(fy_{\eta})_{\xi} - (fy_{\xi})_{\eta} \right]$$

$$f_y = \frac{1}{J} \left[-(fx_{\eta})_{\xi} + (fx_{\xi})_{\eta} \right]$$

where J is the Jacobian of the transformation defined as

$$J = x_{\xi} y_{\eta} - x_{\eta} y_{\xi}$$

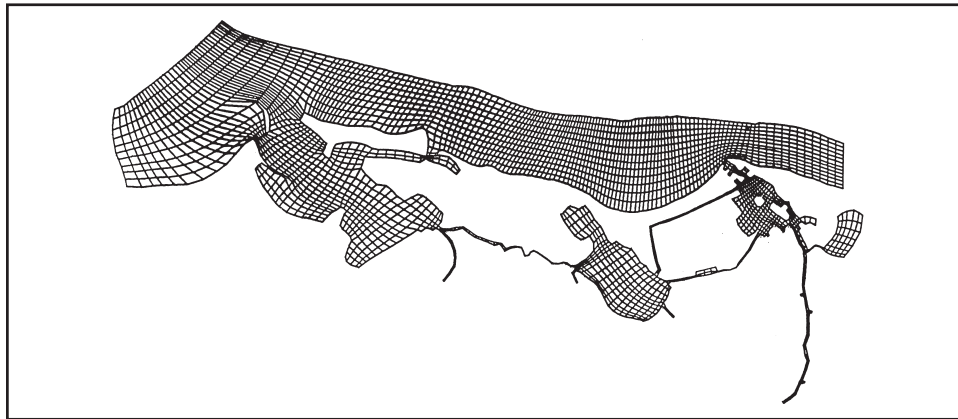


Figure 3-1. Numerical grid of San Juan estuarine system

With the governing equations written in terms of the contravariant components of the velocity, boundary conditions can be prescribed on a boundary-fitted grid in the same manner as on a Cartesian grid since \bar{u} and \bar{v} are perpendicular to the curvilinear cell faces (e.g., at a land boundary, either \bar{u} or \bar{v} is set to zero).

Initially the vertical dimension was handled through the use of what is commonly called a sigma-stretched grid. However, with a sigma-stretched grid, the bottom layer in one column communicates with the bottom layer in an adjacent column. Thus, if depth changes are rather coarsely resolved, channel stratification cannot be maintained. As a result, the governing equations, Equations 3.17-3.21, presented for solution on the Cartesian or z-plane in the vertical direction are the ones constituting the internal mode.

With both the Cartesian coordinates and the Cartesian velocity transformed, the following boundary-fitted equations for \bar{u} , \bar{v} , w , S , and T to be solved in each vertical layer are obtained.

$$\begin{aligned}
\frac{\partial h\bar{u}}{\partial t} = & -h \left(\frac{G_{22}}{J^2} \frac{\partial \zeta}{\partial \xi} - \frac{G_{12}}{J^2} \frac{\partial \zeta}{\partial \eta} \right) + \frac{h}{J} (G_{12}\bar{u} + G_{22}\bar{v}) + \frac{R_o x_\eta}{J^2} \left[\frac{\partial}{\partial \xi} (Jy_\xi h\bar{u}\bar{u}) \right. \\
& + Jy_n h\bar{u}\bar{v}) + \frac{\partial}{\partial \eta} (Jy_\xi h\bar{u}\bar{v} + Jy_n h\bar{v}\bar{v}) \left. \right] - \frac{R_o y_\eta}{J^2} \left[\frac{\partial}{\partial \xi} (Jx_\xi h\bar{u}\bar{u} + Jx_n h\bar{u}\bar{v}) \right. \\
& + \frac{\partial}{\partial \eta} (Jx_\xi h\bar{u}\bar{v} + Jx_n h\bar{v}\bar{v}) \left. \right] - R_o \left[(w\bar{u})_{top} - (w\bar{u})_{bot} \right] \\
& + E_v \left[\left(A_v \frac{\partial \bar{u}}{\partial z} \right)_{top} - \left(A_v \frac{\partial \bar{u}}{\partial z} \right)_{bot} \right] - \frac{R_o h}{Fr_D^2} \left[\int_z^\zeta \left(\frac{G_{22}}{J^2} \frac{\partial \rho}{\partial \xi} \right. \right. \\
& \left. \left. - \frac{G_{12}}{J^2} \frac{\partial \rho}{\partial \eta} \right) dz \right] + \text{Horizontal Diffusion}
\end{aligned} \tag{3.17}$$

$$\begin{aligned}
\frac{\partial h\bar{v}}{\partial t} = & -h \left(-\frac{G_{21}}{J^2} \frac{\partial \zeta}{\partial \xi} + \frac{G_{11}}{J^2} \frac{\partial \zeta}{\partial \eta} \right) - \frac{h}{J} (G_{11}\bar{u} + G_{21}\bar{v}) - \frac{R_o x_\xi}{J^2} \left[\frac{\partial}{\partial \xi} (Jy_\xi h\bar{u}\bar{u}) \right. \\
& + Jy_n h\bar{u}\bar{v}) + \frac{\partial}{\partial \eta} (Jy_\xi h\bar{u}\bar{v} + Jy_n h\bar{v}\bar{v}) \left. \right] + \frac{R_o y_\xi}{J^2} \left[\frac{\partial}{\partial \xi} (Jx_\xi h\bar{u}\bar{u} + Jx_n h\bar{u}\bar{v}) \right. \\
& + \frac{\partial}{\partial \eta} (Jx_\xi h\bar{u}\bar{v} + Jx_n h\bar{v}\bar{v}) \left. \right] - R_o \left[(w\bar{v})_{top} - (w\bar{v})_{bot} \right]
\end{aligned}$$

$$+E_v \left[\left(A_v \frac{\partial \bar{v}}{\partial z} \right)_{top} - \left(A_v \frac{\partial \bar{v}}{\partial z} \right)_{bot} \right] - \frac{R_o h}{Fr_D^2} \left[\int_z^\zeta \left(-\frac{G_{21}}{J^2} \frac{\partial \rho}{\partial \xi} + \frac{G_{11}}{J^2} \frac{\partial \rho}{\partial \eta} \right) dz \right]$$

+ *Horizontal Diffusion*

(3.18)

$$w_{top} = w_{bot} - \frac{1}{J} \left(\frac{\partial J \bar{u} h}{\partial \xi} + \frac{\partial J \bar{v} h}{\partial \eta} \right)$$
(3.19)

$$\frac{\partial h S}{\partial t} = \frac{E_v}{Pr_v} \left[\left(K_v \frac{\partial S}{\partial z} \right)_{top} - \left(K_v \frac{\partial S}{\partial z} \right)_{bot} \right] - \frac{R_o}{J} \left(\frac{\partial h J \bar{u} S}{\partial \xi} + \frac{\partial h J \bar{v} S}{\partial \eta} \right)$$

- $R_o \left[(wS)_{top} - (wS)_{bot} \right]$ + *Horizontal Diffusion*

(3.20)

$$\frac{\partial h T}{\partial t} = \frac{E_v}{Pr_v} \left[\left(K_v \frac{\partial T}{\partial z} \right)_{top} - \left(K_v \frac{\partial T}{\partial z} \right)_{bot} \right] - \frac{R_o}{J} \left(\frac{\partial h J \bar{u} T}{\partial \xi} + \frac{\partial h J \bar{v} T}{\partial \eta} \right)$$

- $R_o \left[(wT)_{top} - (wT)_{bot} \right]$ + *Horizontal Diffusion*

(3.21)

where

$$\begin{aligned} G_{11} &= x_\xi^2 + y_\xi^2 \\ G_{22} &= x_\eta^2 + y_\eta^2 \\ G_{12} &= G_{21} = x_\xi x_\eta + y_\xi y_\eta \end{aligned}$$

Similarly, the transformed external mode equations become:

$$\frac{\partial \zeta}{\partial t} + \beta \left(\frac{\partial \bar{U}}{\partial \xi} + \frac{\partial \bar{V}}{\partial \eta} \right) = 0$$
(3.22)

$$\begin{aligned} \frac{\partial \bar{U}}{\partial t} &= -\frac{H}{J^2} \left(G_{22} \frac{\partial \zeta}{\partial \xi} - G_{12} \frac{\partial \zeta}{\partial \eta} \right) \\ &+ \frac{1}{J} (G_{12} \bar{U} + G_{22} \bar{V}) + \frac{R_o x_n}{J^2 H} \left[\frac{\partial}{\partial \xi} (J y_\xi \bar{U} \bar{U} + J y_\eta \bar{U} \bar{V}) + \frac{\partial}{\partial \eta} (J y_\xi \bar{U} \bar{V} + J y_\eta \bar{V} \bar{V}) \right] \end{aligned}$$

$$\begin{aligned}
& -\frac{R_o y_\eta}{J^2} \left[\frac{\partial}{\partial \xi} (Jx_\xi \bar{U}\bar{U} + Jx_\eta \bar{U}\bar{V}) + \frac{\partial}{\partial \eta} (Jx_\xi \bar{U}\bar{V} + Jx_\eta \bar{V}\bar{V}) \right] \\
& + \tau_{s\xi} - \tau_{b\xi} - \frac{R_o}{Fr_D^2} \frac{H^2}{2} \left(G_{22} \frac{\partial \rho}{\partial \xi} - G_{12} \frac{\partial \rho}{\partial \eta} \right) \\
& + \text{Horizontal Diffusion}
\end{aligned} \tag{3.23}$$

$$\begin{aligned}
\frac{\partial \bar{V}}{\partial t} &= -\frac{H}{J^2} \left(-G_{21} \frac{\partial \zeta}{\partial \xi} + G_{11} \frac{\partial \zeta}{\partial \eta} \right) - \frac{I}{J} (G_{11} \bar{U} + G_{21} \bar{V}) \\
& -\frac{R_o x_\xi}{J^2 H} \left[\frac{\partial}{\partial \xi} (Jy_\xi \bar{U}\bar{U} + Jy_\eta \bar{U}\bar{V}) + \frac{\partial}{\partial \eta} (Jy_\xi \bar{U}\bar{V} + Jy_\eta \bar{V}\bar{V}) \right] \\
& +\frac{R_o y_\xi}{J^2 H} \left[\frac{\partial}{\partial \xi} (Jx_\xi \bar{U}\bar{U} + Jx_\eta \bar{U}\bar{V}) + \frac{\partial}{\partial \eta} (Jx_\xi \bar{U}\bar{V} + Jx_\eta \bar{V}\bar{V}) \right] \\
& + \tau_{s\eta} - \tau_{b\eta} - \frac{R_o}{Fr_D^2} \frac{H^2}{2} \left(-G_{21} \frac{\partial \rho}{\partial \xi} + G_{11} \frac{\partial \rho}{\partial \eta} \right) \\
& + \text{Horizontal Diffusion}
\end{aligned} \tag{3.24}$$

where \bar{U} and \bar{V} are contravariant components of the vertically averaged velocity.

Equations 3.22-3.24 are solved first to yield the water-surface elevations, which are then used to evaluate the water-surface slope terms in the internal mode equations. The horizontal diffusion terms are given in Appendix A.

Numerical Solution Algorithm

Finite differences are used to replace derivatives in the governing equations, resulting in a system of linear algebraic equations to be solved in both the external and internal modes. A staggered grid is used in both the horizontal and vertical directions of the computational domain. In the horizontal directions, a unit cell consists of a ζ -point in the center ($\zeta_{i,j}$), a U-point on its left face ($U_{i,j}$), and a V-point on its bottom face ($V_{i,j}$). In the vertical direction, the vertical velocities are computed at the “full” grid points. Horizontal velocities, temperature, salinity, and density are computed at the “half” grid points (half grid spacing below the full points).

The external mode solution consists of the surface displacement and vertically integrated contravariant unit flows \bar{U} and \bar{V} . All of the terms in the transformed vertically averaged continuity equation are treated implicitly whereas only the water-surface slope terms in the transformed vertically averaged momentum equations are treated implicitly. If the external mode is used purely as a vertically averaged model, the bottom friction is also treated implicitly. Those terms treated implicitly are weighted between the new and old time-steps. The resulting finite difference equations are then factored such that a ξ -sweep followed by an η -sweep of the horizontal grid yields the solution at the new time-step.

Writing Equations 3.11 as

$$\frac{\partial \zeta}{\partial t} + \beta \left(\frac{\partial \bar{U}}{\partial \xi} + \frac{\partial \bar{V}}{\partial \eta} \right) = 0 \quad (3.25)$$

$$\frac{\partial \bar{U}}{\partial t} + \frac{H}{J^2} G_{22} \frac{\partial \zeta}{\partial \eta} = M \quad (3.26)$$

$$\frac{\partial \bar{V}}{\partial t} + \frac{H}{J^2} G_{11} \frac{\partial \zeta}{\partial \xi} = N \quad (3.27)$$

where M and N are the remaining terms in Equations 3.10 and 3.11, the ξ -sweep is

$$\begin{aligned} \xi - sweep &\rightarrow \zeta_{ij}^* + \frac{\beta \theta \Delta t}{\Delta \xi} \left(\bar{U}_{i+1,j}^* - \bar{U}_{ij}^* \right) \\ &= \zeta_{ij}^n (1 - \theta) \frac{\Delta t}{\Delta \xi} \left(\bar{U}_{i+1,j}^n - \bar{U}_{ij}^n \right) \frac{\Delta t}{\Delta \eta} \left(\bar{V}_{ij+1}^n - \bar{V}_{ij}^n \right) \end{aligned} \quad (3.28)$$

where θ is a parameter determining the degree of implicitness and

$$\bar{U}_{ij}^{n+1} + \frac{\theta \Delta t H G_{22}}{\Delta \xi J^2} \left(\zeta_{ij}^* - \zeta_{i-1,j}^* \right) = \bar{U}_{ij}^n - (1 - \theta) \frac{\Delta t H G_{22}}{\Delta \xi J^2} \left(\zeta_{ij}^n - \zeta_{i-1,j}^n \right) + \Delta t M^n \quad (3.29)$$

The η -sweep then provides the updated ζ and \bar{V} at the $n + 1$ time level.

$$\eta - sweep \rightarrow \zeta_{ij}^{n+1} + \frac{\beta \theta \Delta t}{\Delta \eta} \left(\bar{V}_{i,j+1}^{n+1} - \bar{V}_{ij}^{n+1} \right) = \zeta_{i,j}^*$$

$$-(1-\theta)\frac{\Delta t}{\Delta\eta}\left(\bar{V}_{i,j+1}^n - \bar{V}_{i,j}^n\right) + \frac{\Delta t}{\Delta\eta}\left(\bar{V}_{i,j+1}^n - \bar{V}_{i,j}^n\right) \quad (3.30)$$

and

$$\begin{aligned} \bar{V}_{i,j}^{n+1} + \frac{\theta\Delta tHG_{11}}{\Delta\eta J^2}\left(\zeta_{i,j+1}^{n+1} - \zeta_{i,j}^{n+1}\right) \\ = V_{i,j}^n - (1-\theta)\frac{\Delta tHG_{11}}{\Delta\eta J^2}\left(\zeta_{i,j+1}^n - \zeta_{i,j}^n\right) + \Delta tN^n \end{aligned} \quad (3.31)$$

A typical value of θ of 0.55 yields stable and accurate solutions.

The internal mode consists of computations from Equations 3.17-3.21 for the three velocity components \bar{u} , \bar{v} , and w , salinity, and temperature. The same time-step size is used for both internal and external modes. The only terms treated implicitly are the vertical diffusion terms in all equations and the bottom friction and surface slope terms in the momentum equations. Values of the water-surface elevations from the external mode are used to evaluate the surface slope terms in Equations 3.17 and 3.18. As a result, the extremely restrictive speed of a free-surface gravity wave is removed from the stability criteria. Roache's second upwind differencing is used to represent the convective terms in the momentum equations, whereas a spatially third-order scheme developed by Leonard (1979) called QUICKEST is used to represent the advective terms in Equations 3.20 and 3.21 for salinity and temperature, respectively. For example, if the velocity on the right face of a computational cell is positive, then with QUICKEST the value of the salinity used to compute the flux through the face is

$$\begin{aligned} S_R = \frac{1}{2}(S_{i,j,k} + S_{i+1,j,k}) - \frac{1}{6}\left[1 - \left(\frac{\bar{U}_{i+1,j,k}\Delta t}{\Delta\xi}\right)^2\right](S_{i+1,j,k} - 2S_{i,j,k} + S_{i-1,j,k}) \\ - \frac{1}{2}\frac{U_{i+1,j,k}\Delta t}{\Delta\xi}(S_{i+1,j,k} - S_{i,j,k}) \end{aligned} \quad (3.32)$$

Turbulence Parameterization

The effect of vertical turbulence is modeled using the concept of eddy viscosity and diffusivity to parameterize the velocity and density correlation terms that arise from a time averaging of the governing equations. The eddy coefficients are computed through the implementation of what is referred to as a $k-\epsilon$ turbulence model. This model is a two-equation model for the computation of the kinetic energy of the turbulence (k) and the

dissipation of the turbulence (ϵ). Both time evolution and vertical diffusion are retained, and the effects of surface wind shear, bottom shear, velocity gradient turbulence production, dissipation, and stratification are included. The basic idea behind the k - ϵ turbulence model (Rodi 1980) is that the vertical eddy viscosity coefficient can be related to the turbulent kinetic energy per unit mass, k , and its rate of dissipation, ϵ , and an empirical coefficient ($c_v = 0.09$) by:

$$A_z = c_v \frac{k^2}{\epsilon} \quad (3.33)$$

The transport equation for the turbulence quantities are:

$$\frac{\partial(k)}{\partial t} - \frac{\partial}{\partial z} \left(A_z \frac{\partial k}{\partial z} \right) = (P_z - \epsilon + G) \quad (3.34)$$

$$\frac{\partial(\epsilon)}{\partial t} - \frac{\partial}{\partial z} \left(\frac{A_z}{\sigma_\epsilon} \frac{\partial \epsilon}{\partial z} \right) = \left(c_1 \frac{\epsilon}{k} P_z - c_2 \frac{\epsilon^2}{k} \right) \quad (3.35)$$

in which $\sigma_\epsilon = 1.3$, $c_1 = 1.44$, and $c_2 = 1.92$ (Rodi 1980). The source and sink terms on the right-hand side of Equations 3.34 and 3.35 represent mechanical production of turbulence due to velocity gradients, P_z , and buoyancy production or destruction in the stable stratified condition, G . Surface (s) and bottom (b) boundary conditions for the turbulence quantities are specified as:

$$k_{s,b} = \frac{U_*^2}{\sqrt{c_v}} \quad (3.36)$$

$$\epsilon_{s,b} = \frac{U_*^3}{\kappa \frac{\Delta z}{2}} \quad (3.37)$$

where κ is the von Karman constant (≈ 0.4). The friction velocity used for the surface boundary condition is defined as the square root of the resultant wind shear stress divided by the water density. The bottom friction velocity is computed in an identical way with the wind shear stress being replaced by the bottom shear stress. The suppression of the vertical diffusivity by stratification is given by:

$$K_z = A_z (1 + 3R_i)^{-2} \quad (3.38)$$

where R_i is the Richardson Number (Bloss et al. 1988).

Therefore, the number becomes::

$$P_r = (1 + 3R_i)^2 \quad (3.39)$$

Boundary Conditions

The boundary conditions at the free surface are

$$A_v \left(\frac{\partial \bar{u}}{\partial z}, \frac{\partial \bar{v}}{\partial z} \right) = (\tau_{s_\xi}, \tau_{s_\eta}) / \rho = (CW_\xi^2, CW_\eta^2) \quad (3.40)$$

$$\frac{\partial T}{\partial z} = \frac{Pr}{E_v} K(T - T_e) \quad (3.41)$$

$$\frac{\partial S}{\partial z} = 0 \quad (3.42)$$

whereas the boundary conditions at the bottom are

$$A_v \left(\frac{\partial \bar{u}}{\partial z}, \frac{\partial \bar{v}}{\partial z} \right) = (\tau_{b_\xi}, \tau_{b_\eta}) / \rho = \frac{U_r}{A_{vr}} Z_r C_d (\bar{u}_1^2 + \bar{v}_1^2)^{1/2} (\bar{u}_1, \bar{v}_1) \quad (3.43)$$

$$\frac{\partial T}{\partial z} = 0 \quad (3.44)$$

$$\frac{\partial S}{\partial z} = 0 \quad (3.45)$$

where

C = surface drag coefficient

W = wind speed

K = surface heat exchange coefficient

T_e = equilibrium temperature

C_d = bottom friction coefficient

\bar{u}_1, \bar{v}_1 = values of the horizontal velocity components next to the bottom

With z_l equal to one-half the bottom layer thickness, C_d is given by

$$C_d = k^2 [\ln(z_1 / z_0)]^{-2} \quad (3.46)$$

where

k = von Karman constant

z_0 = bottom roughness height

As can be seen from Equation 3.40, the surface shear stress is computed from wind data. Figure 3-2 shows the hourly wind data recorded for each study month at the San Juan International Airport. These data were assumed to be constant over the numerical grid (Figure 3-1).

Manning's formulation is employed for the bottom friction in the external mode equations if the model is used purely to compute vertically averaged flow fields. As presented by Garratt (1977), the surface drag coefficient is computed from

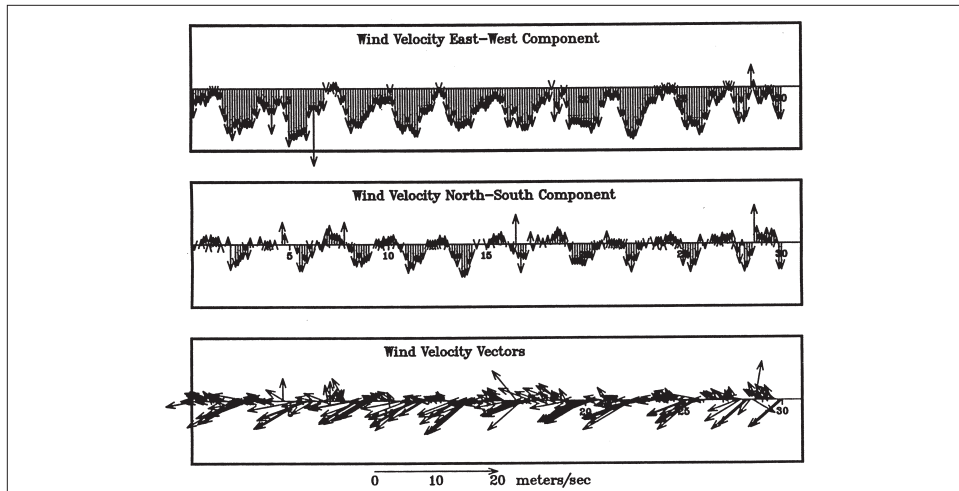
$$C = (0.75 + 0.067W) \times 10^{-3} \quad (3.47)$$

with the maximum allowable value being 0.003.

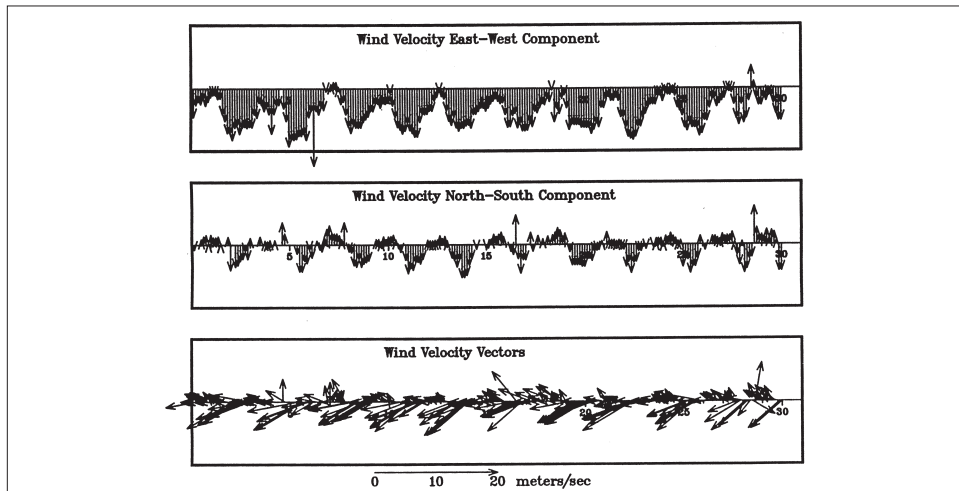
As discussed by Edinger, Brady, and Geyer (1974), the surface heat exchange coefficient, K , and the equilibrium temperature, T_e , are computed from the meteorological data (wind speed, cloud cover, dry bulb air temperatures, and either wet bulb air temperature or relative humidity). However, it should be noted that temperature was not computed in this study. Since there was virtually no change in the temperature during the simulation period, a constant temperature was input and used in the computation of the water density.

At river boundaries, the freshwater inflow and its temperature are prescribed and the salinity is normally assumed to be zero. Freshwater inflows into the San Juan Estuary system occur primarily through the Puerto Nuevo River, Juan Mendez Creek, San Anton Creek, Blasima Creek, and the Malaria Channel (Figure 1-1). As can be seen from an inspection of Figure 3-3, these inflows are quite flashy and, as will be seen in Chapter 6, can result in high salinity stratification in parts of the system. A discussion of the inflow of these data is presented in Chapter 5. The locations of these inflows are shown in Figure 5-4.

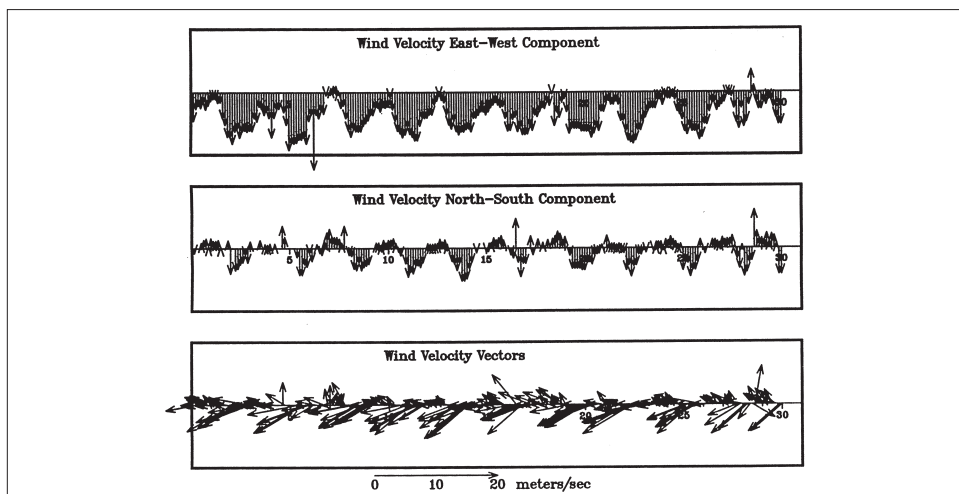
At an ocean boundary, the water-surface elevation is prescribed along with time-varying vertical distributions of salinity and temperature. To prescribe water surface elevations along the open ocean portion of the numerical grid shown in Figure 3-1, a global vertically averaged model called ADCIRC (Westerink et al. 1992) was applied. Figure 3-4 shows the ADCIRC grid which covers the Gulf of Mexico, the Caribbean, and a portion of the Atlantic Ocean. A blowup of the grid surrounding Puerto Rico is shown in Figure 3-5. Time-varying water-surface elevations were saved from the ADCIRC model at several locations along the open ocean grid in



a. June

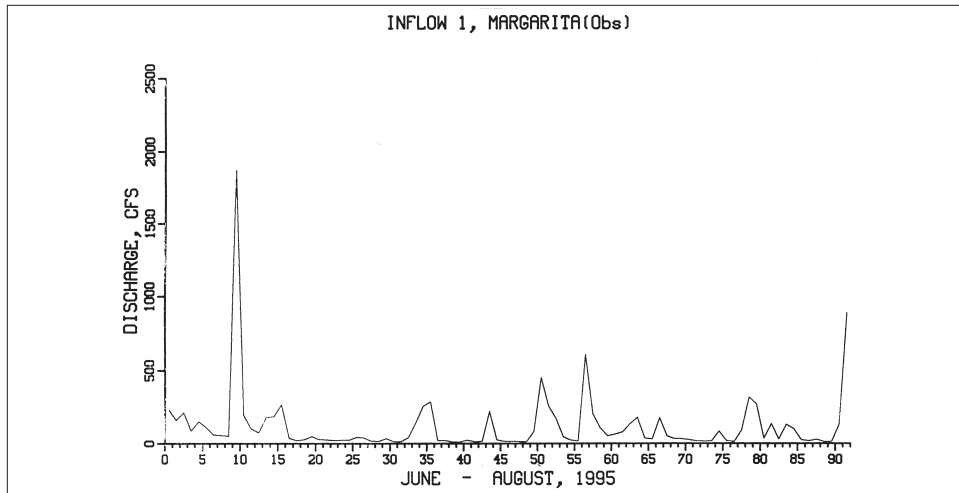


b. July

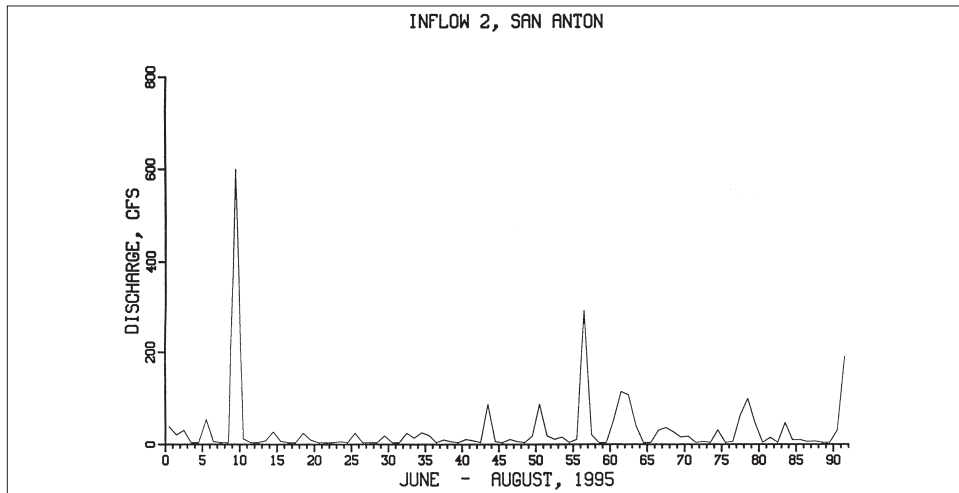


c. August

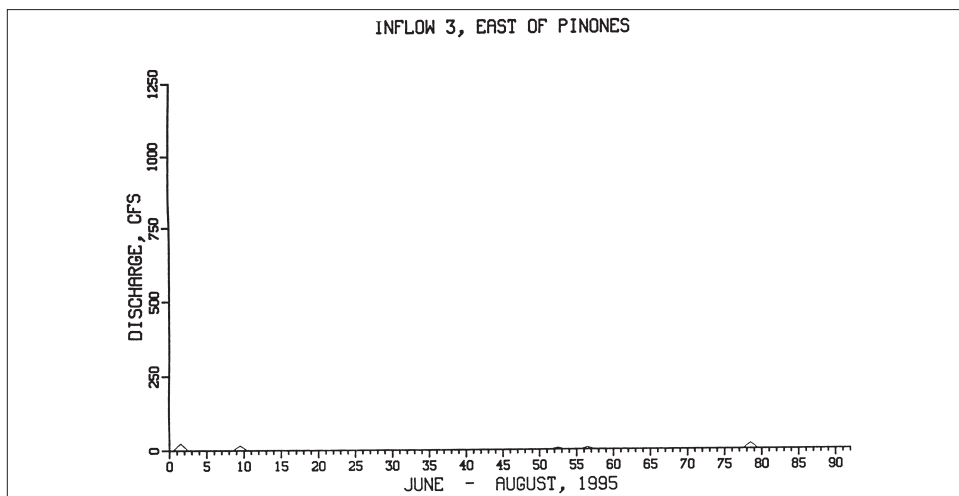
Figure 3-2. San Juan Airport wind data



a. Inflow 1

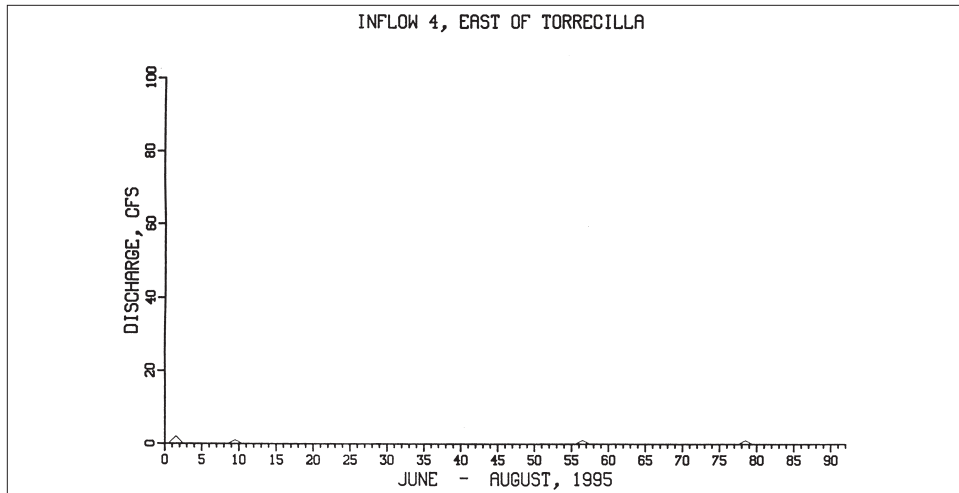


b. Inflow 2

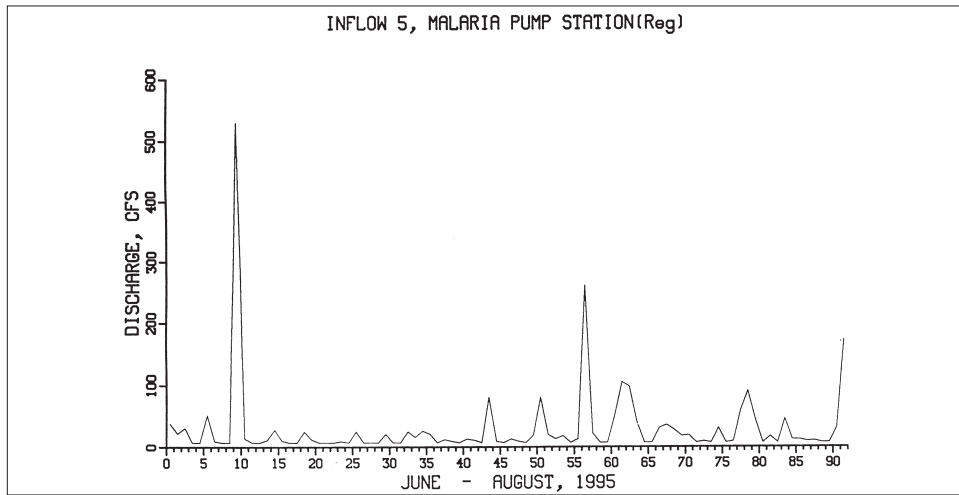


c. Inflow 3

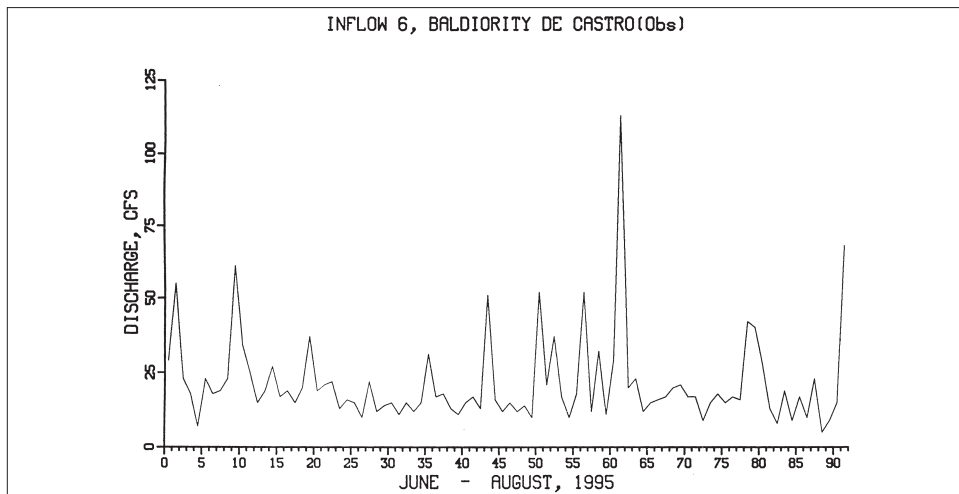
Figure 3-3. Freshwater inflows (continued)



d. Inflow 4

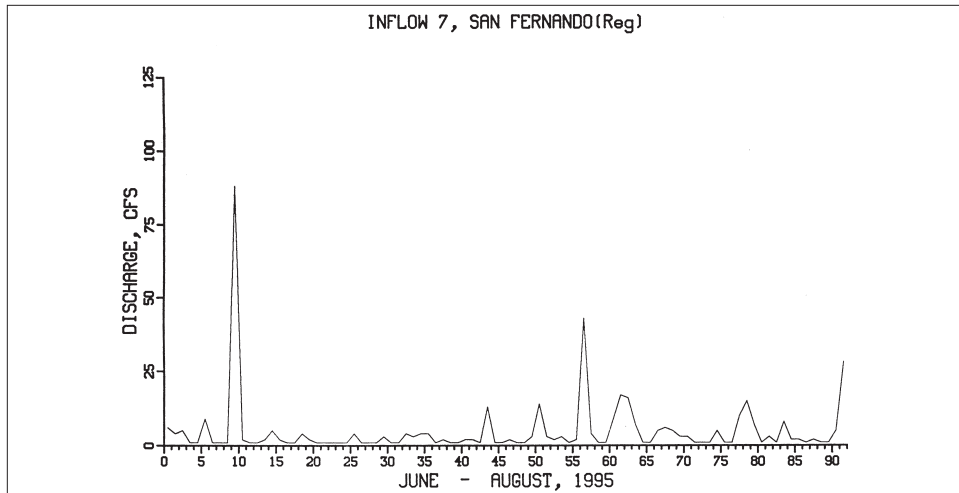


e. Inflow 5

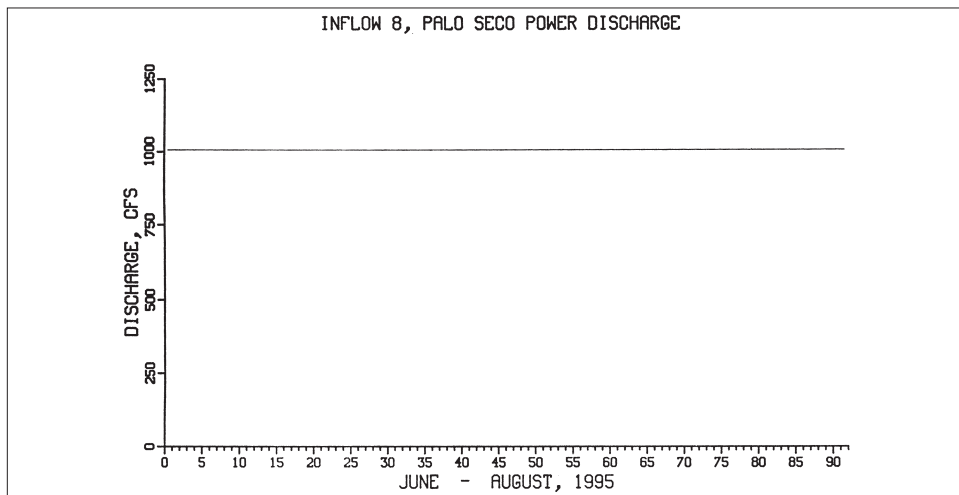


f. Inflow 6

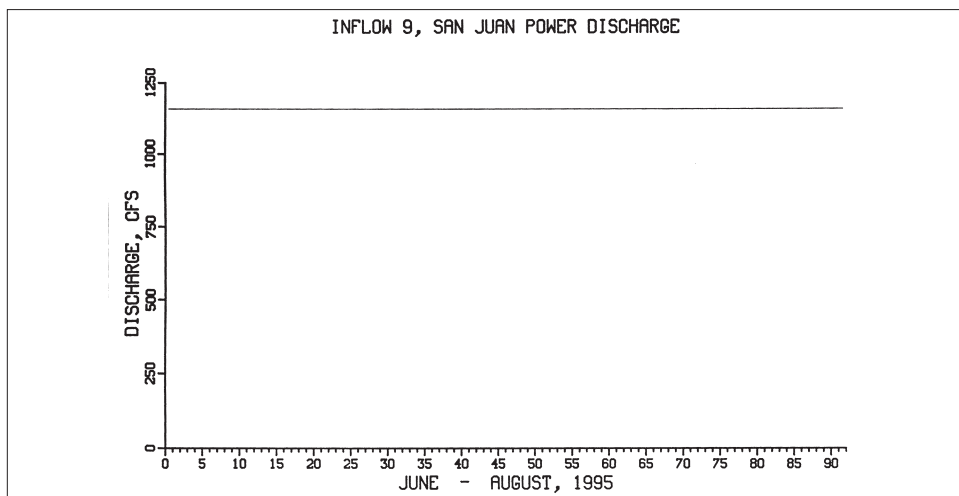
Figure 3-3. Continued



g. Inflow 7

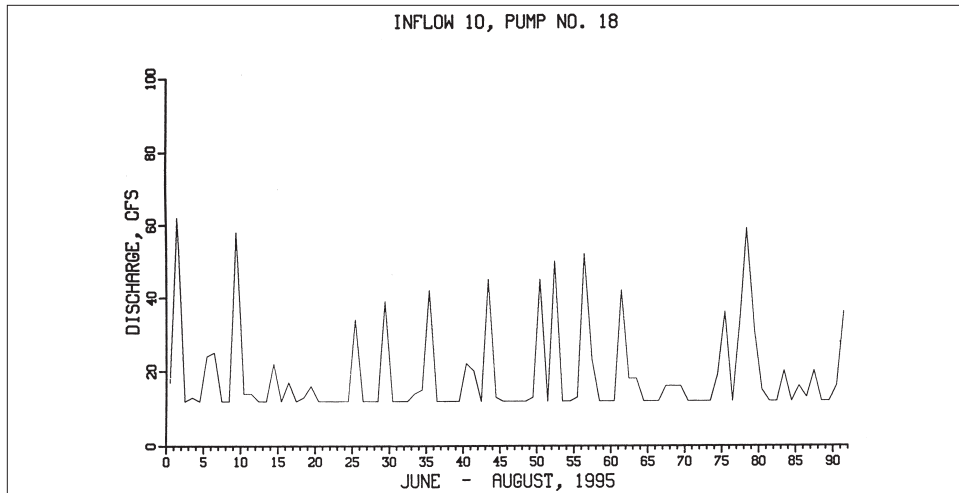


h. Inflow 8

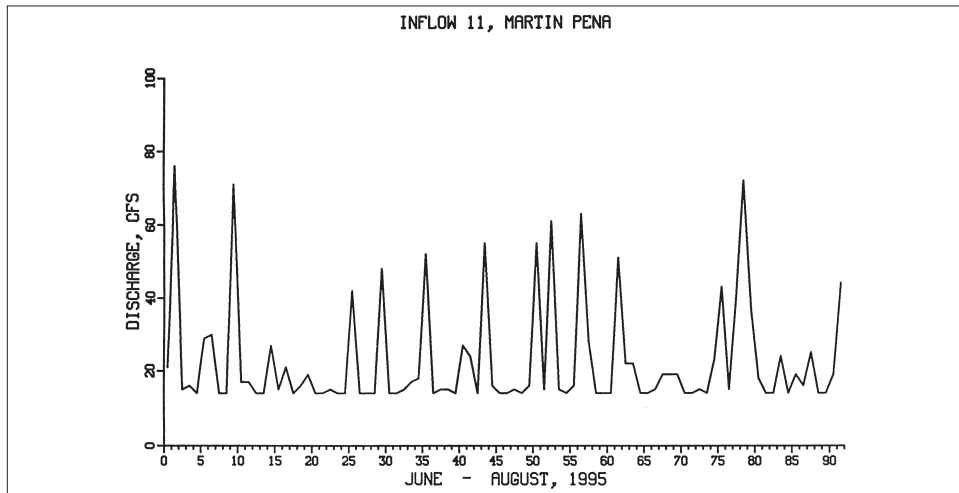


i. Inflow 9

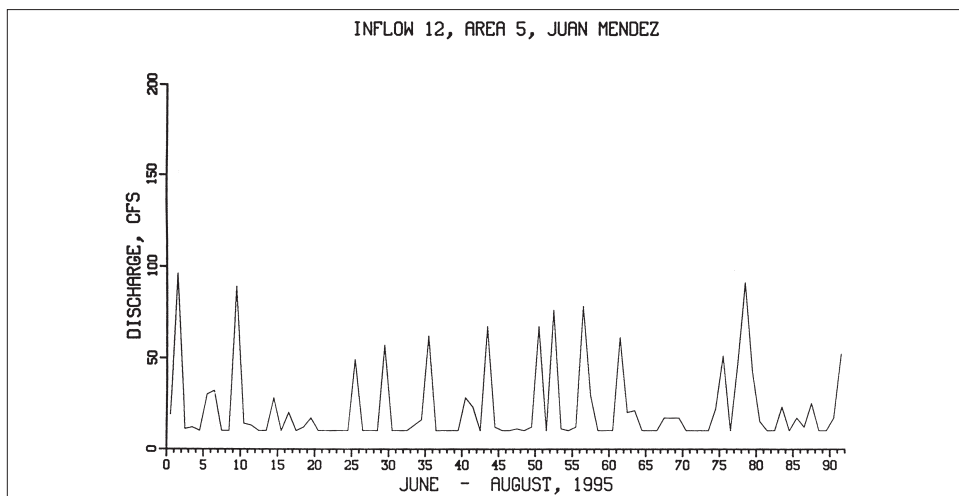
Figure 3-3. Continued



j. Inflow 10

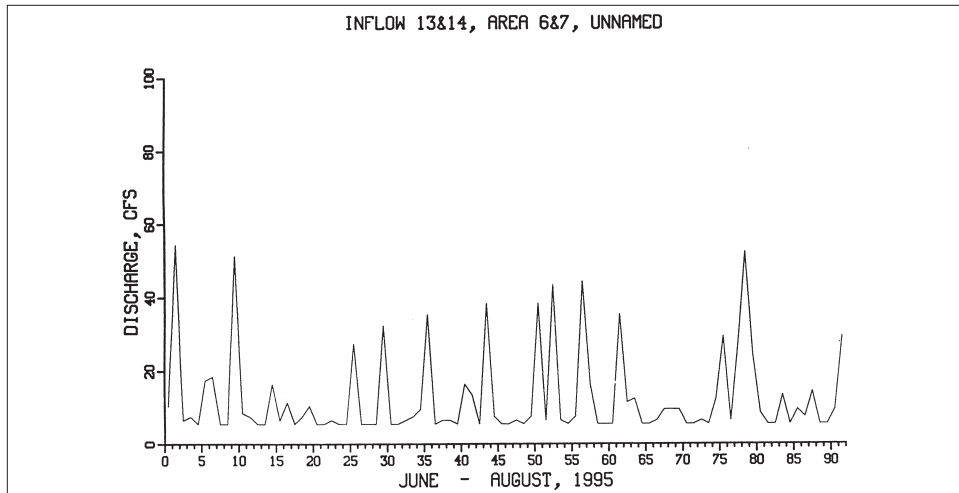


k. Inflow 11

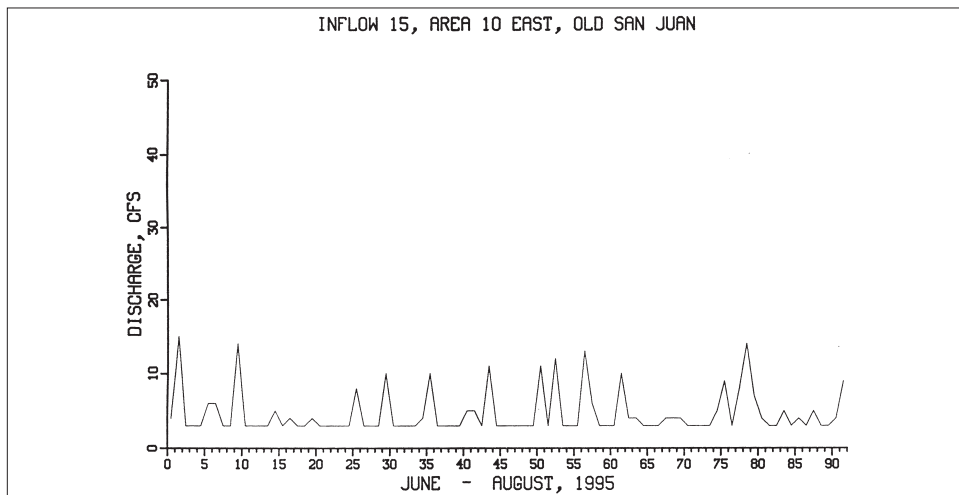


l. Inflow 12

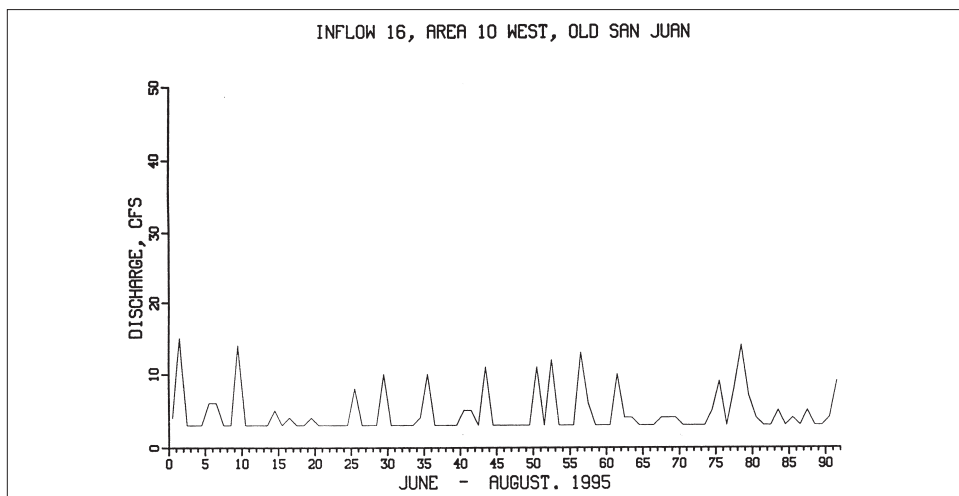
Figure 3-3. Continued



m. Inflow 13 & 14

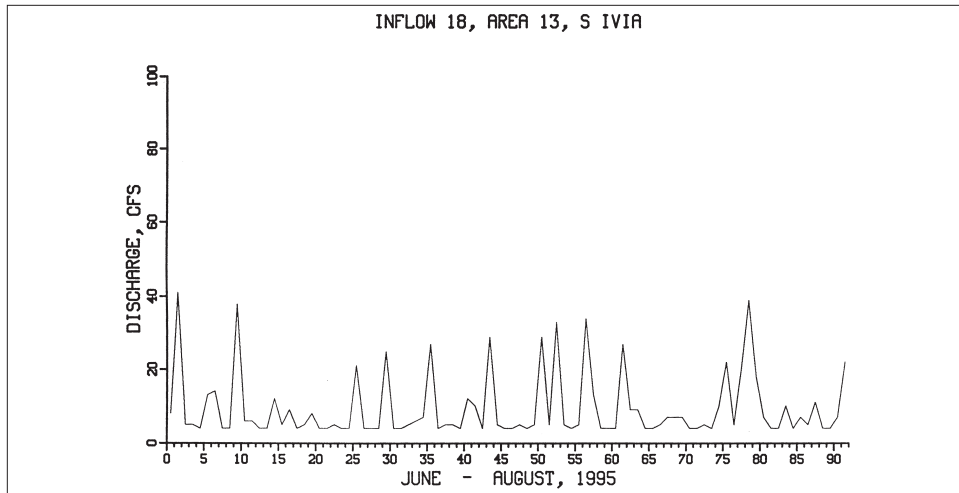


n. Inflow 15

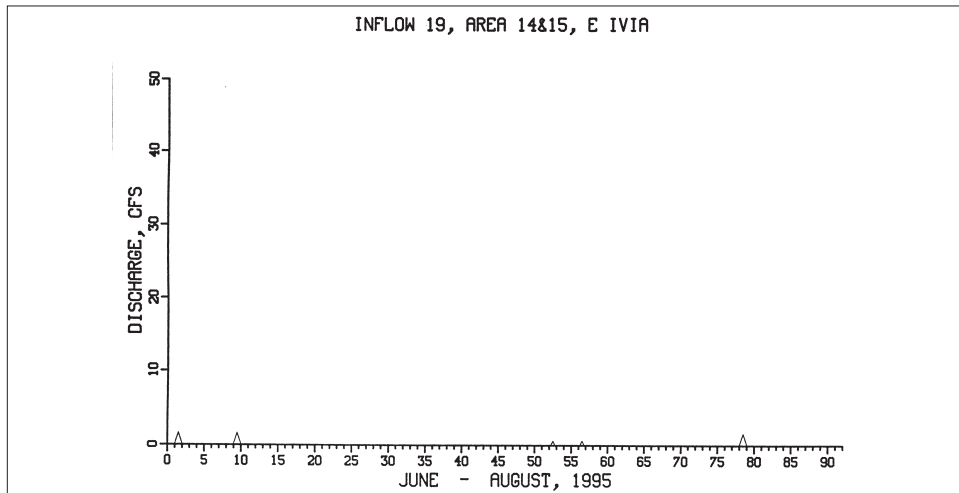


o. Inflow 16

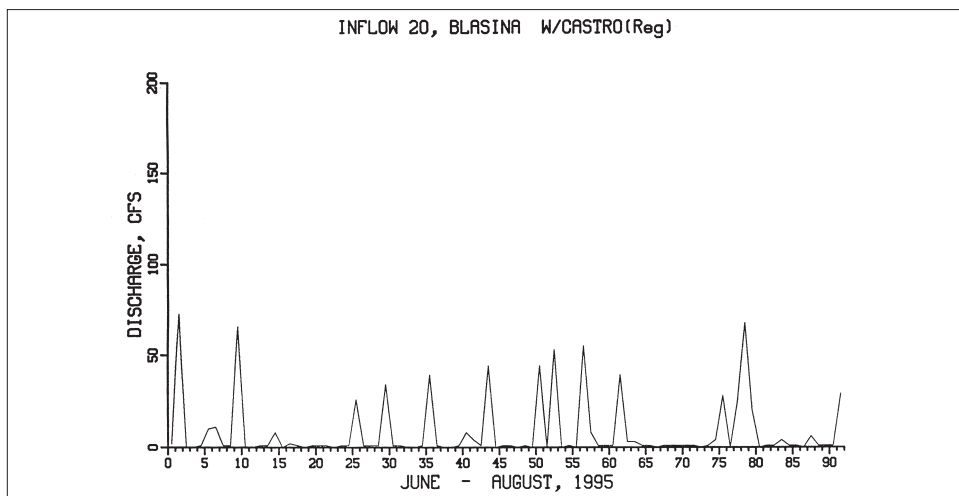
Figure 3-3. Continued



p. Inflow 18

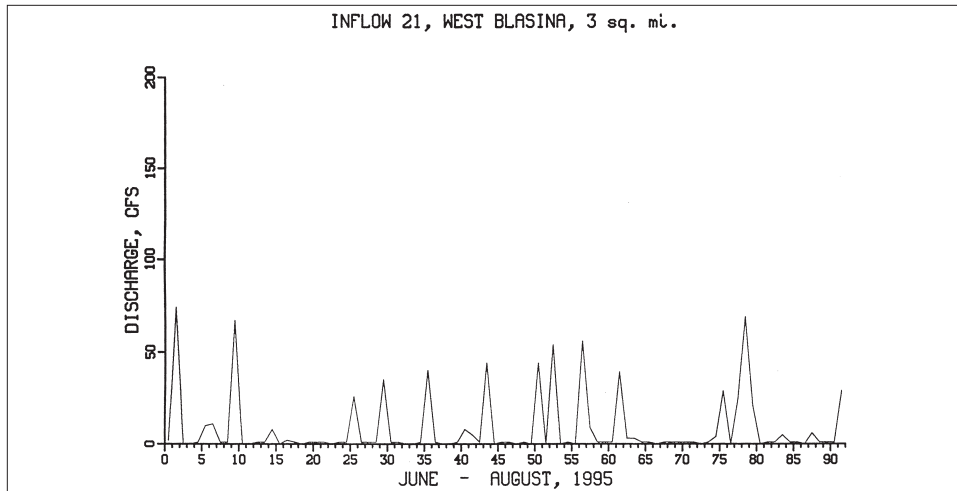


q. Inflow 19

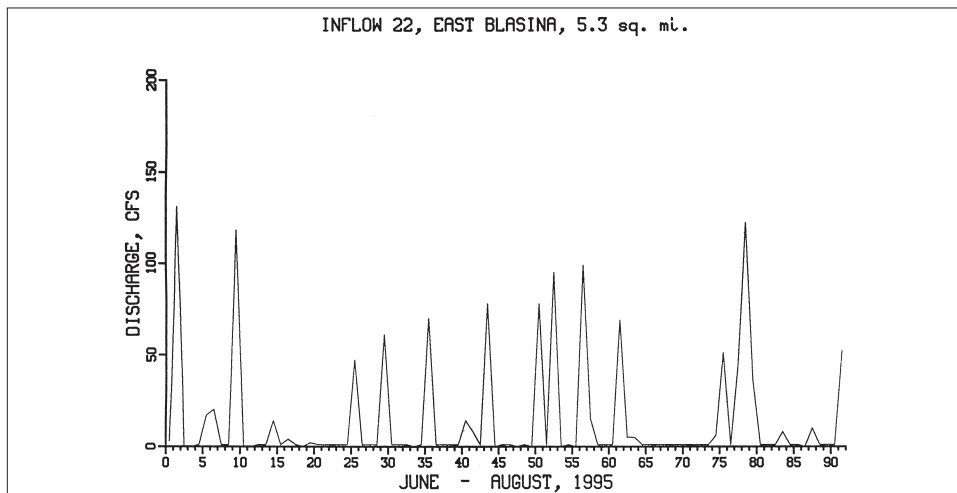


r. Inflow 20

Figure 3-3. Continued



s. Inflow 21



t. Inflow 22

Figure 3-3. Concluded

Figure 3-1. These elevations reflect both the astronomical tide as well as wind effects. An example of the water-surface elevations computed by ADCIRC and used in the CH3D-WES simulation is given in Figure 3-6.

The vertical distribution of salinity along the open ocean grid was specified from data collected by Fagerburg (1998). Since the temperature was specified as a constant, temperatures were not required to be specified along the ocean boundary of the grid. During flood, the specified values of salinity are employed, whereas during ebb, interior values are advected out of the grid. Along a solid boundary, the normal component of the velocity and the viscosity and diffusivity are set to zero.

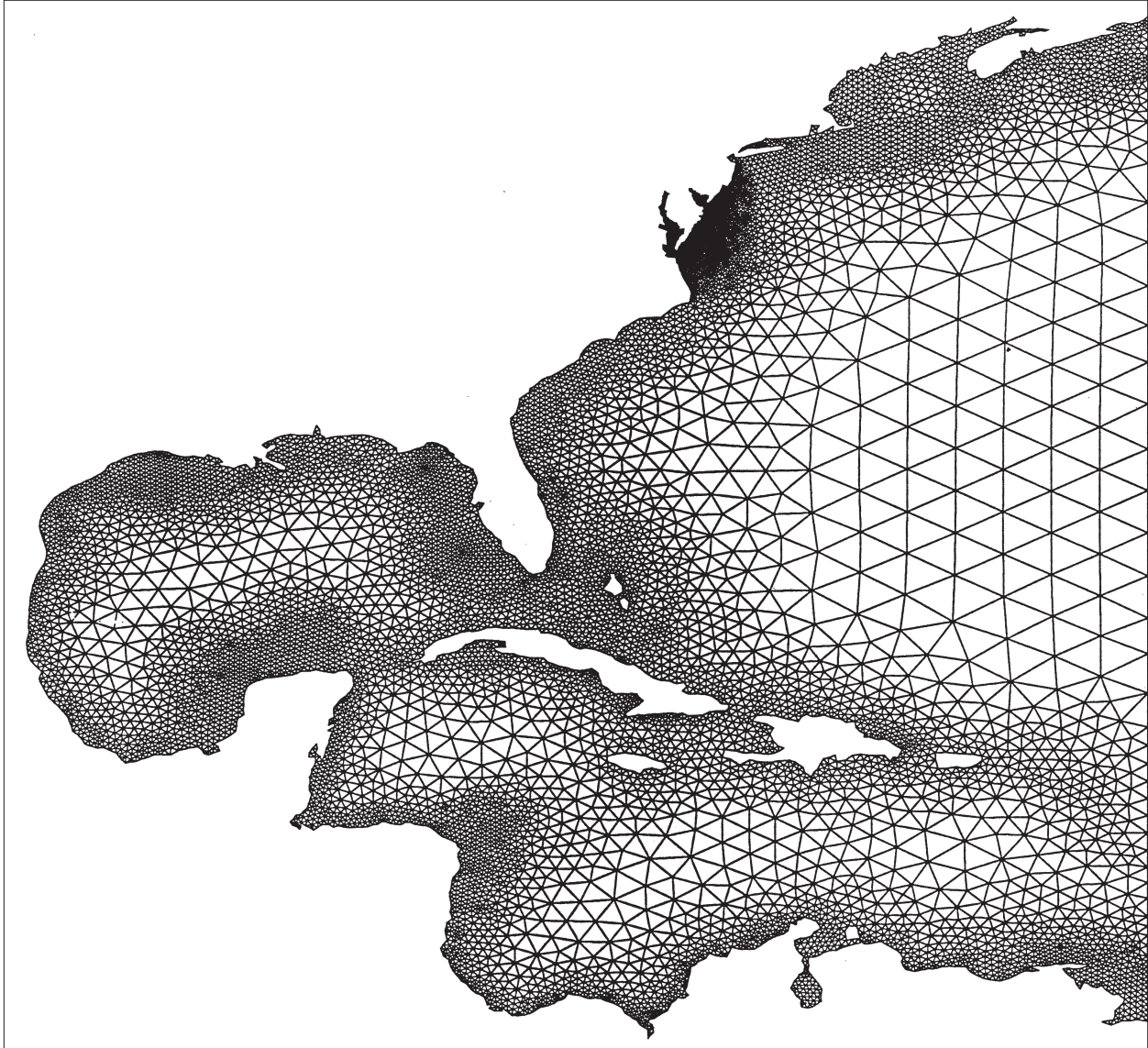


Figure 3-4. ADCIRC numerical grid

Initial Conditions

At the start of a model run, the values of ζ , \bar{u} , \bar{v} , w , \bar{U} , and \bar{V} are all set to zero. Values of the salinity and temperature are read from input files. These initial fields are generated from known data at a limited number of locations. Once the values in individual cells are determined by interpolating from the field data, the resulting 3-D field is smoothed several times. Generally, the salinity and temperature fields are frozen for the first few days of a simulation.

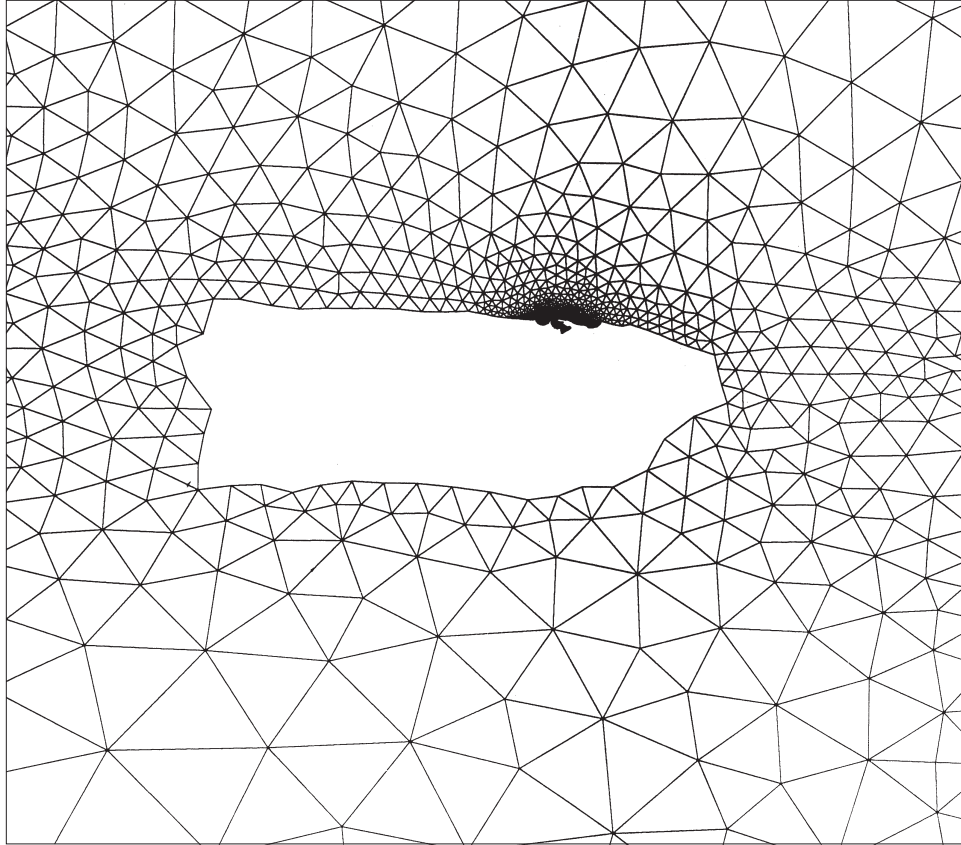


Figure 3-5. ADCIRC grid near Puerto Rico

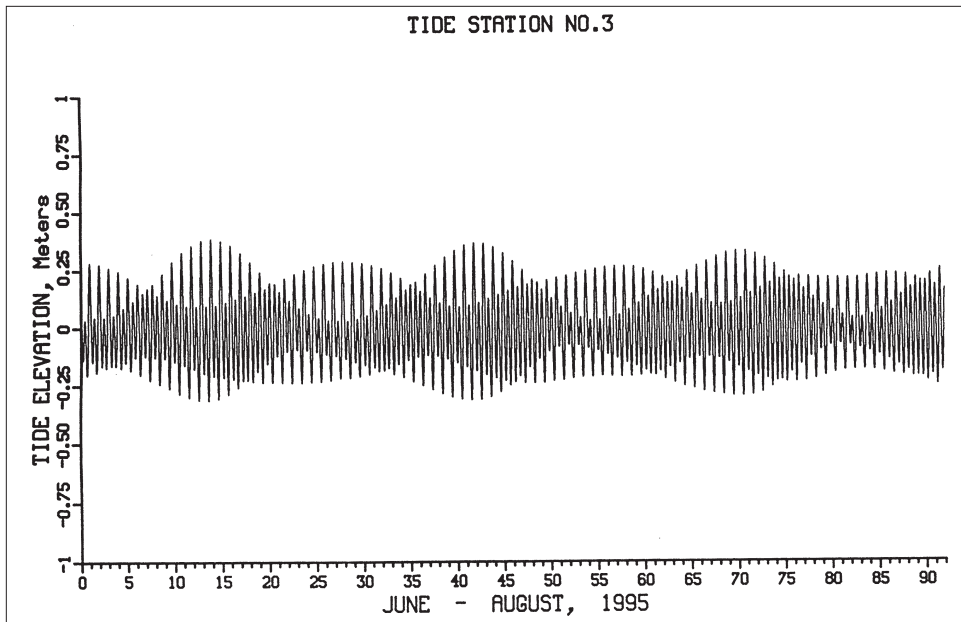


Figure 3-6. Tide computed by ADCIRC and applied on ocean boundary

Numerical Grid

The first step in any numerical modeling study is the generation of a suitable grid that captures the geometry of the modeled system. A map of the San Juan Bay Estuary system is shown in Figure 1-1 with the planform numerical boundary-fitted grid of the system illustrated in Figure 3-1. The numerical grid contains 2690 planform cells with a maximum of 30 vertical layers. Each layer is 3 ft (0.91 m) thick except for the top layer which varies with the tide. With much of the system being very shallow, many of the planform cells are represented by one layer. Thus, the computations involve a mixture of 3D as well as vertically averaged computations. With a total of 28,200 computational cells and a computational time step of 60 seconds, a 3-month simulation requires about 12 CPU hours on a 400 Mhz DEC Alpha work station.

4 Water Quality Model Formulation

Introduction

Kinetics for CE-QUAL-ICM were developed for application of the model to Chesapeake Bay (Cerco and Cole 1994). Model formulations are robust, however, and widely applicable. The model can be configured for specific applications by enabling various user-specified options. The description of the kinetics provided here is for the model as applied to the SJBE system. Descriptions of the complete kinetics are provided by Cerco and Cole (1994, 1995).

The central issues in eutrophication modeling are primary production of carbon by algae and concentration of dissolved oxygen. Primary production provides the energy required by the ecosystem to function. Excessive primary production is detrimental, however, since its decomposition, in the water and sediments, consumes oxygen. Dissolved oxygen is necessary to support the life functions of higher organisms and is considered an indicator of the “health” of estuarine systems. In order to predict primary production and dissolved oxygen, a large suite of model state variables is necessary (Table 4-1).

**Table 4-1.
Water Quality Model State Variables**

Temperature	Salinity
Fecal Coliform Bacteria	Algae
Dissolved Organic Carbon	Labile Particulate Organic Carbon
Refractory Particulate Organic Carbon	Ammonium
Nitrate	Dissolved Organic Nitrogen
Labile Particulate Organic Nitrogen	Refractory Particulate Organic Nitrogen
Total Phosphorus	Dissolved Organic Phosphorus
Labile Particulate Organic Phosphorus	Refractory Particulate Organic Phosphorus
Chemical Oxygen Demand	Dissolved Oxygen

Eutrophication, however, is not the only problem in the San Juan Estuary. Contamination with human and animal waste is also an issue. Consequently, fecal coliform bacteria were added to the suite of eutrophication variables.

Temperature

In some systems, temperature can be a primary determinant of the rate of biochemical reactions. Reaction rates increase as a function of temperature although extreme temperatures result in the mortality of organisms.

Salinity

Salinity is a conservative tracer that provides verification of the transport component of the model and facilitates examination of conservation of mass. Salinity also influences the dissolved oxygen saturation concentration and is used in the determination of kinetics constants that differ in saline and fresh water.

Fecal Coliform Bacteria

Fecal coliform bacteria are commonly found in human and animal waste. Although these organisms are harmless, they indicate waters are contaminated by waste matter.

Algae

Algae are represented in San Juan Estuary as a single group and quantified as carbonaceous biomass. Chlorophyll concentrations, for comparison with observations, are obtained through division of computed biomass by the carbon-to-chlorophyll ratio.

Organic Carbon

Three organic carbon state variables are considered: dissolved, labile particulate, and refractory particulate. Labile and refractory distinctions are based upon the time scale of decomposition. Labile organic carbon decomposes on a time scale of days to weeks while refractory organic carbon requires more time. Labile organic carbon decomposes rapidly in the water column or the sediments. Refractory organic carbon decomposes slowly, primarily in the sediments, and may contribute to sediment oxygen demand years after deposition.

Phosphorus

As with carbon and nitrogen, organic phosphorus is considered in three states: dissolved, labile particulate, and refractory particulate. Only a single mineral form, total phosphate, is considered. Total phosphate exists as two states within the model ecosystem: dissolved phosphate and phosphate incorporated in algal cells. Equilibrium partition coefficients are used to distribute the total among the states.

Nitrogen

Nitrogen is first divided into organic and mineral fractions. Organic nitrogen state variables are: dissolved organic nitrogen, labile particulate organic nitrogen, and refractory particulate organic nitrogen. Two mineral nitrogen forms are considered: ammonium and nitrate. Both are utilized to fulfill algal nutrient requirements although ammonium is preferred from thermodynamic considerations. The primary reason for distinguishing the two is that ammonium is oxidized by nitrifying bacteria into nitrate. This oxidation can be a significant sink of oxygen in the water column and sediments. An intermediate in the complete oxidation of ammonium, nitrite, also exists. Nitrite concentrations are usually much less than nitrate and for modeling purposes nitrite is combined with nitrate. Hence the nitrate state variable actually represents the sum of nitrate plus nitrite.

Chemical Oxygen Demand

Chemical oxygen demand is the concentration of reduced substances that are oxidizable by inorganic means. The primary component of chemical oxygen demand is sulfide released from sediments. Oxidation of sulfide to sulfate may remove substantial quantities of dissolved oxygen from the water column.

Dissolved Oxygen

Dissolved oxygen is required for the existence of higher life forms. Oxygen availability determines the distribution of organisms and the flows of energy and nutrients in an ecosystem. Dissolved oxygen is a central component of the water-quality model.

Conservation of Mass Equation

The foundation of CE-QUAL-ICM is the solution to the three-dimensional mass-conservation equation for a control volume. The control-volume structure was selected to allow maximum flexibility in linkage of CE-QUAL-ICM to alternate hydrodynamic models. Control

volumes in CE-QUAL-ICM correspond to cells in x-y-z space on the CH3D grid. CE-QUAL-ICM solves, for each volume and for each state variable, the conservation of mass equation:

$$\frac{\delta V_i C_i}{\delta t} = \sum_{j=1}^n Q_j C_j^* + \sum_{j=1}^n A_j D_j \frac{\delta C}{\delta x_j} + \sum S_i \quad (4.1)$$

where

- V_i = volume of ith control volume (m^3)
- C_i = concentration in ith control volume ($gm\ m^{-3}$)
- Q_j = volumetric flow across flow face j of ith control volume ($m^3\ sec^{-1}$)
- C_j^* = concentration in flow across flow face j ($gm\ m^{-3}$)
- A_j = area of flow face j (m^2)
- D_j = diffusion coefficient at flow face j ($m^2\ sec^{-1}$)
- n = number of flow faces attached to ith control volume
- S_i = external loads and kinetic sources and sinks in ith control volume ($gm\ sec^{-1}$)
- t, x = temporal and spatial coordinates

Solution to the mass-conservation equation is via the finite-difference method using the QUICKEST algorithm (Leonard 1979) in the horizontal directions and a Crank-Nicolson scheme in the vertical direction.

The majority of this chapter details with the kinetics portion of the mass-conservation equation for each state variable. Parameters are defined where they first appear. All parameters are listed, in alphabetical order, in a glossary (see Table 4-2). For consistency with reported rate coefficients, kinetics are detailed using a temporal dimension of days. Within the CE-QUAL-ICM code, kinetics sources and sinks are converted to a dimension of seconds before employment in the mass-conservation equation.

Algae

Algae play a central role in the carbon and nutrient cycles that comprise the model ecosystem. Sources and sinks of algae are:

- Growth (production)
- Basal metabolism
- Predation
- Settling

The governing equation for algal biomass is:

$$\frac{\delta}{\delta t} B = \left(P - BM - PR - W Sa \frac{\delta}{\delta z} \right) B \quad (4.2)$$

where

B = algal biomass, expressed as carbon (gm C m⁻³)

P = production (day⁻¹)

BM = basal metabolism (day⁻¹)

PR = predation (day⁻¹)

WSa = settling velocity (m day⁻¹)

z = vertical coordinate (m)

Production

Production by phytoplankton is determined by the availability of nutrients, by the intensity of light, and by the ambient temperature. The effects of each are considered to be multiplicative:

$$P = PM f(N)f(I)f(T) \quad (4.3)$$

where

PM = production under optimal conditions (day⁻¹)

f(N) = effect of suboptimal nutrient concentration (0 ≤ f ≤ 1)

f(I) = effect of suboptimal illumination (0 ≤ f ≤ 1)

f(T) = effect of suboptimal temperature (0 ≤ f ≤ 1)

Nutrients

Carbon, nitrogen, and phosphorus are the primary nutrients required for algal growth. Inorganic carbon is usually available in excess and is not considered in the model. The effects of the remaining nutrients on growth are described by the formulation commonly referred to as “Monod kinetics” (Monod 1949). In the Monod formulation (Figure 4-1) growth is dependent upon nutrient availability at low nutrient concentrations but is independent of nutrients at high concentrations. A key parameter in the formulation is the “half-saturation concentration.” Growth rate is half the maximum when available nutrient concentration equals the half-saturation concentration. Liebig’s “law of the minimum” (Odum 1971) indicates growth is determined by the nutrient in least supply:

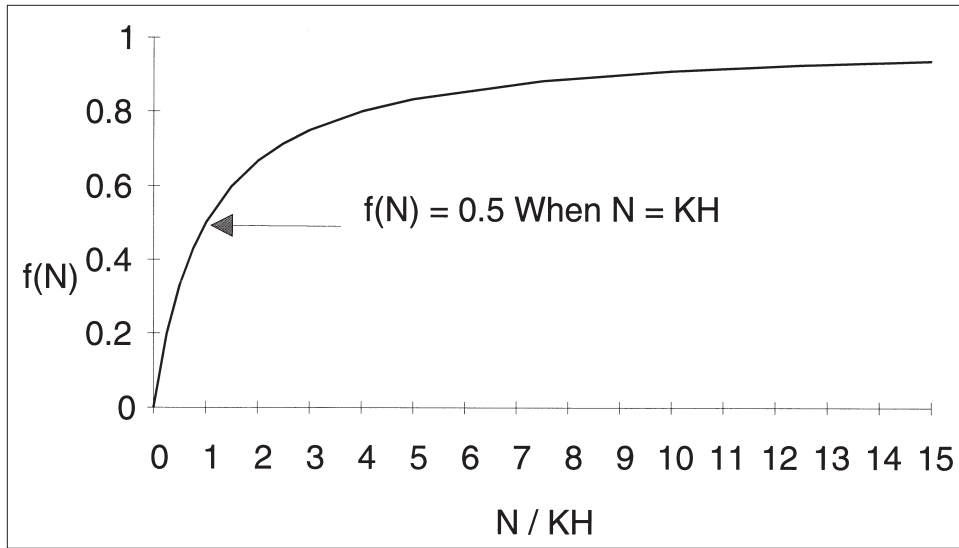


Figure 4-1. The Monod formulation for nutrient-limited growth

$$f(N) = \text{minimum} \left(\frac{NH_4 + NO_3}{KHn + NH_4 + NO_3}, \frac{PO_4d}{KHp + PO_4d} \right) \quad (4.4)$$

where

NH_4 = ammonium concentration (gm N m^{-3})

NO_3 = nitrate concentration (gm N m^{-3})

KHn = half-saturation constant for nitrogen uptake (gm N m^{-3})

PO_4d = dissolved phosphate concentration (gm P m^{-3})

KHp = half-saturation constant for phosphorus uptake (gm P m^{-3})

Light

Algal production increases as a function of light intensity until an optimal intensity is reached. Numerous options are available for a function which represents the increase of production as a function of light intensity. The function employed here is analogous to the Monod function used to compute nutrient limitations:

$$f(I) = \frac{I}{I_h + I} \quad (4.5)$$

where

I = illumination rate (Langley day^{-1})

I_h = half-saturation illumination (Langley day^{-1})

Equation 4.5 describes the instantaneous light limitation at a point in space. The model, however, computes processes integrated over discrete time intervals and aggregated spatially into model segments. Therefore, the equation must be integrated over an appropriate time interval and averaged over the thickness of each model segment. The integration interval selected is one day. This interval does not preclude computation steps less than a day but frees the model from accounting for illumination in “real time.” Daily averaging does preclude computation of diurnal fluctuations in algal production. This restriction is not severe, however, since the classic equations for algal growth are not appropriate for short time scales.

Assuming light intensity declines exponentially with depth, the integrated, averaged form of Equation 4.5 is:

$$f(I) = \frac{FD}{Kess\Delta z} \ln \left(\frac{Ih + I_0 e^{-Kess z_1}}{Ih + I_0 e^{-Kess z_2}} \right) \quad (4.6)$$

where

I_0 = daily illumination at water surface (Langley's day⁻¹)

FD = fractional daylength ($0 \leq FD \leq 1$)

Kess = total light attenuation coefficient (m⁻¹)

Δz = model segment thickness (m)

z_1 = distance from water surface to top of model segment (m)

z_2 = distance from water surface to bottom of model segment (m)

Light attenuation in the water column is composed of two fractions: a background value dependent on water color and concentration of suspended particles, and extinction due to light absorption by ambient chlorophyll:

$$Kess = Keb + Kechl \frac{B}{CChl} \quad (4.7)$$

where

Keb = background light attenuation (m⁻¹)

Kechl = light attenuation coefficient for chlorophyll 'a' (m² mg⁻¹)

CChl = algal carbon-to-chlorophyll ratio (gm C mg⁻¹ chl)

Temperature

Algal production increases as a function of temperature until an optimum temperature or temperature range is reached. Above the optimum, production declines until a temperature lethal to the organisms is attained. Numerous functional representations of temperature effects are available. Inspection of growth versus temperature curves indicates a function similar to a Gaussian probability curve. (Figure 4-2 provides a good fit to observations.)

$$f(T) = e^{-KTg1(T-Tm)^2} \text{ when } T \leq Tm \quad (4.8)$$

$$= e^{-KTg2(Tm-T)^2} \text{ when } T > Tm$$

where

T = temperature (C°)

Tm = optimal temperature for algal growth (C°)

KTg1 = effect of temperature below Tm on growth (C°⁻²)

KTg2 = effect of temperature above Tm on growth (C°⁻²)

Basal Metabolism

As employed here, basal metabolism is the sum of all internal processes that decrease algal biomass. A portion of metabolism is respiration which may be viewed as a reversal of production. In respiration, carbon and nutrients are returned to the environment accompanied by the consumption of dissolved oxygen. A second internal sink of biomass is the excretion of dissolved organic carbon.

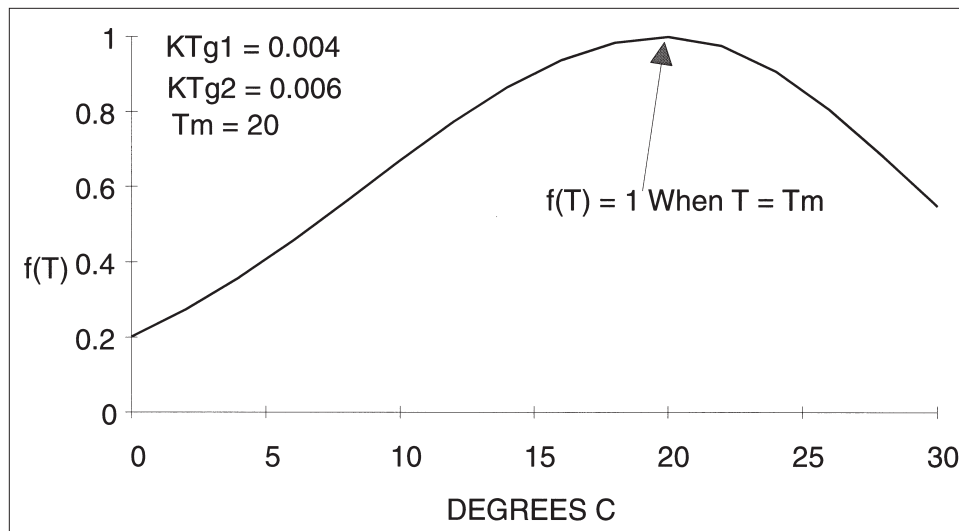


Figure 4-2. Effect of temperature on algal production

Respiration cannot proceed in the absence of oxygen. Basal metabolism cannot decrease in proportion to oxygen availability, however, or algae would approach immortality under anoxic conditions. To solve this dilemma, basal metabolism is considered to be independent of dissolved oxygen concentration but the distribution of metabolism between respiration and excretion is oxygen-dependent. When oxygen is freely available, respiration is a large fraction of the total. When oxygen is restricted, excretion becomes dominant. Formulation of this process is detailed in the following text that describes algal effects on carbon and dissolved oxygen.

Basal metabolism is commonly considered to be an exponentially increasing (Figure 4-3) function of temperature:

$$BM = BMr e^{KTb(T-Tr)} \quad (4.9)$$

where

BMr = metabolic rate at Tr (day^{-1})

KTb = effect of temperature on metabolism (C^{-1})

Tr = reference temperature for metabolism (C°)

Predation

Detailed specification of predation within the water column requires predictive modeling of zooplankton biomass and activity. Absence of data prohibited the modeling of zooplankton in the San Juan Estuary. Consequently, a constant predation rate was specified. This specification implicitly assumed zooplankton biomass is a constant fraction of algal biomass. Zooplankton activity was assumed to be influenced by temperature. The temperature effect was represented by an exponential relationship

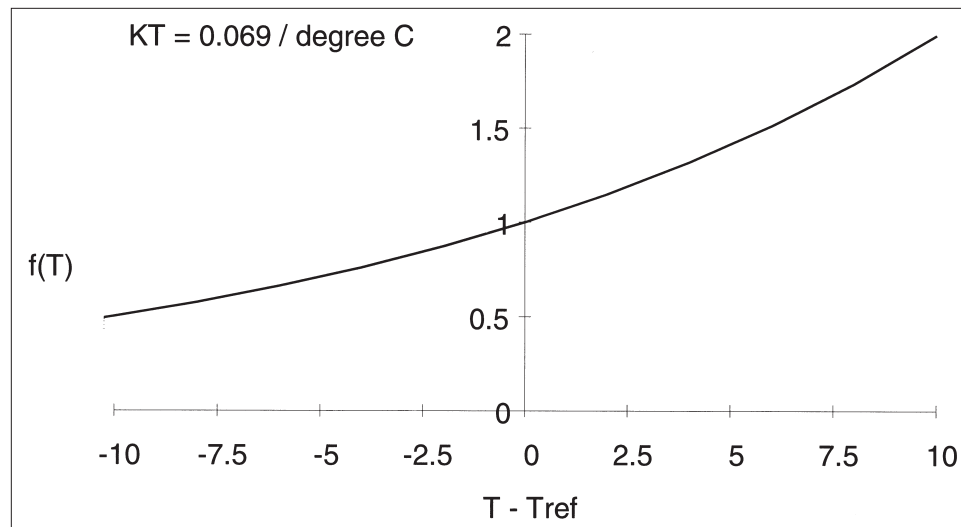


Figure 4-3. Exponential temperature function

(Figure 4-3). The predation formulation is identical to basal metabolism. The difference in predation and basal metabolism lies in the distribution of the end products of these processes.

$$PR = BPR e^{KTb(T-Tr)} \quad (4.10)$$

where

$$BPR = \text{predation rate at } Tr \text{ (day}^{-1}\text{)}$$

Macrobenthic Grazing

A second form of predation on algae is grazing by filter-feeding organisms which inhabit the sediment-water interface. As with zooplankton, detailed specification of predation by macrobenthos requires predictive modeling of macrobenthic activity and biomass. In the absence of a benthos model, a formulation was specified which converted macrobenthic grazing into an equivalent settling rate:

$$WSmb = MBGM FR \frac{DO}{KHomb + DO} \quad (4.11)$$

where

WSmb = equivalent settling rate (m day^{-1})

MBGM = macrobenthic biomass (gm C m^{-2})

FR = filtering rate ($\text{m}^{-3} \text{ gm}^{-1} \text{ C day}^{-1}$)

DO = dissolved oxygen concentration (gm DO m^{-3})

KHomb = dissolved oxygen concentration at which macrobenthic grazing is halved (gm DO m^{-3})

Macrobenthic grazing is implemented only in the model cells which interface with the bottom. Biomass is specified based on the observed distribution of benthos in the system. Incorporation of dissolved oxygen into the relationship accounts for the cessation of filtering and eventual demise of benthos under anoxic conditions. Algal biomass filtered from the water column is routed into the sediment diagenesis portion of the model package.

Effect of Algae on Organic Carbon

During production and respiration, algae primarily take up and produce carbon dioxide, an inorganic form not considered in the model. A small fraction of basal metabolism is exuded as dissolved organic carbon, however, and in the model this fraction increases as dissolved oxygen becomes scarce. Algae also produce organic carbon through the effects of predation. Zooplankton take up and redistribute algal carbon through grazing, assimilation, respiration, and excretion. Since zooplankton are not included in the model, routing of algal carbon through zooplankton is simulated by empirical distribution coefficients. The effects of algae on organic carbon are expressed:

$$\frac{\delta}{\delta t} DOC = \quad (4.12)$$

$$\left[FCD + (1 - FCD) \left(\frac{KHr}{KHr + DO} \right) BM + FC DP PR \right]$$

$$\frac{\delta}{\delta t} LPOC = FCLP PR B \quad (4.13)$$

$$\frac{\delta}{\delta t} RPOC = FCRP PR B \quad (4.14)$$

where

DOC = dissolved organic carbon concentration (gm C m⁻³)

DO = dissolved oxygen concentration (gm O₂ m⁻³)

LPOC = labile particulate organic carbon concentration (gm C m⁻³)

RPOC = refractory particulate organic carbon concentration (gm C m⁻³)

FCD = fraction of basal metabolism exuded as dissolved organic carbon

KHr = half-saturation concentration for algal dissolved organic carbon excretion (gm O₂ m⁻³)

FC DP = fraction of dissolved organic carbon produced by predation

FCLP = fraction of labile particulate carbon produced by predation

FCRP = fraction of refractory particulate carbon produced by predation

The sum of the three predation fractions must equal unity.

Effect of Algae on Phosphorus

Algae take up dissolved phosphate during production and release dissolved phosphate and organic phosphorus through mortality. As with carbon, the fate of algal phosphorus released by metabolism and predation is represented by distribution coefficients. Since the total phosphate state variable includes both intra- and extracellular phosphate, no explicit representation of the effect of algae on phosphate is necessary. Distribution of total phosphate is determined by partition coefficients as detailed in the Phosphorus section of this chapter. The equations that express the effects of algae on organic phosphorus are:

$$\frac{\delta}{\delta t} DOP = (BM FPD + PR FPDP) APC B \quad (4.15)$$

$$\frac{\delta}{\delta t} LPOP = (BM FPL + PR FPLP) APC B \quad (4.16)$$

$$\frac{\delta}{\delta t} RPOP = (BM FPR + PR FPRP) APC B \quad (4.17)$$

where

DOP = dissolved organic phosphorus concentration (gm P m^{-3})

LPOP = labile particulate organic phosphorus concentration
(gm P m^{-3})

RPOP = refractory particulate organic phosphorus concentration
(gm P m^{-3})

APC = phosphorus-to-carbon ratio of all algal groups ($\text{gm P gm}^{-1} \text{C}$)

FPD = fraction of dissolved organic phosphorus produced by
metabolism

FPL = fraction of labile particulate phosphorus produced by
metabolism

FPR = fraction of refractory particulate phosphorus produced by
metabolism

FPDP = fraction of dissolved organic phosphorus produced by
predation

FPLP = fraction of labile particulate phosphorus produced by
predation

FPRP = fraction of refractory particulate phosphorus produced by
predation

The sums of the metabolism and respiration fractions must each be less than or equal to unity.

Effect of Algae on Nitrogen

Algae take up ammonium and nitrate during production and release ammonium and organic nitrogen through mortality. Nitrate is internally reduced to ammonium before synthesis into biomass occurs (Parsons et al. 1984). Trace concentrations of ammonium inhibit nitrate reduction so that, in the presence of ammonium and nitrate, ammonium is utilized first. The “preference” of algae for ammonium can be expressed empirically (Thomann and Fitzpatrick 1982):

$$PN = NH_4 \frac{NO_3}{(KHn + NH_4)(KHn + NO_3)} + NH_4 \frac{KHn}{(NH_4 + NO_3)(KHn + NO_3)} \quad (4.18)$$

where

$$PN = \text{algal preference for ammonium uptake } (0 \leq PN \leq 1)$$

The ammonium preference function (Figure 4-4) has two limiting values. When nitrate is absent, the preference for ammonium is unity. When ammonium is absent, the preference is zero. In the presence of ammonium and nitrate, the preference depends on the abundance of both forms relative to the half-saturation constant for nitrogen uptake. When both ammonium and nitrate are abundant, the preference for ammonium approaches unity. When ammonium is scarce but nitrate is abundant, the preference decreases in magnitude and a significant fraction of algal nitrogen requirement comes from nitrate.

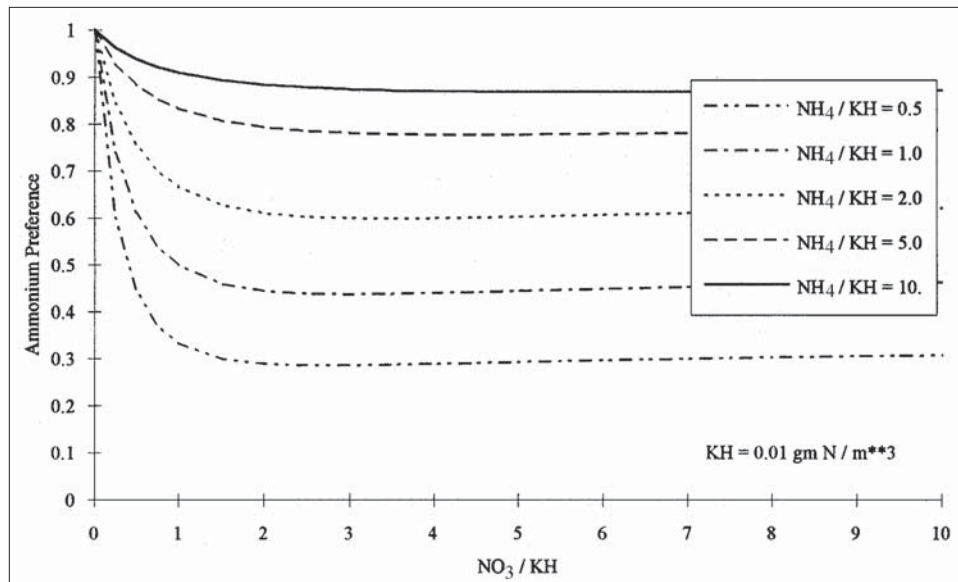


Figure 4-4. The ammonium preference function

The fate of algal nitrogen released by metabolism and predation is represented by distribution coefficients. The effects of algae on the nitrogen state variables are expressed:

$$\frac{\delta}{\delta t} NH_4 = (BM FNI + PR FNIP - PN P)ANC B \quad (4.19)$$

$$\frac{\delta}{\delta t} NO_3 = (PN - 1)P ANC B \quad (4.20)$$

$$\frac{\delta}{\delta t} DON = (BM FND + PR FNDP)ANC B \quad (4.21)$$

$$\frac{\delta}{\delta t} LPON = (BM FNL + PR FNL P)ANC B \quad (4.22)$$

$$\frac{\delta}{\delta t} RPON = (BM FNR + PR FNR P)ANC B \quad (4.23)$$

where

DON = dissolved organic nitrogen concentration ($gm N m^{-3}$)

LPON = labile particulate organic nitrogen concentration ($gm N m^{-3}$)

RPON = refractory particulate organic nitrogen concentration
($gm N m^{-3}$)

ANC = nitrogen-to-carbon ratio of algae ($gm N gm^{-1} C$)

FNI = fraction of inorganic nitrogen produced by metabolism

FND = fraction of dissolved organic nitrogen produced by
metabolism

FNL = fraction of labile particulate nitrogen produced by
metabolism

FNR = fraction of refractory particulate nitrogen produced by
metabolism

FNIP = fraction of inorganic nitrogen produced by predation

FNDP = fraction of dissolved organic nitrogen produced by predation

FNLP = fraction of labile particulate nitrogen produced by predation

FNR P = fraction of refractory particulate nitrogen produced by
predation

The sums of the metabolism fractions and the predation fractions must each equal unity.

Algal Stoichiometry

Algal biomass is quantified in units of carbon. In order to express the effects of algae on nitrogen and phosphorus, the ratios of nitrogen-to-carbon and phosphorus-to-carbon in algal biomass must be specified. Global mean values of these ratios are well known (Redfield et al. 1966). Algal composition varies, however, especially as a function of nutrient availability. As nitrogen and phosphorus become scarce, algae adjust their composition so that smaller quantities of these vital nutrients are required to produce carbonaceous biomass (Droop 1973; DiToro 1980; Parsons et al. 1984).

Observations from upper Chesapeake Bay were examined to assess the potential variability of algal stoichiometry. Data employed were collected by the Maryland Department of the Environment from June 1985 to December 1987. This subset of the monitoring database was selected since it contained direct laboratory analysis of particulate nutrients. Examination was restricted to surface (≤ 2 m) data to maximize the fraction of algae in the particulate analyses. The ratio of particulate carbon-to-nitrogen was plotted as a function of ammonium plus nitrate concentration (Figure 4-5). The ratio of particulate carbon-to-phosphorus was plotted as a function of dissolved phosphate concentration (Figure 4-6). (These ratios were plotted to correspond to conventional reporting of algal composition. Their inverses are used in the model.) The variation of carbon-to-nitrogen stoichiometry in the upper Bay was small. No altered composition as a function of diminished nutrient availability was evident. As a consequence of these observations, the model formulation specified constant algal nitrogen-to-carbon ratio, ANC. Large variations in carbon-to-phosphorus ratio occurred, however. The carbon-to-phosphorus ratio in seston more than doubled as dissolved phosphate concentration diminished. To account for this effect, a variable algal phosphorus-to-carbon ratio, APC, was specified in the model.

Calculation of APC requires specification of three parameters:

- APCmin = minimum phosphorus-to-carbon ratio ($\text{gm P gm}^{-1} \text{ C}$);
- APCmax = maximum phosphorus-to-carbon ratio ($\text{gm P gm}^{-1} \text{ C}$);
and
- PO₄dmax = dissolved phosphate concentration at which algal phosphorus-to-carbon ratio achieves its maximum value (gm P m^{-3}).

The minimum phosphorus-to-carbon ratio is assumed to occur when dissolved phosphate is zero. The ratio increases linearly from the minimum to the maximum which occurs when dissolved phosphate equals PO₄dmax:

$$APC = APC \text{ min} + \frac{APC \text{ max} - APC \text{ min}}{PO_4 d \text{ max}} PO_4 d \quad (4.24)$$

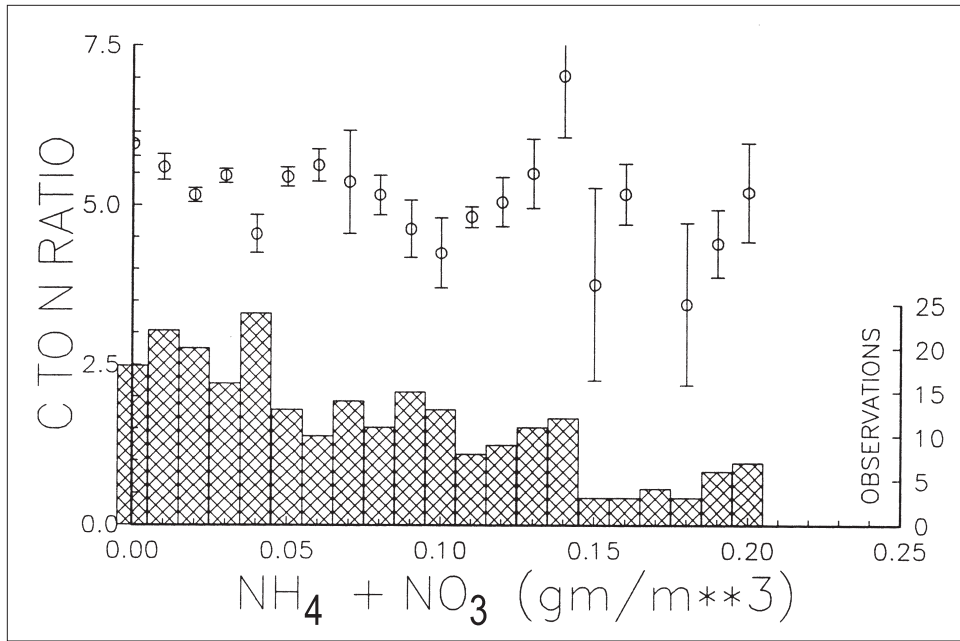


Figure 4-5. Carbon-to-nitrogen ratio (mean and standard error) of seston in upper Chesapeake Bay. Bars show number of observations

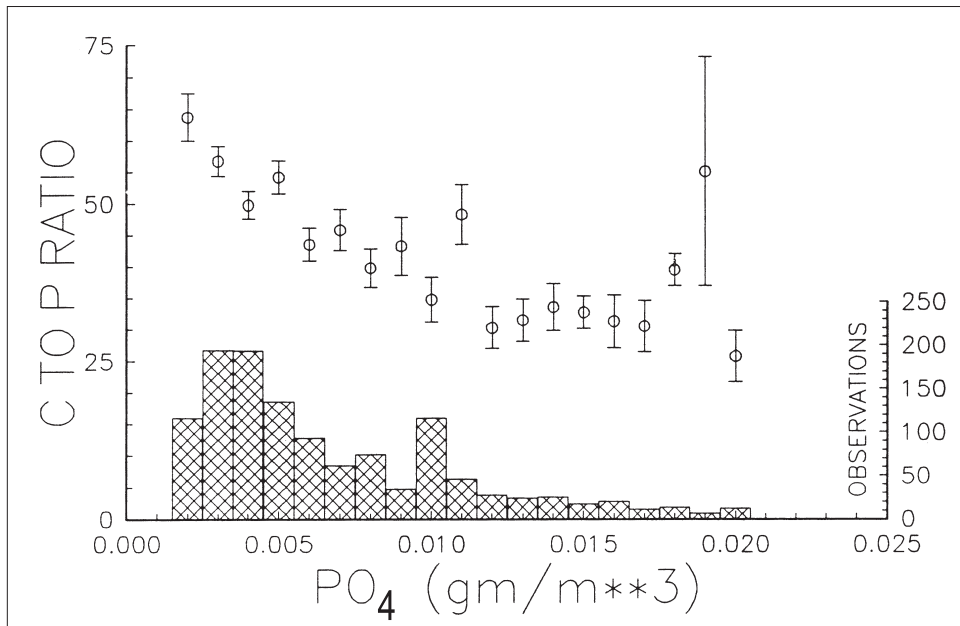


Figure 4-6. Carbon-to-phosphorus ratio (mean and standard error) of seston in upper Chesapeake Bay. Bars show number of observations

where

$$\text{APC} = \text{algal phosphorus-to-carbon ratio (gm P gm}^{-1}\text{ C)}$$

When dissolved phosphate exceeds PO_4dmax , APC is held at its maximum value (Figure 4-7).

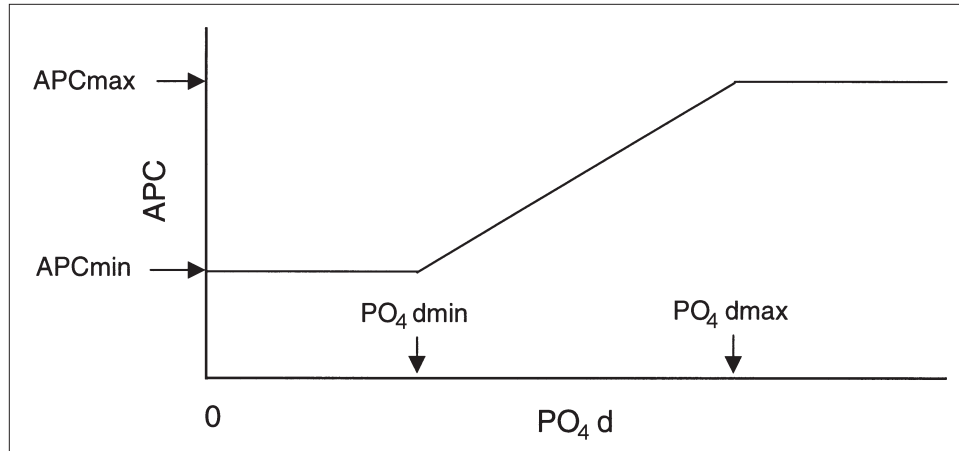
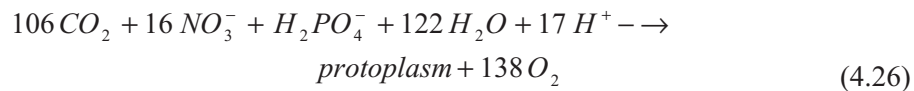
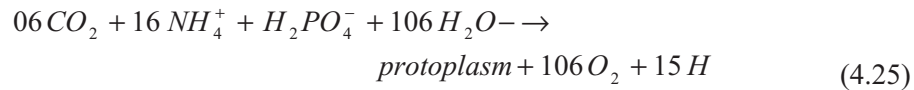


Figure 4-7. Model algal phosphorus-to-carbon ratio

Effect of Algae on Dissolved Oxygen

Algae produce oxygen during photosynthesis and consume oxygen through respiration. The quantity produced depends on the form of nitrogen utilized for growth. More oxygen is produced, per unit of carbon fixed, when nitrate is the algal nitrogen source than when ammonium is the source. Equations describing algal uptake of carbon and nitrogen and production of dissolved oxygen (Morel 1983) are:



When ammonium is the nitrogen source, one mole oxygen is produced per mole carbon dioxide fixed. When nitrate is the nitrogen source, 1.3 moles oxygen are produced per mole carbon dioxide fixed.

The equation that describes the effect of algae on dissolved oxygen in the model is:

$$\frac{\delta}{\delta t} DO = \left[(1.3 - 0.3 PN)P - (1 - FCD) \frac{DO}{KHr + DO} BM \right] AOCR B \quad (4.27)$$

where

$$AOCR = \frac{\text{dissolved oxygen-to-carbon ratio in respiration}}{(2.67 \text{ gm O}_2 \text{ gm}^{-1} \text{ C})}$$

The magnitude of AOCR is derived from a simple representation of the respiration process:



The quantity $(1.3 - 0.3 PN)$ is the photosynthesis ratio and expresses the molar quantity of oxygen produced per mole carbon fixed. The photosynthesis ratio approaches unity as the algal preference for ammonium approaches unity.

Organic Carbon

Organic carbon undergoes innumerable transformations in the water column. The model carbon cycle (Figure 4-8) consists of the following elements:

- Phytoplankton production
- Phytoplankton exudation
- Predation on phytoplankton
- Dissolution of particulate carbon
- Heterotrophic respiration
- Denitrification
- Settling

Algal production is the primary carbon source although carbon also enters the system through external loading. Predation on algae releases particulate and dissolved organic carbon to the water column. A fraction of the particulate organic carbon undergoes first-order dissolution to dissolved organic carbon. The remainder settles to the sediments. Dissolved organic carbon produced by phytoplankton exudation, by predation, and by dissolution is respired or denitrified at a first-order rate to inorganic carbon. No carbon is recycled from the sediments to the water column although oxygen demand created by carbon diagenesis is included in the model.

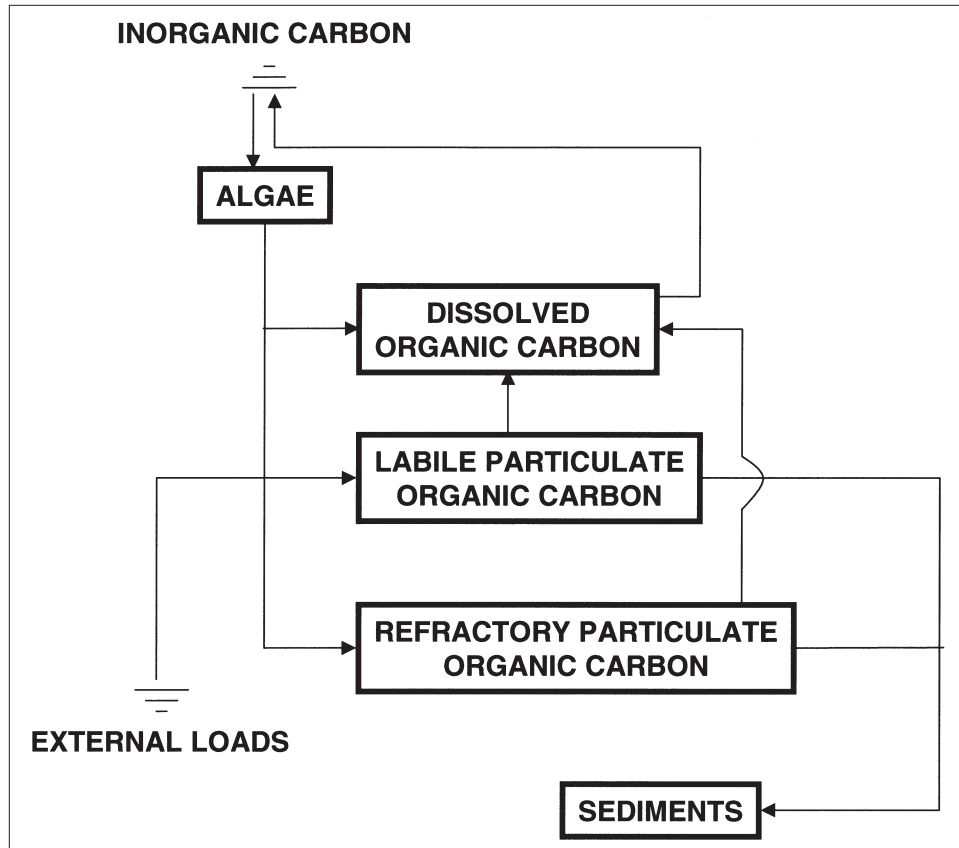


Figure 4-8. Model carbon cycle

Dissolution and Respiration Rates

Dissolution and respiration rates depend on the availability of carbonaceous substrate and on heterotrophic activity. Heterotrophic activity and biomass have been correlated with algal activity and biomass across a wide range of natural systems (Bird and Kalff 1984; Cole et al. 1988). Consequently, algal biomass can be incorporated into dissolution and respiration rate formulations as a surrogate for heterotrophic activity. The correlation between algae and heterotrophs occurs because algae produce labile carbon that fuels heterotrophic activity. Dissolution and respiration processes do not require the presence of algae, however, and may be fueled entirely by external carbon inputs. Representation of dissolution and respiration in the model allows specification of algal-dependent and algal-independent rates:

$$K_{doc} = K_{dc} + K_{dcalg} B \quad (4.29)$$

where

K_{doc} = respiration rate of dissolved organic carbon (day^{-1})

K_{dc} = minimum respiration rate (day^{-1})

$$Kd_{alg} = \text{constant that relates respiration to algal biomass} \\ (\text{m}^3 \text{ gm}^{-1} \text{ C day}^{-1})$$

$$Kl_{poc} = Klc + Kl_{alg} B \quad (4.30)$$

where

$$Kl_{poc} = \text{dissolution rate of labile particulate organic carbon (day}^{-1}\text{)}$$

$$Klc = \text{minimum dissolution rate (day}^{-1}\text{)}$$

$$Kl_{alg} = \text{constant that relates dissolution to algal biomass} \\ (\text{m}^3 \text{ gm}^{-1} \text{ C day}^{-1})$$

$$Kl_{rpo} = Krc + Krc_{alg} B \quad (4.31)$$

where

$$Kl_{rpo} = \text{dissolution rate of refractory particulate organic carbon} \\ (\text{day}^{-1})$$

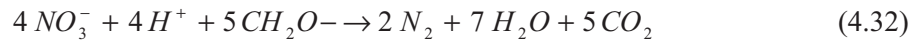
$$Krc = \text{minimum dissolution rate (day}^{-1}\text{)}$$

$$Krc_{alg} = \text{constant that relates dissolution to algal biomass} \\ (\text{m}^3 \text{ gm}^{-1} \text{ C day}^{-1})$$

An exponential function (Figure 4-3) relates dissolution and respiration to temperature.

Denitrification

As oxygen is depleted from natural systems, oxidation of organic matter is affected by the reduction of alternate oxidants (referred to as “alternate electron acceptors”). The sequence in which alternate acceptors are employed is determined by the thermodynamics of oxidation-reduction reactions. The first substance reduced in the absence of oxygen is nitrate. A representation of the denitrification reaction can be obtained by balancing standard half-cell redox reactions (Stumm and Morgan 1981):



Equation 4-32 describes the stoichiometry of the denitrification reaction. The kinetics of the reaction, represented in the model, are first-order. The dissolved organic carbon respiration rate, K_{doc} , is modified so that significant decay via denitrification occurs only when nitrate is freely available and dissolved oxygen is depleted (Figure 4-9). A parameter is included so that the anoxic respiration rate is slower than oxic respiration:

$$Denit = \frac{KH_{doc}}{KH_{doc} + DO} \frac{NO_3}{KH_{dn} + NO_3} AANOX K_{doc} \quad (4.33)$$

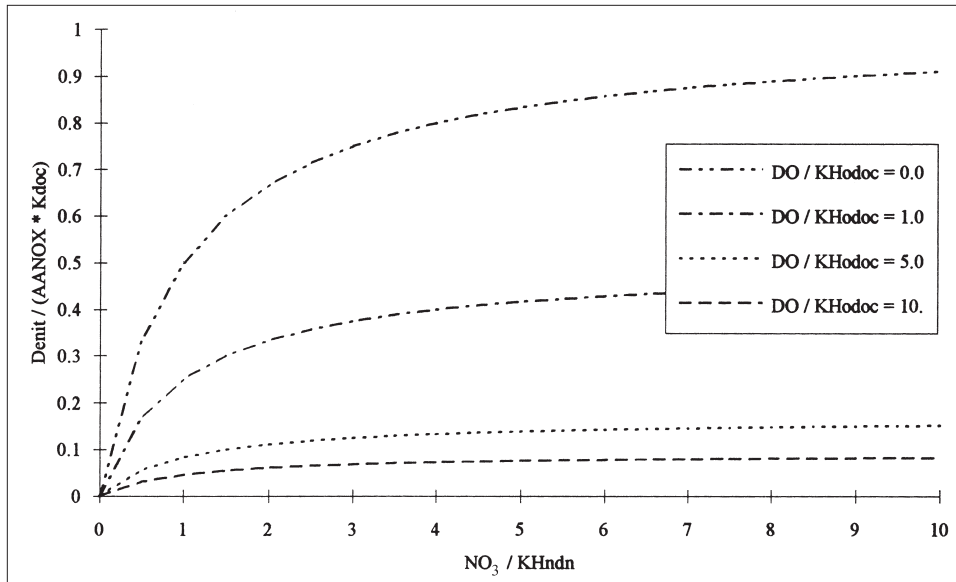


Figure 4-9. Effect of nitrate and dissolved oxygen on denitrification rate

where

Denit = denitrification rate of dissolved organic carbon (day^{-1})

AANOX = ratio of denitrification to oxic carbon respiration rate
($0 \leq \text{AANOX} \leq 1$)

KHodoc = half-saturation concentration of dissolved oxygen required
for oxic respiration ($\text{gm O}_2 \text{ m}^{-3}$)

KHndn = half-saturation concentration of nitrate required for
denitrification (gm N m^{-3})

An exponential function (Figure 4-3) relates denitrification to temperature. Parameter values in the function are the same as those for dissolved organic carbon respiration.

Dissolved Organic Carbon

The complete representation of all dissolved organic carbon sources and sinks in the model ecosystem is:

$$\begin{aligned} \frac{\delta}{\delta t} \text{DOC} = & \left(\text{FCD} + (1 - \text{FCD}) \frac{\text{KHr}}{\text{KHr} + \text{DO}} \text{BM} + \text{FCDP PR} \right) \text{B} \\ & + \text{Klpoc LPOC} + \text{Krpoc RPOC} - \frac{\text{DO}}{\text{KHodoc} + \text{DO}} \text{Kdoc DOC} \\ & - \text{Denit DOC} \end{aligned} \quad (4.34)$$

Labile Particulate Organic Carbon

The complete representation of all labile particulate organic carbon sources and sinks in the model ecosystem is:

$$\frac{\delta}{\delta t} LPOC = FCLP PR B - Klpoc LPOC - WSl \frac{\delta}{\delta z} LPOC \quad (4.35)$$

where

WSl = settling velocity of labile particles (m day⁻¹)

Refractory Particulate Organic Carbon

The complete representation of all refractory particulate organic carbon sources and sinks in the model ecosystem is:

$$\frac{\delta}{\delta t} RPOC = FCRP PR B - Krpoc RPOC - WSr \frac{\delta}{\delta z} RPOC \quad (4.36)$$

where

WSr = settling velocity of refractory particles (m day⁻¹)

Phosphorus

The model phosphorus cycle (Figure 4-10) includes the following processes:

- Algal production and metabolism
- Predation
- Hydrolysis of particulate organic phosphorus
- Mineralization of dissolved organic phosphorus
- Settling

External loads provide the ultimate source of phosphorus to the system. Dissolved phosphate is incorporated by algae during growth and released as phosphate and organic phosphorus through respiration and predation. A portion of the particulate organic phosphorus hydrolyzes to dissolved organic phosphorus. The balance settles to the sediments. Dissolved organic phosphorus is mineralized to phosphate. Within the sediments, particulate phosphorus is mineralized and recycled to the water column as dissolved phosphate.

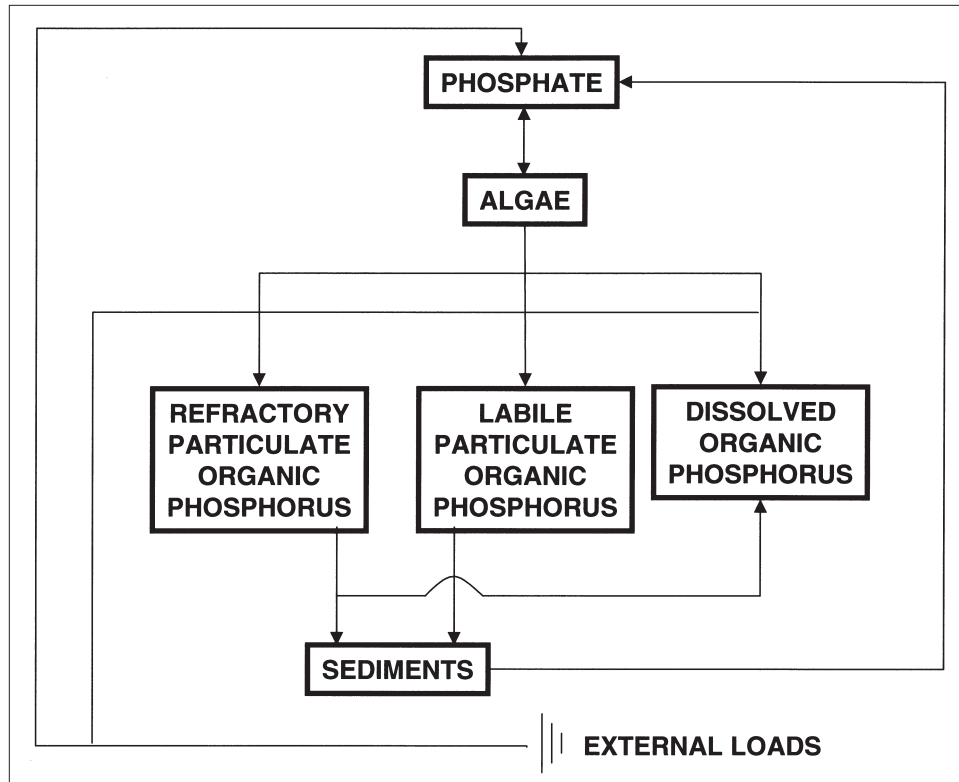


Figure 4-10. Model phosphorus cycle

Effects on phosphorus of algal production, metabolism, and predation have already been detailed. Descriptions of hydrolysis and mineralization and of the total phosphate system follow.

Hydrolysis and Mineralization

Within the model, hydrolysis is defined as the process by which particulate organic substances are converted to dissolved organic form. Mineralization is defined as the process by which dissolved organic substances are converted to dissolved inorganic form. Conversion of particulate organic phosphorus to phosphate proceeds through the sequence of hydrolysis and mineralization. Direct mineralization of particulate organic phosphorus does not occur.

Mineralization of organic phosphorus is mediated by the release of nucleotidase and phosphatase enzymes by bacteria (Ammerman and Azam 1985; Chrost and Overbeck 1987) and algae (Matavulj and Flint 1987; Chrost and Overbeck 1987; Boni et al. 1989). Since the algae themselves release the enzyme and since bacterial abundance is related to algal biomass, the rate of organic phosphorus mineralization is related, in the model, to algal biomass. A most remarkable property of the enzyme process is that alkaline phosphatase activity is inversely proportional to ambient phosphate concentration (Chrost and Overbeck 1987; Boni et al. 1989).

Put in different terms, when phosphate is scarce, algae stimulate production of an enzyme that mineralizes organic phosphorus to phosphate. This phenomenon is simulated by relating mineralization to the algal phosphorus nutrient limitation. Mineralization is highest when algae are strongly phosphorus limited and is least when no limitation occurs.

Expressions for mineralization and hydrolysis rates are:

$$K_{dop} = K_{dp} + \frac{KH_p}{KH_p + PO_4} K_{dpalg} B \quad (4.37)$$

where

K_{dop} = mineralization rate of dissolved organic phosphorus (day^{-1})

K_{dp} = minimum mineralization rate (day^{-1})

K_{dpalg} = constant that relates mineralization to algal biomass
($\text{m}^3 \text{ gm}^{-1} \text{ C day}^{-1}$)

$$K_{lpop} = K_{lp} + \frac{KH_p}{KH_p + PO_4} K_{lpalg} B \quad (4.38)$$

where

K_{lpop} = hydrolysis rate of labile particulate phosphorus (day^{-1})

K_{lp} = minimum hydrolysis rate (day^{-1})

K_{lpalg} = constant that relates hydrolysis to algal biomass
($\text{m}^3 \text{ gm}^{-1} \text{ C day}^{-1}$)

$$K_{rpop} = K_{rp} + \frac{KH_p}{KH_p + PO_4} K_{rpalg} B \quad (4.39)$$

where

K_{rpop} = hydrolysis rate of refractory particulate phosphorus (day^{-1})

K_{rp} = minimum hydrolysis rate (day^{-1})

K_{rpalg} = constant that relates hydrolysis to algal biomass
($\text{m}^3 \text{ gm}^{-1} \text{ C day}^{-1}$)

An exponential function (Figure 4-3) relates mineralization and hydrolysis rates to temperature.

Potential effects of algal biomass and nutrient limitation on mineralization and hydrolysis rates are shown in Figure 4-11. When nutrient concentration greatly exceeds the half-saturation concentration for algal uptake, the rate roughly equals the minimum. Algal biomass has little influence. As nutrient becomes scarce relative to the half-saturation concentration,

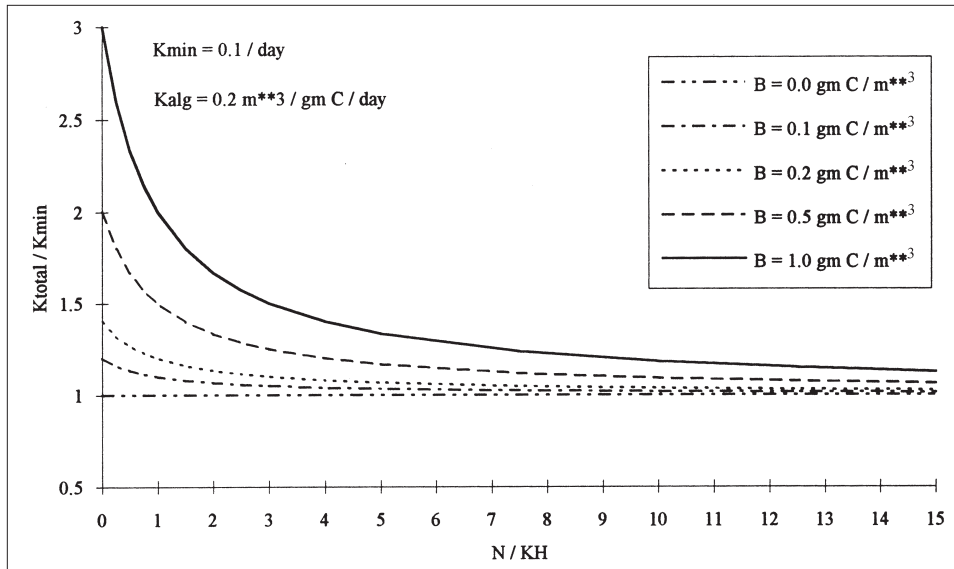


Figure 4-11. Effect of algal biomass and nutrient concentration on hydrolysis and mineralization

the rate increases. The magnitude of increase depends on algal biomass. Factor of two to three increases are feasible.

The Total Phosphate System

One fraction of total phosphorus in the water column is phosphorus incorporated in algal biomass. This fraction is computed in the model as the product of algal biomass and APC, the phosphorus-to-carbon ratio. In the environment, algae adjust their phosphorus content in response to external conditions. Algal phosphorus content is high when external phosphorus is abundant, and phosphorus content is low when phosphorus is scarce. The adaptation of algae to their environment indicates phosphorus-to-carbon ratio should be a variable in the model. Treatment of the ratio as a variable, however, greatly complicates computation of phosphorus transport due to the mixture of algal masses of different composition. The complication is avoided if intracellular and extracellular phosphorus are treated and transported as a single state variable. Intracellular and extracellular concentrations are determined by equilibrium partitioning of their sum.

The model phosphate state variable is defined as the sum of dissolved phosphate and algal phosphorus content:

$$PO_4t = PO_4d + PO_4a \quad (4.40)$$

where

$$PO_4t = \text{total phosphate (gm P m}^{-3}\text{)}$$

$$PO_4d = \text{dissolved phosphate (gm P m}^{-3}\text{)}$$

$$PO_4a = \text{algal phosphorus (gm P m}^{-3}\text{)}$$

Computation of Algal Phosphorus

Algal phosphorus is defined:

$$PO_4 a = APC B \quad (4.41)$$

The phosphorus-to-carbon ratio is calculated by the empirical function expressed in Equation 4.24.

The expressions 4.24 and 4.40 form a set of simultaneous equations in which APC depends on $PO_4 d$ and $PO_4 d$ depends on APC. The equations can be solved directly for APC:

$$APC = \frac{APCMIN + APCRAT PO_4 t}{1 + APCRAT B} \quad (4.42)$$

in which:

$$APCRAT = \frac{APCMAX - APCMIN}{PO_4 d \max} \quad (4.43)$$

The computation of APC takes place only when $PO_4 d < PO_4 d \max$. Otherwise, APC takes the value APCMAX.

Effect of Variable Phosphorus Stoichiometry

The effect of the variable phosphorus-to-carbon ratio and the operation of the total phosphate system is best seen by an example. The model was applied to a chemostat supplied with unlimited inorganic nitrogen. Phosphorus recycling was eliminated in the water and sediments so that only the initial phosphate was available to the algae. The chemostat was simulated for thirty days. Midway through the simulation, a phosphate load, equivalent to the initial mass in the chemostat, was injected. Simulations were conducted with and without variable stoichiometry.

Algal production was initially identical with and without variable stoichiometry (Figure 4-12). As dissolved phosphate became scarce in the constant-stoichiometry chemostat, algal production diminished so that respiration exceeded growth prior to day five. Biomass decreased until the phosphate injection at day fifteen. In the variable-stoichiometry chemostat, algae responded to diminished phosphate availability by reducing their phosphorus-to-carbon ratio. Because less phosphorus was required per unit carbonaceous biomass formed, growth exceeded respiration beyond day five and maximum biomass exceeded biomass formed under constant stoichiometry. Upon injection of new phosphate, algal production increased with and without variable stoichiometry. Algae with variable stoichiometry responded with increased phosphorus-to-carbon ratio as well as increased production. As a result of the altered ratio,

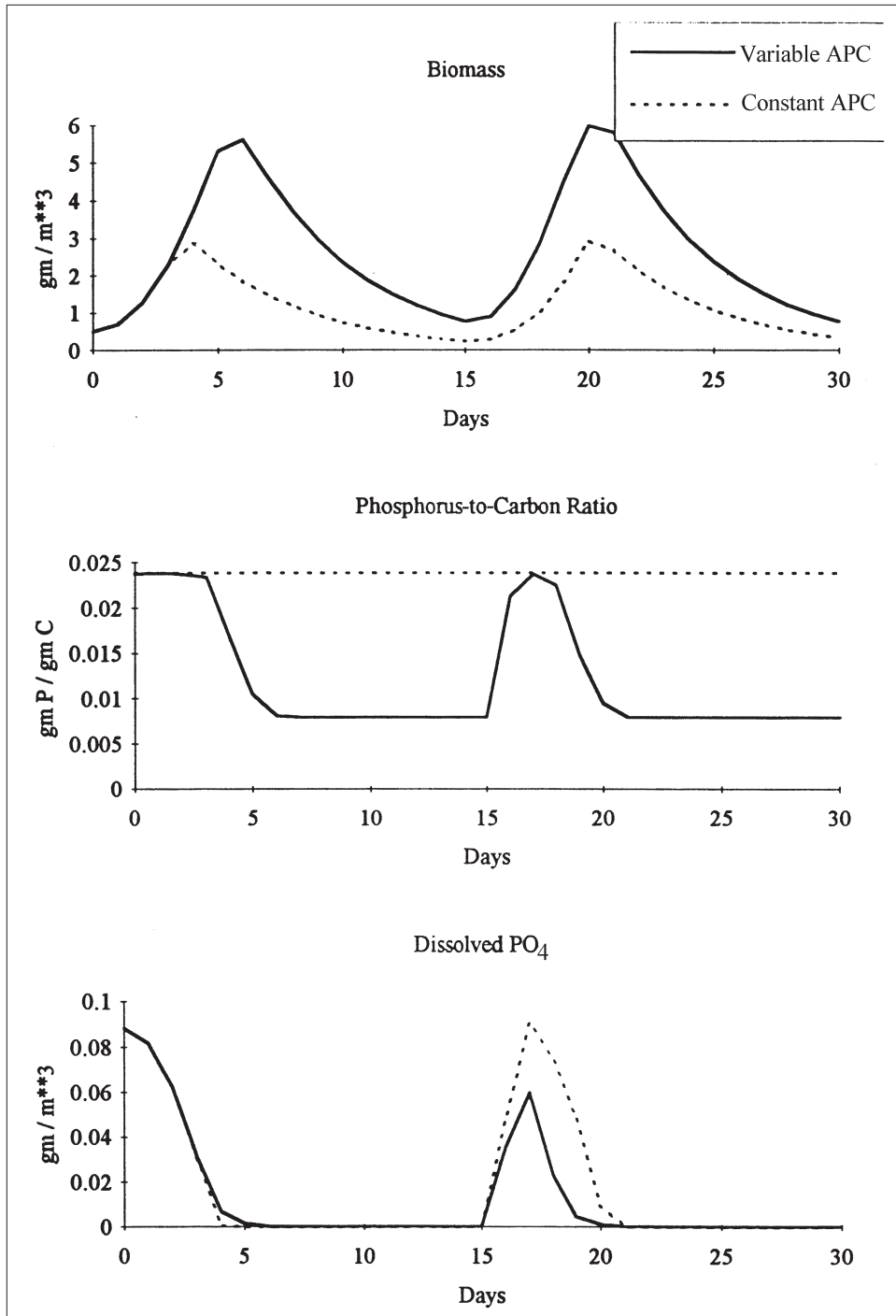


Figure 4-12. Chemostat simulation with and without variable phosphorus stoichiometry

dissolved phosphate peaked at a lower concentration in the presence of variable stoichiometry. The ability of algae to diminish phosphorus-to-carbon ratio still allowed algae in the variable-stoichiometry chemostat to exceed biomass formed in the constant-stoichiometry chemostat, however.

Phosphate

Once the interactions of dissolved and algal phosphate are made explicit, the balance of the equations describing phosphorus are straightforward summations of previously described sources and sinks:

$$\frac{\delta}{\delta t} PO_4 = -WSa \frac{\delta}{\delta z} APC B + K_{dop} DOP \quad (4.44)$$

Algal uptake and release of phosphate represents an exchange of phosphate fractions rather than a phosphate source or sink. Consequently, no algal source or sink terms are included in the phosphate mass-conservation equation. The settling term is required to represent the settling of particulate phosphate incorporated in algal biomass.

Dissolved Organic Phosphorus

$$\begin{aligned} \frac{\delta}{\delta t} DOP = & (BM_{FPD} + PR_{FPDO}) APC B \\ & + K_{lpop} LPOP + K_{rpop} RPOP - K_{dop} DOP \end{aligned} \quad (4.45)$$

Labile Particulate Organic Phosphorus

$$\begin{aligned} \frac{\delta}{\delta t} LPOP = & (BM_{FPL} + PR_{FPLP}) APC B \\ & - K_{lpop} LPOP - WSI \frac{\delta}{\delta z} LPOP \end{aligned} \quad (4.46)$$

Refractory Particulate Organic Phosphorus

$$\begin{aligned} \frac{\delta}{\delta t} RPOP = & (BM_{FPR} + PR_{FPRP}) APC B \\ & - K_{rpop} RPOP - WSR \frac{\delta}{\delta z} RPOP \end{aligned} \quad (4.47)$$

Nitrogen

The model nitrogen cycle (Figure 4-13) includes the following processes:

- Algal production and metabolism
- Predation
- Hydrolysis of particulate organic nitrogen
- Mineralization of dissolved organic nitrogen
- Settling

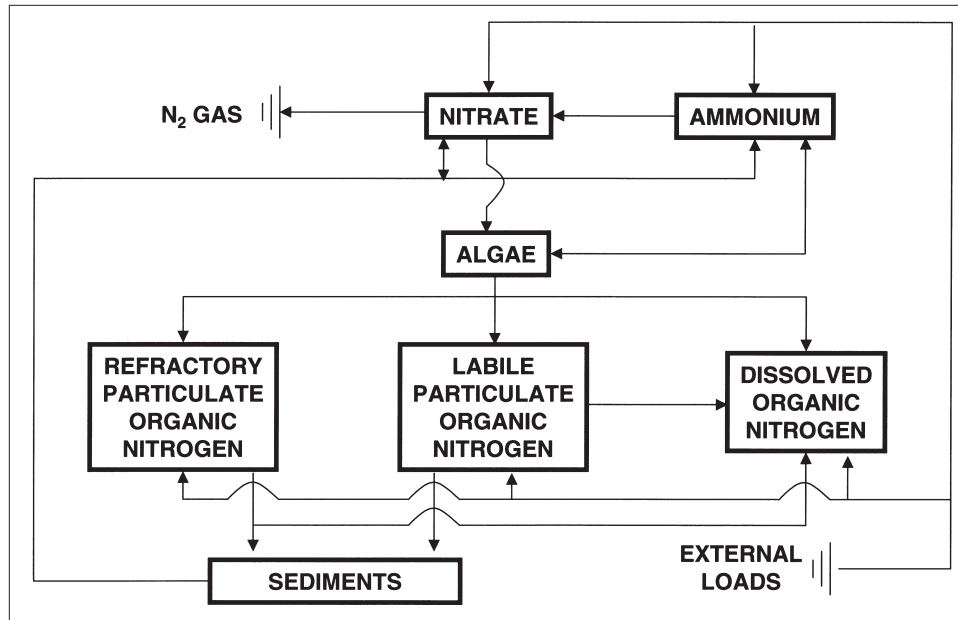


Figure 4-13. Model nitrogen cycle

- Nitrification
- Denitrification

External loads provide the ultimate source of nitrogen to the system. Inorganic nitrogen is incorporated by algae during growth and released as ammonium and organic nitrogen through respiration and predation. A portion of the particulate organic nitrogen hydrolyzes to dissolved organic nitrogen. The balance settles to the sediments. Dissolved organic nitrogen is mineralized to ammonium. In an oxygenated water column, a fraction of the ammonium is subsequently oxidized to nitrate through the nitrification process. In anoxic water, nitrate is lost to nitrogen gas through denitrification. Particulate nitrogen that settles to the sediments is mineralized and recycled to the water column, primarily as ammonium. Nitrate moves in both directions across the sediment-water interface, depending on relative concentrations in the water column and sediment interstices.

Effects on nitrogen of algal production, metabolism, and predation have already been detailed. Descriptions of hydrolysis, mineralization, nitrification, and denitrification follow.

Hydrolysis and Mineralization

In the model, particulate organic nitrogen is converted to the dissolved organic form via hydrolysis. Dissolved organic nitrogen is converted to ammonium through mineralization. Conversion of particulate nitrogen to ammonium proceeds through the sequence of hydrolysis and mineralization. Direct mineralization of particulate nitrogen does not occur. The

argument for accelerated hydrolysis and mineralization during nutrient-limited conditions is not as clear for nitrogen as for phosphorus. The same formulations are made available for nitrogen as for phosphorus, however. Accelerated processes can be activated or deactivated through parameter selection. The nitrogen hydrolysis and mineralization formulations are:

$$K_{don} = K_{dn} + \frac{KHn}{KHn + NH_4 + NO_3} K_{dnalg} B \quad (4.48)$$

where

K_{don} = mineralization rate of dissolved organic nitrogen (day^{-1})

K_{dn} = minimum mineralization rate (day^{-1})

K_{dnalg} = constant that relates mineralization to algal biomass
($\text{m}^3 \text{gm}^{-1} \text{C day}^{-1}$)

$$K_{lpon} = K_{ln} + \frac{KHn}{KHn + NH_4 + NO_3} K_{lnalg} B \quad (4.49)$$

where

K_{lpon} = hydrolysis rate of labile particulate nitrogen (day^{-1})

K_{ln} = minimum hydrolysis rate (day^{-1})

K_{lnalg} = constant that relates hydrolysis to algal biomass
($\text{m}^3 \text{gm}^{-1} \text{C day}^{-1}$)

$$K_{rpon} = K_{rn} + \frac{KHn}{KHn + NH_4 + NO_3} K_{rnalg} B \quad (4.50)$$

where

K_{rpon} = hydrolysis rate of refractory particulate nitrogen (day^{-1})

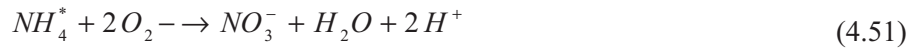
K_{rn} = minimum hydrolysis rate (day^{-1})

K_{rnalg} = constant that relates hydrolysis to algal biomass
($\text{m}^3 \text{gm}^{-1} \text{C day}^{-1}$)

An exponential function (Figure 4-3) relates mineralization and hydrolysis rates to temperature.

Nitrification

Nitrification is a process mediated by specialized groups of autotrophic bacteria that obtain energy through the oxidation of ammonium to nitrite and oxidation of nitrite to nitrate. A simplified expression for complete nitrification (Tchobanoglous and Schroeder 1987) is:



The equation indicates that two moles of oxygen are required to nitrify one mole of ammonium into nitrate. The simplified equation is not strictly true, however. Cell synthesis by nitrifying bacteria is accomplished by the fixation of carbon dioxide so that less than two moles of oxygen are consumed per mole ammonium utilized (Wezernak and Gannon 1968).

The kinetics of complete nitrification are modeled as a function of available ammonium, dissolved oxygen, and temperature:

$$NT = \frac{DO}{KH_{ont} + DO} \frac{NH_4}{KH_{nnt} + NH_4} f(T) NTm \quad (4.52)$$

where

NT = nitrification rate ($\text{gm N m}^{-3} \text{ day}^{-1}$)

KH_{ont} = half-saturation constant of dissolved oxygen required for nitrification ($\text{gm O}_2 \text{ m}^{-3}$)

KH_{nnt} = half-saturation constant of NH₄ required for nitrification (gm N m^{-3})

NT_m = maximum nitrification rate at optimal temperature ($\text{gm N m}^{-3} \text{ day}^{-1}$)

The kinetics formulation (Figure 4-14) incorporates the products of two “Monod” functions. The first function diminishes nitrification at low dissolved oxygen concentration. The second function expresses the influence of ammonium concentration on nitrification. When ammonium concentration is low, relative to KH_{nnt}, nitrification is proportional to ammonium concentration. For NH₄ << KH_{nnt}, the reaction is approximately first-order. (The first-order decay constant \approx NT_m/KH_{nnt}.) When ammonium concentration is large, relative to KH_{nnt}, nitrification approaches a maximum rate. This formulation is based on a concept proposed by Tuffey et al. (1974). Nitrifying bacteria adhere to benthic or suspended sediments. When ammonium is scarce, vacant surfaces suitable for nitrifying bacteria exist. As ammonium concentration increases, bacterial biomass increases, vacant surfaces are occupied, and the rate of nitrification increases. The bacterial population attains maximum density when all surfaces suitable for bacteria are occupied. At this point, nitrification proceeds at a maximum rate independent of additional increase in ammonium concentration.

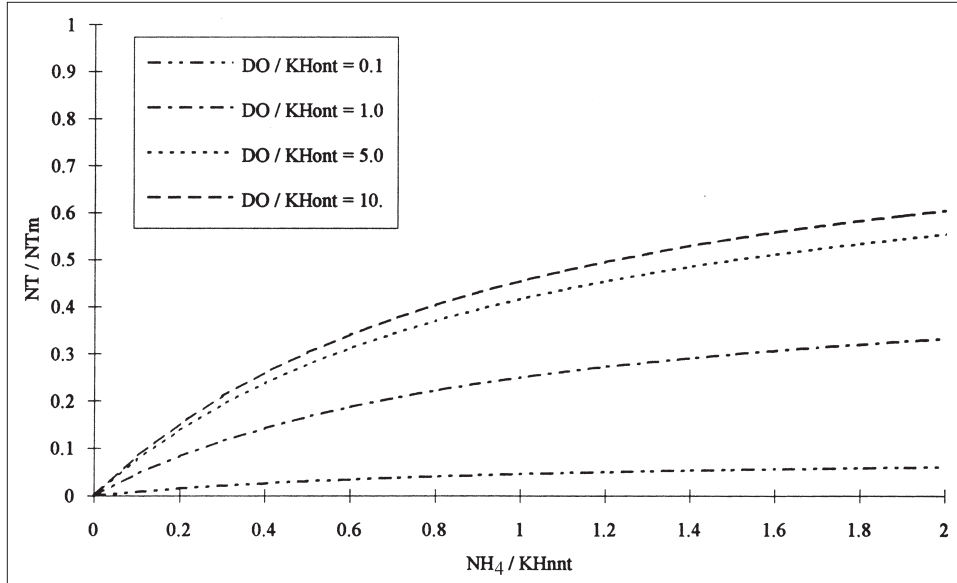


Figure 4-14. Effect of dissolved oxygen and ammonium concentration on nitrification rate

The optimal temperature for nitrification may be less than peak temperatures that occur in coastal waters. To allow for a decrease in nitrification at superoptimal temperature, the effect of temperature on nitrification is modeled in the Gaussian form of Equation 4.8.

Effect of Nitrification on Ammonium

$$\frac{\delta}{\delta t} NH_4 = -NT \quad (4.53)$$

Effect of Nitrification on Nitrate

$$\frac{\delta}{\delta t} NO_3 = NT \quad (4.54)$$

Effect of Nitrification on Dissolved Oxygen

$$\frac{\delta}{\delta t} DO = -AONT NT \quad (4.55)$$

where

AONT = mass dissolved oxygen consumed per mass
ammonium-nitrogen nitrified ($4.33 \text{ gm O}_2 \text{ gm}^{-1} \text{ N}$)

Effect of Denitrification on Nitrate

The effect of denitrification on dissolved organic carbon has been described. Denitrification removes nitrate from the system in stoichiometric proportion to carbon removal:

$$\frac{\delta}{\delta t} NO_3 = -ANDC \text{ Denit DOC} \quad (4.56)$$

where

ANDC = mass nitrate-nitrogen reduced per mass dissolved organic carbon oxidized ($0.933 \text{ gm N gm}^{-1} \text{ C}$)

Nitrogen Mass Balance Equations

The mass-balance equations for nitrogen state variables are written by summing all previously described sources and sinks:

Ammonium

$$\begin{aligned} \frac{\delta}{\delta t} NH_4 = & (BM \text{ FNI} + PR \text{ FNIP} - PN \text{ P})ANC \text{ B} \\ & + Kdon \text{ DON} - NT \end{aligned} \quad (4.57)$$

Dissolved Organic Nitrogen

$$\begin{aligned} \frac{\delta}{\delta t} DON = & (BM \text{ FND} + PR \text{ FNDP})ANC \text{ B} \\ & + Klpon \text{ LPON} + Krpon \text{ RPON} - Kdon \text{ DON} \end{aligned} \quad (4.58)$$

Labile Particulate Organic Nitrogen

$$\begin{aligned} \frac{\delta}{\delta t} LPON = & (BM \text{ FNL} + PR \text{ FNLP})ANC \text{ B} \\ & - Klpon \text{ LPON} - WSl \frac{\delta}{\delta z} LPON \end{aligned} \quad (4.59)$$

Refractory Particulate Organic Nitrogen

$$\begin{aligned} \frac{\delta}{\delta t} RPON = & (BM \text{ FNR} + PR \text{ FNRP})ANC \text{ B} \\ & - Krpon \text{ RPON} - WSr \frac{\delta}{\delta z} RPON \end{aligned} \quad (4.60)$$

Nitrate

$$\frac{\delta}{\delta t} NO_3 = (PN - 1)P ANC B + NT - ANDC Denit DOC \quad (4.61)$$

Chemical Oxygen Demand

Chemical oxygen demand is the concentration of reduced substances that are oxidizable through inorganic means. The source of chemical oxygen demand in saline water is sulfide released from sediments. A cycle occurs in which sulfate is reduced to sulfide in the sediments and reoxidized to sulfate in the water column. In freshwater, methane is released to the water column by the sediment model. Both sulfide and methane are quantified in units of oxygen demand and are treated with the same kinetics formulation:

$$\frac{\delta}{\delta t} COD = - \frac{DO}{KHocod + DO} Kcod COD \quad (4.62)$$

where

COD = chemical oxygen demand concentration (gm O₂-equivalents m⁻³)

KHocod = half-saturation concentration of dissolved oxygen required for exertion of chemical oxygen demand (gm O₂ m⁻³)

Kcod = oxidation rate of chemical oxygen demand (day⁻¹)

An exponential function (Figure 4-3) describes the effect of temperature on exertion of chemical oxygen demand.

Dissolved Oxygen

Sources and sinks of dissolved oxygen in the water column (Figure 4-15) include:

- Algal photosynthesis
- Atmospheric reaeration
- Algal respiration
- Heterotrophic respiration
- Nitrification
- Chemical oxygen demand

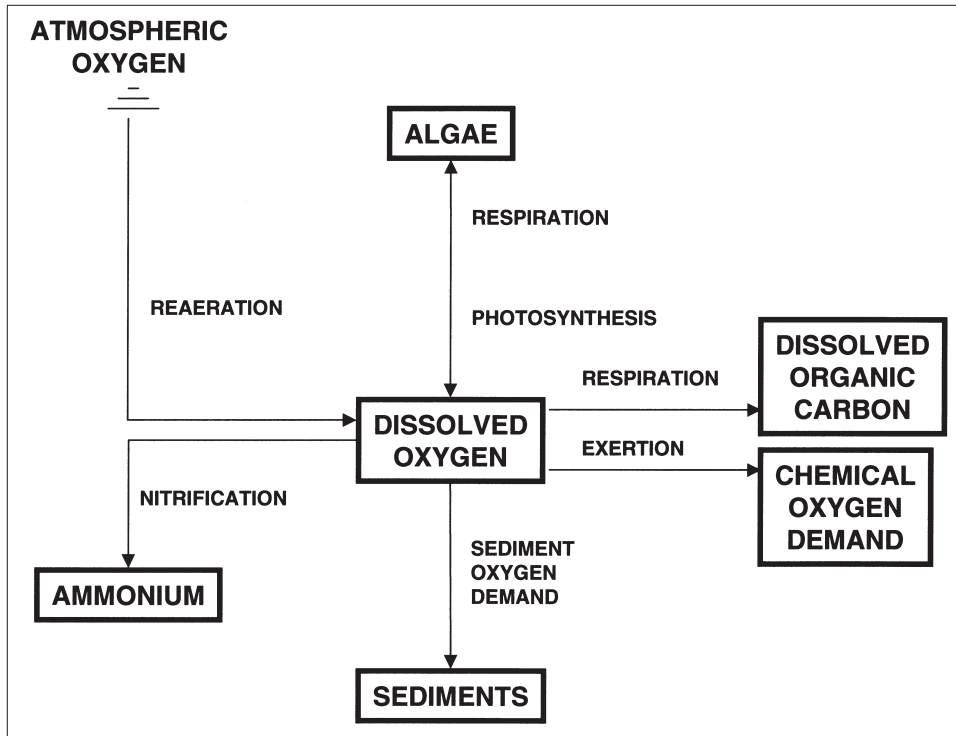


Figure 4-15. Model dissolved oxygen cycle

Reaeration

The rate of reaeration is proportional to the dissolved oxygen deficit in model segments that form the air-water interface:

$$\frac{\delta}{\delta t} DO = \frac{Kr}{\Delta z} (DO_s - DO) \quad (4.63)$$

where

Kr = reaeration coefficient ($m \text{ day}^{-1}$)

DO_s = dissolved oxygen saturation concentration ($gm \text{ O}_2 \text{ m}^{-3}$)

In shallow water (e.g. free-flowing streams), the reaeration coefficient depends largely on turbulence generated by bottom shear stress (O'Connor and Dobbins 1958). In deeper systems (e.g. estuaries), however, wind effects may dominate the reaeration process (O'Connor 1983). The reaeration coefficient is also influenced by temperature (ASCE 1961) and salinity (Wen et al. 1984). No universal formula for evaluation of the reaeration coefficient exists. In the model, the reaeration coefficient is treated as a user-supplied parameter.

Saturation dissolved oxygen concentration diminishes as temperature and salinity increase. An empirical formula that describes these effects (Genet et al. 1974) is:

$$DO_s = 14.5532 - 0.38217 T + 0.0054258 T^2 - CL(1.665 \times 10^{-4} - 5.866 \times 10^{-6} T + 9.796 \times 10^{-8} T^2) \quad (4.64)$$

where

$$CL = \text{chloride concentration (} = \text{salinity}/1.80655)$$

Summary of Dissolved Oxygen Sources and Sinks

The complete kinetics for dissolved oxygen are:

$$\begin{aligned} \frac{\delta}{\delta t} DO = & \left((13 - 0.3PN)P - \frac{DO}{KHr + DO} BM \right) AOCR B \\ & - AONT NT - \frac{DO}{KHodoc + DO} AOCR Kdoc DOC \\ & - \frac{DO}{KHocod + DO} Kcod COD + \frac{Kr}{\Delta z} (DO_s - DO) \end{aligned} \quad (4.65)$$

Salinity

No internal sources or sinks of salinity exist. Salinity is included to verify proper transport and linkage to the HM.

Temperature

A conservation of internal energy equation can be written analogous to the conservation of mass equation. The only source or sink of internal energy considered is exchange with the atmosphere. Although solar radiation can penetrate several meters into the water column, radiation-induced increases in internal energy are here assigned entirely to the surface model layer.

For practical purposes, the internal-energy equation can be written as a conservation of temperature equation. Change of temperature due to atmospheric exchange is considered proportional to the temperature difference between the water surface and a theoretical equilibrium temperature (Edinger et al. 1974):

$$\frac{\delta T}{\delta t} = \frac{KT}{\rho C_p \Delta z} (T_e - T) \quad (4.66)$$

where

T_e = equilibrium temperature (C°)

KT = heat exchange coefficient ($\text{watt m}^{-2} C^\circ^{-1}$)

C_p = specific heat of water ($4200 \text{ watt sec kg}^{-1} C^\circ^{-1}$)

ρ = density of water (1000 kg m^{-3})

Fecal Coliform

Mortality of fecal coliform bacteria in the environment is represented as a first-order loss process:

$$\frac{\delta FC}{\delta t} = -K_{fc} FC \quad (4.67)$$

where

K_{fc} = decay rate of fecal coliform (day^{-1})

Glossary

Table 4-2 presents a glossary of terms employed in water-column kinetics described in this chapter.

**Table 4-2.
Terms in Kinetics Equations**

Symbol	Definition	Units
A_j	Area of flow face j	m^2
AANOX	Ratio of denitrification to oxic carbon respiration rate	
ANC	Nitrogen-to-carbon ratio of algae	$gm\ N\ gm^{-1}\ C$
AOCR	Dissolved oxygen-to-carbon ratio in respiration	$gm\ O_2\ gm^{-1}\ C$
AONT	Mass dissolved oxygen consumed per mass ammonium nitrified	$gm\ O_2\ gm^{-1}\ N$
ANDC	Mass nitrate-nitrogen consumed per mass carbon oxidized	$gm\ N\ gm^{-1}\ C$
APC	Algal phosphorus-to-carbon ratio	$gm\ P\ gm^{-1}\ C$
APCmin	Minimum phosphorus-to-carbon ratio	$gm\ P\ gm^{-1}\ C$
APCmax	Maximum phosphorus-to-carbon ratio	$gm\ P\ gm^{-1}\ C$
APCRAT	Change in phosphorus-to-carbon ratio per unit change in dissolved phosphate	C^{-1}
BMr	Basal metabolic rate of algae at reference temperature T_r	day^{-1}
BPR	Predation rate on algae at reference temperature T_r	day^{-1}
B	Biomass of algae	$gm\ C\ m^{-3}$
C_i	Concentration in ith control volume	$gm\ m^{-3}$
C_j^*	Concentration in flow across face j	$gm\ m^{-3}$
CChl	Carbon-to-chlorophyll ratio of algae	$gm\ C\ mg^{-1}\ chl$
CL	Chloride concentration	ppt
COD	concentration of chemical oxygen demand	$gm\ m^{-3}$
C_p	specific heat of water	$watt\ sec\ kg^{-1}\ ^\circ C^{-1}$
D_j	Diffusion coefficient at flow face j	$m^2\ sec^{-1}$
Denit	Denitrification rate of dissolved organic carbon	day^{-1}
DO	Dissolved oxygen	$gm\ O_2\ m^{-3}$
DOC	Dissolved organic carbon	$gm\ C\ m^{-3}$
DON	Dissolved organic nitrogen	$gm\ N\ m^{-3}$
DOP	Dissolved organic phosphorus	$gm\ P\ m^{-3}$
DOs	Saturation dissolved oxygen concentration	$gm\ O_2\ m^{-3}$
FCD	Fraction of basal metabolism exuded as dissolved organic carbon by algae	$0 \leq FCDx \leq 1$
FCDP	Fraction of dissolved organic carbon produced by predation	$0 \leq FCDP \leq 1$
FCLP	Fraction of labile particulate carbon produced by predation	$0 \leq FCLP \leq 1$
FCRP	Fraction of refractory particulate carbon produced by predation	$0 \leq FCRP \leq 1$
FD	Daylight fraction of total daylength	$0 \leq FD \leq 1$
$f(l)$	Effect of suboptimal illumination on algal production	$0 \leq f(l) \leq 1$

(Sheet 1 of 5)

Table 4-2. Continued

Symbol	Definition	Units
f(N)	Effect of suboptimal nutrient concentration on algal production	$0 \leq f(N) \leq 1$
FNI	Fraction of inorganic nitrogen produced by metabolism of algae	$0 \leq FNI \leq 1$
FNIP	Fraction of inorganic nitrogen produced by predation	$0 \leq FNIP \leq 1$
FND	Fraction of dissolved organic nitrogen produced by metabolism of algae	$0 \leq FND \leq 1$
FNDP	Fraction of dissolved organic nitrogen produced by predation	$0 \leq FNDP \leq 1$
FNL	Fraction of labile particulate nitrogen produced by metabolism of algae	$0 \leq FNL \leq 1$
FNLP	Fraction of labile particulate nitrogen produced by predation	$0 \leq FNLP \leq 1$
FNR	Fraction of refractory particulate nitrogen produced by metabolism of algae	$0 \leq FNR \leq 1$
FNRP	Fraction of refractory particulate nitrogen produced by predation	$0 \leq FNRP \leq 1$
FPD	Fraction of dissolved organic phosphorus produced by metabolism by algae	$0 \leq FPD \leq 1$
FPDP	Fraction of dissolved organic phosphorus produced by predation	$0 \leq FPDP \leq 1$
FPI	Fraction of inorganic phosphorus produced by metabolism of algae	$0 \leq FPI \leq 1$
FPIP	Fraction of inorganic phosphorus produced by predation	$0 \leq FPIP \leq 1$
FPL	Fraction of labile particulate phosphorus produced by metabolism of algae	$0 \leq FPL \leq 1$
FPLP	Fraction of labile particulate phosphorus produced by predation	$0 \leq FPLP \leq 1$
FPR	Fraction of refractory particulate phosphorus produced by metabolism of algae	$0 \leq FPR \leq 1$
FPRP	Fraction of refractory particulate phosphorus produced by predation	$0 \leq FPRP \leq 1$
FR	Macrobenthic filtration rate	$\text{m}^3 \text{gm}^{-1} \text{C day}^{-1}$
f(T)	Effect of suboptimal temperature on algal production	$0 \leq f(T) \leq 1$
I	Illumination rate	Langley's day ⁻¹
I _h	Illumination rate at which algal production is halved	Langley's day ⁻¹
I _o	Daily illumination at water surface	Langley's day ⁻¹
K _{cod}	Oxidation rate of chemical oxygen demand	day ⁻¹
K _{dc}	Minimum respiration rate of dissolved organic carbon	day ⁻¹
K _{dcalg}	Constant that relates respiration rate to algal biomass	$\text{m}^3 \text{gm}^{-1} \text{C day}^{-1}$
K _{d_n}	Minimum mineralization rate of dissolved organic nitrogen	day ⁻¹
K _{d_nalg}	Constant that relates mineralization rate to algal biomass	$\text{m}^3 \text{gm}^{-1} \text{C day}^{-1}$
K _{doc}	Dissolved organic carbon respiration rate	day ⁻¹

(Sheet 2 of 5)

Table 4-2. Continued

Symbol	Definition	Units
Kdon	Dissolved organic nitrogen mineralization rate	day ⁻¹
Kdop	Dissolved organic phosphorus mineralization rate	day ⁻¹
Kdp	Minimum mineralization rate of dissolved organic phosphorus	day ⁻¹
Kdpalg	Constant that relates mineralization rate to algal biomass	m ³ gm ⁻¹ C day ⁻¹
Keb	Background light attenuation	m ⁻¹
Kechl	Light attenuation coefficient for chlorophyll 'a'	m ² mg ⁻¹
Kess	Total light attenuation	m ⁻¹
Kfc	Decay rate of fecal coliform	day ⁻¹
KHn	Half-saturation concentration for nitrogen uptake by algae	gm N m ⁻³
KHndn	Half-saturation concentration of nitrate required for denitrification	gm N m ⁻³
KHnnt	Half-saturation concentration of NH ₄ required for nitrification	gm N m ⁻³
KHocod	Half-saturation concentration of dissolved oxygen required for exertion of COD	gm O ₂ m ⁻³
KHodoc	Half-saturation concentration of dissolved oxygen required for oxidic respiration	gm O ₂ m ⁻³
KHomb	Dissolved oxygen concentration at which macrobenthic grazing is halved	gm O ₂ m ⁻³
KHont	Half-saturation concentration of dissolved oxygen required for nitrification	gm O ₂ m ⁻³
KHp	Half-saturation concentration for phosphorus uptake by algae	gm P m ⁻³
KHr	Half-saturation concentration for dissolved organic carbon excretion by algae	gm O ₂ m ⁻³
Klc	Minimum dissolution rate of labile particulate carbon	day ⁻¹
Klcalg	Constant that relates dissolution rate to algal biomass	m ³ gm ⁻¹ C day ⁻¹
Kln	Minimum dissolution rate of labile particulate nitrogen	day ⁻¹
Klnalg	Constant that relates dissolution rate to algal biomass	m ³ gm ⁻¹ C day ⁻¹
Klp	Minimum dissolution rate of labile particulate phosphorus	day ⁻¹
Klpalg	Constant that relates dissolution rate to algal biomass	m ³ gm ⁻¹ C day ⁻¹
Klpoc	Labile particulate organic carbon dissolution rate	day ⁻¹
Klpon	Labile particulate organic nitrogen hydrolysis rate	day ⁻¹
Klpop	Labile particulate organic phosphorus hydrolysis rate	day ⁻¹
Kr	Reaeration coefficient	m day ⁻¹
Krc	Minimum dissolution rate of refractory particulate carbon	day ⁻¹
Krcalg	Constant that relates dissolution rate to algal biomass	m ³ gm ⁻¹ C day ⁻¹
Krn	Minimum dissolution rate of refractory particulate nitrogen	day ⁻¹
Krnalg	Constant that relates dissolution rate to algal biomass	m ³ gm ⁻¹ C day ⁻¹

(Sheet 3 of 5)

Table 4-2. Continued

Symbol	Definition	Units
Krp	Minimum dissolution rate of refractory particulate phosphorus	day ⁻¹
Krpalg	Constant that relates dissolution rate to algal biomass	m ³ gm ⁻¹ C day ⁻¹
Krpoc	Refractory particulate organic carbon dissolution rate	day ⁻¹
Krpon	Refractory particulate organic nitrogen hydrolysis rate	day ⁻¹
Krpop	Refractory particulate organic phosphorus hydrolysis rate	day ⁻¹
KT	Surface heat exchange coefficient	watt m ⁻² °C ⁻¹
KTb	Effect of temperature on basal metabolism of algae	°C ⁻¹
KTcod	Effect of temperature on oxidation of chemical oxygen demand	°C ⁻¹
KTg1	Effect of temperature below T _m on growth of algae	°C ⁻²
KTg2	Effect of temperature above T _m on growth of algae	°C ⁻²
KThdr	Constant that relates hydrolysis rates to temperature	°C ⁻¹
KTmnl	Constant that relates mineralization rates to temperature	°C ⁻¹
KTnt1	Effect of temperature below T _{mnt} on nitrification	°C ⁻²
KTnt2	Effect of temperature above T _{mnt} on nitrification	°C ⁻²
LPOC	Labile particulate organic carbon	gm C m ⁻³
LPON	Labile particulate organic nitrogen	gm N m ⁻³
LPOP	Labile particulate organic phosphorus	gm P m ⁻³
MBGM	Macrobenthic biomass	gm C m ⁻²
NH ₄	Ammonium concentration	gm N m ⁻³
NO ₃	Nitrate+nitrite concentration	gm N m ⁻³
NT	Nitrification rate	gm N m ⁻³ day ⁻¹
NTm	Maximum nitrification rate at optimal temperature	gm N m ⁻³ day ⁻¹
PM	Production rate of algae under optimal conditions	day ⁻¹
PN	Preference for ammonium uptake by algae	0 ≤ PN ≤ 1
PO ₄ a	Phosphate in algal biomass	gm P m ⁻³
PO ₄ d	Dissolved phosphate concentration	gm P m ⁻³
PO ₄ dmax	Dissolved phosphate concentration at which algal phosphorus-to-carbon ratio achieves its maximum value	gm P m ⁻³
PO ₄ t	Total phosphate concentration	gm P m ⁻³
PR	Rate of predation on algae	day ⁻¹
P	Production rate of algae	day ⁻¹
Q _j	Volumetric flow across flow face j	m ³ sec ⁻¹
RPOC	Refractory particulate organic carbon	gm C m ⁻³
RPON	Refractory particulate organic nitrogen	gm N m ⁻³

(Sheet 4 of 5)

Table 4-2. Concluded		
Symbol	Definition	Units
RPOP	Refractory particulate organic phosphorus	gm P m ⁻³
S	Salinity	ppt
S _i	External loads and kinetics sources and sinks in ith control volume	gm sec ⁻¹
t	Temporal coordinate	sec
T	temperature	°C
Te	Equilibrium temperature	°C
Tm	Optimal temperature for growth of algae	°C
Tmnt	Optimal temperature for nitrification	°C
Tr	Reference temperature for metabolism	°C
Trcod	Reference temperature for COD oxidation	°C
Trhdr	Reference temperature for hydrolysis	°C
Trmnl	Reference temperature for mineralization	°C
V _i	Volume of ith control volume	m ³
WSl	Settling velocity of labile particles	m day ⁻¹
WSr	Settling velocity of refractory particles	m day ⁻¹
WSa	Settling velocity of algae	m day ⁻¹
WSmb	Equivalent settling rate induced by macrobenthic grazing	m day ⁻¹
x	Spatial coordinate	m
z	Vertical coordinate	m
z ₁	Distance from water surface to top of model segment	m
z ₂	Distance from water surface to bottom of model segment	m
Δz	Model segment thickness	m
ρ	Density of water	kg m ⁻³
<i>(Sheet 5 of 5)</i>		

Predictive Sediment Submodel

The predictive sediment submodel was developed as one component of the Chesapeake Bay eutrophication model study (Cercio and Cole 1994). The need for a predictive benthic sediment model was made apparent by the results of a preceding steady-state model study of the bay (HydroQual 1987). The study indicated sediments were the dominant source of phosphorus and ammonium during the summer period of minimum dissolved oxygen. Increased sediment oxygen demand and nutrient releases were implicated in a perceived dissolved oxygen decline from 1965 to 1985. No means existed to predict how these sediment processes would respond to

nutrient load reductions, however. Neither was the time scale for completion of the responses predictable.

For management purposes, a sediment model was required with two fundamental capabilities: (1) predict effects of management actions on sediment-water exchange processes, and (2) predict time scale for alterations in sediment-water exchange processes.

The model (Figure 4-16) was driven by net settling of organic matter from the water column to the sediments. In the sediments, the model simulated the diagenesis (decay) of the organic matter. Diagenesis produced oxygen demand and inorganic nutrients. Oxygen demand, as sulfide (in salt water) or methane (in fresh water), took three paths out of the sediments: export to the water column as chemical oxygen demand, oxidation at the sediment-water interface as sediment oxygen demand, or burial to deep, inactive sediments. Inorganic nutrients produced by diagenesis took two paths out of the sediments: release to the water column, or burial to deep, inactive sediments.

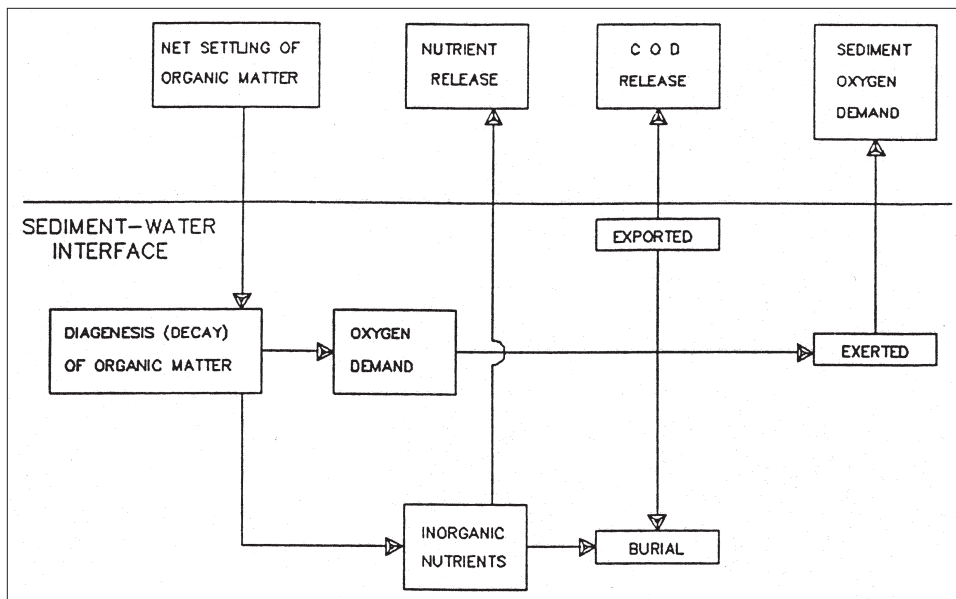


Figure 4-16. Sediment model schematic

Additional details of the model, required to understand the coupling of the sediment submodel to the model of the water column, are provided below. Complete model documentation is provided by DiToro and Fitzpatrick (1993). A listing of sediment model state variables and predicted sediment-water fluxes is provided in Table 4-3.

**Table 4-3.
Sediment Model State Variables and Fluxes**

State Variable	Sediment-Water Flux
Temperature	
Particulate Organic Carbon	Sediment Oxygen Demand
Sulfide/Methane	Release of Chemical Oxygen Demand
Particulate Organic Nitrogen	
Ammonium	Ammonium Flux
Nitrate	Nitrate Flux
Particulate Organic Phosphorus	
Phosphate	Phosphate Flux

Description of Sediment Model

Benthic sediments are represented as two layers with a total depth of 10 cm (Figure 4-17). The upper layer, in contact with the water column, may be oxic or anoxic depending on dissolved oxygen concentration in the water. The lower layer is permanently anoxic. The thickness of the upper layer is determined by the penetration of oxygen into the sediments. At its maximum thickness, the oxic layer depth is only a small fraction of the total.

The sediment model consists of three basic processes. The first is deposition of particulate organic matter from the water column to the sediments. Due to the negligible thickness of the upper layer, deposition proceeds from the water column directly to the lower, anoxic layer. Within the lower layer, organic matter is subject to the second basic process, diagenesis (or decay). The third basic process is flux of substances produced by diagenesis to the upper sediment layer, to the water column, and to deep, inactive sediments. The flux portion of the model is the most complex. Computation of flux requires consideration of reactions in both sediment layers, of partitioning between particulate and dissolved fractions in both layers, of sedimentation from the upper to lower layer and from the lower layer to deep inactive sediments, of particle mixing between layers, of diffusion between layers, and of mass transfer between the upper layer and the water column.

Deposition

Deposition is one process which couples the model of the water column with the model of the sediments. Consequently, deposition is represented in both the sediment and water-column models. In the water column, deposition is represented with a modification of the mass-balance equation applied only to cells that interface the sediments:

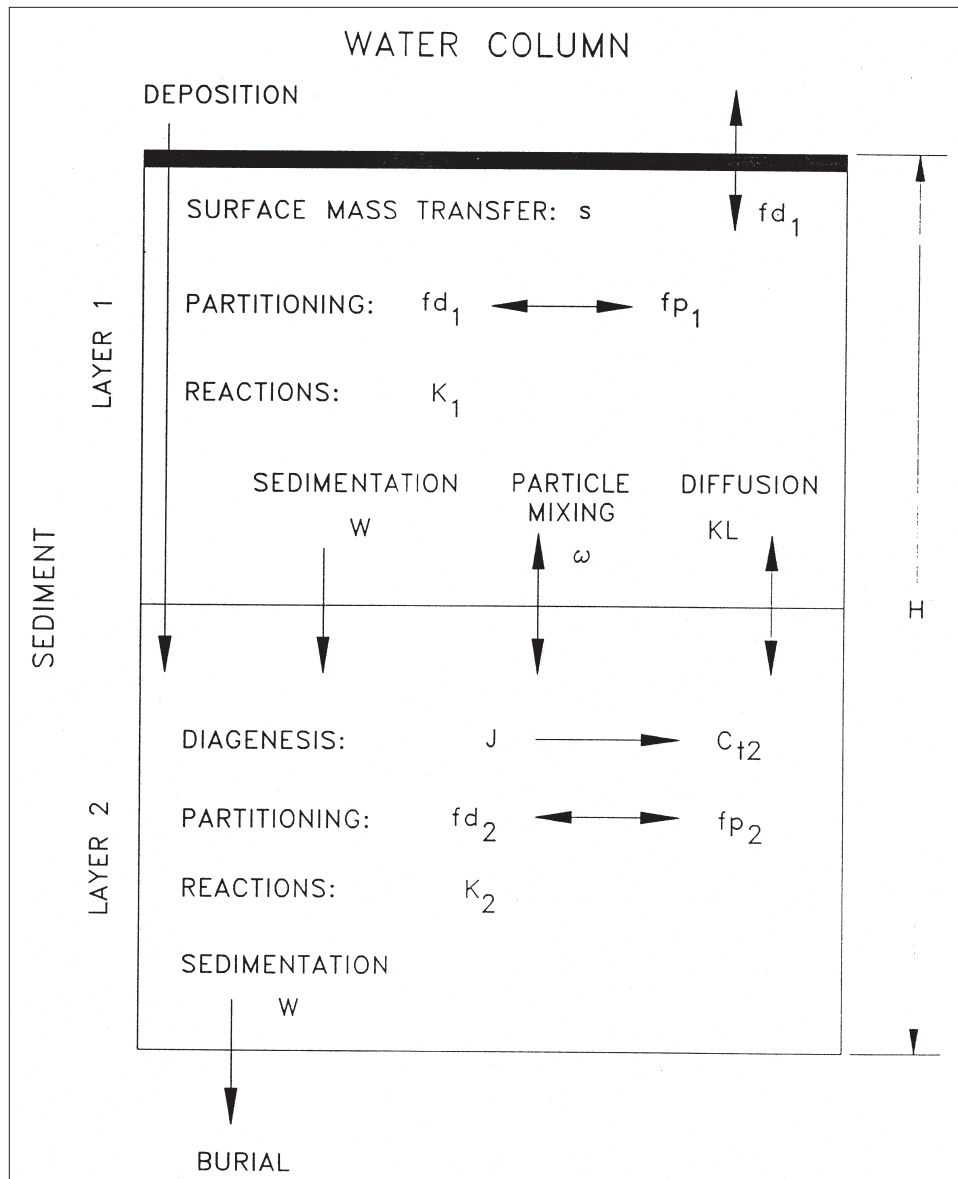


Figure 4-17. Sediment model layers and definitions

$$\frac{\delta C}{\delta t} = [\text{transport}] + [\text{kinetics}] + \frac{WS}{\Delta z} C_{up} - \frac{W_{net}}{\Delta z} C \quad (4.68)$$

where

C = concentration of particulate constituent (gm m^{-3})

WS = settling velocity in water column (m day^{-1})

C_{up} = constituent concentration two cells above sediments (gm m^{-3})

W_{net} = net settling to sediments (m day^{-1})

$\Delta z =$ cell thickness (m)

Net settling to the sediments may be greater or lesser than settling in the water column. Sediment resuspension is implied when settling to the sediments is less than settling through the water column. Net settling that exceeds particle settling velocity implies active incorporation of particles into sediment by biota or other processes.

Diagenesis

Organic matter in the sediments is divided into three G classes or fractions, in accordance with principles established by Westrich and Berner (1984). Division into G classes accounts for differential decay rates of organic matter fractions. The G1, labile, fraction has a half life of 20 days. The G2, refractory, fraction has a half life of one year. The G3, inert, fraction undergoes no significant decay before burial into deep, inactive sediments. Each G class has its own mass-conservation equation:

$$H \frac{\delta G_i}{\delta t} = W_{net} f_i C - W G_i - H K_i G_i \theta_i^{(T-20)} \quad (4.69)$$

where

- H = total thickness of sediment layer (m)
- G_i = concentration organic matter in G class i (gm m^{-3})
- f_i = fraction of deposited organic matter assigned to G class I
- W = burial rate (m day^{-1})
- K_i = decay rate of G class i (day^{-1})
- θ_i = constant that expresses effect of temperature on decay of G class i

Since the G3 class is inert, $K_3 = 0$.

Total diagenesis is the rate at which oxygen demand and nutrients are produced by diagenesis of the G1 and G2 fractions:

$$J = H \left[K_1 G_1 \theta_1^{(T-20)} + K_2 G_2 \theta_2^{(T-20)} \right] \quad (4.70)$$

where

$$J = \text{total diagenesis } (\text{gm m}^{-2} \text{ day}^{-1})$$

Flux

Total diagenesis provides the driving force for the flux portion of the model. Computation of flux requires mass-balance equations for oxygen demand and nutrients in both sediment layers. The upper layer is thin such that a steady-state approximation is appropriate:

$$s \, fd_1 \, Ct_1 = \omega(fp_2Ct_2 - fp_1Ct_1) + KL(fd_2Ct_2 - fd_1Ct_1) - W \, Ct_1 \pm \sum K_1 \quad (4.71)$$

where

Ct_1 = total concentration in upper layer (gm m^{-3})

Ct_2 = total concentration in lower layer (gm m^{-3})

fd_1 = dissolved fraction of total substance in upper layer
($0 \leq fd \leq 1$)

fd_2 = dissolved fraction of total substance in lower layer

fp_1 = particulate fraction of total substance in upper layer = $1 - fd_1$

fp_2 = particulate fraction of total substance in lower layer

s = sediment-water mass-transfer coefficient (m day^{-1})

ω = particle mixing velocity (m day^{-1})

KL = diffusion velocity for dissolved fraction (m day^{-1})

$\sum K_1$ = sum of all sources and sinks due to reactions in upper layer
($\text{gm m}^{-2} \text{day}^{-1}$)

The left-hand side of Equation 4-71 represents flux to the water column under the assumption that dissolved concentration in the water column is negligibly small compared to the sediments. The assumption is made here for notational simplicity. Effects of concentration in the overlying water are computed in the sediment model code. The terms on the right-hand side are mass transport due to particle mixing, diffusion of dissolved substance, deposition to the lower layer, and reactive sources and sinks. The reactions include, for example, the oxidation of sulfide that results in sediment oxygen demand. The equation states that flux to the water column, deposition from surficial sediments, and reactive sources and sinks are balanced by mixing and diffusion from deeper sediments.

The mass balance equation for the lower layer accounts for temporal concentration variations:

$$\begin{aligned} \frac{\delta Ct_2}{\delta t} = & \frac{J}{H} - \frac{\omega}{H}(fp_2Ct_2 - fp_1Ct_1) - \frac{KL}{H}(fd_2Ct_2 - fd_1Ct_1) \\ & + \frac{W}{H}(Ct_1 - Ct_2) \pm \sum K_2 \end{aligned} \quad (4.72)$$

where

$$\Sigma K_2 = \text{sum of all sources and sinks due to reactions in lower layer} \\ (\text{gm m}^{-2} \text{ day}^{-1})$$

The first term on the right of Equation 4.72 represents the diagenetic source of oxygen demand or nutrient. The second term represents exchange of the particulate fraction with the upper layer. The third term represents exchange of the dissolved fraction with the upper layer. The fourth term represents deposition of total substance from the upper layer to the lower layer and burial from the lower layer to deep, inactive sediments. The last term is the sum of all internal sources and sinks due to reactions.

The mass balance equations, with appropriate sources and sinks, are solved within the sediment model for sulfide, methane, ammonium, nitrate, phosphate, and silica. Details of the reactions and solution scheme may be found in the model documentation (DiToro and Fitzpatrick 1993).

The water-quality and sediment models interact on a time scale equal to the integration time step of the water-quality model. After each integration, predicted particle deposition, temperature, nutrient and dissolved oxygen concentrations are passed from the water-quality model to the sediment model. The sediment model computes sediment-water fluxes of dissolved nutrients and oxygen based on predicted diagenesis and concentrations in the sediments and water. The computed sediment-water fluxes are incorporated by the water-quality model into appropriate mass balances and kinetic reactions.

5 Water Quality Model Input

The CE-QUAL-ICM (ICM) requires various forms of information in order to accurately predict water quality. Types of input data required include hydrodynamic, meteorological, initial conditions, boundary conditions and external loadings, and also parameters. Descriptions of these inputs for this study are presented below. Parameters include kinetic rate coefficients, half saturation constants, stoichiometry, and other coefficients used in water quality reactions. Parameters used in this study are presented in Chapter 7.

Hydrodynamics

CH3D-WES (see Chapter 3) was the source for all hydrodynamic information for ICM during this study. The hydrodynamic information generated by CH3D can be described as time-invariant and time-varying. Time-invariant data are the information obtained from CH3D which do not change, or are constant, during the ICM simulation. Time-varying data are information which change during the simulation and which must be updated in ICM at each hydrodynamic update interval.

Time-invariant hydrodynamic data consist of: cell areas (m^2) in planform, i.e., in the horizontal plane; initial cell volumes (m^3) for all computational cells; distances (m) between neighboring cell centroids; and initial subsurface horizontal flow-face areas (m^2) between all cells. With the z-plane version of CH3D-WES, which was used for this study, the horizontal flow-face areas and volumes of cells below the surface layer do not change over time. However, since the surface layer thicknesses increase and decrease with the tides, horizontal flow-face areas and cell volumes in the surface layer do change over time.

Time-varying data consist of three-dimensional flows (m^3/sec) between computational cells, horizontal flow-face areas (m^2) for surface layer cells, cell volumes (m^3) for the surface layer, and vertical diffusivities (m^2/sec) between layers. The flows, facial areas, and diffusivities are updated within ICM at each hydrodynamic update interval, but they are held constant in ICM between hydrodynamic updates. Volumes are used for

comparison purposes during each hydrodynamic update to ensure that the internally computed volume of ICM is consistent with CH3D-WES volumes, i.e., to check for preservation of volume conservation.

A calibrated version of CH3D-WES must be applied for the same period over which the WQM is to be applied. A processor is appended as subroutines to the CH3D-WES source code. The processor computes time-averaged flows, surface layer flow-face areas, and vertical diffusivities throughout the ICM grid for each hydrodynamic update interval and then writes these values to an output file that is subsequently used by ICM. For the SJBE study, the averaging interval, or hydrodynamic update interval was fifteen minutes. Processing the hydrodynamic information separately and storing it in a file allows a set of hydrodynamic information to be generated once and used repeatedly for WQM application. Details of the hydrodynamic model and its application are covered in Chapter 3.

For this study, a one-to-one correspondence of the HM and WQM grids was used, i.e., the same grid was used for both models. Since water levels are used to drive the ocean boundaries of the HM, the outermost row of cells is not used within the WQM grid. It is possible for the WQM to use either a coarser overlay of the HM grid or an entirely different grid and project mass conserving flow fields from the HM grid to the WQM. The latter approach has been developed recently and is still undergoing testing.

For this study, a modification was made to the grid. The areas of concern in this study were in the interior bays and canals of the system and not the offshore regions. There are large differences in depth (and the number of layers) between the areas of concern and the offshore waters. Numerous areas in the interior of the system had depths of approximately 3 ft and were modeled as one layer. Offshore regions were over 90 ft deep or 30 layers. The large numbers of cells required offshore resulted in un-necessarily long computational requirements. To alleviate this problem, an additional four rows of cells were removed along the ocean boundary. The final grid shown in Figure 5-1 contained 1,923 surface cells and 10,600 total cells. The deepest portion of the reduced grid was directly offshore of the mouth of San Juan Bay which was 30 layers or approximately 90 ft deep.

Meteorological Data

ICM utilizes meteorological information in the computation of temperature and algal growth. Daily meteorological observations were obtained for the National Weather Service Station at the San Juan International Airport for the period May through September 1995. Data obtained consisted of daily average values for dry bulb temperature, wet bulb temperature, cloud cover, and wind speed. With this information values for equilibrium temperature, heat exchange coefficient, daily solar illumination, and

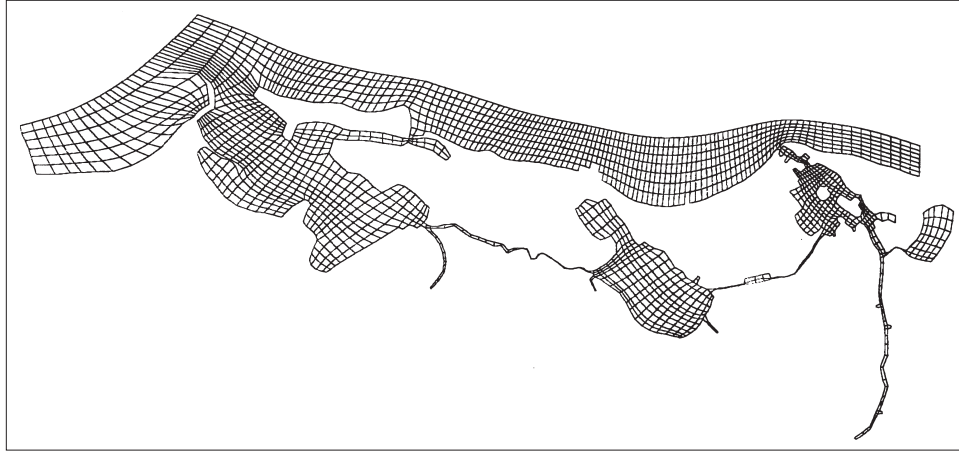


Figure 5-1. Water quality model grid, reduced from hydrodynamic model grid

fractional day length were computed. Details of the computational procedures used are found in Edinger et al. (1974).

Initial Conditions

ICM requires initial concentrations for all modeled constituents in all water column and sediment cells. These values must be realistic, otherwise model results can be biased by the initial conditions and may not fully reflect the loading and hydrodynamic processes occurring during simulation. Appropriate initial conditions for the sediment model are especially crucial since sediment model cells respond more slowly to changes in the loads and processes than does the water column.

Initial conditions were generated by spinning up the model. Spinning up was accomplished by initiating model calibration with a set of uniform initial conditions for water column cells based upon sampling data. Initial conditions in the sediments were specified in a similar manner. ICM was run using the calibration period hydrodynamics, loads, and boundary conditions. At the end of the first calibration run, the concentrations of all constituents in all water column and sediment cells were stored in a binary file. This file was then used as the initial conditions for a second calibration run. At the completion of the second calibration run, concentrations for all cells were again written to a binary file which was used as the initial conditions for the third calibration run. This process was repeated in subsequent calibration runs until a quasi steady-state condition (in terms of initial conditions) was reached in both the water column and sediment cells. This process required approximately 12 runs. Once a quasi steady-state set of initial conditions existed, all subsequent runs were made using the same set of initial conditions. The same iterative procedure was used to establish initial conditions for scenario runs. The scenario simulation period was run multiple times using results from the previous run to

establish a new set of initial conditions. The process was repeated until a quasi steady-state set of initial conditions existed between runs.

Boundary Concentrations and Loading Estimates

Water quality boundary conditions for this study can be divided into two forms, ocean and terrestrial. Atmospheric loadings were not included. Ocean boundary conditions are concentrations set along the open ocean boundary. These concentrations are used for all flow conditions during which flow is coming into the water quality model grid at the edge of the grid along the ocean boundary. Terrestrial boundary concentrations or loads are specified for inflows entering the water quality model grid from tributary headwaters, local, nonpoint source runoff directly from land into the bays, and point source loads. Point source loads are usually used to account for discharges from treatment plants, wastewater, combined sewer overflows, pumping plants, and other sources of pollutants at specified locations. Point and nonpoint source loadings are usually treated as loads, which means they are input as mass/time (the product of flow times concentration) at the appropriate grid locations and are not tied to a HM tributary inflow. Boundary concentrations are usually specified to the WQM for tributaries since flows are passed from the HM to the WQM for all tributaries. However, for this study, the tributary loads were computed and input for all constituents, except temperature and DO for which concentration boundary conditions were input.

Ocean Boundary Concentrations

The values used for the ocean boundary were obtained from the data collected at stations AO-1 and AO-2 (Kennedy et al., 1996). Analysis of data at these stations indicates that there is little variation in the data between the stations, and there was no vertical stratification. Nutrient levels were low relative to levels inside the SJBE system. Consequentially, these data were averaged and a single value was determined which was used for all ocean boundary faces (Table 5-1). Ocean boundary concentrations varied over time and were updated periodically as shown in Table 5-1.

**Table 5-1.
Ocean Boundary Concentrations**

Parameter	Day 0	Day 38	Day 52	Day 66	Day 81
Temperature, °C	28.0	28.0	28.3	28.2	28.9
Salinity, ppt	37.9	36.6	36.2	37.9	37.1
Total Suspended Solids, mg/l	0.0	0.0	0.0	0.0	0.0
Chlorophyll-a, µg/l	0.48	0.37	0.48	0.23	0.50
DOC, mg/l	3.12	0.94	3.15	8.47	1.98
POC, mg/l	0.38	0.43	0.38	1.50	0.32
NH ₄ , mg/l	0.0	0.09	0.0	0.03	0.16
NO ₃ , mg/l	0.01	0.01	0.0	0.0	0.0
TON, mg/l	0.0	0.0	0.0	0.0	0.0
TIP, mg/l	0.002	0.002	0.001	0.001	0.003
DOP, mg/l	0.003	0.017	0.0	0.007	0.007
POP, mg/l	0.001	0.006	0.003	0.0	0.004
DO, mg/l	6.2	6.1	5.9	5.3	4.8

Loading Estimates

External loads of constituents are separated into two categories, point source and nonpoint source. Point source loads are traditionally defined as those which are attributable to a single location or “point.” Examples include effluent pipes from municipal or industrial wastewater treatment facilities. Nonpoint source loads are defined as those whose origin is distributed over a widely spaced area. A traditional example is runoff from a local subwatershed along the model shoreline. Nonpoint source loads can also include loads which are truly point source in nature but which occur in the watershed and not at the model boundary.

When commencing this study, an extensive effort was made to identify significant point source and nonpoint source loads for the SJBE system. Many possible sources of pollution were identified as reasons for poor water quality in various regions of the system. Unfortunately, little documentation was discovered which substantiated these theories. Part of the problem is that in some cases it is hard to quantify the loads due to their distributed nature. Other cases, such as sewer pump station overflows, are intermittent and the quantity of water and load cannot be easily determined. In other instances, data on concentration or flow were lacking.

A review of EPA permit records indicated that there were no major municipal wastewater treatment plants or industrial point source dischargers for nutrients or oxygen-depleting substances that were releasing effluents directly into the SJBE system. Treatment plant effluents are removed via a Puerto Rico Aqueduct and Sewer Authority (PRASA) pipeline for ocean disposal beyond the boundary of the water quality model grid. Two Puerto Rico Electric Power Association (PREPA) power plants

discharge cooling water to San Juan Bay. The net effect of these two power plants is that they increase the temperature of the cooling water. Therefore, all of the external loads can be considered as nonpoint source loads.

Estimation of Flows. While there are officially no major point source dischargers to the system, the system receives significant loads in the form of runoff loads from the adjacent watershed and storm water pump stations. Prior to estimation of these loads, two pieces of information are required, flow and concentration. Two forms of flow data were available, Rio Piedras (see Figure 1-1) flow records and storm water pump station records.

Rio Piedras at Hato Rey flow records for the period being modeled were obtained from the USGS. The frequency of these data were 15 minutes. A review of the records for the calibration period indicated that observed flows varied from 0.11 to 236.6 m³/s (4 to 8355 ft³/s), see Figures 5-2a through 5-2d for June through September 1995. Daily averages of flow were used in the hydrodynamic model for the Rio Piedras inflow.

Records for storm water pump stations operated by the Puerto Rico Department of Natural Resources were obtained. The only pump station whose records overlapped the calibration period was the Baldorioty de Castro Pump Station on San José Lagoon. (Records for the calibration period for the other pump stations were unavailable.) Information on these records consisted of hours of operation for pumps from which the daily pumping duration could be obtained. The daily total water volume pumped was determined by multiplying the pump capacity by the daily pumping duration. This volume was then converted into an equivalent daily flow rate as shown in Figure 5-3.

The SJBE watershed was divided into 21 sub-basins as shown in Figure 5-4 based upon information extracted from USGS topographic maps. Areas for each sub-basin were determined and are listed in Table 5-2. Freshwater flows were introduced in the HM at each location where there is an arrow shown in Figure 5-4. There are more arrows than sub-basins since flows were put in and taken out at two power plants and in several cases more than one flow location was used for a sub-basin. For all cases, except Caño Martín Peña, the HM inflow was treated as a tributary (i.e., quantity with momentum). For Caño Martín Peña, inflow was distributed along the canal as a lateral flow, i.e., no momentum.

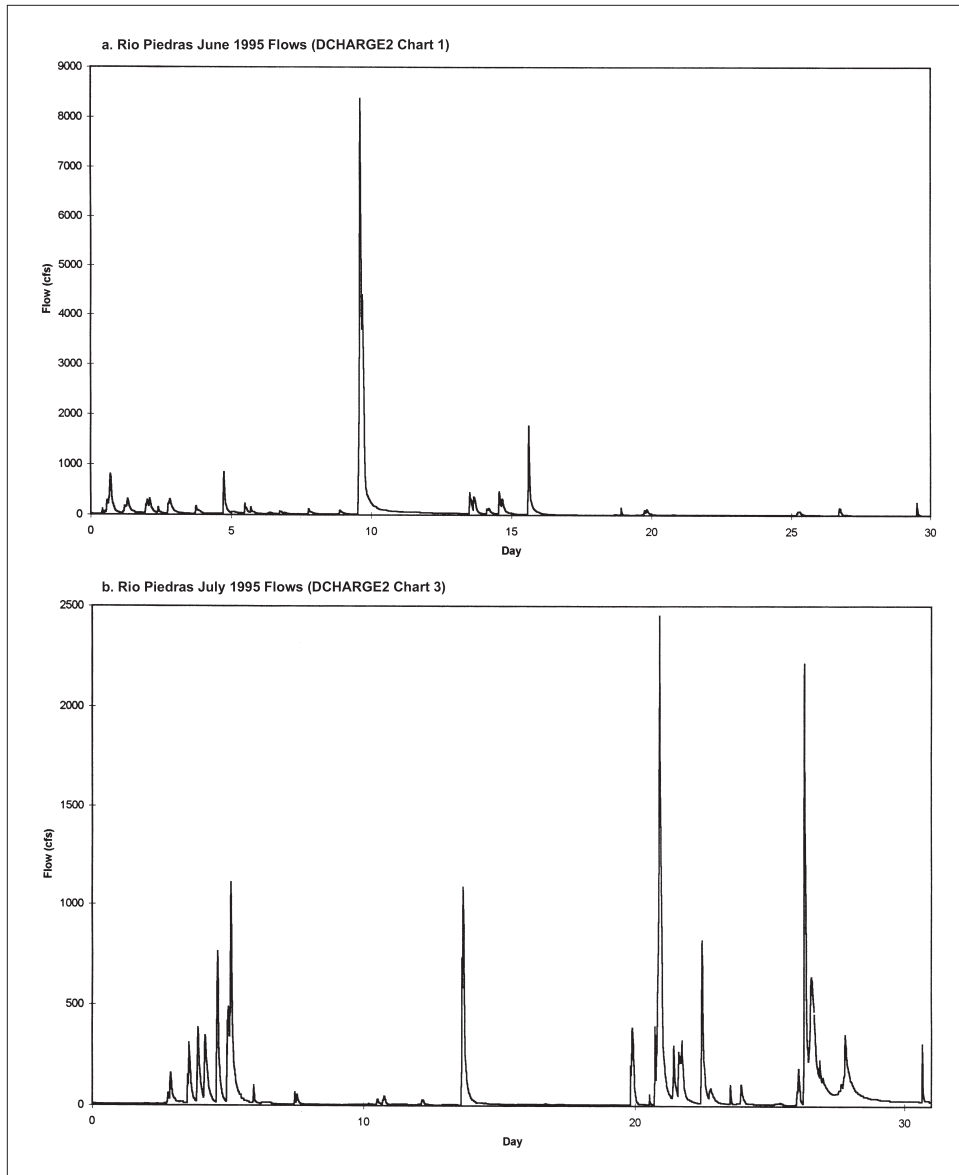


Figure 5-2. Flows observed at Hato Rey, Rio Piedras, June-September 1995 (continued)

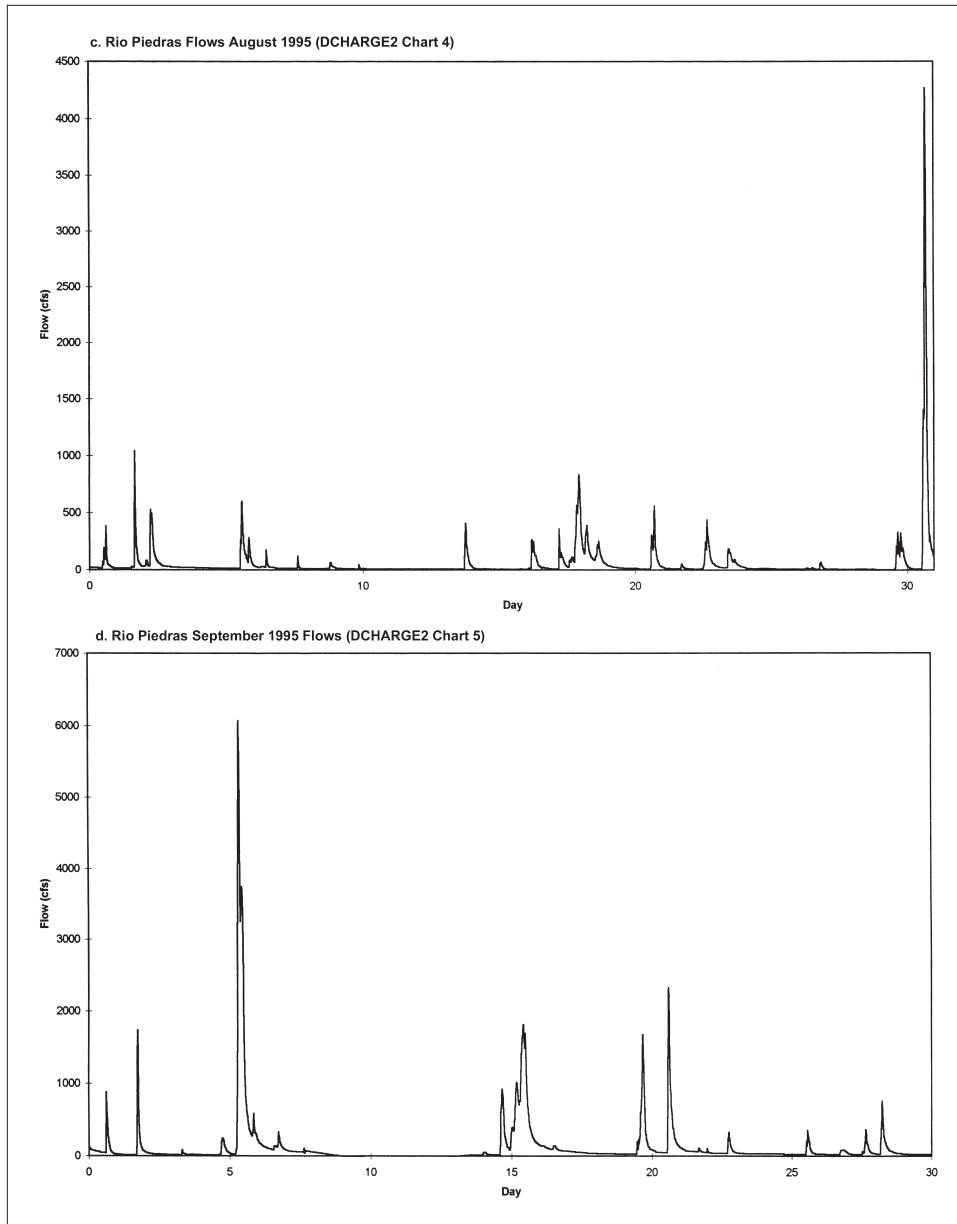


Figure 5-2. (concluded)

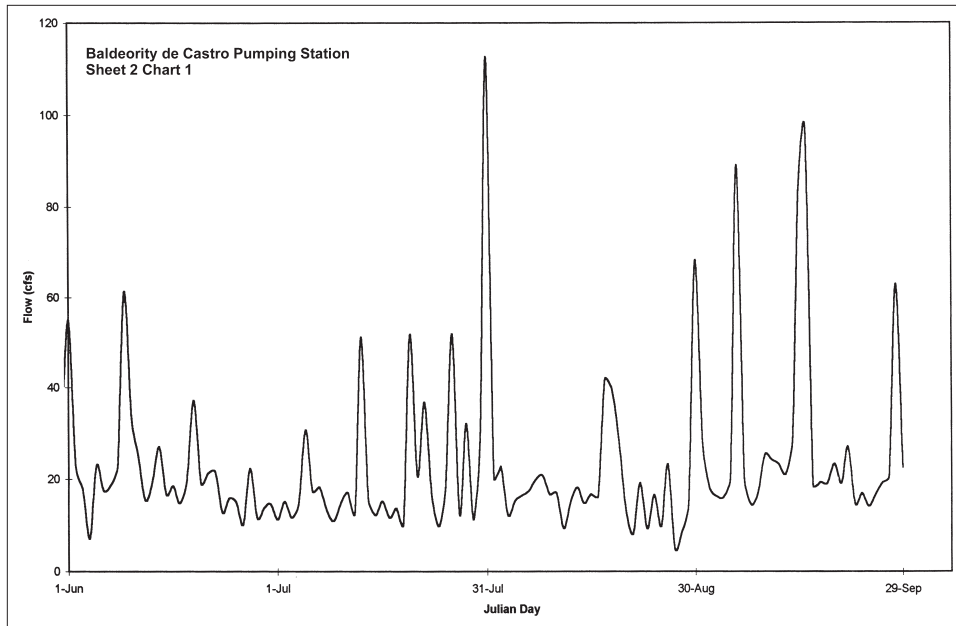


Figure 5-3. Flows for Baldeority de Castro Pump Station computed from pumping records for June-September 1995

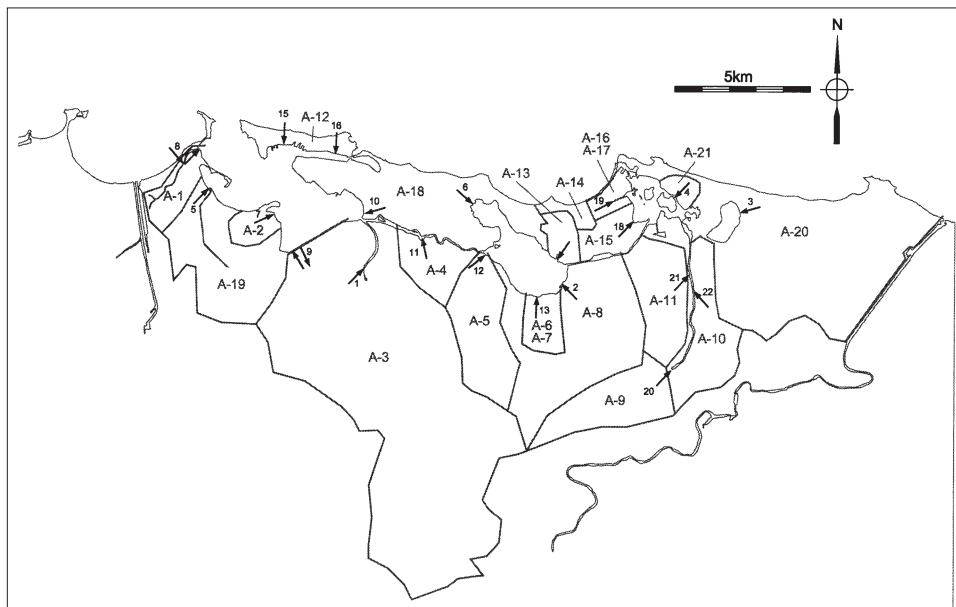


Figure 5-4. Model sub-basins of the San Juan Bay Estuary System with model locations of freshwater inflows indicated by the arrows

**Table 5-2.
SJBE Sub-Basins and Areas**

Sub-basin	Name	Size (mi ²)
A1	Bayamon	1.35
A2	San Fernando	1.0
A3	Rio Piedras	27.1
A4	Martin Peña	2.3
A5	Juan Mèndez	3.2
A6	Unnamed creek sw Laguna San José	0.9
A7	Unnamed creeks Laguna San José	0.9
A8	Quebrada San Antòn	6.8
A9	Quebrada Blasina	2.96
A10	Eastern Blasina	5.3
A11	Western Blasina	3.0
A12	Old San Juan	0.9
A13	Western End of Airport	0.9
A14	Northern End of Airport	0.45
A15	Southern End of Airport	1.35
A16	Eastern End of Airport 1	0.22
A17	Eastern End of Airport 2	0.23
A18	Santurce	5.86
A19	Malaria	6.0
A20	Piñones	13.0
A21	East of Torrecilla	1.0

Using the USGS gaged flow records from Hato Rey and the Baldorioty de Castro Pump Station pumping records, flow relationships were derived for each sub-basin of the watershed. However, prior to the derivation of any flow relationships, the observed flows for the two locations had to be converted to inches per day of runoff. This was accomplished by dividing the equivalent daily volume of flow by the area of the respective sub-basin expressed in square feet. The resulting height of runoff was then converted from ft/day to in./day. Sub-basin area used for the Rio Piedras regression was the area upstream of the USGS flow gage at Hato Rey (15.2 mi²). A contributing area of 1.94 mi² was used for the Baldorioty de Castro sub-basin.

Rainfall records for the calibration period were available from the National Weather Service station at the San Juan International Airport and for a number of USGS rainfall collection stations in the basin. Using rainfall records from the USGS rain gage at Rio Piedras and flow records from the USGS flow gage at Hato Rey, a type II regression was performed to determine a relationship between rainfall and runoff. A similar procedure was followed using pumping records from Baldorioty de Castro Pump Station and National Weather Service rainfall records. The rainfall-runoff

relationships developed for Rio Piedras at Hato Rey and Baldorioty de Castro Pump Station, respectively, are

$$q_P = 0.046 + 0.7468 * \text{rain} \quad (5.1)$$

where

q_P = Rio Piedras flow at Hato Rey, inches/day
rain = daily rainfall observed at the Rio Piedras rain gage,
inches/day

and

$$q_B = 0.232 + 0.9 * \text{rain} \quad (5.2)$$

where

q_B = Baldorioty de Castro Pump Station flow, inches/day
rain = daily rainfall observed at the San Juan International Airport,
inches/day

Figures 5-5 and 5-6 show the relationship between Equations 5.1 and 5.2 and the observed rainfall and flow. The first term in Equations 5.1 and 5.2 represents a base flow and the second a runoff flow. The base flow occurs whether there is any rainfall or not. Runoff flow only occurs when there has been rainfall. The values computed in the above equations are in inches per day of flow which were converted to ft³/s for each sub-basin by the following relationship

$$Q = 5.093 \times 10^{-3} q A_{\text{Basin}} \quad (5.3)$$

where

A_{Basin} = measured area of sub-basin in mi²

Initially, Equations 5.1 - 5.3 were used to compute runoff flows for all sub-basins for which there were no observed flows, which included all the sub-basins except for Rio Piedras and the Baldorioty de Castro Pump Station. For Rio Piedras, flows observed at Hato Rey were multiplied by 1.78 to account for contributions from the portion of the watershed below the stream gage.

Refinements were made to several of the other sub-basins after tests with the hydrodynamic model indicated that the predicted inflows were too high to maintain proper salinity. Because water levels and flows through transects compared favorably with measured data, it was assumed that estimated flows were probably too high rather than ocean exchange too low. Inflows for the several sub-basins around Quebrada Blasina and Laguna de Piñones were computed using the SCS Curve Number Method (Mississippi

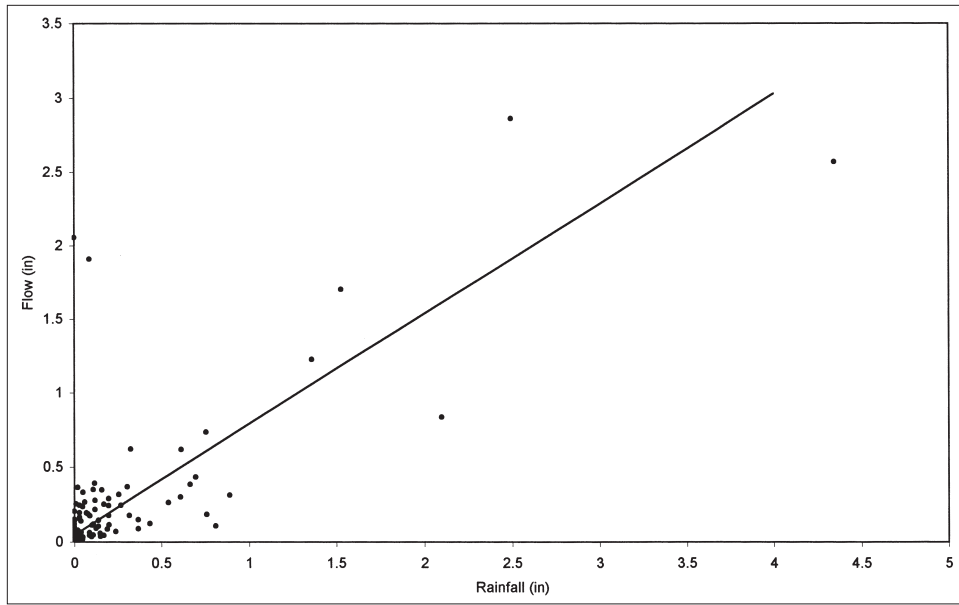


Figure 5-5. Observed flows for Rio Piedras at Hato Rey versus observed rainfall plotted with the best-fit regression line

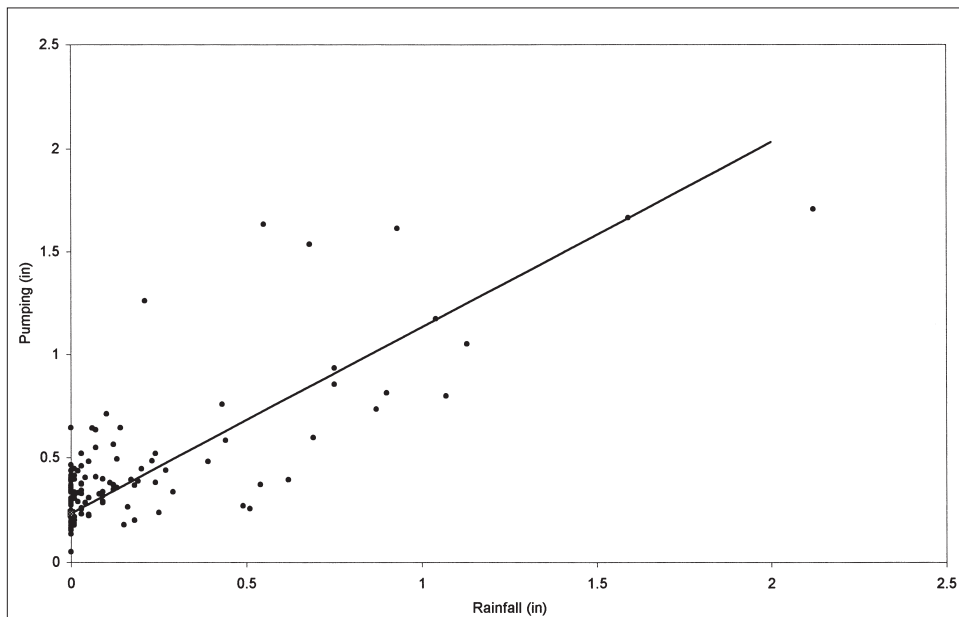


Figure 5-6. Computed flows based on pumping records for Baldorioty de Castro Pump Station versus observed rainfall plotted with the best-fit regression line

Department of Environmental Quality et al. 1994) to estimate runoff flows per unit area (inches/day).

$$q = \frac{\left(\text{rain} + 0.2 * \left(\frac{1000}{CN} - 10 \right) \right)^2}{\text{rain} + 0.8 * \left(\frac{1000}{CN} - 10 \right)} \quad (5.4)$$

where

rain = rainfall at International Airport, inches/day

CN = SCS Curve Number

Curve Numbers were selected based on land use, land cover, and soil type and are shown in Table 5-3. The unit areal flows computed from Equation 5.4 were used with Equation 5.3 to calculate volumetric flows (m³/sec). Rationale for re-computing flows for these basins was twofold. The region east of Piñones is undeveloped and flat and would therefore have a longer retention time and slower response than the developed, hilly Rio Piedras watershed. Secondly, flows for the region surrounding Laguna de Piñones were being over-predicted by the regression developed from the Baldorioty de Castro Pump Station. The Santurce region served by the Baldorioty de Castro Pump Station is a highly developed region of the San Juan metropolitan area. Due to limited infiltration as a result of impervious land cover, this region has a high percentage of runoff (90%). In addition, there is a substantial base flow which is thought to be due to leaking sewer pipes and undocumented sewer connections to the storm-water collection system. Neither the base flow nor the high runoff coefficient for the Baldorioty de Castro regression was appropriate for the Piñones and Blasina sub-basins.

**Table 5-3.
SJBE Sub-Basin Curve Numbers**

Sub-Basin	Name	SCS Curve Number
A9	Quebrada Blasina	98
A10	Eastern Blasina	98
A11	Western Blasina	98
A13	Western End of Airport	84
A16	Eastern End of Airport 1	86
A17	Eastern End of Airport 2	86
A20	Piñones	76
A21	East of Torrecilla	76

Flows for the remaining regions were analyzed in conjunction with hydrodynamic calibration runs. It became apparent that the estimated inflows were also too high in the interior of the system, specifically San José Lagoon. In order to improve the salinity predictions in San José, base flows for the sub-basins flowing into San José were reduced by 50%. Table 5-4 summarizes the sources of and methods used to obtain runoff for each sub-basin.

Sub-Basin	Name	Method
A1	Bayamon	Rio Piedras Regression
A2	San Fernando	Rio Piedras Regression
A3	Rio Piedras	USGS Observed Flows
A4	Martin Peña	Baldorioty de Castro Regression
A5	Juan Mendez	Baldorioty de Castro Regression
A6	Unnamed creek sw Laguna San José	Baldorioty de Castro Regression
A7	Unnamed creek sw Laguna San José	Baldorioty de Castro Regression
A8	Quebrada San Anton	Baldorioty de Castro Regression
A9	Quebrada Blasina	SCS Curve Number Method
A10	Eastern Blasina	SCS Curve Number Method
A11	Western Blasina	SCS Curve Number Method
A12	Old San Juan	SCS Curve Number Method
A13	Western End of Airport	SCS Curve Number Method
A14	Northern End of Airport	SCS Curve Number Method
A15	Southern End of Airport	SCS Curve Number Method
A16	Eastern End of Airport 1	SCS Curve Number Method
A17	Eastern End of Airport 2	SCS Curve Number Method
A18	Santurce	Baldorioty de Castro Records and Regression
A19	Malaria	Rio Piedras Regression
A20	Piñones	SCS Curve Number Method
A21	East of Torrecilla	SCS Curve Number Method

Runoff Concentrations. Runoff concentrations are required to set tributary boundary concentrations and/or to compute tributary and local runoff loads. Most of the runoff entering into the San Juan estuaries system is not routinely sampled. As a result, the most comprehensive database available for the calibration period was the tributary sampling conducted in conjunction with the open water monitoring study conducted for model calibration (Kennedy et al. 1996). Due to the limited number of observations on any one tributary and the similarity of most of the watershed, the data for all were combined together into a database from which a single average value was determined and used (see Table 5-5) for each constituent concentration. These values were held constant for the duration of the calibration simulation and applied with the following exceptions discussed below to estimate all loads, including tributary inflows, local, storm-water runoff, and storm-water pumping plant discharges. With this approach, loads vary with flow since they are the product of flow and concentration. However,

the limited information on loadings to the system is a major source for model error and uncertainty and a recognized future monitoring need.

Constituent	Value Used
Temperature, °C	27.9
Salinity, ppt	0.0
Total Suspended Solids, mg/l	12.0
DOC, mg/l	13.2
POC, mg/l	2.0
NH ₄ , mg/l	1.035
NO ₃ , mg/l	0.15
TON, mg/l	0.16
DIP, mg/l	0.23
DOP, mg/l	0.025
POP, mg/l	0.20
DO, mg/l	5.84
Fecal Coliform, mpn/100ml	1.6 × 10 ⁶

Exceptions to uniform concentrations are presented in Table 5-6. Exceptions included DO concentrations in the flows from Malaria Canal where DO was set to 2.0 mg/l instead of the 5.84 mg/l value used elsewhere (Table 5-5). The highest DO observation in Malaria during the sampling study was 2.53 mg/l, while the lowest was 0.5 mg/l. Malaria is reputed to have poor water quality resulting from sewage overflows and discharges and as such warrants a lower DO concentration. Headwater boundary TSS concentrations on the Rio Piedras were set to 114 mg/l while those on the Quebrada San Anton were set to 57 mg/l. TSS levels in these two streams were much higher than the other tributaries. Chlorophyll loads were introduced for only the sub-basins shown in Table 5-6, whereas for other sub-basins, the chlorophyll load was zero. Finally, fecal coliform bacteria levels for Rio Bayamon were set to 215 mpn/100 ml. This value is the average of the samples collected in that stream. The reason that Rio Bayamon observations were so low is unclear. Rio Bayamon serves as the receptor for cooling water discharges from the Palo Seco Power Plant, one of two power plants in the SJBE System. The intake water for this plant comes from offshore and should have very low levels of fecal coliform. The power plant uses approximately 650x10⁶ gal/day or 28.5 m³/s (1,006 ft³/s), which when discharged to the Rio Bayamon would then simply be diluting the upstream fecal coliform levels thereby resulting in the low counts obtained during sampling. Tributary loads for Rio Bayamon were computed using only the computed tributary flow based upon drainage area.

**Table 5-6.
Modified Runoff Concentrations**

Sub-Basin	DO mg/l	TSS mg/l	Chlorophyll µg/l	Fecal Coliform mpn/100 ml
Rio Piedras	5.84	112	3.33	1.6×10^6
Malaria	2.0	12	2.5	1.6×10^6
Bayamon	5.84	12	82	215
San Fernando	5.84	12	27	1.6×10^6
Quebrada Blasina	5.84	12	1	1.6×10^6
Runoff into Eastern Blasina	5.84	12	1	1.6×10^6
Runoff into Western Blasina	5.84	12	1	1.6×10^6
Runoff into Caño Martín Peña	5.84	12	4	1.6×10^6
Juan Méndez	5.84	47	3	1.6×10^6
Un-named creeks sw Laguna San José	5.84	12	4	1.6×10^6
Un-named creeks Laguna San José	5.84	12	4	1.6×10^6
Quebrada San Antòn	5.84	12	11	1.6×10^6
Runoff into Airport area	5.84	12	4	1.6×10^6
Runoff into Laguna de Piñones	5.84	12	1	1.6×10^6

The second power plant located in the system, the San Juan Power Plant, withdraws and discharges to San Juan Bay near the Military Terminal. The maximum cooling water flow for this facility is 700×10^6 gal/day or $32.8 \text{ m}^3/\text{s}$ ($1159 \text{ ft}^3/\text{s}$). These power plants are treated as a special type of boundary in the WQM. At the intakes, water is removed from the model grid. The water is then returned to the model at the outfall location without any change in water quality other than a temperature increase of 5°C resulting from process unit cooling. Concentrations of other constituents are introduced unchanged at the outfall.

Initial sub-basin loads to the WQM were computed by multiplying the daily flows for each sub-basin by the concentrations for the various constituents indicated in Tables 5-5 and 5-6. It is pointed out that for all sub-basins not indicated in Table 5-6, the uniform concentrations of Table 5-5 were used to compute loads. Additional loads were identified and implemented during calibration and are discussed in Chapter 7.

The model requires that loads of organic carbon, nitrogen, and phosphorus be split into model state variables. These variables represent dissolved organic, labile particulate organic, and refractory particulate organic constituents. Laboratory analyses do not always directly indicate these splits. In that case, values observed in other systems are adapted and refined, if necessary, in the model calibration process.

Dissolved organic carbon (DOC) was directly analyzed. Particulate organic carbon (POC) was obtained by subtracting DOC from total organic carbon. POC was split evenly between labile and refractory fractions. This split includes more labile material than is normally employed. In Chesapeake Bay, for example, the split is 10% labile and 90% refractory. More labile material was required in San Juan to create oxygen demand and match observed low dissolved oxygen concentrations in system bottom waters. The split suggests loads to the SJBE system contain more fresh organic matter (algal, raw sewage) than runoff to temperate estuaries.

Total organic nitrogen (TON) was obtained by subtracting ammonium from total Kjeldahl nitrogen (TKN). Guidance for splitting TON into dissolved and particulate forms was obtained from ammonium and TKN data collected in receiving waters adjacent to tributaries. The split was 10% dissolved and 90% particulate. Particulate organic nitrogen was split evenly into labile and refractory fractions, consistent with the splits for POC.

The majority of phosphorus observations in the tributaries were of total phosphorus (TP) and total dissolved phosphorus (TDP). Roughly 20% of the observations also included dissolved inorganic phosphorus (DIP) and particulate inorganic phosphorus (PIP). The DIP measures were used to guide specification of DIP in the loads. Subtraction of DIP from TDP yielded concentration of dissolved organic phosphorus (DOP) for use in the model. Subtraction of TDP from TP yielded total particulate phosphorus. The total particulate phosphorus included labile and refractory organic particles as well as particulate inorganic particles. PIP contains mineral forms that are not biologically available. Since the model does not include detailed representation of PIP chemistry, PIP is assigned to the refractory particulate organic fraction. Consequently, the split of particulate phosphorus into labile and refractory fractions included more refractory matter than for carbon or nitrogen. The splits used in the model were 12.5% labile and 87.5% refractory.

6 Hydrodynamic Model Adjustment and Skill Assessment

As previously discussed, a field data collection effort provided data for boundary conditions as well as interior data for comparison with model results (Fagerburg 1998). Water-surface elevations, salinity, and water-velocity data were collected at several locations throughout the system during June-August 1995. Both long-term as well as short-term data were collected. The short-term data were collected over 17-19 August 1995 when the crew returned to remove the long-term instruments. These data included ADCP data collected over several ranges in an attempt to define the water flux through the connecting canals of the system. Due to fouling of the long-term meters, very little useful long-term velocity and salinity data were obtained. Most salinity data employed were collected by Kennedy et al. (1996) during their collection of water quality data. Locations of data stations used in the skill assessment of CH3D are shown in Figure 6-1. Assessing the ability of the numerical model to simulate the hydrodynamics of the system has primarily revolved around reproducing the observed tides throughout the system, reproducing the extreme stratification in salinity that often exists during storm events, and reproducing the net flux through Caño Martín Peña and Canal Suárez.

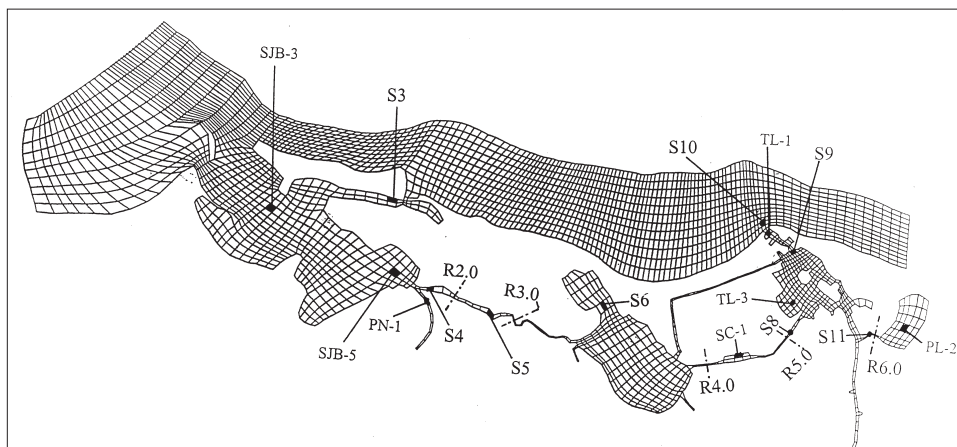


Figure 6-1. Location of data stations

Tide Reproduction

As illustrated in Figure 3-6, the tide in San Juan Harbor is mixed, with the M2 component being the largest. To better illustrate comparisons of the observed and computed tides throughout the system, comparisons for a three-day period in July 1995 are shown in Figures 6-2 - 6-6. It can be seen that the range and phase are reproduced fairly well, with phase errors on the order of perhaps 30 minutes occurring in some places. Figure 6-7 shows the computed and observed tide at a station in Laguna San José. The extreme reduction in the tide in Laguna San José as a result of the constriction in the eastern end of Martín Peña Canal and a bridge constriction in Canal Suárez is clearly illustrated. Obviously, there is little tidal flushing of Laguna San José, resulting in the poor water quality observed there.

Table 6-1 shows a comparison of the M2 and O1 computed and observed harmonic components of the tides at stations in San Juan Bay, Laguna San José, Laguna La Torrecilla, and Laguna de Piñones. Phasing is relative to the tide in San Juan Harbor. The letter **R** stands for the ratio of the ranges and **L** is the lag in phase in hours. It can be seen that the greatest reduction is in the higher frequency components. This agrees with the analytical analysis for a simplified co-oscillating system. Generally the comparison of the computed constituents with those determined from the observed data is good.

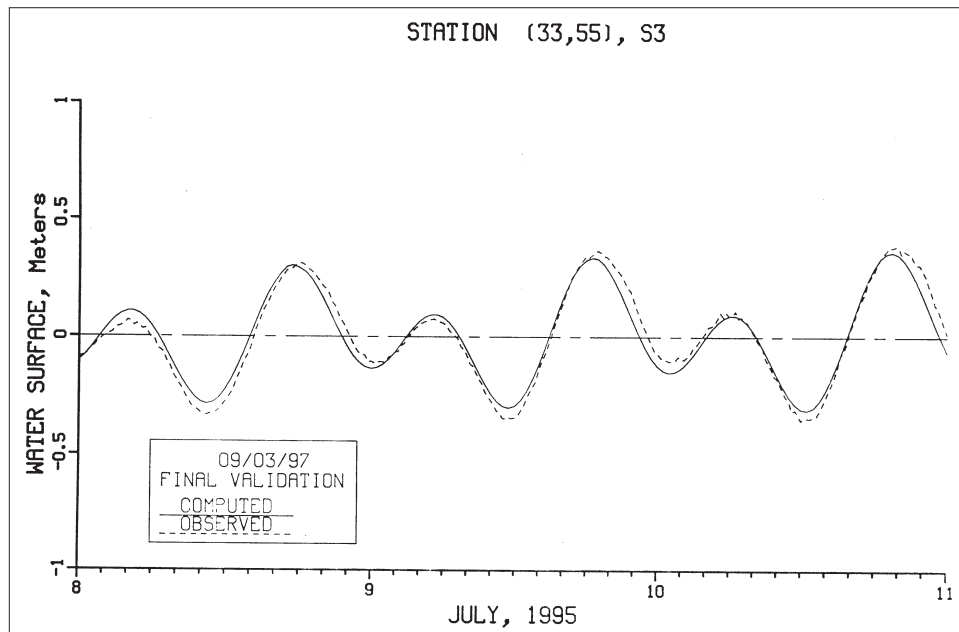


Figure 6-2. Comparison of computed and observed tide at S3

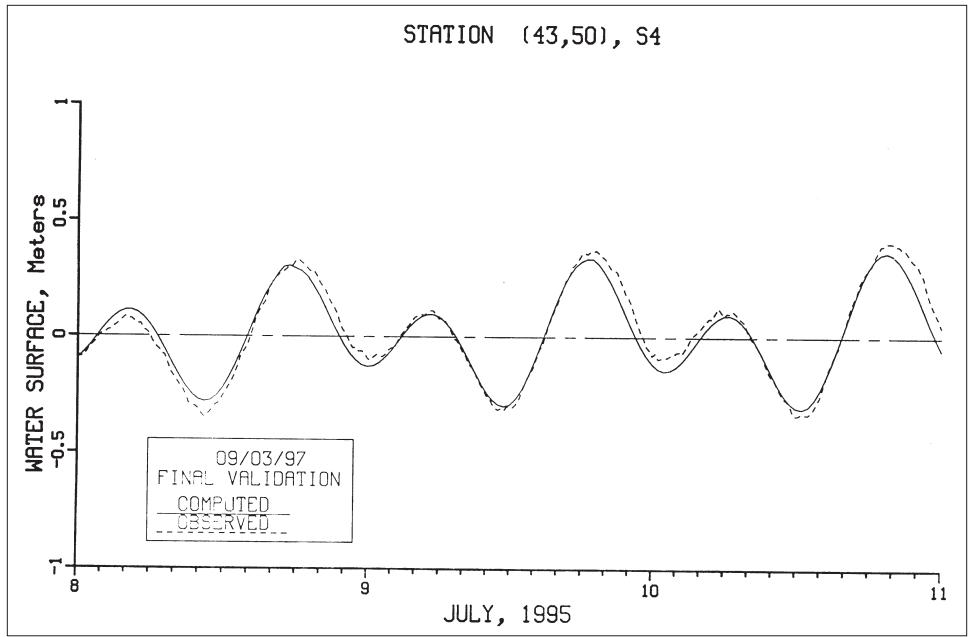


Figure 6-3. Comparison of computed and observed tide at S4

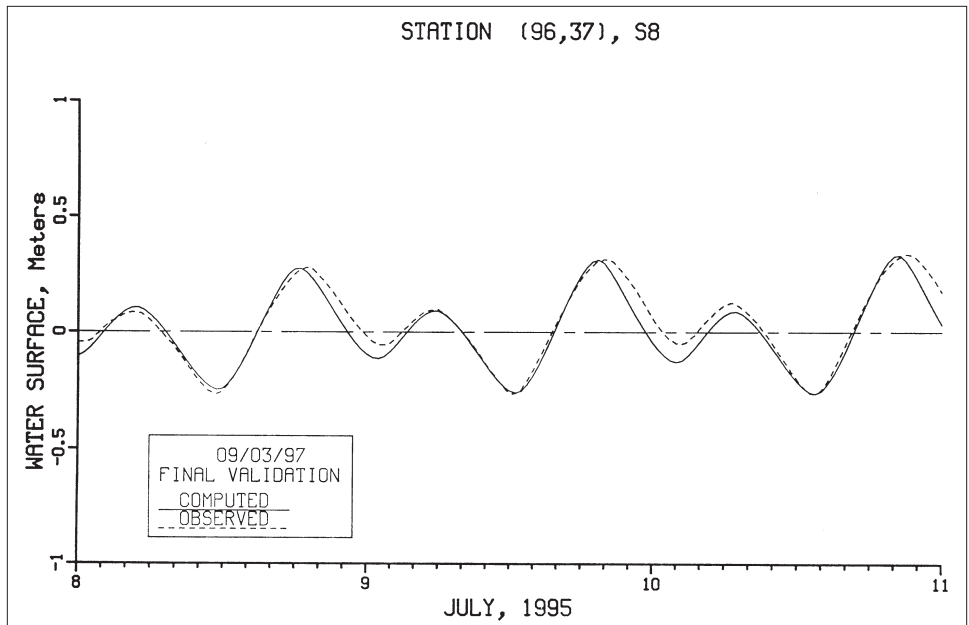


Figure 6-4. Comparison of computed and observed tide at S8

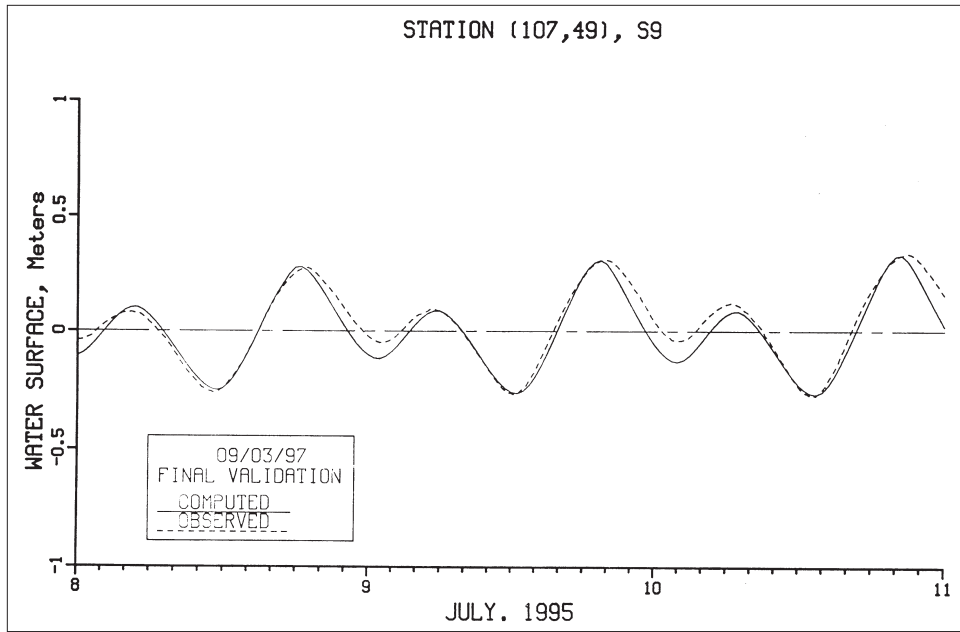


Figure 6-5. Comparison of computed and observed tide at S9

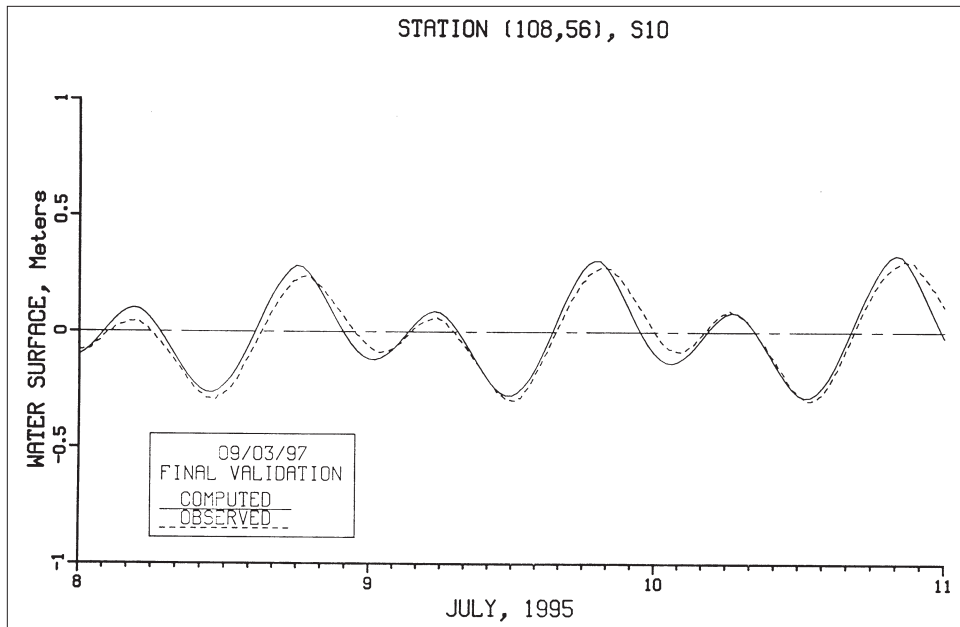


Figure 6-6. Comparison of computed and observed tide at S10

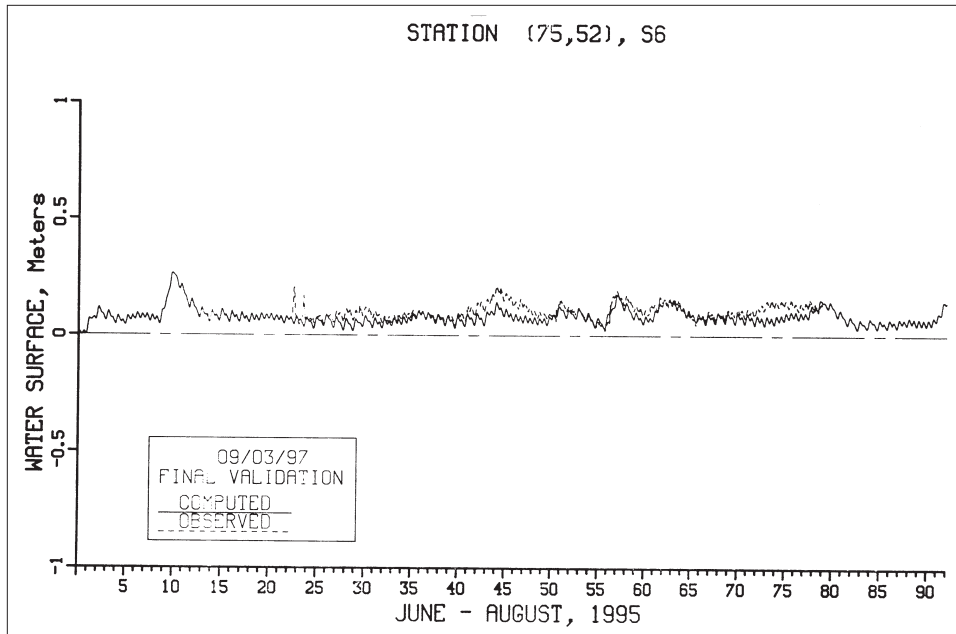


Figure 6-7. Comparison of computed and observed tide at S6

Table 6-1.
Comparison of Harmonic Constituents of Tide Relative to San Juan Bay Tide

Location	M2				O1			
	Model		Data		Model		Data	
	R	L	R	L	R	L	R	L
San José	0.06	3.69	0.06	3.85	0.16	5.42	0.10	6.47
Torreçilla	0.90	0.37	0.81	0.41	0.92	0.64	0.87	0.83
Piñones	0.12	4.01	0.12	3.67	0.23	6.01	0.23	6.18

Salinity Reproduction

The numerical model was run for the period 1 June - 31 August 1995. Boundary forcings are presented and discussed in Chapter 3. Although initial conditions on water-surface elevation and water velocity aren't too important since the effect of those initial conditions are flushed from the system within a few tidal cycles, the specification of the initial salinity field is much more important. Model stability was fairly sensitive to the initial salinity prescribed. In previous applications of CH3D, this behavior has not been observed. To overcome this problem, the model was initiated with a constant salinity over the entire grid and run for the month of June. The computed salinity field was then saved and used as the initial salinity field in all subsequent simulations for the entire three months. This

procedure yielded an initial salinity field that was close to observed data and resulted in a stable model.

Figures 6-8 through 6-19 show the ability of the numerical model to reproduce salinity throughout the system. In most plots, both near-surface salinity (layer 30) and near-bottom (layers less than 30) are shown. However, in some locations the depth is so shallow, e.g., Station S6 in Laguna San José (Figure 6-13), that only near-surface salinity is presented. An inspection of the salinity plots reveals that the Kennedy data (Kennedy et. al. 1996) are the primary salinity data available for skill assessment. Due to fouling of the long-term meters in the tropical waters of the SJBE system, most of the salinity data from those meters weren't useful. Figure 6-15 which shows a comparison of salinity at Station S8 collected by a long-term meter with model results is an example. Some salinity data collected during the 17-19 August short-term survey were of use, e.g., see Figure 6-11.

During periods of high freshwater inflow, a freshwater lens of 30-60 cm flows on the surface of some portions of the system, resulting in high salinity stratification. An example of this occurring can be observed in the western end of Martín Peña Canal. Field data show that the surface salinity is reduced to 5-10 ppt with salinity near the bottom being greater than 30 ppt. Figure 6-10 illustrates the model's ability to reproduce this extreme stratification after a large freshwater inflow event (relative to other flows during the study period) that occurred around the 9th of June (see Figure 3-4 showing the freshwater inflows). Note that the Kennedy data displayed in the salinity plots labeled near surface (layer 30) were collected at 0.5 m and 1.0 m, whereas the model results correspond to the middle of the top layer, which varies in thickness with the tide. The observed extreme stratification is reproduced well in the numerical model even though each layer in the vertical is 0.91 m thick.

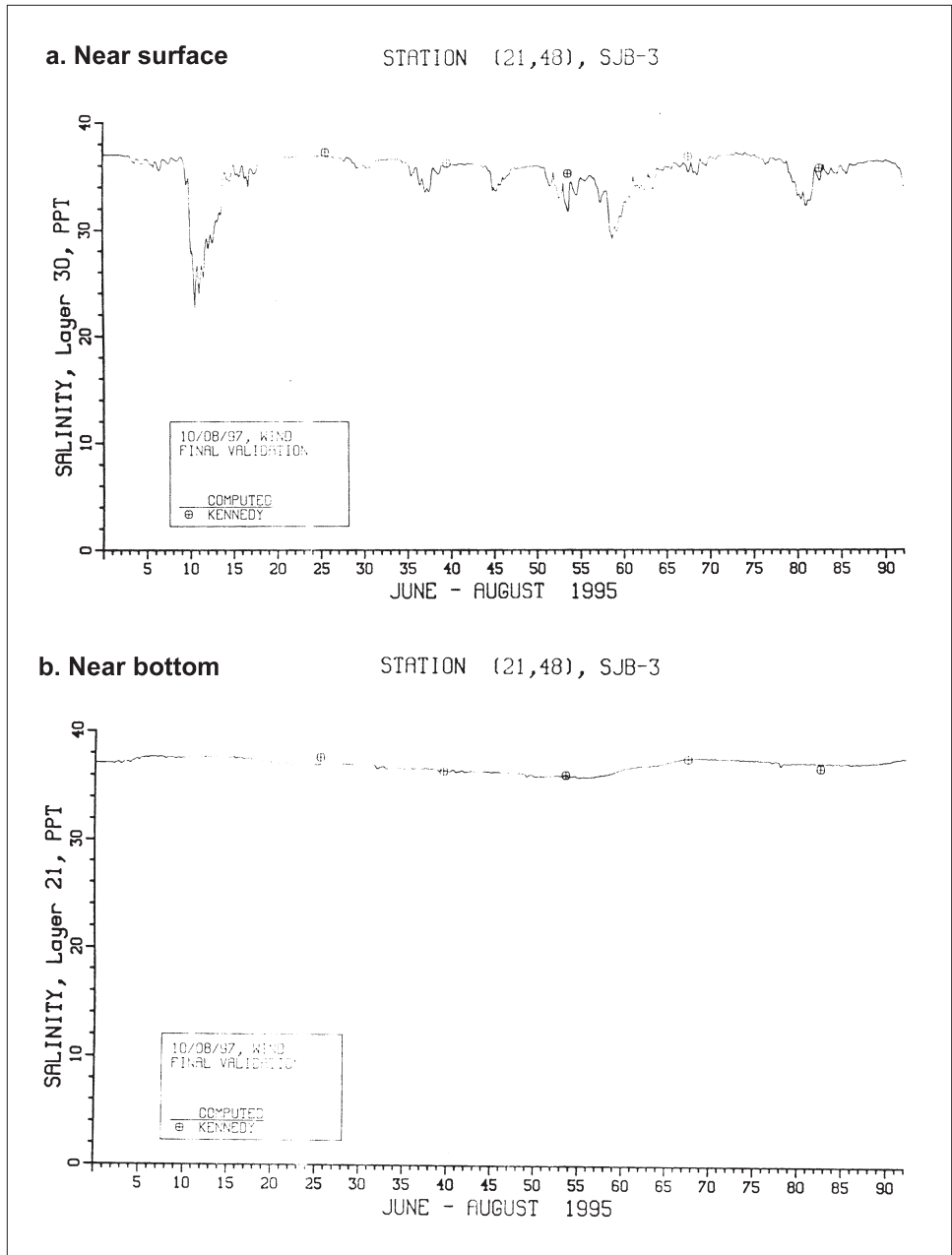


Figure 6-8. Comparison of computed and observed salinity at SJB-3

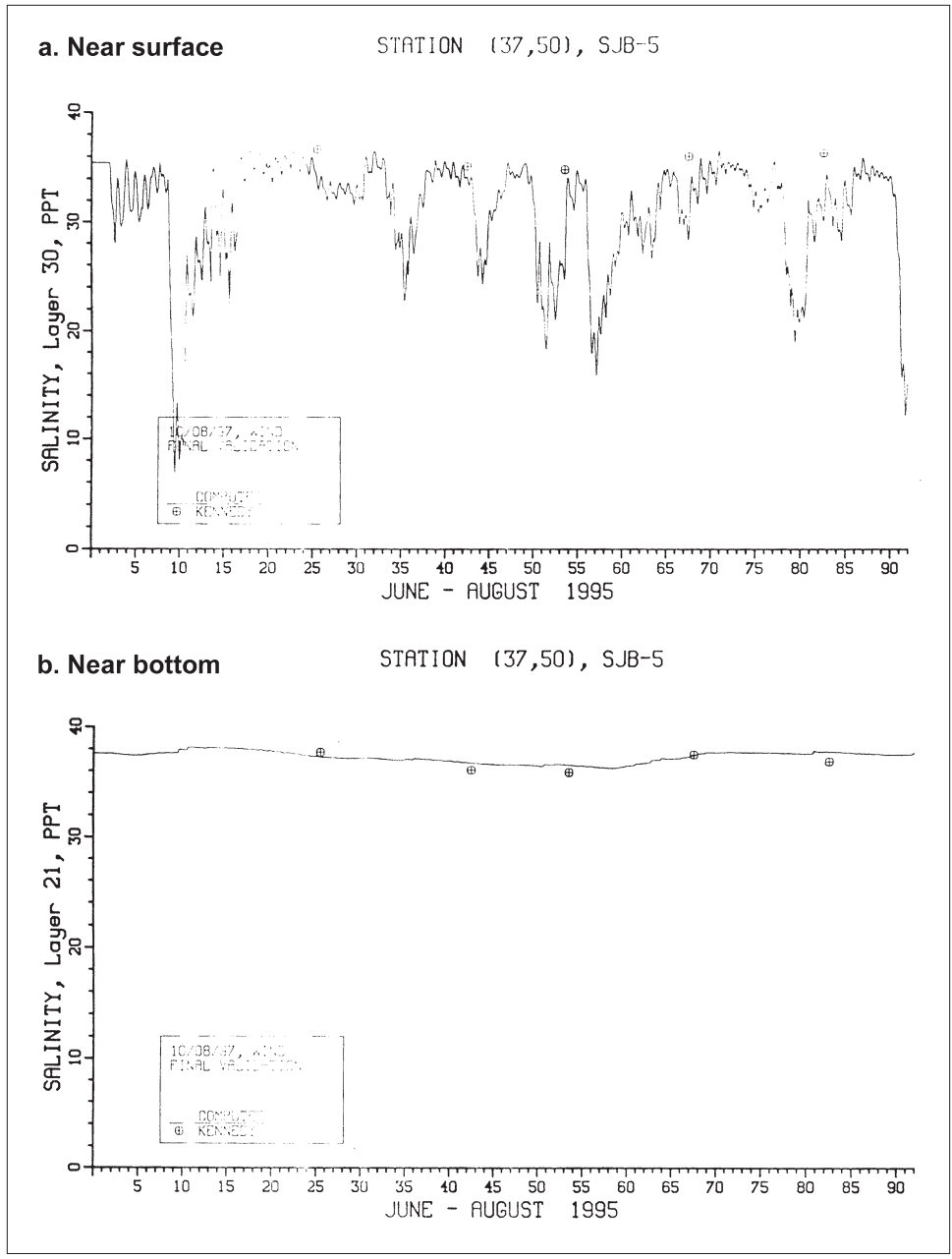


Figure 6-9. Comparison of computed and observed salinity at SJB-5

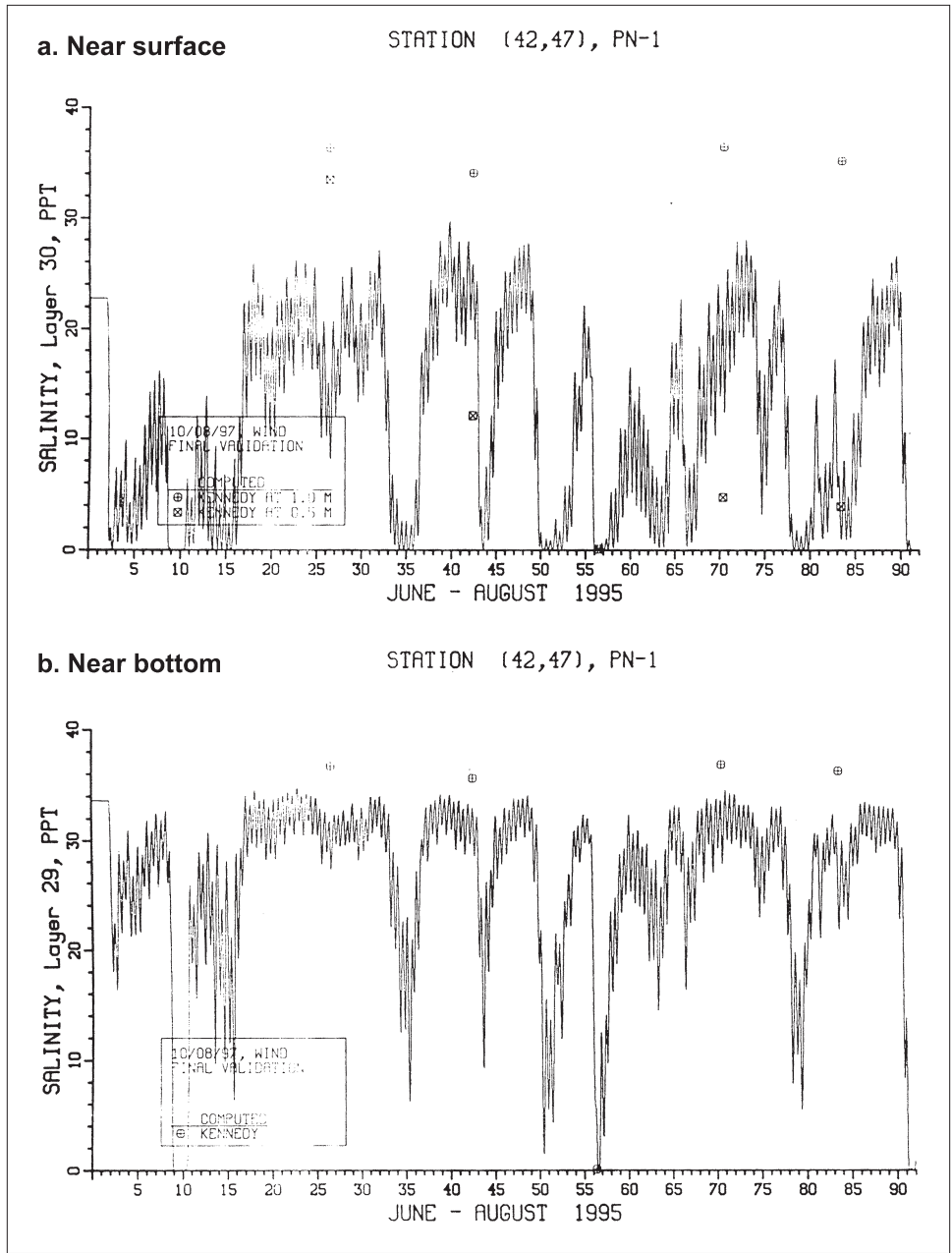


Figure 6-10. Comparison of computed and observed salinity at PN-1

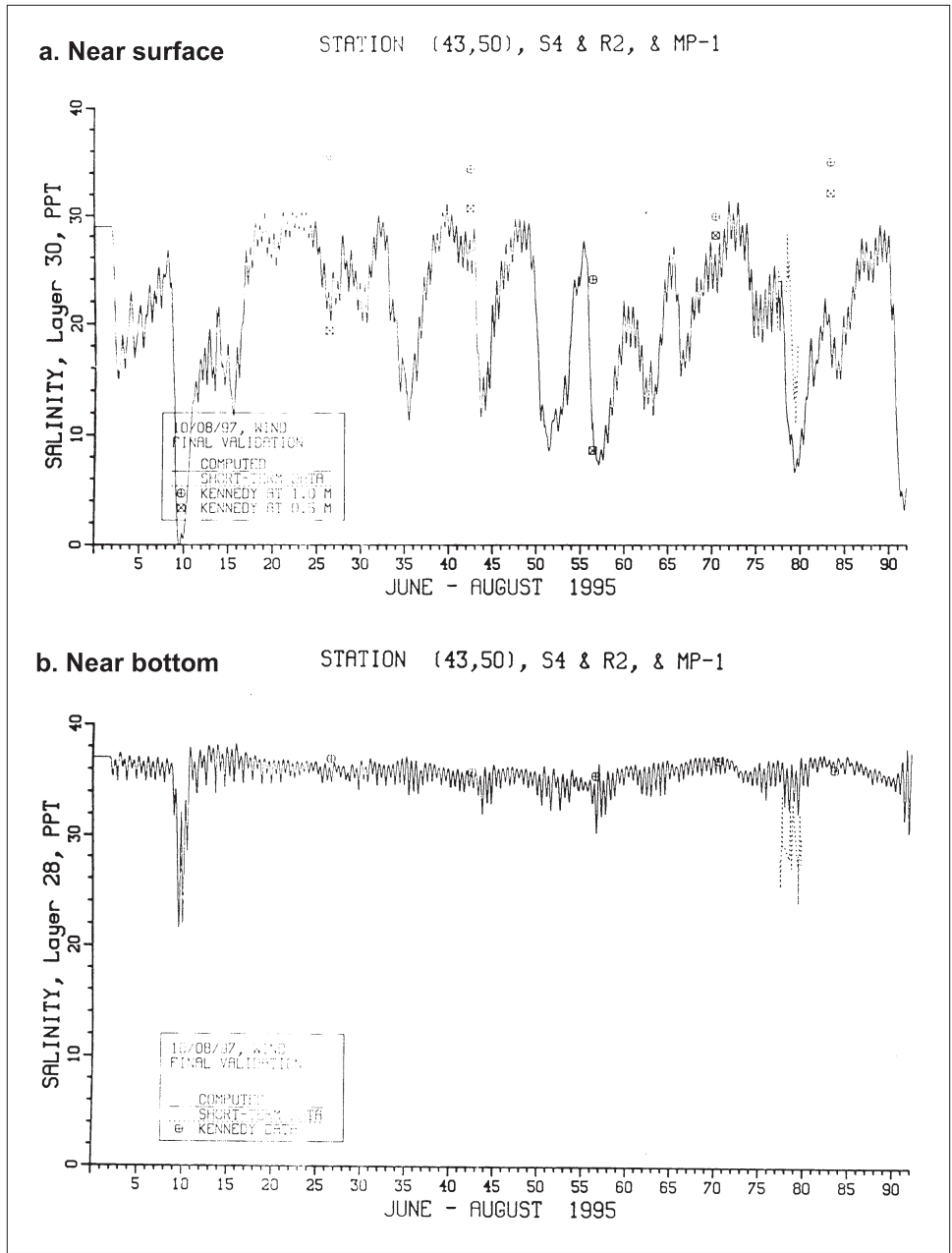


Figure 6-11. Comparison of computed and observed salinity at S4

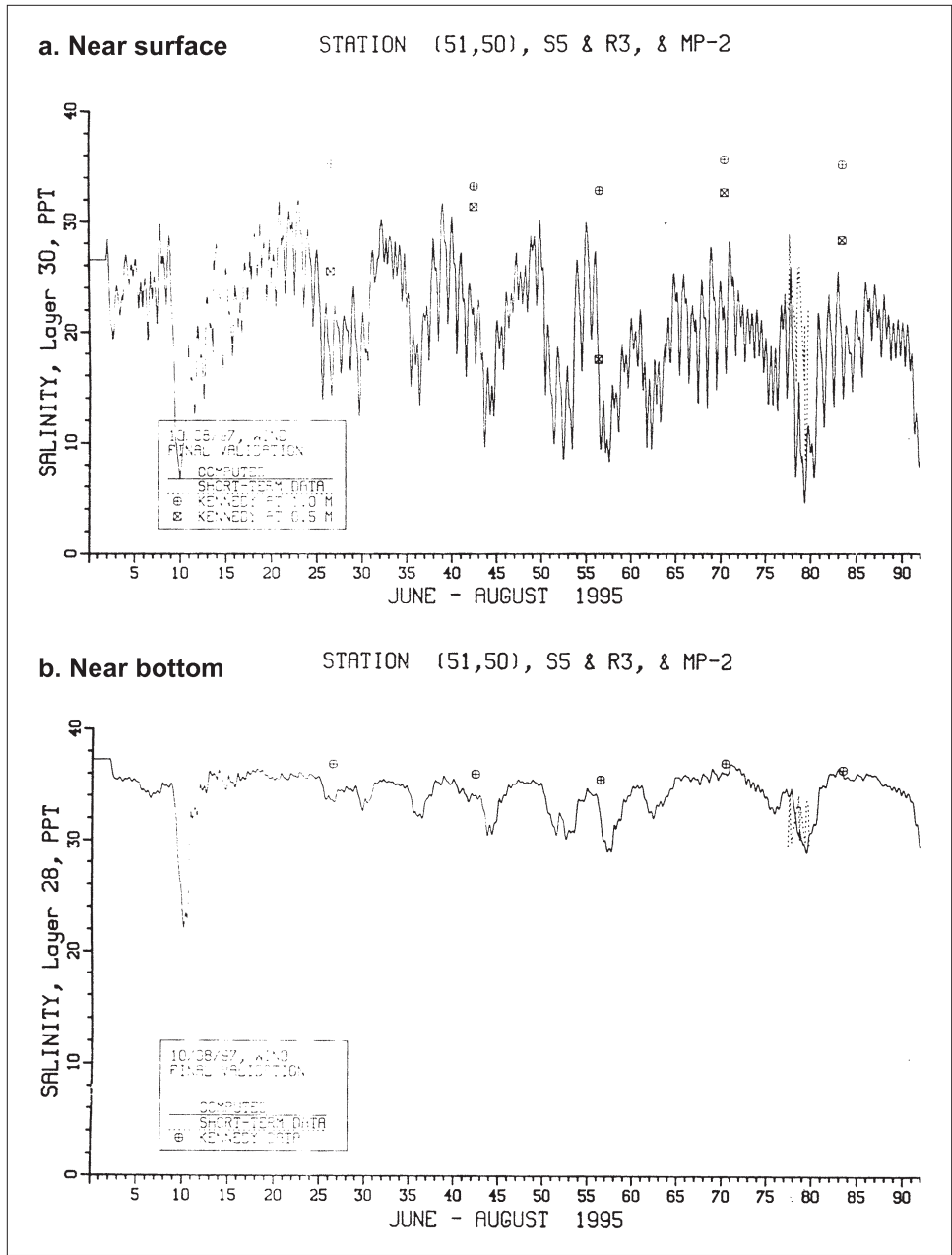


Figure 6-12. Comparison of computed and observed salinity at S5

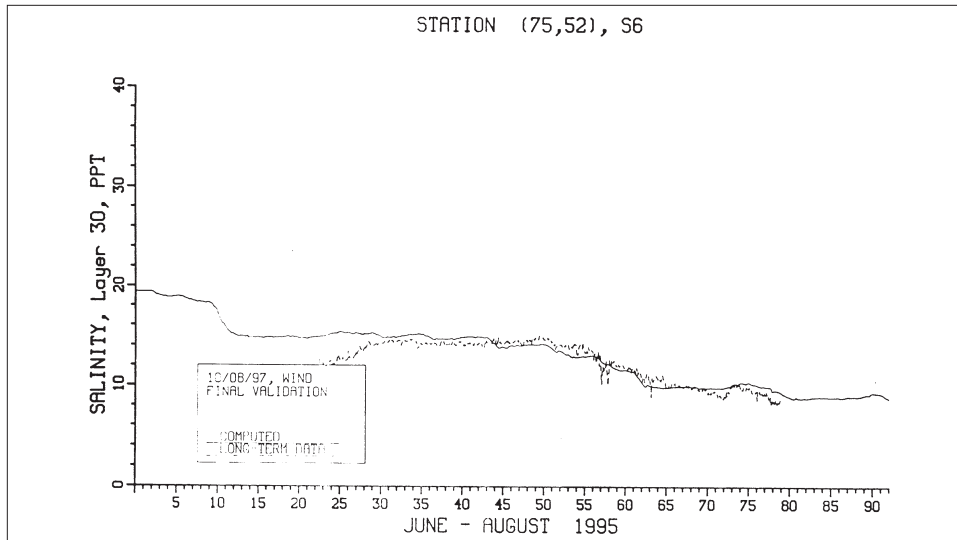


Figure 6-13. Comparison of computed and observed salinity at S6

Reproduction of the Exchange Between Canals

An important component of the skill assessment of the model is the illustration that the model can accurately compute the exchange between the various lagoons, especially the exchange between San Juan Bay and Laguna San José and between Laguna La Torrecilla and Laguna San José since this will have a major impact on water quality computations in Laguna San José and the viability of various management strategies to improve flushing. Figures 6-20 through 6-22 show the computed flux at the eastern end of Martín Peña Canal, the western end of Canal Suárez and between Laguna La Torrecilla and Laguna de Piñones. Total flux volumes in cubic meters for the entire three months have been computed and are shown on the plots. The net flux through Caño Martín Peña is about 1/4 of that through Canal Suárez and is directed toward San Juan Bay, whereas the flux through Canal Suárez is directed toward Torrecilla. The net flux through the Torrecilla - Piñones canal is directly into Torrecilla. These fluxes, of course, represent the sum of the net freshwater inflows into the various lagoons minus the volume of water evaporated. An evaporation rate of 82 in./yr was assumed in the computations.

The bounds on flux determined from a USGS survey (Ellis et. al. 1976) over one tidal cycle in 1974 are superimposed on the plots. It can be seen that the computed bounds in Canal Suárez and the Torrecilla - Piñones canal agree with the USGS data quite well. The bounds on the computed flux through Martín Peña Canal don't agree as well, but conditions in the eastern end of Martín Peña are different from those that existed in 1974. Significant sedimentation and the disposal of debris has occurred in this part of the system since 1974, resulting in the eastern end of Caño Martín Peña becoming clogged. As a result, special model adjustments were necessary as discussed in the next section.

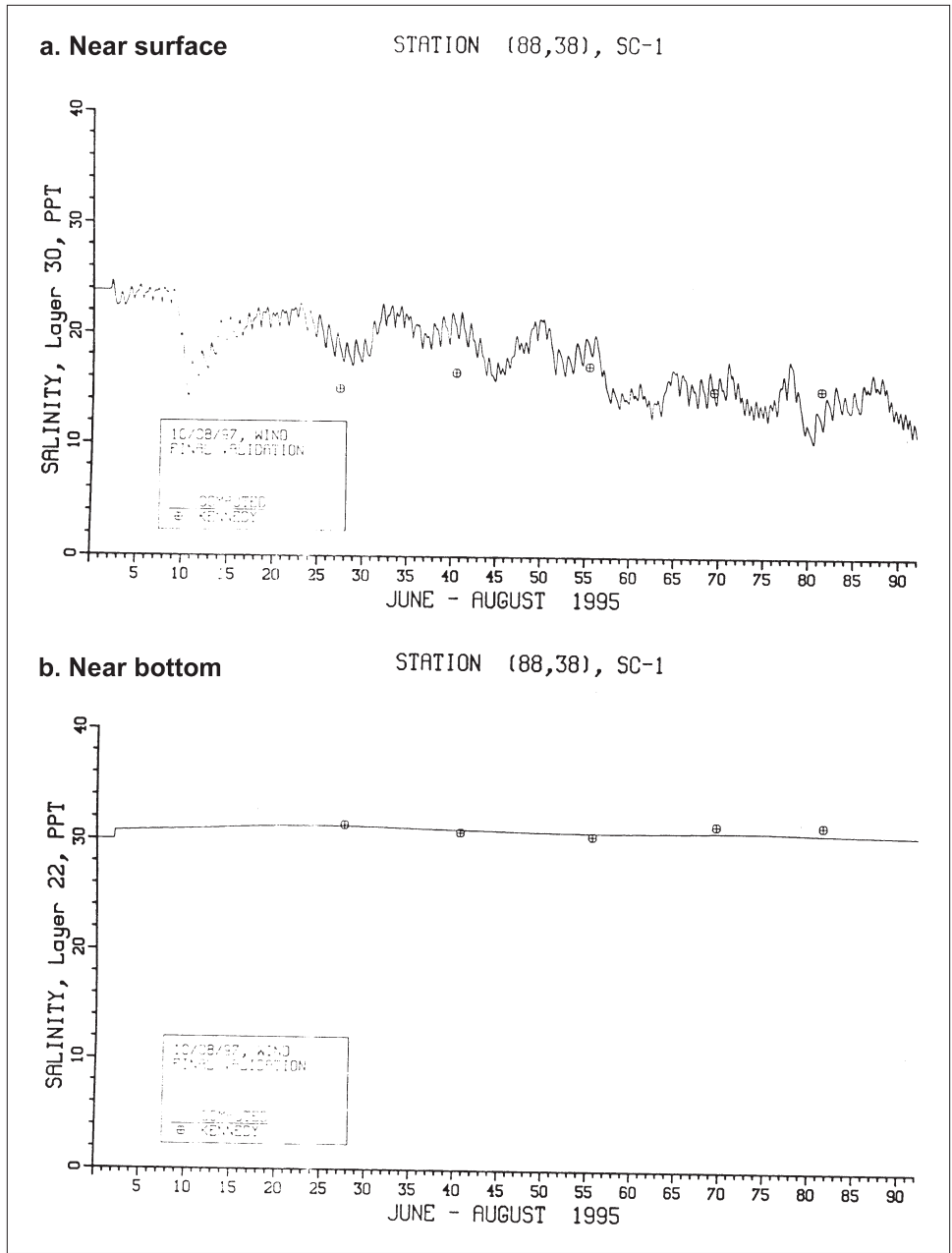


Figure 6-14. Comparison of computed and observed salinity at SC-1

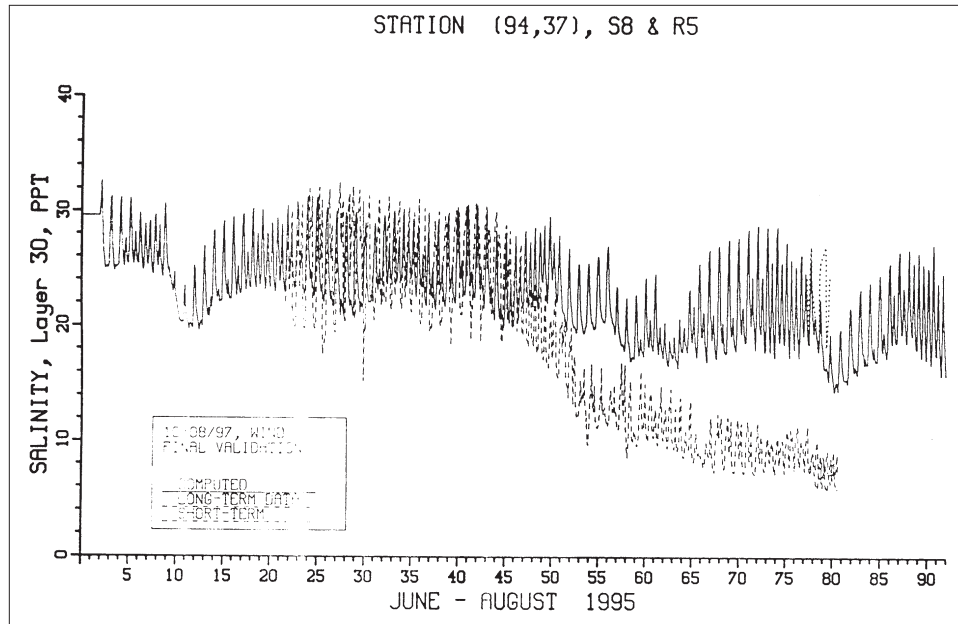


Figure 6-15. Comparison of near surface computed and observed salinity at S8

Figures 6-23 through 6-25 show comparisons of computed flux in Martín Peña Canal, Canal Suárez, and the Torrecilla-Piñones canal with the flux determined from the ADCP data collected during 17-19 August 1995. Generally the agreement is quite good and, with the USGS data agreement, increases confidence that the hydrodynamic model computes the proper exchange between the various bodies of water comprising the SJBE system.

Model Coefficients

The only model parameters available for variation during skill assessment of the hydrodynamic model are the bottom friction, or drag coefficient, horizontal diffusion coefficient, and minimum and maximum values of the vertical diffusion coefficients for momentum and salinity. The value of the bottom drag coefficient was set to 0.002 throughout most of the system. The major exception was in the eastern end of Caño Martín Peña and the canal connecting Torrecilla and Laguna de Piñones. As previously discussed, the eastern end of Martín Peña is severely constricted with debris such as old refrigerators that have been dumped into the canal over the past few years. Values of the bottom drag coefficient specified in these areas were 0.0075 and 0.0040, respectively.

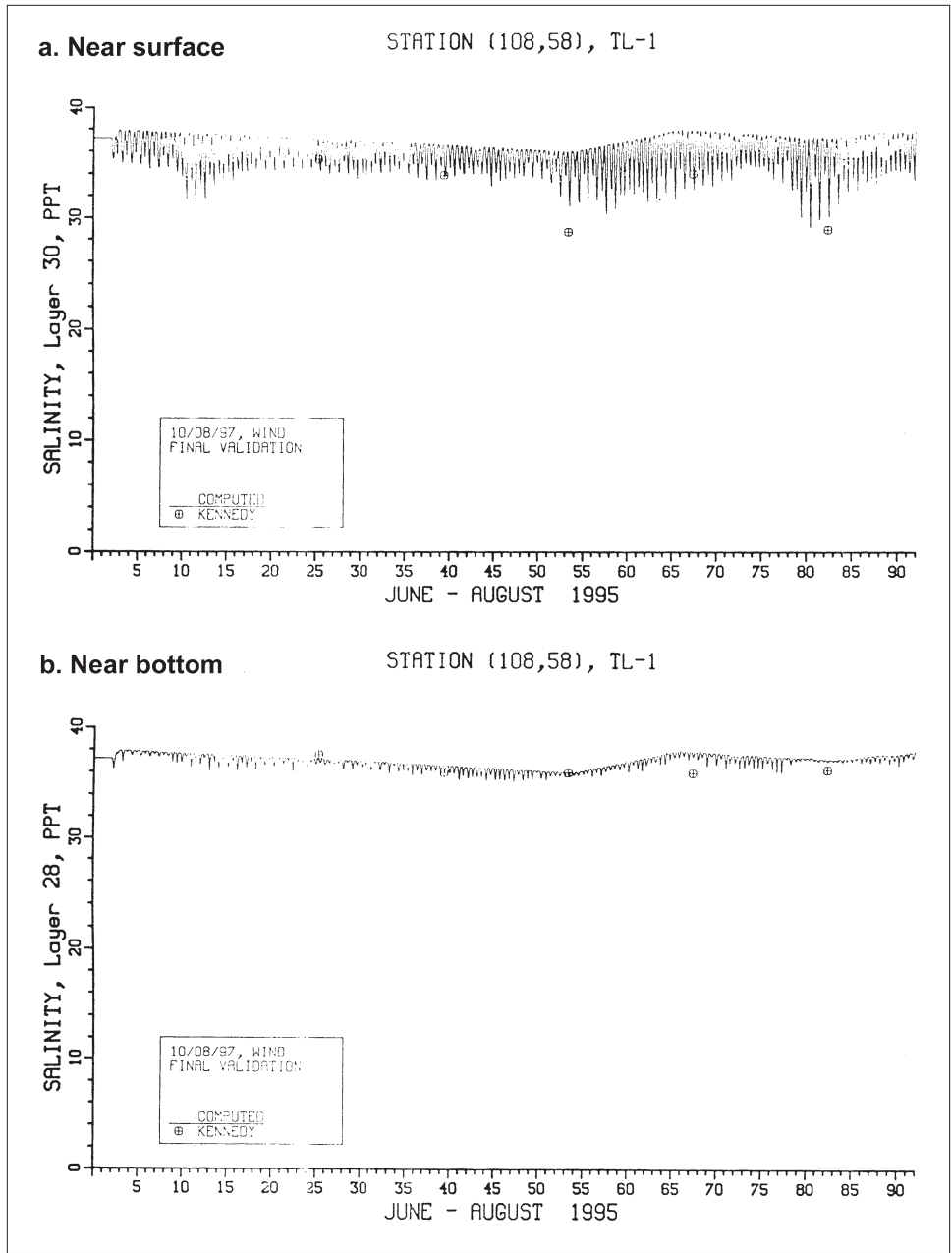


Figure 6-16. Comparison of computed and observed salinity at TL-1

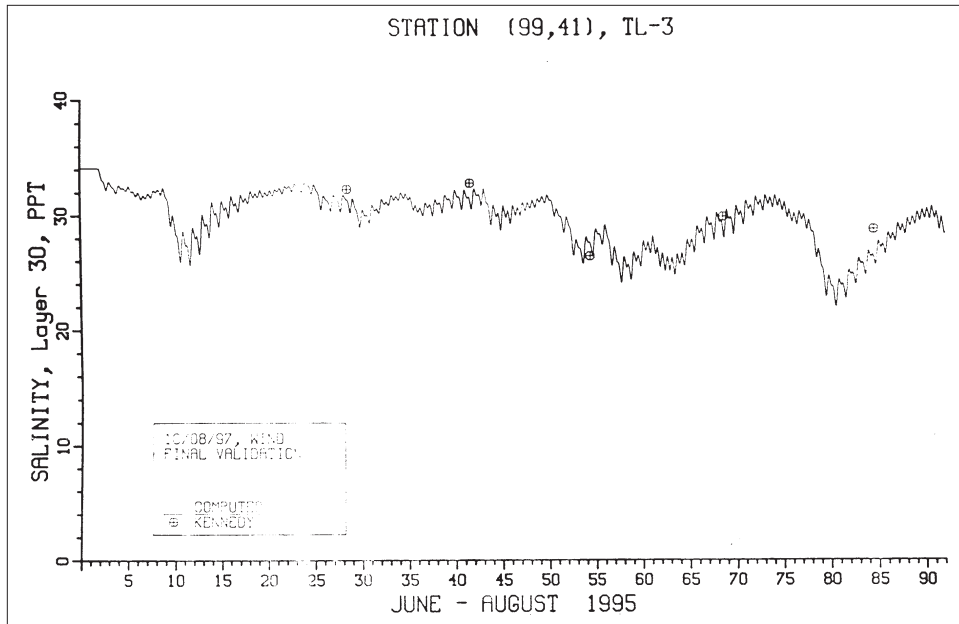


Figure 6-17. Comparison of near surface computed and observed salinity at TL-3

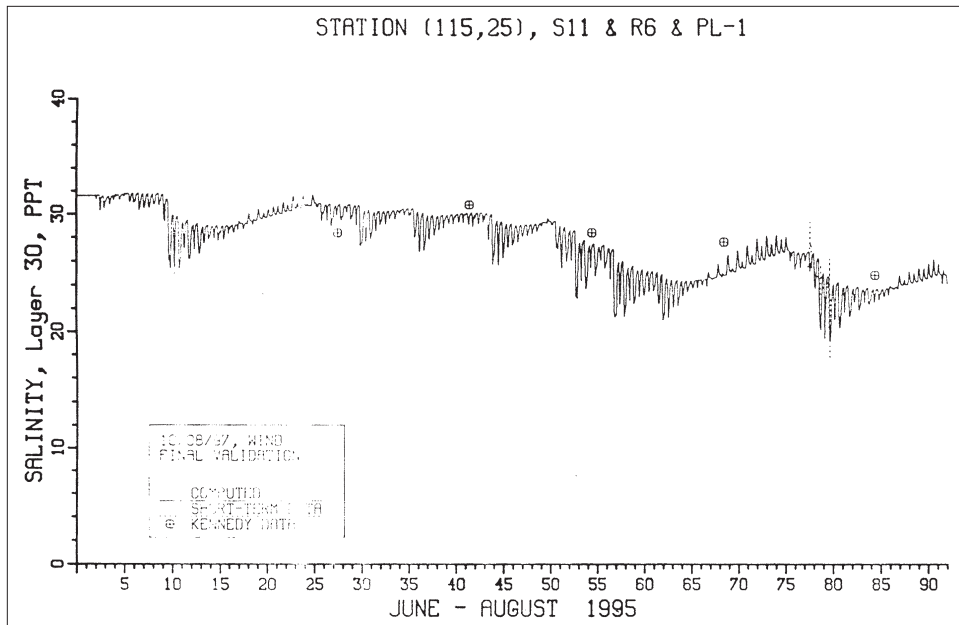


Figure 6-18. Comparison of near surface computed and observed salinity at PL-1

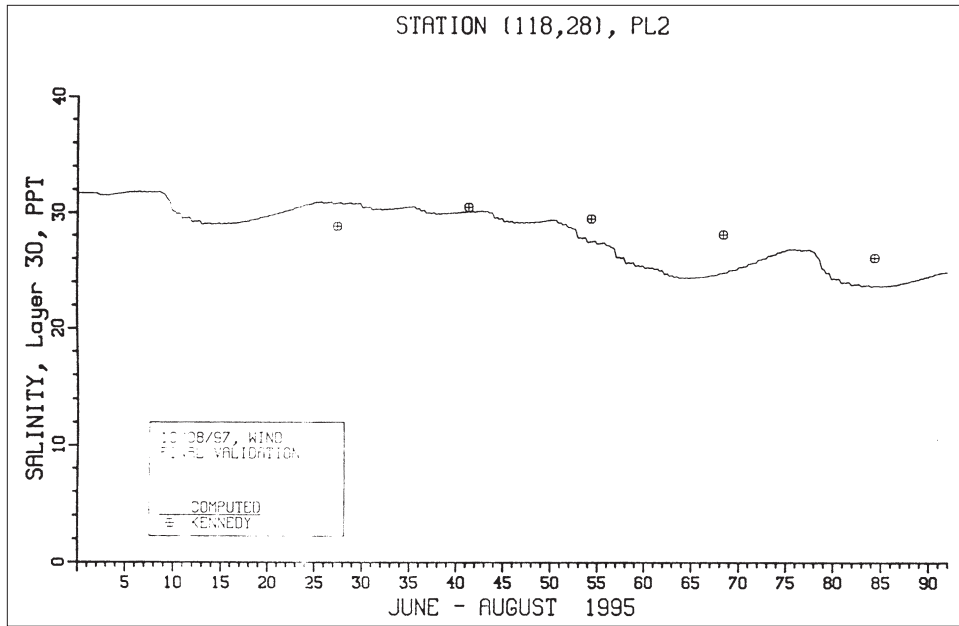


Figure 6-19. Comparison of near surface computed and observed salinity at PL-2

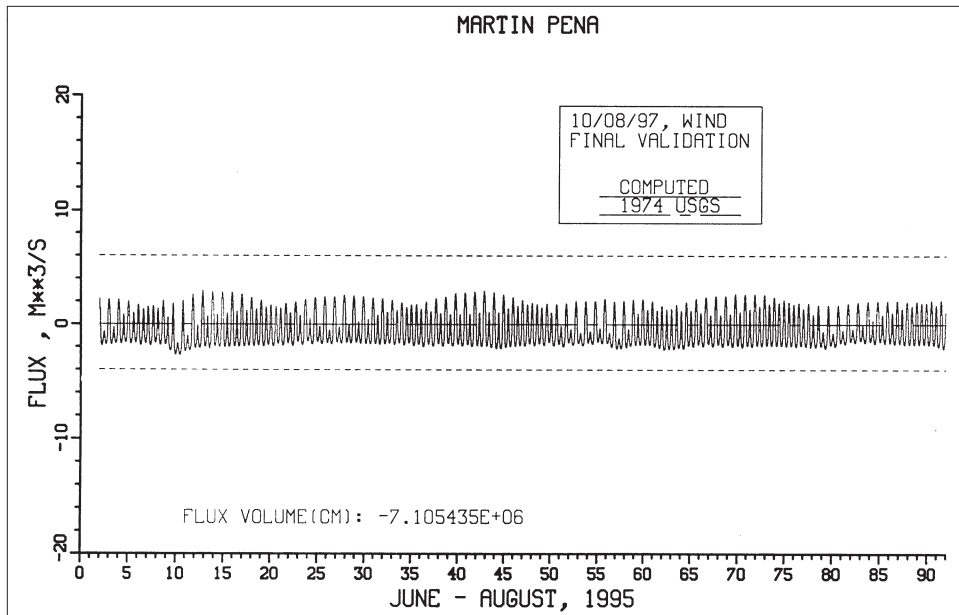


Figure 6-20. Computed flux through Martin Pena Canal compared with USGS data

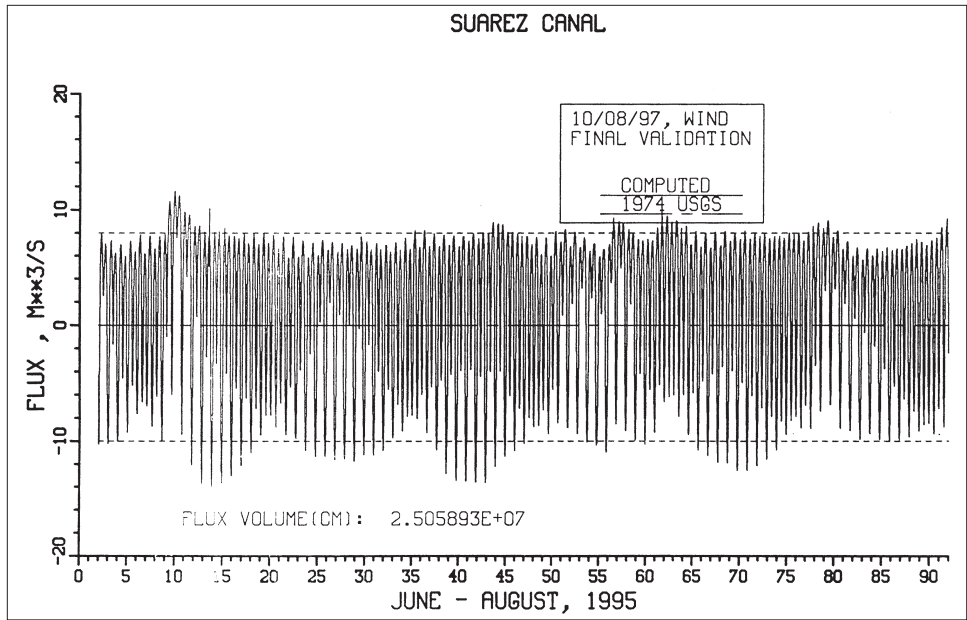


Figure 6-21. Computed flux through Suarez Canal compared with USGS data

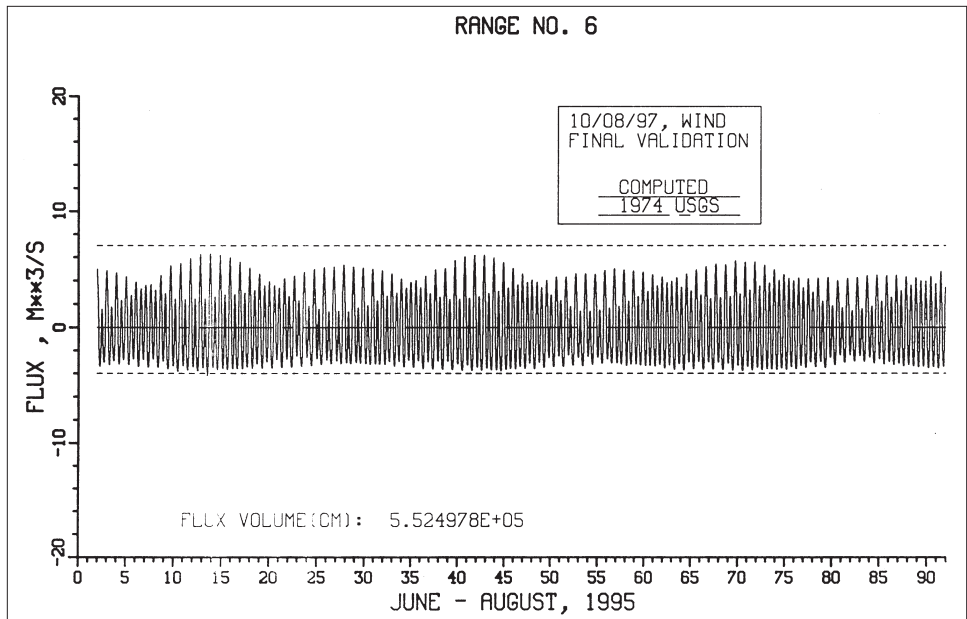


Figure 6-22. Computed flux through Torrecilla - Pinones Canal compared with USGS data

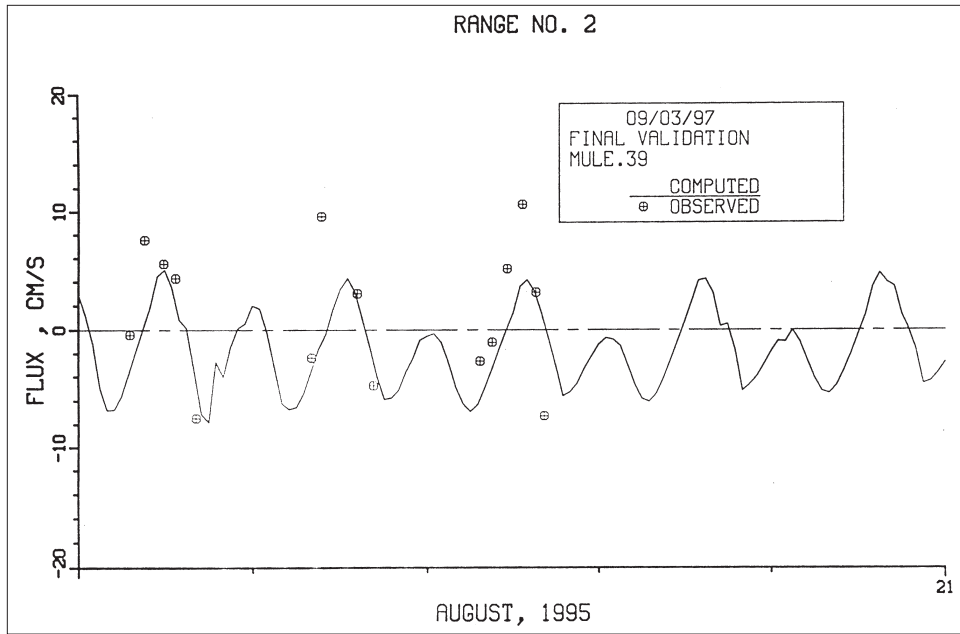


Figure 6-23. Comparison of computed flux at Range 2 with flux determined from ADCP data

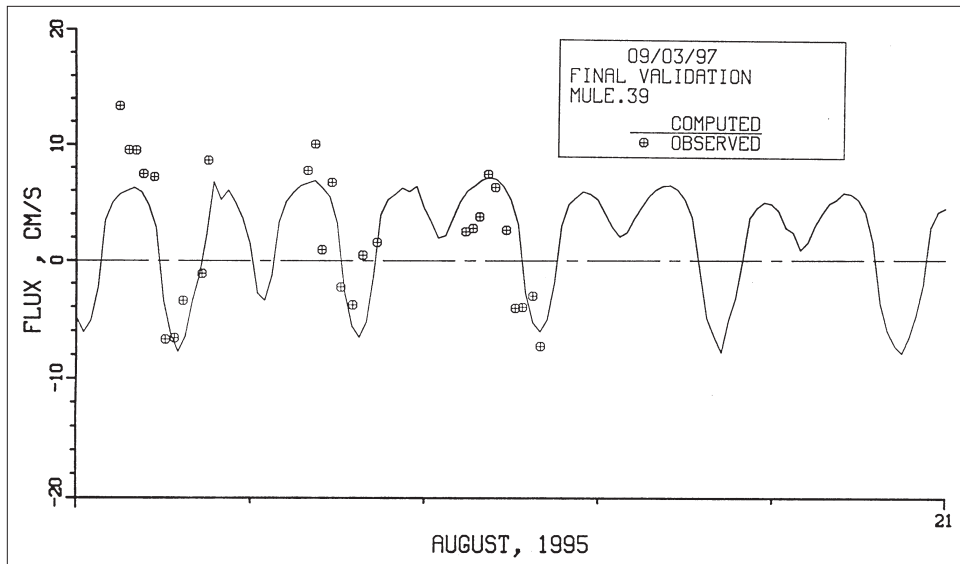


Figure 6-24. Comparison of computed flux at Range 4 with flux determined from ADCP data

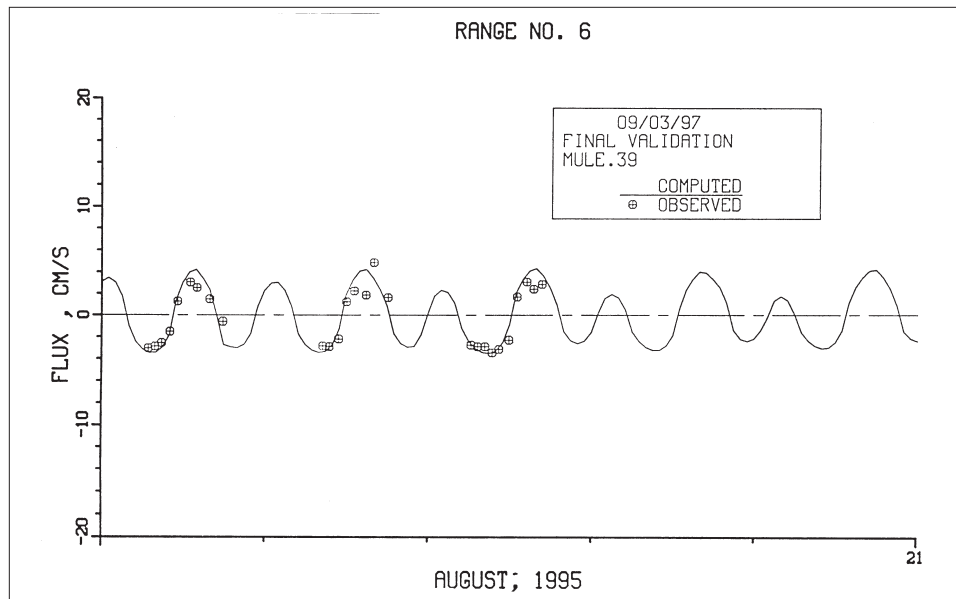


Figure 6-25. Comparison of computed flux at Range 6 with flux determined from ADCP data

The horizontal diffusion coefficient is the same in both horizontal directions. The value selected was $10 \text{ m}^2/\text{sec}$. This value is typical of values employed in other studies as well as values reported in the literature by other modelers.

With the coefficients in the vertical turbulence k-e model being considered as universal coefficients, the only parameters available for variation are the bounds on the computed vertical eddy viscosity and diffusion coefficients. The minimum values specified for the vertical viscosity and vertical diffusivity were 5 and $0.001 \text{ cm}^2/\text{sec}$, respectively, whereas, the maximum value for both was set to $500 \text{ cm}^2/\text{sec}$. These minimum and maximum limits are the same as previously employed in a study on Chesapeake Bay (Johnson et. al. 1991).

Conclusions

Skill assessment of the hydrodynamic model focused on illustrating the ability of the model to reproduce tides throughout the SJBE system; to reproduce the salinity throughout the modeled system, with particular focus on reproducing the extreme stratification that develops during storm events; and to properly compute the exchange of water between the various lagoons in the system. Although data for comparison with the model were limited due to fouling of the long-term meters by the warm tropical waters of the SJBE system, enough data were available to create confidence that the hydrodynamic model reproduces the basic hydrodynamics of the SJBE system so that model results can be used to provide transport for the water quality model.

7 Water Quality Model Calibration and Skill Assessment

The purpose of calibration is to demonstrate that the model can adequately simulate observed conditions. Once this is done, then the model can be used as a predictive tool to determine what effect a proposed action might have. Over 50 simulations were made during calibration. During these simulations, kinetic coefficients were adjusted within accepted tolerances, estimated loads were reviewed and adjusted if necessary, and new processes were added to the WQM. The results presented here represent the culmination of the knowledge gained during the 50 plus calibration simulations. Listed in Table 7-1 are values for the calibration parameters described in Chapter 4 and Table 4-2.

The period 1 June through 31 August 1995 was used for WQM calibration. Model calibration was assessed via plots of model output and observed data. Scatter plots of model output and observed data provide an indication of overall model performance. Calibration period-average longitudinal transect plots were used during calibration as they are indicative of model performance at a variety of locations during the simulation. Time-series plots for selected locations demonstrate the WQM output agreement with observations in specific locations over time.

Table 7-1. Parameter Values		
Symbol	Value	Units
AANOX	0.5	
ANC	0.167	gm N gm ⁻¹ C
AOCR	2.67	gm O ₂ gm ⁻¹ C
AONT	4.33	gm O ₂ gm ⁻¹ N
ANDC	0.933	gm N gm ⁻¹ C
APCmin	0.01	gm P gm ⁻¹ C
APCmax	0.024	gm P gm ⁻¹ C

(Sheet 1 of 3)

Table 7-1. (Continued)

Symbol	Value	Units
BMr	0.01	day ⁻¹
BPR	0.215	day ⁻¹
CChl	60	gm C mg ⁻¹ chl
FCD	0.0	0 ≤ FCDx ≤ 1
FCDP	0.1	0 ≤ FCDP ≤ 1
FCLP	0.55	0 ≤ FCLP ≤ 1
FCRP	0.35	0 ≤ FCRP ≤ 1
FNI	0.0	0 ≤ FNIx ≤ 1
FNIP	0.0	0 ≤ FNIP ≤ 1
FND	1.0	0 ≤ FNDx ≤ 1
FNDP	0.1	0 ≤ FNDP ≤ 1
FNL	0.0	0 ≤ FNLx ≤ 1
FNLP	0.55	0 ≤ FNLP ≤ 1
FNR	0.0	0 ≤ FNRx ≤ 1
FNRP	0.35	0 ≤ FNRP ≤ 1
FPD	1.0	0 ≤ FPDx ≤ 1
FPDP	0.5	0 ≤ FPDP ≤ 1
FPI	0.0	0 ≤ FPI ≤ 1
FPIP	0.2	0 ≤ FPIP ≤ 1
FPL	0.0	0 ≤ FPLx ≤ 1
FPLP	0.2	0 ≤ FPLP ≤ 1
FPR	0.0	0 ≤ FPRx ≤ 1
FPRP	0.1	0 ≤ FPRP ≤ 1
FR	5.6	m ⁻³ gm ⁻¹ C day ⁻¹
Ih	50	Langleys day ⁻¹
Kcod	30	day ⁻¹
Kdc	0.025 to 0.25	day ⁻¹
Kdcalg	0.0	m ³ gm ⁻¹ C day ⁻¹
Kdn	0.2 to 2.0	day ⁻¹
Kdnalg	0.0	m ³ gm ⁻¹ C day ⁻¹
Kdp	0.05	day ⁻¹
Kdpalg	0.2	m ³ gm ⁻¹ C day ⁻¹
Keb	0.09 to 2.8	m ⁻¹
Kechl	0.029	m ² mg ⁻¹
Kfc	5.0	day ⁻¹
KHn	0.01	gm N m ⁻³
KHndn	0.1	gm N m ⁻³
KHnt	1.0	gm N m ⁻³
KHocod	0.5	gm O ₂ m ⁻³
KHodoc	0.5	gm O ₂ m ⁻³
KHomb	2.0	gm O ₂ m ⁻³
KHont	1.0	gm O ₂ m ⁻³

(Sheet 2 of 3)

Table 7-1. (Concluded)

Symbol	Value	Units
KHp	0.001	gm P m ⁻³
KHr	0.5	gm O ₂ m ⁻³
Klc	0.15 to 1.5	day ⁻¹
Klcalg	0.0	m ³ gm ⁻¹ C day ⁻¹
Kln	0.3 to 3.0	day ⁻¹
Klnalg	0.0	m ³ gm ⁻¹ C day ⁻¹
Klp	0.075	day ⁻¹
Klpalg	0.0	m ³ gm ⁻¹ C day ⁻¹
Kr	2.44	m day ⁻¹
Krc	0.005	day ⁻¹
Krcalg	0.0	m ³ gm ⁻¹ C day ⁻¹
Krn	0.005	day ⁻¹
Krnalg	0.0	m ³ gm ⁻¹ C day ⁻¹
Krp	0.005	day ⁻¹
Krpalg	0.0	m ³ gm ⁻¹ C day ⁻¹
KTb	0.069	°C ⁻¹
KTcod	0.041	°C ⁻¹
KTg1	0.008	°C ⁻²
KTg2	0.01	°C ⁻²
KThdr	0.069	°C ⁻¹
KTmhl	0.069	°C ⁻¹
KTnt1	0.09	°C ⁻²
KTnt2	0.09	°C ⁻²
MBGM	0.0 to 0.16	gm C m ⁻²
NTm	0.07 to 0.7	gm N m ⁻³ day ⁻¹
PM	3.0	day ⁻¹
PO ₄ dmax	0.01	gm P m ⁻³
Tm	30	°C
Tmnt	30	°C
Tr	30	°C
Trcod	23	°C
Trhdr	20	°C
Trmnl	20	°C
WSl	0.3	m day ⁻¹
WSr	0.3	m day ⁻¹
WSa	0.05	m day ⁻¹

(Sheet 3 of 3)

Scatter Plots

Figure 7-1 contains calibration period scatter plots. The locations of circles indicate the correlation between model predictions and observed data. A perfect match between model and observed data is indicated by the diagonal line on each graph. Circles above the line indicate that the model is overpredicting for that observation. Circles below the line indicate that the model is underpredicting the observation. Observations used in these plots were typically obtained by means of a grab sample or in situ measurement and reflect the conditions in the water column at that instant. Model outputs used in these plots are the daily averages of the constituents of interest in cells corresponding to the sample site location. Some of the scatter in these plots can be attributed to the phasing resulting from comparison of instantaneous observations with daily average model results. Shown with each plot are the mean error (ME), absolute mean error (AME), root mean square (RMS) error, and relative error (RE) which is expressed as percent.

The mean error is a summary of the model tendency to overestimate or underestimate the observed data. Mean error can be zero even though large discrepancies exist in individual model-data comparisons. Mean error is computed as follows:

$$ME = \frac{\sum(O - P)}{n} \quad (7-1)$$

where

- ME = mean error
- O = observation
- P = model prediction
- n = number of observations

The absolute mean error is a measure of the average discrepancy between observations and model results. No differentiation is made between overestimation or underestimation. Absolute mean error is computed as follows:

$$AME = \frac{\sum|O - P|}{n} \quad (7-2)$$

where

- AME = absolute mean error

The root mean square error is an indication of the average discrepancy between observations and model results. It is computed as follows:

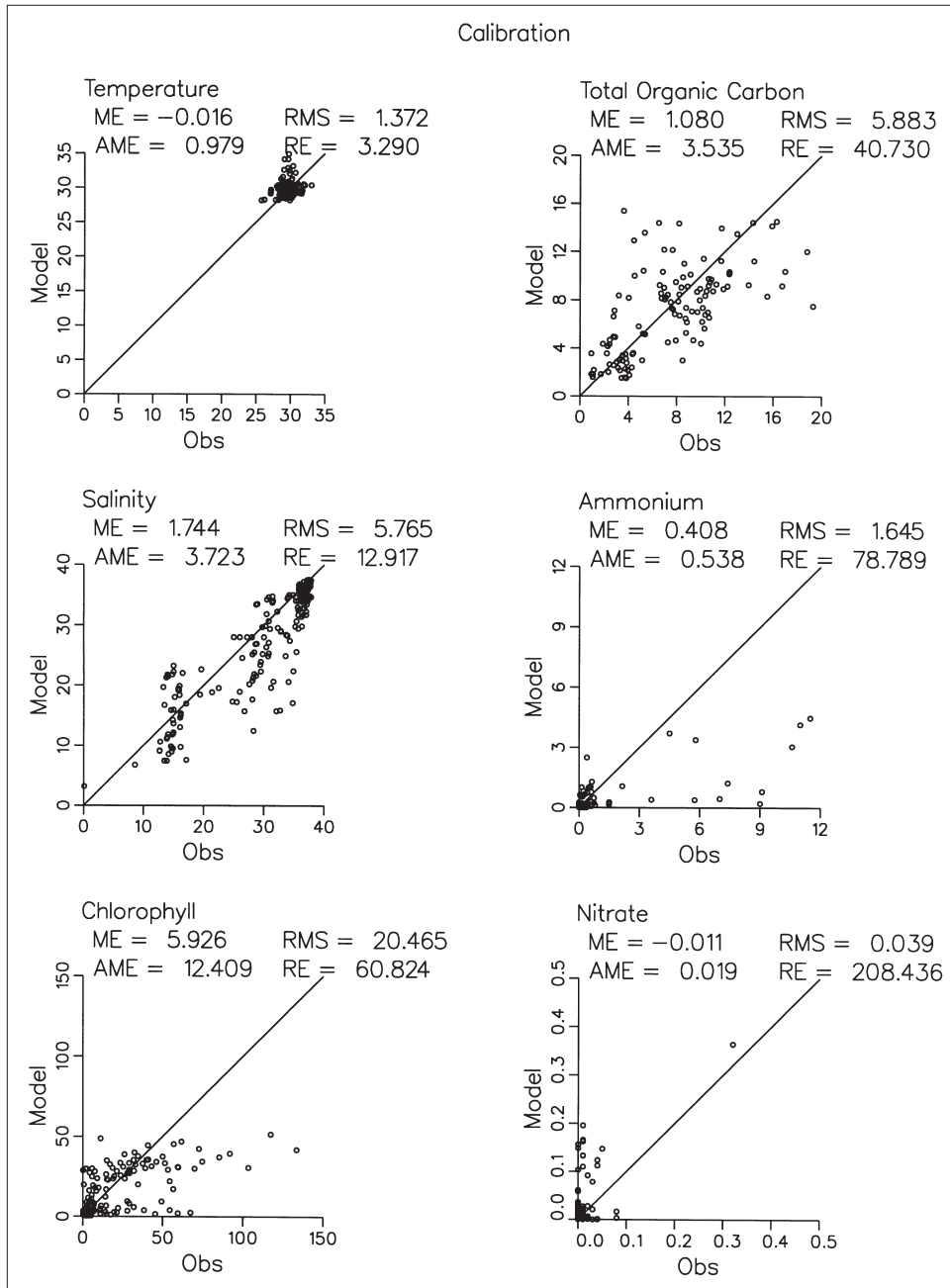


Figure 7-1. Calibration period scatter plots (continued)

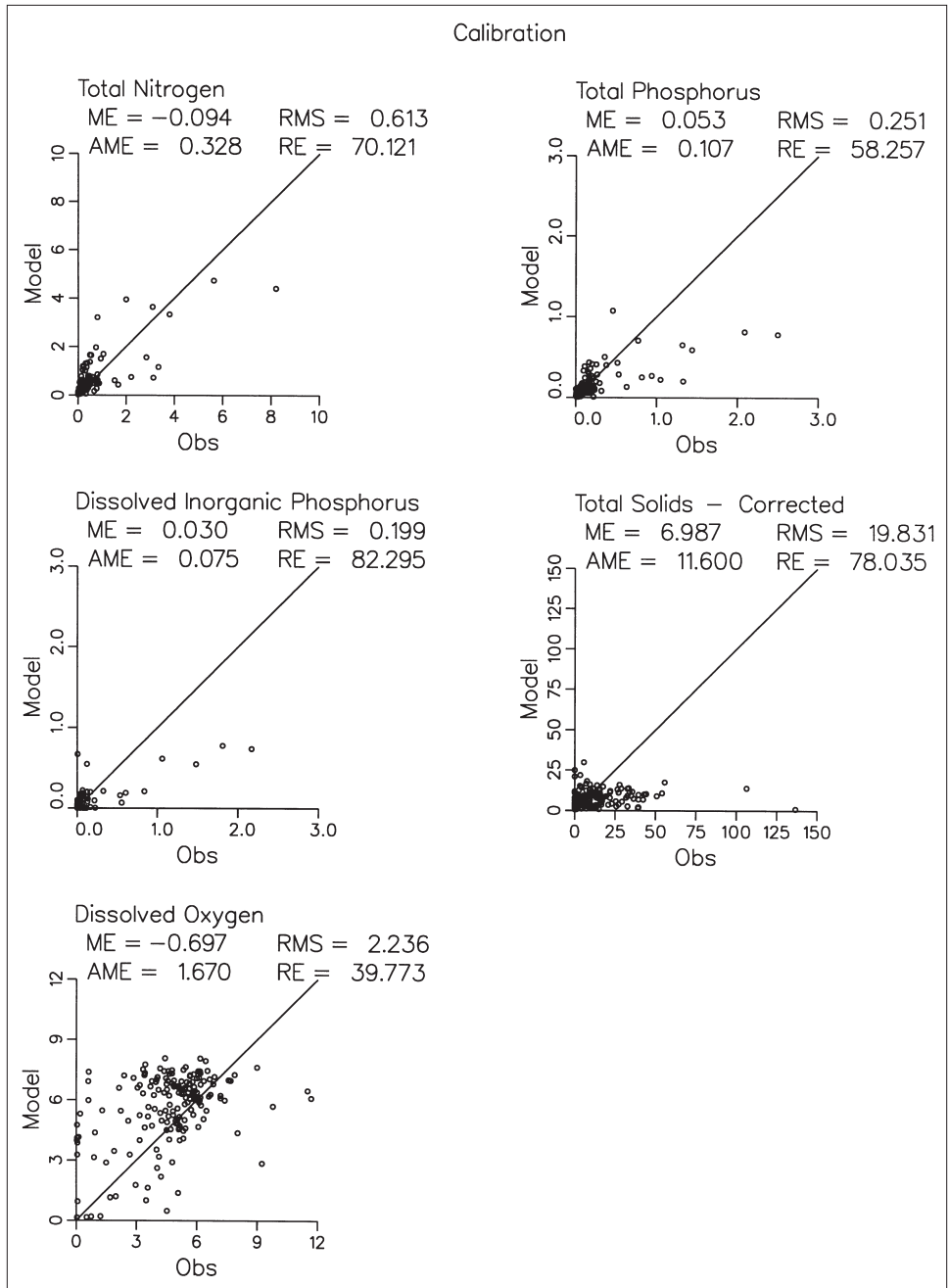


Figure 7-1. (concluded)

$$RMS = \sqrt{\frac{\sum(O - P)^2}{n}} \quad (7-3)$$

where

RMS = root mean square

The relative error is the absolute mean error normalized by the magnitude of the observations. It is expressed as a percent and is computed as follows:

$$RE = \frac{\sum|O - P|}{\sum O} \quad (7-4)$$

where

RE = relative error

Overall, the model does well for all constituents. The scatter plot for temperature indicates that the model results are in agreement with observations. The scatter plot for salinity indicates that model predictions agree reasonably well over a range of conditions. While not evident from these plots, ICM underpredicts salinity in Caño Martín Peña, Laguna de Piñones, and the southern portion of Laguna La Torrecilla. Results for chlorophyll indicate that ICM underpredicts extremely high values (over 75 ug/l) but does reasonably well for lower values. The total organic carbon scatter plot exhibits a significant amount of variability around the diagonal indicating that the model is reasonable over a range of conditions but underpredicts some high values.

The ammonium scatter plot indicates that the model underpredicts when concentrations are greater than 1 mg/l. Concentrations of this level and higher were typically only observed in borrow pits in the interior of the SJBE system. Observed nitrate concentrations were low with most being at or just above detection levels. The model indicates a few higher nitrate concentrations but most are very low, as are the observations. Model predictions agreed well with observations for total nitrogen over the 0- to 3-mg/l range but overpredict for the few observations greater than 3 mg/l.

Model predictions for dissolved inorganic phosphorus and total phosphorus are good with the exception of the model underpredicting concentrations exceeding 1 mg/l.

Overall the model overpredicts DO by about 0.70 mg/l, primarily on the surface in the eastern portion of the system, possibly due to overestimation of reaeration. Generally, bottom DO predictions agree favorably with observations. ICM underpredicts DO when concentrations are greater than 8 mg/l, which are supersaturated DO concentrations for the temperature and salinity of this system. Dissolved oxygen supersaturation is a result of

photosynthesis during daylight hours. The model uses calculated daily-average light; thus, photosynthesis and its contribution to DO production are daily-average values, whereas photosynthesis actually follows a sinusoidal pattern that peaks during daylight hours. All observations were collected during the day. Therefore, the model always tends to underpredict DO when supersaturated conditions prevail.

The scatter plot reveals that the WQM overpredicted anoxic and hypoxic conditions in some cases. Upon further investigation it was determined that half of these cases were occurring at stations in upper Laguna La Torrecilla, Blasina Canal, and in the canal leading to Laguna de Piñones. All five bottom observations at TL-5 indicated DO levels lower than 1 mg/l. Corresponding WQM results ranged from 3.14 to 5.3 mg/l. Dissolved oxygen observations in Piñones Canal at station PL-1 ranged from 0.6 mg/l to 3.7 mg/l. Corresponding model predictions ranged from 6.6 to 7.2 mg/l. Reasons for the poor model performance at these locations are several. First, Piñones Canal is influenced by the mangroves which it flows through. Loadings from the mangroves are not accounted for in the model. Second, Piñones Canal is modeled as one layer deep in the model which precludes any simulated stratification. Loads from Piñones Canal are discharged into Blasina Canal at TL-5 which would impact water quality at that location. Furthermore, observations at TL-5 indicate that the water column is stratified. Although Blasina Canal is modeled with two layers, this amount of resolution was insufficient to resolve the rather strong stratification observed in the field in this reach.

Model DO overprediction occurred at station MP-2 in Caño Martín Peña in the surface layer. Surface water at this station was influenced by thin, freshwater lenses which were too thin for the model to accurately resolve. Finally, there are stations where the model computed anoxic DO when anoxic DO existed, such as the bottom layer of MP-2. However, plots of anoxic observations against anoxic model predictions on the scatter plot yielded a single point rather than multiple points, which gives a false impression that the model rarely computes low DO when low, observed DO conditions existed.

The remaining cases where low DO conditions were overpredicted were distributed among the sampling stations. Three were from the bottom of Laguna San José at different sampling stations, one at the bottom of Laguna del Condado, and one at the bottom of San Antonio Canal. Reasons for overpredictions at any of these stations would be speculative. One of these overpredictions occurred at station SJ-1 (Laguna Los Corozos) whose time series results are shown in Figure 7-7. No clear reason is evident for this overprediction. This observation was the first at this station. All subsequent observations were much higher and agreed favorably with model results. Possibly, the first sample was obtained in a slightly different location or in a slug of “dirty water” recently discharged from the Baldorioty de Castro Pump Station.

Total suspended solids scatter plots indicate that the model performs reasonably well. During model calibration a problem with the total suspended solids data was discovered. Total suspended solids data had been collected and filtered but not rinsed with distilled water. Since some of the samples were collected in waters that were saline, the filtered material contained salt. When the filter was dried the salt remained and its weight was incorrectly attributed to suspended solids. In an attempt to compensate for this error, observed total suspended solids data were corrected by using the following relationship.

$$TSS_{new} = TSS_{obs} - \frac{C_{sal}}{C_{ocean}} TSS_{ocean} \quad (7.5)$$

where

TSS_{new} = new total suspended solids concentration

TSS_{obs} = observed total suspended solids concentration

C_{sal} = observed salinity at sampling location

C_{ocean} = observed salinity at ocean boundary

TSS_{ocean} = observed total suspended solids concentration at AO-1 and AO-2 (see Figure 2-1)

With this correction implemented, the agreement of model predictions and observations improved. ICM still underpredicted observations greater than 25 mg/l. All total suspended solids data presented in this report have been corrected in the manner described above.

Longitudinal Transect Comparisons

Calibration period-average longitudinal transect plots were made for a transect beginning at the mouth of San Juan Bay, passing through Caño Martín Peña, Laguna San José, Canal Suárez, ending at the mouth of Laguna La Torrecilla (see Figure 7-2). The route of this transect was selected so as to pass through five of the major features of the SJBE system. Two transects are shown for each constituent. One transect is for cells in the surface layer while the other is for cells in the bottom layer. Due to the bathymetry of the system, there are locations where the grid is only one layer thick which results in the same cell appearing in both the surface and bottom transects. Locations where this occurs include eastern Caño Martín Peña, Laguna San José, and Laguna La Torrecilla. The model average for the calibration period is shown on the transect plots as a solid line. The range of model predictions during the simulation is illustrated by the shaded region. Average values of sampling observations are indicated as a circle while the ranges of observations are indicated by the vertical bar through the circle. The model results presented here are averages over the

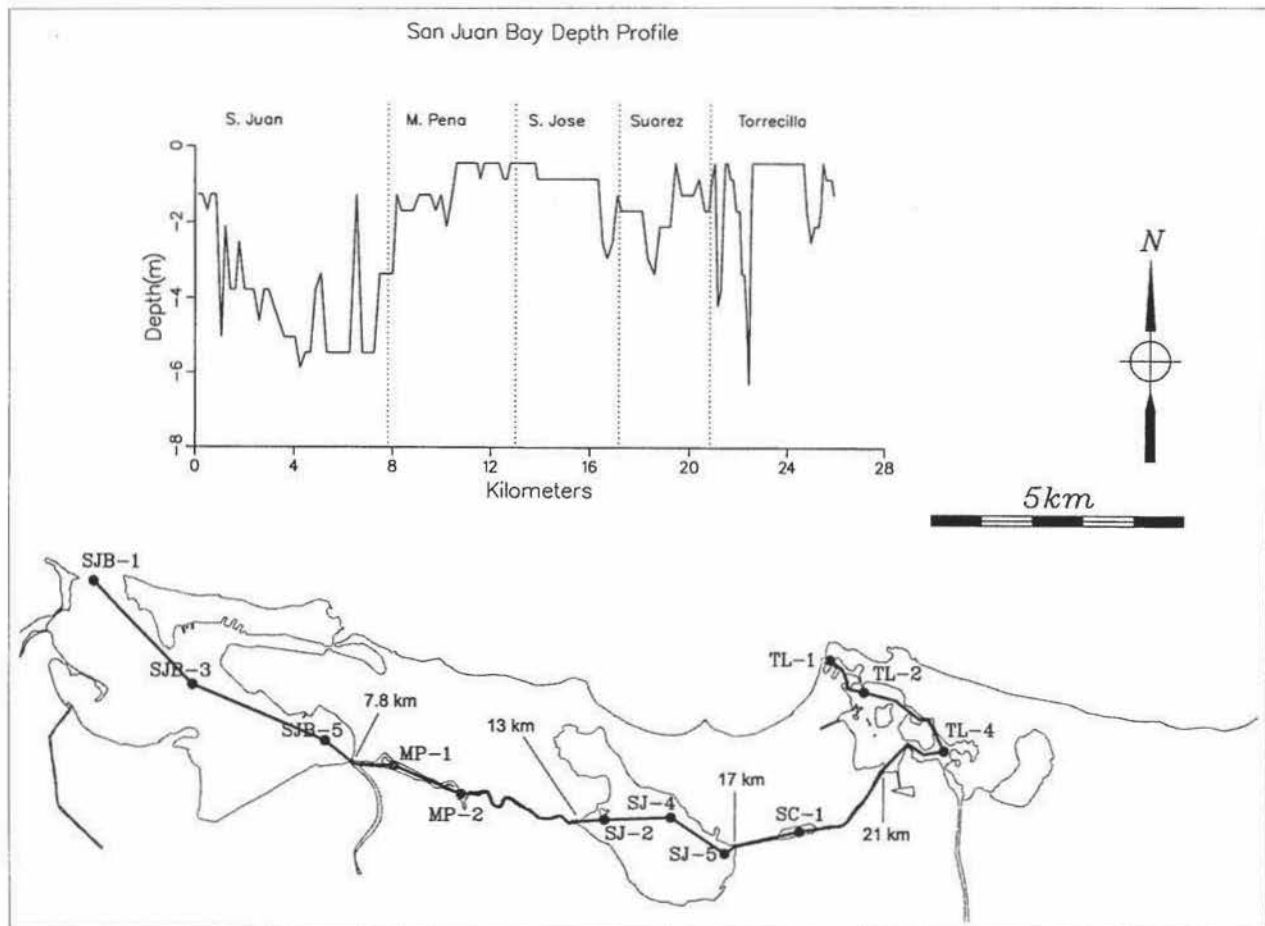


Figure 7-2. Longitudinal transect and observation stations used for preparing calibration-period average transect plots

whole calibration period and as such do not relate the effects of any temporal activity which might be reflected in the observed data.

Overall, as these plots indicate (see Figure 7-3), the model performs well. There are locations where the line denoting the model calibration average and the average of the observed data do not agree. However, the model does capture most of the means of the observations and their range.

As indicated in the description of the transect route, this transect passes through water bodies with very different characteristics. San Juan Bay is well flushed via tidal exchange with the Atlantic Ocean at its mouth and a secondary channel on the northeastern side, i.e., Caño de San Antonio. Due to the extensive exchange with the ocean, water quality in San Juan Bay is similar to that of the ocean. Laguna San José, which is located along the middle of the transect is completely landlocked with only limited exchange with the ocean via Caño Martín Peña and Canal Suárez. As a result, salinity in Laguna San José is less than half of ocean values. Laguna La Torrecilla on the eastern end of the system is a transition region between the interior of the system and the ocean. Water quality near the

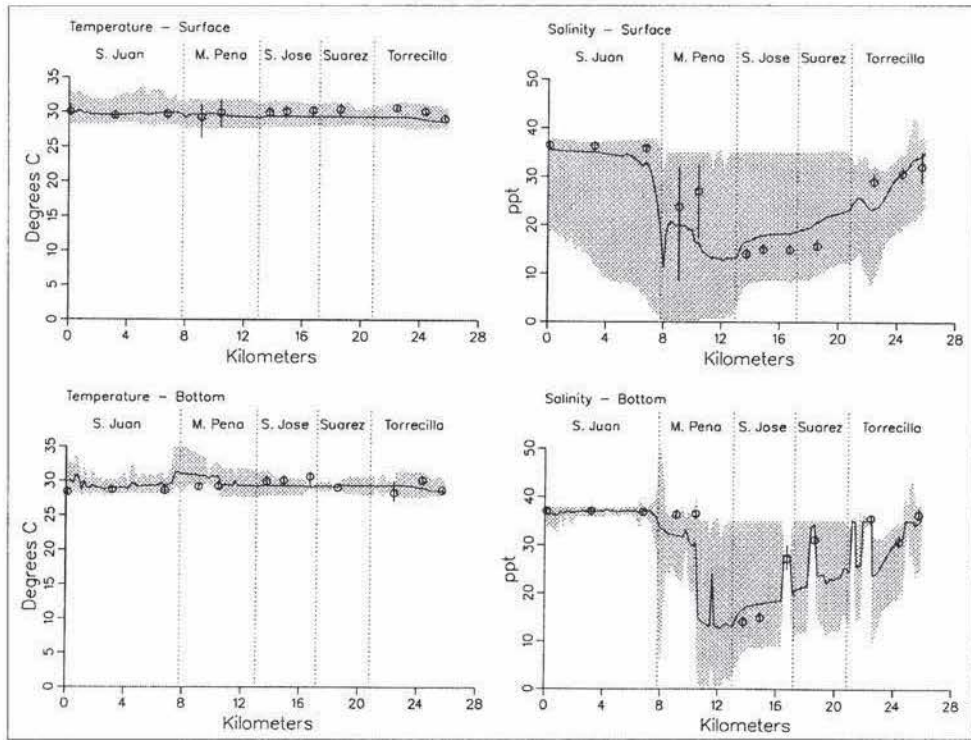


Figure 7-3. Calibration-period average, longitudinal transect plot of computed and observed water quality variables resulting from model calibration for summer 1995 (Sheet 1 of 8)

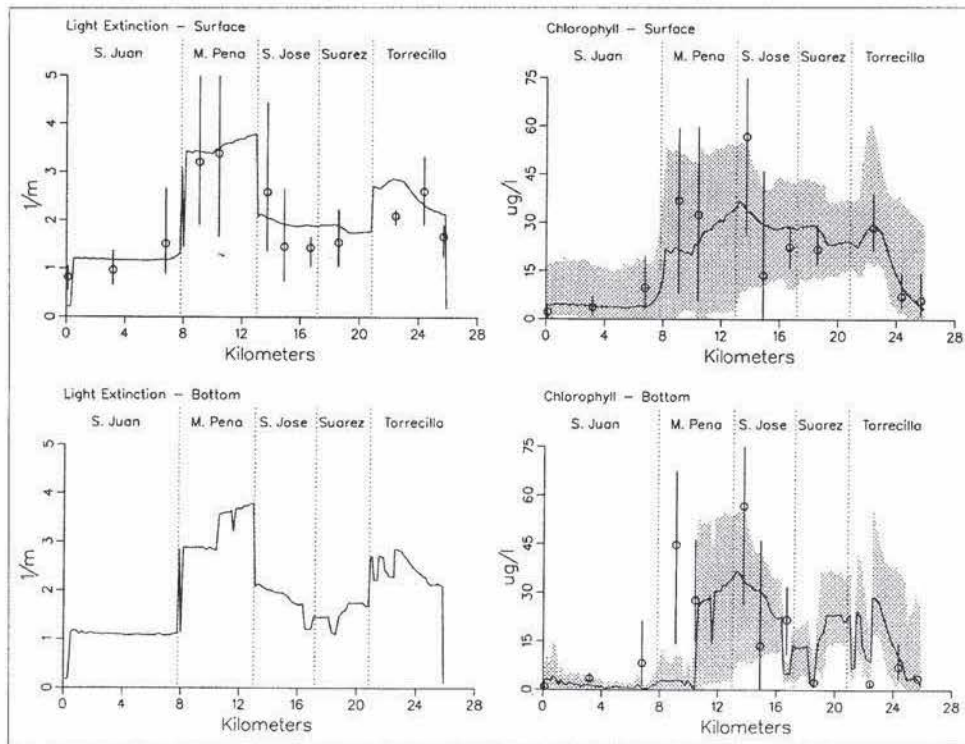


Figure 7-3. (Sheet 2 of 8)

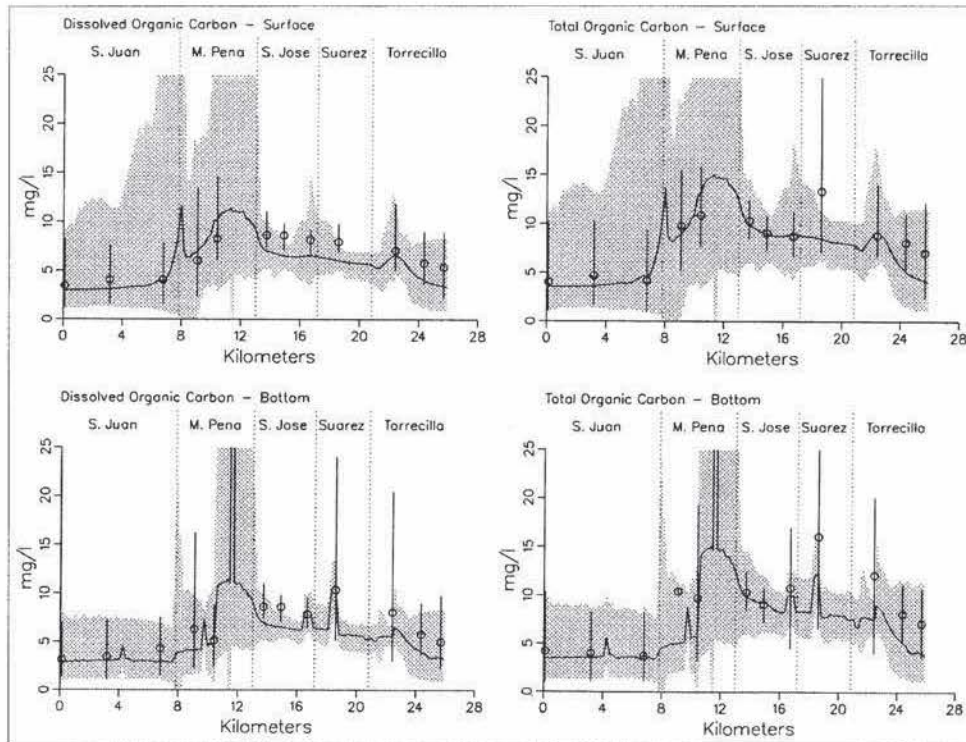


Figure 7-3. (Sheet 3 of 8)

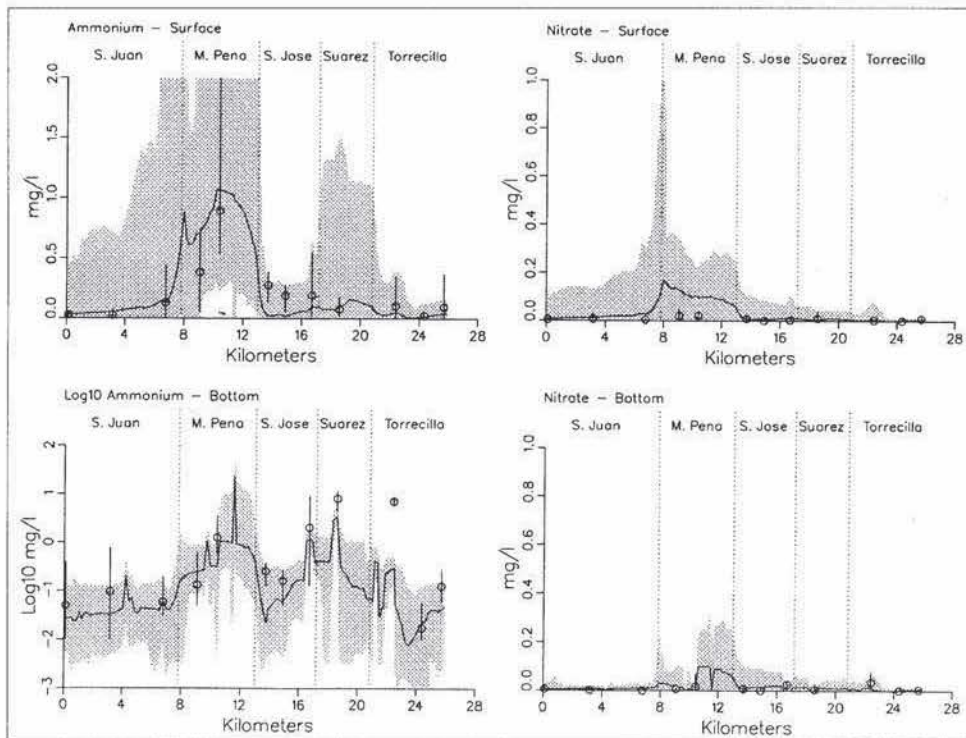


Figure 7-3. (Sheet 4 of 8)

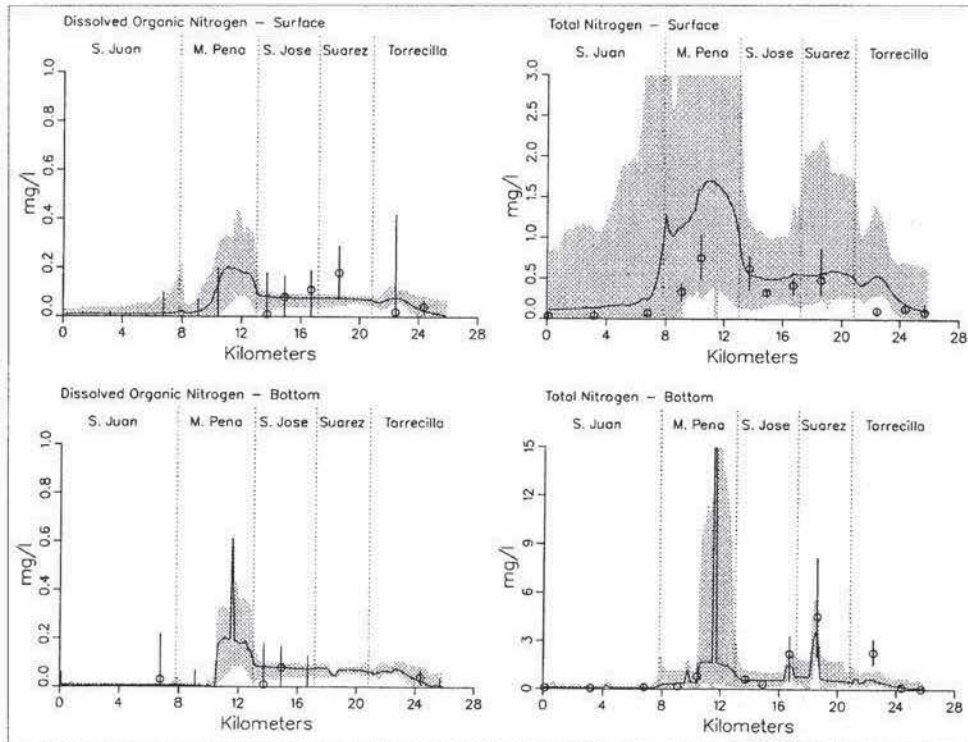


Figure 7-3. (Sheet 5 of 8)

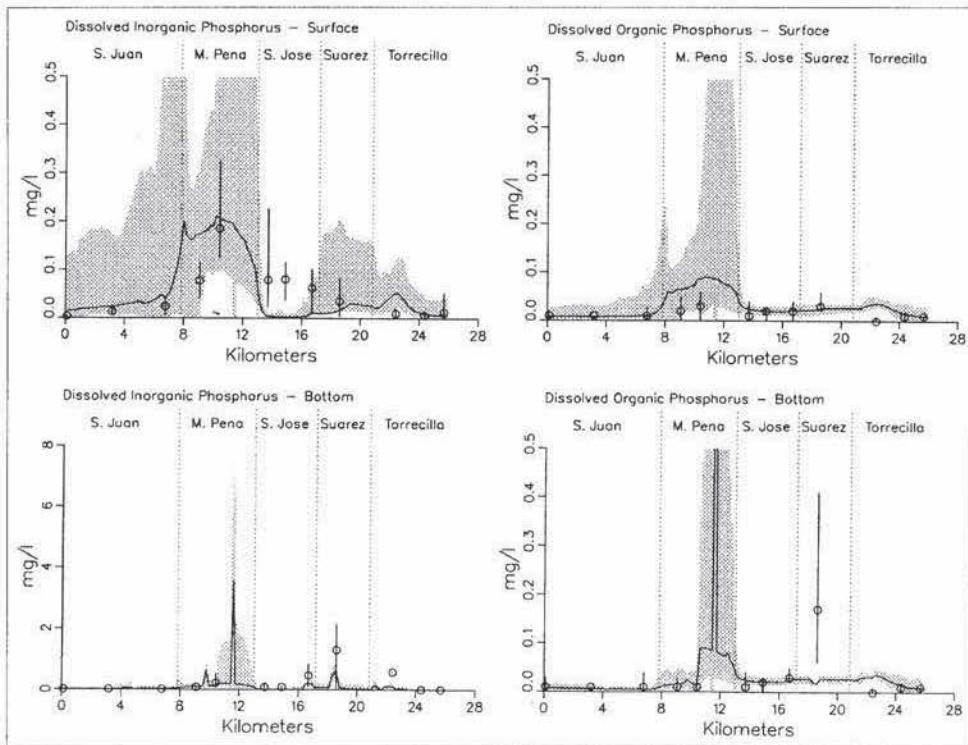


Figure 7-3. (Sheet 6 of 8)

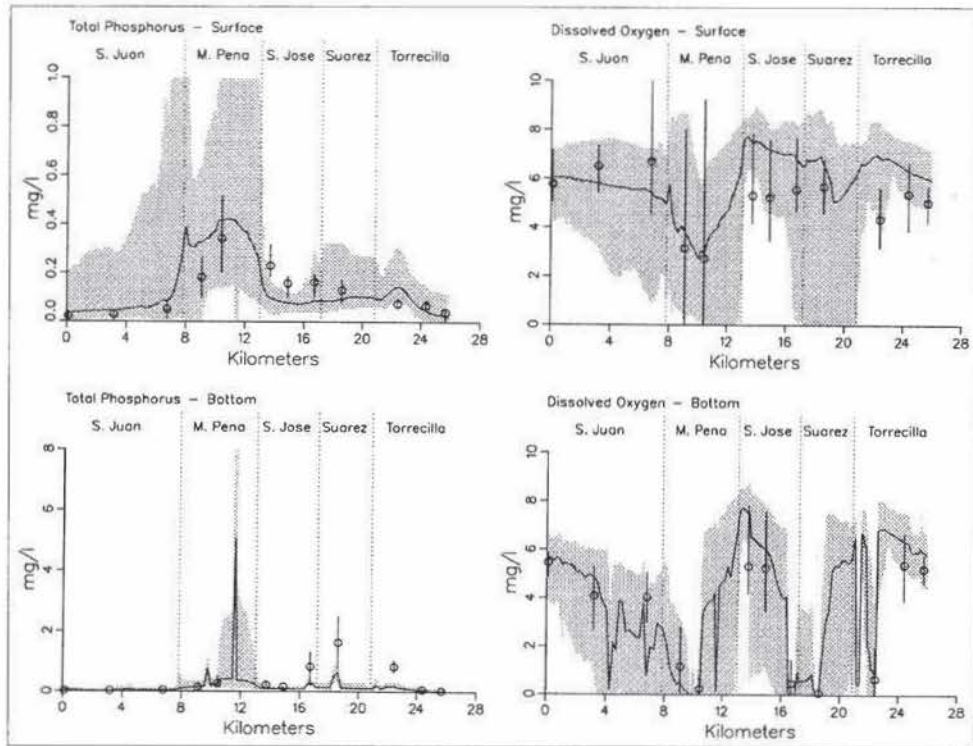


Figure 7-3. (Sheet 7 of 8)

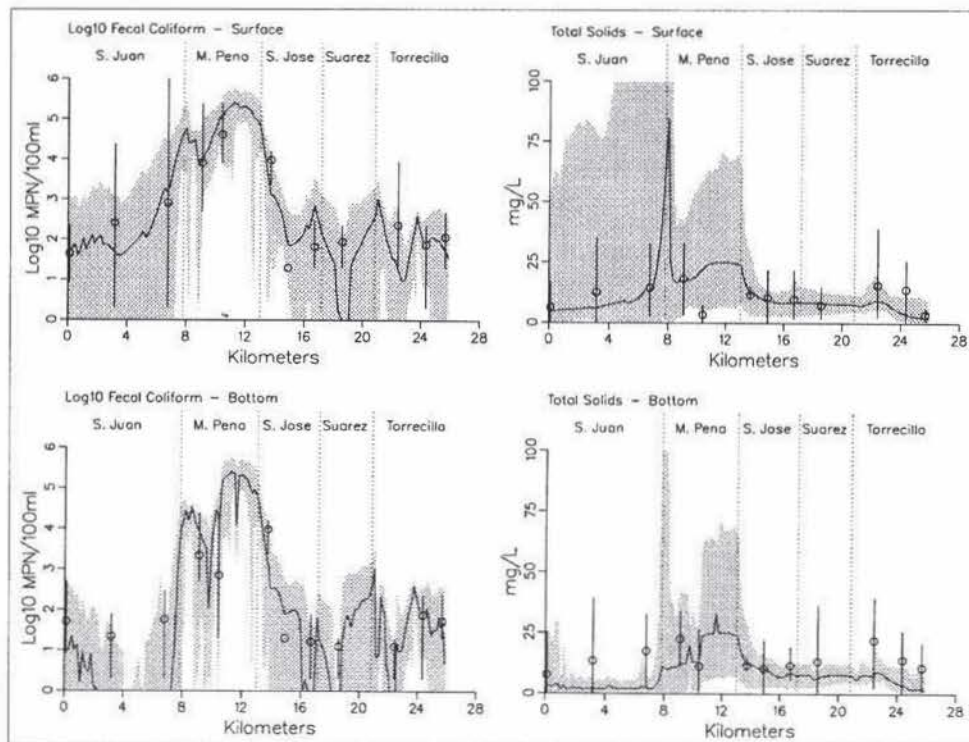


Figure 7-3. (Sheet 8 of 8)

mouth of Laguna La Torrecilla is similar to offshore conditions while water quality in the other areas is more like that found in Canal Suárez. Each constituent is discussed in the order it is presented in the transect plots.

Temperature

Temperature transect plots indicate that there is little variation in the model predictions for temperature along the transect, Figure 7-3. Likewise there was little variation in observed temperature readings. Model results agree favorably with observations indicating that the model is predicting temperature accurately. The lack of significant temperature differences between the surface and bottom transects is an indication that the system is not thermally stratified.

Salinity

Salinity transects, unlike the temperature transects, indicate significant variation. Model results and observed data for San Juan Bay exhibit average salinity approximately equal to that found offshore. Near the mouth of Caño Martín Peña, surface salinity drops in response to freshwater inflows from Río Piedras and the flow from Caño Martín Peña. Bottom salinity decreases slightly in the dredged portion of Caño Martín Peña with the model average being lower than the observed data. However, the observed data for both surface and bottom samples at this location do fall within the range of model predictions.

The degree of variation in observed salinity supports the model results which indicate that there are significant swings in salinity as a result of fresher flows from eastern Caño Martín Peña and runoff into Laguna San José. These fresher flows remain near the surface and override the bottom waters of western Caño Martín Peña resulting in a 10- to 15-ppt difference in salinity between surface and bottom waters. Eastern Caño Martín Peña is shallow and modeled as one layer in most places. This results in the surface and bottom salinity plots being identical for this region. The only exception occurs near km 12 where there is a small hole. At this location, the model grid is two layers deep while the cells upstream and downstream are only one layer deep. The cell in the “hole” cannot have advection into or out of it due to the one-cell isolation. The only means for moving material into or out of this cell are diffusion and settling. Salinity being a dissolved substance does not settle but can diffuse depending upon the overlying water salinity. At the same time, salinity is not taken up by the sediments so the salinity that diffuses into the “hole” is only removed by diffusion when the overlying water is fresher.

Predicted surface salinity in Laguna San José is slightly higher than observations for the calibration period. The surface and bottom salinity values at SJ-2 and SJ-4 are identical as this is a location where the system

is relatively shallow and there is no stratification. At station SJ-5, there is a significant difference in surface and bottom salinity. This location is a dredge material borrow pit which is 6.8 m deep. These pits are located throughout Laguna San José, Canal Suárez, and Laguna La Torrecilla. Just as the small hole in Caño Martín Peña, these holes have limited exchange with surface waters. Some holes are large enough that they cover multiple model cells and can therefore accommodate advection which should allow these holes to freshen. However, observed data indicated that surface salinity at these holes was much lower than bottom salinity. Numerous theories were developed as to why the salinity in these holes should be so much higher than that at the surface. The theories included groundwater intrusion from the ocean into the holes. Whatever the mechanism, it was beyond the capability of CH3D and ICM to simulate it without modification.

In an attempt to incorporate the effects of these holes on water quality, the salinity in these deep holes was “nudged” toward higher values throughout the simulation. The same procedures were used in both the HM and WQM. During each model time-step iteration, the salinity in the holes where nudging was employed was adjusted toward a predetermined, higher concentration according to the relationship

$$C_{new} = C + 0.1 * (C_{nudge} - C) \quad (7.6)$$

where

C_{new} = new salinity concentration

C = previously computed salinity concentration

C_{nudge} = reference salinity concentration

The result of nudging was that these dredge material borrow pits became pseudo-salinity boundaries representing sources of ocean salinity. Nudging was only employed in cells located more than three layers deep in dredge material borrow pits. A value of $C_{nudge} = 28$ ppt was used for holes in Laguna San José while a value of $C_{nudge} = 35$ ppt was used for dredge borrow pits in Laguna La Torrecilla. In locations where nudging was employed, little fluctuation in salinity occurred. Examples of the effects of nudging can be seen in the bottom salinity transect plots between km 16 and km 24.

Transect salinity continues to increase as the transect passes through Canal Suárez. There is a slight decrease in salinity as the transect passes around an island in Laguna La Torrecilla in the vicinity of TL-4 at which time it is exposed more to the fresher Blasina flows. Salinity continues to rise as the transect continues through Torrecilla to the ocean.

Light Extinction

The background light extinction was specified spatially based upon observations. Model values vary some during the simulation due to the effects of algae. Only the model mean values are plotted in Figure 7-3 for interpretive purposes. These values were adjusted so that the model light extinction closely followed the observed. Although the model surface and bottom light extinction values are very similar for surface and bottom layers, the amount of light remaining in the bottom layers can be quite different from that in the surface layers. Light extinction measurements were taken only for the surface.

Chlorophyll

Modeled chlorophyll levels along the transect in San Juan Bay are low, averaging 4 $\mu\text{g/l}$. There is a slight gradient in the observed values in San Juan Bay with the observations near the mouth of Caño Martín Peña being the highest. The average and range of chlorophyll observations fall within the range of the WQM simulation for San Juan Bay. Chlorophyll levels increase significantly just inside Caño Martín Peña. Model levels remain constant throughout the western dredged portion of Martín Peña and begin to increase once the undredged eastern portion of the canal is reached.

Computed chlorophyll concentrations at the juncture between Caño Martín Peña and Laguna San José are the highest of any location on the transect. Chlorophyll concentrations remain high throughout San José and into Canal Suárez. Average chlorophyll observations in San José exhibited temporal and spatial variability which made calibration problematic. Attempts to make the WQM match the higher chlorophyll observations at SJ-2 would make it overpredict the much lower average at SJ-4 even more. Attempts to obtain a better match at SJ-4 would result in the WQM underpredicting even more at SJ-2 which in turn would cause lower chlorophyll predictions throughout Martín Peña. The surface waters of San José serve as an incubator for chlorophyll with ample light and nutrients to promote growth.

Macrobenthic grazing was added to the model in order to aid in chlorophyll calibration in Laguna San José. Benthic organisms remove algae via filtration of the overlying cell, consequentially, the waters above bivalve beds have lower levels of algae and other particulates. Light penetration increases in the waters above clam beds in response to the decrease in suspended matter.

Bivalve beds were observed at different locations in Laguna San José during the sampling study. Bivalves were placed into the southern half of Laguna San José in the WQM, Figure 7-4. Macrobenthic grazing is dependent upon dissolved oxygen levels. Bivalves require dissolved oxygen to live. In the WQM the higher the dissolved oxygen the better the conditions for grazing, the lower the dissolved oxygen the worse.

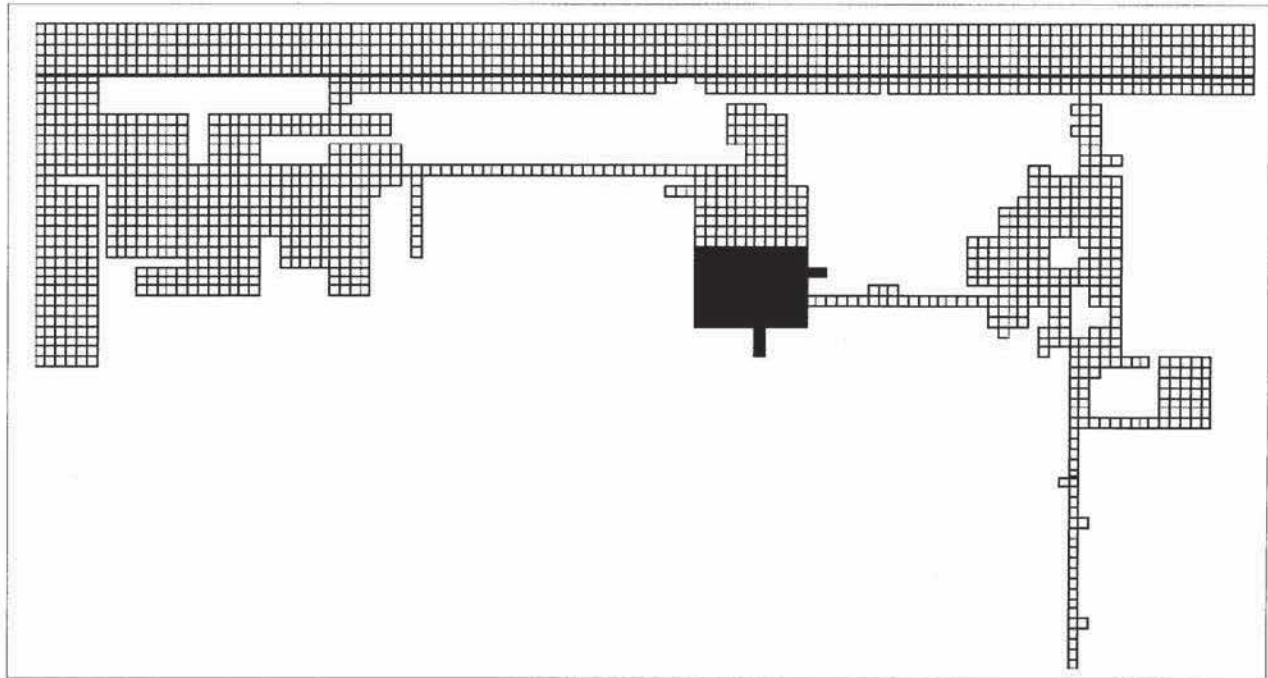


Figure 7-4. Location of clams in the WQM

Macrobenthic grazing will not occur in bottom cells with anoxic conditions even if bivalves are present.

Incorporation of macrobenthic grazing allowed greater spatial variability in Laguna San José chlorophyll concentrations. The net impact was that chlorophyll levels decreased in the southern portion of Laguna San José in the presence of the bivalve beds.

Canal Suárez chlorophyll levels were lower than either Laguna San José or Laguna La Torrecilla but still higher than any other location along the transect. Model surface chlorophyll concentrations along the transect in Torrecilla were highest at TL-4. Levels at TL-1 and TL-2 are relatively low reflecting the influence of the ocean water exchange through the Laguna La Torrecilla inlet.

Bottom chlorophyll concentrations along the transect are typically low. The exception occurs at locations where the model grid is only one layer deep which results in the same cell being on both the surface and bottom transects. Light limitation is the major limiting factor for algal growth in the deeper waters of the system with the exception of the regions offshore. Typically, algae found in the bottom waters were transported there by settling and vertical flows.

Organic Carbon

The WQM simulated three forms of organic carbon: dissolved, labile particulate, and refractory particulate. Results are shown for dissolved organic carbon (DOC) and total organic carbon (TOC) which is the sum of DOC and the two particulate fractions. The DOC and TOC transects have similar shapes which is expected since DOC is the major component of TOC. Concentrations at both the San Juan Bay and Laguna La Torrecilla inlets reflect the conditions offshore. The interior portions of the transect have elevated levels that are the result of anthropogenic loadings. The highest surface concentrations occur at the Rio Piedras - Caño Martín Peña confluence and in the eastern portion of Caño Martín Peña. The high concentrations at the Rio Piedras - Caño Martín Peña juncture result from the Rio Piedras loadings. Transect plots indicate that this load is rapidly disseminated into the waters of San Juan Bay by the combined Rio Piedras and Caño Martín Peña flows.

Surface DOC and TOC concentrations in eastern Caño Martín Peña are high as a result of the organic carbon component of the un-sewered loads. This region is reported to directly receive substantial discharges of untreated wastewater. The exact quantity was unknown and could only be estimated. Based upon calibration results and demographic information, a loading of 400 kg/day of organic carbon split evenly between dissolved and labile particulate fractions was distributed along the eastern half of Caño Martín Peña. In addition, loadings of 62.5 kg/day of ammonia, 37.5 kg/day of dissolved organic nitrogen, 12.5 kg/day of dissolved inorganic phosphorus, and 7.5 kg/day of dissolved organic phosphorus were also added. The carbon/nitrogen/phosphorus (C/N/P) ratio of this load was 20/5/1 which is typical of that indicated for medium strength wastewater (Metcalf and Eddy 1979). Based on a daily per-capita total organic carbon loading of 75 g/person/day (0.17 lb/person/day) this loading was equivalent to that of approximately 5300 persons. The un-sewered loadings into eastern Caño Martín Peña were required not only to bring the DOC and TOC up but to increase the levels of other nutrients and decrease dissolved oxygen. The impact of the un-sewered loads on these and other variables is discussed below in the corresponding sections.

Model surface DOC concentrations match observed data quite well throughout the system except for Laguna La Torrecilla where model predictions were slightly low. One possible explanation for the model being low in this region is that the model does not include the organic carbon loading coming from the mangroves around Torrecilla. Surface model DOC concentrations in San José and Canal Suárez are slightly low in comparison to observed data. However, model predictions for TOC at these stations indicate that the model average agrees with the observed averages at stations SJ-2, SJ-4, SJ-5, and SC-1. Any attempt to increase DOC concentrations in the model would increase TOC concentrations and result in a poorer model performance in San José and Canal Suárez.

Model bottom DOC levels are similar to surface levels for most of the transect. In the dredged western portion of western Caño Martín Peña, bottom DOC levels are lower than surface waters. A possible reason for this is that there is some salinity stratification in this portion of the canal which decreases surface-bottom water mixing. Over the remainder of the transect, model surface and bottom DOC concentrations are comparable except for holes and dredge material borrow pits. At these locations, DOC concentrations are elevated as a result of the dissolution of settled particulate organic carbon and the respiration and decay of algae that settle into these cells. As a result, the DOC levels in these holes are higher as there is no mechanism to readily remove the DOC other than vertical diffusion. Observed bottom DOC and TOC concentrations at SJ-5, SC-1 and TL-4 indicate elevated concentrations similar to those predicted by the model.

Nitrogen

Results for three model constituents, ammonium, nitrate, and dissolved organic nitrogen (DON) are shown as well as results for total nitrogen. The dominant feature of the nitrogen transects are the high observed values of ammonium in Caño Martín Peña. The high observed ammonium levels in Caño Martín Peña are further evidence of substantial discharges of untreated wastewater directly into Caño Martín Peña. The sources of this ammonium are direct loading, mineralization of DON, and diagenesis of settled particulate organic nitrogen in the sediments. Mineralization occurs in the water column but as indicated in the transect plots, little DON was observed in Caño Martín Peña. Diagenesis occurs in the sediments and is a likely source of the ammonium especially in the holes and dredged borrow pits. At these locations, particulate organic matter in these cells will eventually be settled and undergo diagenesis. The ammonium released can only be removed via diffusion. Consequentially observed ammonium levels greater than 1 mg/l were observed and predicted along the bottom.

In the deeper portions of Caño Martín Peña, Laguna San José, and Canal Suárez, sediments act as a source of ammonium to the water column. Model sediment fluxes of 25 mg/m²/day or greater are common in Laguna San José and Canal Suárez. Benthic algae in the shallow portions of the eastern portion of Caño Martín Peña and Laguna San José take up ammonium as it is being released from the sediments to the water column. Without these algae, ammonium levels in Caño Martín Peña and Laguna San José would be even higher. The spatial extent of the benthic algae is limited by the availability of light and nutrients.

Computed and observed nitrate levels were low throughout the system. The model slightly overpredicts nitrate in Caño Martín Peña, possibly due to under-estimation of sediment denitrification or algal uptake of nitrate. Computed and observed dissolved organic nitrogen is also relatively low with more present in the eastern half of the system. Surface transect plots indicate that model total nitrogen levels were higher in Caño Martín Peña

than observed values but agreed well with observations in Laguna San José. Total nitrogen transect plots for the bottom indicate that the model performs well for the whole system. Model predictions are low for the first station in Laguna La Torrecilla, TL-4, but this is mainly the result of the ammonium prediction for this station being low.

Phosphorus

Dissolved inorganic phosphorus (DIP) transects have a look similar to that of ammonium. Low predicted and observed surface concentrations occurred throughout the system with the exception of Caño Martín Peña. DIP concentrations approaching 0.2 mg/l were predicted for the length of Caño Martín Peña which matched well with observations at MP-2 but were slightly above the observations at MP-1. The sediments of the dredged western portion of Caño Martín Peña are a source of DIP with sediment flux rates reaching a maximum of 20 mg/m²/day near MP-2. Eastern Caño Martín Peña sediments serve as a sink for DIP with the benthic algae community at this location taking DIP from the water column. Eastern Caño Martín Peña receives a phosphorus loading of 20 kg/day as part of the un-sewered area loadings. Surface water predictions from the model are lower than observations in Laguna San José but are representative in Canal Suárez and Laguna La Torrecilla. The reason for low predictions in Laguna San José appear to be benthic and planktonic algal nutrient uptake. Much of Laguna San José is relatively shallow so that the bottom waters at certain locations receive adequate light for benthic algae to flourish. Where benthic algae are active their role is the sequestration of sediment releases of nutrients, notably DIP and ammonia. If conditions are appropriate, the benthic algae can uptake the complete sediment release of a nutrient and still remove nutrients from the overlying water column. Incorporation of benthic algae into the WQM improved the calibration by muting sediment releases at certain locations and increasing the uptake of nutrients from the water column.

Model predictions for DIP for the bottom transect agree well with observed data. Again the holes and dredged borrow pits have elevated levels of DIP which the model captures. Model results for surface water dissolved organic phosphorus indicate that the model slightly overpredicts in Caño Martín Peña but does well in the remainder of the system. Overall, transects for total phosphorus demonstrate that the model tracks well with the observed data for both surface and bottom waters throughout the system.

Dissolved Oxygen

Observed data for the surface water dissolved oxygen (DO) transect indicate that levels are relatively high throughout the system with the exception of Caño Martín Peña. The least variability in DO is observed at the stations located at the mouths of San Juan Bay and Laguna La Torrecilla. These locations are the most influenced by the ocean and therefore reflect ocean conditions of constant salinity, temperature, and low levels of algae. Model predictions for DO decrease slightly along the transect between the mouth of San Juan Bay and Caño Martín Peña. Averages for observed data at stations SJB-3 and SJB-5 are higher than model predictions along the surface but the range of observations overlap the range of model predictions. The highest of the observed DO concentrations exceed saturation and are indicative of the diurnal effects of algal photosynthesis. The inability of the WQM to capture DO supersaturation at these stations is probably due to the fact that ICM does not incorporate diurnal effects in the algal process computations.

Model surface calibration average and range match observed data well in Caño Martín Peña. Observed data in this region indicate large fluctuations in DO which the model is able to capture. Model surface DO levels increased in eastern Caño Martín Peña as a result of algal photosynthesis. Calibration averages were slightly higher than observed data averages in Laguna San José and Canal Suárez; however, the range of model predictions encompassed the observed averages.

Bottom water model calibration results indicate numerous locations with anoxic conditions. Portions of Caño Martín Peña are anoxic on the bottom due to high DO demands exceeding reaeration. Additionally, holes and dredged borrow pits are anoxic as a result of sediment releases of ammonium in addition to poor circulation and exchange with the aerated surface waters. Sediment oxygen demand (SOD) also removes DO from the water column but only in areas where the water has DO. Consequentially, locations with high SODs are also locations where the bottom water is not anoxic but instead has adequate DO.

Fecal Coliform

The only source of fecal coliform bacteria in the model is from external loads. Once introduced to the system, fecal coliform can only be transported and die. Highest fecal coliform levels are found near the loading sources. The highest fecal coliform observation occurred in the interior of the system in Caño Martín Peña and western Laguna San José. Transect plots indicate that model output matches observations well for both the average and range throughout the system.

Total Suspended Solids

Total suspended solids (TSS) include both inorganic and organic suspended solids. TSS plots indicate that the model performs well along the transect. Model predictions are higher than observations at MP-2 but match observations at the closest two stations MP-1 and SJ-2. The dominant feature of the surface transect is the spike at km 8. This spike results from the Rio Piedras sediment load. As indicated by the plot, this load is disseminated rapidly in the system. The plot for the bottom transect indicates that the model performs well in the interior of the system but tends to be low in San Juan Bay and Laguna La Torrecilla.

Benthic Algae

ICM has no mechanism for the transport, transplantation, or propagation of benthic algae from one cell to another. Consequentially, benthic algae exist at the sediment water interface of every water column in the model. If the light or nutrients are inadequate, the algae are dormant and have no effect on water quality or sediment processes. Where nutrient and light levels are conducive the algae grow. The kinetic processes of benthic algae are similar to those of phytoplankton which were described earlier in Chapter 4. Specific information of benthic algal processes can be found in Cerco and Seitzinger (1998). As indicated in Figure 7-5, the presence of benthic algae in an appreciable amount is limited to relatively few locations along the transect. Nutrients are abundant for the length of the transect and throughout the SJBE system. However light at the sediment water interface is adequate at only a few locations. Most locations along the transect are too deep and the light extinction too high for appreciable levels of light to penetrate to the sediment water interface. The highest benthic algae biomass levels were at the mouths of San Juan Bay and Laguna La Torrecilla where levels approaching 20 g C/m^2 were computed. Light extinction at these locations is low as a result of water clarity and low chlorophyll levels. Adequate nutrients from the interior of the system are also available which allow the benthic algae to thrive. Two locations in the interior of the system, one in Laguna San José and one in Canal Suárez, also have elevated levels of benthic algae. Both of these locations are shallow and represented in the model as one layer deep. Benthic algae at the Laguna San José location receive ample nutrients from Caño Martín Peña while the Canal Suárez benthic algae receive nutrients exiting from Laguna San José via Canal Suárez.

In Laguna La Torrecilla and Caño Martín Peña there are locations where the benthic algal biomass is between 0.1 gm C/m^2 and 2 gm C/m^2 . Even at these levels the algae play an important role in the water quality of the system. At all locations along the transect where benthic algae are growing, it is sequestering sediment nutrient releases notably ammonium and phosphate. At these locations the sediments are sinks for ammonium and phosphate while at the locations where benthic algae are dormant the sediments can be sources.

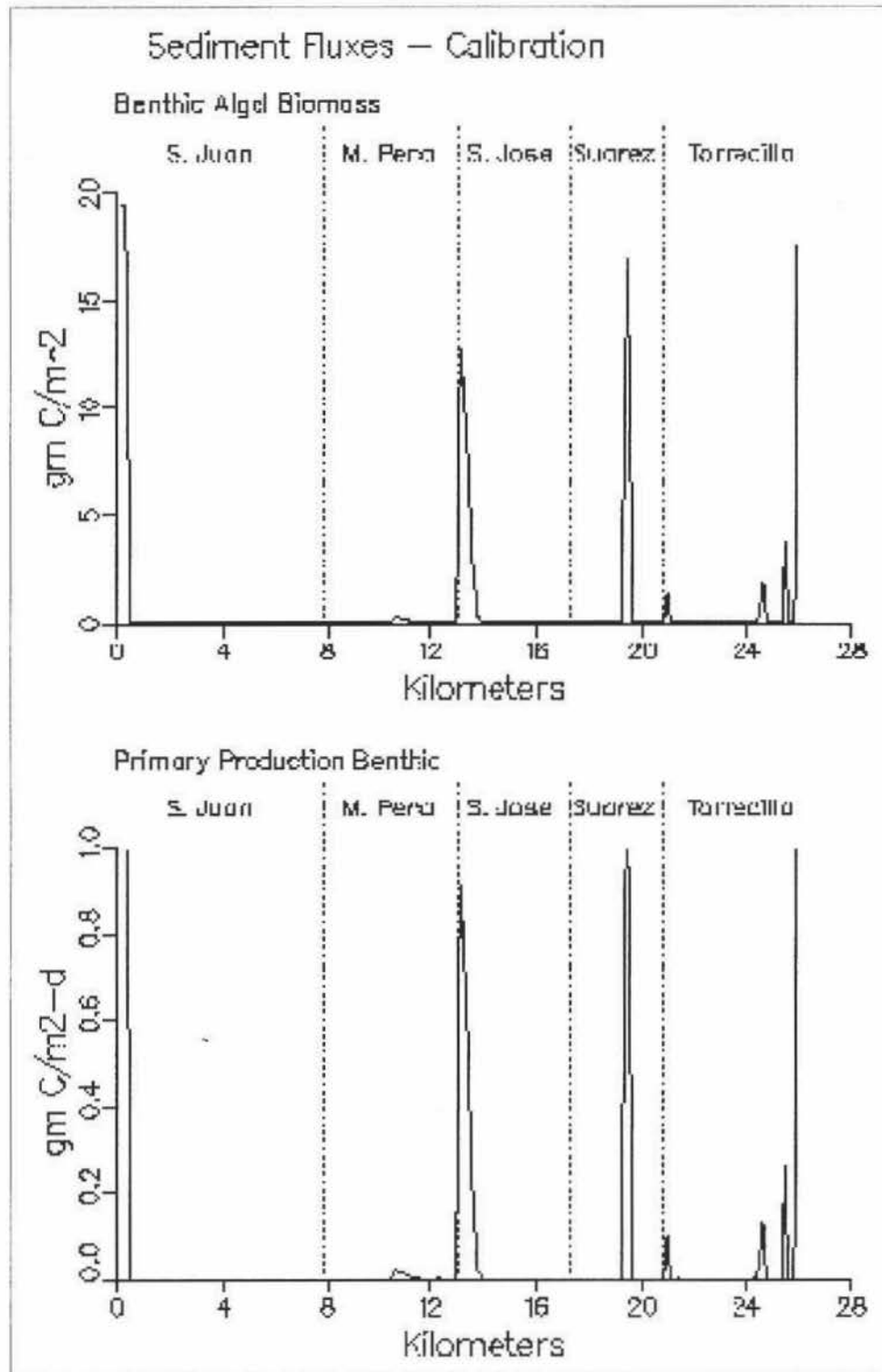


Figure 7-5. Longitudinal transect calibration period average benthic algae

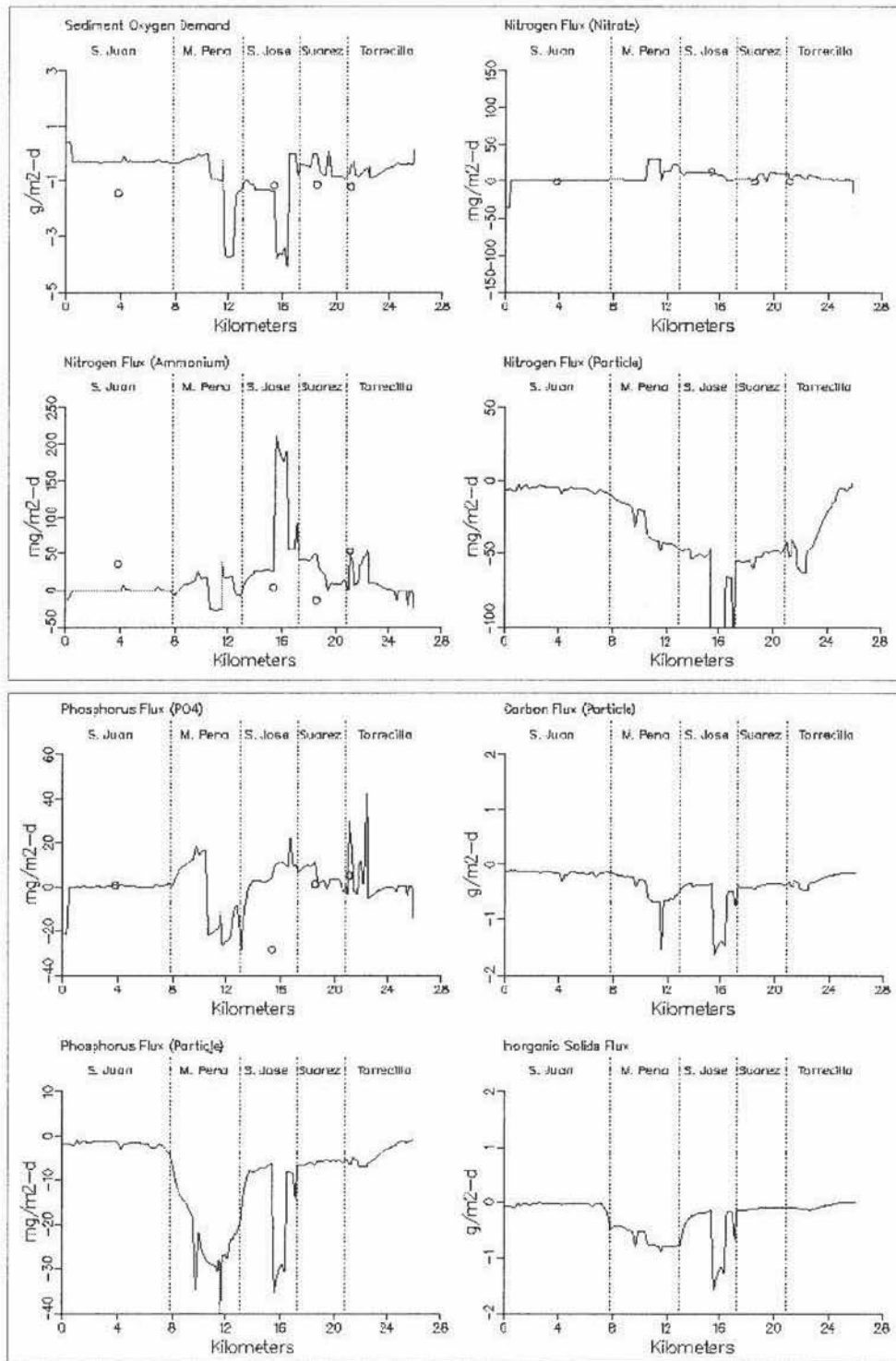


Figure 7-6. Longitudinal transect calibration period average sediment fluxes

Sediment Fluxes

Calibration period averages for sediment fluxes along the transect are shown in Figure 7-6. Negative values indicate that there is a transfer from the water column to the sediment while positive values indicate that there is a transfer from the sediments to the water column.

The calibration period average for sediment oxygen demand indicates that except for Caño Martín Peña and Laguna San José the sediment oxygen demand was between 0 and -1 gm/m^2 -day. In eastern Caño Martín Peña and eastern Laguna San José the sediment oxygen demand increases to -4 gm/m^2 -day. These high sediment oxygen demand rates occur in the vicinity of holes and borrow pits which have limited flushing. An oddity of sediment oxygen demand is that there must be oxygen present in the water column for the sediment oxygen demand to have a value as the sediment oxygen demand is indicative of the *transfer* of oxygen from the water column to the sediments. The processes that create a sediment oxygen demand continue in the absence of water column dissolved oxygen. Under these conditions, the demand is transported to the water column as a chemical oxygen demand. Consequently, the highest sediment oxygen demands are in the areas adjacent to the anoxic holes and borrow pits. The sediment oxygen demand in the cells comprising the anoxic pits and borrow holes are 0 gm/m^2 -day. On both ends of the transect and at one location in Canal Suárez, the sediment oxygen demand was greater than 0 gm/m^2 -day which is indicative of the sediments being a dissolved oxygen source (i.e. releasing dissolved oxygen to the water column). Conditions at these locations (adequate light and nutrients) are conducive to benthic algal growth and photosynthesis which is the source of the dissolved oxygen.

Sediment ammonia fluxes along the transect varied from -25 mg/m^2 -day to 200 mg/m^2 -day. Locations where the ammonia flux was negative are due to the presence of active benthic algae which are taking up ammonia releases from the sediments and ammonia from the water column. Sediment fluxes for Caño Martín Peña, Laguna San José, and Canal Suárez indicate that the sediments in the interior of the system serve as an ammonia source. The highest fluxes tend to be associated with holes and borrow pits in which dissolved oxygen is low or absent.

The highest nitrate fluxes occur in the central portion of Caño Martín Peña on the western end of the undredged eastern portion. Fluxes approaching 30 mg/m^2 -day were predicted for this location. Lower positive fluxes were predicted along the remainder of the transect through Laguna San José, Canal Suárez, and Laguna La Torrecilla.

Particulate nitrogen flux results indicate that the Caño Martín Peña, Laguna San José, Canal Suárez, and Laguna La Torrecilla all are sinks for particulate nitrogen. The bathymetry of this portion of the system when combined with the proximity of the tributary and anthropogenic loads results in the high level of deposition occurring.

Phosphorus sediment flux plots had many similarities to the nitrogen sediment flux plots. Benthic algae located at the mouths of San Juan Bay and Laguna La Torrecilla cause the sediments at these locations to be phosphate sinks. There is little sediment flux of phosphate in San Juan Bay due to the low deposition rate of particulate phosphorus at this location and to the oxic bottom dissolved oxygen levels. The sediments of the dredged western end of Caño Martín Peña are a source of phosphate for the water column while the undredged eastern end is a sink. The bottom waters of the western end have low dissolved oxygen or are anoxic which contributes to the sediment phosphorus release. The eastern end of Caño Martín Peña has high dissolved oxygen due to reaeration and its shallow depth. In addition, this reach of Caño Martín Peña receives the un-sewered loads. These factors combine to cause the eastern part of Caño Martín Peña to act as a sink for dissolved inorganic phosphorus. The water column of Caño Martín Peña has the highest levels of dissolved inorganic phosphorus found in the SJBE system. Most of this phosphorus originates with the un-sewered and lateral inflow loads into Caño Martín Peña. Elevated dissolved inorganic phosphorus flux rates occur in eastern Laguna San José and Laguna La Torrecilla in the vicinity of hypoxic pits and dredge borrow pits.

Time Series Comparisons

Located in Laguna Los Corozos, which is in the northern portion of Laguna San José, is station SJ-1 (see Figure 2-1). This portion of the bay is the receiving water for the Baldorioty de Castro Pump Station. ICM results for temperature agree well with observations at SJ-1 for the duration of the calibration period, Figure 7-7. Surface salinity results indicated that ICM agrees favorably with the first three observations but slightly underpredicts observations at the end of the calibration period. ICM chlorophyll results agree well with the first four observations but are much lower than the fifth observed concentration of 92 mg/l. ICM results agreed well with surface ammonium and nitrate observations for SJ-1 which were low for the duration of the calibration period. The time series plot for total nitrogen indicates that overall the model is performing adequately for nitrogen at this station. Dissolved inorganic phosphorus results from ICM underpredict the first two observations but agree well with the last three. Time series of total phosphorus indicate that the model performs adequately.

Algal growth in the surface layer is limited by nitrogen availability more so than phosphorus. The average concentration of 0.01 mg/l of phosphorus available is more than adequate to maintain algal levels at their current state. Under some conditions, nitrogen is even more limiting than light at this location. Occasionally nitrogen limitation on algal growth relaxes when large flows and accompanying loads are discharged from the Baldorioty de Castro storm water pump station.

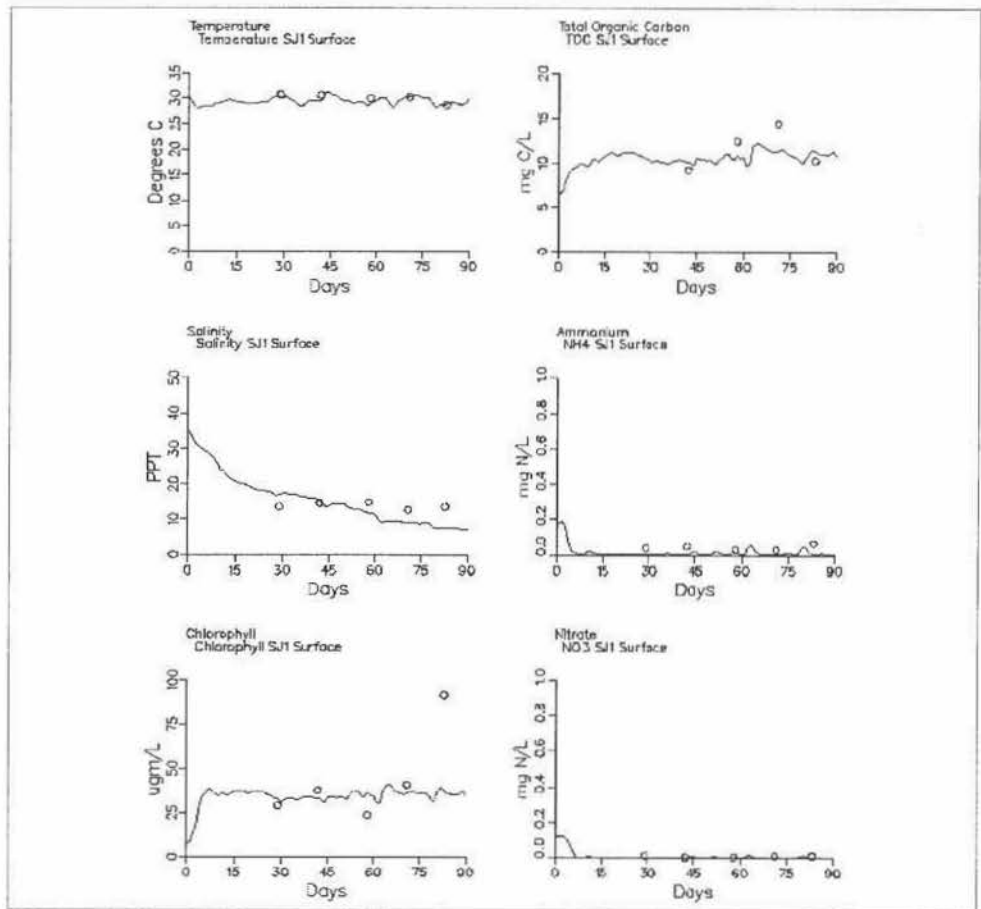


Figure 7-7. Laguna Los Corozos (Northern Laguna San José) calibration period time series (Sheet 1 of 4)

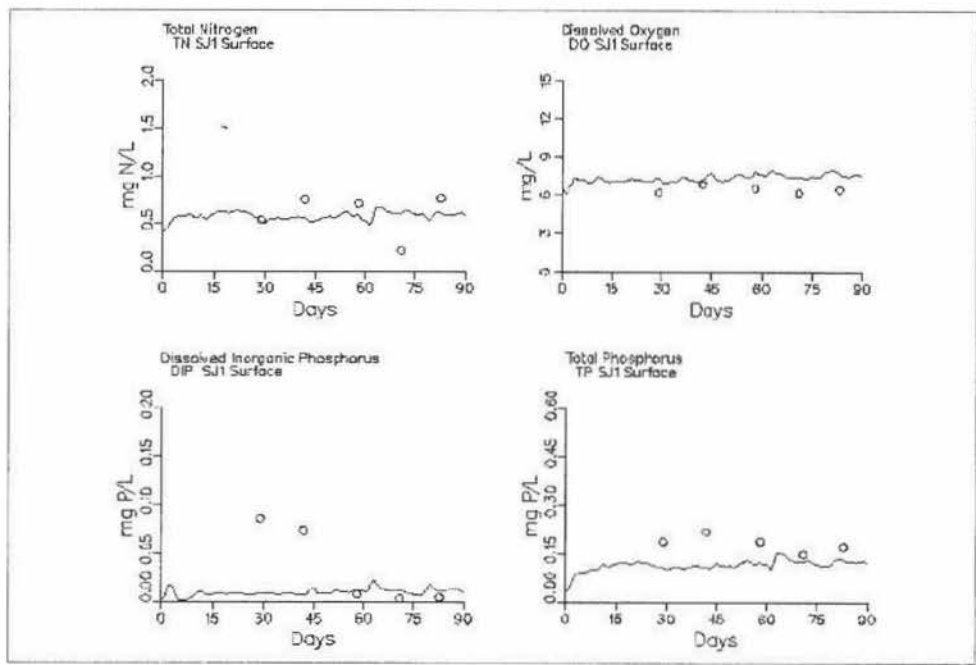


Figure 7-7. (Sheet 2 of 4)

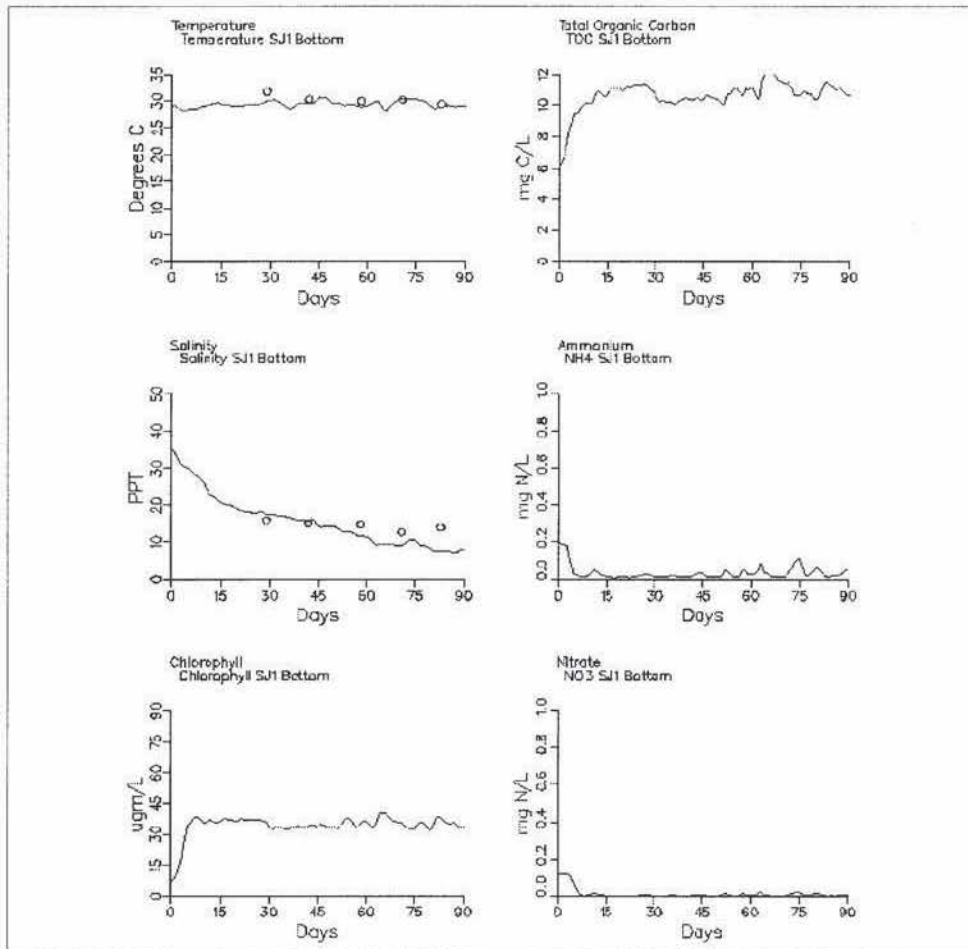


Figure 7-7. (Sheet 3 of 4)

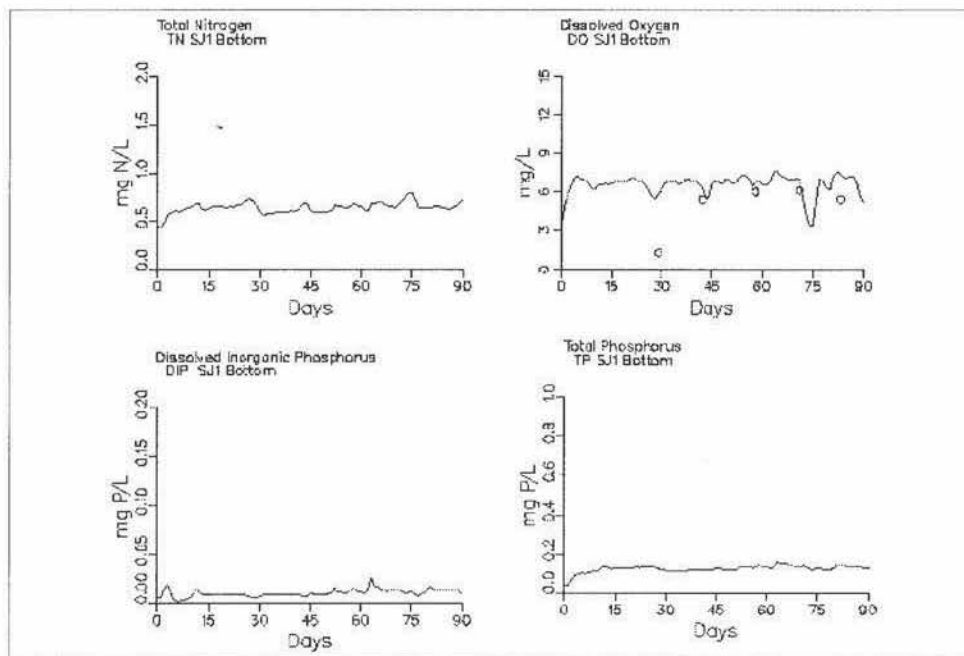


Figure 7-7. (Sheet 4 of 4)

Dissolved oxygen observations are slightly lower than model predictions in the surface layer. The model predictions are near saturation for the salinity and temperature conditions in this system. Sampling results indicate that the surface water dissolved oxygen was consistently around 6 mg/l. Both the model and the observed data indicate that dissolved oxygen levels are relatively high in spite of the high organic carbon concentrations. Algal photosynthesis maintains surface dissolved oxygen levels near saturation for the temperature and salinity conditions present. Dissolved oxygen results for the bottom layer indicate more variability than the dissolved oxygen in the surface layer. The observed data indicate that there was little difference in surface and bottom dissolved oxygen on four of the five sampling dates. This observation when combined with the salinity and temperature surface and bottom time series observations indicate that there is little stratification at this location.

Time series plots for station MP-2 located in Caño Martín Peña are shown in Figure 7-8. This station is located midway between San Juan Bay and Laguna San José at the eastern end of the dredged channel. Water quality at this location is affected by the conditions in Laguna San José, eastern Caño Martín Peña, the Caño Martín Peña watershed, and San Juan Bay.

ICM results for surface water temperature at MP-2 matched observed values well. Temperature predictions for the bottom layer were slightly higher than the observations. Surface salinity observations varied from 17.1 to 32.7 ppt. ICM surface salinity results also indicated significant variation but were still less than the observed data. Salinity swings of 10 ppt were repeatedly predicted at MP-2 during calibration. The timing of these salinity swings corresponds with the occurrence of increases in runoff in the Caño Martín Peña watershed in response to a storm event, Figure 3-3. It must be noted that the ICM results are daily averages while the salinity observations are instantaneous. As such, a portion of the difference between the ICM results and the observed salinities could be attributed to timing.

Bottom salinity observations at this station ranged from 35.4 to 37 ppt during the calibration period. Salinity observations this high indicate that salt water is intruding along the bottom of Caño Martín Peña. Station MP-2 is located near the farthest extent of the intrusion as it is at the end of the dredged section of the canal. ICM bottom salinity results, while lower than the observations, are consistently over 30 ppt. Just as with the surface salinity, some fluctuations are evident in response to runoff events in the Caño Martín Peña sub-basin. When both the surface and bottom observations are viewed together, it is evident that the surface salinity is consistently lower than the bottom salinity. This difference is due to the lower salinity “fresh” water from Laguna San José and eastern Caño Martín Peña overriding the denser high salinity water infiltrating up western Caño Martín Peña from San Juan Bay. A review of the salinity transect plots, Figure 7-3, indicates that this salinity stratification continues to the western end of Caño Martín Peña. Rio Piedras inflows aid in keeping the surface salinity decreased in western Caño Martín Peña.

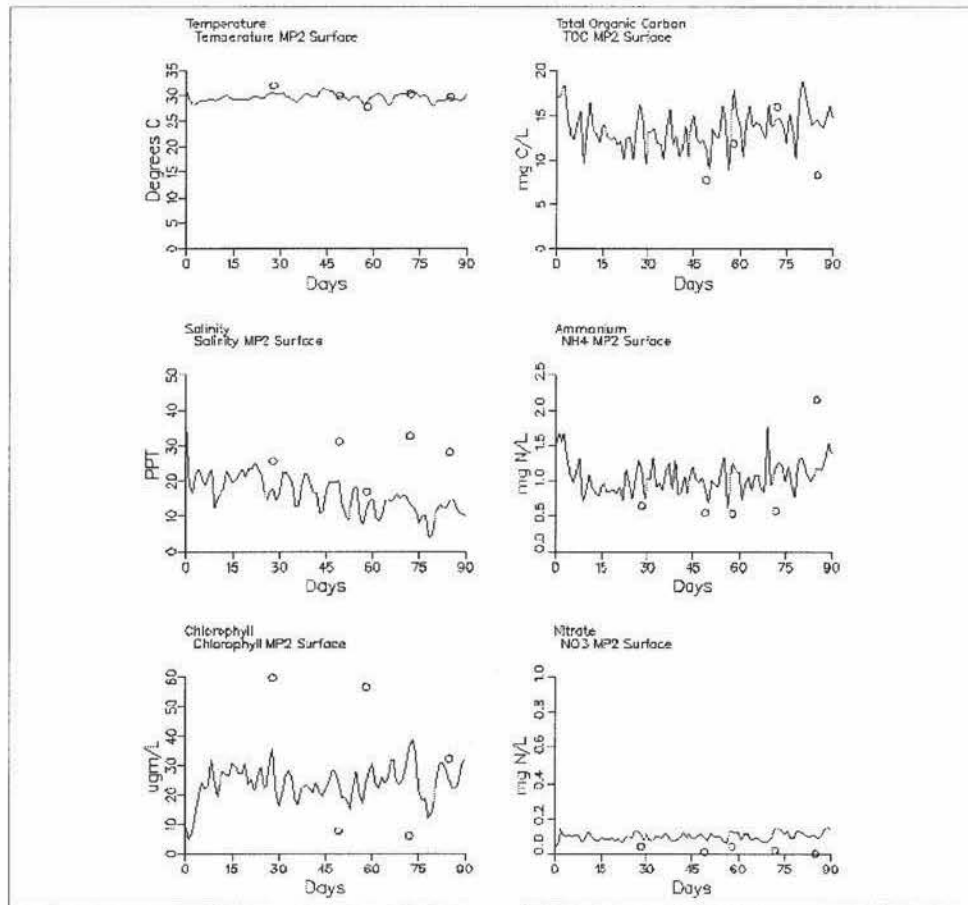


Figure 7-8. Caño Martín Peña station MP-2 calibration period time series (Sheet 1 of 4)

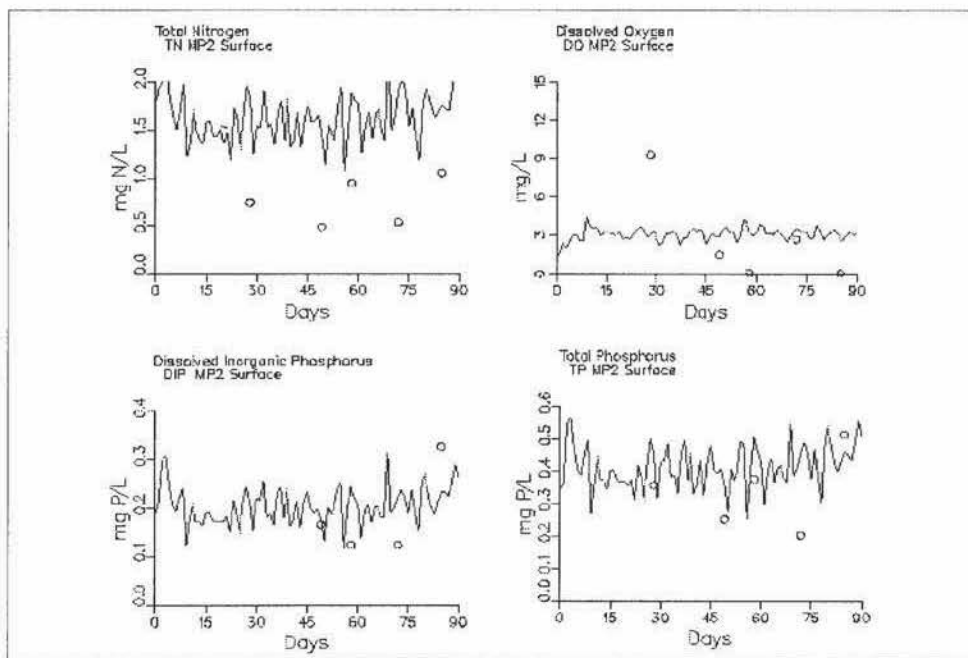


Figure 7-8. (Sheet 2 of 4)

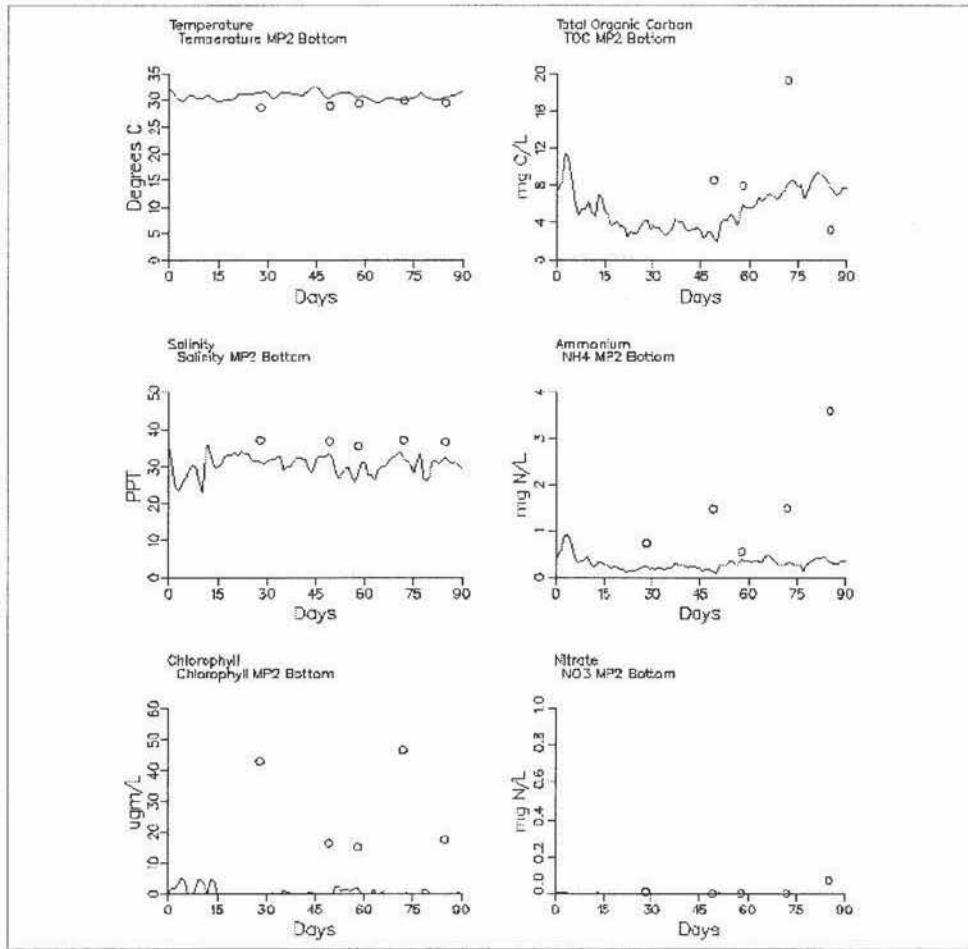


Figure 7-8. (Sheet 3 of 4)

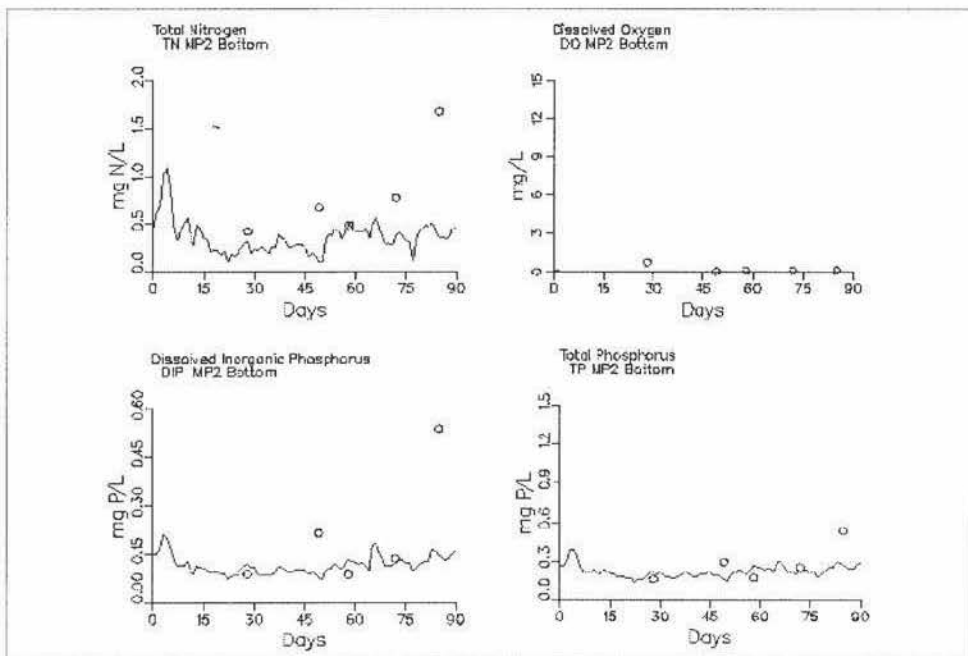


Figure 7-8. (Sheet 4 of 4)

Observed chlorophyll levels at MP-2 varied from 6 ug/l to 60 ug/l. Algae observed at station SJ-2 most likely originate in Laguna San José and are flushed down Caño Martín Peña by runoff-producing events. This is substantiated by the following. The two highest chlorophyll observations at MP-2 correspond to the lowest salinity concentrations. The lowest two chlorophyll observations correspond to the highest surface salinity observations. Runoff events generate higher flows in Caño Martín Peña which transport the chlorophyll quickly past MP-2. High light extinction and resulting low water column light levels in Caño Martín Peña are not conducive to algal growth, so the only way that elevated levels can exist is that they are generated elsewhere. ICM chlorophyll results exhibit significant variation in response to flow conditions. However, they do not indicate the degree of variability seen in the observations. As with salinity, this could be the result of comparing daily average model output with instantaneous observations at a location where things are sensitive to tidal action and flow conditions. Bottom chlorophyll observations exhibited significant variation too. Observations ranged from 15 ug/l to 47 ug/l. ICM chlorophyll results at this location are low. The only means by which algae can reach the bottom waters at station MP-2 are settling or transport with the intruding salt water. There are ample nutrients in the water to support algae but negligible light. The absence of light results in algal mortality before adequate time has passed for the algae to reach this location.

Total organic carbon surface observations ranged from 7.6 to 15.9 mg/l while bottom observations were between 7.9 mg/l and 19.3 mg/l. ICM results for the surface ranged from approximately 9 mg/l to 19 mg/l. The ICM results exhibited considerable variation in response to tidal action and eastern Caño Martín Peña flows but were representative of the observations. ICM bottom total organic carbon results were lower than the surface results and tended to be lower than the observed data. This is expected since the chlorophyll predictions were low at this location.

Observed ammonium levels in the surface water were elevated. Four of the observations were between 0.54 mg/l and 0.68 mg/l while the fifth was 2.15 mg/l. ICM results showed considerable fluctuation in response to hydrodynamic conditions but overall were representative of the observed data. Bottom water ammonia predictions were lower than the observations but still relatively high. Ammonium sediment flux rates at this station average 25 mg/m² day. Since the surface water ammonium levels are higher than the bottom water levels and the sediment flux of ammonia is not huge, it appears that the source of the ammonium in the surface water at MP-2 is eastern Caño Martín Peña. Little nitrate is found in the water at MP-2. ICM surface nitrate levels at MP-2 were slightly higher than the observations which were in the 0-mg/l to 0.04-mg/l range. ICM bottom nitrate predictions for MP-2 were essentially 0 mg/l which matched four of the five observations. Sediment nitrate fluxes at MP-2 were essentially 0 mg/m² day. Anoxic conditions along the bottom prevent nitrification from transforming ammonia into nitrate.

ICM dissolved oxygen concentrations in the surface fluctuated around 3 mg/l throughout the calibration period. Four of the observations during the calibration period were less than 3 mg/l with two being less than 0.12 mg/l. One observation was in excess of 9 mg/l which was in excess of saturation for the temperature and salinity at that time. A dissolved oxygen level this high results from algal photosynthesis. Bottom dissolved oxygen observations ranged from 0.04 mg/l to 0.79 mg/l. ICM results for bottom dissolved oxygen were 0 mg/l for the duration of the calibration period. When both surface and bottom dissolved oxygen concentrations are considered, ICM does a good job of matching observed conditions. The conditions existing at MP-2 result from two things. First, the high nutrient and organic carbon loading of eastern Caño Martín Peña. These oxygen-depleting substances remove the dissolved oxygen from the water faster than reaeration can replace it. Secondly, its location at the upper end of the dredging allows the waters from eastern Caño Martín Peña to override the denser waters infiltrating from San Juan Bay. Limited mixing between the surface and bottom waters at this location contributes to the dissolved oxygen depletion.

Overall ICM performs well at station MP-2. Conditions at this location are very dynamic. Major influences at this site are two. First is the flow from San José Bay into eastern Caño Martín Peña which is high in nutrients, algae, and oxygen demand. Second is the infiltration of salt water along the bottom of western Caño Martín Peña from San Juan Bay. ICM is able to reproduce many of the conditions observed during calibration even though conditions at this site are continually changing.

Station LC-1 is located in Laguna Condado. Temperature and salinity plots of results indicate that ICM matches observations in LC-1 well, Figure 7-9. Both temperature and salinity at this location reflect offshore conditions. ICM results match surface chlorophyll observations which are low, ranging from 0.5 to 3.2 ug/l. Total organic carbon observations for the surface and bottom exhibit the same behavior which mimics the observations at AO-1. ICM total organic carbon results indicate the same pattern as the observations. Ammonia observations at the surface ranged from 0 mg/l to 0.41 mg/l and from 0 mg/l to 0.6 mg/l at the bottom. ICM ammonia results were low, typically less than 0.05 mg/l in both the surface and bottom. ICM ammonia results were much lower than the extreme observations at this location. The validity of the extreme values at this station is uncertain since they are much greater than the TKN observations. At the end of the calibration period ICM ammonia concentrations are increasing in response to increases in the ammonia concentration specified at the ocean boundary. Nitrate levels, observed and computed in ICM, are near or are 0 mg/l for the duration of the calibration period in both surface and bottom waters. ICM dissolved inorganic phosphorus and total phosphorus levels agreed well with observations in both the surface and bottom waters at station LC-1. ICM dissolved oxygen results agreed well with all but one dissolved oxygen observation.

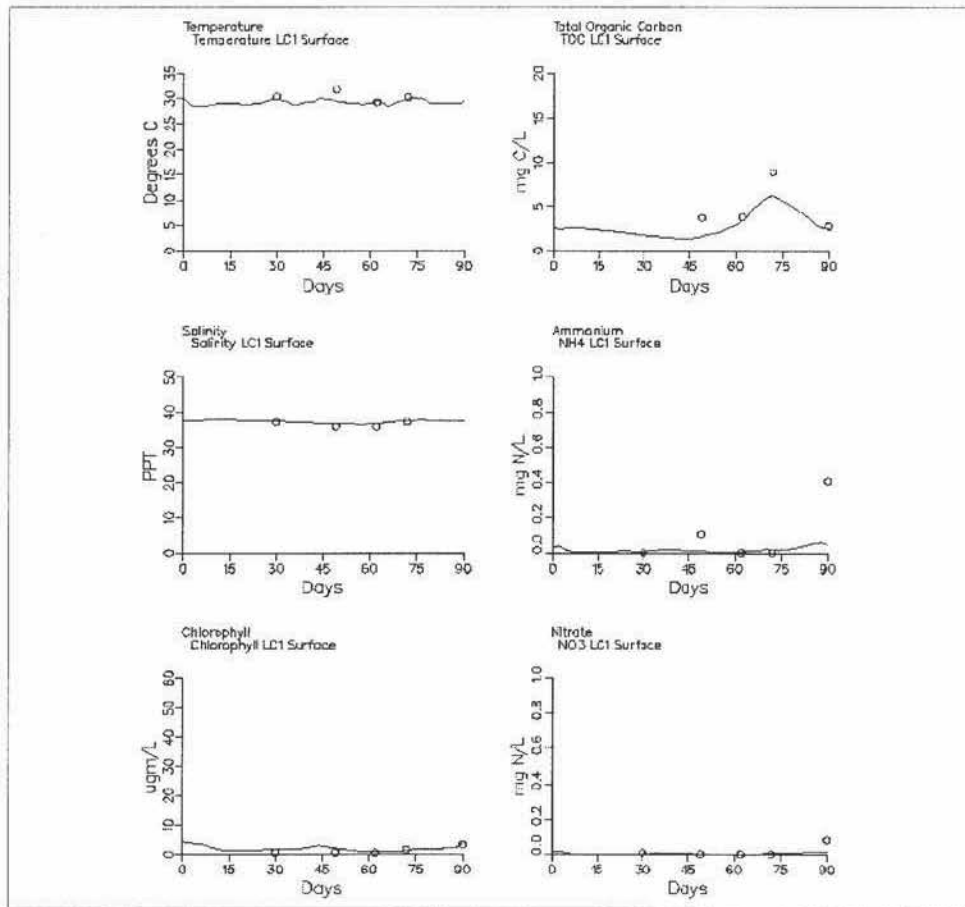


Figure 7-9. Laguna Condado station LC-1 calibration period time series (Sheet 1 of 4)

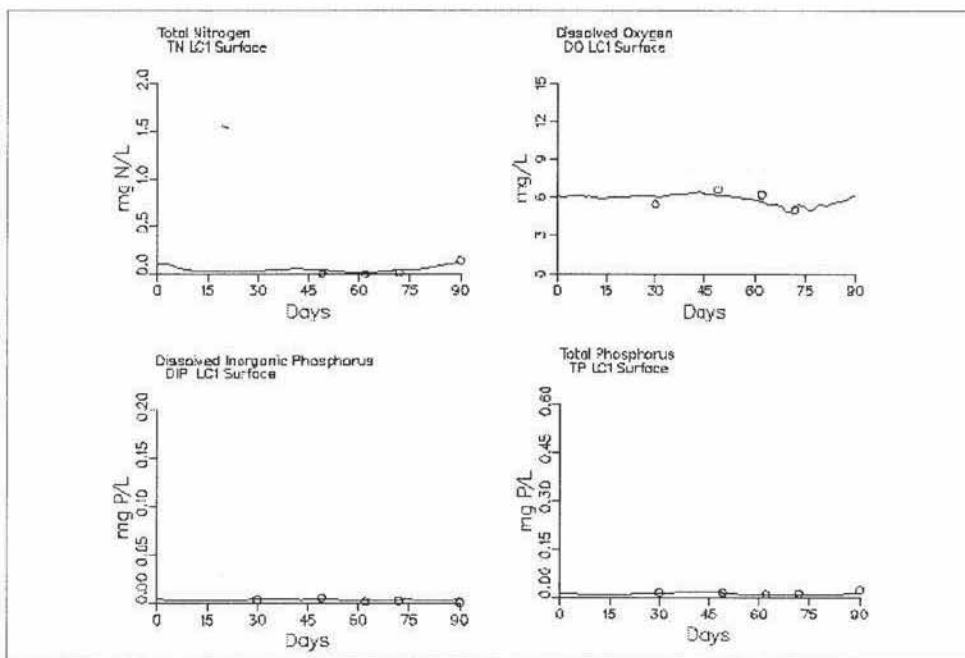


Figure 7-9. (Sheet 2 of 4)

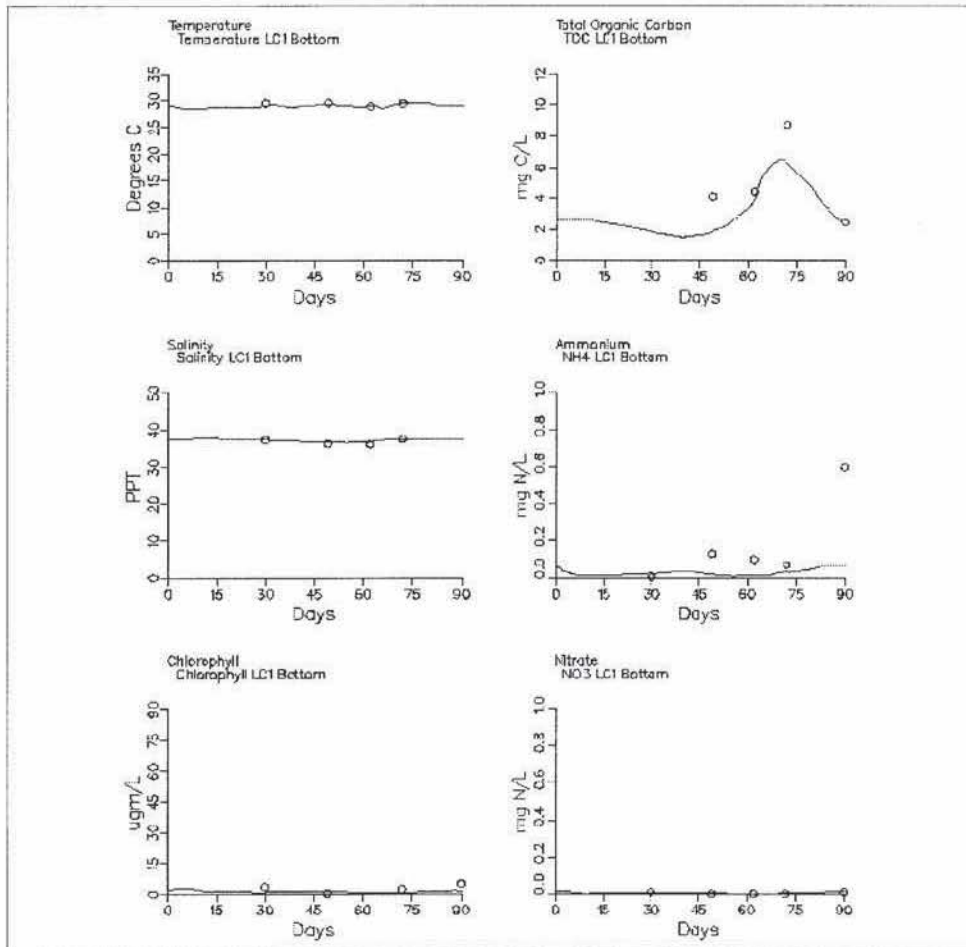


Figure 7-9. (Sheet 3 of 4)

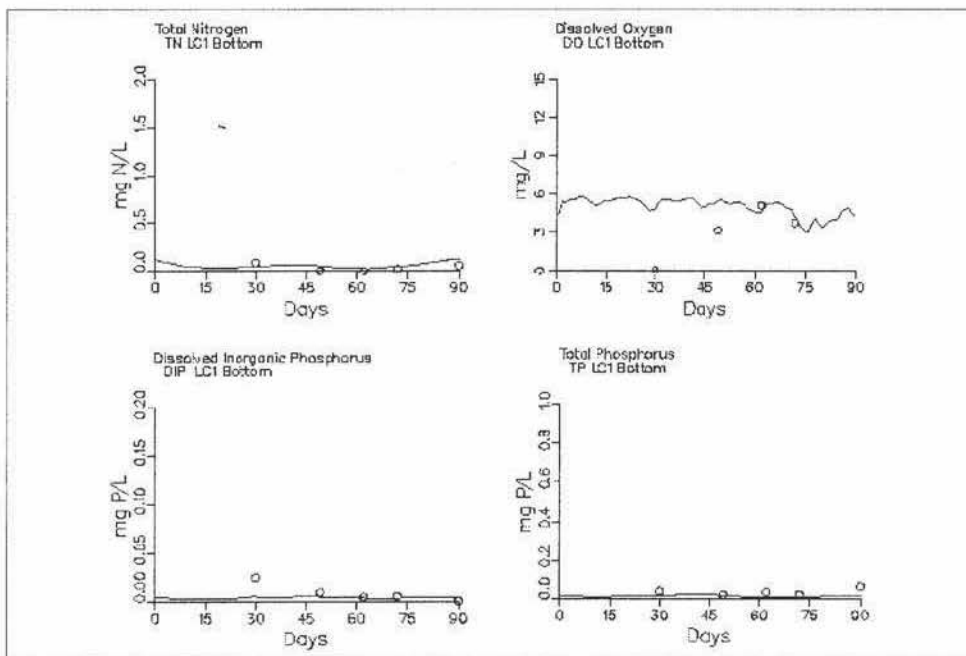


Figure 7-9. (Sheet 4 of 4)

Overall, the results indicate that ICM is performing well at this location. No attempts were made to calibrate ICM for Laguna Condado. A large part of ICM's performance at this location is attributable to the amount of exchange that occurs between Laguna Condado and the ocean. Constituent concentrations in Laguna Condado are similar to those specified at the ocean boundary. This is further evidence of the dominance of offshore conditions on this body.

Station SA-1 is located in Caño San Antonio which lies along the north-east side of San Juan Bay. Temperature and salinity observations in the surface and at the bottom at SA-1 location reflect conditions observed offshore at stations AO-1 and AO-2 indicating a high degree of exchange with the ocean. ICM results for both temperature and salinity correspond well with these observations, Figure 7-10. Surface chlorophyll observations were less than 5 ug/l. ICM chlorophyll results for the surface were typically 2 ug/l or less. Bottom water observations were less than 2.5 ug/l with the exception of one observation which was 17.6 ug/l. ICM results for the bottom of SA-1 indicated that chlorophyll levels were of 1-2 ug/l which agreed well with all but one observation. Total organic carbon surface and bottom observations at SA-1 demonstrated the same behavior observed at the offshore stations AO-1 and AO-2 with an increase in total organic carbon at calibration day 68. ICM results were similar to these observations. ICM results for ammonia, nitrate, and total nitrogen agreed well with both surface and bottom observations at SA-1. Dissolved organic phosphorus and total phosphorus ICM results likewise agreed well with surface and bottom observations at SA-1. Surface dissolved oxygen observations at SA-1 ranged from 5.16 to 9.78 mg/l while bottom dissolved oxygen levels ranged from 3.57 to 4.71 mg/l. As the ranges of observations indicate, the bottom dissolved oxygen concentration was considerably lower than the surface. ICM results adequately matched both surface and bottom dissolved oxygen levels when it is remembered that ICM results are daily averages and do not reflect any diurnal variation due to algal activity.

Laguna de Piñones is one of the major bodies of water in the SJBE system. Its location prevented its inclusion in the transect. Laguna de Piñones is located to the east of Laguna La Torrecilla and resides within a mangrove forest. Laguna de Piñones is connected to the southern end of Laguna La Torrecilla via a narrow canal. The region surrounding Laguna de Piñones is largely undeveloped and the flows and loads it receives are naturally occurring. Laguna de Piñones is shallow and was modeled as one layer in ICM.

Two stations are located in Laguna de Piñones. PL-1 is located in the canal that connects Laguna de Piñones and Laguna La Torrecilla. PL-2 is located on the eastern side of the lagoon. Model results indicate only slight fluctuations in temperature during the calibration period at both stations (Figure 7-11). Salinity predictions are adequate for the first portion of the calibration period but are low by day 90 of the simulation. This is indicative of freshwater flows from the watershed possibly being too high

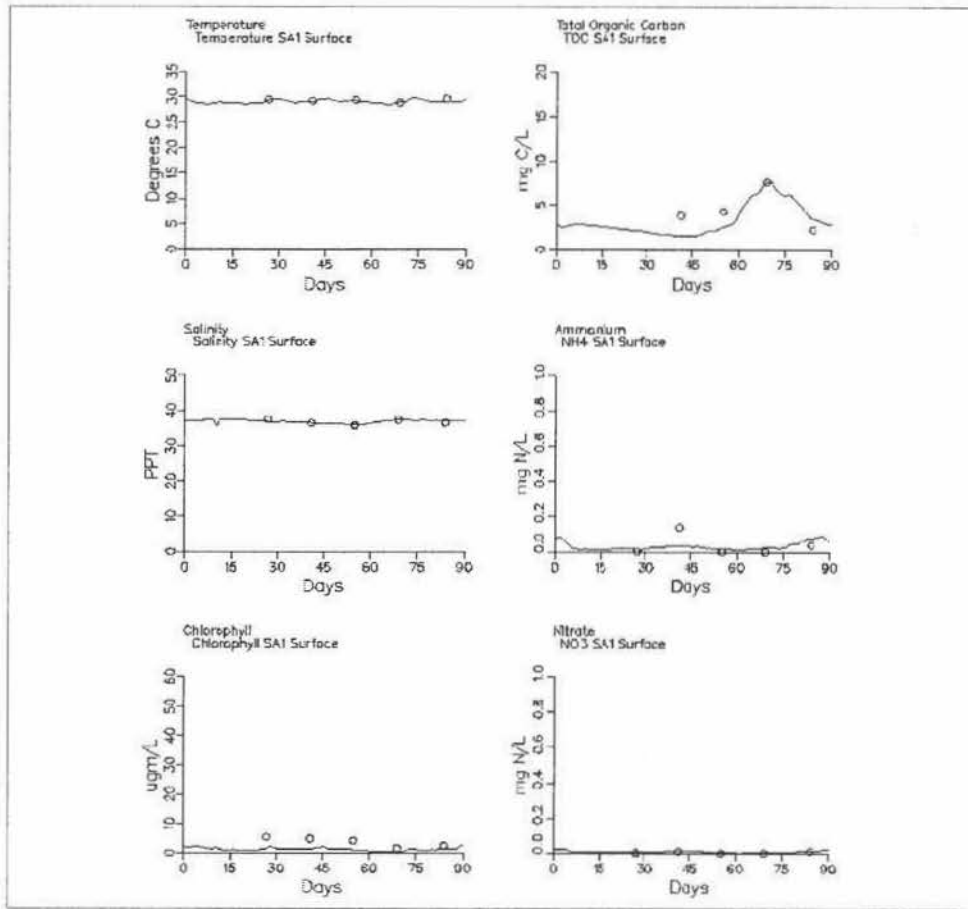


Figure 7-10. Caño San Antonio station SA-1 calibration period time series (Sheet 1 of 4)

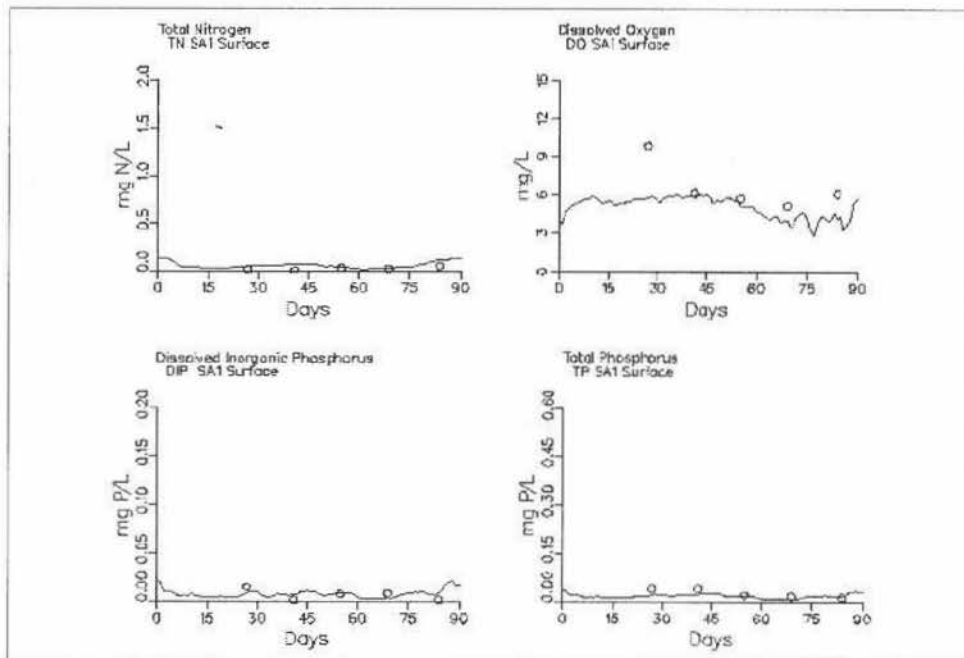


Figure 7-10. (Sheet 2 of 4)

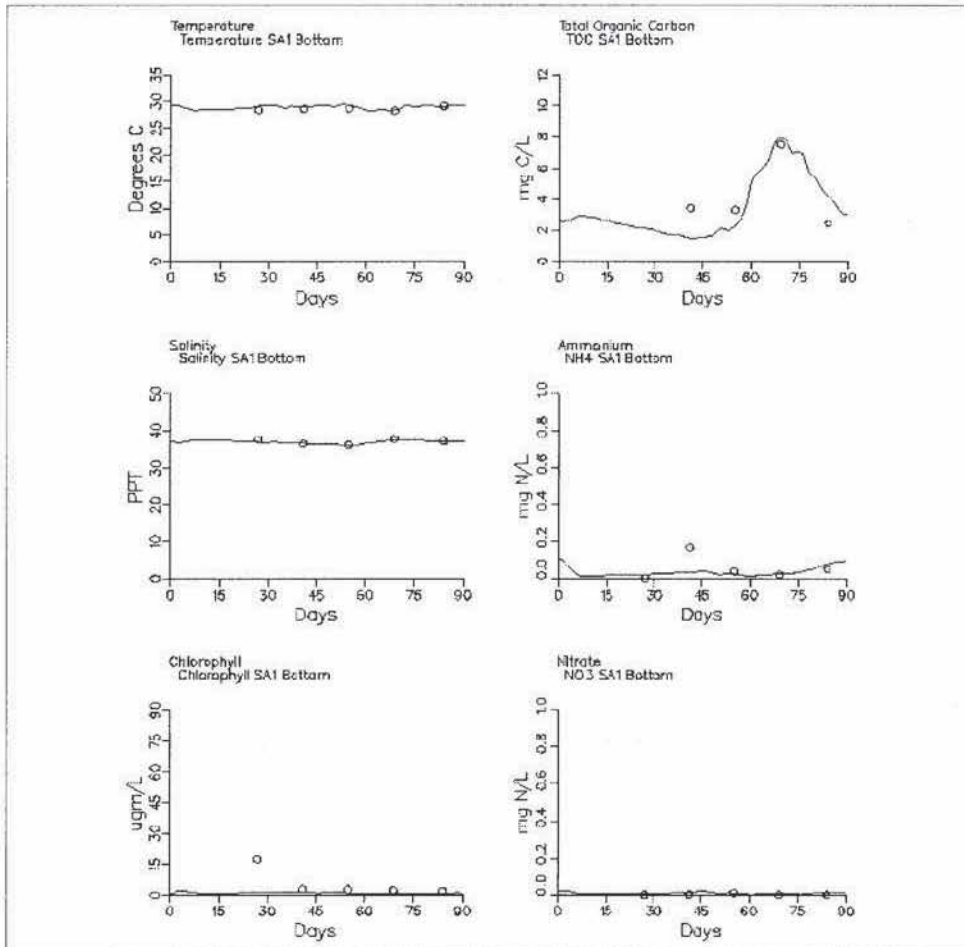


Figure 7-10. (Sheet 3 of 4)

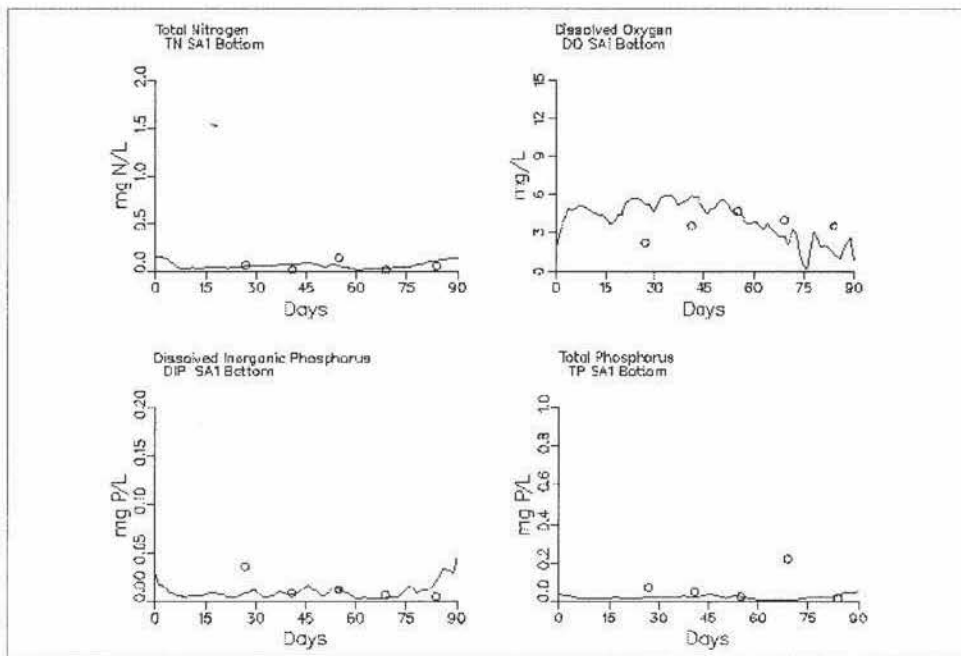


Figure 7-10. (Sheet 4 of 4)

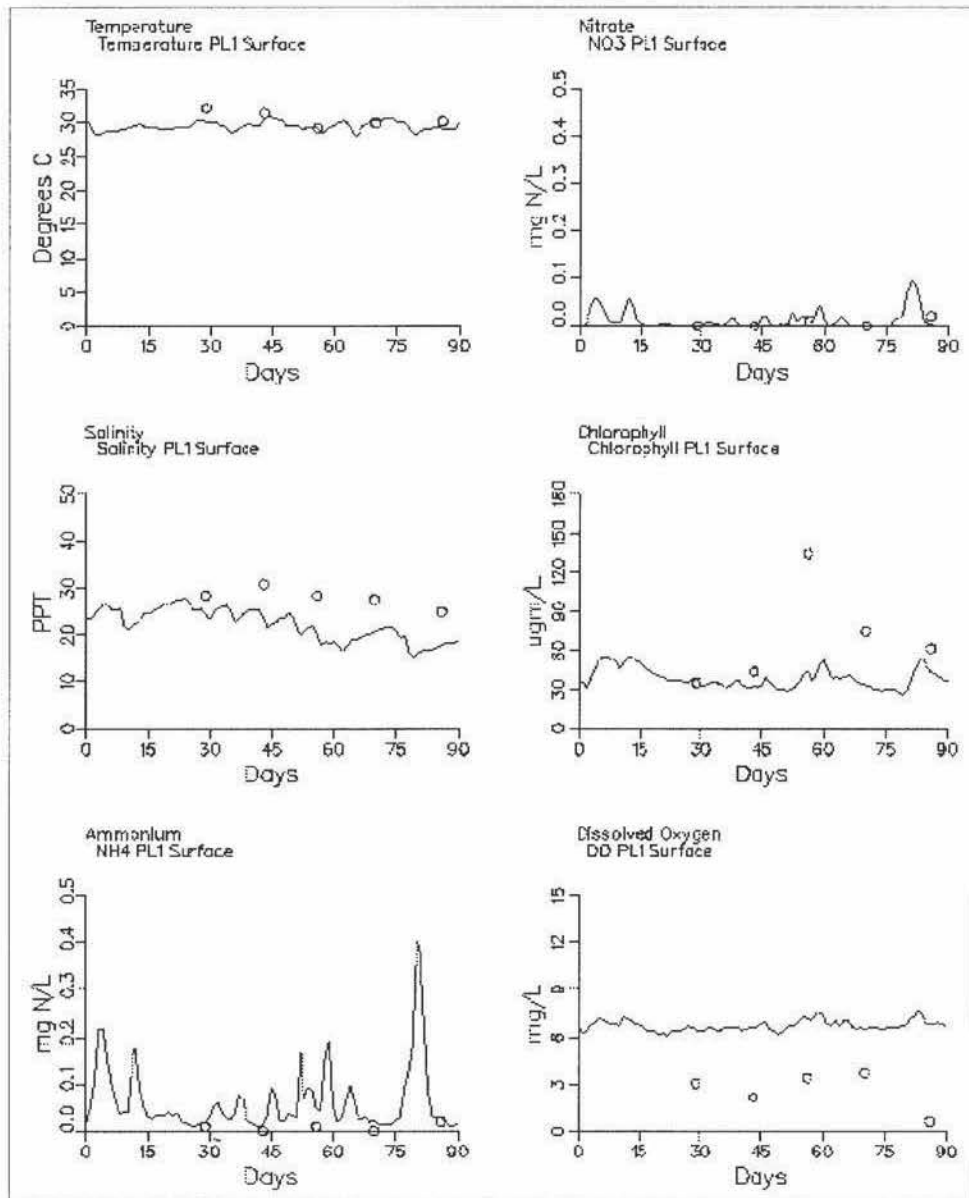


Figure 7-11. Computed and observed water quality variables at stations PL1 and PL2 (Laguna de Piñones) resulting from model calibration for summer 1995 (Sheet 1 of 4)

or too little salt water being able to enter Laguna de Piñones from Laguna La Torrecilla. Early on during calibration it was evident that the original loadings to Piñones were too low. Algae were too low as were nitrogen and organic carbon while dissolved oxygen was too high. Additional loads of nitrogen and carbon were added to the Piñones inflows to compensate for irregular inflow events and possible underestimation of loads. Organic carbon loads were increased from a daily average of 31.4 kg/d to 314.5 kg/day and total nitrogen loadings were increased from 4.5 kg/day to 36.1 kg/day. With these loads model chlorophyll predictions did increase but remained slightly low as a result of nutrient limitations retarding algal growth. Results for ammonium and dissolved inorganic phosphorus

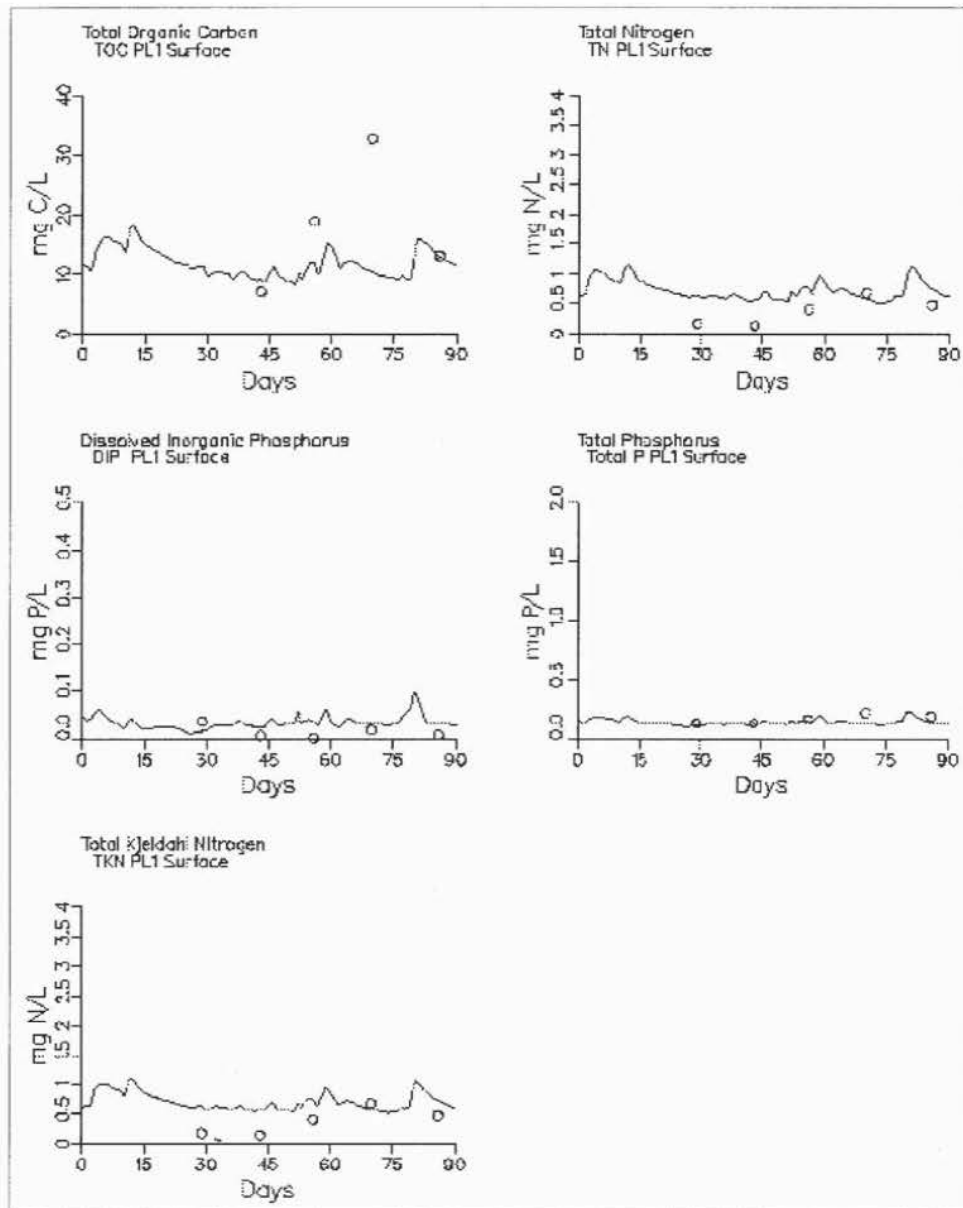


Figure 7-11. (Sheet 2 of 4)

indicate that as soon as a runoff event has deposited these nutrients into the system, algal growth (expressed by chlorophyll levels) increases until the nutrients are removed. At that time, chlorophyll levels cease to increase and actually begin to decrease until the next influx of nutrients occurs. Model predictions for total nitrogen and total phosphorus match the observations well. Model output for total organic carbon underpredicted the observed data continually even with the additional loading. Underprediction of TOC is possibly due to the presence of the mangrove forest which contributes organic carbon. No attempt was made to simulate the effects of the mangroves surrounding the lagoon. Model dissolved oxygen levels remained relatively constant throughout the

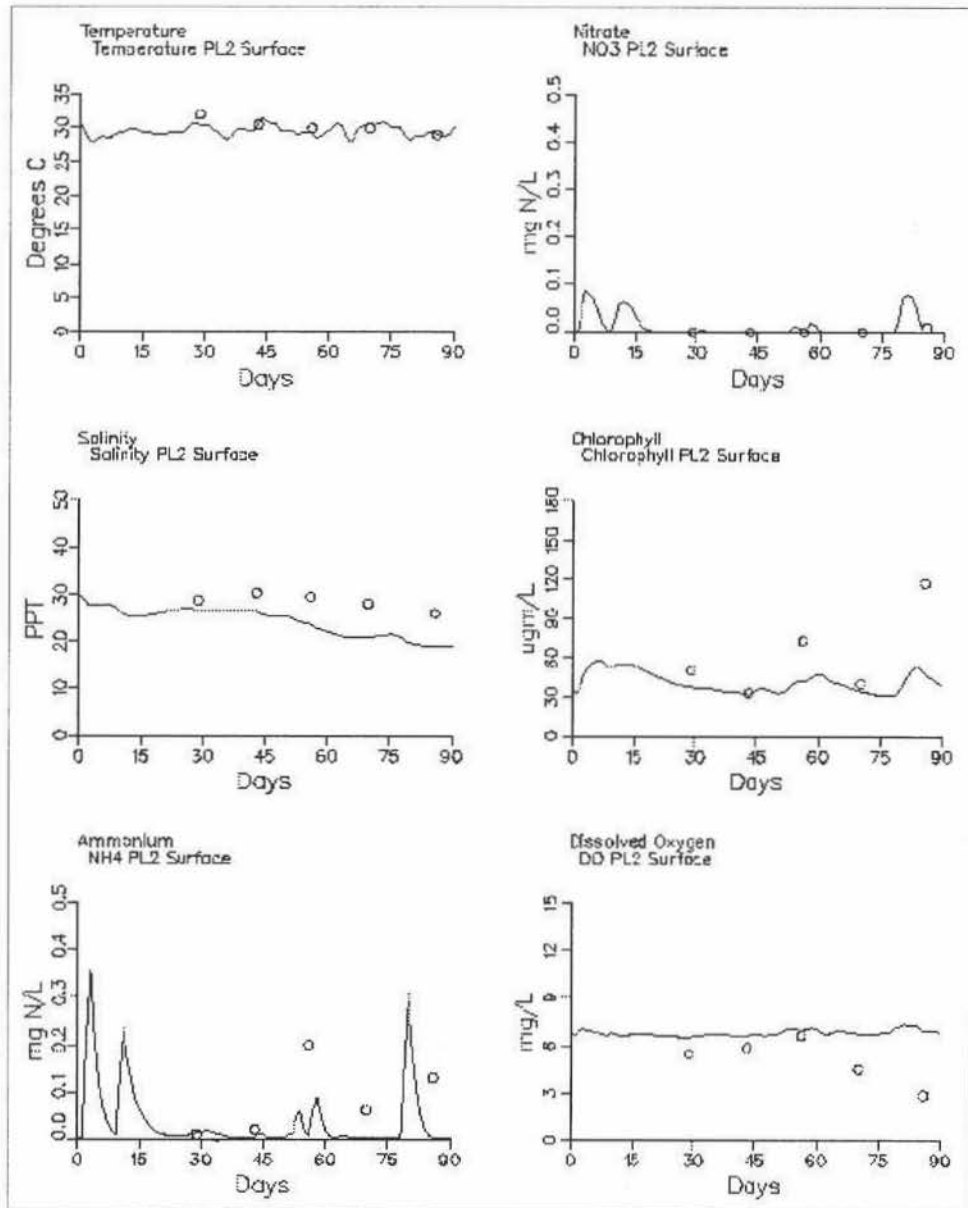


Figure 7-11. (Sheet 3 of 4)

calibration period and are overpredicted compared with observed, especially in the lagoon connecting canal. Possibly SOD is underpredicted due to TOC loadings from the mangroves, or the problem could be related to the inability of the model to resolve thin layers of stratification. Stratified water columns with thin (i.e., < 0.5 m) freshwater lenses are common in estuaries such as the SJBE.

Laguna de Piñones is located on the periphery of the SJBE system. None of the scenarios conducted involved Laguna de Piñones. Thus, the calibration results for Laguna de Piñones are adequate for the purposes of this study.

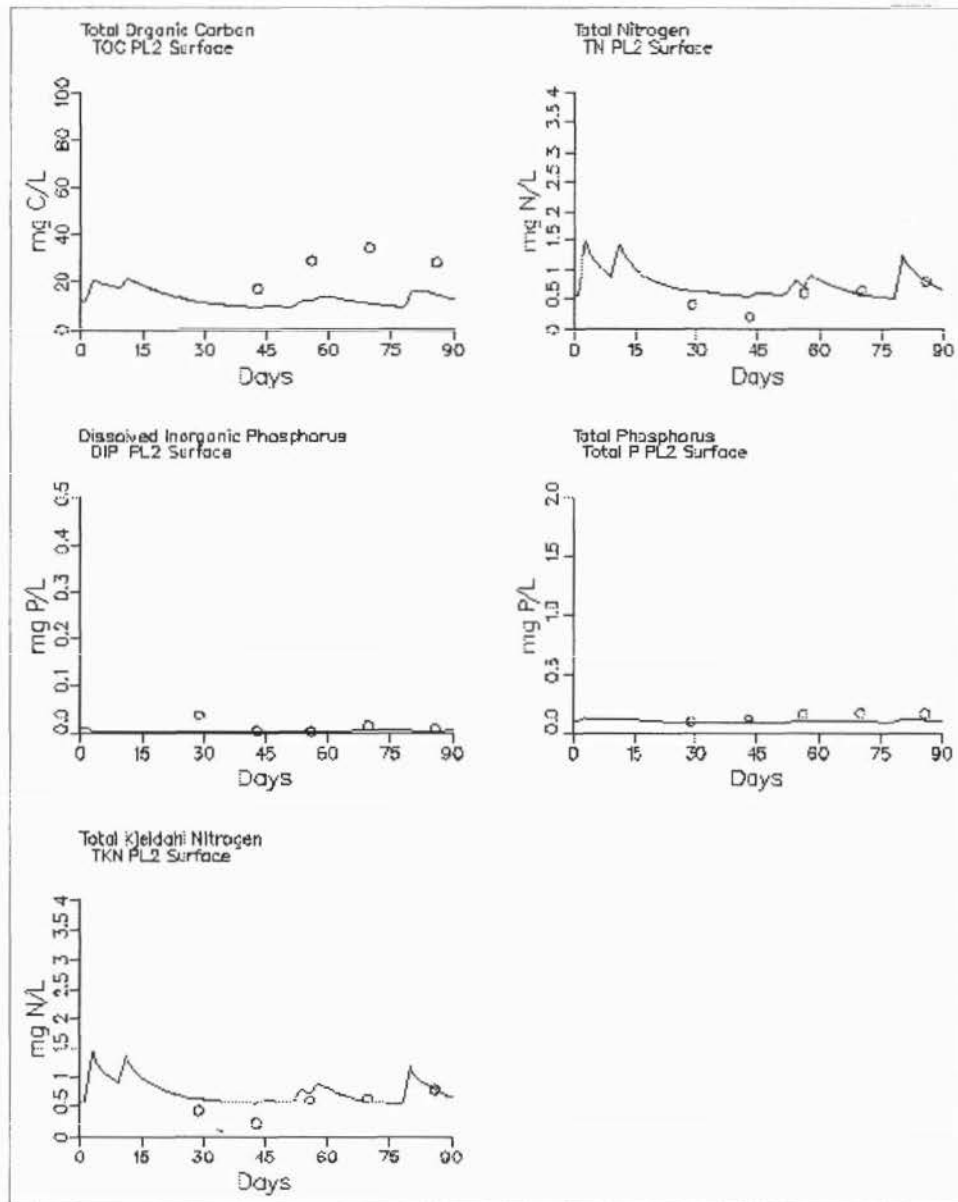


Figure 7-11. (Sheet 4 of 4)

Calibration Conclusions

Model calibration has resulted in a useful tool which adequately replicates observed behavior in the SJBE system. Though the SJBE system is not large it is very heterogeneous with numerous bays, lagoons, and canals which complicated WQM calibration and affected performance. Often, attempts to improve calibration in one constituent or region had detrimental consequences on the calibration elsewhere. Further improvements in calibration were hindered by the limitations of the loading data. A comprehensive database of loading information did not exist and the loads used for calibration were estimates. The actual SJBE system is subjected to

highly variable (both spatially and temporally) loadings resulting from runoff events and localized anthropogenic loadings. Great effort was expended in developing and implementing loads in the WQM which would be representative of these conditions. However, these estimates might not always agree with actual loads resulting from short-term events. Consequently, model calibration is impacted as the WQM may not match observations at locations with large temporal fluctuations in water quality resulting from runoff.

Another consideration when reviewing calibration results is the scale at which processes occur in the real system. Vertical resolution in the WQM is limited to the layer thicknesses used in the hydrodynamic model which were in turn limited by model stability requirements. Consequentially, processes such as stratification in shallow water or the simulation of over-riding, thin, freshwater lenses are beyond the capability of the WQM to resolve.

Overall model calibration was judged to be acceptable for scenario testing by the modelers and the model review group. In scenario testing, the model is run with a modification (scenario) and the results compared to a simulation with no modifications (base) and the relative differences determined. Any calibration deficiencies are present in both the base and scenario simulations and therefore tend to cancel out when the focus is on relative differences between base and scenario results.

8 Management Scenarios

Methods

The model was used to evaluate the effectiveness of various management alternatives (i.e., scenarios) for improving water quality. This section describes the methods used for conducting the management scenario simulations.

The overall strategy consisted of developing a scenario test period (STP) that was used for all scenarios so that comparisons of the relative worth of various management options could be evaluated. Both the HM and WQM had to be executed for each scenario, since the flows from the HM are used to drive the WQM, and in most cases the proposed management alternative affects the flows. However, as discussed further below, it was not necessary to run the HM for the same length of time as the WQM since the HM output is saved and can be used in a repetitive fashion throughout the WQM simulation, as was done for WQM calibration. To properly compare different management options, the WQM was run until it reached an equilibrium condition, i.e., a cyclic, steady-state condition. As the hydrodynamics, inflows, and loadings of the STP were cycled multiple times through the WQM, the WQM eventually arrived at an equilibrium condition that was time-varying, but repeated itself for each STP cycle. The time to reach equilibrium depended on the time it took for the sediments and water column to reach equilibrium, which was on the order of about 8 months.

The calibration period of summer 1995 was chosen for the STP. This period was chosen since it allowed comparison of each scenario against baseline conditions that existed in 1995 when observed data were available. The STP extended for one complete lunar month (28.25 days) using the conditions extending from 10 July through 7 August 1995, which contained a storm event around 1 August. A few extra days were executed on the front end of each HM run for model spin-up. The observed conditions for tides, wind, and freshwater flows were used. Output from the HM was saved and used repeatedly by the WQM throughout the longer, multimonth WQM simulation. Thus, the hydrodynamics used for each month of the WQM simulation were identical for a given scenario. When recycling

hydrodynamics in this fashion, there is a requirement that the system water depths and volumes be nearly equivalent at the beginning and end of the HM simulation to avoid building up or depleting too much water over the long-term WQM simulation. This requirement was satisfied by carefully choosing the beginning and ending time for the STP.

Each WQM scenario STP was run for eight times to spin-up the new conditions, thus achieving a new dynamic steady-state. Only results from the final 28.25-day STP are presented here.

The STP constituent loadings for the WQM were the same as those used for the calibration, except for the loading reduction scenarios where loads were reduced. Meteorological conditions for the WQM for all scenarios were based upon the average July period of record observations at San Juan International Airport and are presented in Table 8-1. Observed, hourly varying July winds were used for the HM scenario runs since winds can affect residual circulation.

Table 8-1. Scenario Meteorological Conditions	
Dry Bulb Temperature	82°F
Dew Point Temperature	73°F
Wind Speed	8.5 mph
Cloud Cover	60%

Scenario Descriptions

Ten sets of simulations (Table 8-2) were run to assess the impact proposed remediation management strategies would have upon water quality. Scenario 1a was a base condition against which the other nine would be judged. Five scenarios (1b, 1c, 2, 3, and 4) involved some form of channel/bathymetric modification in either Caño Martín Peña, Laguna San José, or Canal Suárez and Laguna La Torrecilla which would result in a redistribution of flows. Scenarios 5a and 5b involved only loading reductions while scenarios 6a and 6b combined channel/bathymetric modifications and loading reductions. The channel/bathymetric modifications called for by many of these scenarios resulted in a reconfiguration of ICM grid (see Table 8-3) as well as running new conditions in the HM (see Table 8-2). The scenarios evaluated are described further below, and the results are discussed in the subsequent sections of this chapter.

**Table 8-2.
Management Water Quality Scenarios**

Scenario	Description	Hydrodynamic Scenario
1a	Base condition with approved dredging in San Juan Bay and Rio Piedras implemented	1a
1b	1a plus clearing and widening eastern end of Caño Martín Peña to 50 ft	1b
1c	1a plus widening Caño Martín Peña to 150 ft and deepening to 9 ft	1c
2	1a plus filling all dredge material borrow pits to 6-ft depth	2
3	1a plus removing the constriction at the Loiza Expressway bridge on Suárez Canal by widening by 100 ft and deepening to 12 ft	3
4	Conditions of Scenario 3 plus installation of 1-way tide gate in Canal Suárez	4
5a	1a plus loading reduction in Caño Martín Peña Canal (removal of un-sewered loadings)	1a
5b	1a plus loading reduction in San José (removal of Baldorioty de Castro pump station loadings)	1a
6a	1c plus 5a and 5b	1c
6b	6a plus 2	6b

**Table 8-3.
ICM Grid for Each Scenario**

Scenario	Surface Cells	Total Cells	Total Flow Faces	Horizontal Flow Faces
1a	1923	10731	28230	19422
1b	1923	10731	28230	19422
1c	1923	10769	28309	19463
2	1923	10341	27451	19033
3	1923	10734	28238	19427
4	1923	10734	28238	19427
5a	1923	10731	28230	19422
5b	1923	10731	28230	19422
6a	1923	10769	28309	19463
6b	1923	10379	27530	19047

Scenario 1a, Baseline Conditions

The baseline simulation was similar to conditions that existed during the summer of 1995 and used the same boundary conditions and loadings as those used for model calibration. The geometry and bathymetry of the system were the same as the *existing* conditions with the exception of minor geometric changes related to dredge and fill improvements that were approved and have either been implemented or are underway. These improvements involved deepening the San Juan Harbor channel to 11.9 m (39 ft) and deepening the Puerto Nuevo flood control channel to 7.32 m (24 ft). Scenario 1a served as the baseline, or *existing*, conditions against which all other scenarios were compared to evaluate their effectiveness.

Scenarios 1b and 1c, Channel Improvements in Caño Martín Peña

The eastern portion of Caño Martín Peña is considered to severely hinder flushing of the inner part of the system. Thus, two scenarios simulations were conducted to evaluate channel improvements for the eastern portion of Caño Martín Peña. The first channel improvement, Scenario 1b, consisted of clearing the channel to a nominal 15.2-m (50-ft) width from about 7 m (25 ft). The model bottom drag coefficient was also changed to reflect clearing of the channel for Scenario 1b. The second channel improvement, Scenario 1c, consisted of a channel widened to a minimum width of 45.7 m (150 ft) and deepened to a minimum depth of 2.74 m (9 ft). Both scenarios were run with all other conditions and configurations set the same as those for Scenario 1a. The HM grid was modified for each channel configuration, and the HM was executed for the STP to generate flows for the WQM. Then the WQM was run to equilibrium using the new HM output and *existing* loads for the STP.

Scenario 2, Filling of Submerged Borrow Pits

This scenario consisted of Scenario 1a conditions plus filling of submerged borrow pits within Laguna San José and Laguna La Torrecilla. These pits are the result of sand and fill mining for development of residential and service facilities. The deep holes have low DO and are sources for nutrients that diffuse from bottom sediments under low DO conditions. The bathymetry for model grids cells representing the pits was reduced to a depth of 1.83 m (6 ft). The HM was executed for the STP with the new depths. The WQM was then run to equilibrium using this HM output and *existing* loads.

Scenario 3, Loiza Expressway Bridge Constriction in Suárez Canal Removed

For the most part, Suárez Canal does not restrict flushing, with the exception of a constriction at the Loiza Expressway bridge, where the canal is only about 15 m (50 ft) wide and 0.91 m (3 ft) deep. Thus, a scenario was conducted to investigate removing the Loiza Expressway bridge constriction by enlarging the canal at the bridge to 30.5 m (100 ft) wide by 3.66 m (12 ft) deep. The HM grid was adjusted to represent the proposed Suárez Canal improvement, and the model was run using Scenario 1a conditions for all other geometric features and boundary conditions. The WQM was then run to equilibrium using this HM output and *existing* loads.

Scenario 4, Tide Gate in Suárez Canal with Bridge Constriction Removed

Scenario 4 investigated a tide gate installed and operated in Suárez Canal where the gate was open during flood flow through Suárez Canal and closed during ebb flow to force water out through Caño Martín Peña. The HM was modified to allow simulation of a tide gate operating in the western portion of Suárez Canal, and the HM was executed for the STP with the tide gate combined with Scenario 1a conditions plus the bridge constriction removed (Scenario 3). The bridge constriction was removed too for this scenario since this improvement is considered likely to occur if a tide gate is built. The WQM was then run to equilibrium using this HM output and *existing* loads.

Scenarios 5a and 5b, Loading Reductions

Considerable loadings of nutrients and fecal coliform bacteria occur within the SJBE system. Therefore, management actions to reduce these loadings is a potential effective means of improving water quality. To evaluate the effectiveness of loading reductions, it was necessary to conduct these simulations with *existing* conditions for other boundary conditions and system geometry and bathymetry. Therefore, the loading reductions were conducted with Scenario 1a hydrodynamics imposed. So it was not necessary to re-run the HM for Scenarios 5a and 5b. The loadings in the WQM prescribed in Scenario 1a were reduced as described below, and the WQM was run to a new equilibrium condition.

Scenario 5a consisted of eliminating local, nonpoint source loadings along Caño Martín Peña. These loads are significant and represent untreated sewage from un-sewered residential areas. Removing these loads is a very likely management scenario.

Scenario 5b consisted of diverting all pollutant loadings that enter Laguna San José via the Baldorioty de Castro storm water pump station.

The flows from the plant were still introduced, but the constituent concentrations were removed.

Scenarios 6a and 6b, Combinations

Following review of results from the previous scenarios, the SJBEP recommended two combination scenarios be run to evaluate the cumulative effectiveness.

Scenario 6a consisted of the combination of management alternatives prescribed by Scenarios 1c, 5a, 5b. Thus, Scenario 6a contained the improved Caño Martín Peña (45.7 m or 150 ft wide and 2.74 m or 9 ft deep) along with the elimination of loadings in Caño Martín Peña and from the Baldorioty de Castro storm water pump station. Otherwise, other geometry, bathymetry, and boundary conditions were the same as those for Scenario 1a. Thus, HM output from run 1c was used to drive the WQM to a new equilibrium condition using the reduced loadings for Scenarios 5a and 5b.

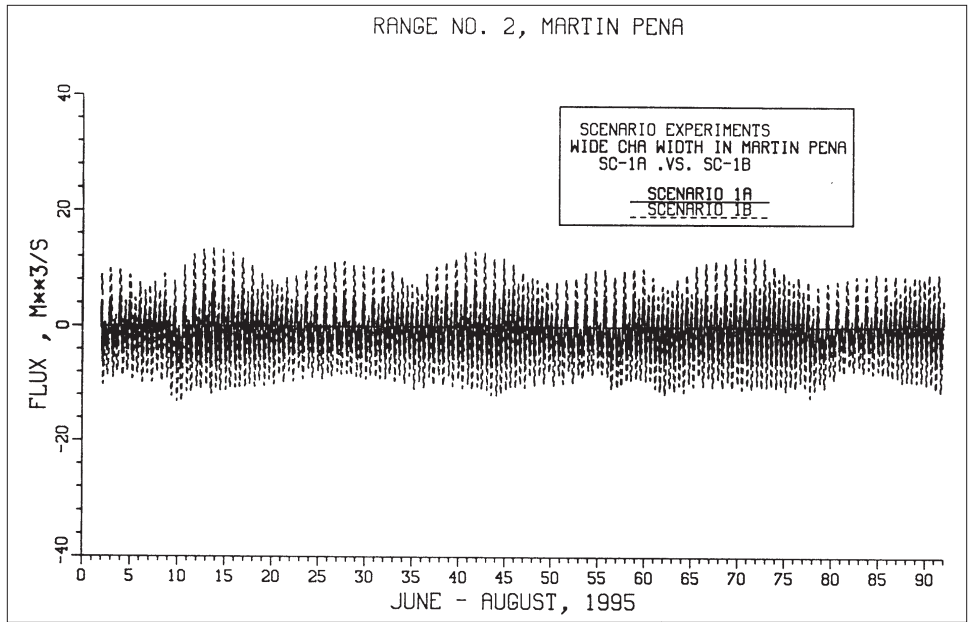
Scenario 6b consisted of the combination of management alternatives prescribed by Scenarios 1c, 2, 5a, and 5b. Thus, Scenario 6b included conditions for Scenario 6a plus Scenario 2, i.e., submerged borrow pits filled. Scenario 6b required re-running the HM with the combination of Scenarios 1c and 2 management alternatives. These HM results were used to drive the WQM to a new equilibrium condition with Scenarios 5a and 5b loading reductions imposed.

Hydrodynamic Model Results

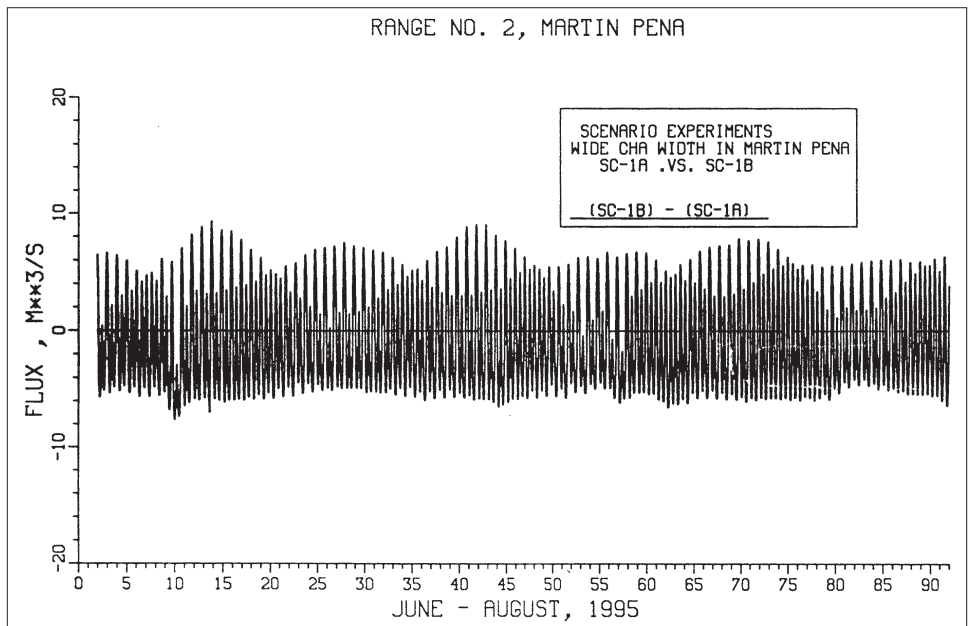
This section discusses the scenarios that were simulated by the HM. Comparisons of HM results from each of the scenarios with results from Scenario 1a are presented and discussed below.

Scenario 1b Results

As can be seen from Figures 8-1 and 8-2, the impact of slightly widening the eastern end of Martín Peña and reducing the friction is to increase the tidal flux through the Martín Peña Canal while slightly decreasing the flux through Canal Suárez. Figure 8-3 shows essentially no change in the tidal range in Laguna San José, but a slight setdown in the water level is computed. This is likely due to more of the Laguna San José freshwater inflow being able to move out of the lagoon more quickly through the improved Martín Peña Canal. As a result of the increased flow of freshwater, one might expect that the salinity in Martín Peña would decrease. Figure 8-4 shows this to be the case. Likewise, due to the decreased amount of San José freshwater inflow moving out through the Canal

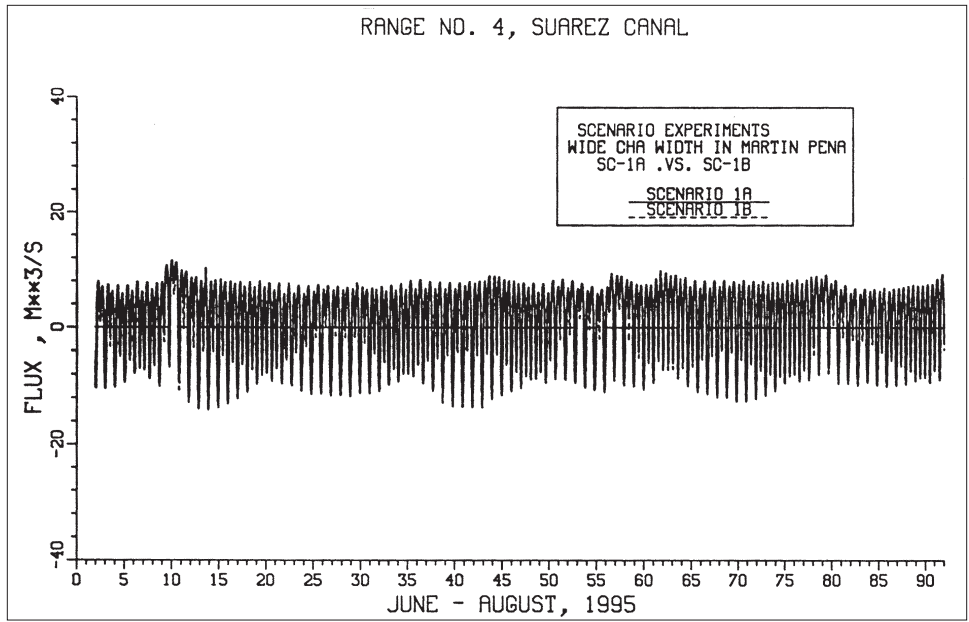


a. Both 1a and 1b

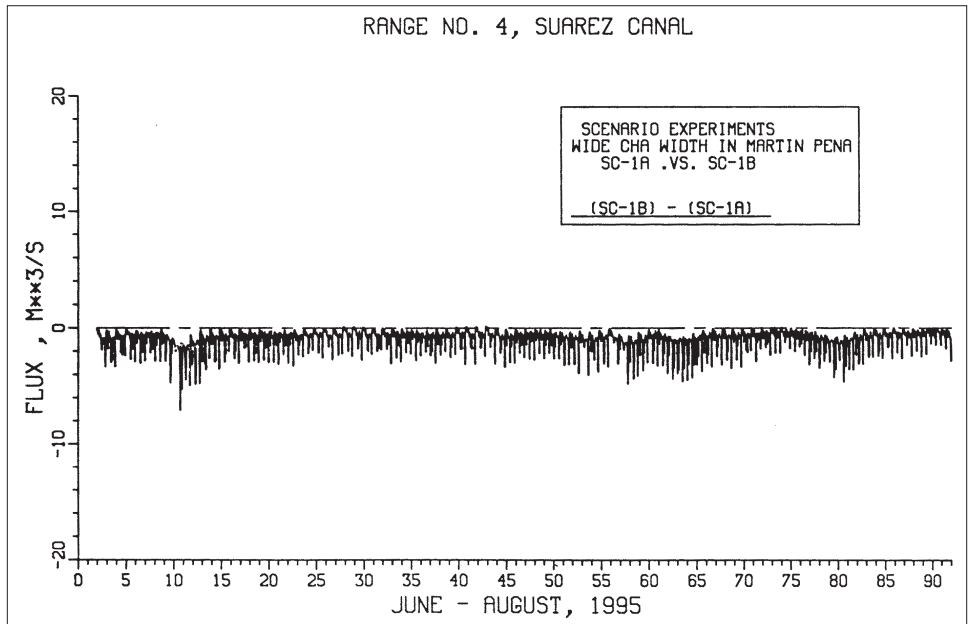


b. Difference between 1a and 1b

Figure 8-1. Comparison of flux through Martin Pena Canal between Scenarios 1a and 1b



a. Both 1a and 1b



b. Difference between 1a and 1b

Figure 8-2. Comparison of flux through Suarez Canal between Scenarios 1a and 1b

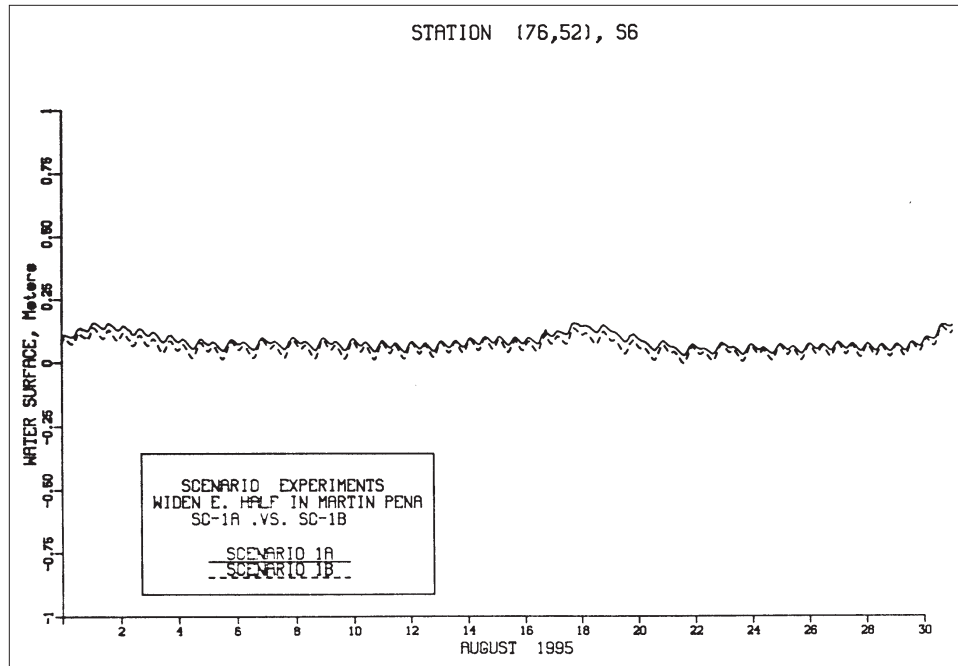


Figure 8-3. Comparison of tide at S6 between Scenarios 1a and 1b

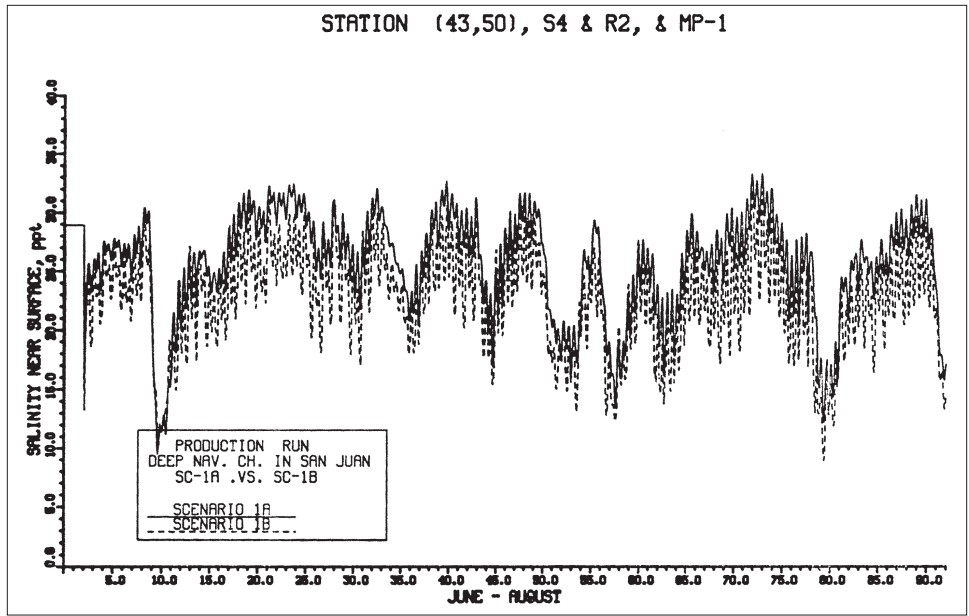
Suárez, Figure 8-5 shows that the salinity in Suarez increases. With the salinity in Suarez being higher, higher saline water flows into Laguna San José during flood, resulting in higher salinity in San José. This is illustrated in Figure 8-6.

Scenario 1c Results

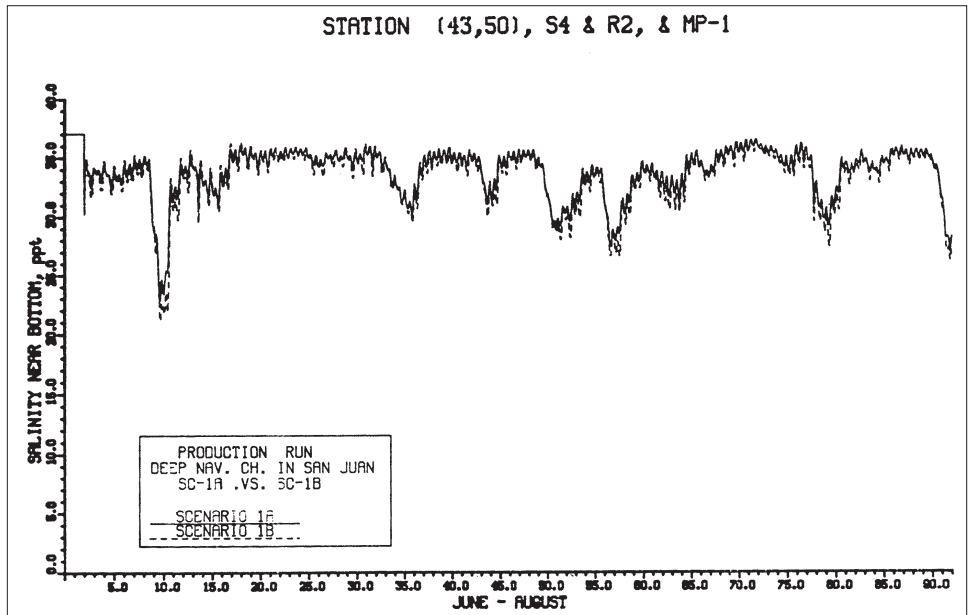
With a substantial increase in width and depth in Martín Peña Canal for this scenario, Figure 8-7 illustrates that the tide range in Laguna San José increases from less than 5 cm (0.164 ft) to 30-35 cm (0.984 - 1.148 ft). As illustrated in Figure 8-8, the tidal flushing between San Juan Bay and Laguna San José increases by more than an order of magnitude. However, as with Scenario 1b, improvements in Martín Peña Canal result in less flushing through Canal Suárez (Figure 8-9). With the tremendous increase in tidal flushing through Martín Peña Canal, the high saline waters of San Juan Bay move into Laguna San José, resulting in increases in salinity in Martín Peña and San José (Figures 8-10 and 8-11). Likewise, with the increased salinity in San José, as water moves from San José into Canal Suárez, salinity in Canal Suárez increases (Figure 8-12).

Scenario 2 Results

As illustrated in Figures 8-13 - 8-15, filling the holes in the system had virtually no impact on flux through the canals nor on the tidal range in Laguna San José. However, as shown in Figures 8-16 - 8-18, decreases in salinity in Martín Peña, San José, and Suarez were computed. Data from

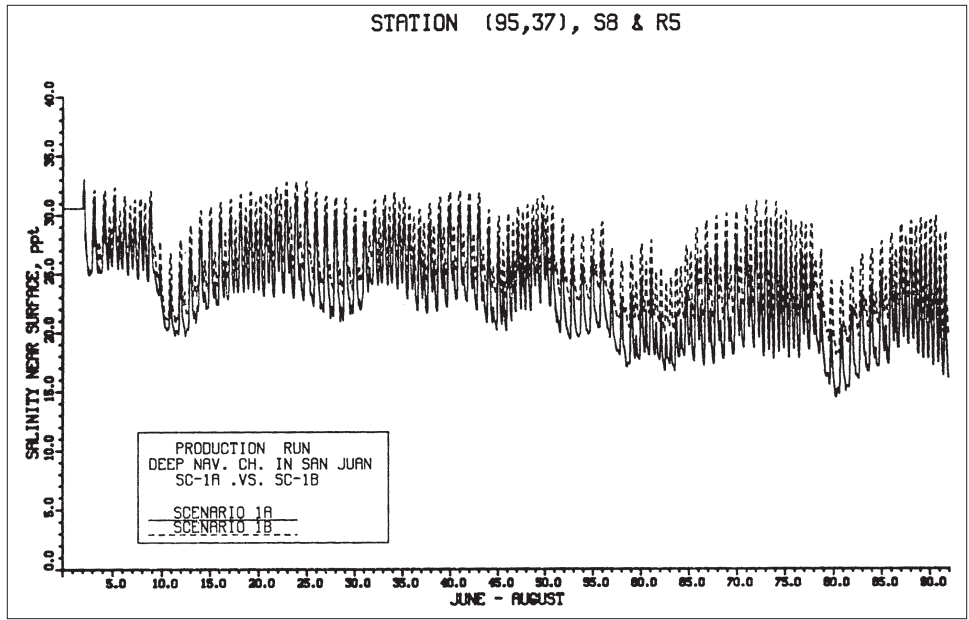


a. Near surface

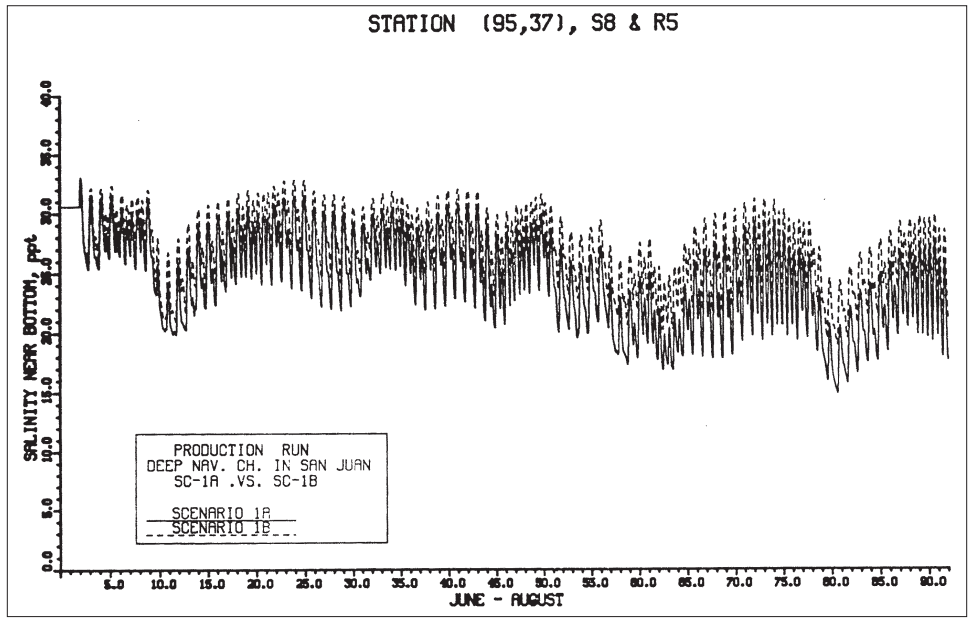


b. Near bottom

Figure 8-4. Comparison of salinity at S4 between Scenarios 1a and 1b



a. Near surface



b. Near bottom

Figure 8-5. Comparison of salinity at S8 between Scenarios 1a and 1b

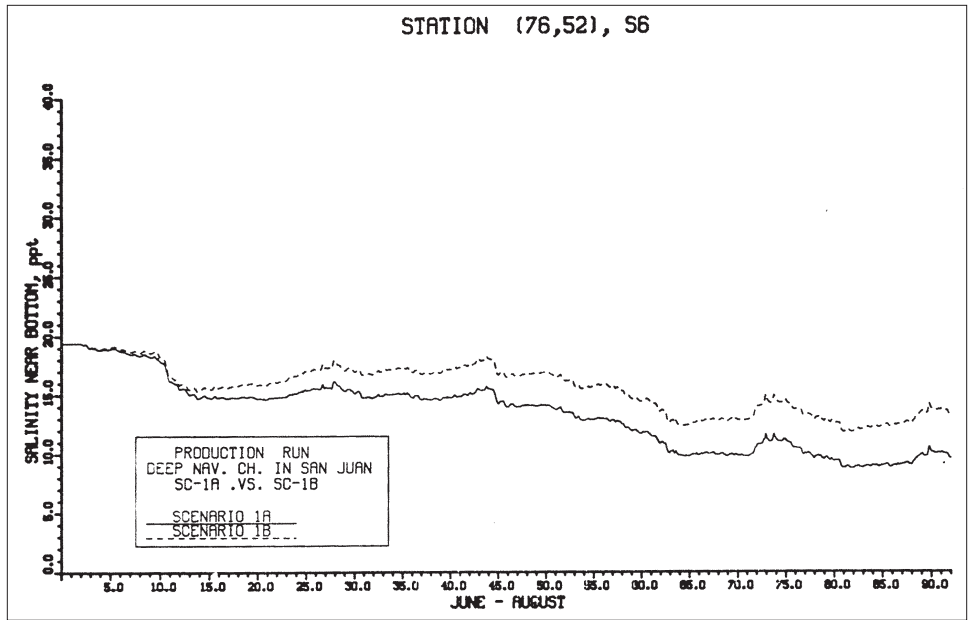


Figure 8-6. Comparison of salinity at S6 between Scenarios 1a and 1b

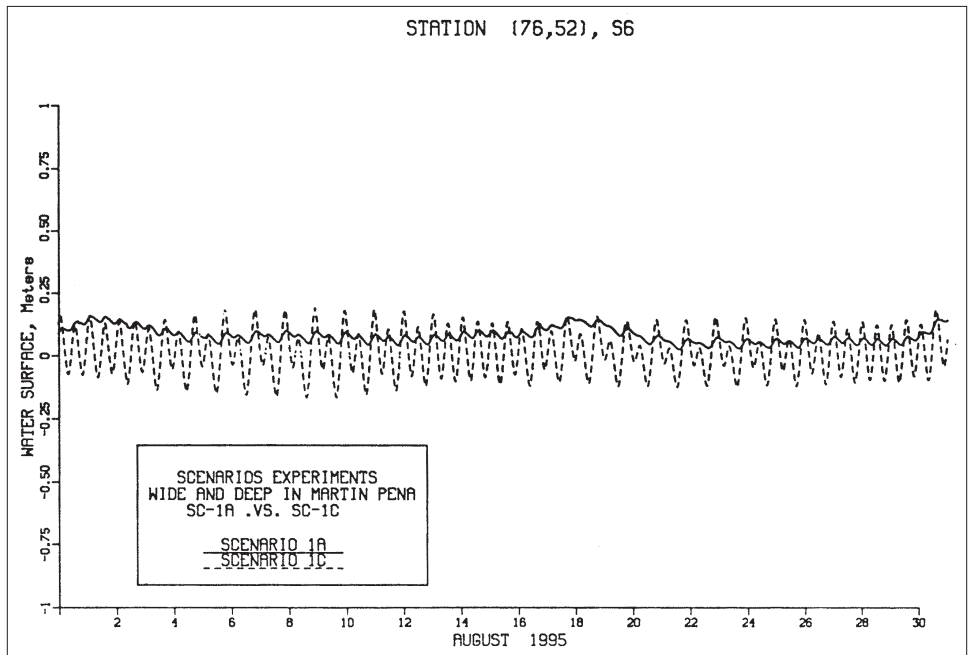
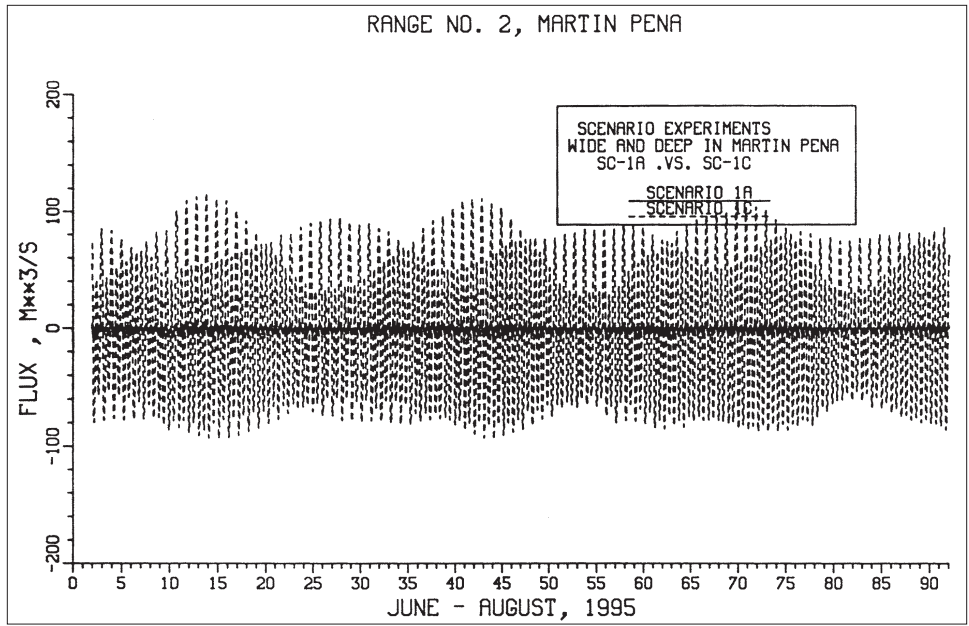
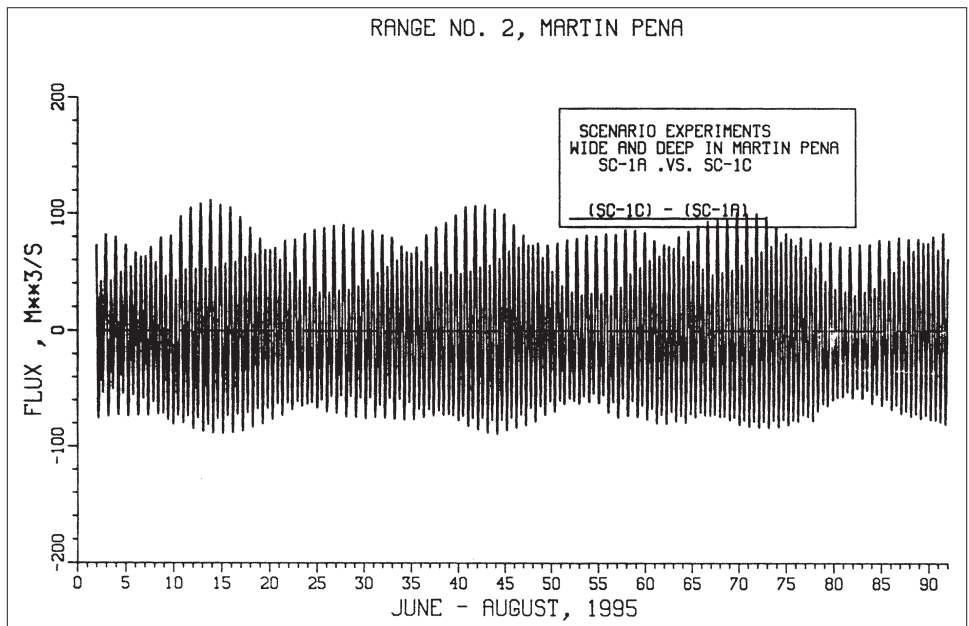


Figure 8-7. Comparison of tide at S6 between Scenarios 1a and 1c

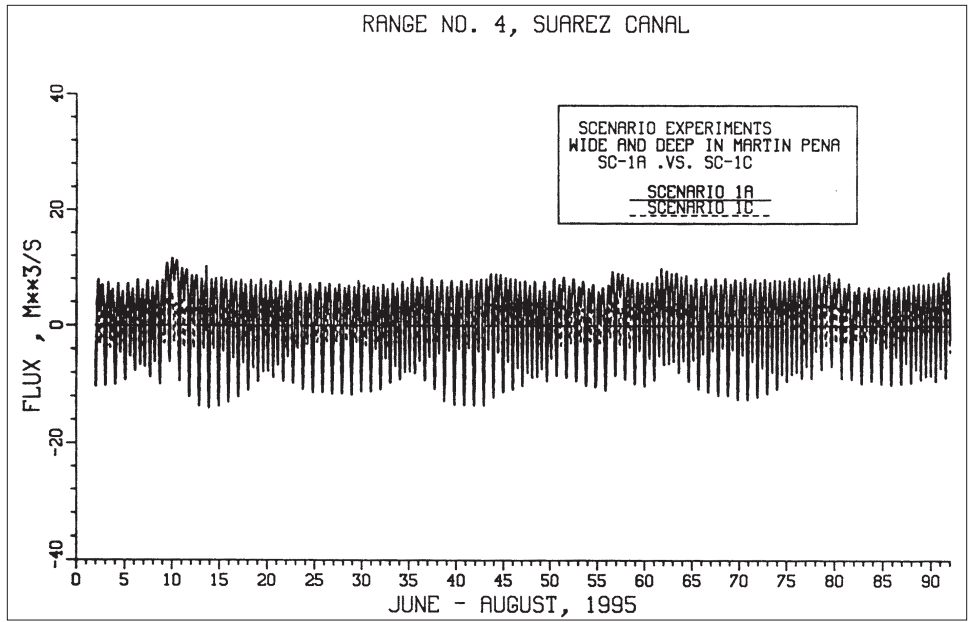


a. Both 1a and 1c

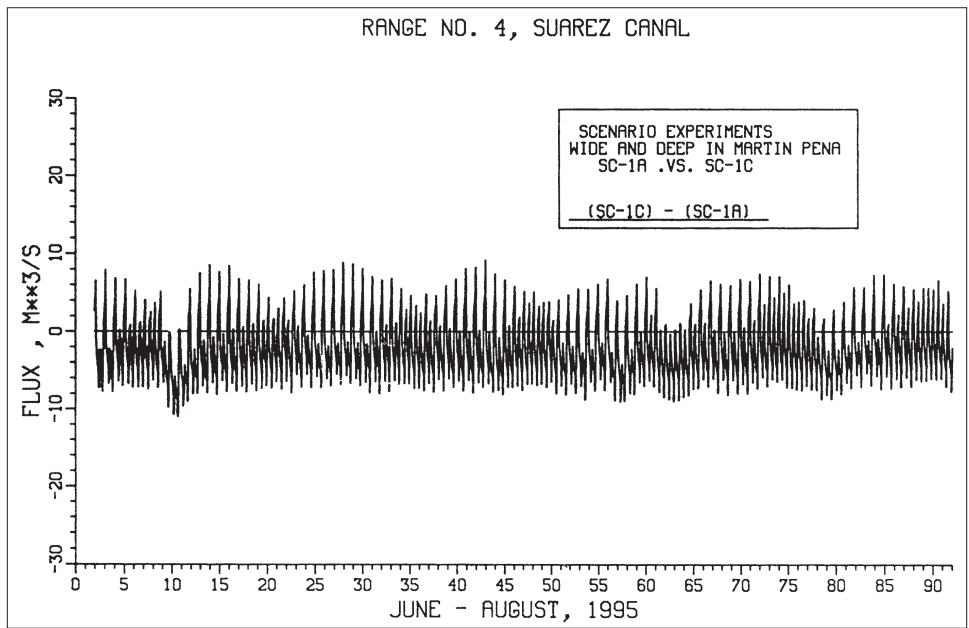


b. Difference between 1a and 1c

Figure 8-8. Comparison of flux at Range 2 between Scenarios 1a and 1c

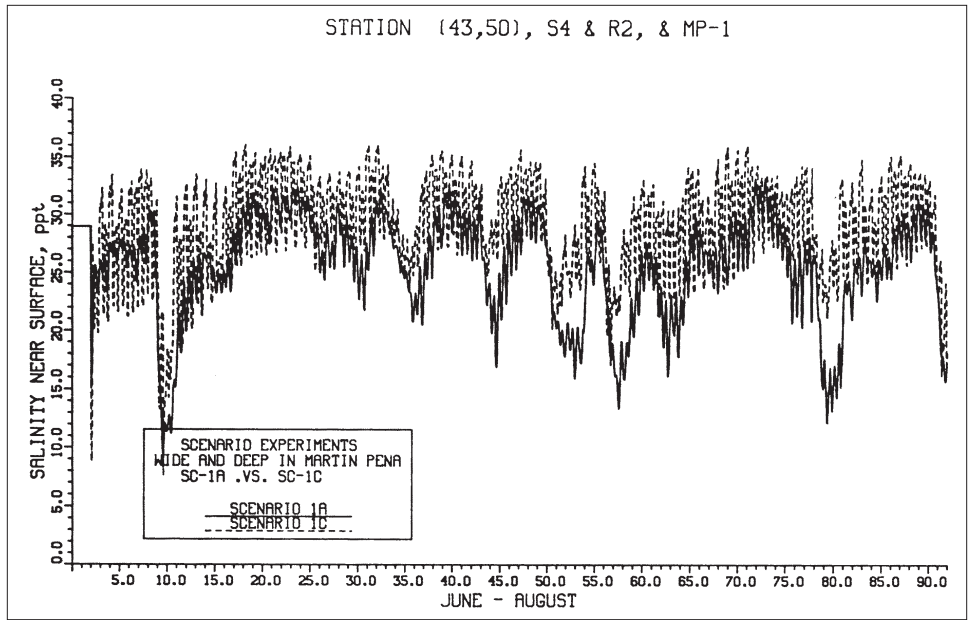


a. Both 1a and 1c

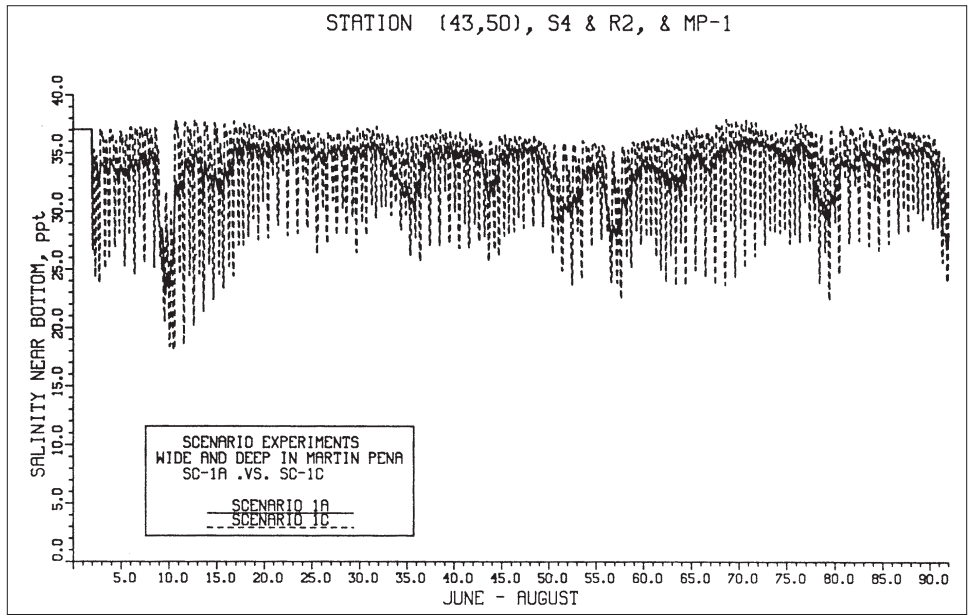


b. Difference between 1a and 1c

Figure 8-9. Comparison of flux at Range 4 between Scenarios 1a and 1c



a. Near surface



b. Near bottom

Figure 8-10. Comparison of salinity at S4 between Scenarios 1a and 1c

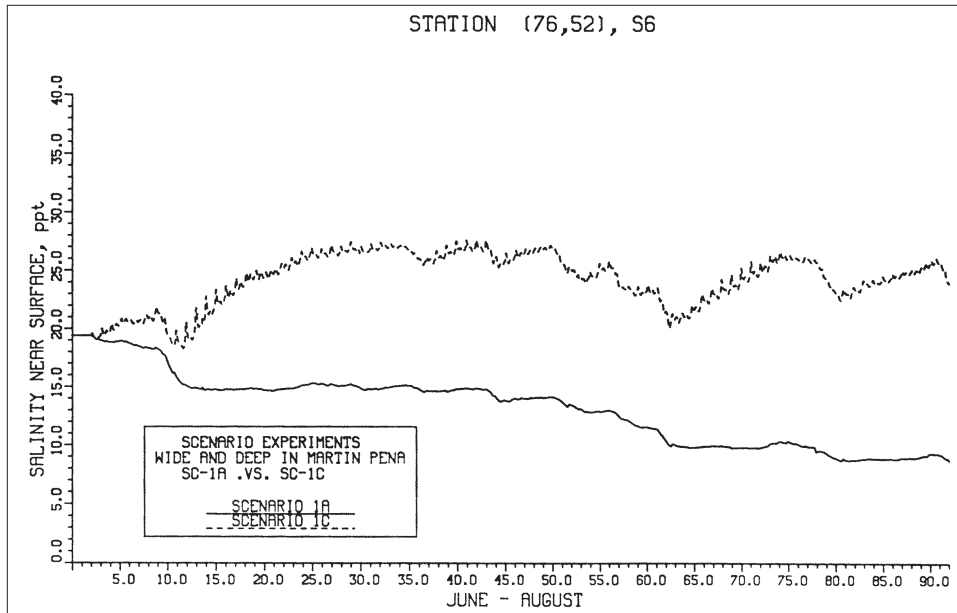
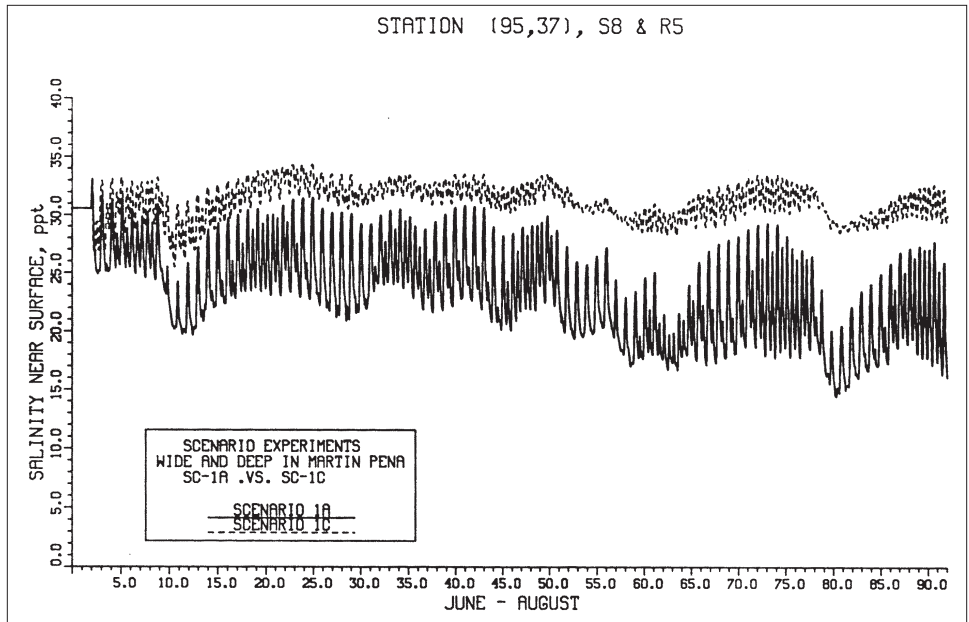


Figure 8-11. Comparison of salinity at S6 between Scenarios 1a and 1c

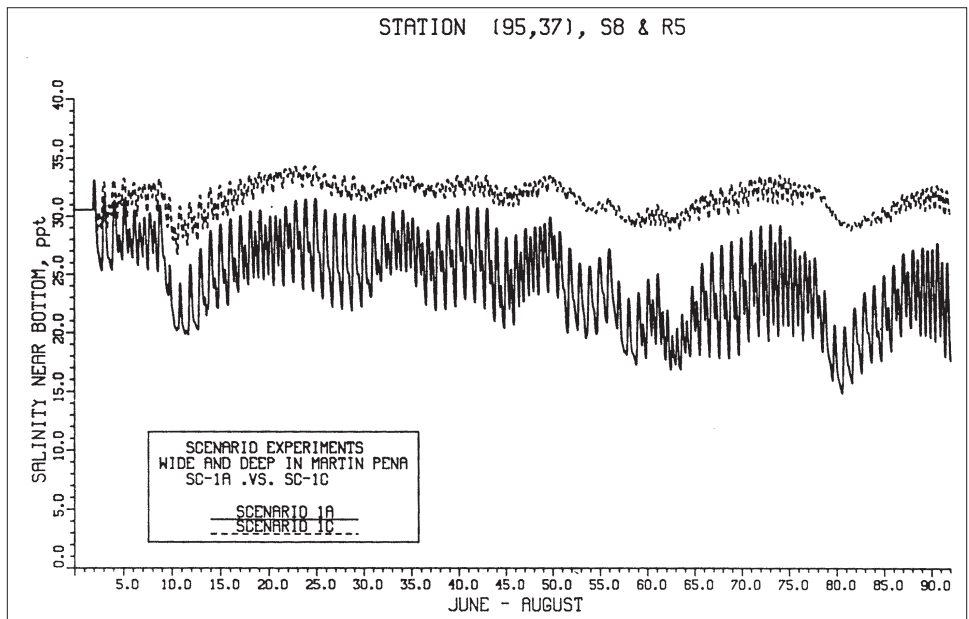
the field collection effort previously discussed show that high salinity exists in the dredged holes in Laguna San José and one hole in Canal Suárez. It has been speculated that high salinity groundwater from the ocean maintains the high salinity in the holes. To simulate this behavior in the model, salinity in the holes was nudged (see Chapter 7) to match the field data. Thus, when the holes were filled, this source of salinity was removed, resulting in the lower computed salinity in Laguna San José and Canal Suárez.

Scenario 3 Results

This scenario involved widening and deepening the constriction in Canal Suárez. As can be seen from Figure 8-19, opening this constriction results in the tide range in San José increasing from less than 5 cm (0.164 ft) to 20-25 cm (0.656 - 0.820 ft), with the resulting tidal flux through Canal Suárez (Figure 8-20) being increased by a factor of 5 or so. Figure 8-21 shows that the impact on the flux through Martín Peña is to increase the flux slightly on flood (water moving into Laguna San José). This results in the salinity in Martín Peña being slightly increased (Figure 8-22). With the increased tidal exchange between San José and Laguna La Torrecilla, salinity in both San José and Suarez increases (Figures 8-23 and 8-24). One noticeable exception in Suarez is around the 9th of June when a storm event resulted in a considerable runoff of freshwater into Laguna San José (see inflows in Figure 3-3). With the less constricted Canal Suárez, a larger portion of the San José freshwater inflow moves through the canal than before.

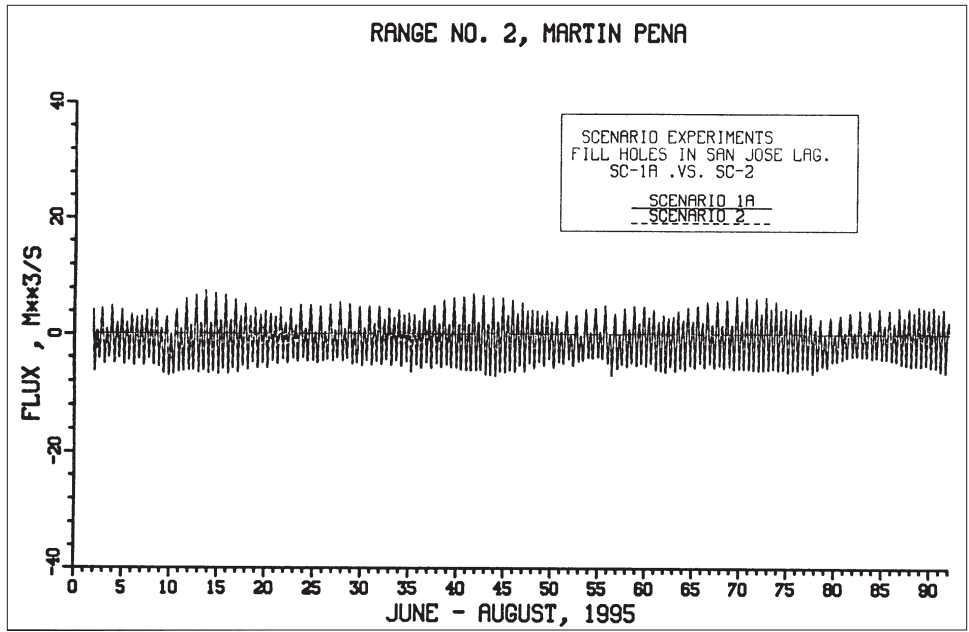


a. Near surface

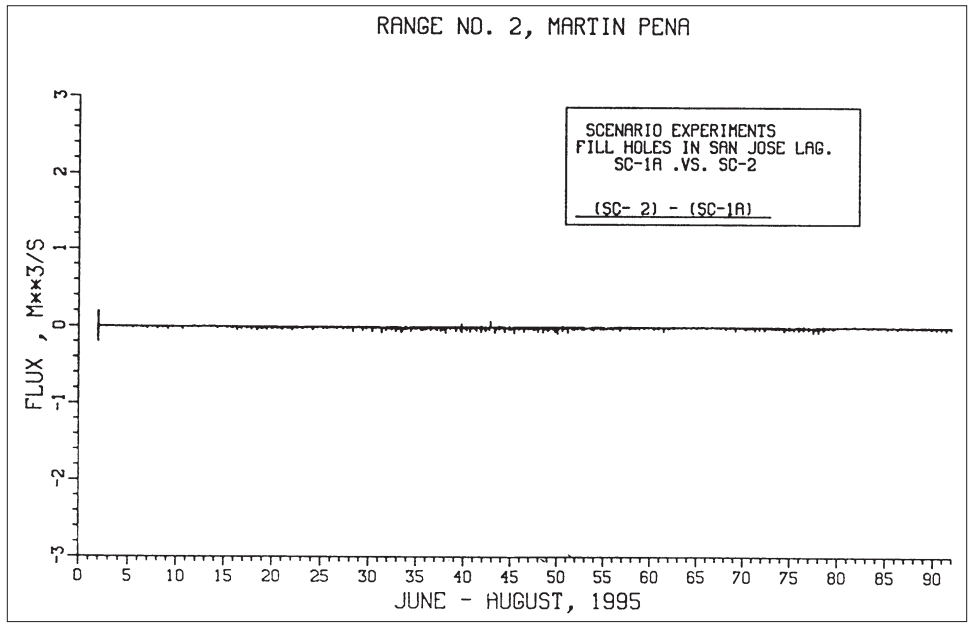


b. Near bottom

Figure 8-12. Comparison of salinity at S8 between Scenarios 1a and 1c

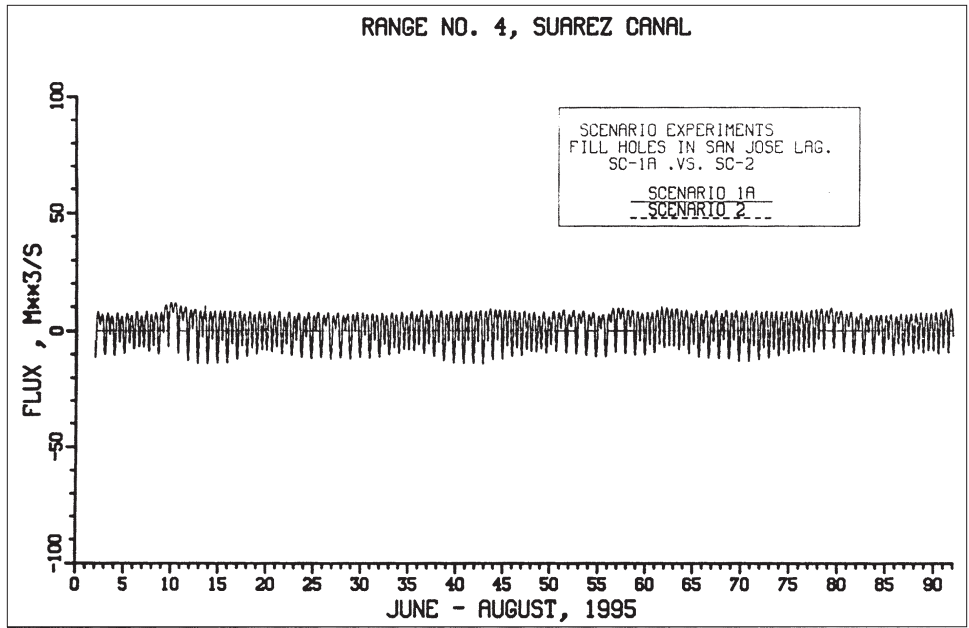


a. Both 1a and 2

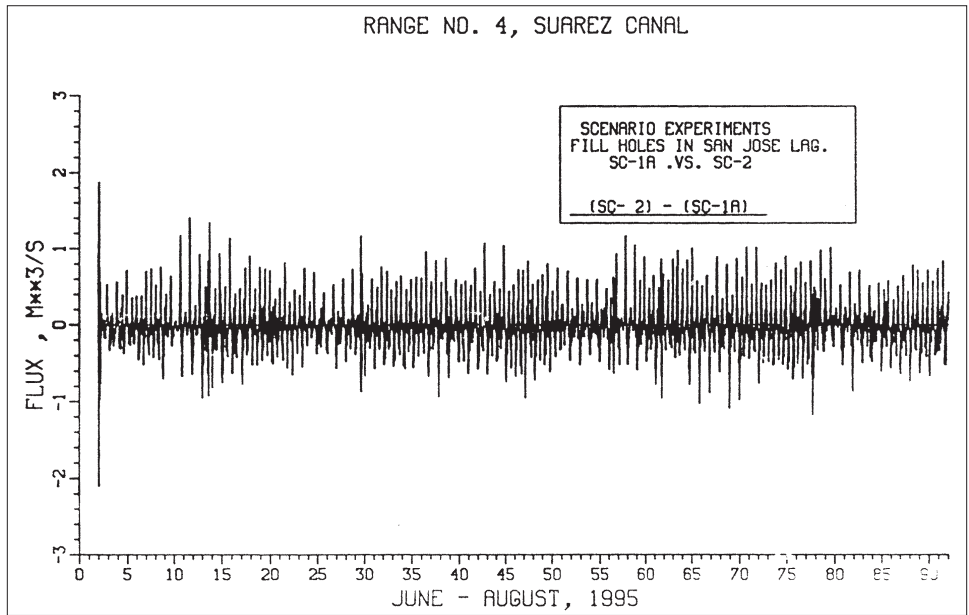


b. Difference between 1a and 2

Figure 8-13. Comparison of flux at Range 2 between Scenarios 1a and 2



a. Both 1a and 2



b. Difference between 1a and 2

Figure 8-14. Comparison of flux at Range 4 between Scenarios 1a and 2

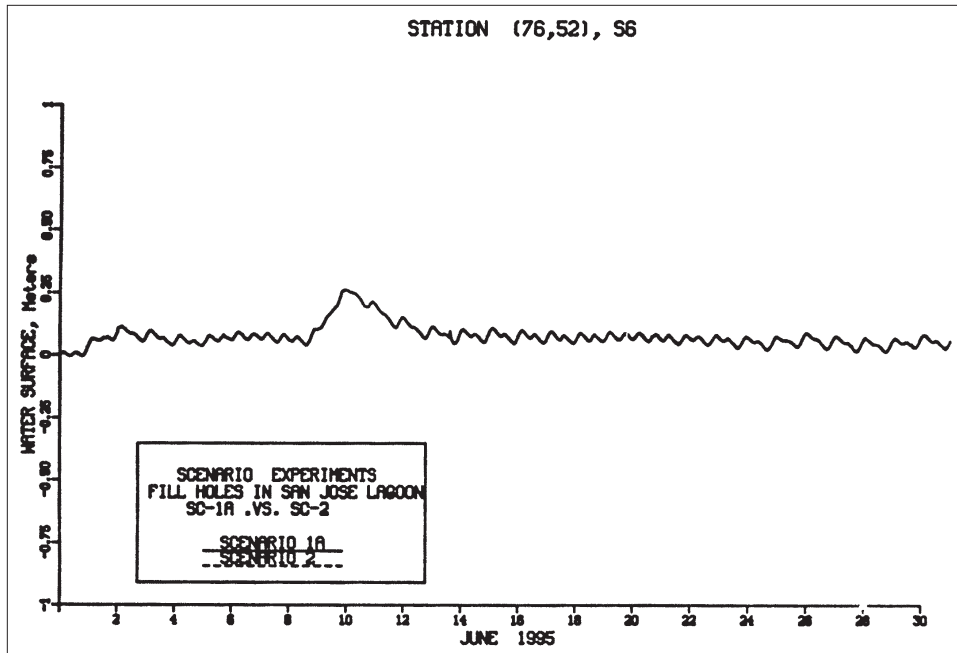
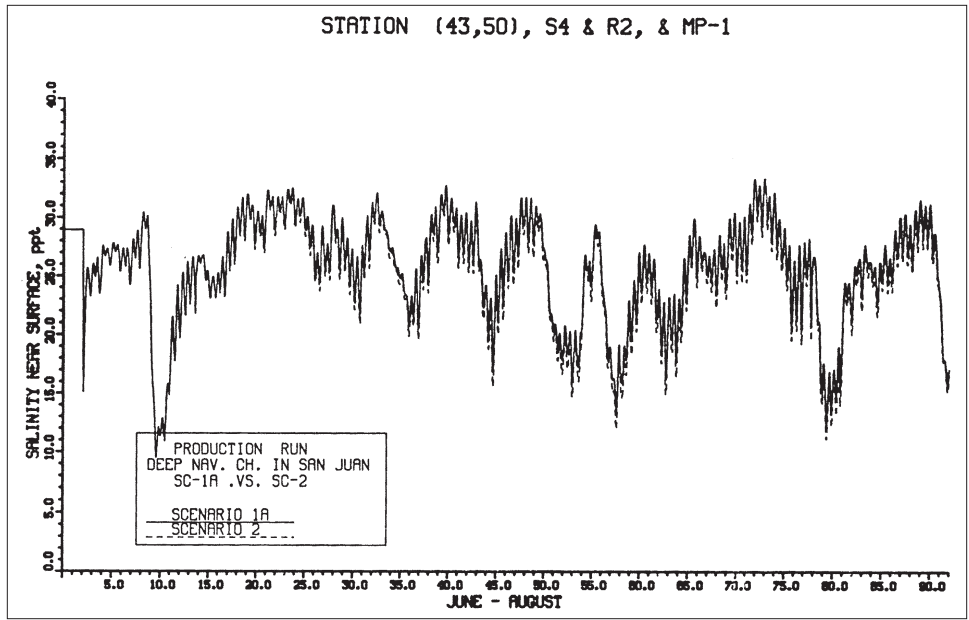


Figure 8-15. Comparison of tide at S6 between Scenarios 1a and 2

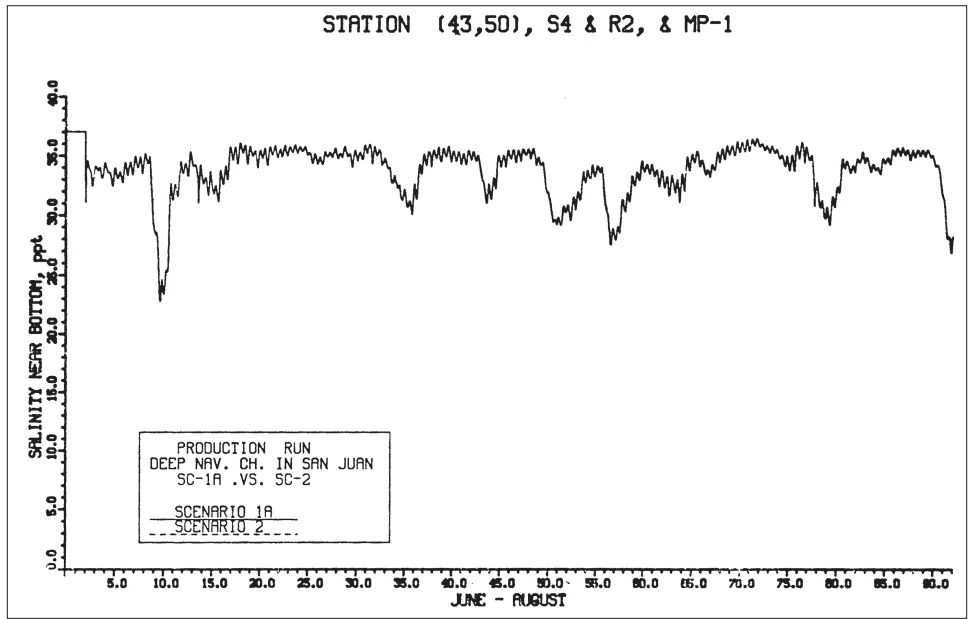
Scenario 4 Results

Scenario 4 has the Loiza Expressway bridge constriction removed in the Canal Suárez along with a tide gate installed in the canal. Simulation of the tide gate was accomplished by setting an internal boundary condition to cut off flow from San José through Canal Suárez to Torrecilla when the water surface elevation is higher on the San José side of the gate. The basic operation of the tide gate was expected to be such that tidal-floodwaters from Torrecilla would move into San José and would then be trapped in San José and forced to flow out through Martín Peña Canal. However, for the vast majority of the time, the water-surface elevation on the San José side of the gate remains higher than on the Torrecilla side of the gate, resulting in virtually no flux through Canal Suárez (Figure 8-25). Thus, only occasionally does the gate allow tidal-floodwaters from Laguna La Torrecilla into Laguna San José. The reason is that with the Martín Peña Canal so constricted, water can't easily pass out of San José, resulting in a buildup of the water-surface elevation in Laguna San José. This buildup of the San José water-surface elevation can be seen in Figure 8-26. Figure 8-27 shows the increased flux during ebb (water moving toward San Juan Bay) through Martín Peña.

An interesting observation from Figure 8-26 is that there is essentially no tidal fluctuation in Laguna San José with Canal Suárez blocked. Thus, the small tidal fluctuation observed in San José for the existing state of the system (Figure 6-7) is almost totally due to the tide moving through Canal Suárez. The tidal effect on Laguna San José due to Martín Peña Canal is essentially zero.



a. Near surface



b. Near bottom

Figure 8-16. Comparison of salinity at S4 between Scenarios 1a and 2

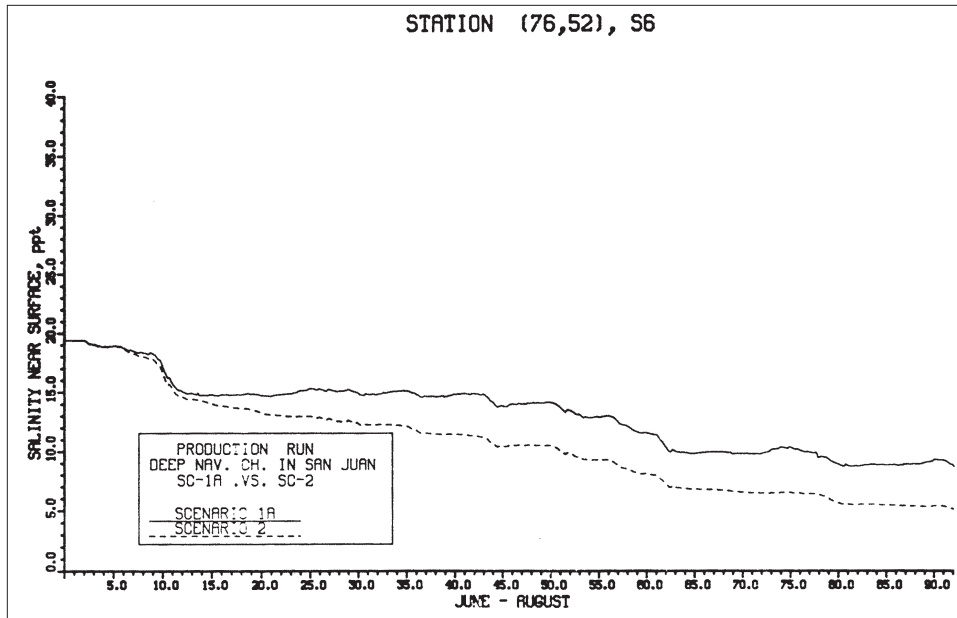
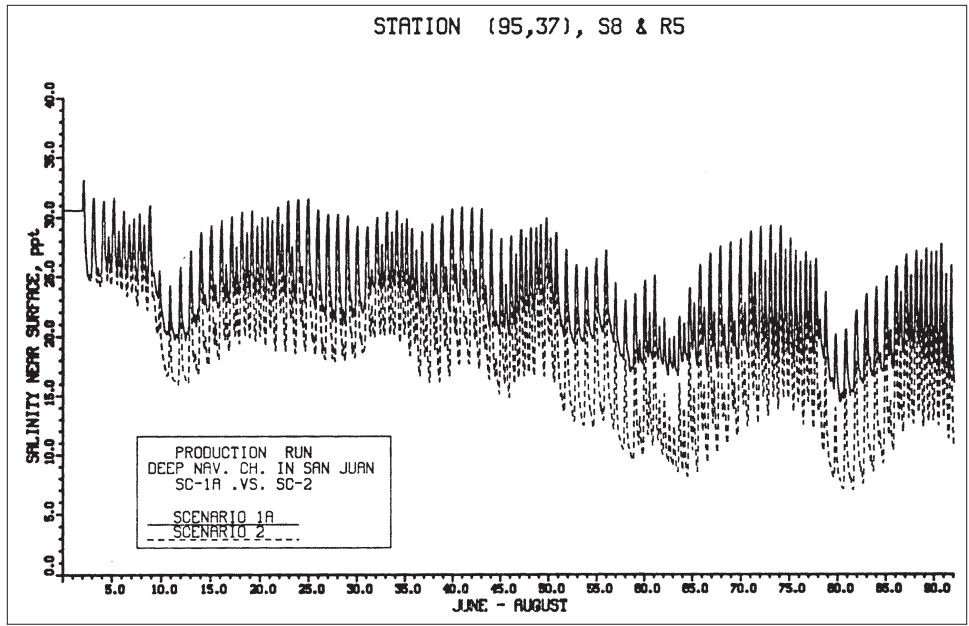


Figure 8-17. Comparison of salinity at S6 between Scenarios 1a and 2

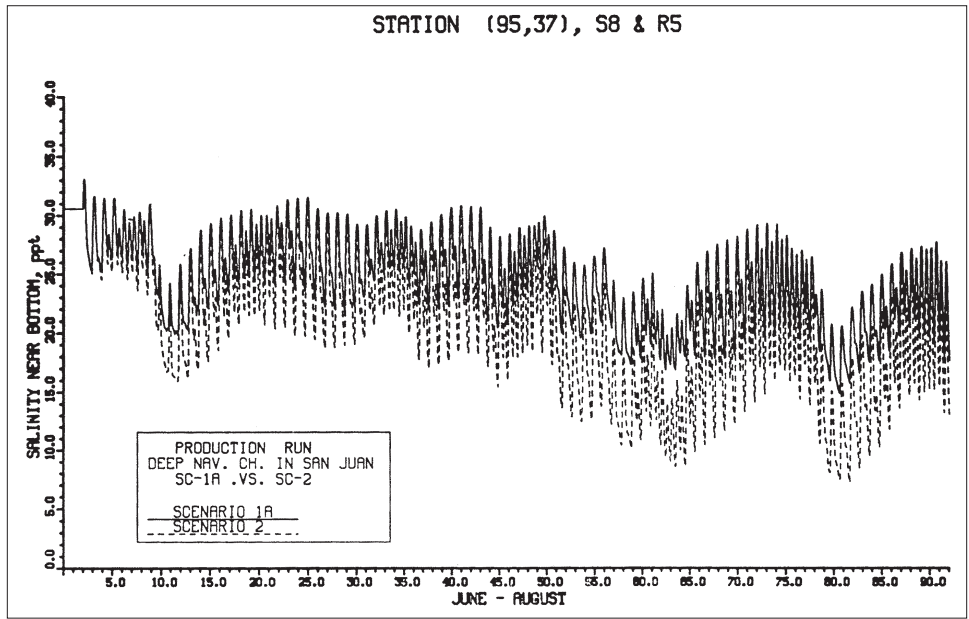
With all of the freshwater inflow into Laguna San José having to pass through Martín Peña Canal, Figure 8-28 shows that the impact is a reduction in salinity in Martín Peña. However, as illustrated in Figures 8-29 and 8-30, salinity in Laguna San José and Canal Suárez increases. With no flow from Laguna San José into Torecilla Lagoon, salinity in Suarez on the Torecilla side of the tide gate builds up. Thus, during the few times that tidal-flood flow in the Canal Suárez is allowed through the tide gate into San José, much higher salinity is flushed into San José, resulting in increased salinity in Laguna San José.

Scenario 6b Results

As previously discussed, this scenario is a combination of Scenario 1c and Scenario 2. In other words, the eastern end of Martín Peña is widened to a minimum of 150 ft (45.7 m) and deepened to 9 ft (2.74 m) and the dredged holes are filled. An inspection of the results from this scenario (Figures 8.31 -8.36) along with those from Scenario 1c (Figures 8.7 -8.12) reveals virtually no difference in the computed tide in Laguna San José nor in the computed flux and salinity in the Martín Peña and Canal Suarez from those obtained for Scenario 1c. Although Scenario 2 by itself does result in a decrease in salinity in Laguna San José and the connecting canals (Figures 8.16 - 8.18), evidently the hydrodynamic impact of Scenario 1c is so large that the influence of Scenario 2 is miniscule when the two are combined. An inspection of Figure 8.8 of the flux through Canal Martín Peña for Scenario 1c shows that during flood (flow into Canal Martín Peña from San Juan Bay) the average flux is about 50 m³/sec. Thus, on each flood cycle about 2.25 million m³ of high saline San Juan Bay water moves into Laguna San José. With the total volume of Laguna San



a. Near surface



b. Near bottom

Figure 8-18. Comparison of salinity at S8 between Scenarios 1a and 2

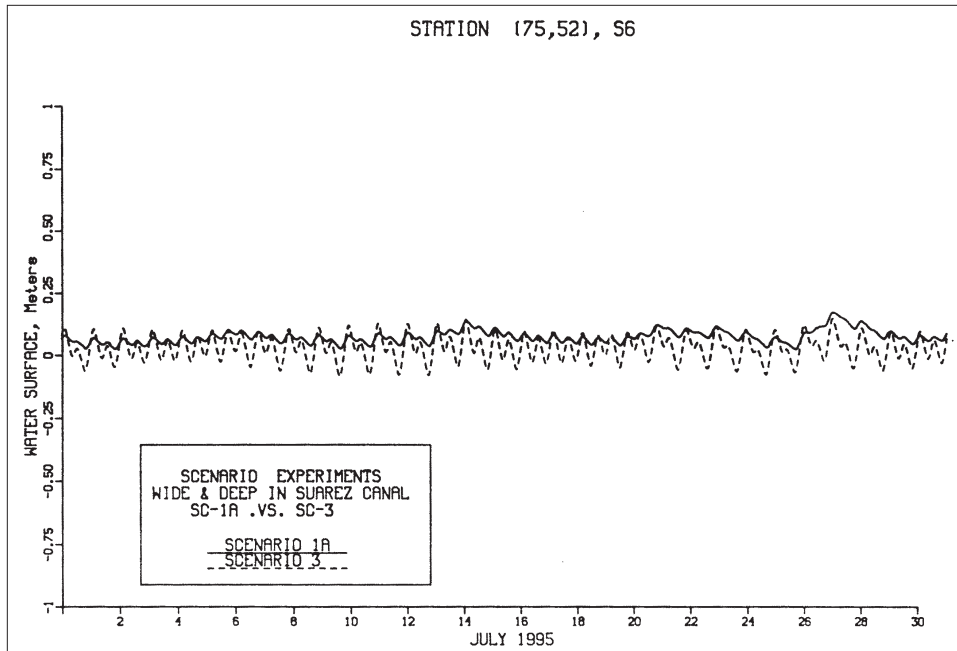


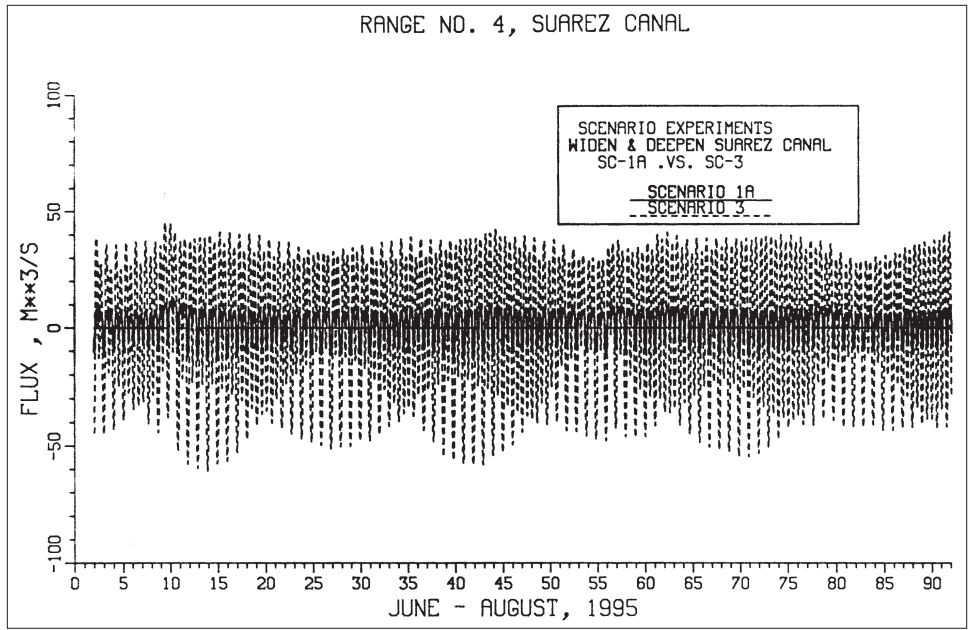
Figure 8-19. Comparison of tide at S6 between Scenarios 1a and 3

José being about 7.5 million m³, it only takes three to four flood cycles to totally replace the waters of Laguna San José. This illustrates the enormous impact of Scenario 1c.

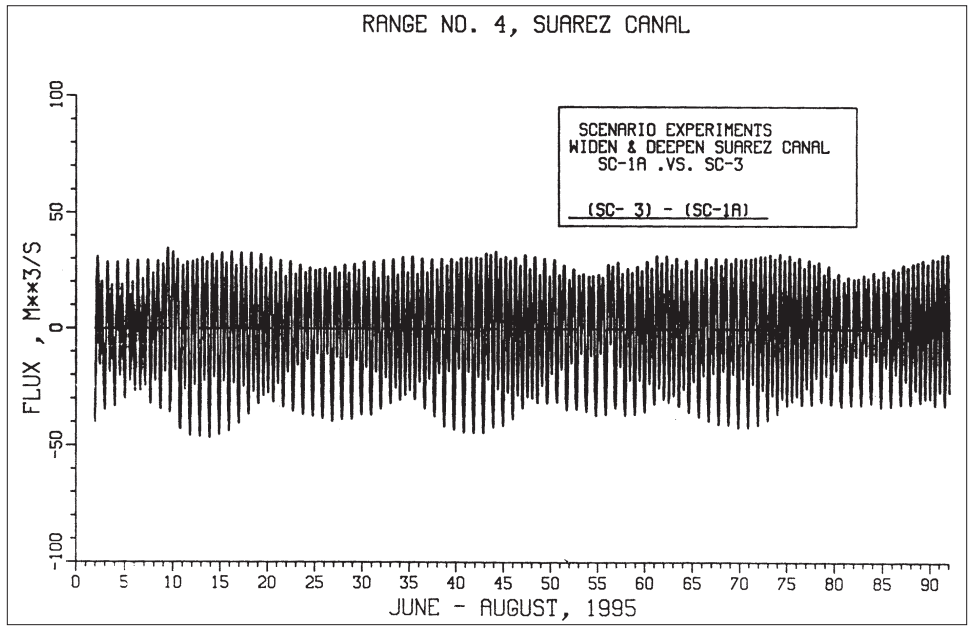
Conclusions

The major goal to be accomplished through physical changes to the SJBE system is to increase tidal flushing in Martín Peña Canal and Laguna San José. The results from the various scenarios discussed above show that Scenario 1c accomplishes this goal the best, if the desire is to increase the exchange between San José and San Juan Bay. Scenario 3 also significantly increases the tidal flushing of Laguna San José, but the exchange is with Laguna La Torrecilla waters rather than San Juan Bay waters. It is doubtful that mixing the relatively polluted San José waters with the relatively clean waters of Torrecilla is desirable.

The final scenario simulated was a combination of Scenario 1c and Scenario 2. Although Scenario 2 has little impact on tidal flushing in Laguna San José, the belief (from a HM perspective without including any benefits of pollutant load reductions) is that with the increased tidal flushing resulting from significantly widening and deepening the Martín Peña Canal, along with filling the highly polluted deep holes in San José and other areas of the system, the combination of Scenarios 1c and 2 offers the best hope for improving the water quality of Laguna San José.

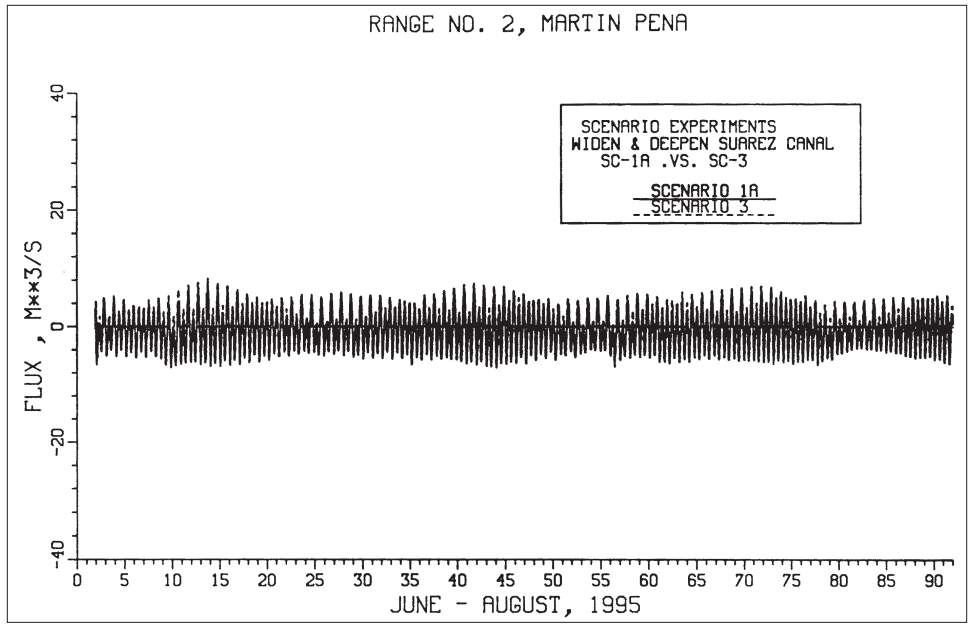


a. Both 1a and 3

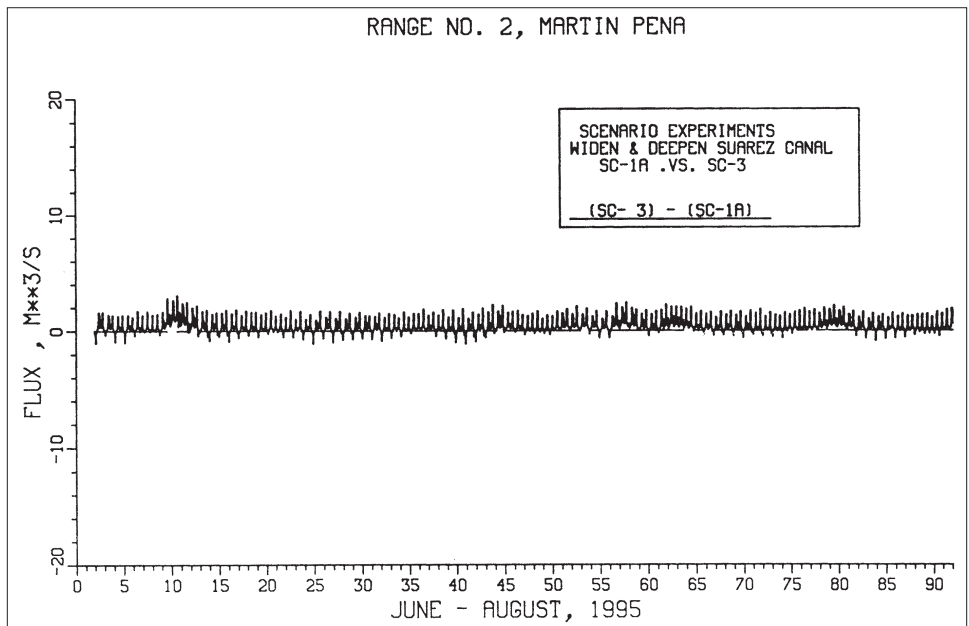


b. Difference between 1a and 3

Figure 8-20. Comparison of flux at Range 4 between Scenarios 1a and 3

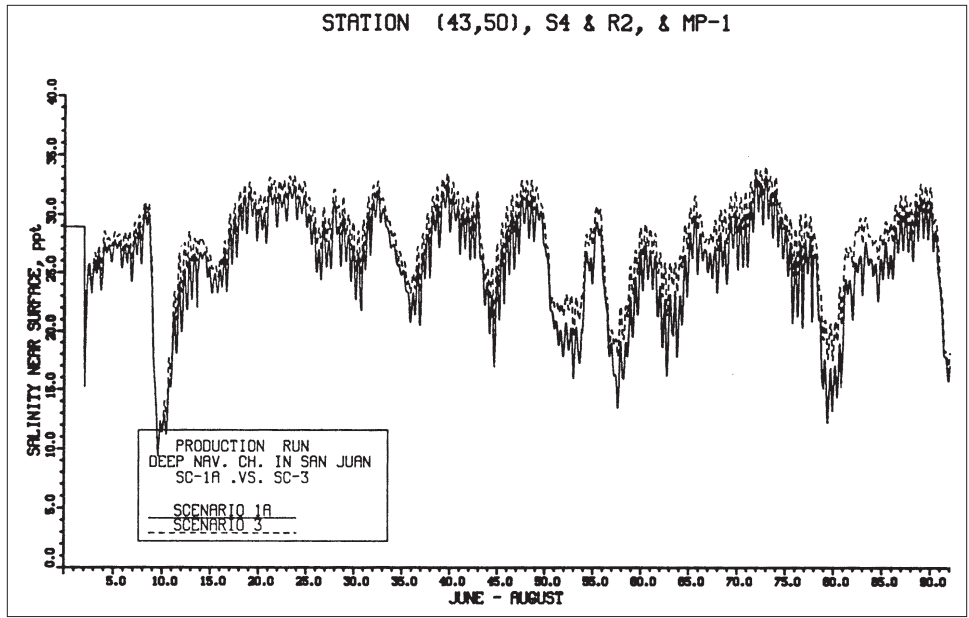


a. Both 1a and 3

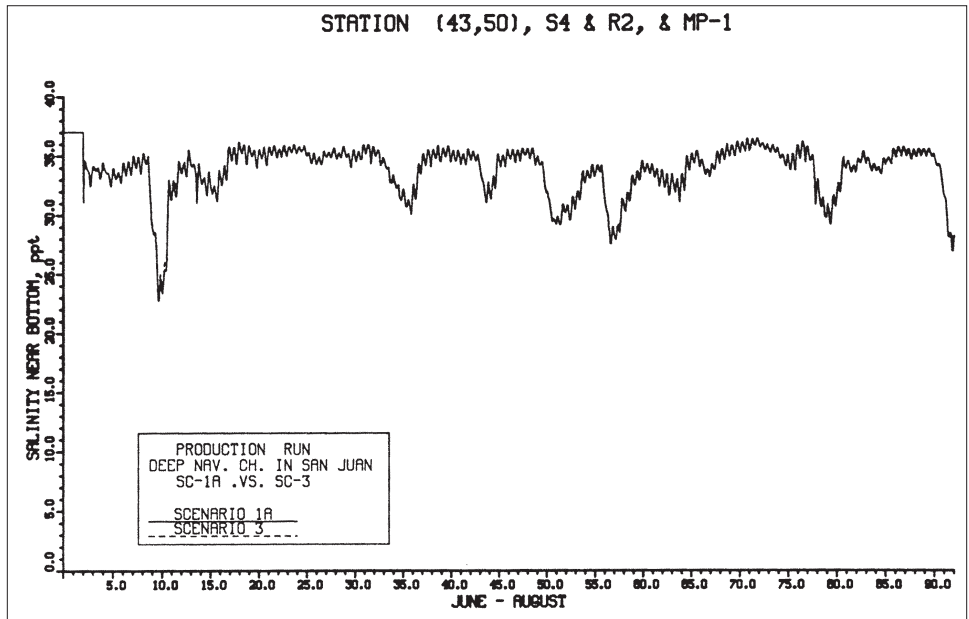


b. Difference between 1a and 3

Figure 8-21. Comparison of flux at Range 2 between Scenarios 1a and 3



a. Near surface



b. Near bottom

Figure 8-22. Comparison of salinity at S4 between Scenarios 1a and 3

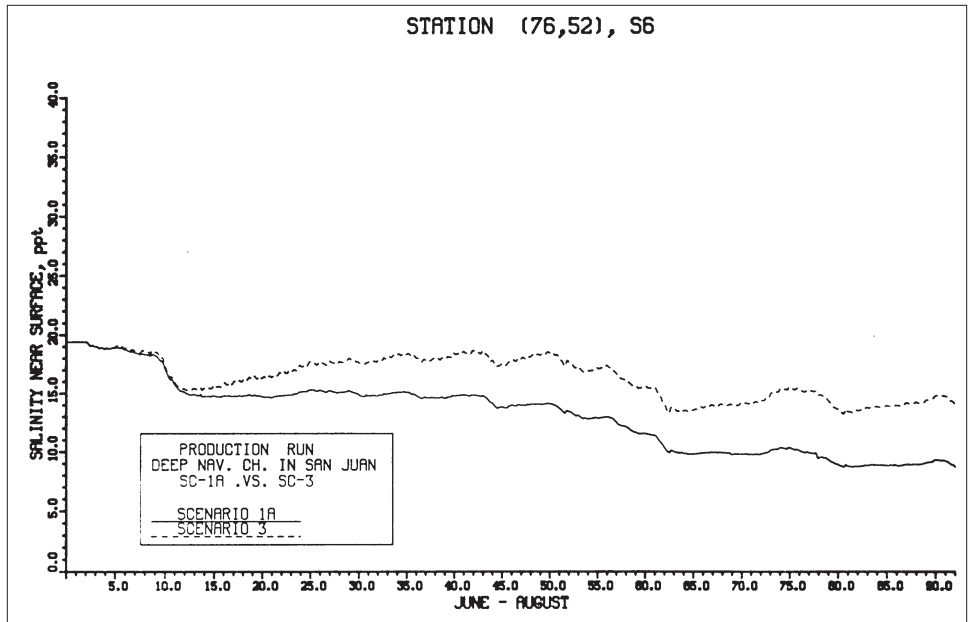
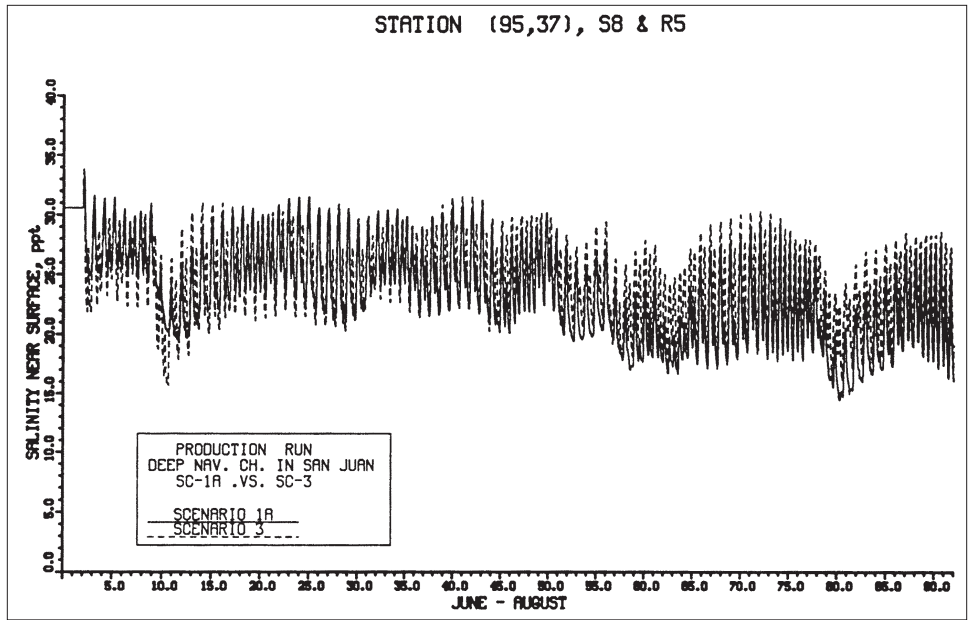
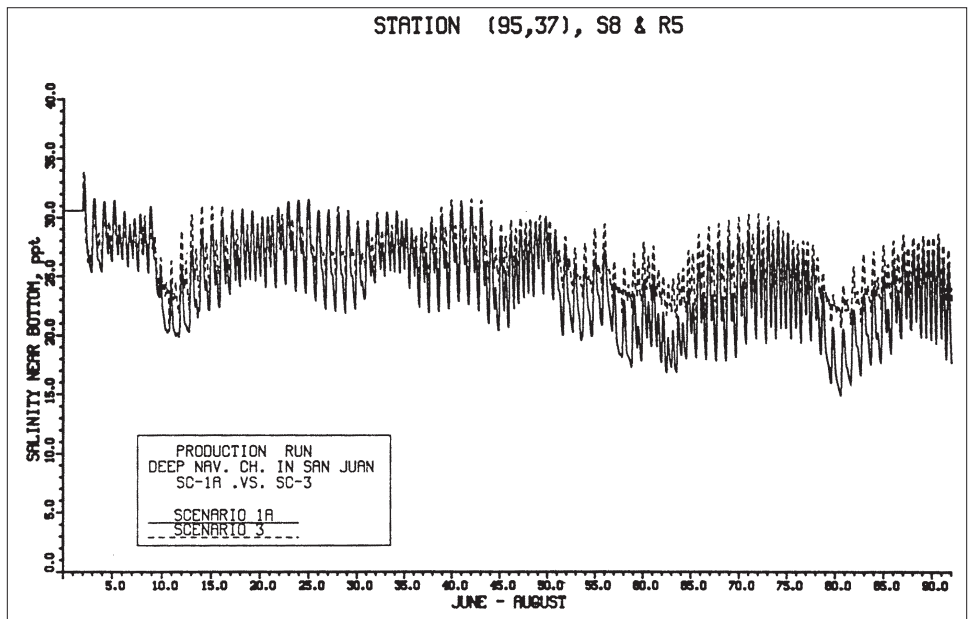


Figure 8-23. Comparison of salinity at S6 between Scenarios 1a and 3

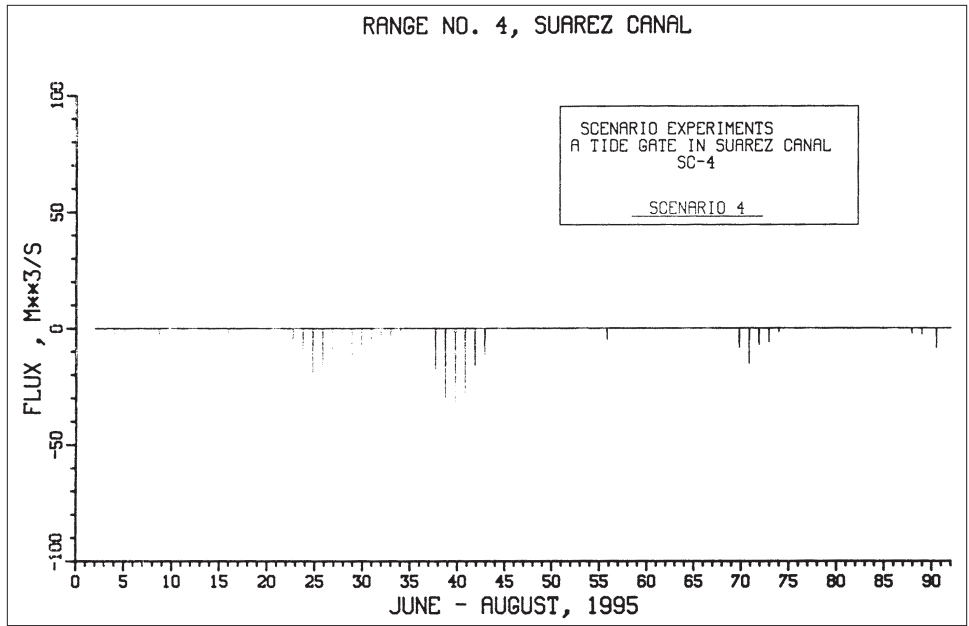


a. Near surface

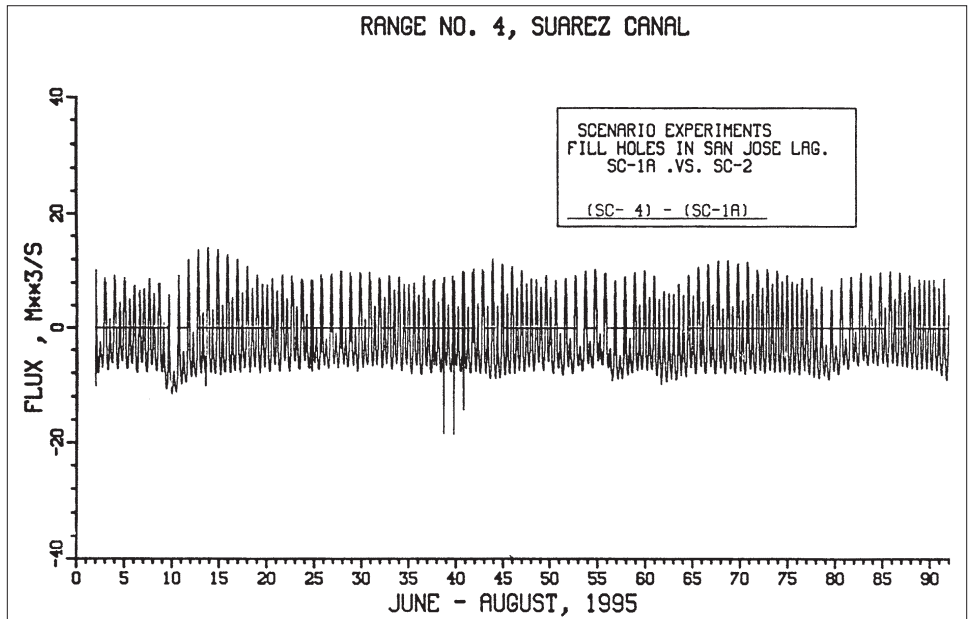


b. Near bottom

Figure 8-24. Comparison of salinity at S8 between Scenarios 1a and 3



a. Only 4



b. Difference between 1a and 4

Figure 8-25. Comparison of flux at Range 4 between Scenarios 1a and 4

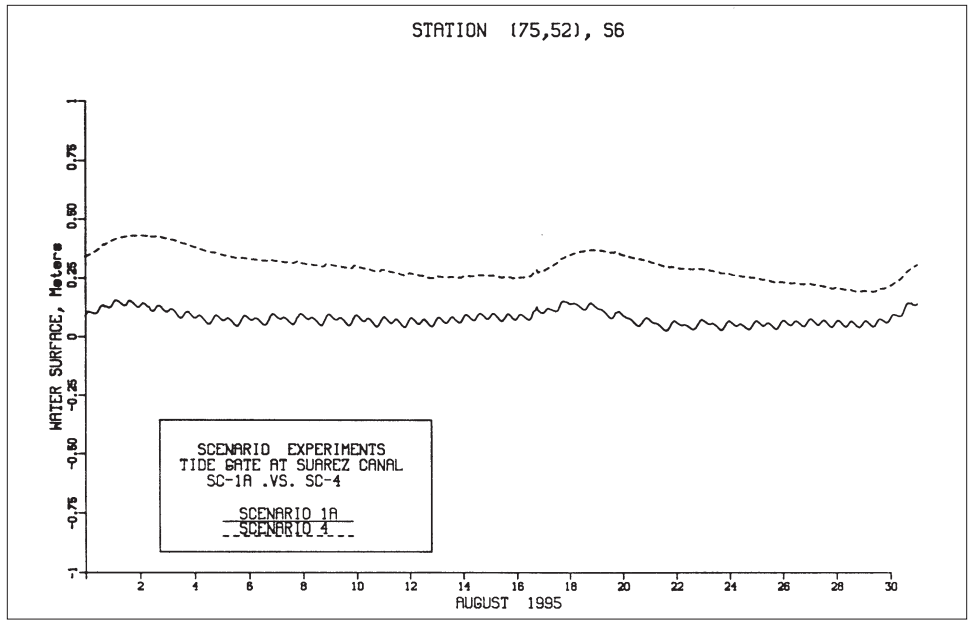
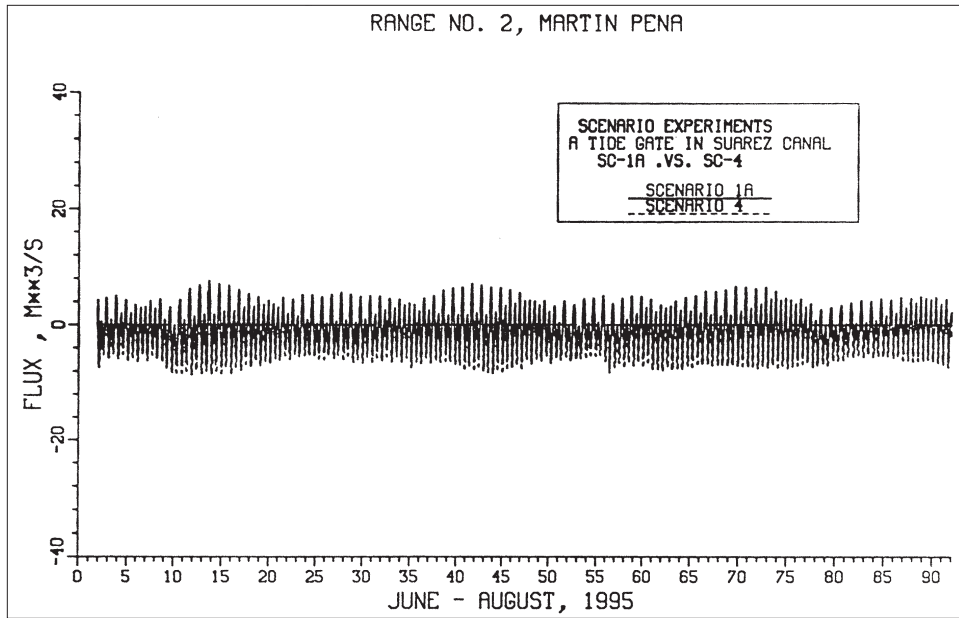
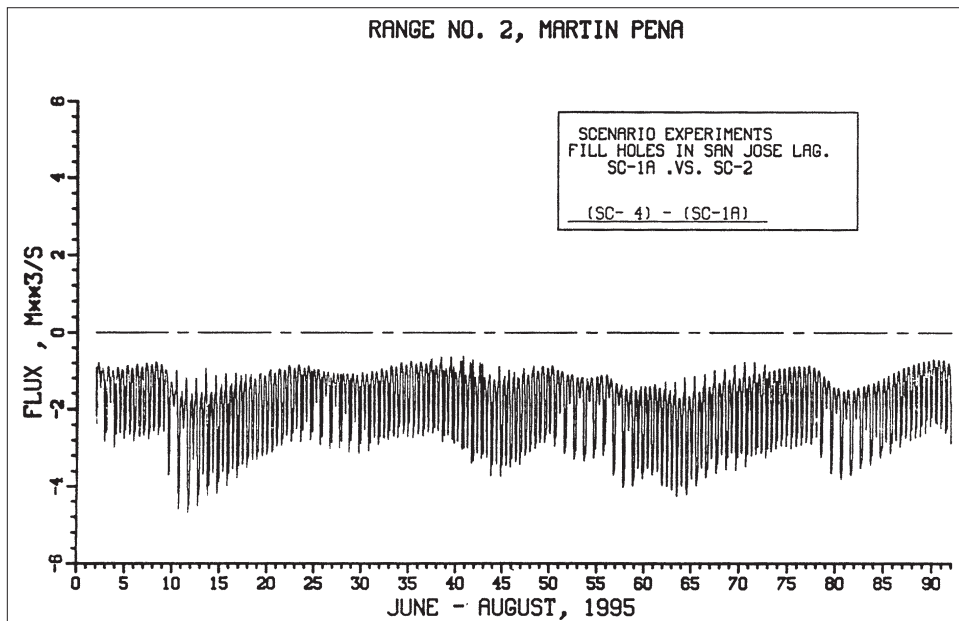


Figure 8-26. Comparison of tide at S6 between Scenarios 1a and 4

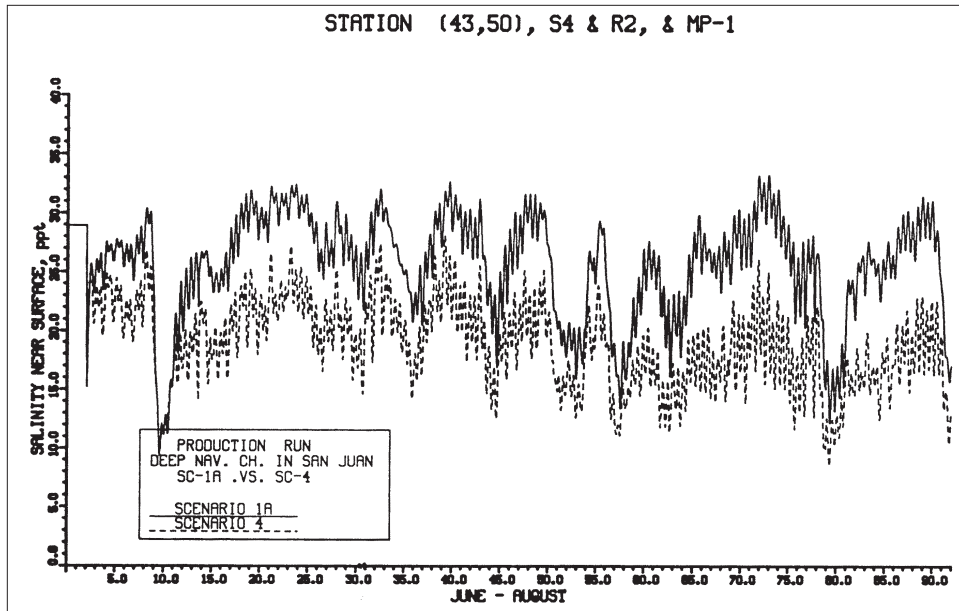


a. Both 1a and 4

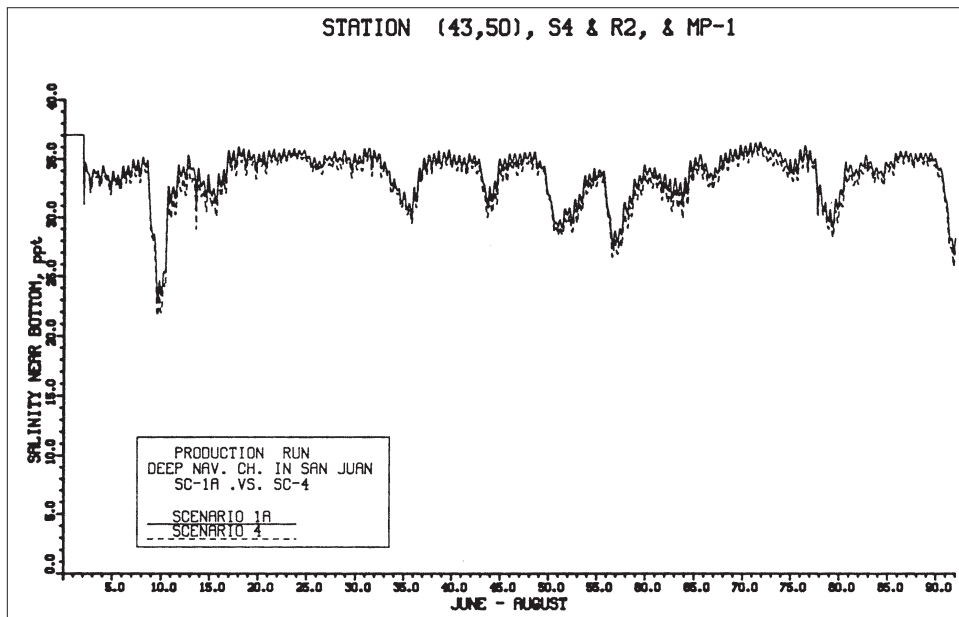


b. Difference between 1a and 4

Figure 8-27. Comparison of flux at Range 2 between Scenarios 1a and 4



a. Near surface



b. Near bottom

Figure 8-28. Comparison of salinity at S4 between Scenarios 1a and 4

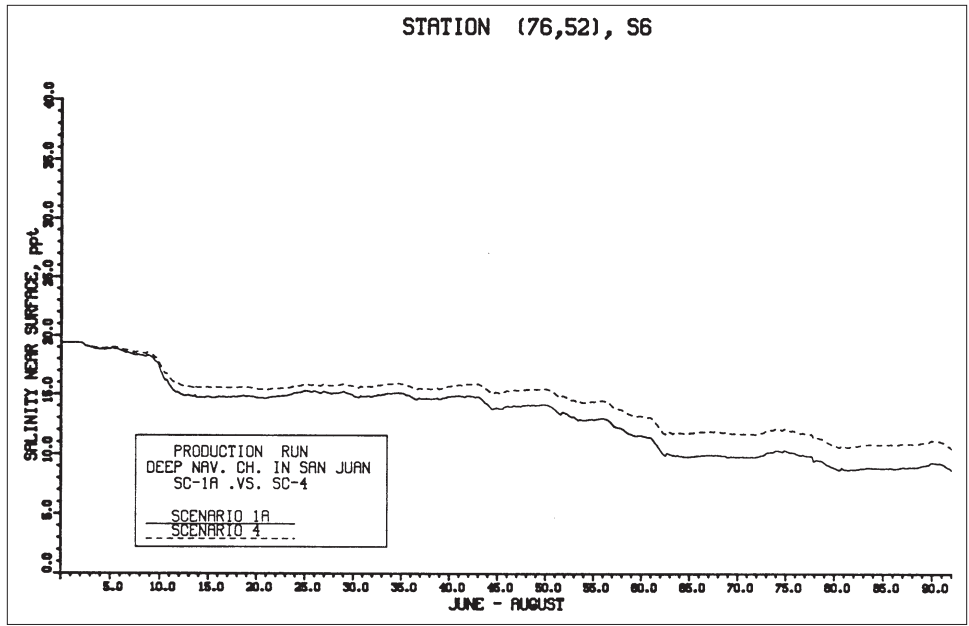
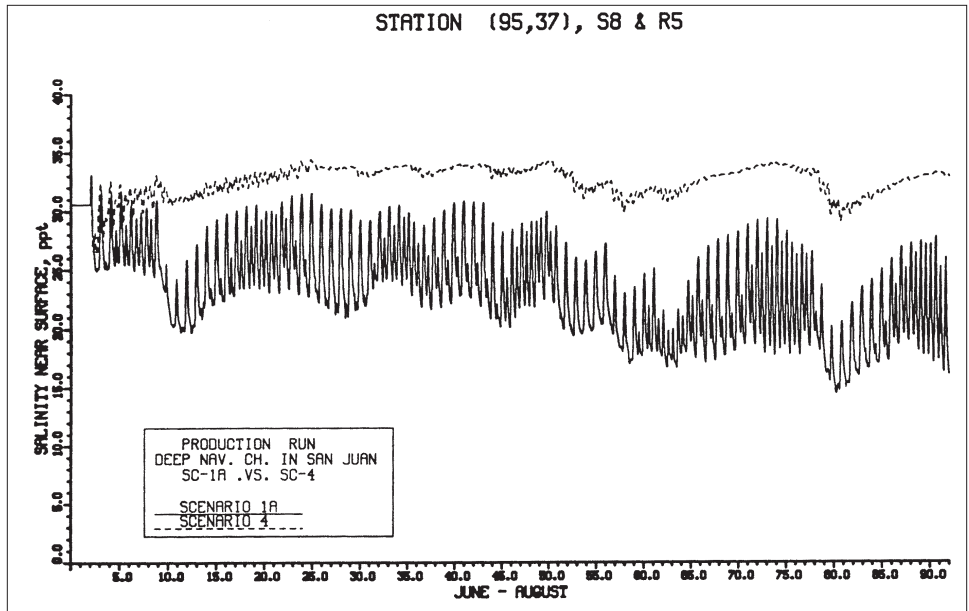
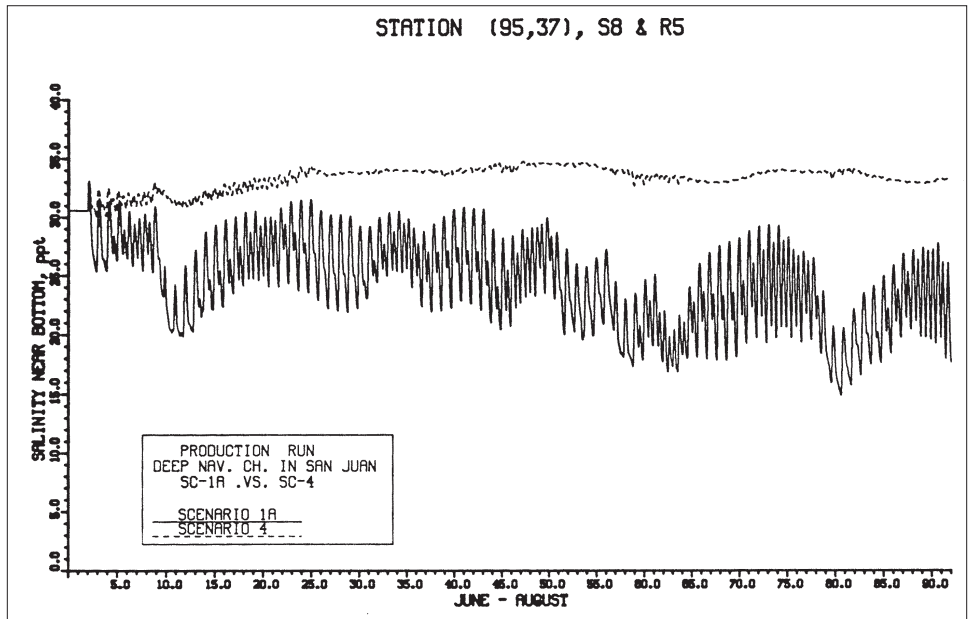


Figure 8-29. Comparison of salinity at S6 between Scenarios 1a and 4



a. Near surface



b. Near bottom

Figure 8-30. Comparison of salinity at S8 between Scenarios 1a and 4

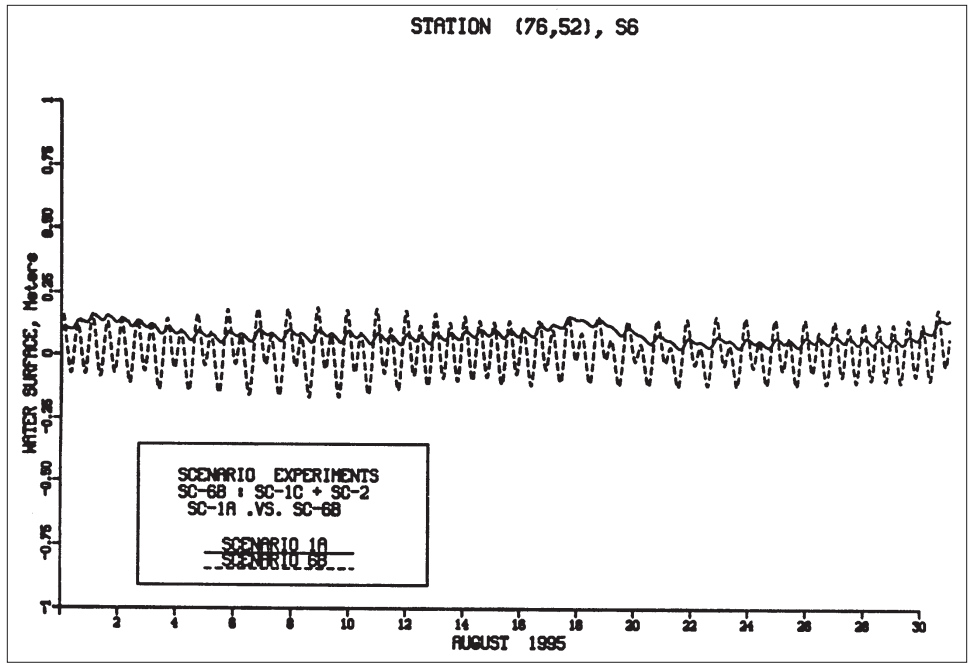
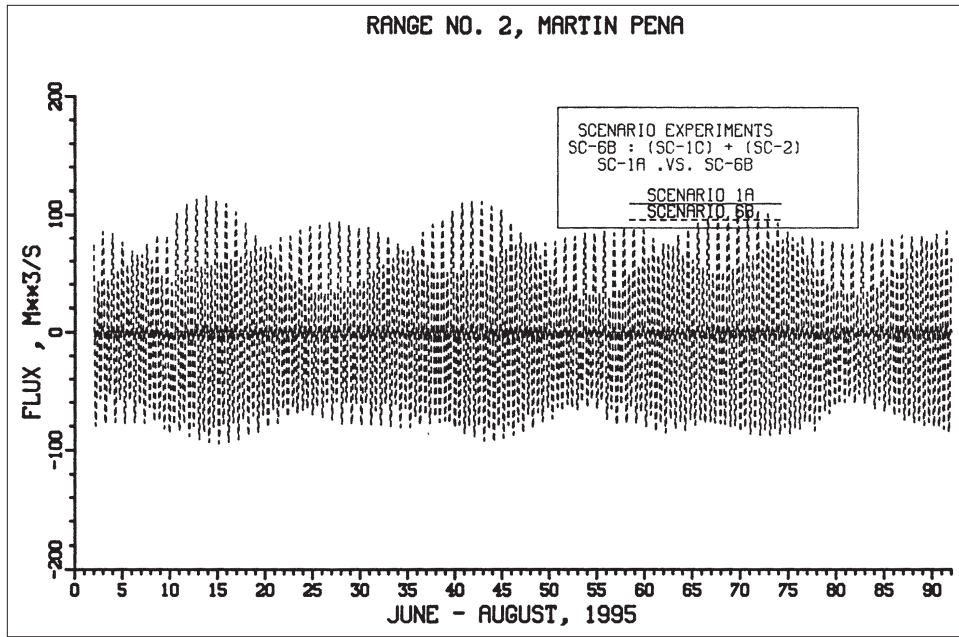
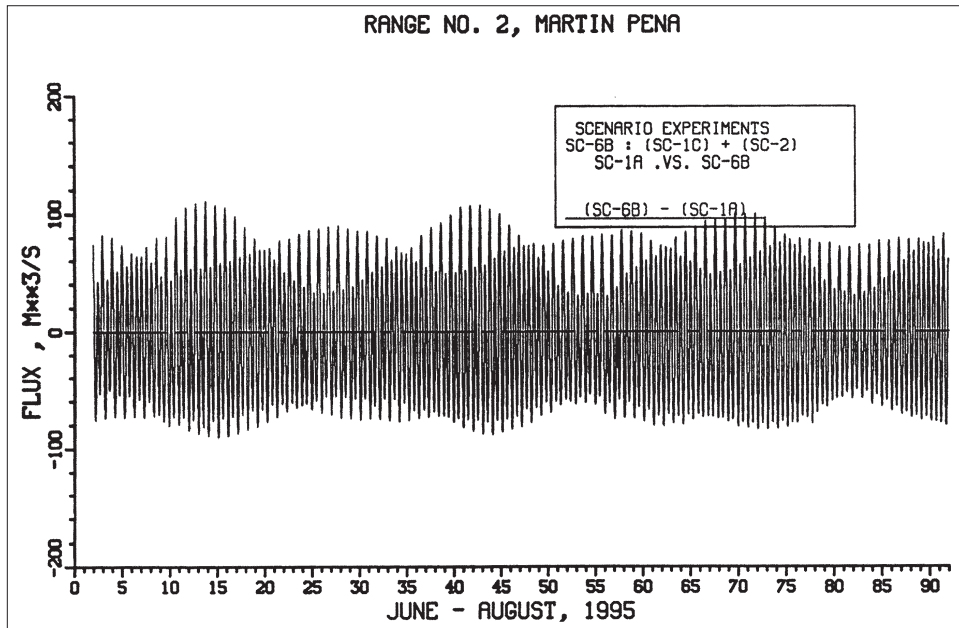


Figure 8-31. Comparison of tide at S6 between Scenarios 1a and 6b

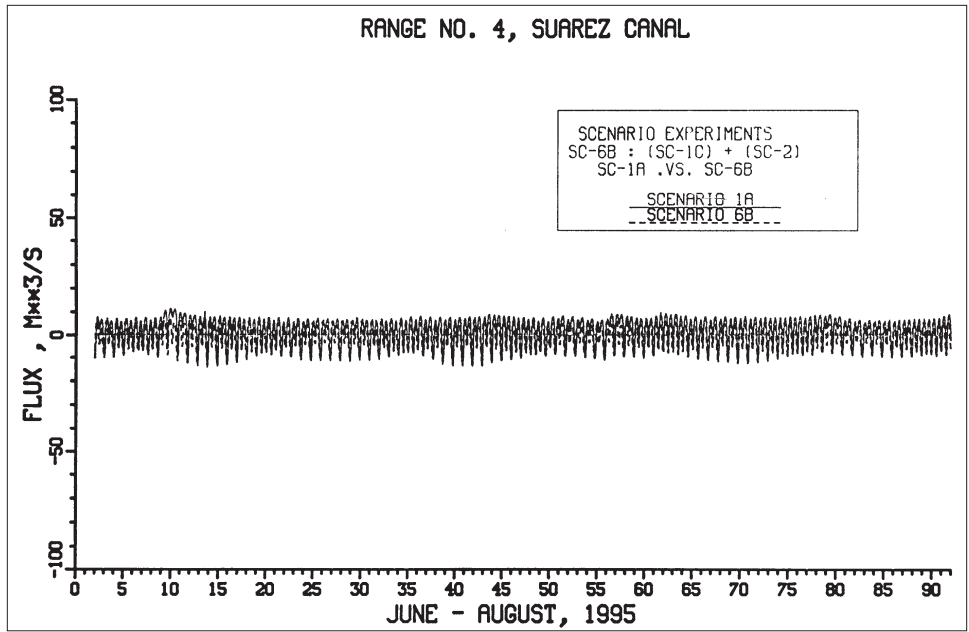


a. Both 1a and 6b

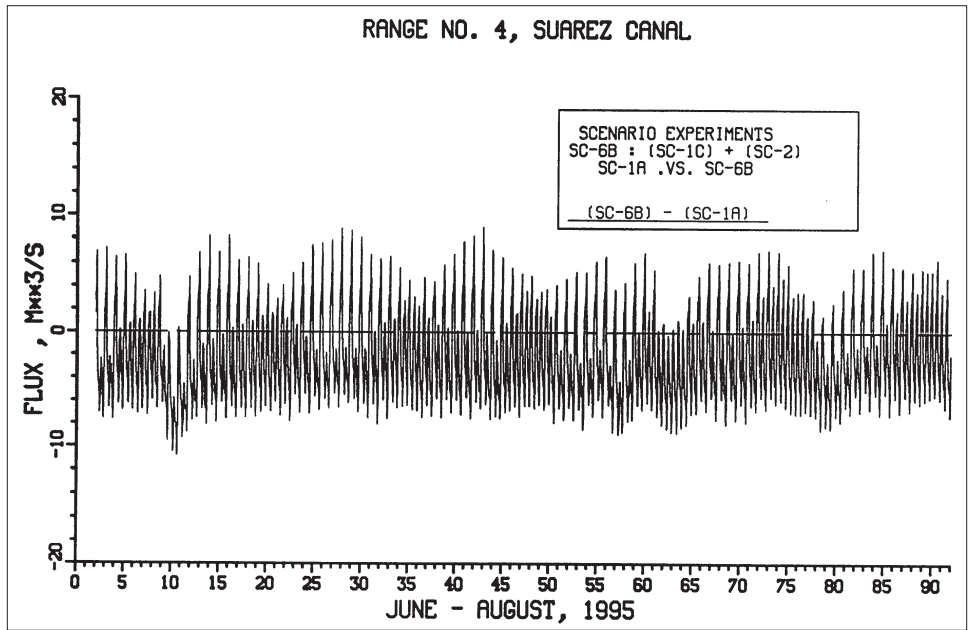


b. Difference between 1a and 6b

Figure 8-32. Comparison of flux at Range 2 between Scenarios 1a and 6b

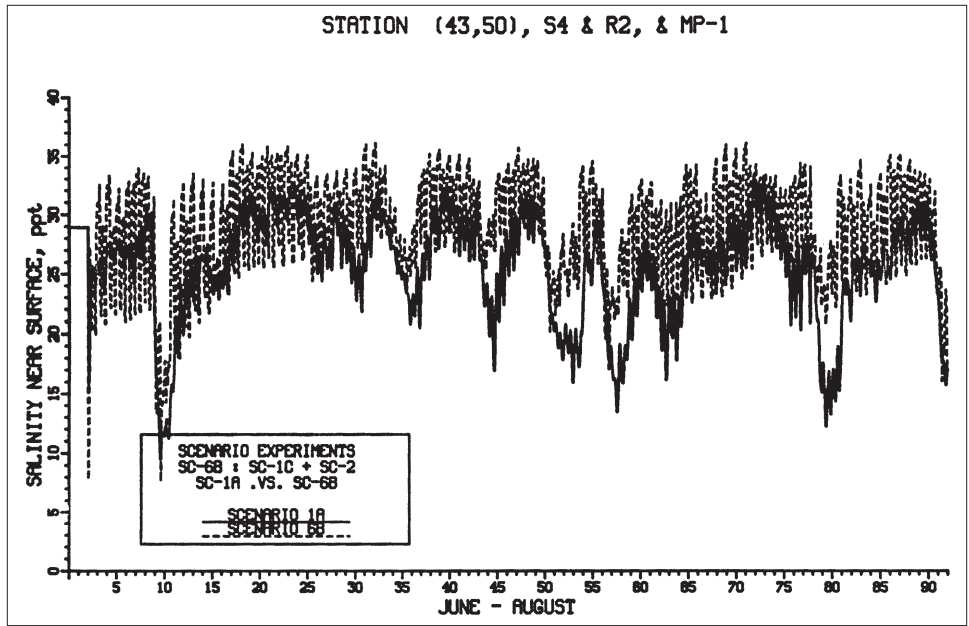


a. Both 1a and 6b

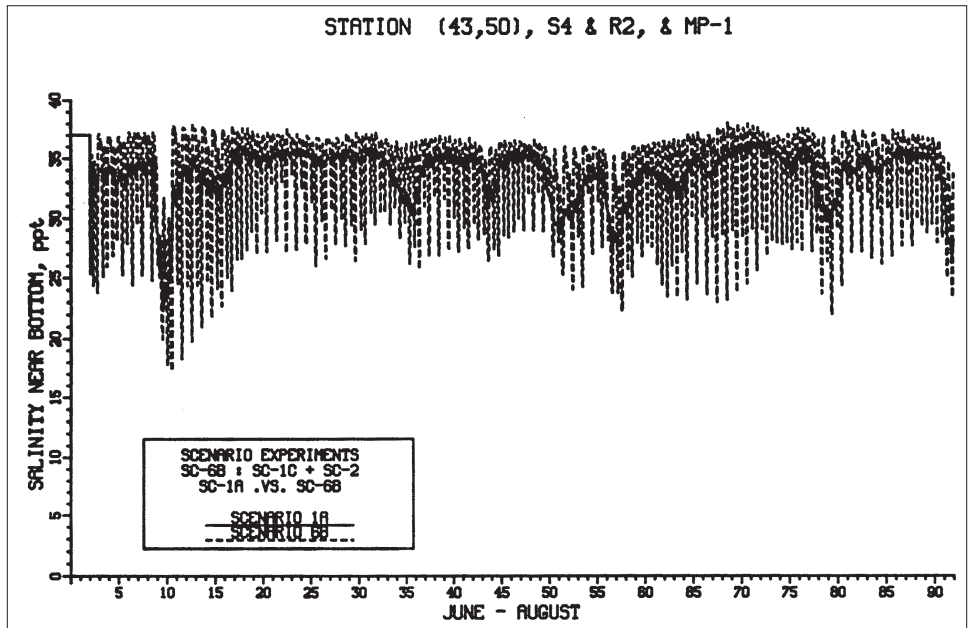


b. Difference between 1a and 6b

Figure 8-33. Comparison of flux at Range 4 between Scenarios 1a and 6b

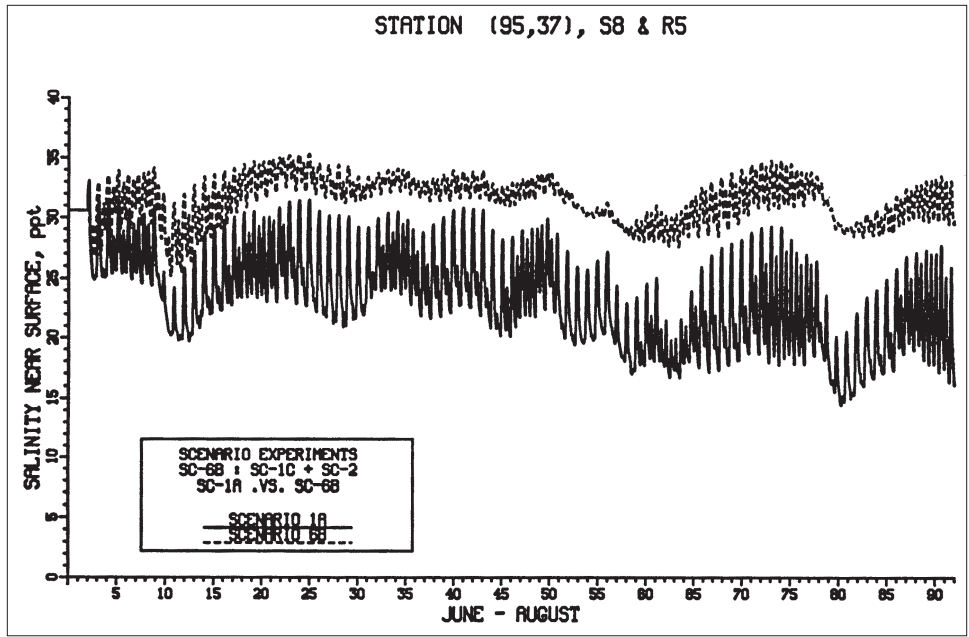


a. Near surface

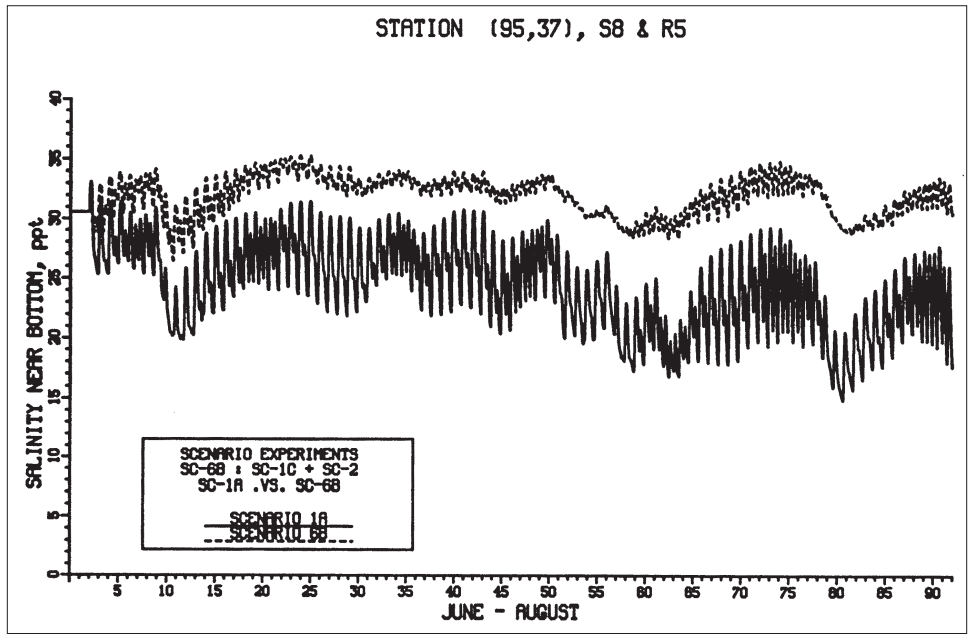


b. Near bottom

Figure 8-34. Comparison of salinity at S4 between Scenarios 1a and 6b



a. Near surface



b. Near bottom

Figure 8-36. Comparison of salinity at S8 between Scenarios 1a and 6b

Water Quality Model Results

All scenarios required a common set of initial conditions for the water column and the sediments so that any differences observed between the scenarios would be attributable to the modifications imposed by the scenario. Ideally, the spatially varying set of initial conditions for the water column and sediments generated during calibration would be used. Unfortunately, the addition and deletion of water quality cells resulting from channel modification caused the number of cells and cell numbering to vary among scenarios. All scenarios had the same plan view so the number of surface cells remained unchanged, only subsurface cells were added or deleted in response to scenario dredging and filling activities.

To circumvent the problems with cell numbers and numbering in the scenarios, each scenario began with a uniform set of initial conditions in the water column as shown in Table 8-4. The WQM was run for the duration of the scenario, the final concentrations saved to a file which was then used as the initial conditions for the next run of that scenario. Sediment initial conditions were more problematic. Since sediments respond more slowly to changes in flow patterns and loadings than the water column does, beginning each scenario with a spatially uniform set of sediment initial conditions was undesirable due to the length of simulation required to reach a dynamic steady-state condition. Instead, the first run of every scenario began with the same sediment initial conditions used during calibration. These had been established over numerous calibration runs and were in equilibrium with calibration water column conditions.

Scenario results were compared using the same longitudinal transect as used during calibration. Results from each scenario were averaged over the STP and plotted with results from the base scenario, 1a, in order to assess the impact resulting from the scenario. Since all conditions in the scenarios were identical except for the change mandated by that scenario, deviations between the results of an individual scenario and 1a were wholly due to the conditions of the scenario.

Results from Scenarios 1b through 4 indicate changes in water quality that are totally due to changes in circulation resulting from channel/bathymetric modifications in Caño Martín Peña, Laguna San José, Canal Suárez, and Laguna La Torrecilla. As such, results from these scenarios all have similar characteristics.

In the following sections, Scenarios 1b through 6b are discussed. Results from all are compared to the base scenario, 1a. Observations are made as to the effects of the scenario conditions on each water quality constituent.

**Table 8-4.
Scenario Uniform Initial Conditions for Water Column**

Constituent	Value	Units
Temperature	30	ppt
Salinity	30	°C
Total Solids	10	g m ⁻³
Algae	0.6	g m ⁻³
Dissolved Organic Carbon	5	g m ⁻³
Labile Particulate Organic Carbon	1	g m ⁻³
Refractory Particulate Organic Carbon	1	g m ⁻³
Ammonium	0.1	g m ⁻³
Nitrate	0.02	g m ⁻³
Dissolved Organic Nitrogen	0.05	g m ⁻³
Labile Particulate Organic Nitrogen	0.2	g m ⁻³
Refractory Particulate Organic Nitrogen	0.2	g m ⁻³
Total Phosphorus	0.03	g m ⁻³
Dissolved Organic Phosphorus	0.02	g m ⁻³
Labile Particulate Organic Phosphorus	0.04	g m ⁻³
Refractory Particulate Organic Phosphorus	0.04	g m ⁻³
Chemical Oxygen Demand	0.1	g m ⁻³
Dissolved Oxygen	6	g m ⁻³
Fecal Coliform	100	mpn/100ml

Scenario 1b

The WQM grid for Scenario 1b was the same as the one used in 1a as widening Caño Martín Peña did not change the number of cells or flow faces. Figure 8-37 indicates the effect Scenario 1b had on the various water quality constituents. Temperature was unchanged between Scenario 1a and 1b as was expected. Salinity levels in San Juan Bay were only slightly changed but both surface and bottom salinity levels along the remainder of the transect were altered significantly. Surface salinity in western Caño Martín Peña decreased slightly in Scenario 1b while salinity in the eastern portion increased. This is due to the widening of the channel promoting increased exchange between the eastern and western ends of the canal. Surface salinity increased in Laguna San José as a result of increased flushing with San Juan Bay through Caño Martín Peña. Net flow from Laguna San José to Caño Martín Peña increased from 0.5 m³/s to 1.45 m³/s. Surface salinity also increased in Canal Suárez and La Torrecilla as a result of more of the freshwater flows into Laguna San José being removed via Caño Martín Peña. Net flow from Laguna San José to Canal Suárez decreased from 1.98 m³/s to 1.08 m³/s. Bottom salinity also

increased throughout the interior portion of the system as a result of greater exchange with San Juan Bay and the ocean.

Chlorophyll levels in the surface layer of western Caño Martín Peña increased as a result of additional flushing from Laguna San José. Correspondingly, there were decreases in chlorophyll over the eastern end of the transect as a result of chlorophyll leaving Laguna San José. The redistribution in chlorophyll had a slight effect on predicted light extinction values in the interior portions of the system as the self-shading component was affected. Phytoplankton production decreased in San José from 6093 kg C/day in 1a to 5825 kg C/day in 1b as a result of lower algae levels due to increased flushing.

Transect plots for carbon indicate that levels in the interior portions of the system decrease in Scenario 1b. This results from increased exchanges between Caño Martín Peña and San Juan Bay and Laguna San José and Caño Martín Peña. Carbon daily flux rates between Laguna San José and Caño Martín Peña increase from 454 kg/day in 1a to 1311 kg/day in 1b, while daily flux rates from Caño Martín Peña to San Juan Bay increased from 4860 kg/day to 5674 kg/day. As a result of the widening of Caño Martín Peña, less carbon was leaving Laguna San José by Canal Suárez in 1b (769 kg/day) than in 1a (1631 kg/day) which results in a decrease in carbon levels expressed as DOC and TOC in Canal Suárez and Laguna La Torrecilla.

Results similar to those for carbon were seen for nitrogen and phosphorus. The widening of Caño Martín Peña in Scenario 1b resulted in more nitrogen and phosphorus leaving Laguna San José via Caño Martín Peña rather than through Canal Suárez. This did not have much effect on concentrations in Laguna San José as concentrations were already low. There was a slight decrease in sediment ammonium flux rates over the length of Canal Suárez which resulted in ammonium release for Scenario 1b dropping to 8.9 kg/day from 10.2 kg/day in 1a. Both surface and bottom ammonium concentrations in Canal Suárez dropped in response to this and the decrease in nitrogen fluxes from Laguna San José. Nitrogen levels in surface and bottom waters decreased in Caño Martín Peña as a result of increased flushing and a slight decrease in ammonium releases from 3.95 kg/day in 1a to 3.67 kg/day in 1b. Dissolved organic phosphorus and dissolved inorganic phosphorus concentrations dropped in both the surface and subsurface waters of Caño Martín Peña. Again the decrease appears to be the result of increased flushing moving the flow and loading out of Caño Martín Peña faster.

Dissolved oxygen levels improved considerably over the length of Caño Martín Peña in 1b. The largest increase occurred near the middle of Caño Martín Peña at the end of the dredged portion where dissolved oxygen levels increased from 3 mg/l to over 5.5 mg/l. Bottom dissolved oxygen levels increased slightly in eastern Caño Martín Peña, Canal Suárez, and Laguna La Torrecilla. Fecal coliform levels remained relatively unchanged along the transect except for a slight decrease in eastern Caño

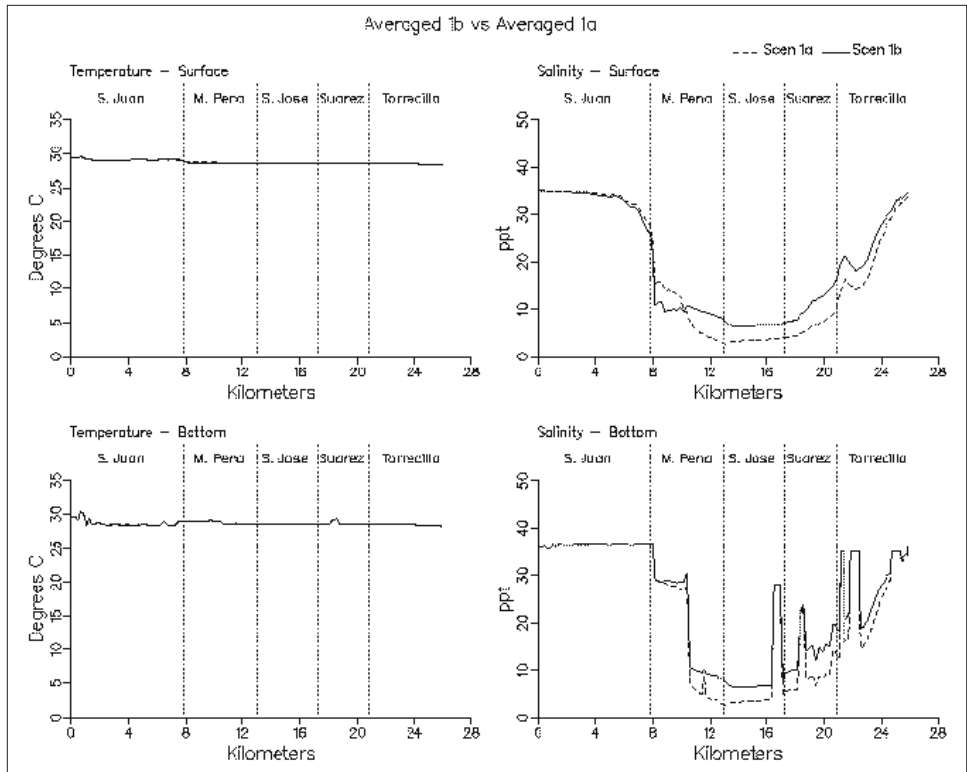


Figure 8-37. Simulation averaged transect plots and sediment flux plots comparing Scenario 1b with Scenario 1a (Sheet 1 of 11)

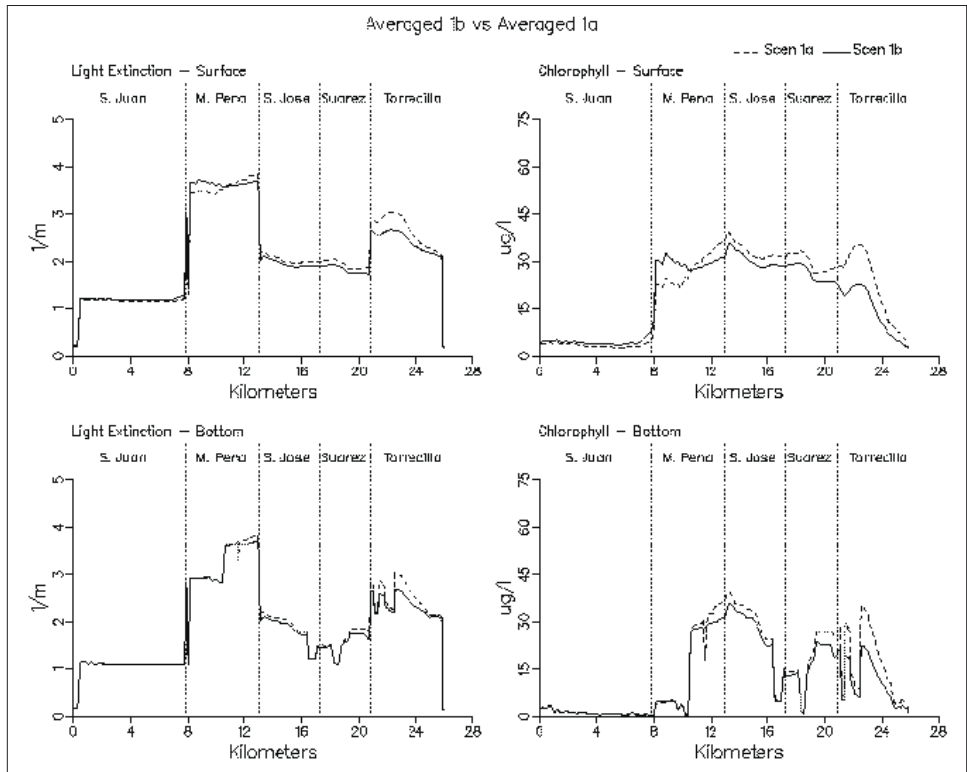


Figure 8-37. (Sheet 2 of 11)

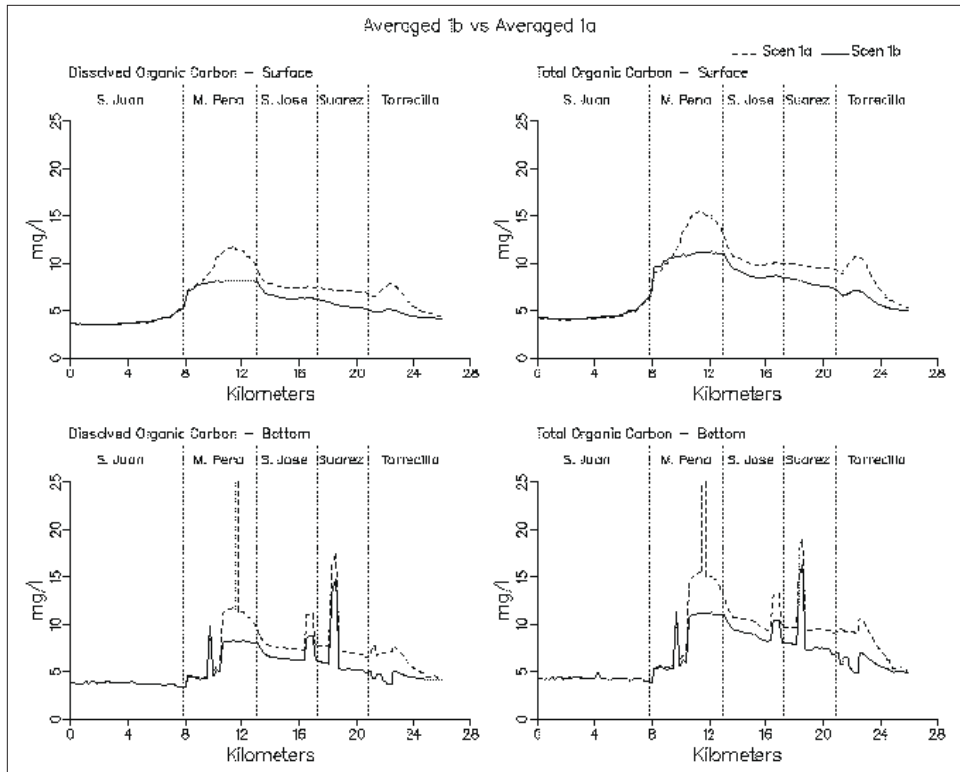


Figure 8-37. (Sheet 3 of 11)

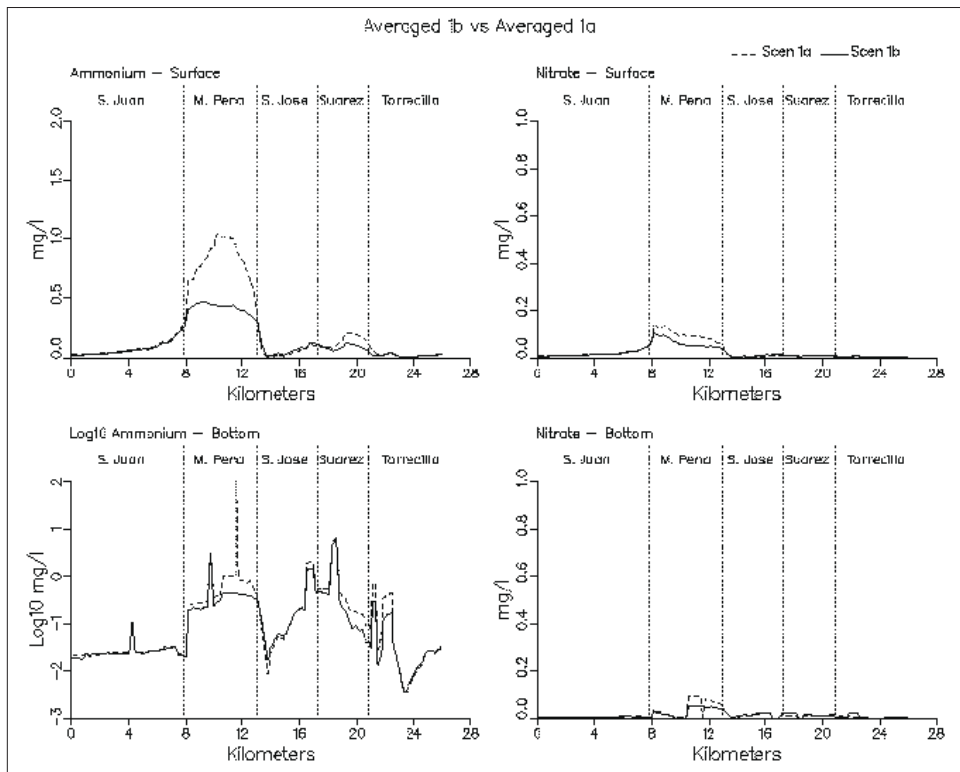


Figure 8-37. (Sheet 4 of 11)

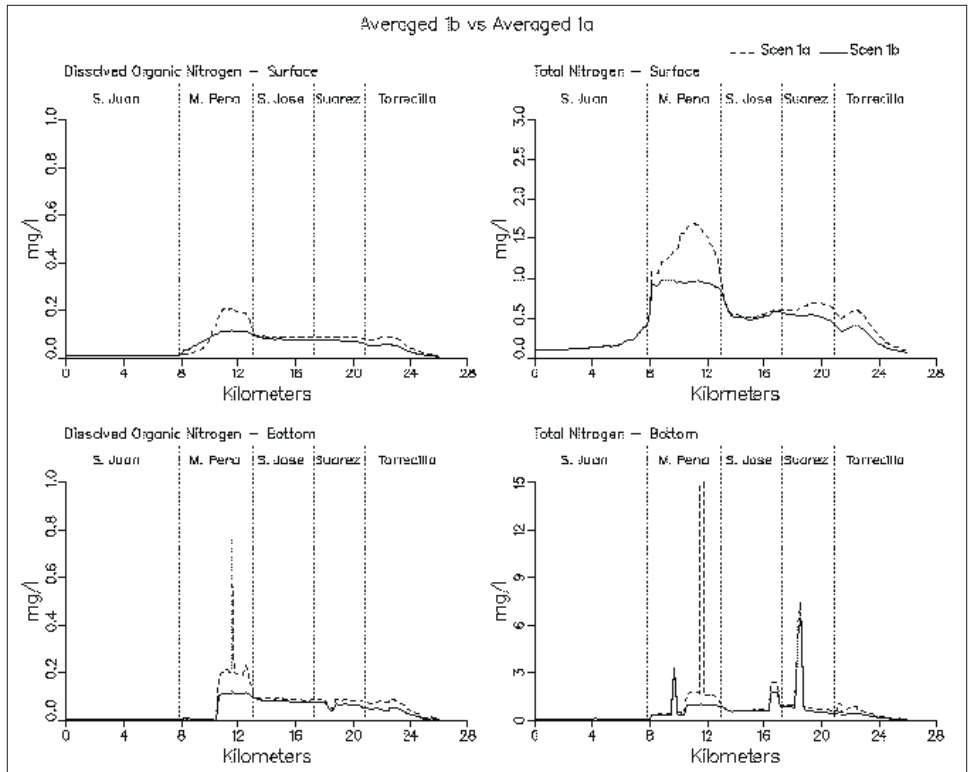


Figure 8-37. (Sheet 5 of 11)

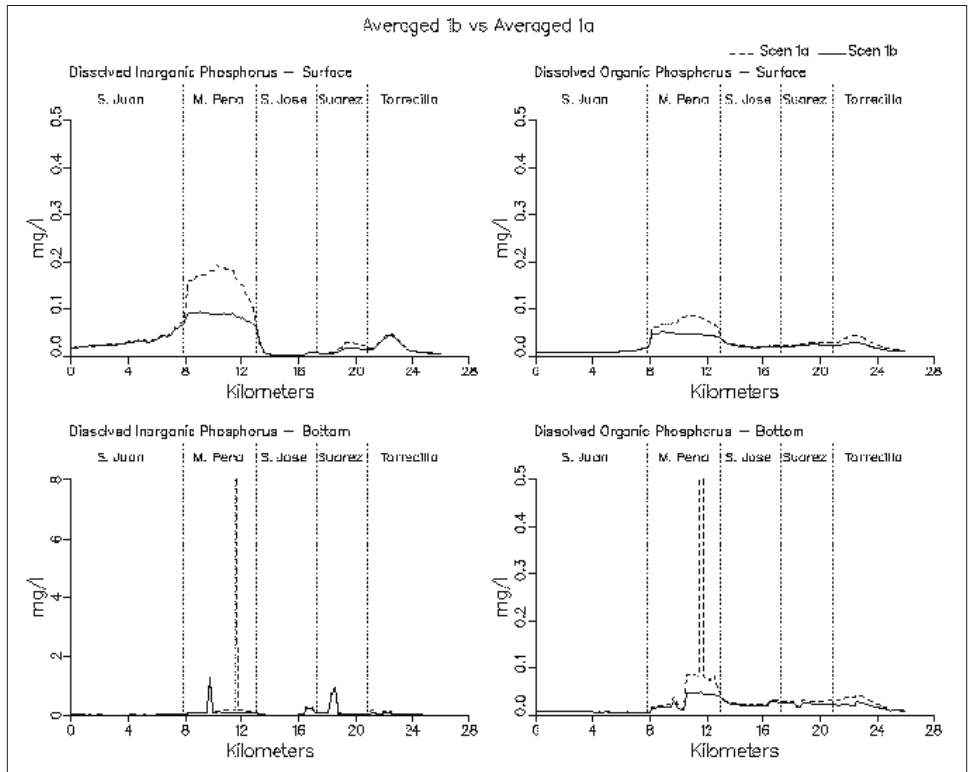


Figure 8-37. (Sheet 6 of 11)

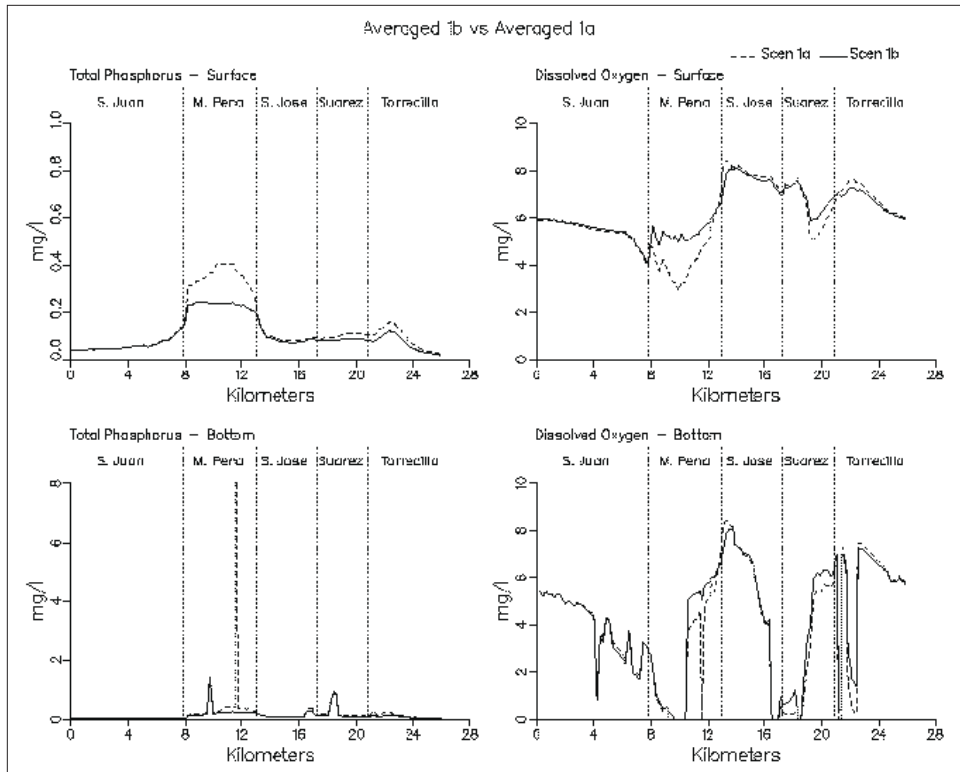


Figure 8-37. (Sheet 7 of 11)

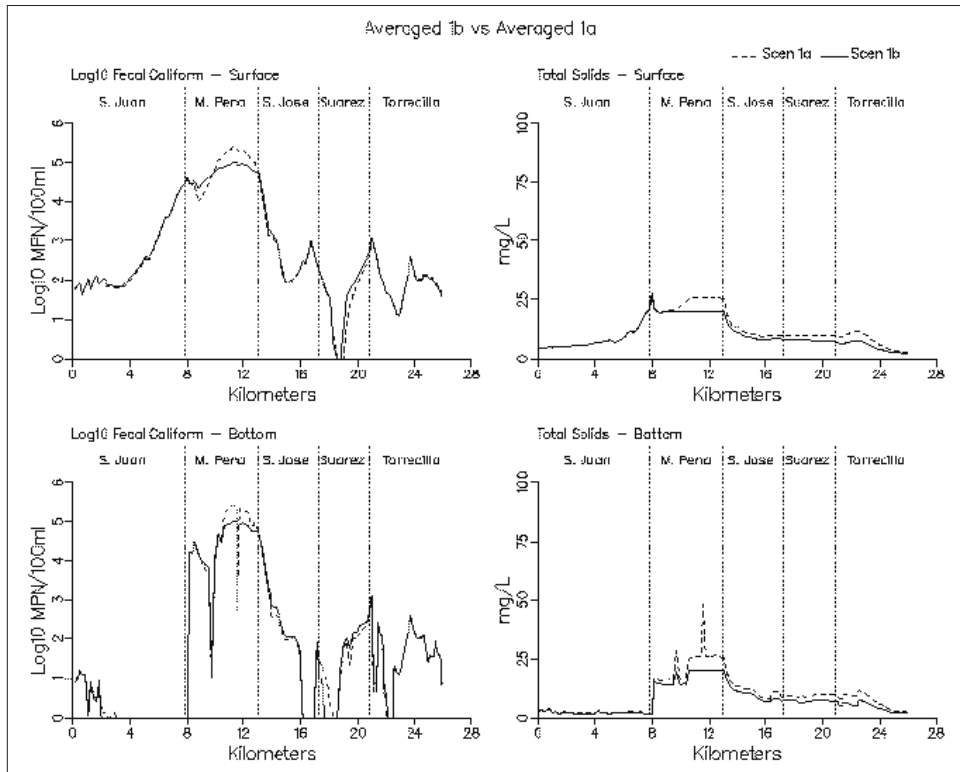


Figure 8-37. (Sheet 8 of 11)

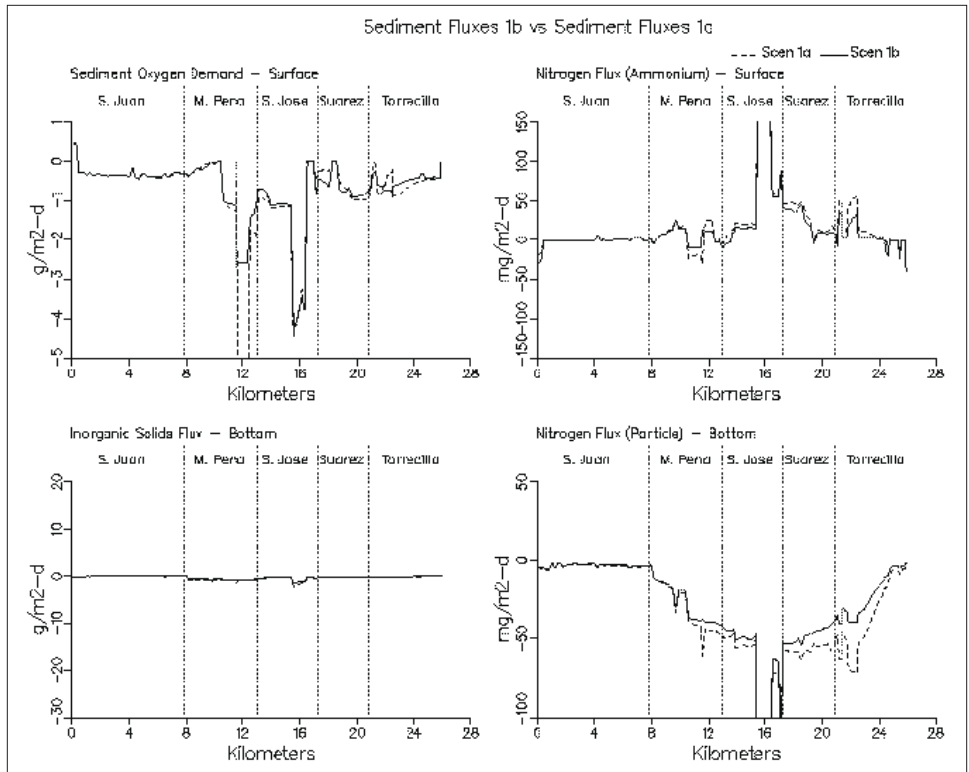


Figure 8-37. (Sheet 9 of 11)

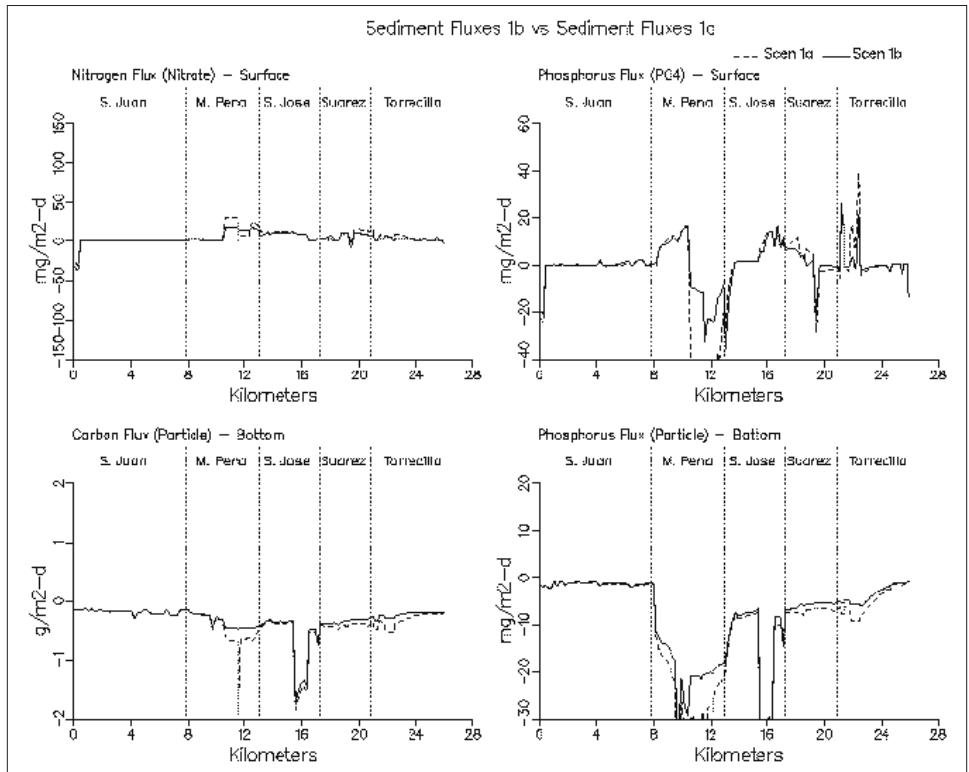


Figure 8-37. (Sheet 10 of 11)

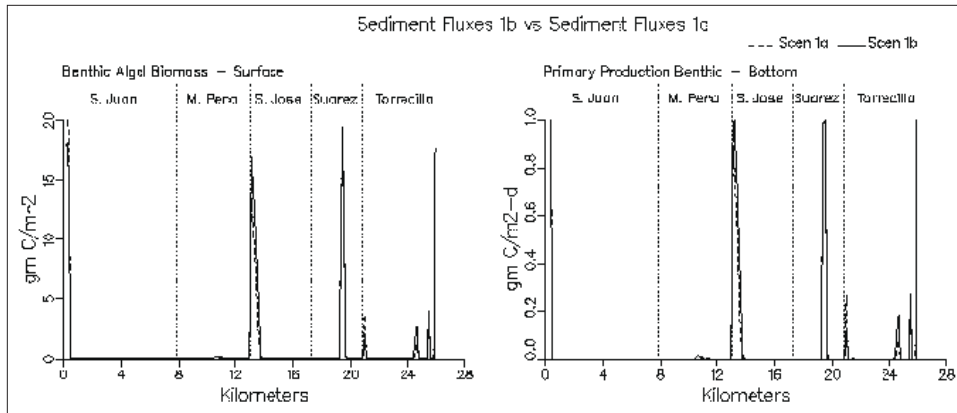


Figure 8-37. (Sheet 11 of 11)

Martín Peña as a result of increased flushing. Total solids transect plots also indicated decreases in the interior of the system as a result of additional flushing.

In summary, Scenario 1b resulted in an increase in the flow from Laguna San José through Caño Martín Peña. At the same time, there was a corresponding decrease in flow from Laguna San José through Canal Suárez. There were corresponding decreases in the mass of carbon, nitrogen, and phosphorus leaving Laguna San José via Canal Suárez which had the end result of improving water quality by decreasing nutrients and increasing salinity in Canal Suárez. The decrease in Laguna San José flow through Canal Suárez had the result of increasing ocean water influx through the Laguna La Torrecilla inlet which raised salinity levels. Nutrient levels in Caño Martín Peña were typically decreased by the nearly three-fold increase in flushing through the eastern end of the canal. The additional load due to the flux of Laguna San José waters through Caño Martín Peña was more than offset by the additional exchange with San Juan Bay.

Scenario 1c

The channel modifications for this scenario required that a new grid be generated (Table 8-3). Widening and deepening Caño Martín Peña had a significant effect on the distribution of flows from Laguna San José. Average discharge from Laguna San José through Caño Martín Peña increased to over $3 \text{ m}^3/\text{s}$. In the base Scenario 1a, discharge through this same path was only $0.5 \text{ m}^3/\text{s}$. Flow from Laguna San José via Canal Suárez in the base scenario had been nearly $2 \text{ m}^3/\text{s}$. In Scenario 1c, there is a reversal of the net flow so that there is now an average inflow of water from Canal Suárez to Laguna San José of $0.4 \text{ m}^3/\text{s}$. In effect, a clockwise circulation pattern has been established through the interior of the system from Laguna La Torrecilla to the mouth of San Juan Bay.

The change in circulation described above had significant effects upon water quality. Average salinity levels in Caño Martín Peña, Laguna San José, and Canal Suárez increased to approximately 23 ppt, Figure 8-38. There was a slight decrease in surface salinity in San Juan Bay as a result of more of the freshwater flows from Laguna San José being discharged through Caño Martín Peña. Bottom water salinity levels in Caño Martín Peña, Laguna San José, and Canal Suárez had increases similar to those of the surface waters, reaching concentrations of 25 ppt or greater. Chlorophyll levels in Caño Martín Peña, Laguna San José, Canal Suárez, and Laguna La Torrecilla decreased. Only San Juan Bay indicated any increase in chlorophyll when compared to Scenario 1a. Surface chlorophyll concentrations increased to 7 µg/l in San Juan Bay as a result of chlorophyll from Laguna San José being transported down Caño Martín Peña. Phytoplankton production levels increased in San Juan Bay in 1c to 5300 kg C/day. In 1a, phytoplankton production levels were 3586 kg C/day. By comparison, phytoplankton production levels in Laguna San José were 5860 kg C/day in Scenario 1c and 6093 kg C/day in Scenario 1a. So while there was a significant change in chlorophyll levels between 1a and 1c in Laguna San José, the change was not the result of decreased algal activity but was instead the result of algae being discharged to San Juan Bay via Caño Martín Peña. A slight change in light extinction rates occurs along the transect as a result of changes in algal self-shading due to changes in algae concentration.

Surface dissolved organic carbon levels decreased in Caño Martín Peña, Laguna San José, Canal Suárez, and Laguna La Torrecilla. Concentrations in eastern Caño Martín Peña decreased from 12 mg/l to 5 mg/l. To some degree decreases in this area can be attributed to the canal dredging increasing receiving water volume for the un-sewered loadings. Total organic carbon levels showed results similar to those of dissolved organic carbon. Particulate organic carbon sediment deposition rates were decreased in eastern Caño Martín Peña from 0.5 g/m²-day to 0.1 g/m²-day. Carbon fluxes from Laguna San José to Caño Martín Peña in Scenario 1c were 3530 kg/day. Carbon fluxes from Canal Suárez to Laguna San José were 166 kg/day. Therefore, Canal Suárez transferred organic carbon into Caño Martín Peña for 1c.

Surface and bottom ammonium levels decreased all along the transect with the exception of a slight increase (0.05 mg/l) in the vicinity of station SJ-2 in Laguna San José. The greatest decreases in surface waters occurred in eastern Caño Martín Peña where ammonium levels decreased from as high as 1 mg/l to 0.1 mg/l. Surface levels decreased in western Caño Martín Peña but not to the same degree as in the eastern end of the canal. One possible explanation for this is the effects of the Rio Piedras inflows into Caño Martín Peña at its juncture with San Juan Bay. Ammonium levels decreased in the anoxic holes throughout the system. The most substantial decreases occurred in Caño Martín Peña as a result of the channelization removing the hole from the eastern end. The decreases in eastern Laguna San José, Canal Suárez, and Laguna La Torrecilla result from the clockwise circulation pattern established through the interior.

Nitrate levels decreased in the surface waters of Caño Martín Peña and were unchanged elsewhere. Dissolved organic nitrogen levels decreased along the transect from Caño Martín Peña eastward. An insignificant increase occurred in San Juan Bay at its confluence with Caño Martín Peña. Laguna San José discharged 186.7 kg/day of nitrogen into Caño Martín Peña and imported 5 kg/day from Canal Suárez.

Phosphorus results for Scenario 1c were similar to nitrogen results. Laguna San José discharged 15.3 kg/day of phosphorus into Caño Martín Peña and imported 2.3 kg/day from Canal Suárez. Dissolved inorganic phosphorus levels dropped in Caño Martín Peña surface waters and in the bottom waters all along the transect. Dissolved organic phosphorus levels also dropped in Caño Martín Peña in 1c and remained unchanged elsewhere along the transect. Total phosphorus results indicated the greatest decrease occurred in Caño Martín Peña. Slight decreases in total phosphorus occurred in Canal Suárez and Laguna La Torrecilla as a result of the flow reversal from 1a to 1c in Canal Suárez.

Surface dissolved oxygen levels increased in Caño Martín Peña to the 5-mg/l to 6-mg/l range in 1c. No bottom waters in Caño Martín Peña were anoxic in 1c although at least one location had an average dissolved oxygen less than 1 mg/l. Overall, bottom water dissolved oxygen levels in Caño Martín Peña were greater than 3 mg/l. Laguna San José, Canal Suárez, Laguna La Torrecilla all saw some degree of dissolved oxygen decrease in the surface and bottom waters. These decreases appear to be the result of diminished algal concentrations resulting in less photosynthesis. Bottom anoxic conditions at the confluence of Laguna San José and Canal Suárez were raised to a minimum of 2 mg/l and as high as 5 mg/l. Only the deep hole in Canal Suárez remained anoxic.

Fecal coliform levels decreased in Caño Martín Peña by an order of magnitude in part due to additional receiving water volume being present. Levels increased insignificantly in San Juan Bay as a result of additional flushing through Caño Martín Peña. A slight increase also occurred along the transect in Laguna San José as a result of Caño Martín Peña being opened. Total solids levels decreased throughout the system in 1c with the greatest decreases occurring in Caño Martín Peña.

In summary, Scenario 1c resulted in an increase in the discharge of Laguna San José through Caño Martín Peña. At the same time, there was a reversal in net flow in Suárez Canal which resulted in the establishment of a clockwise circulation pattern through the interior of the system. Canal Suárez exported nutrients into Laguna San José in 1c. All water quality variables, except DO, showed improvement in Scenario 1c when compared to 1a in all bodies of water examined. There were decreases in surface dissolved oxygen levels in Laguna San José, Canal Suárez, and Laguna La Torrecilla as a result of decreased algal photosynthesis. Nevertheless, surface dissolved oxygen levels in these waters remained in the 6-mg/l to 7-mg/l range and were the highest along the transect.

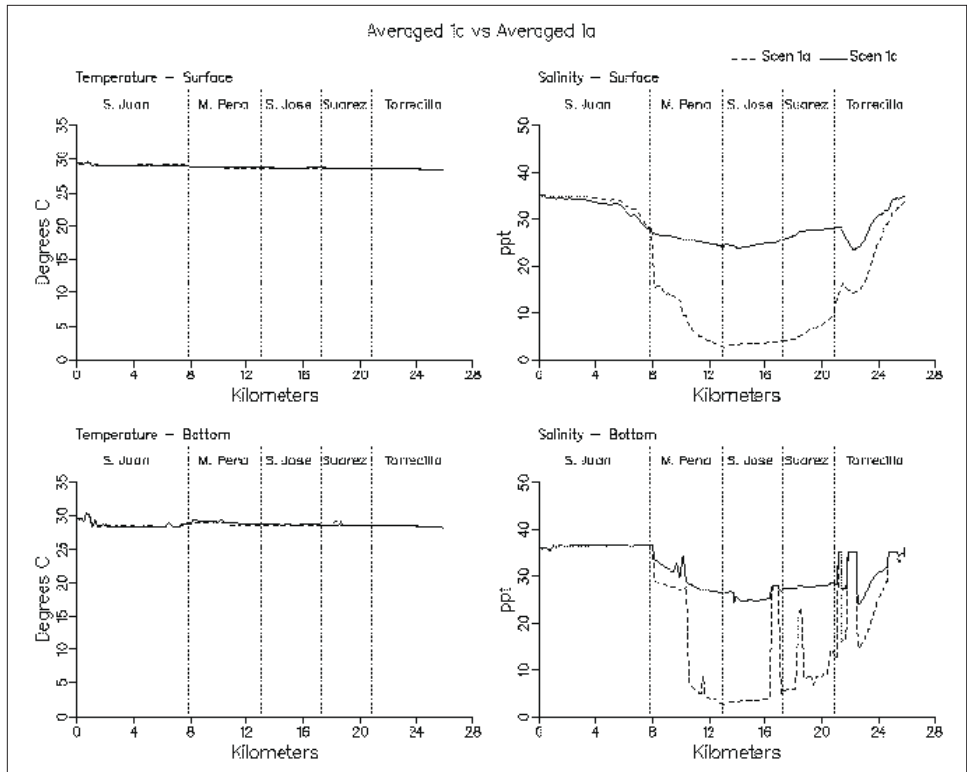


Figure 8-38. Simulation averaged transect plots comparing Scenario 1c with Scenario 1a (Sheet 1 of 11)

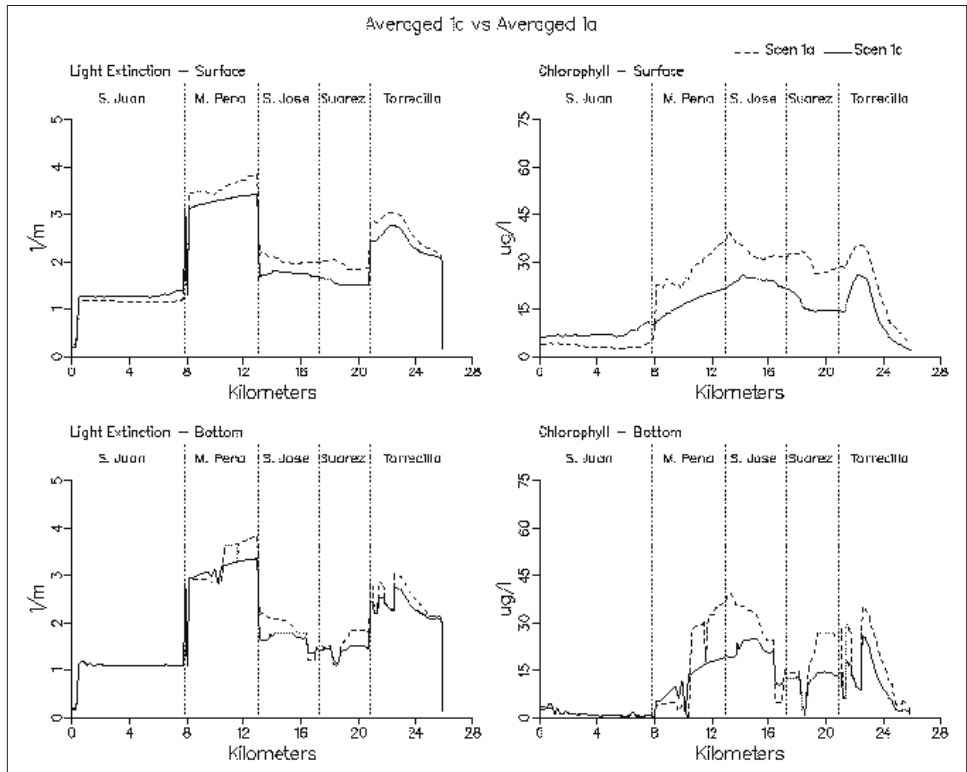


Figure 8-38. (Sheet 2 of 11)

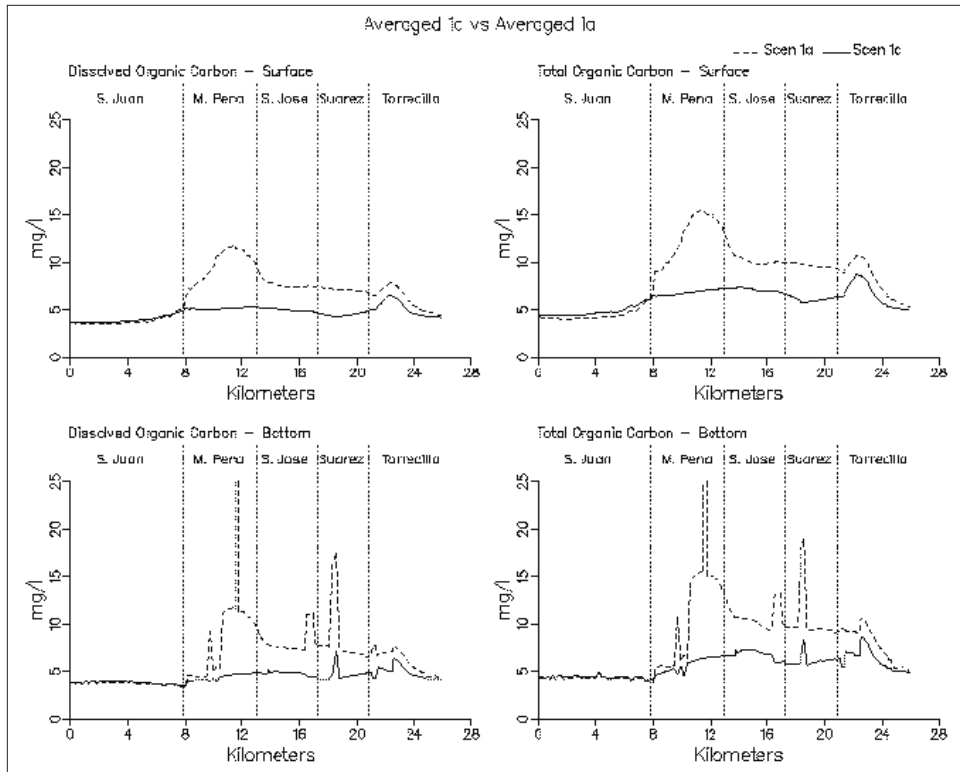


Figure 8-38. (Sheet 3 of 11)

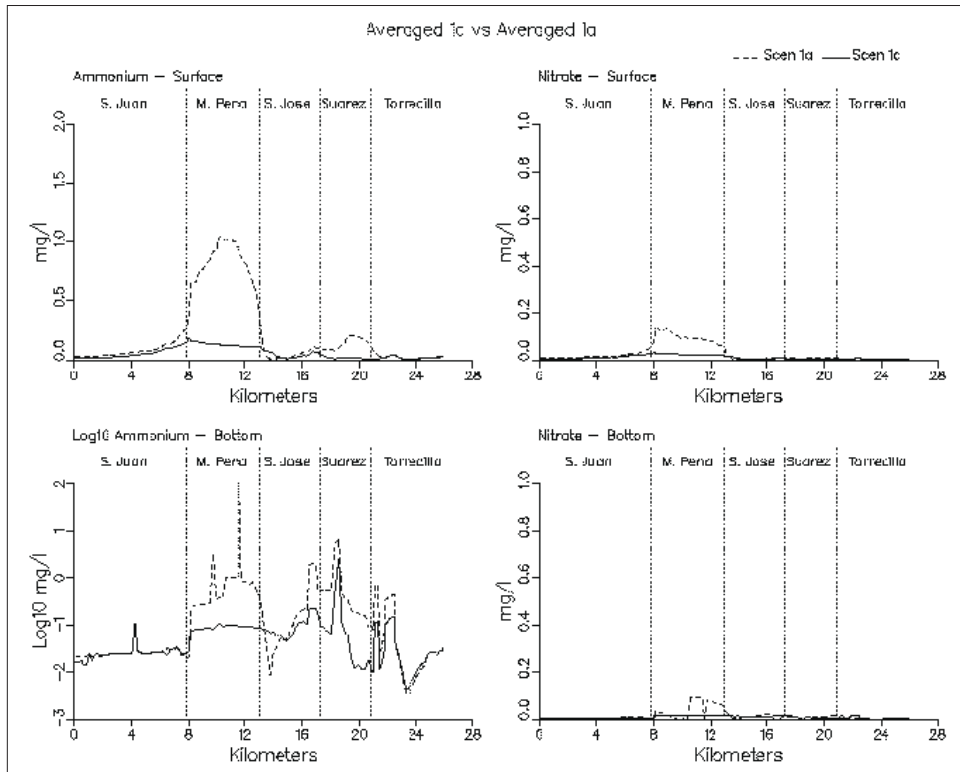


Figure 8-38. (Sheet 4 of 11)

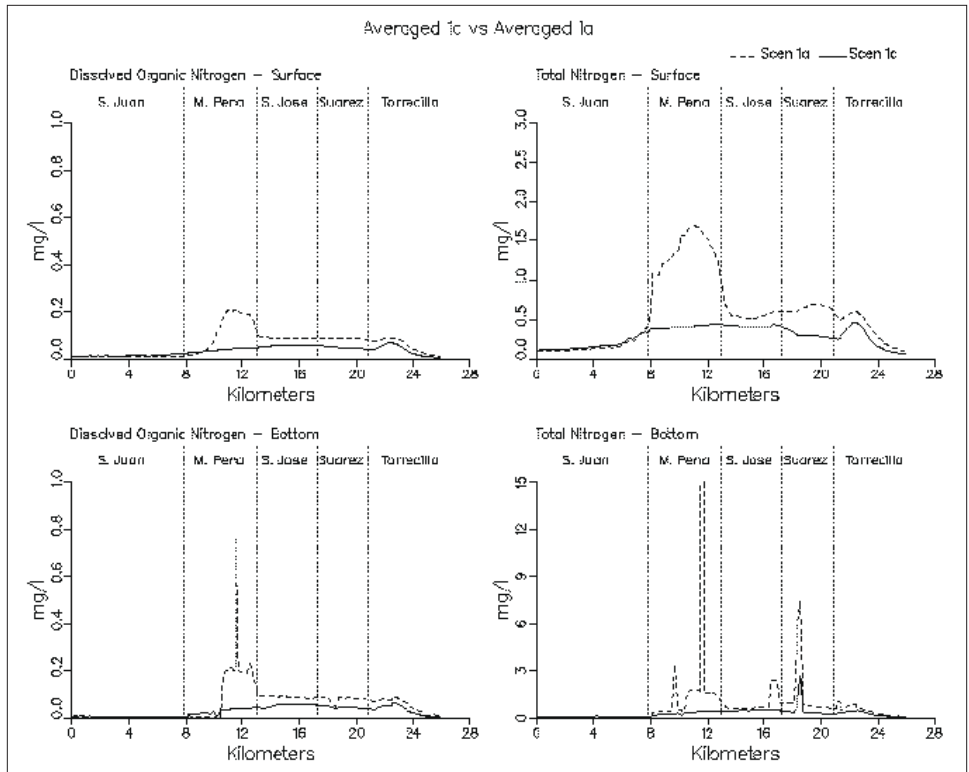


Figure 8-38. (Sheet 5 of 11)

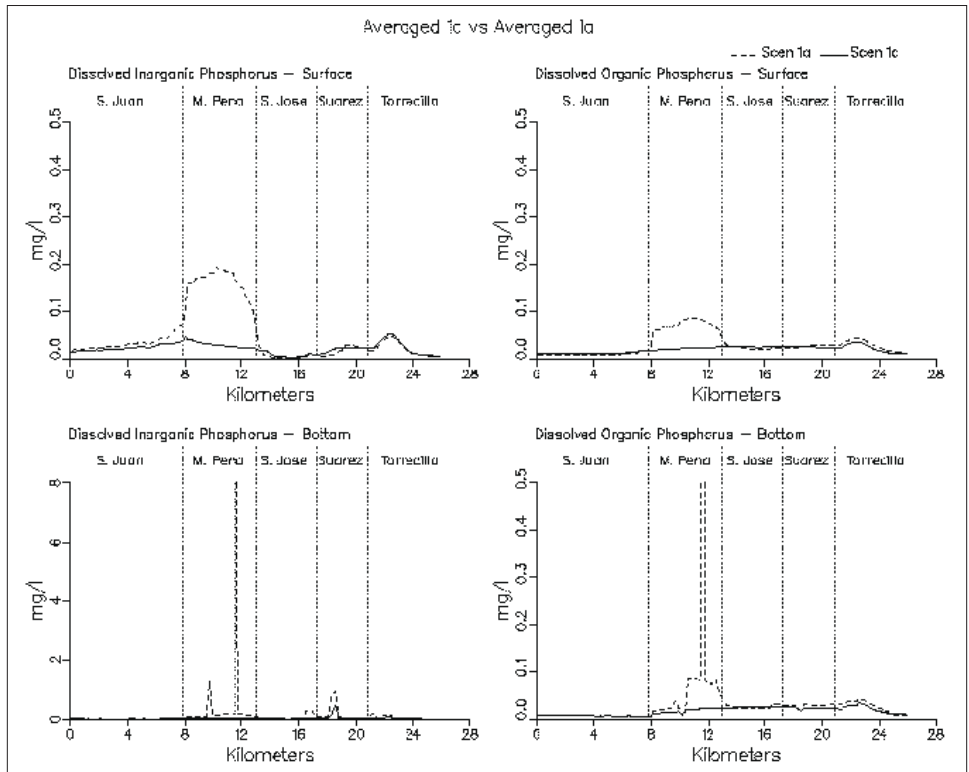


Figure 8-38. (Sheet 6 of 11)

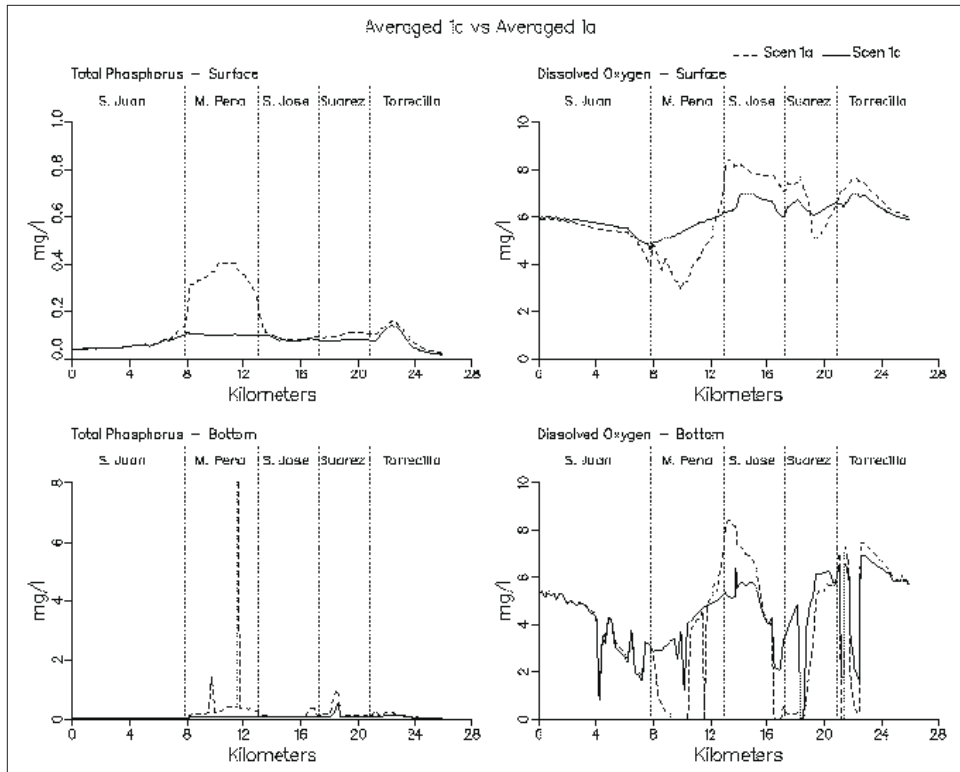


Figure 8-38. (Sheet 7 of 11)

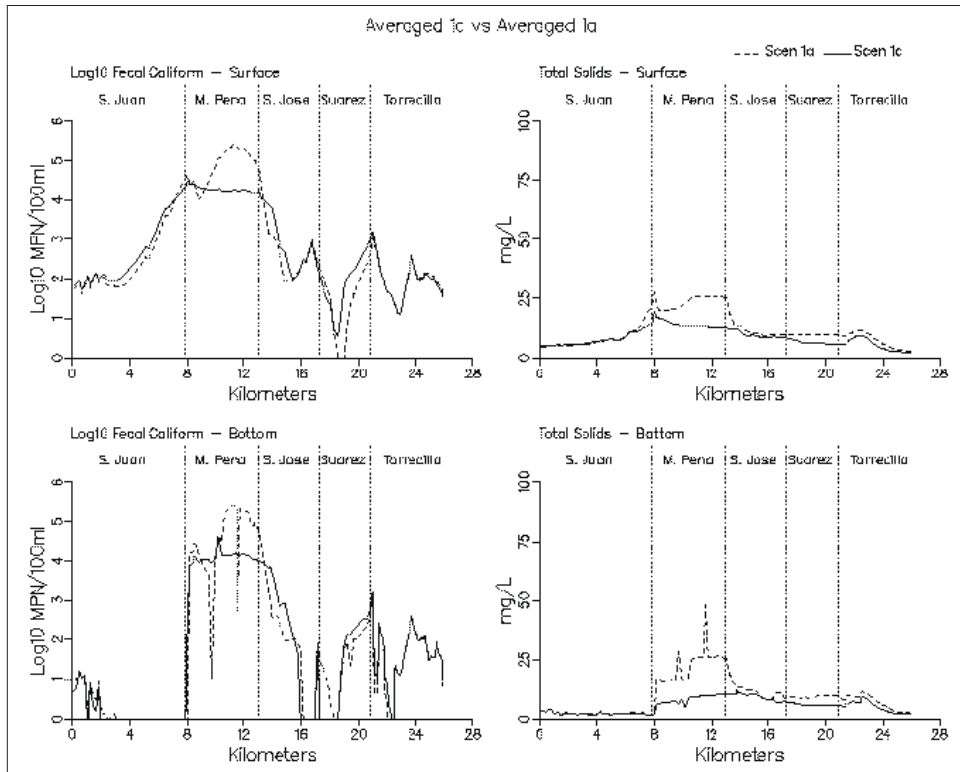


Figure 8-38. (Sheet 8 of 11)

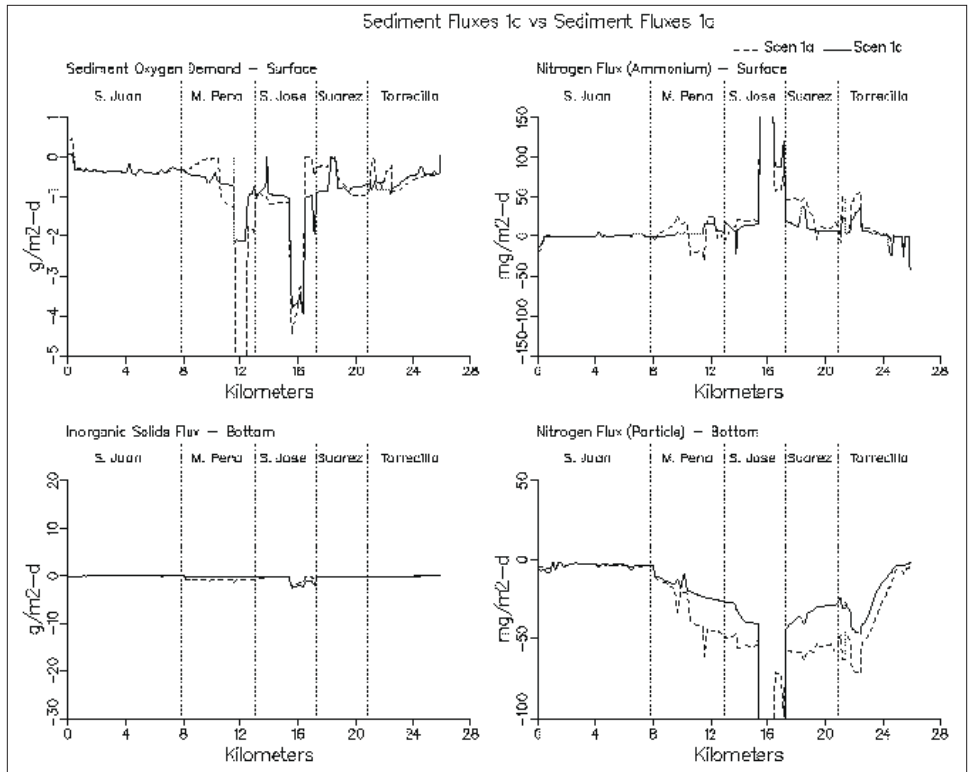


Figure 8-38. (Sheet 9 of 11)

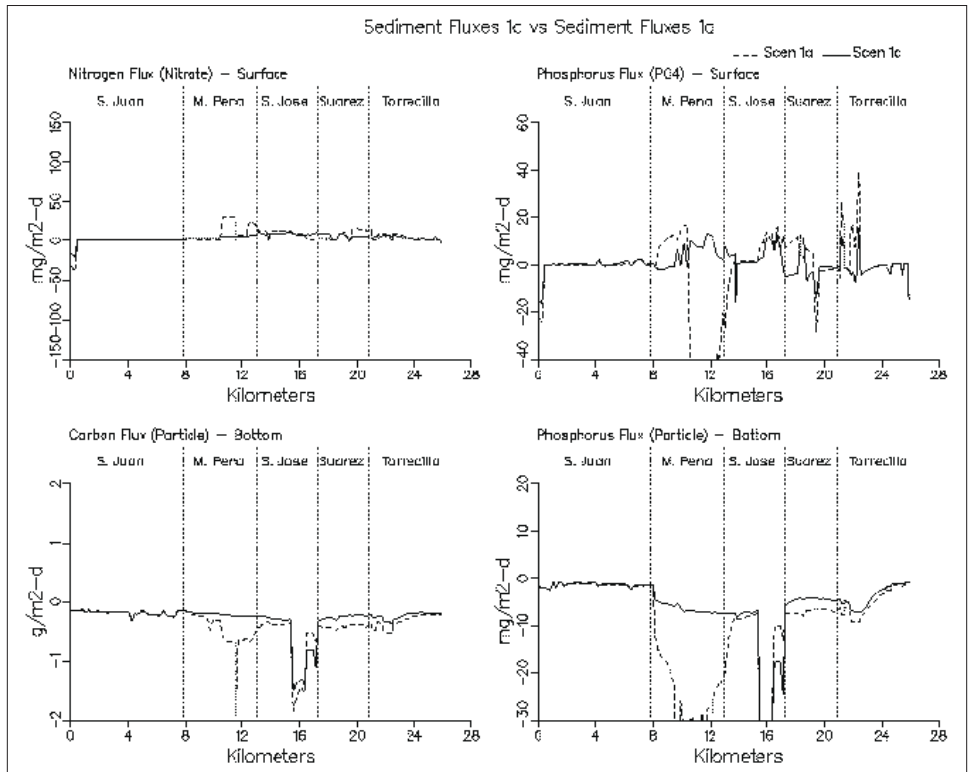


Figure 8-38. (Sheet 10 of 11)

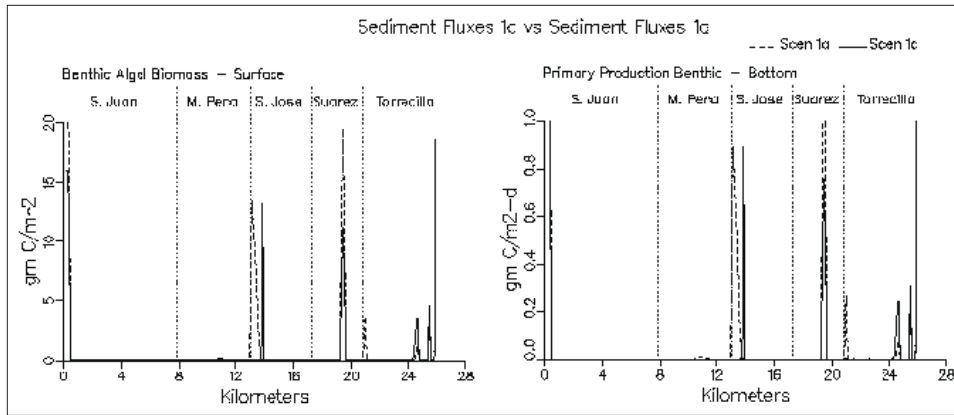


Figure 8-38. (Sheet 11 of 11)

Scenario 2

Scenario 2 was unique among scenarios in that nothing was done which would improve circulation and flushing of Laguna San José, Caño Martín Peña, or Canal Suárez. Neither would the features of Scenario 2 result in any decrease in tributary or runoff loads to the system. Instead, by filling the anoxic holes of Laguna San José, sediment nutrient fluxes and the oxygen demand arising from these holes should be decreased. The volume of Laguna San José in Scenario 1a was 12,781,933 m³ which was decreased to 9,507,690 m³ in Scenario 2. The distribution of flows leaving Laguna San José in Scenario 2 was identical to the flow distribution in 1a.

Results from Scenario 2 indicate that the surface temperatures in San Juan Bay are slightly cooler than 1a (Figure 8-39). Salinity transects show more differences. Filling in the holes resulted in there being no “nudging” of salinity. As a result, this internal salinity boundary condition was lost. The spin-up runs required to equilibrate the sediments effectively flushed the salt out of Laguna San José and Canal Suárez. As a result, the waters being flushed down Caño Martín Peña are too fresh and actually decrease the salinity of San Juan Bay.

Chlorophyll levels in Scenario 2 are much lower throughout the interior of the system. Tributary loads of chlorophyll are unchanged, thus the reason appears to be nutrient limitation. In Scenario 2, Laguna San José sediments take up 105.5 kg/day of ammonium and 28.9 kg/day of phosphate. In comparison, the sediments gave off 436 kg/day of ammonium and 20 kg/day of phosphate in Scenario 1a.

Dissolved organic carbon levels are decreased in Scenario 2 apparently as a result of the decrease in algae productivity. Carbon fluxes from Laguna San José to Caño Martín Peña were 329 kg/day. Fluxes from Laguna San José to Canal Suárez were 1060 kg/day.

Ammonium levels in Caño Martín Peña were unchanged in Scenario 2. Levels in Canal Suárez did drop to near 0 mg/l. Nitrate levels were unchanged throughout the system. Dissolved organic nitrogen levels decreased from the middle of Caño Martín Peña eastward in response to a decrease in algal levels. Total nitrogen levels indicated considerable decreases in Laguna San José and Canal Suárez when compared to Scenario 1a. Nitrogen fluxes from Laguna San José to Caño Martín Peña were 8.8 kg/day while fluxes from Laguna San José to Canal Suárez were 18.4 kg/day.

Dissolved inorganic phosphorus concentrations actually increased in Caño Martín Peña, Laguna San José, and Canal Suárez in Scenario 2. This is felt to be in response to the decreased levels of algae in Laguna San José. Also, the presence of phosphorus and the near absence of ammonium indicate that nitrogen is probably the limiting factor in algal growth. Dissolved organic phosphorus levels along the transect were relatively unchanged in Scenario 2. Total phosphorus levels were unchanged in Scenario 2 except for slight decreases in the eastern end of Canal Suárez. Phosphorus fluxes from Laguna San José to Caño Martín Peña in Scenario 2 were 2 kg/day. Phosphorus fluxes from Laguna San José to Canal Suárez were 12.9 kg/day.

Surface dissolved oxygen levels showed little change in Scenario 2. There were slight increases in DO in San Juan Bay but this is undoubtedly due to the decrease in salinity. Bottom dissolved oxygen levels increased significantly in Laguna San José as a result of the removal of the ammonium fluxes and sediment oxygen demand associated with the anoxic holes. Fecal coliform levels were unchanged. Total solids transect plots indicated a slight decrease in the interior system which is the result of decreased algal levels in these waters.

In summary, Scenario 2 improved water quality by removing internal nutrient sources which resulted in a decrease in algal concentrations. The extensive spin-up period resulted in the flushing of the salinity out of the interior of the system but does not appear to have influenced other water quality constituents significantly.

Scenario 3

Scenario 3 involved Scenario 1a plus removal of the bridge constriction on Canal Suárez. Net flow from Laguna San José to Canal Suárez increased from less than 2 m³/s in Scenario 1a to over 2.5 m³/s for Scenario 3. Flow from Laguna San José to Caño Martín Peña decreased from 0.5 m³/s in 1a to less than 0.1 m³/s in Scenario 3. In essence, all of Laguna San José's exchange with the ocean is via Canal Suárez in Scenario 3.

Results for Scenario 3 indicate that salinity increases in Caño Martín Peña, Laguna San José, and Canal Suárez when compared to 1a (Figure

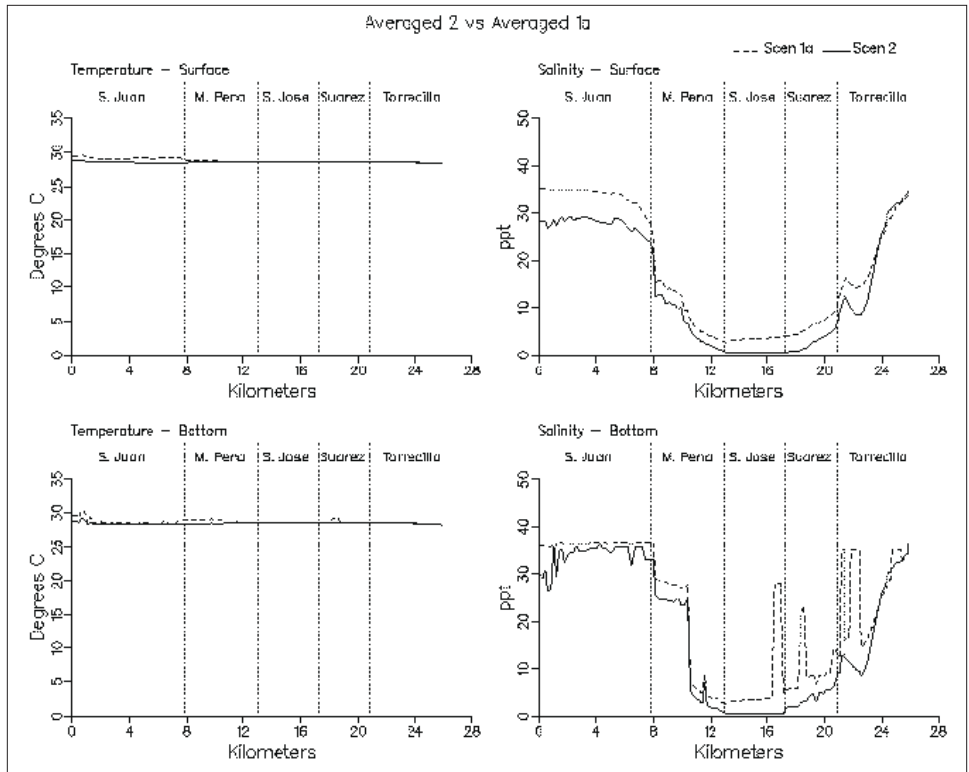


Figure 8-39. Simulation averaged transect plots comparing Scenario 2 with Scenario 1a (Sheet 1 of 11)

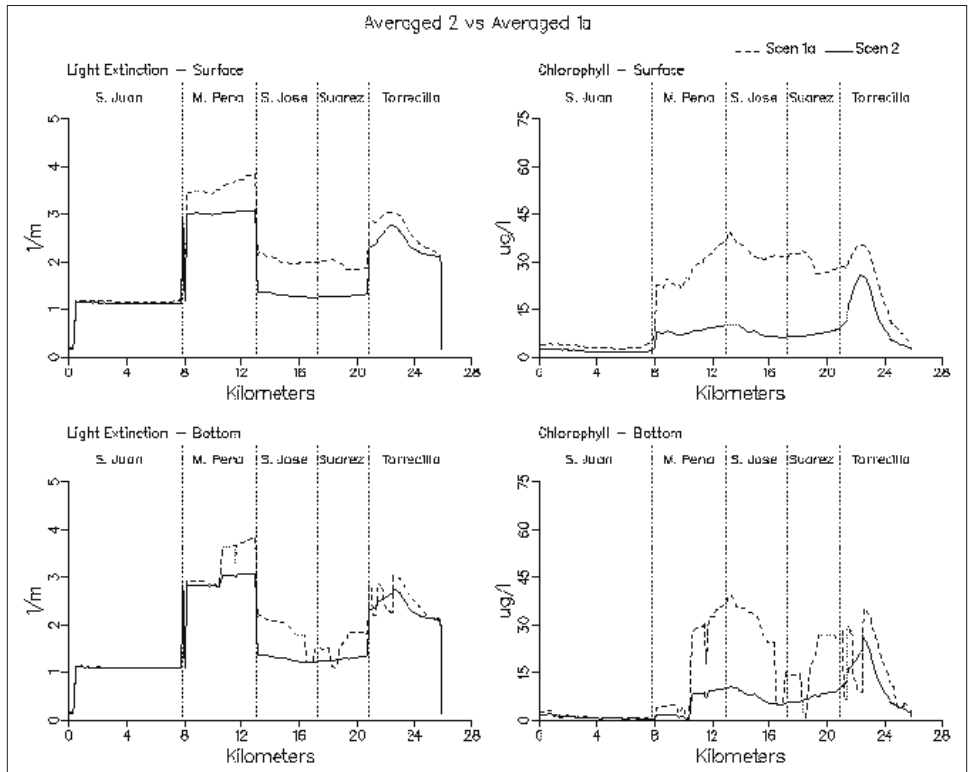


Figure 8-39. (Sheet 2 of 11)

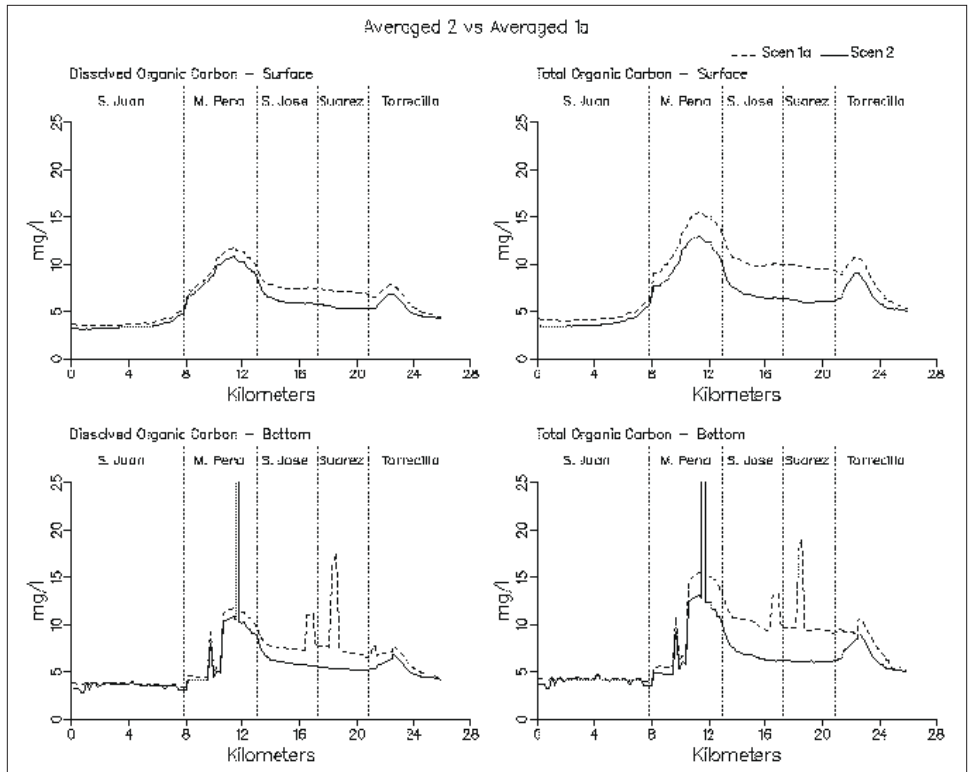


Figure 8-39. (Sheet 3 of 11)

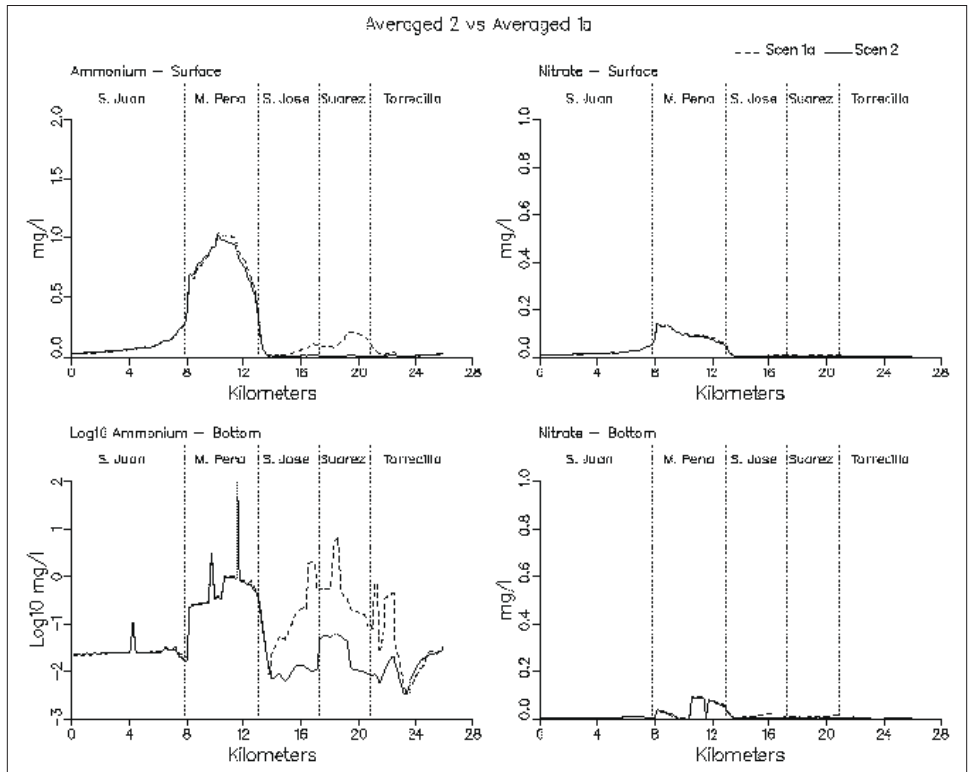


Figure 8-39. (Sheet 4 of 11)

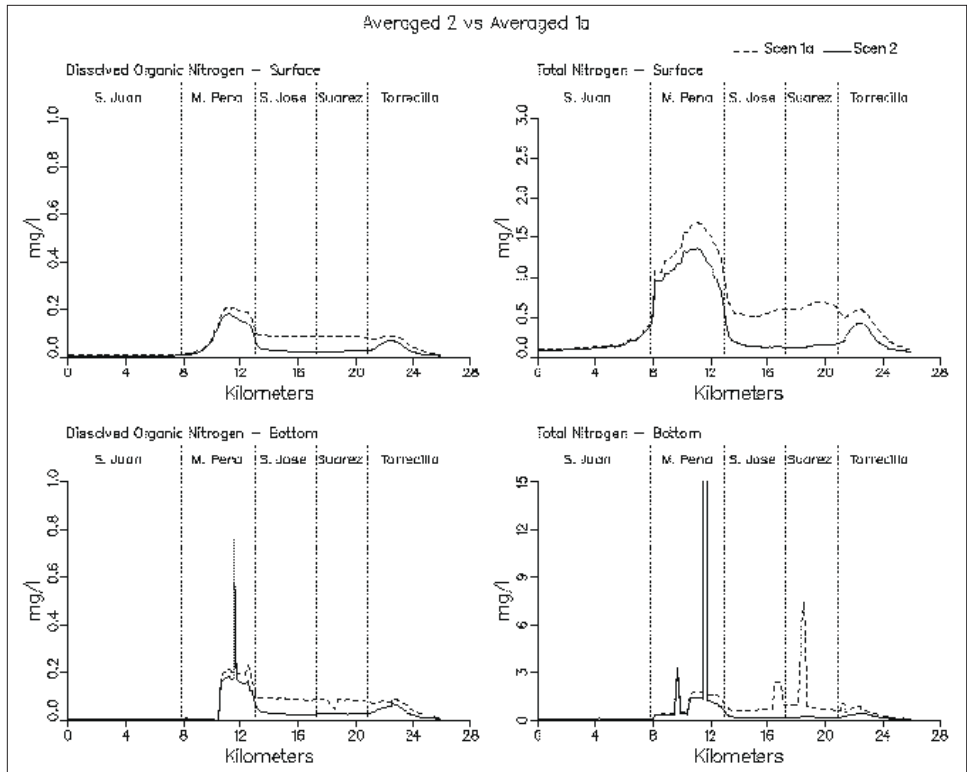


Figure 8-39. (Sheet 5 of 11)

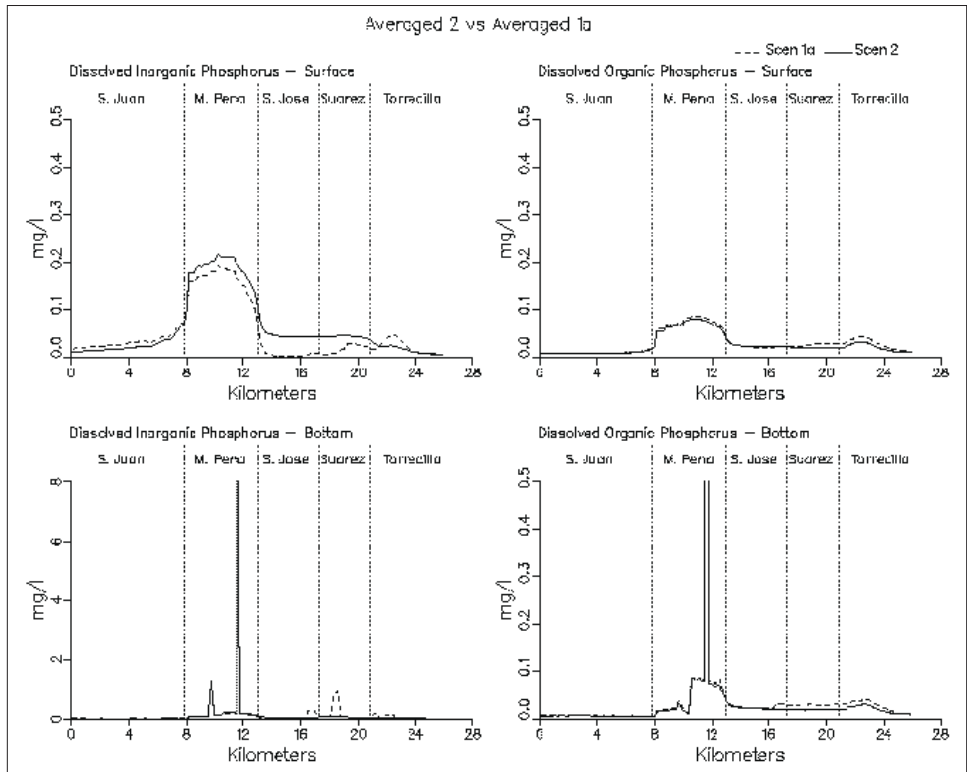


Figure 8-39. (Sheet 6 of 11)

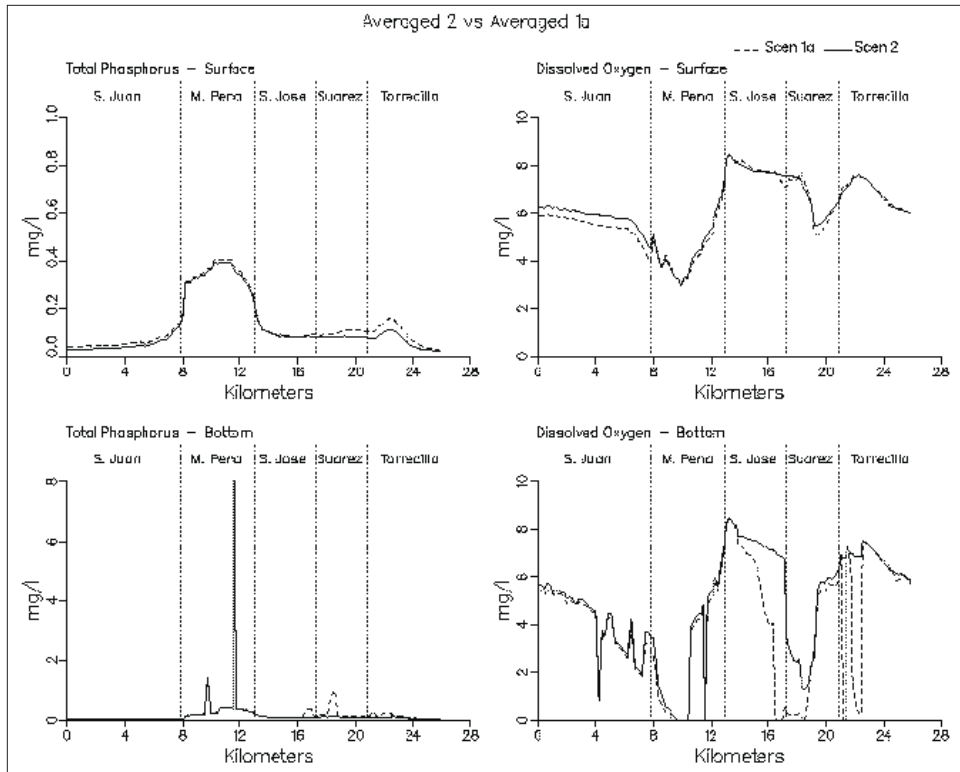


Figure 8-39. (Sheet 7 of 11)

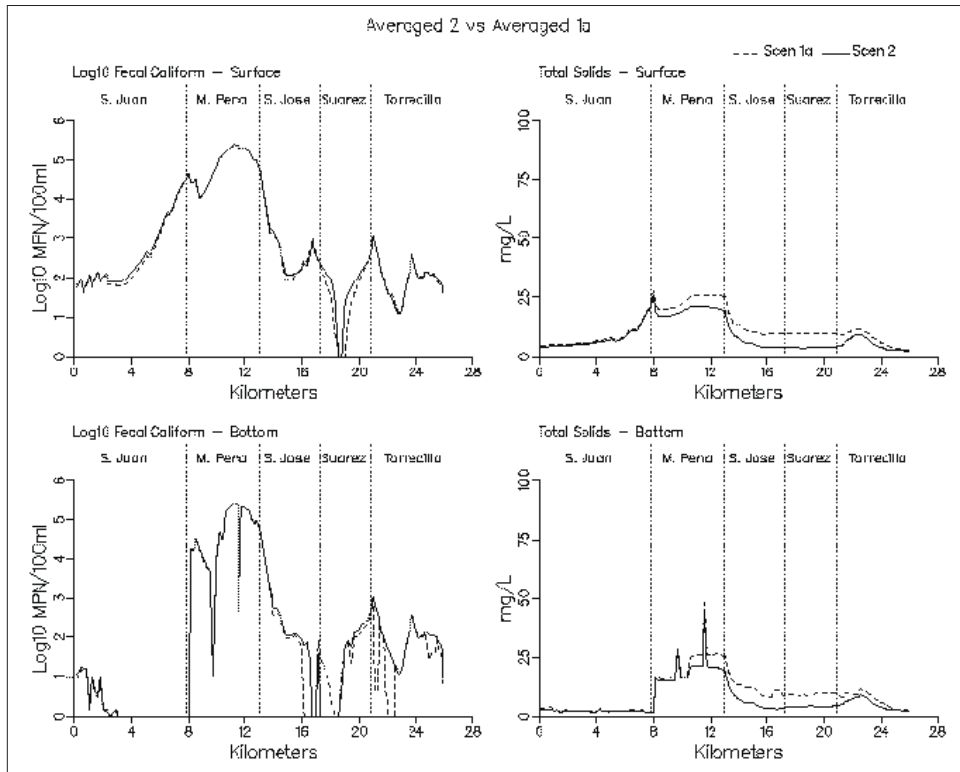


Figure 8-39. (Sheet 8 of 11)

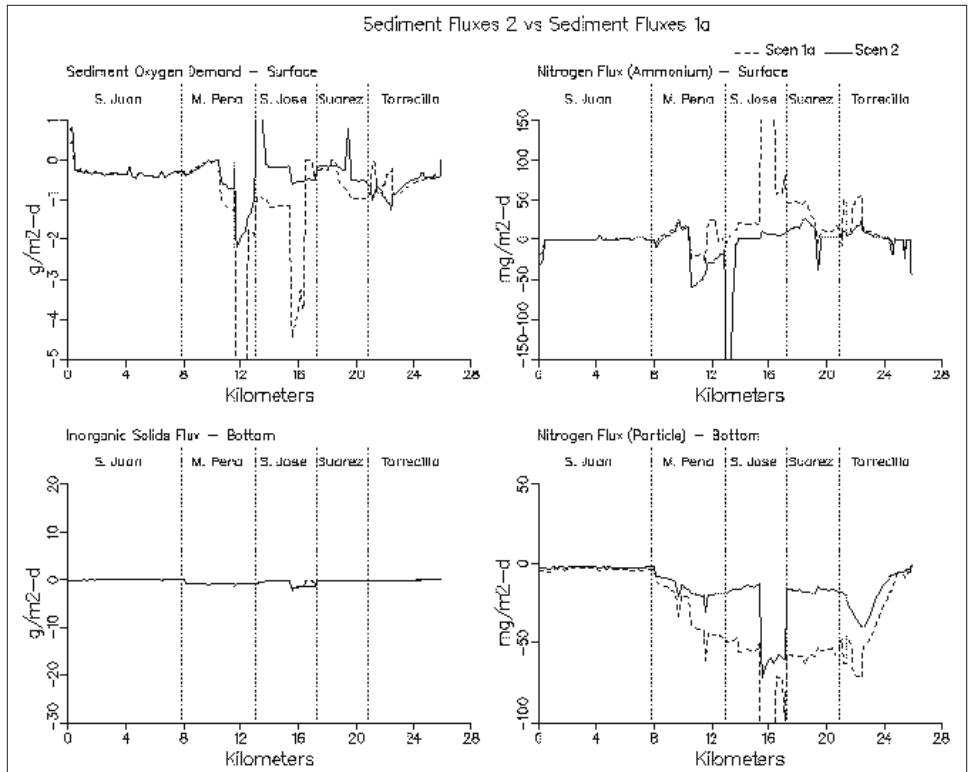


Figure 8-39. (Sheet 9 of 11)

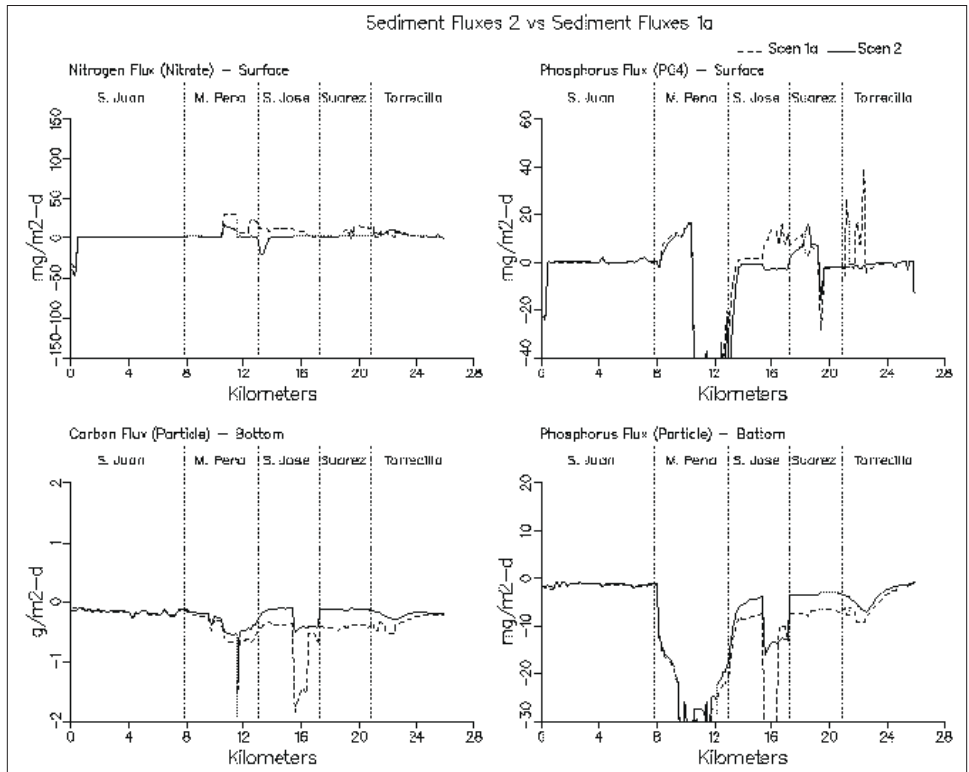


Figure 8-39. (Sheet 10 of 11)

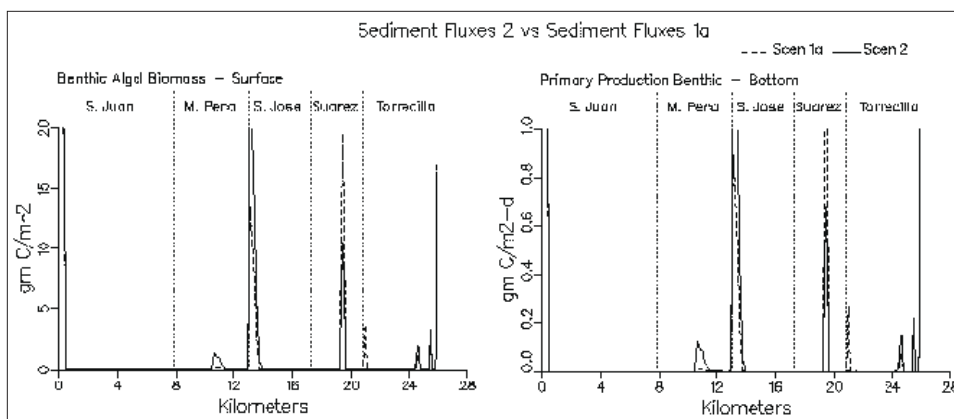


Figure 8-39. (Sheet 11 of 11)

8-40). Increases in Caño Martín Peña are probably the result of saltwater intrusion farther up the canal. Increases in Laguna San José and Canal Suárez result from more exchange with the ocean via Laguna La Torrecilla. Chlorophyll levels remained relatively unchanged in Laguna San José, Canal Suárez, and Laguna La Torrecilla in Scenario 3 compared to Scenario 1a, but decreased in western Caño Martín Peña by $10 \mu\text{g/l}$ due to bay water intrusion up the canal and less algae exchange with Laguna San José. Light extinction levels were unchanged except for Caño Martín Peña where there was a slight decrease due to a decrease in algal self-shading. Only slight changes were observed in organic carbon levels in Scenario 3. Surface dissolved organic carbon levels decreased slightly in western and increased slightly in the eastern portions of Caño Martín Peña. Although total organic carbon concentrations in Laguna San José in Scenario 3 are nearly identical to those in 1a, the flux of carbon from Laguna San José to Canal Suárez is 2261 kg/day versus 1631 kg/day in 1a. Caño Martín Peña actually exports a slight amount of carbon (35.5 kg/day) to Laguna San José in Scenario 3.

Surface water ammonium concentrations increased in the eastern undredged portion of Caño Martín Peña as a result of lower flushing from Laguna San José. Bottom water ammonium levels increased slightly in the undredged portion of Caño Martín Peña to 1 mg/l . Surface water ammonium levels in eastern Canal Suárez decreased from 0.2 mg/l to less than 0.1 mg/l . Bottom ammonia concentrations decreased the entire length of Canal Suárez in part due to a decrease in sediment ammonium fluxes in the western portion of the canal. Nitrate levels exhibited only the slightest change in Caño Martín Peña. Dissolved organic nitrogen levels were relatively unchanged in Scenario 3. Changes in transect plots for total nitrogen between 1a and Scenario 3 are attributable to the changes in ammonium concentrations in Caño Martín Peña and Canal Suárez. Laguna San José exported 178 kg/day of nitrogen through Canal Suárez in Scenario 3 versus 138 kg/day in Scenario 1a. Laguna San José also imported 38.2 kg/day from Caño Martín Peña in Scenario 3 where it had exported 7.5 kg/day in Scenario 1a.

Scenario 3 phosphorus results were similar to those of nitrogen. Increases occurred in dissolved inorganic phosphorus in the undredged eastern portion of Caño Martín Peña and decreases occurred in the eastern end of Canal Suárez. Bottom dissolved inorganic phosphorus levels decreased in the hole in Caño Martín Peña. Dissolved organic phosphorus levels increased slightly in eastern Caño Martín Peña. DIP and DOP levels elsewhere did not change. Laguna San José imported 9.4 kg/day of phosphorus from Caño Martín Peña and exported 23.4 kg/day through Canal Suárez.

Dissolved oxygen levels in Scenario 3 were similar to those in Scenario 1c. Dissolved oxygen decreased slightly in eastern Caño Martín Peña probably as a result of decreased photosynthesis. Surface dissolved oxygen levels did increase in the eastern portion of Canal Suárez. Anoxic conditions in the western end of Canal Suárez were relieved. Fecal coliform levels were unchanged throughout the system except for a slight increase in Canal Suárez. Little change in total solids transect plots occurred as a result of Scenario 3 modifications.

In summary, the modifications of Scenario 3 did little to improve overall water quality when compared to Scenario 1a. Salinity in Laguna San José was increased over 1a results. However, even though there was still a slight discharge from Laguna San José to Caño Martín Peña, Caño Martín Peña became a source of nutrients to Laguna San José. Nutrient concentrations increased in the undredged section of Caño Martín Peña with the diminished flushing from Laguna San José.

Scenario 4

Scenario 4 like Scenario 3 centered on modifications to Canal Suárez without any channel modifications elsewhere. In Scenario 4, a one-way tide gate was installed in the western section of Canal Suárez, along with the removal of the bridge constriction. The tide gate would allow flows in Canal Suárez to move in an east to west fashion but not west to east. This prevented Laguna San José from discharging via Canal Suárez and forced all flow leaving Laguna San José to exit via Caño Martín Peña. No additional channel modifications were made to Caño Martín Peña other than those performed for Scenario 1a.

Scenario 4 results indicated significant change in salinity when compared to results for Scenario 1a (see Figure 8-41). Salinity levels decreased in Caño Martín Peña in response to increased flow from Laguna San José. Average net flow from Laguna San José to Caño Martín Peña increased from 0.5 m³/s in Scenario 1a to 2.55 m³/s in Scenario 4. For comparisons' sake, the net discharge from Laguna San José to Caño Martín Peña in Scenario 1c where Caño Martín Peña had been widened and deepened was 3.05 m³/s. A net inflow of water from Canal Suárez to Laguna San José of 0.2 m³/s occurred in Scenario 4. Salinity levels on the ocean

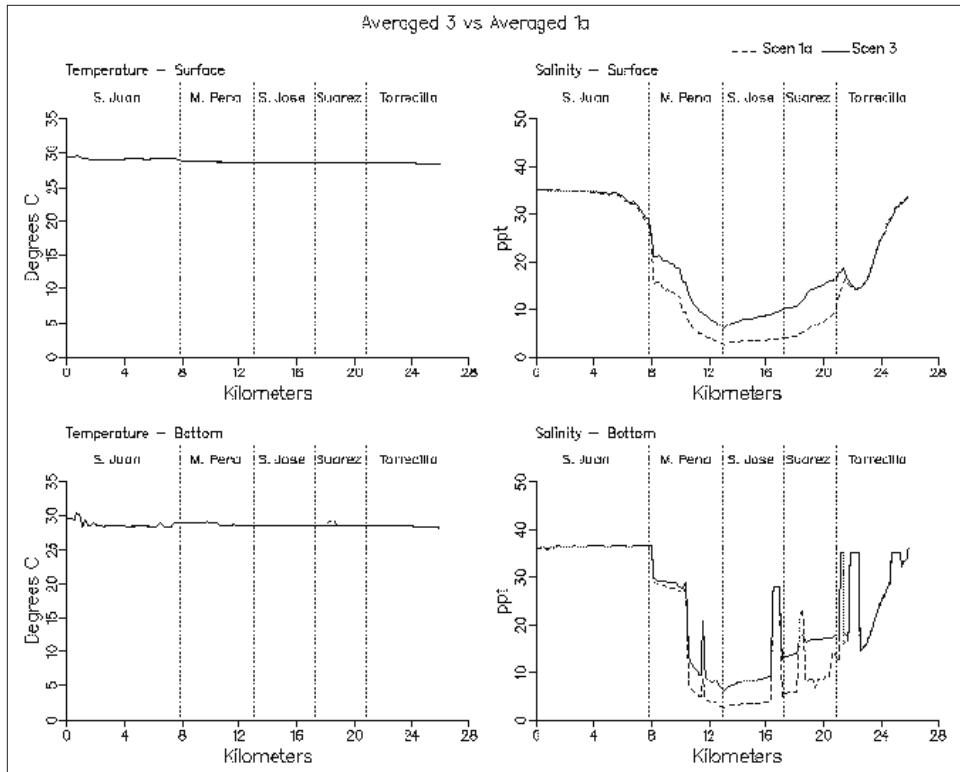


Figure 8-40. Simulation averaged transect plots comparing Scenario 3 with Scenario 1a (Sheet 1 of 11)

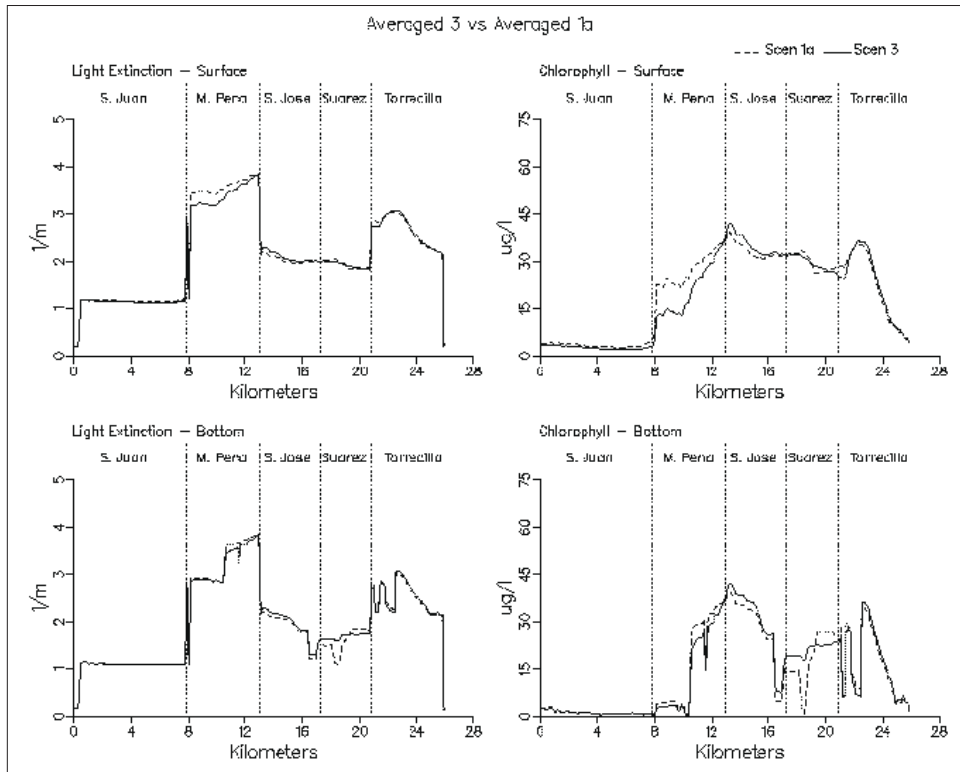


Figure 8-40. (Sheet 2 of 11)

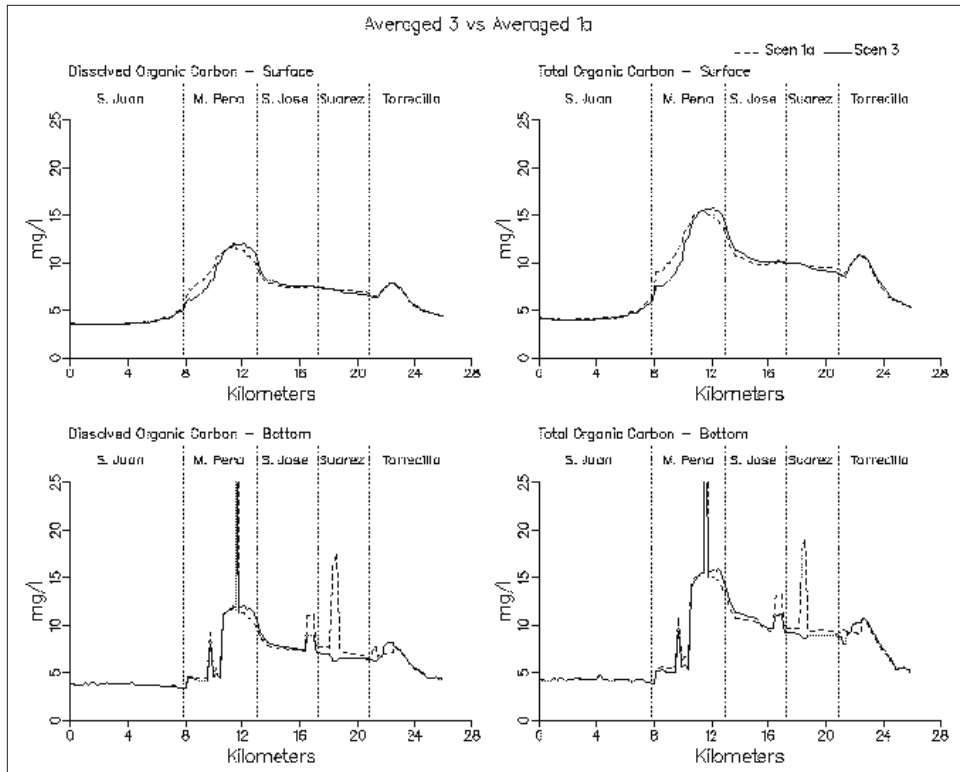


Figure 8-40. (Sheet 3 of 11)

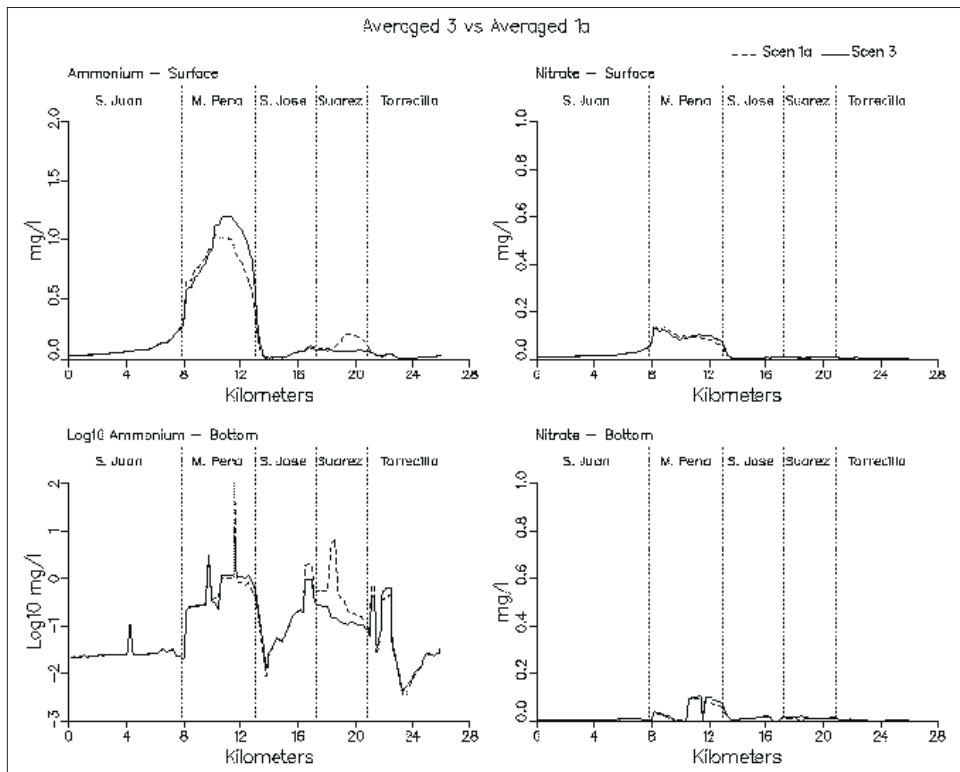


Figure 8-40. (Sheet 4 of 11)

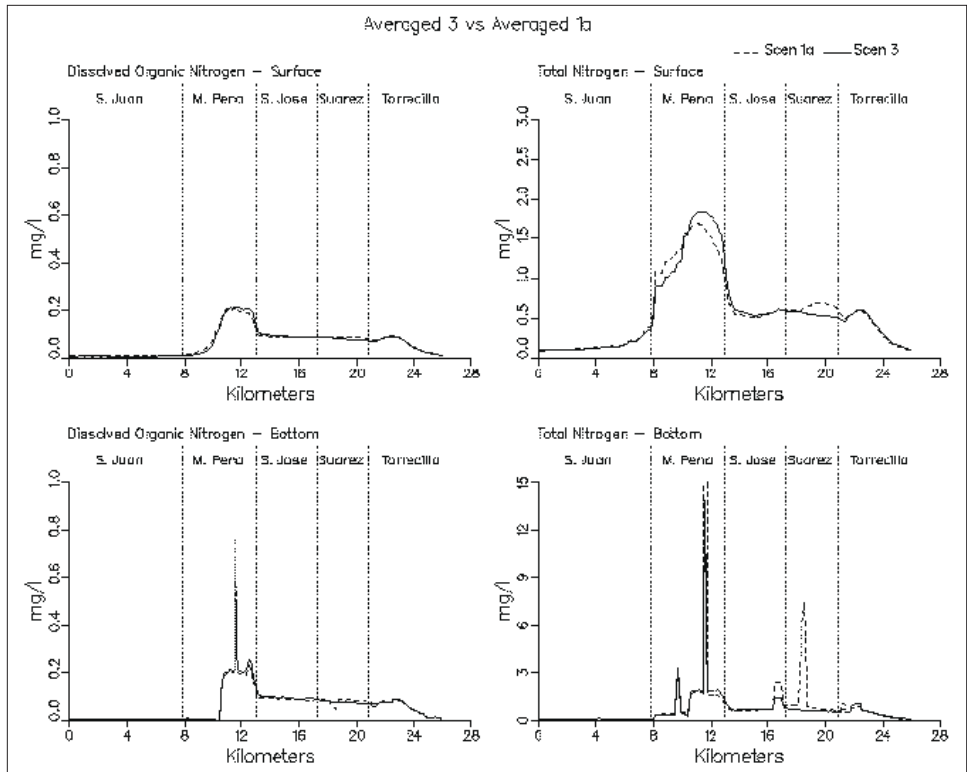


Figure 8-40. (Sheet 5 of 11)

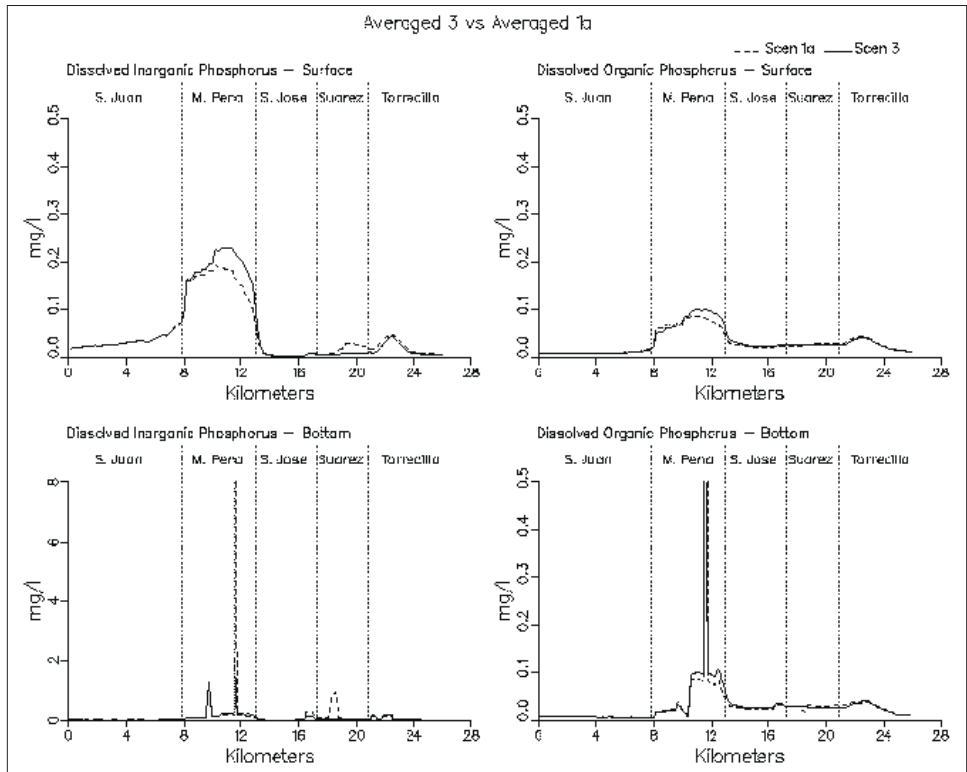


Figure 8-40. (Sheet 6 of 11)

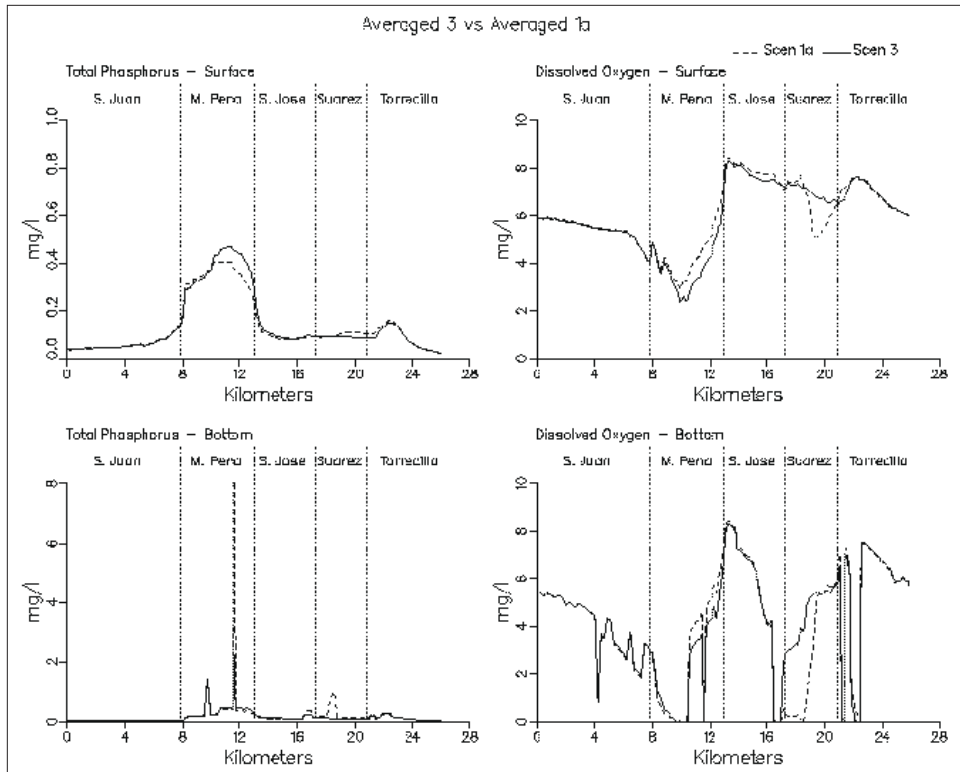


Figure 8-40. (Sheet 7 of 11)

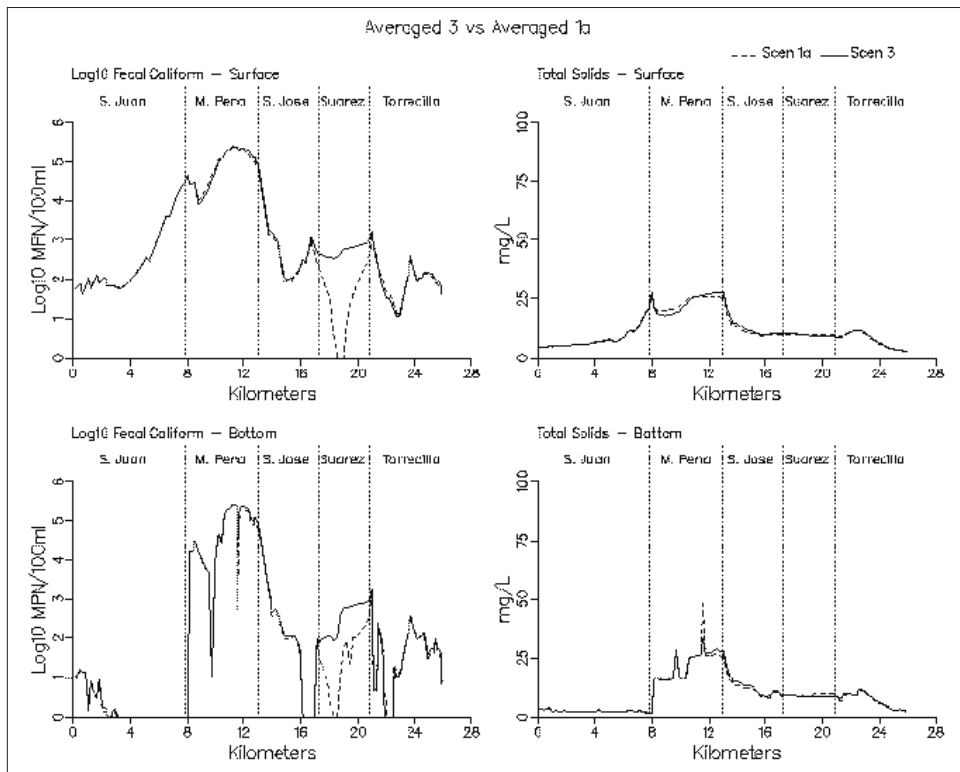


Figure 8-40. (Sheet 8 of 11)

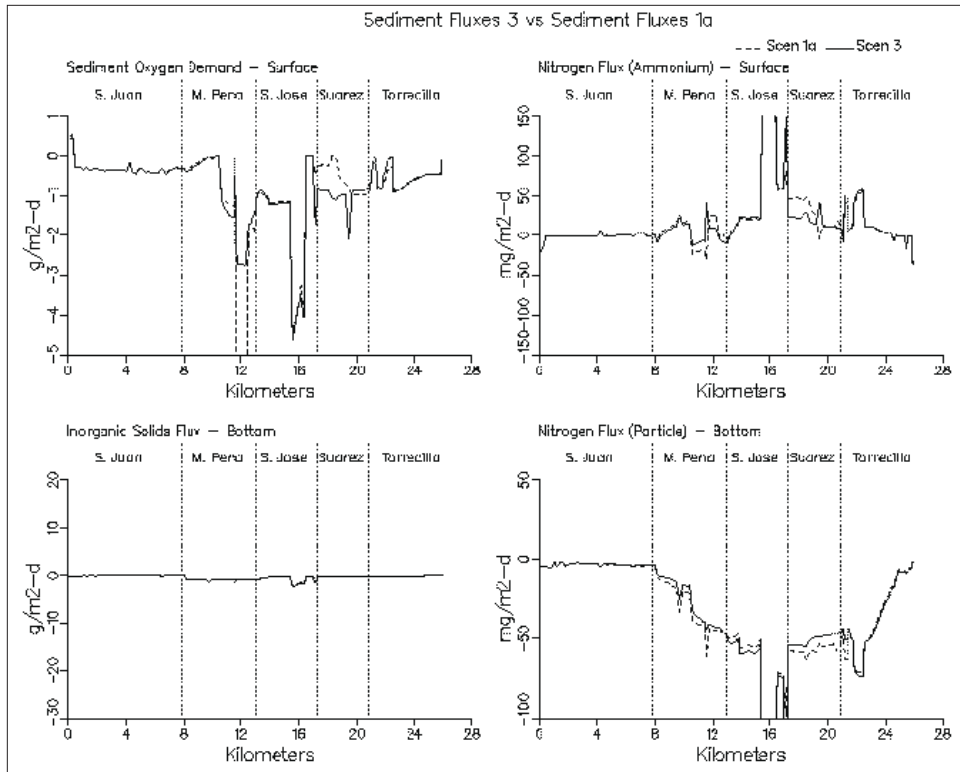


Figure 8-40. (Sheet 9 of 11)

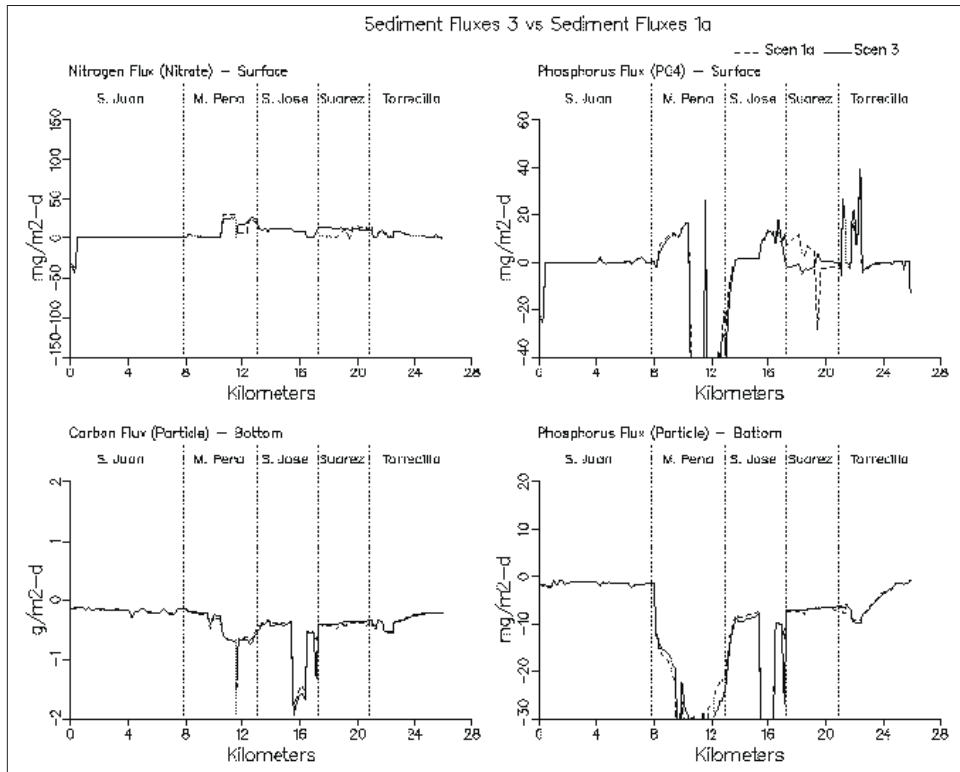


Figure 8-40. (Sheet 10 of 11)

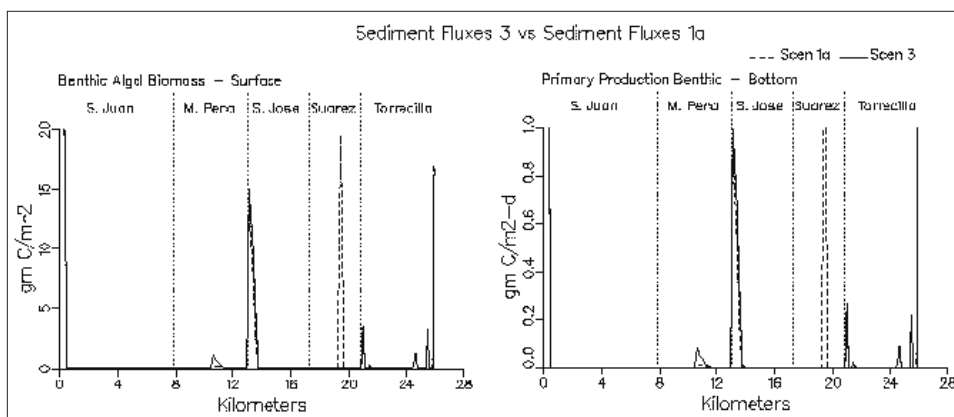


Figure 8-40. (Sheet 11 of 11)

side of the tide gate in Canal Suárez increased in response to the lack of flow from Laguna San José.

Chlorophyll results indicate that chlorophyll levels in Caño Martín Peña increased in Scenario 4. Laguna San José chlorophyll levels were relatively unchanged in comparison to 1a which indicates that the rise observed in Caño Martín Peña is due to the algae from Laguna San José being forced out through Caño Martín Peña. Addition of the tidal gate does not significantly decrease algae levels in Laguna San José. Chlorophyll levels do decrease on the ocean side of the tide gate in Canal Suárez once again because flows from Laguna San José are cut off.

Transect plots for carbon for Scenario 4 indicate patterns that are repeated in other water-quality constituents. The tide gate acts as a wall preventing waters from Laguna San José, which typically have higher concentrations of carbon, nitrogen, and phosphorus, from entering Canal Suárez. As a result, concentrations in Suarez decrease. Dissolved organic carbon concentrations on the ocean side of the tide gate decreased by 4 mg/l. Concentrations in eastern Caño Martín Peña also decreased but this decrease was in response to the increased flushing resulting from the higher flows. Total organic carbon profiles exhibited the same behavior as dissolved organic carbon. Carbon fluxes from Laguna San José to Caño Martín Peña were 2415 kg/day. Daily carbon imports from Canal Suárez to Laguna San José were 73 kg/day.

Surface ammonium concentrations decreased in Caño Martín Peña in response to the increased flushing and dilution through the canal. Surface ammonium concentrations on the ocean side of the tide gate decreased to nearly 0 mg/l. Bottom water ammonia concentrations at this location decreased to approximately 0.02 mg/l. This decrease is attributed to a decrease in particulate nitrogen deposition to the sediments and its subsequent decay and release as ammonium. Nitrate levels in the surface waters of Caño Martín Peña decreased by 0.05 mg/l. Dissolved organic nitrogen levels on the ocean side of the tide gate decreased to 0.05 mg/l while those

in Laguna San José were unchanged. Dissolved organic nitrogen levels in eastern Caño Martín Peña decreased, but concentrations on the western end increased as a result of the higher flows redistributing the un-sewered organic nitrogen loads. Total nitrogen daily fluxes from Laguna San José to Caño Martín Peña were 141 kg/day. Total daily imports of nitrogen from Canal Suárez were 2 kg/day.

Dissolved inorganic phosphorus levels in Caño Martín Peña decreased in Scenario 4. Levels on the ocean side of the tide gate increased in Canal Suárez in response to lower levels of algae. Higher levels of algae and increased dilution are probably the reason for the dissolved inorganic phosphorus decrease in Caño Martín Peña. Dissolved organic phosphorus levels indicated decreases in Caño Martín Peña with slight increases on the eastern side of Laguna San José. Concentrations on the ocean side of the tide gate were relatively unaffected. Daily phosphorus flux from Laguna San José to Caño Martín Peña were 32 kg/day. An average of 1 kg/day was imported from Canal Suárez to Laguna San José.

Dissolved oxygen levels increased in Scenario 4 in Caño Martín Peña as a result of the increased flushing of high dissolved oxygen concentration water from Laguna San José. Anoxic conditions that occurred in the bottom waters of western Caño Martín Peña were unaffected by the additional flushing. Dissolved oxygen levels on the ocean side of the tide gate decreased slightly as a result of decreased algal photosynthesis. Fecal coliform levels throughout most of the system remained unchanged except for Canal Suárez which saw a slight decrease as a result of loading from Laguna San José being cut off. Total solids levels decreased slightly in Caño Martín Peña as a result of additional flushing. Solids concentrations on the ocean side of the tide gate decreased slightly again because the source of the solids in Laguna San José had been cut off.

In summary, Scenario 4 tended to improve water quality conditions in Canal Suárez since it prevented the more polluted water from Laguna San José from entering. Any improvements seen in Caño Martín Peña appear to be due to increased flow through the canal resulting in an increased volume of receiving water for runoff.

Scenario 5a

In Scenario 5a the un-sewered loads were removed from Caño Martín Peña. These loads were not redirected any place but were simply removed from the model. A total of 400 kg/day of carbon, 100 kg/day of nitrogen, and 20 kg/day of phosphorus were removed. An additional reduction was made to the fecal coliform loading for the Martín Peña sub-basin to approximate the effect of removal of fecal coliform loading associated with these loads would have.

Scenario 5a was run using Scenario 1a hydrodynamics. Scenario 5a temperature and salinity were identical to those of 1a (see Figure 8-42).

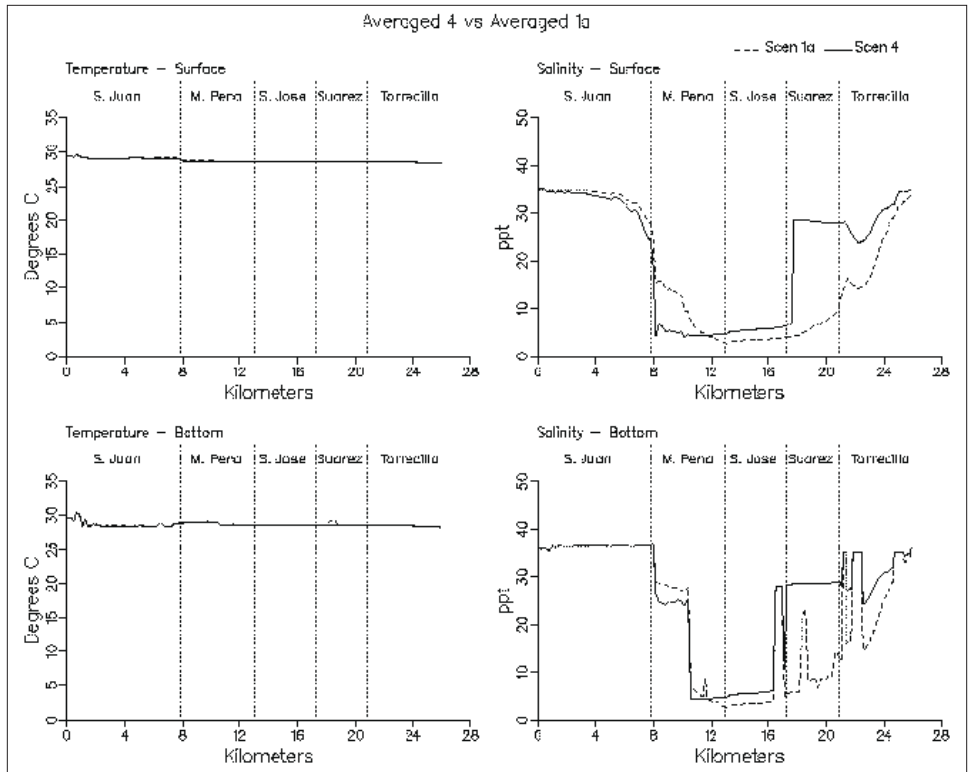


Figure 8-41. Simulation averaged transect plots comparing Scenario 4 with Scenario 1a (Sheet 1 of 11)

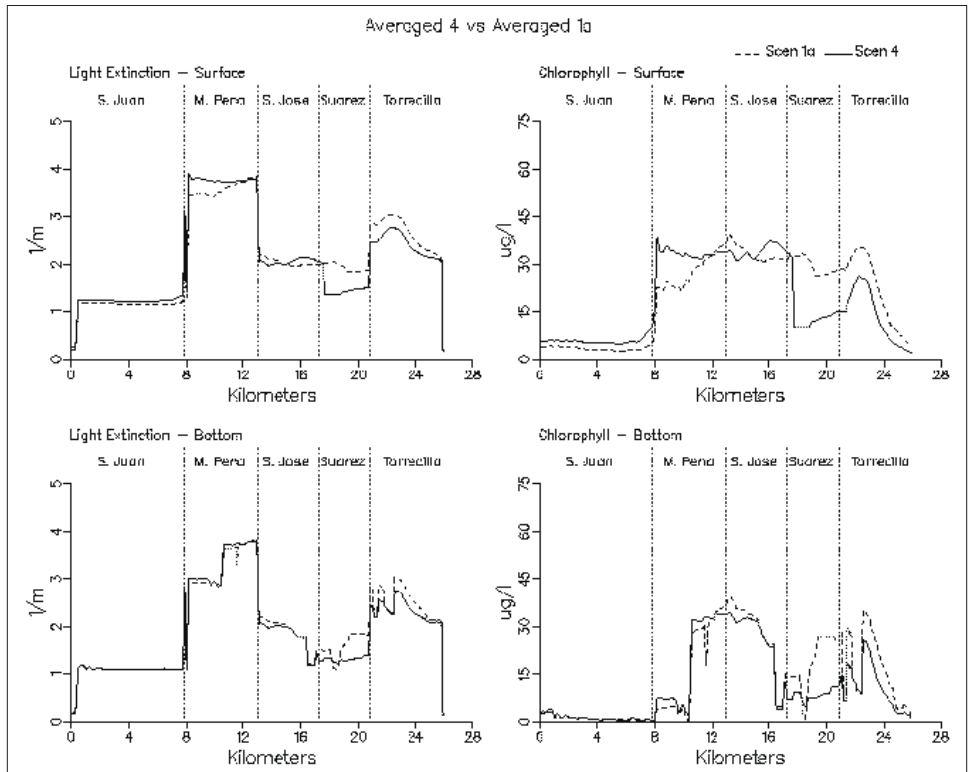


Figure 8-41. (Sheet 2 of 11)

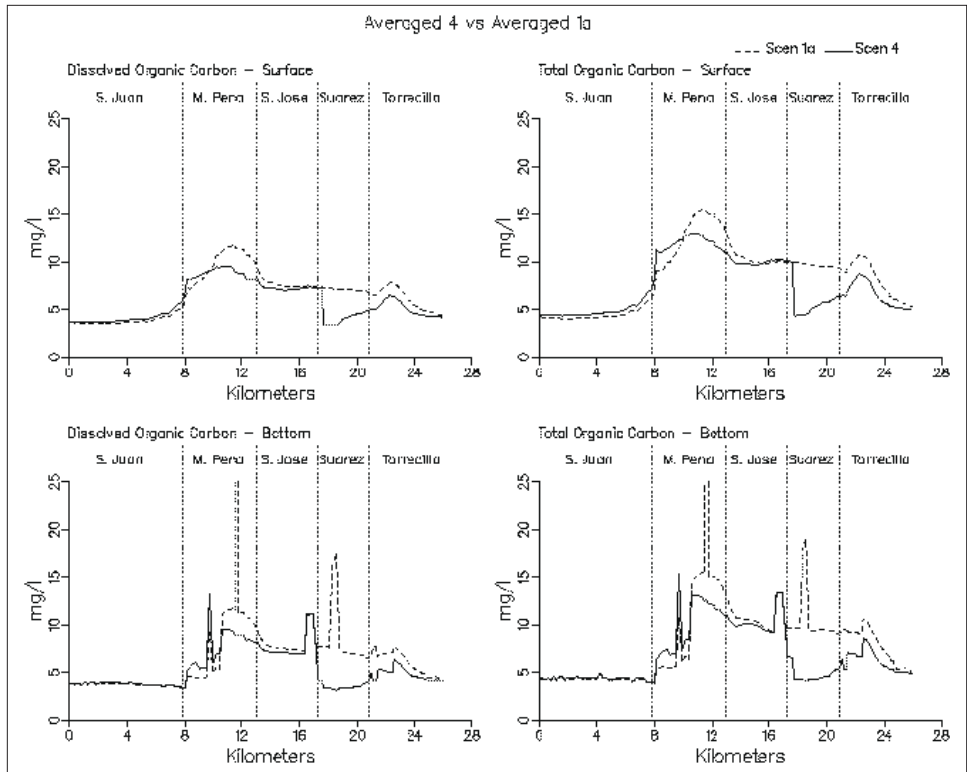


Figure 8-41. (Sheet 3 of 11)

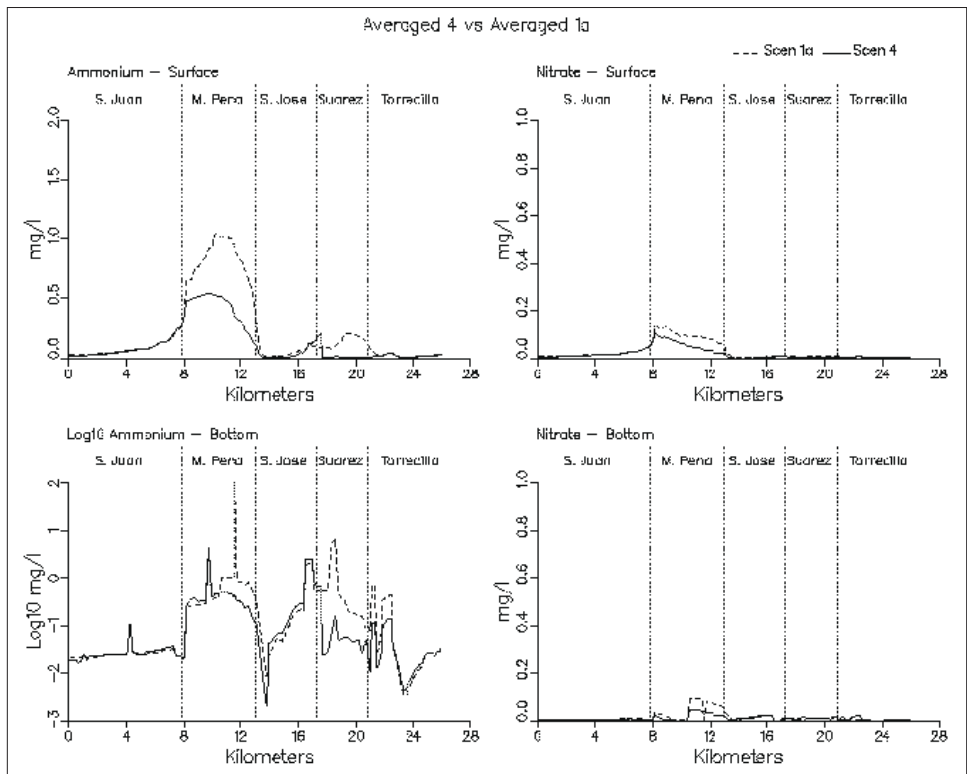


Figure 8-41. (Sheet 4 of 11)

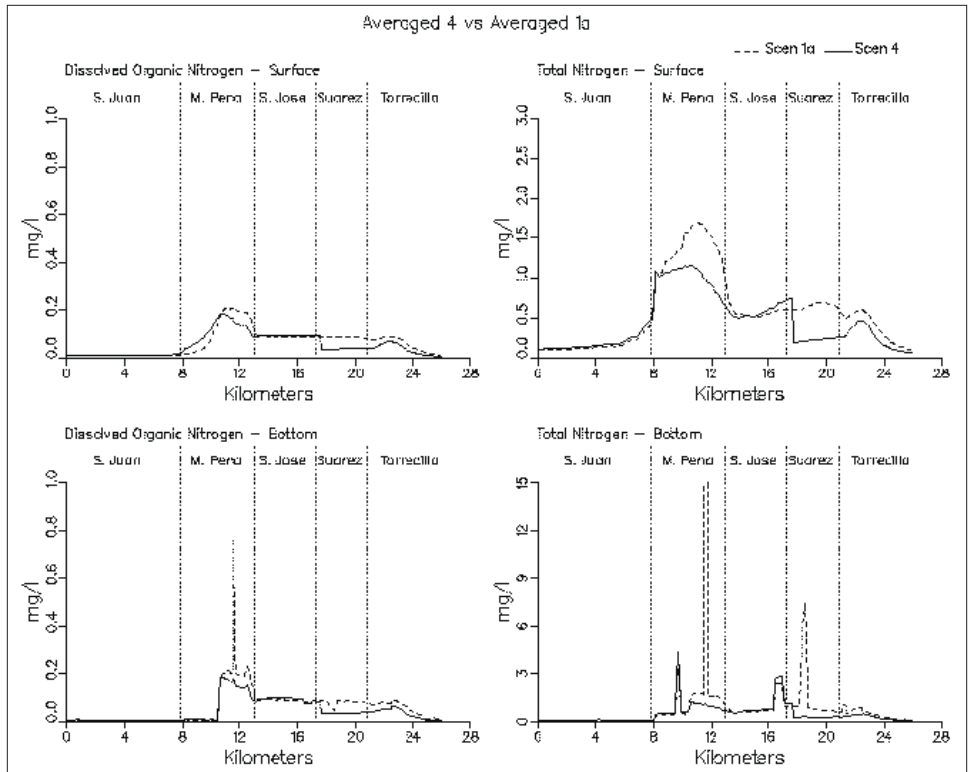


Figure 8-41. (Sheet 5 of 11)

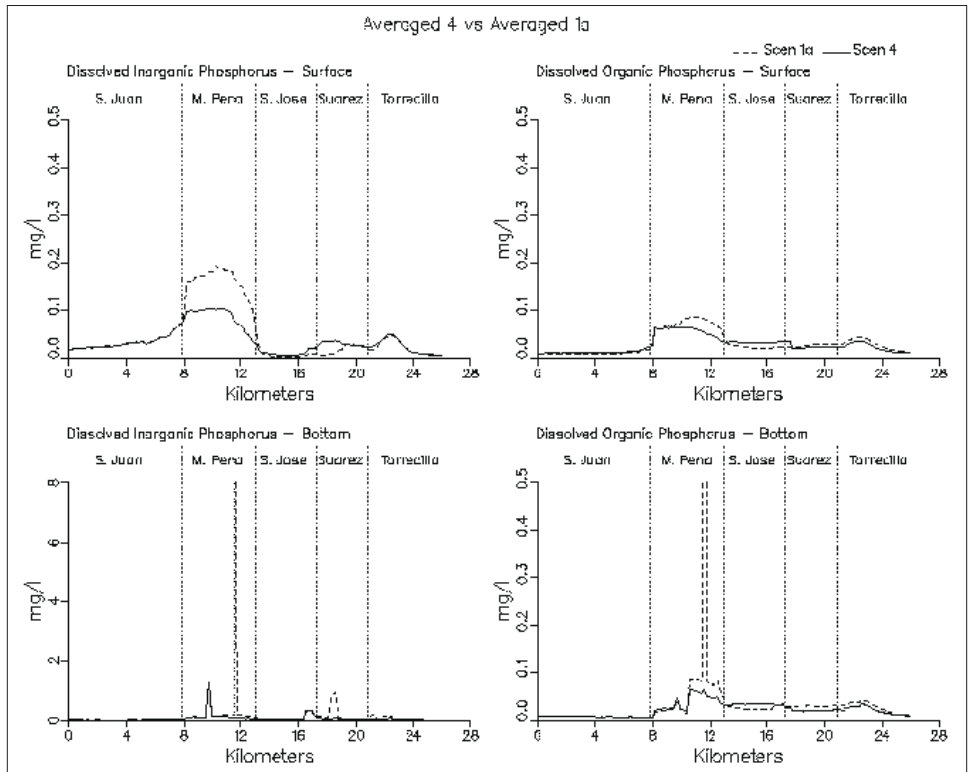


Figure 8-41. (Sheet 6 of 11)

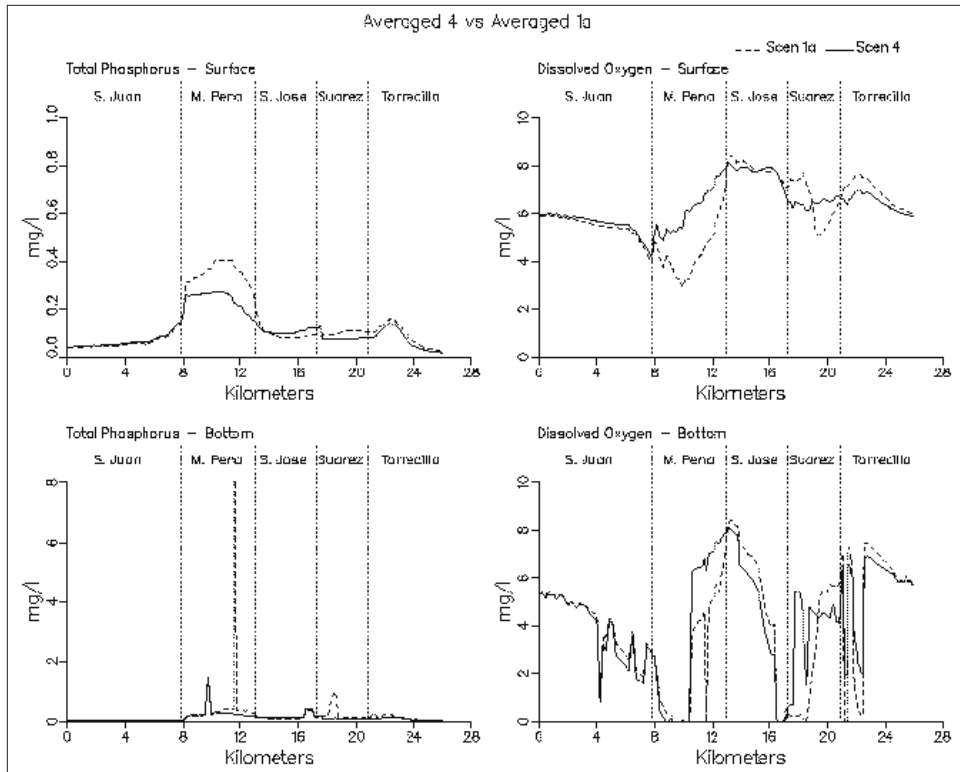


Figure 8-41. (Sheet 7 of 11)

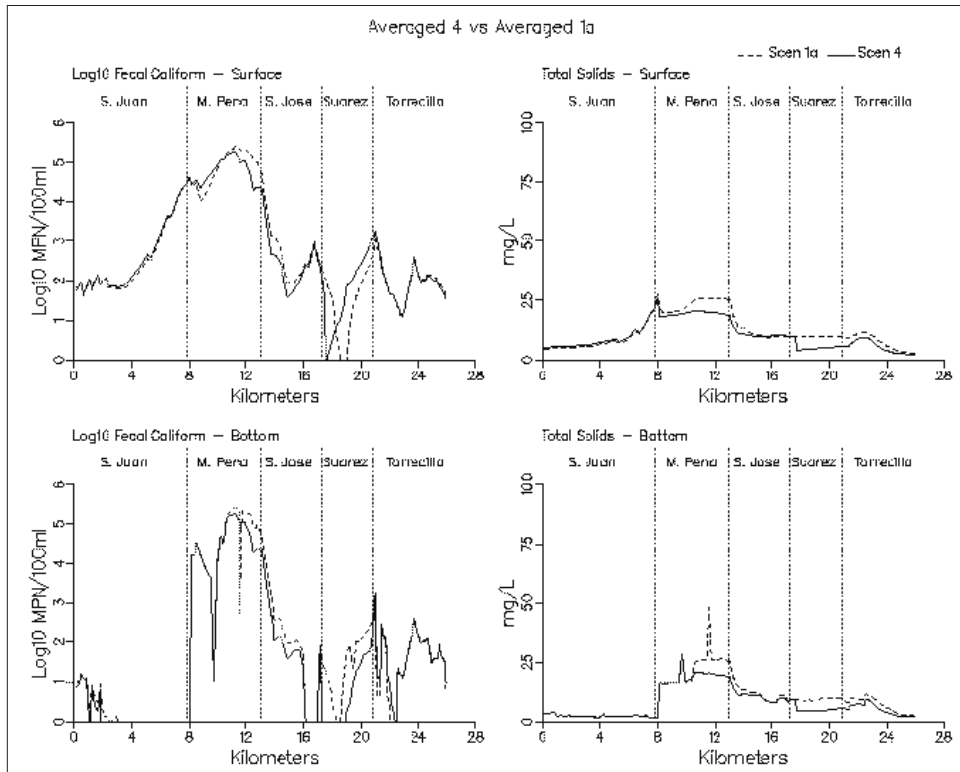


Figure 8-41. (Sheet 8 of 11)

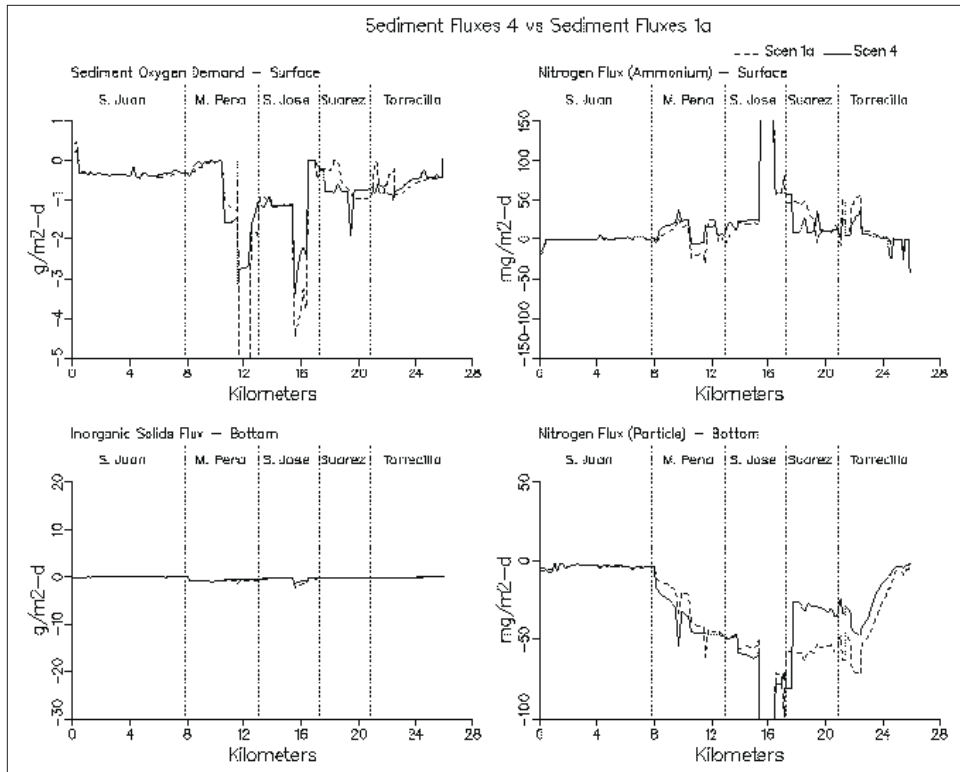


Figure 8-41. (Sheet 9 of 11)

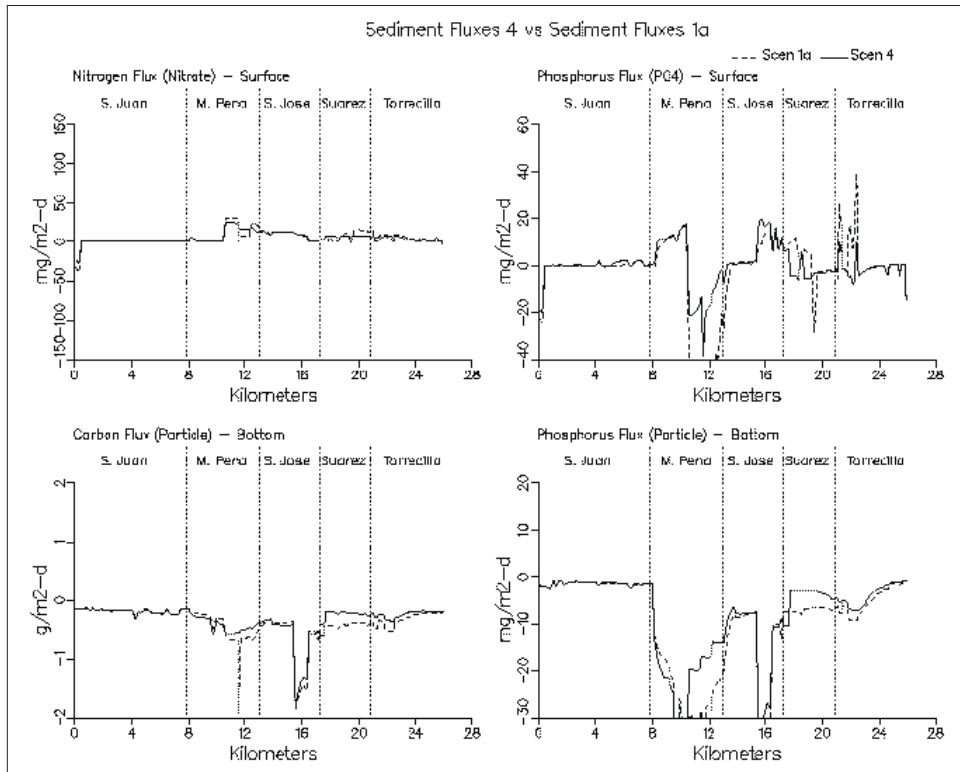


Figure 8-41. (Sheet 10 of 11)

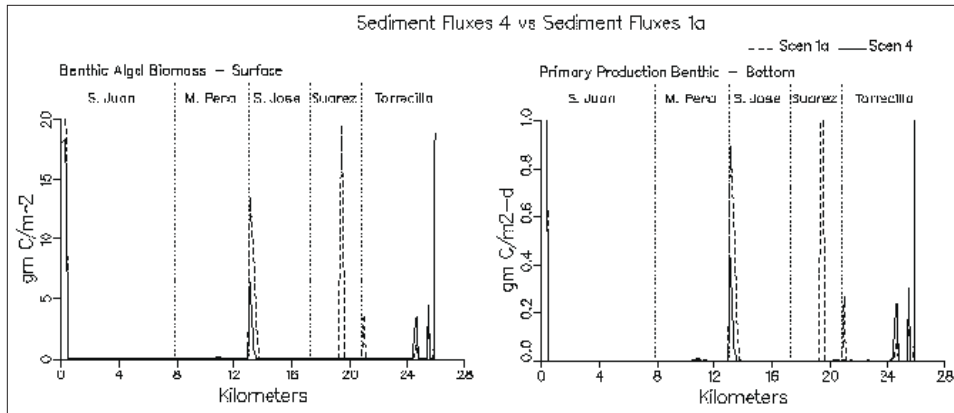


Figure 8-41. (Sheet 11 of 11)

Chlorophyll levels decreased slightly in Caño Martín Peña, Laguna San José, and Canal Suárez. The amount of the decrease was a maximum of 4 $\mu\text{g/l}$. Dissolved organic carbon levels decreased by 3 mg/l in Caño Martín Peña. Total carbon levels in Caño Martín Peña decreased by 4 mg/l. There was a slight decrease in DOC and TOC in Laguna San José and Canal Suárez.

Ammonium levels in Caño Martín Peña decreased from a maximum of 1.0 mg/l to 0.4 mg/l. No changes occurred elsewhere along the transect. Nitrate levels also decreased in Caño Martín Peña in response to the loading reduction. Dissolved organic nitrogen levels decreased significantly in Caño Martín Peña with the removal of the un-sewered loads. Surface total nitrogen levels decreased by nearly 1 mg/l in Caño Martín Peña. Concentrations at this location are still the highest along the transect.

Removal of the un-sewered loads resulted in a decrease in dissolved inorganic phosphorus levels in Caño Martín Peña of 0.1 mg/l, while dissolved organic phosphorus levels decreased to Laguna San José levels. No other significant change occurred in phosphorus concentrations elsewhere along the transect.

The DO transect indicates a slight improvement (0.3 mg/l) in Caño Martín Peña. No other changes were observed. Fecal coliform levels showed some decrease in Caño Martín Peña. Effects did not extend beyond the confluence of Caño Martín Peña and San Juan Bay. A slight increase in total solids resulting from a decrease in algae occurred in Caño Martín Peña.

In summary, impacts resulting from Scenario 5a conditions were confined for the most part to Caño Martín Peña. Other than in Caño Martín Peña, these effects were insignificant.

Scenario 5b

Scenario 5b like 5a involved a loading reduction. In this scenario, the loading reduction was the removal of loads originating from the Baldeorioty de Castro storm water pumping station. Upper Laguna San José serves as the receiving waters for this load. An average loading of 906 kg/day of carbon, 79.2 kg/day of nitrogen, and 27.2 kg/day of phosphorus was removed. All other conditions and loads were the same as those used in Scenario 1a. The pumping discharges remained without the loads.

Salinity and temperature were identical in Scenario 5b to those of 1a (see Figure 8-43). Chlorophyll levels decreased by a maximum of approximately 8 µg/l in Laguna San José and Canal Suárez. Smaller decreases were predicted in Caño Martín Peña.

Dissolved organic carbon levels decreased approximately 2 mg/l in Laguna San José and Canal Suárez. Total organic carbon levels indicated a similar decrease. Carbon fluxes from Laguna San José to Caño Martín Peña were 369 kg/day. Carbon fluxes from Laguna San José to Canal Suárez were 1240 kg/day.

Neither ammonium nor nitrate discharges indicated any change along the transect in Scenario 5b when compared with Scenario 1a. Any ammonium discharged by the pump station is rapidly taken up and doesn't remain in the system long enough to influence ammonium concentrations along the transect. Dissolved organic nitrogen levels decreased slightly in response to lower chlorophyll levels in Laguna San José and Canal Suárez. Nitrogen flux rates from Laguna San José to Caño Martín Peña averaged 10.2 kg/day. Nitrogen flux rates from Laguna San José to Canal Suárez averaged 109.9 kg/day.

The only change in phosphorus levels along the transect in Scenario 5b occurred as a result of decreased algae levels. Dissolved inorganic phosphorus levels in Scenario 5b were unchanged from 1a. Dissolved organic phosphorus levels showed only the slightest decrease in Laguna San José. Phosphorus flux rates from Laguna San José to Caño Martín Peña averaged 1 kg/day. Phosphorus flux rates from Laguna San José to Canal Suárez averaged 15.5 kg/day.

Dissolved oxygen, fecal coliform, and total solids levels along the transect were relatively unaffected by the loading reductions of Scenario 5b.

In summary, the effects of the loading reduction of Scenario 5b were limited to a great extent to Laguna San José. The reduction in nutrients resulted in a decrease in algae which did affect organic carbon levels in Caño Martín Peña and Canal Suárez. Nitrogen levels were affected slightly in Laguna San José and Canal Suárez. Substantial impacts in nutrients were not observed along the transect since this loading reduction

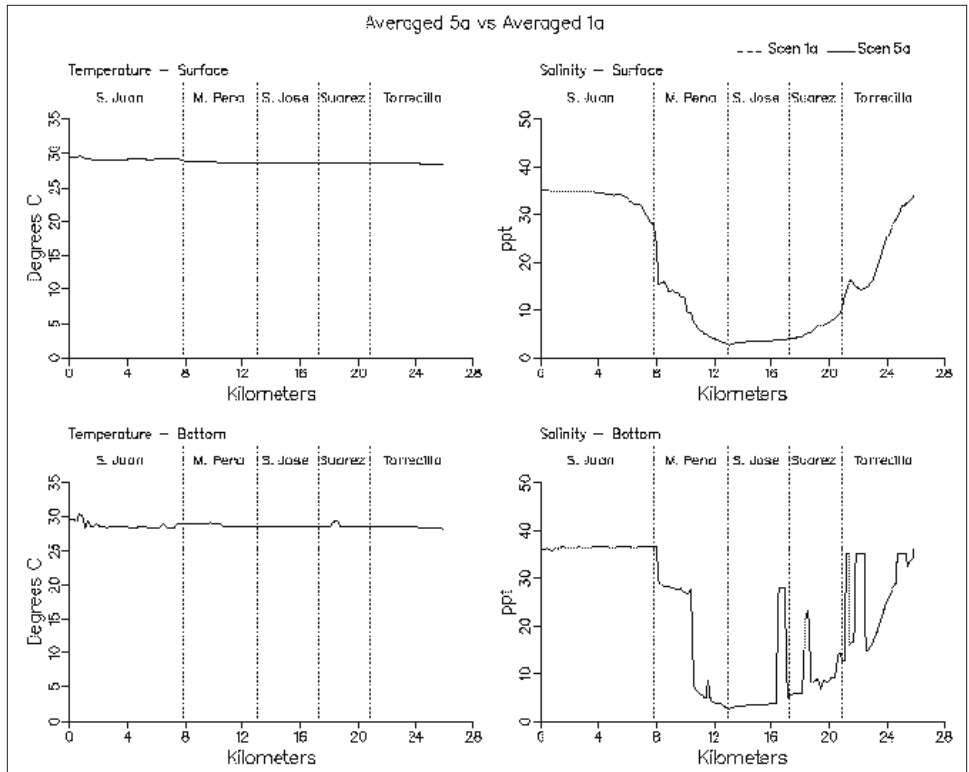


Figure 8-42. Simulation averaged transect plots comparing Scenario 5a with Scenario 1a (Sheet 1 of 11)

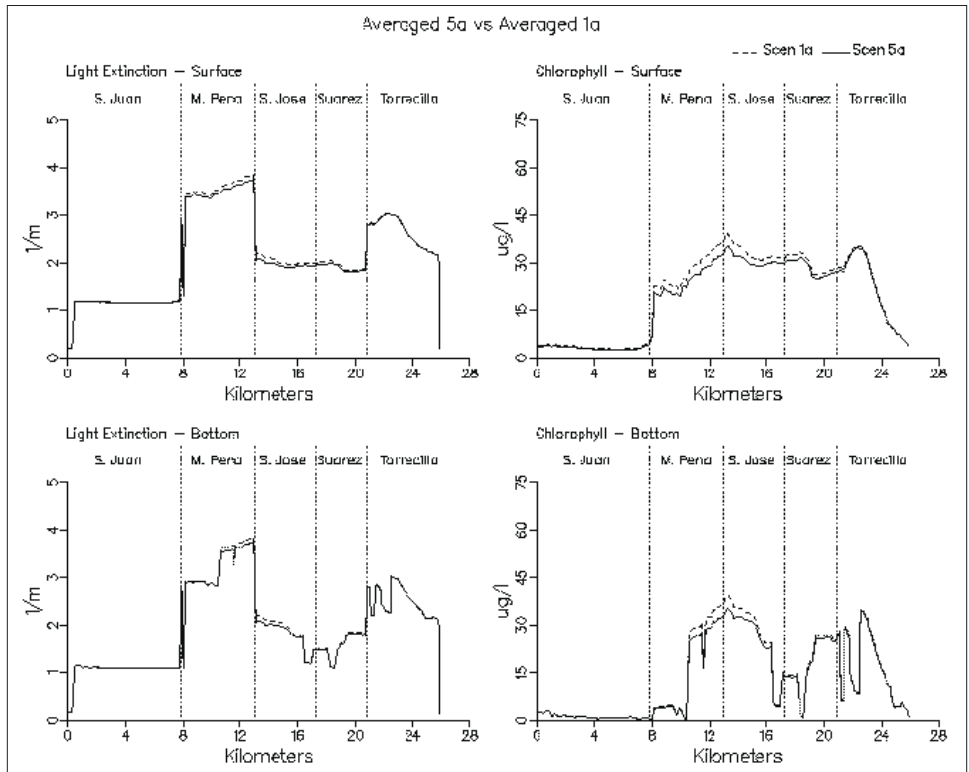


Figure 8-42. (Sheet 2 of 11)

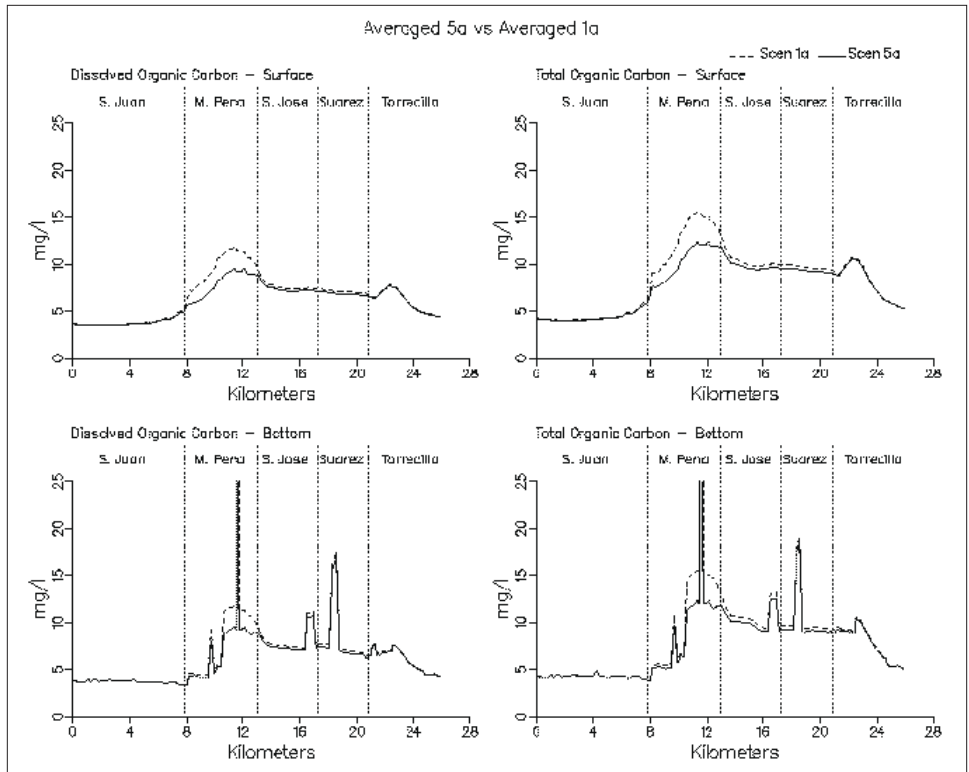


Figure 8-42. (Sheet 3 of 11)

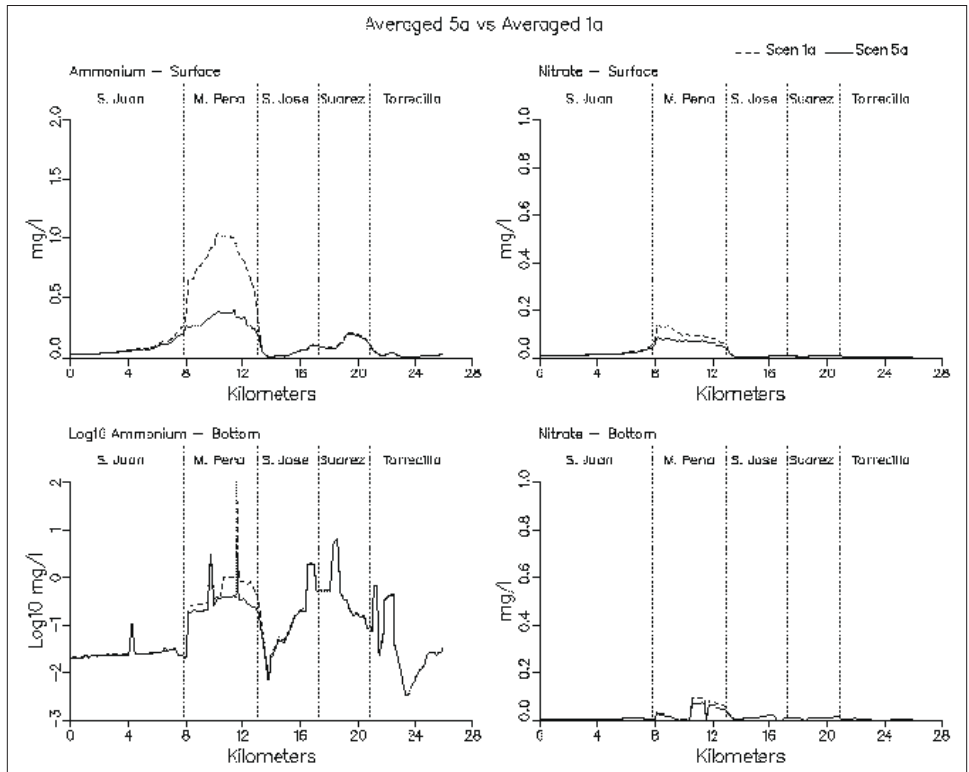


Figure 8-42. (Sheet 4 of 11)

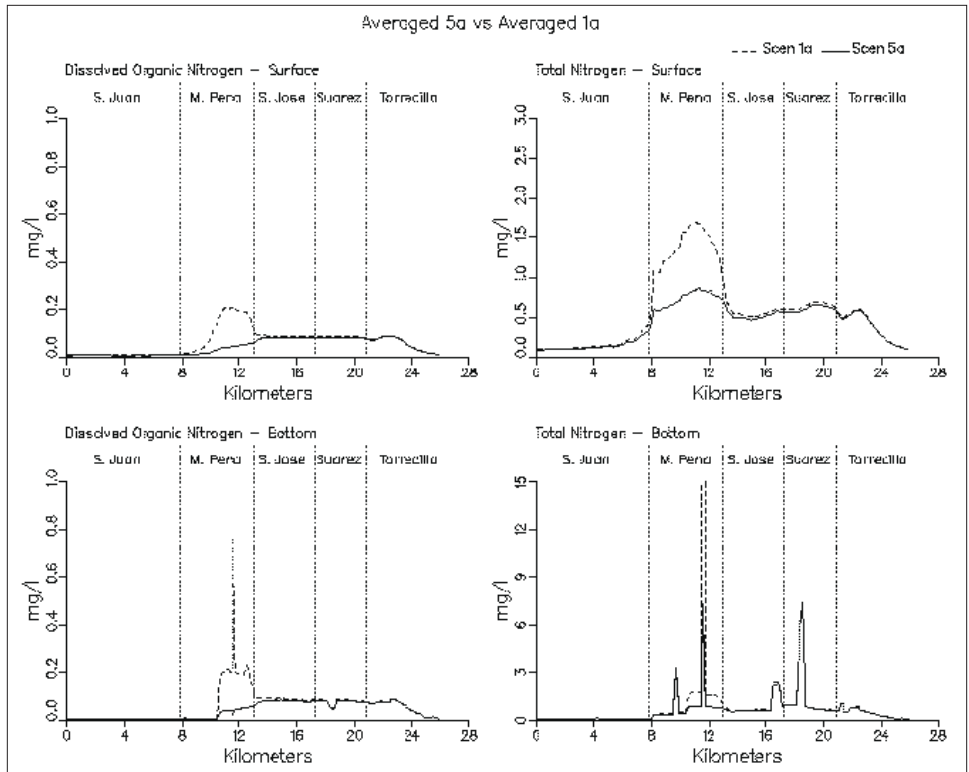


Figure 8-42. (Sheet 5 of 11)

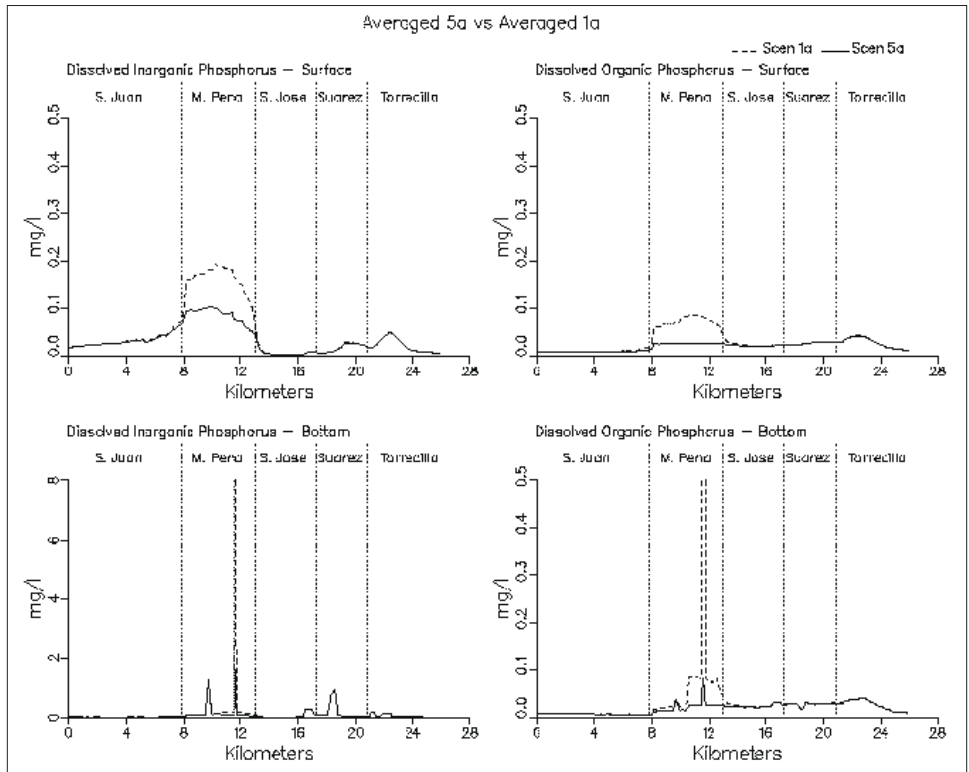


Figure 8-42. (Sheet 6 of 11)

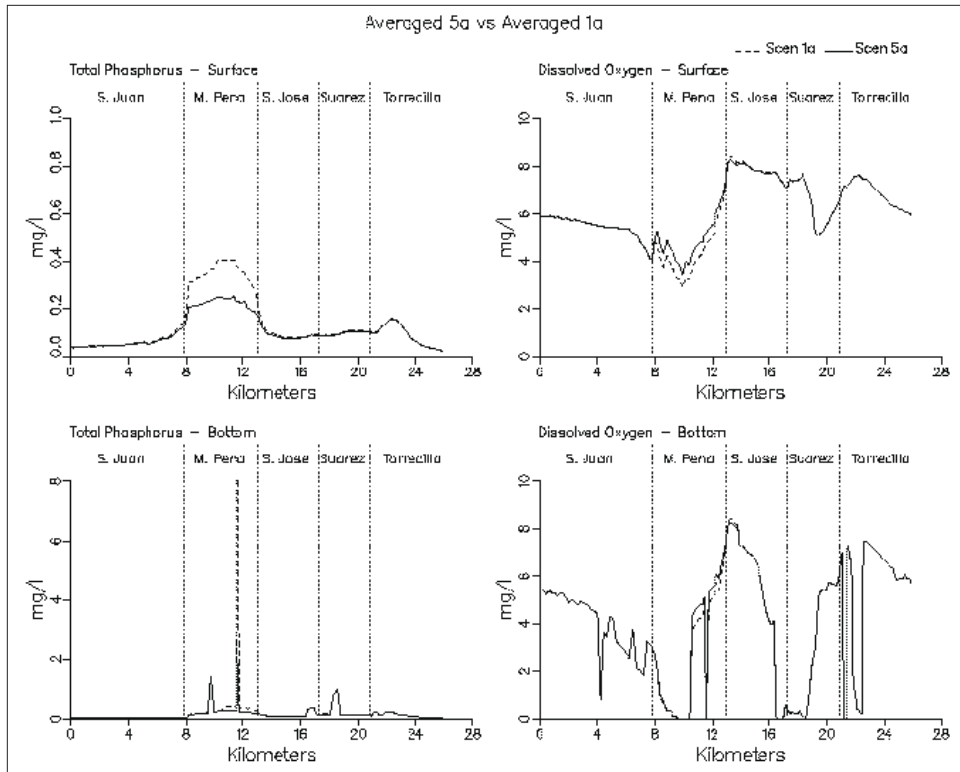


Figure 8-42. (Sheet 7 of 11)

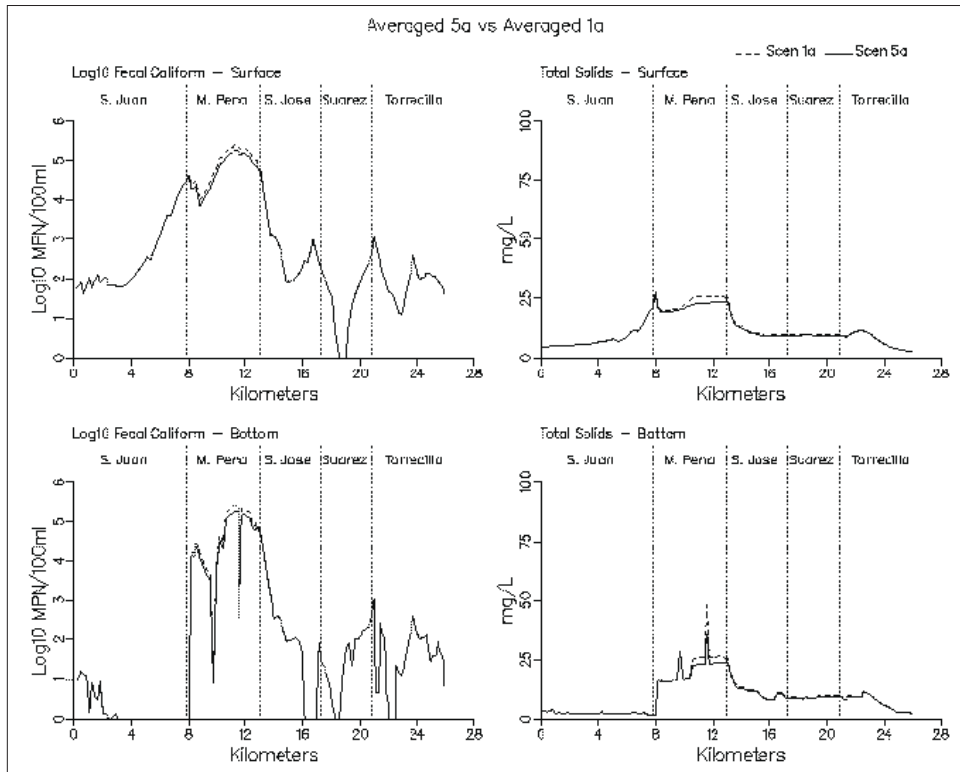


Figure 8-42. (Sheet 8 of 11)

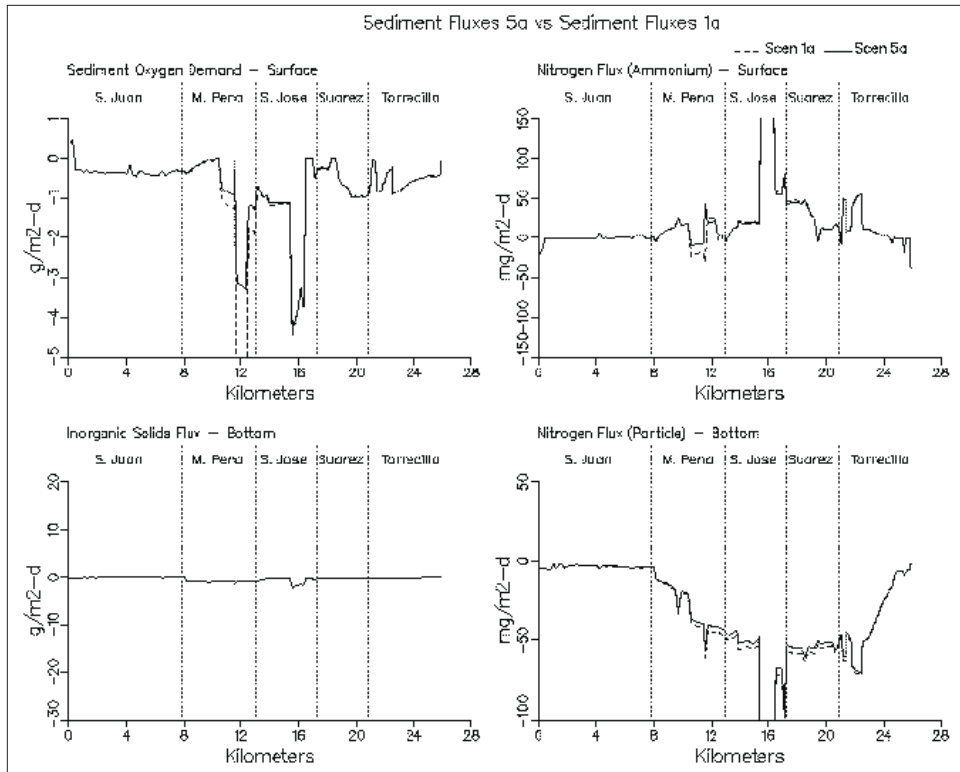


Figure 8-42. (Sheet 9 of 11)

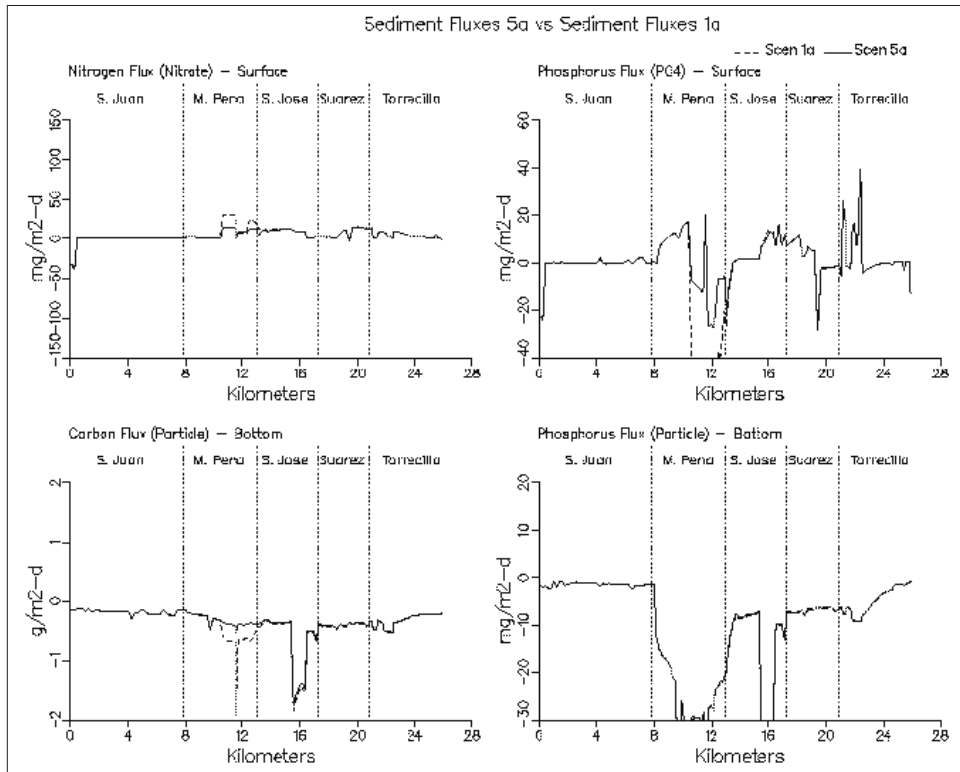


Figure 8-42. (Sheet 10 of 11)

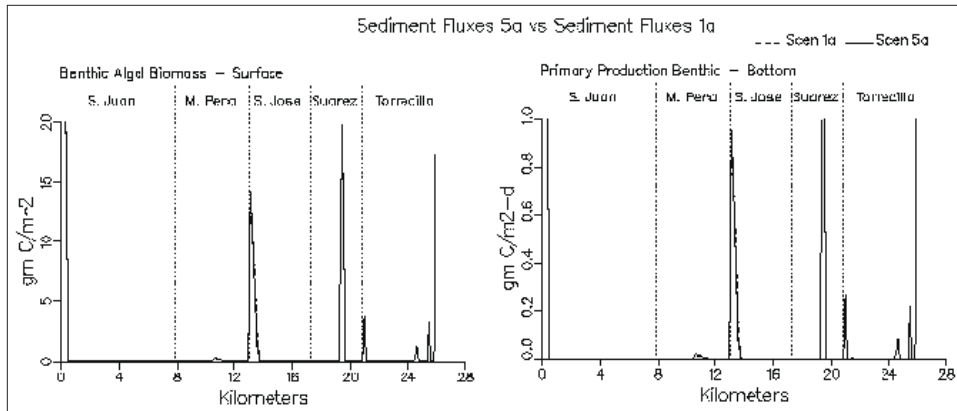


Figure 8-42. (Sheet 11 of 11)

is relatively far from the transect. Changes in nutrients loadings are rapidly compensated by algal uptake near the point of discharge.

Scenario 6a

Scenario 6a combined the loading reductions of Scenarios 5a and 5b with the channel modification to Caño Martín Peña of Scenario 1c. Since the loading reductions of 5a and 5b did not require the grid to be reconfigured, the grid and hydrodynamic data for Scenario 1c could be used for Scenario 6a. In essence, Scenario 6a is a repeat of Scenario 1c with loading reductions in Laguna San José and Caño Martín Peña.

As expected, temperature and salinity transects for Scenario 6a (see Figure 8-44) were identical to results for Scenario 1c. Chlorophyll levels for Scenario 6a are lower than those of Scenario 1a for all of the transect except San Juan Bay where levels increased by 3 $\mu\text{g/l}$. Chlorophyll levels in Laguna San José are typically 15 $\mu\text{g/l}$ lower than those of Scenario 1a with the greatest decrease occurring at the confluence of Caño Martín Peña and Laguna San José. At this location, chlorophyll levels were approximately 23 $\mu\text{g/l}$ lower in Scenario 6a than in Scenario 1a. Surface chlorophyll levels in Scenario 6a were lower than those predicted in Scenario 1c. The average surface chlorophyll level in Laguna San José was approximately 7 $\mu\text{g/l}$ lower in Scenario 6a than that in Scenario 1c. Chlorophyll levels decreased in Caño Martín Peña by 2 $\mu\text{g/l}$ on the western end and as much as 5 $\mu\text{g/l}$ on the eastern end in Scenario 6a when compared to results from Scenario 1c. A decrease of 6 $\mu\text{g/l}$ of chlorophyll occurred in western Canal Suárez in Scenario 6a when compared to Scenario 1c. The decreases in chlorophyll observed between Scenarios 6a and 1c result from the removal of the un-sewered loads for Caño Martín Peña and the loads for the Baldeoroty de Castro Pump Station. Since neither one of these sources input a chlorophyll load, the decrease in chlorophyll levels observed is the result of a decrease in nutrients.

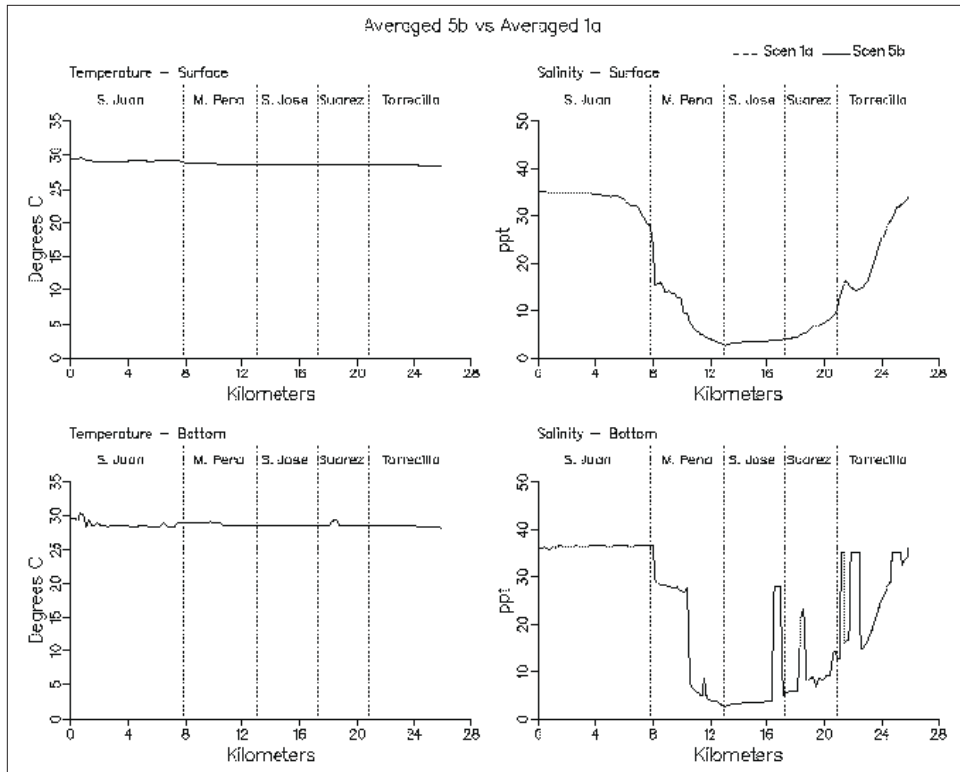


Figure 8-43. Simulation averaged transect plots comparing Scenario 5b with Scenario 1a (Sheet 1 of 11)

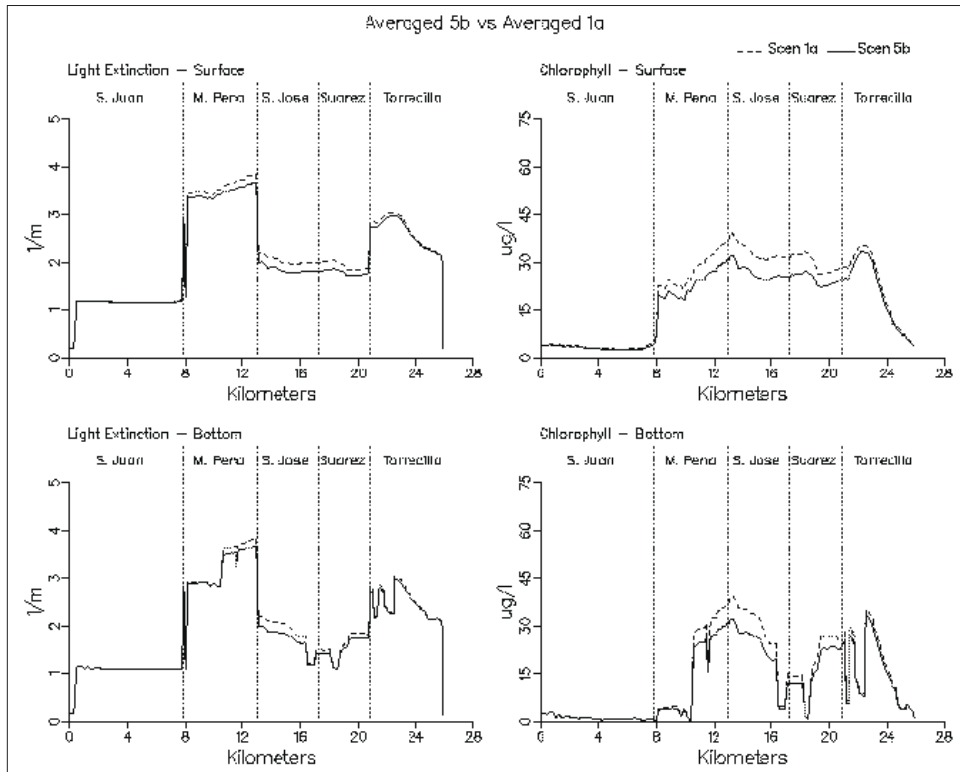


Figure 8-43. (Sheet 2 of 11)

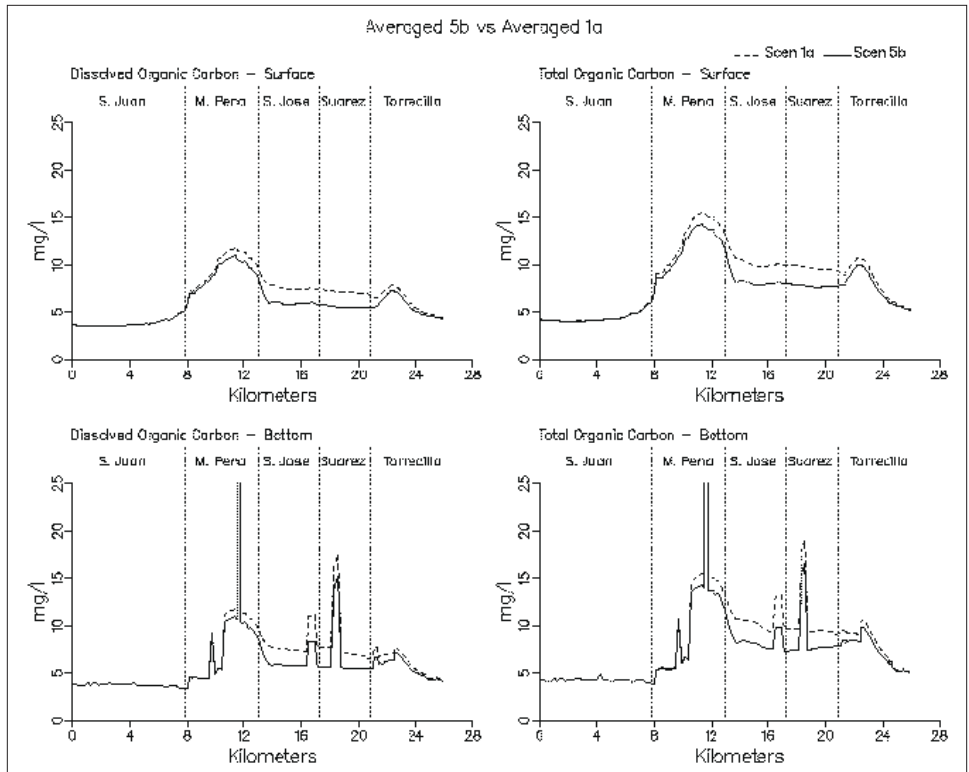


Figure 8-43. (Sheet 3 of 11)

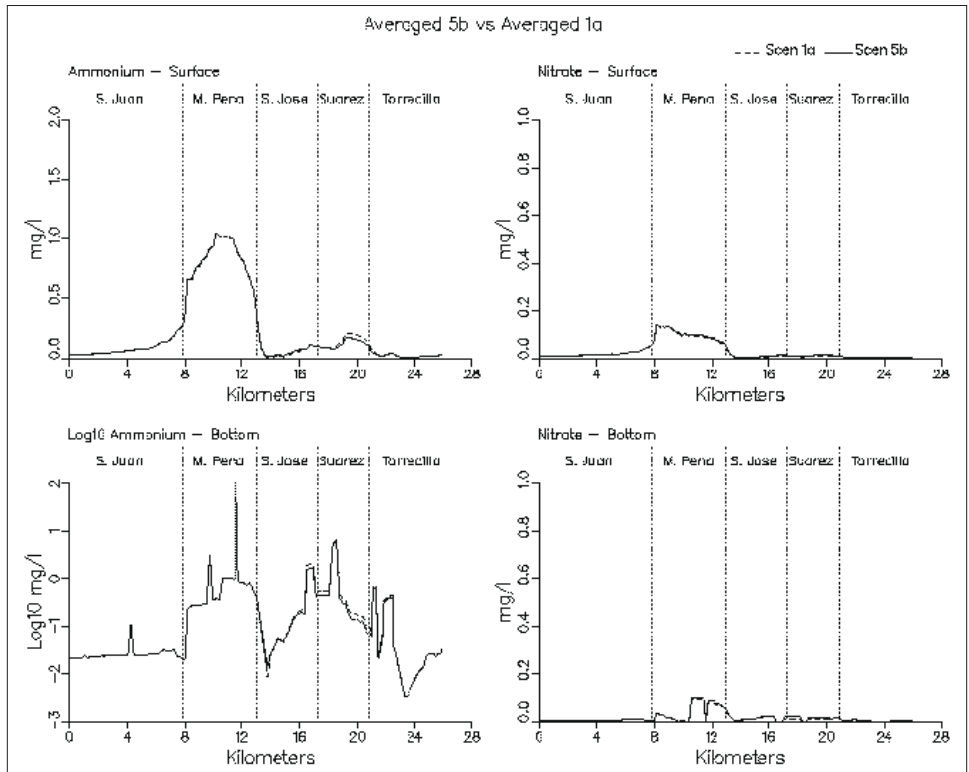


Figure 8-43. (Sheet 4 of 11)

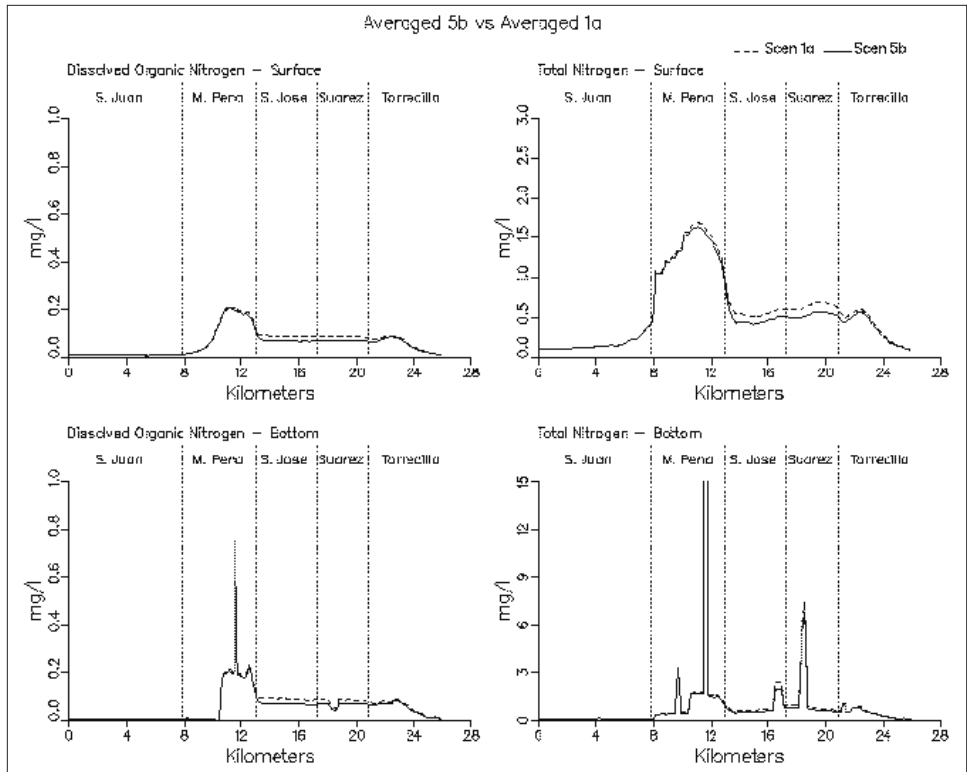


Figure 8-43. (Sheet 5 of 11)

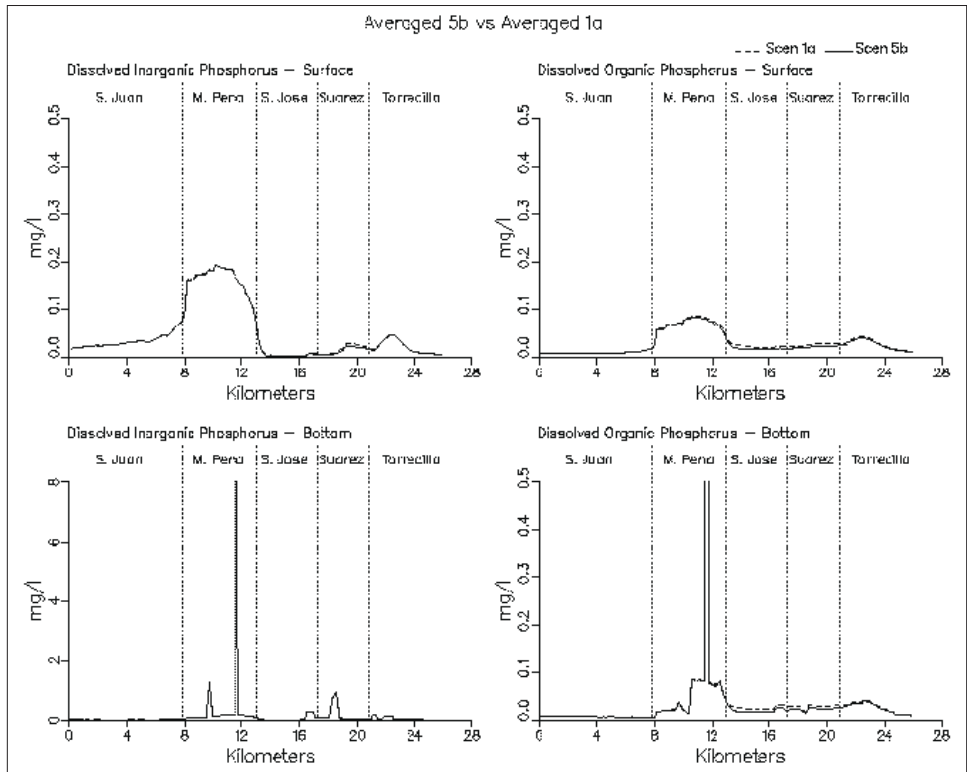


Figure 8-43. (Sheet 6 of 11)

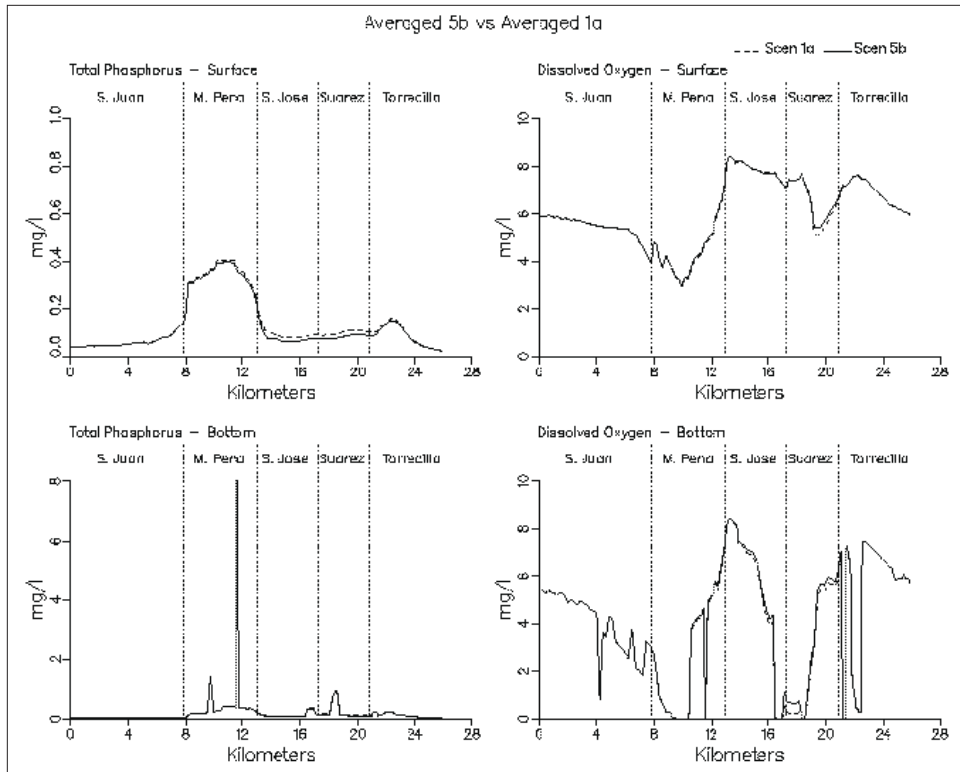


Figure 8-43. (Sheet 7 of 11)

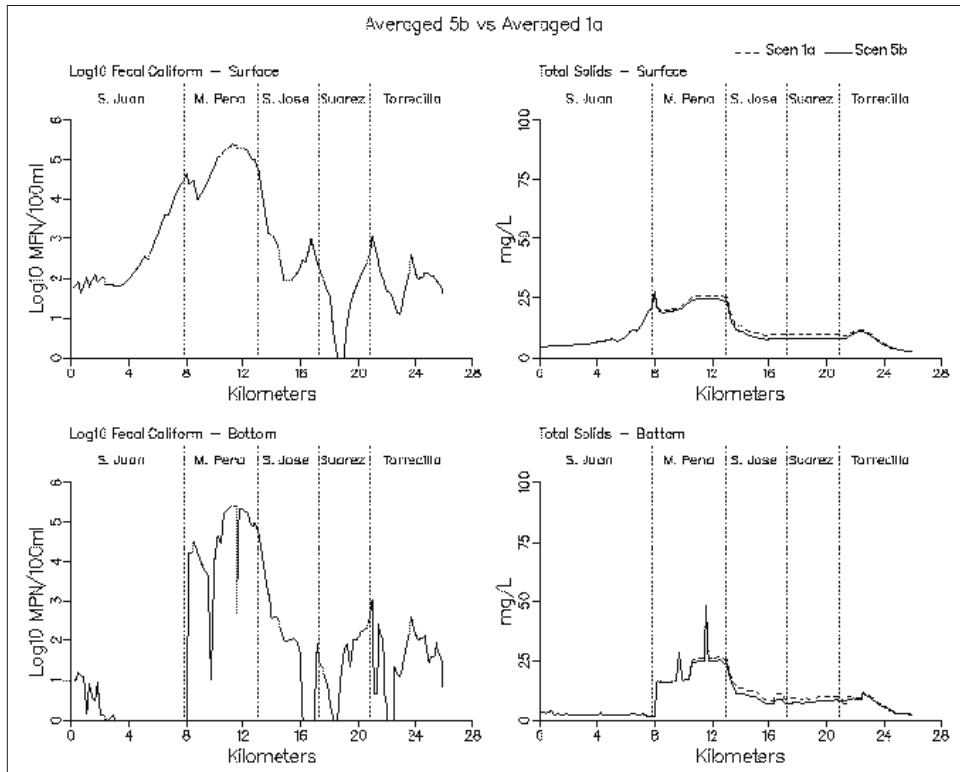


Figure 8-43. (Sheet 8 of 11)

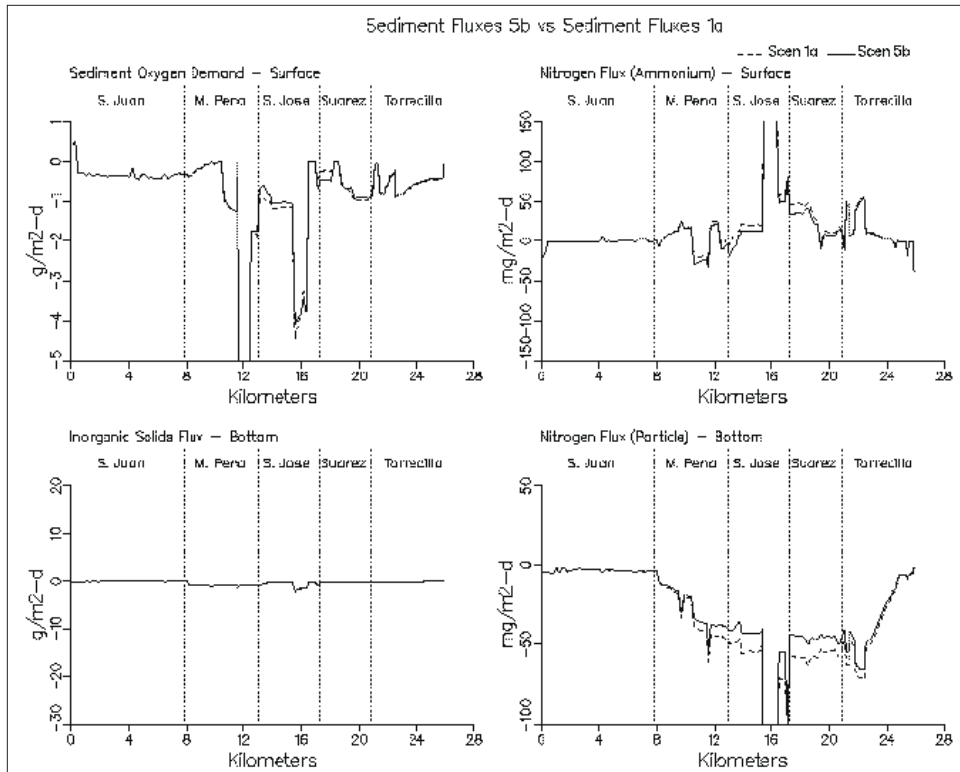


Figure 8-43. (Sheet 9 of 11)

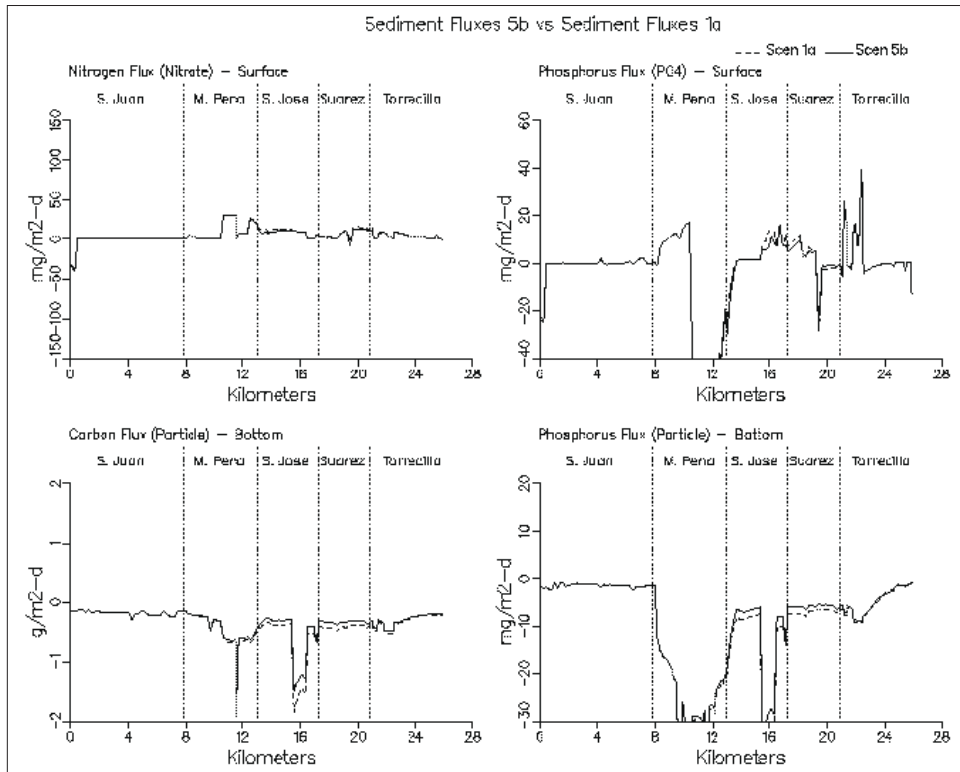


Figure 8-43. (Sheet 10 of 11)

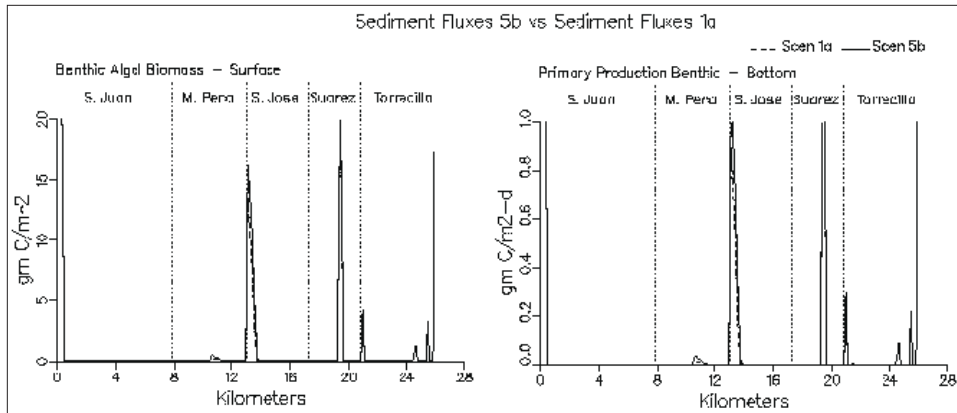


Figure 8-43. (Sheet 11 of 11)

Organic carbon concentrations decreased in Caño Martín Peña, Laguna San José, Canal Suárez, and Laguna La Torrecilla in Scenario 6a when compared to 1a. Dissolved organic carbon levels decreased by 8 mg/l in eastern Caño Martín Peña, 4 mg/l in Laguna San José, 3 mg/l in Canal Suárez, and 1 mg/l in upper Laguna La Torrecilla. Similar decreases in total organic carbon levels occurred in Scenario 6a. Comparison of Scenario 6a results with those of 1c indicates that dissolved organic carbon levels decreased by 1 mg/l in Caño Martín Peña and 1.5 mg/l in Laguna San José. In Scenario 6a, Laguna San José exported 2558 kg/day of carbon to Caño Martín Peña and imported 174 kg/day from Canal Suárez.

Caño Martín Peña surface ammonium levels in Scenario 6a were much lower than those of 1a and slightly lower than those of 1c as a result of the removal of the un-sewered loadings. In Scenario 6a, the maximum ammonium concentration in Caño Martín Peña occurs in the western end and is the result of Rio Piedras inflows. Caño Martín Peña nitrate concentrations decreased in Scenario 6a by 0.1 mg/l in comparison to Scenario 1a levels but were identical to Scenario 1c levels. Dissolved organic nitrogen decreased in Caño Martín Peña, Laguna San José, Canal Suárez, and Laguna La Torrecilla in Scenario 6a. The greatest decrease occurred in eastern Caño Martín Peña. When compared to 1a results, dissolved organic nitrogen concentrations decreased 0.18 mg/l at this location in Scenario 6a. However, when compared to Scenario 1c, it is evident that most of this decrease is the result of the channelization of Caño Martín Peña as the dissolved organic nitrogen levels in Scenario 1c are only 0.02 mg/l higher than those of 6a. In Scenario 6a, Laguna San José dissolved organic nitrogen levels were half of what they had been in Scenario 1a. These levels were also 0.03 mg/l lower than they had been in Scenario 1c. Total nitrogen levels in Scenario 6a were significantly lower in Scenario 6a than in 1a as a result of the decreases in ammonium, dissolved organic nitrogen, and particulate organic nitrogen. In Scenario 6a, Laguna San José discharged 161 kg/day of nitrogen to Caño Martín Peña and imported 7 kg/day from Canal Suárez.

Scenario 6a phosphorus levels indicated large decreases in Caño Martín Peña when compared to results for Scenario 1a. Dissolved inorganic phosphorus levels decreased from as much as 0.2 mg/l in Caño Martín Peña in 1a to 0.04 mg/l in 6a. However, comparison of results from 1c to those of 6a indicates that this decrease results from the channelization of Caño Martín Peña and not from the removal of the un-sewered loads as the concentrations for dissolved inorganic phosphorus in Caño Martín Peña in Scenarios 1c and 6a are identical. Scenario 6a dissolved organic phosphorus levels and total phosphorus levels in Caño Martín Peña and Laguna San José also indicate decreases when compared to Scenario 1a. The largest decreases occur in Caño Martín Peña and are a result of both the channelization and loading reductions as dissolved organic phosphorus and total phosphorus levels are lower in Scenario 6a than in Scenario 1c. In Scenario 6a, Laguna San José exports 14.6 kg/day of phosphorus to Caño Martín Peña and imports 2.5 kg/day from Canal Suárez.

Dissolved oxygen levels in Scenario 6a increased significantly in Caño Martín Peña when compared to Scenario 1a results. Dissolved oxygen levels decreased in Laguna San José, Canal Suárez, and Laguna La Torrecilla as a result of lower algal photosynthesis. Both surface and bottom dissolved oxygen results from Scenario 6a are nearly identical to the results for Scenario 1c which indicates that, at least along the transect, the removal of the un-sewered loads and the storm water loads had less of an effect than channelization of Caño Martín Peña. It must be remembered that surface dissolved oxygen levels in Scenario 1c and 6a are relatively high and cannot go any higher without algal photosynthesis. Dissolved oxygen levels along the bottom of Laguna San José in Scenario 6a did increase slightly when compared to Scenario 1c indicating that the loading removal did have some effect.

Fecal coliform levels in Scenario 6a exhibited the same behavior as those of 1a except for Caño Martín Peña where levels were one order of magnitude lower. Total solids transects for Scenario 6a were lower than the results for Scenario 1a. Scenario 6a results exhibited the same pattern as the results of Scenario 1c but were slightly lower. The decrease in total solids that occurs between Scenarios 1c and 6a results from a decrease in the solids load at Baldeorioty de Castro Pump Station and the decrease in algae brought upon by lower nutrient levels.

In summary, the conditions simulated in Scenario 6a improved water quality throughout the interior portions of the system. Opening Caño Martín Peña established a clockwise circulation through the interior system which promotes flushing. The most significant feature that the loading reductions added was a decrease in chlorophyll levels in Laguna San José in turn decreasing levels in Canal Suárez and Caño Martín Peña. Decreases in algae levels in these bodies translated into decreases in organic carbon, nitrogen, phosphorus, and total solids.

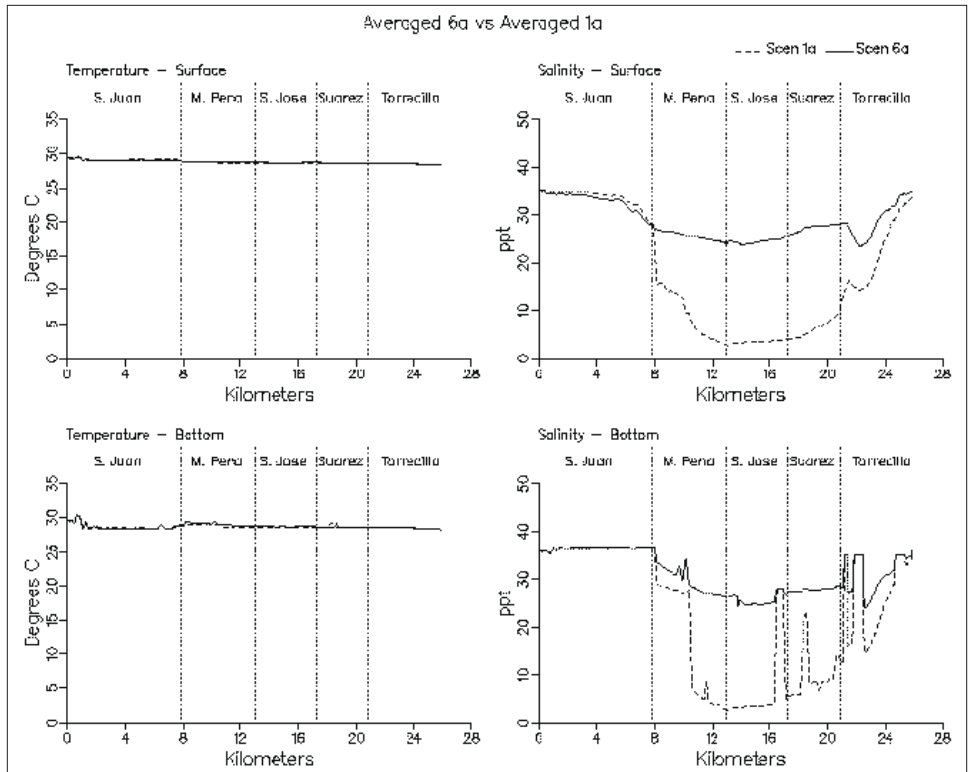


Figure 8-44. Simulation averaged transect plots comparing Scenario 6a with Scenario 1a (Sheet 1 of 11)

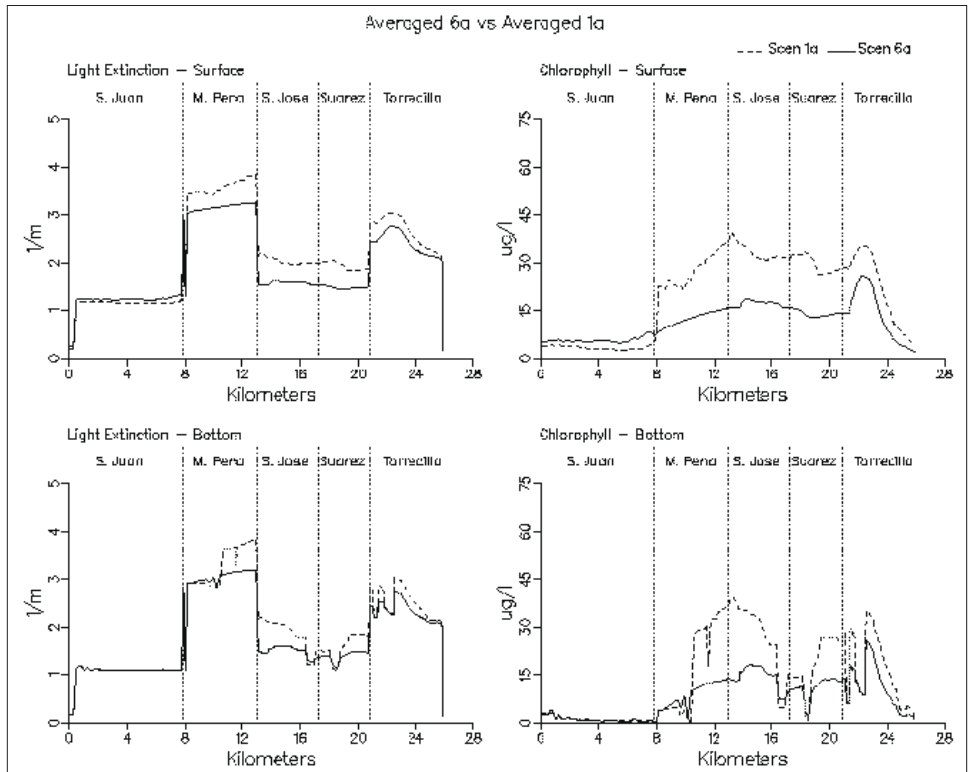


Figure 8-44. (Sheet 2 of 11)

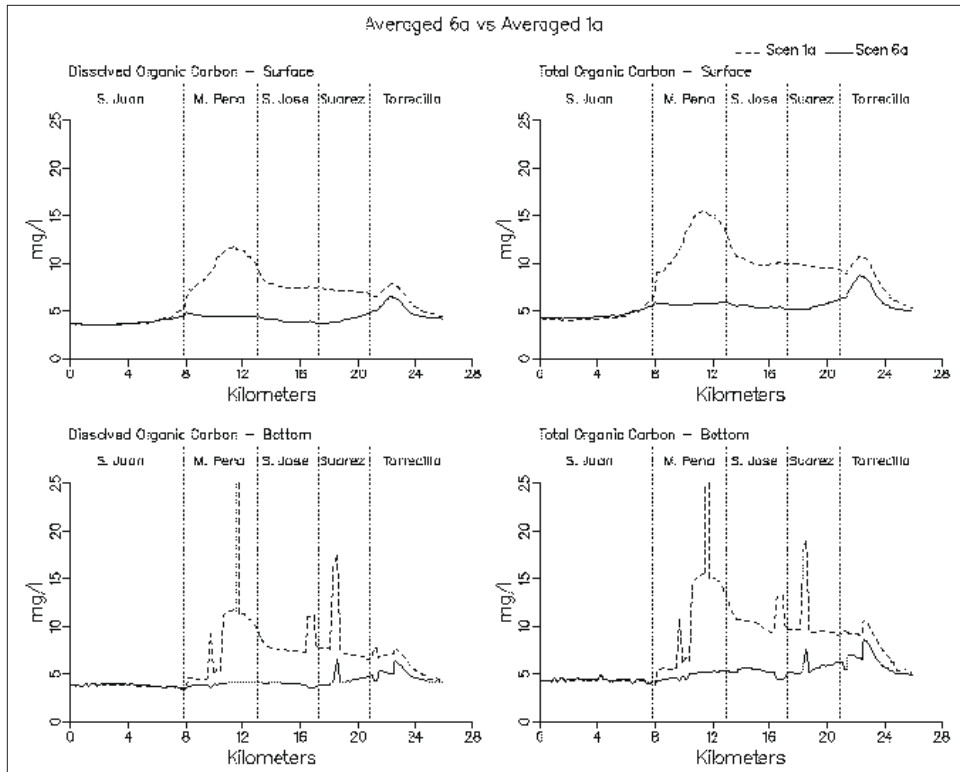


Figure 8-44. (Sheet 3 of 11)

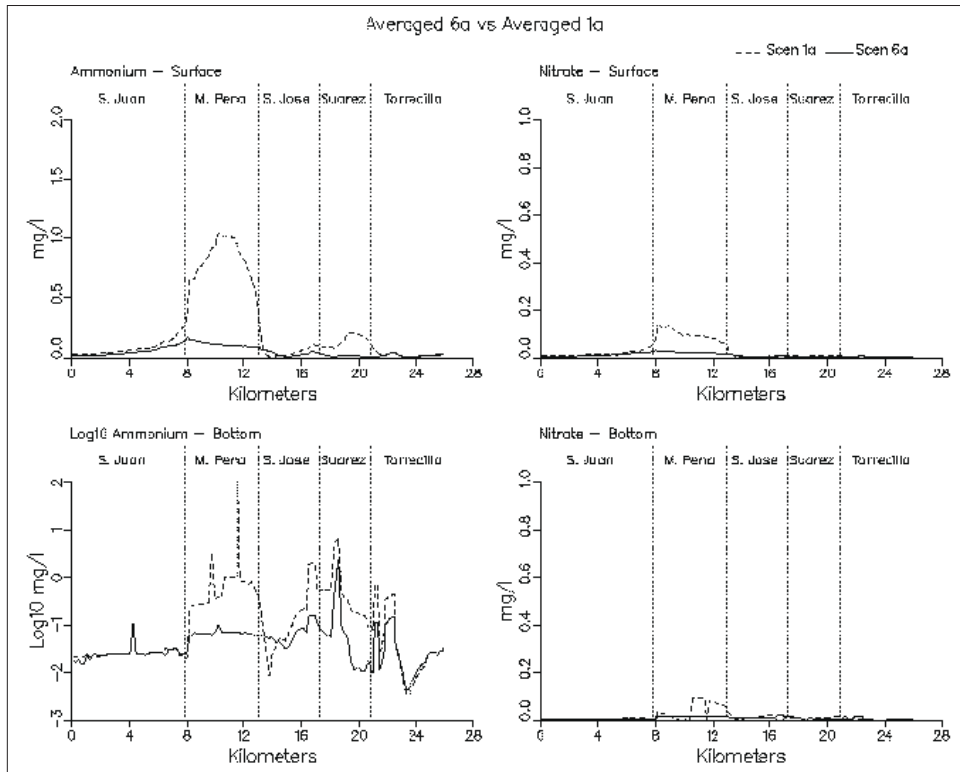


Figure 8-44. (Sheet 4 of 11)

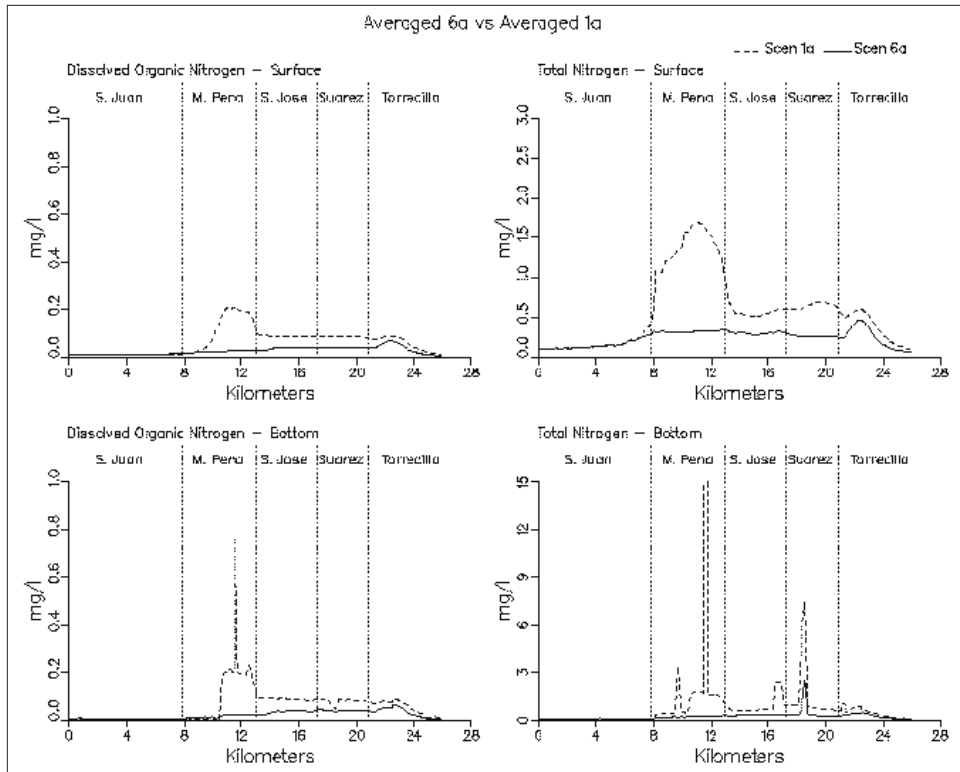


Figure 8-44. (Sheet 5 of 11)

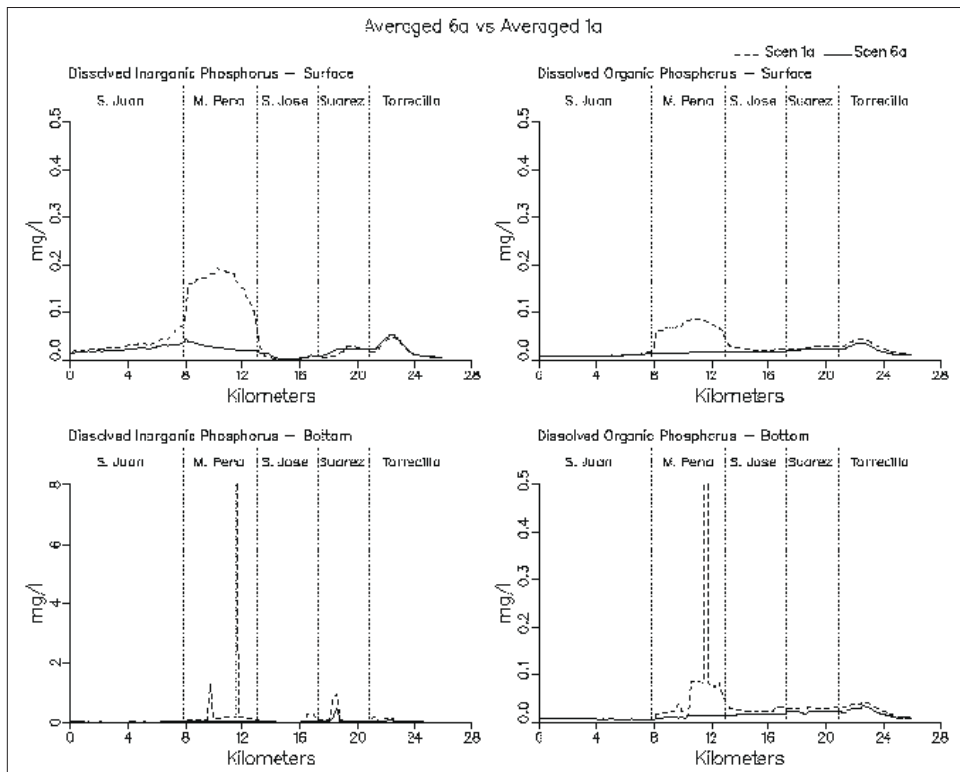


Figure 8-44. (Sheet 6 of 11)

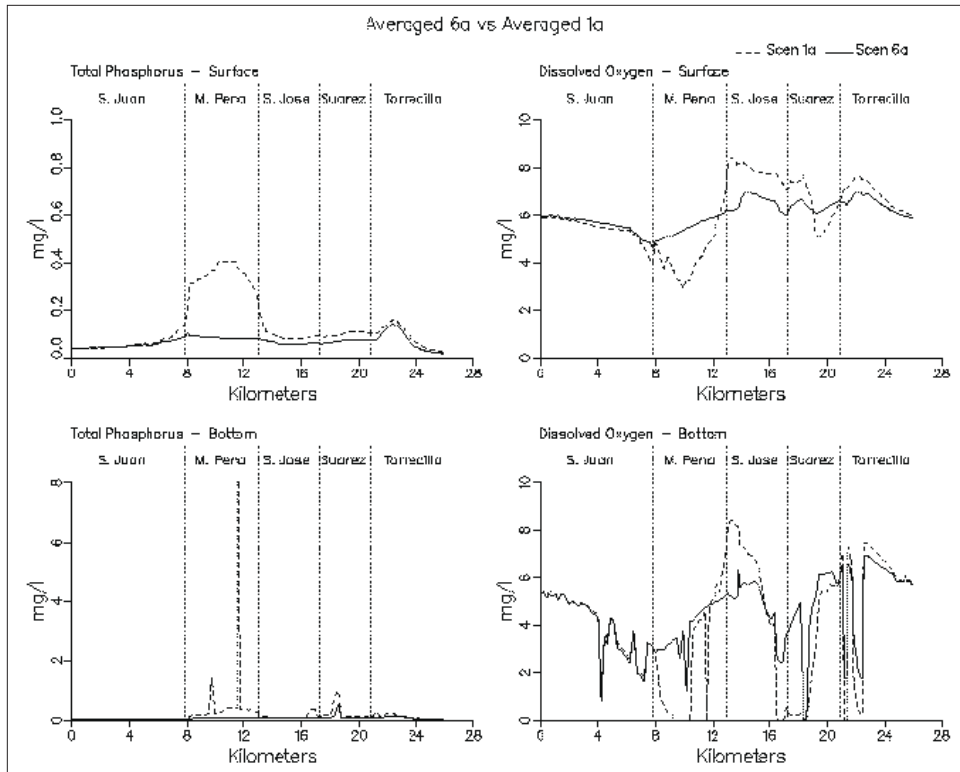


Figure 8-44. (Sheet 7 of 11)

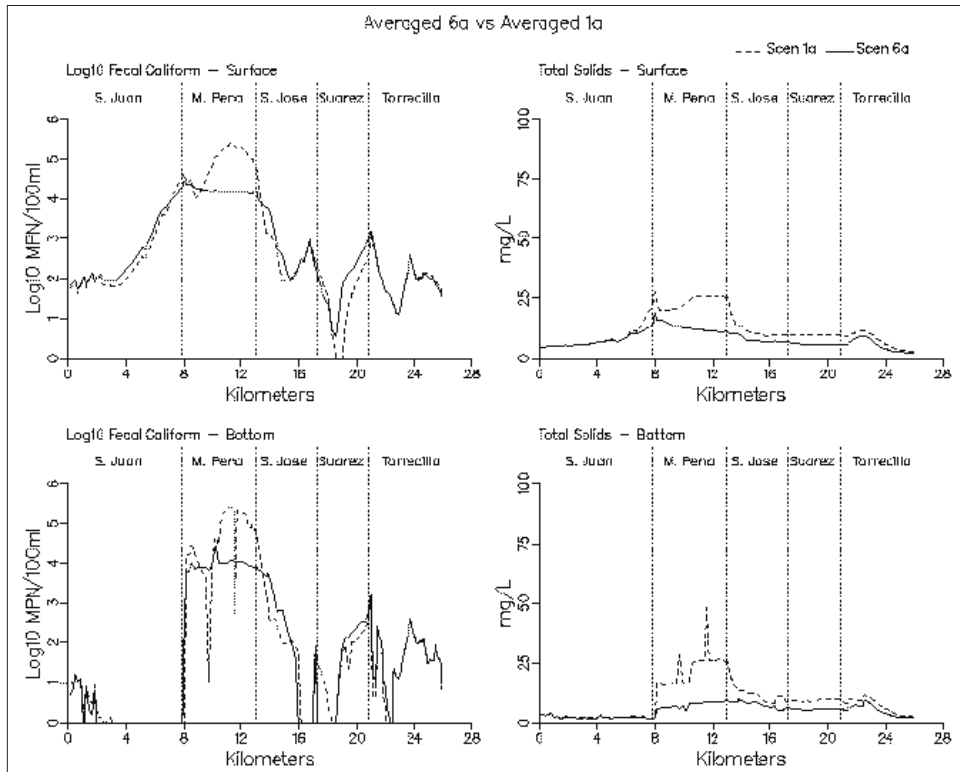


Figure 8-44. (Sheet 8 of 11)

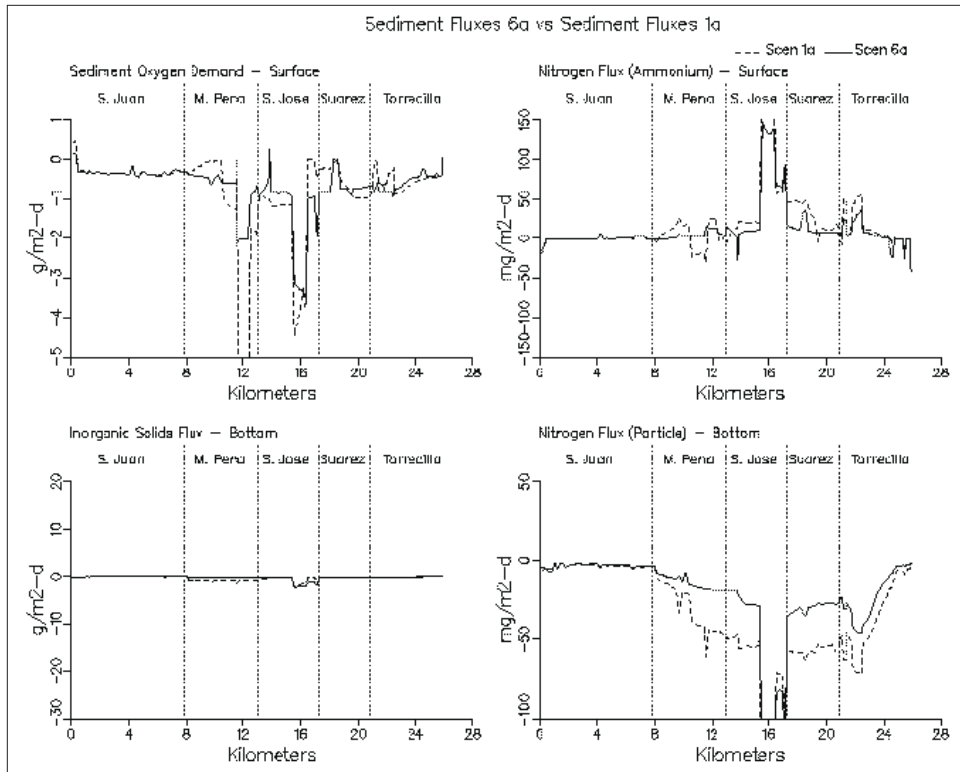


Figure 8-44. (Sheet 9 of 11)

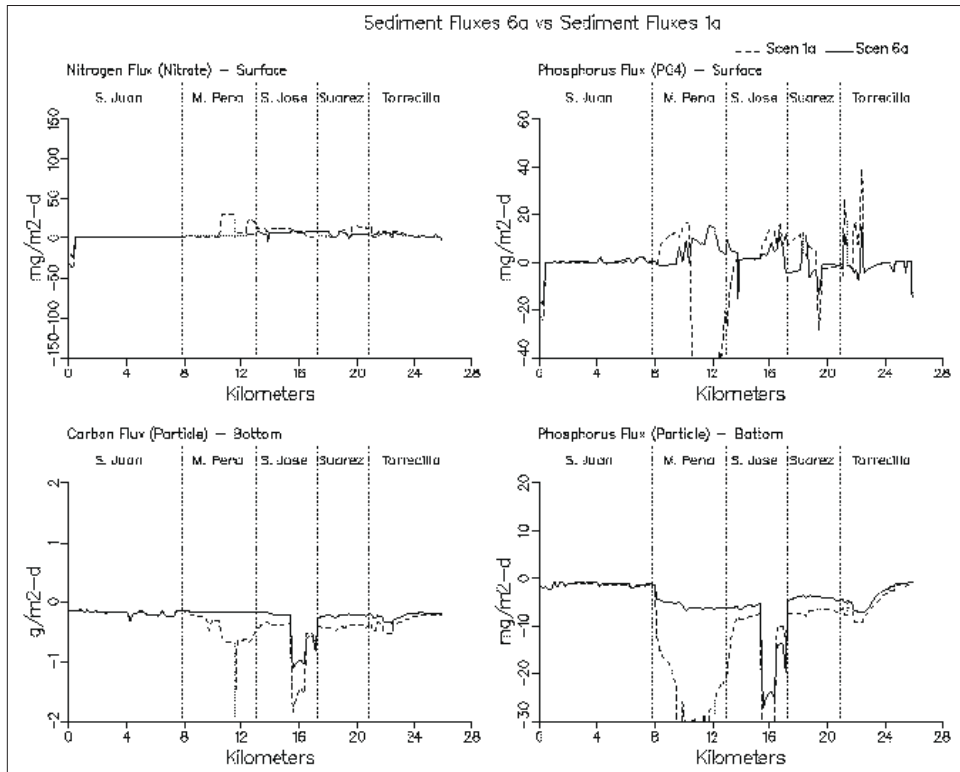


Figure 8-44. (Sheet 10 of 11)

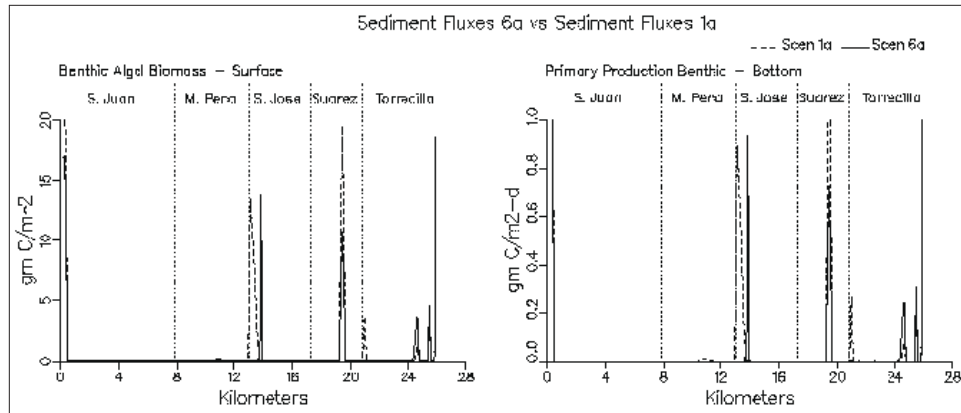


Figure 8-44. (Sheet 11 of 11)

Scenario 6b

Scenario 6b combines all of the loading reductions and channelization of Scenario 6a with the filling of anoxic dredge material borrow pits in Scenario 2. Flows from Laguna San José to Caño Martín Peña were $3.05 \text{ m}^3/\text{s}$ and flows from Canal Suárez into Laguna San José were $0.4 \text{ m}^3/\text{s}$. Since Scenario 6b is a hybrid version of Scenario 6a, this discussion will focus more on the changes that occurred between Scenarios 6a and 6b, than between 6b and 1a.

Temperature results from Scenario 6b indicate that surface temperatures are slightly cooler in San Juan Bay (see Figure 8-45) compared with Scenario 1a. Salinity in Laguna San José increased in Scenario 6b over what it was in either Scenarios 1a or Scenario 2 but is still below what it was for Scenario 1c. The reason for the increase is obviously the channelization of Caño Martín Peña which is why the salinity is higher than it was in either Scenario 1a or 2. The reason that the salinity in Scenario 6b is lower than that of Scenario 1c appears to be the effects of spin-up runs without nudging on. As discussed earlier, nudging acts as a pseudo-salinity-boundary condition inside Laguna San José. Without nudging, the cells in the anoxic holes freshened up. While the opening of Caño Martín Peña allowed more saltwater intrusion into Laguna San José, the freshwater inflows diluted the waters of the lagoon which resulted in a decrease in the salinity of San Juan Bay.

Scenario 6b chlorophyll levels indicated the same behavior as observed in Scenario 6a. There was a slight decrease of $1 \text{ }\mu\text{g/l}$ to $2 \text{ }\mu\text{g/l}$ in surface chlorophyll levels in Caño Martín Peña and Laguna San José. This decrease resulted from the additional reduction in nutrient releases from the anoxic holes. When comparing Scenario 6b to 6a, sediment ammonium releases decreased in Laguna San José and dissolved inorganic phosphorus releases decreased in eastern Caño Martín Peña. Phytoplankton primary production in Laguna San José decreased in Scenario 6b to 3470 kg C/day

from 3972 kg C/day in Scenario 6a. For comparison, Laguna San José phytoplankton primary production was 6093 kg C/day in Scenario 1a.

Dissolved and total organic carbon results for Scenario 6b are similar to those of 6a. Both dissolved and total organic carbon levels are slightly lower in San Juan Bay and slightly higher in Canal Suárez and upper Laguna La Torrecilla. Laguna San José organic carbon exports to Caño Martín Peña were 2650 kg/day and imports from Canal Suárez were 190 kg/day.

Scenario 6b surface ammonium results were very similar to those of 6a. Slight decreases in Laguna San José occurred as a result of decreases in sediment ammonium fluxes. There were also slight decreases in bottom ammonium levels mainly in eastern Laguna San José and in Canal Suárez. Nitrate levels were unchanged between Scenario 6a and 6b. Dissolved organic nitrogen and total nitrogen also exhibited no change. Nitrogen exports from Laguna San José via Caño Martín Peña in Scenario 6b were 167 kg/day and imports from Canal Suárez were 7.3 kg/day.

Dissolved inorganic phosphorus levels in Scenarios 6b were slightly lower than those of 6a. The largest decreases, 0.03 mg/l, occurred in Canal Suárez and Laguna La Torrecilla as a result of decreases in sediment fluxes in those regions. A slight decrease was observed in the surface waters of San Juan Bay and appears to be the result of decreased releases in Caño Martín Peña. Dissolved organic phosphorus transects for 6b and 6a were identical. Total phosphorus plots for 6a and 6b appear to be the same except for the differences due to dissolved inorganic phosphorus. Phosphorus exports in Scenario 6b from Laguna San José via Caño Martín Peña were 15.3 kg/day while imports from Canal Suárez were 1.6 kg/day.

Dissolved oxygen results for Scenario 6b were similar to those of 6a. Surface dissolved oxygen levels show increases over those of 6a but these are due to an increase in the saturation concentration of dissolved oxygen resulting from decreased salinity. Since the reason for the decreases in salinity are not fully understood at present, it is felt that the conditions of Scenario 6b did not improve the surface dissolved oxygen significantly. The conditions of Scenario 6b did improve the bottom dissolved oxygen in Laguna San José and Canal Suárez. Fecal coliform and total solids levels in Scenario 6b were not appreciably different from levels in 6a.

In summary, Scenario 6b indicated some improvements in water quality over Scenario 6a. Chlorophyll levels decreased slightly as did some nutrient releases. Significant effects were observed in dissolved oxygen levels in the locations where the anoxic holes in eastern Laguna San José and Canal Suárez were filled in.

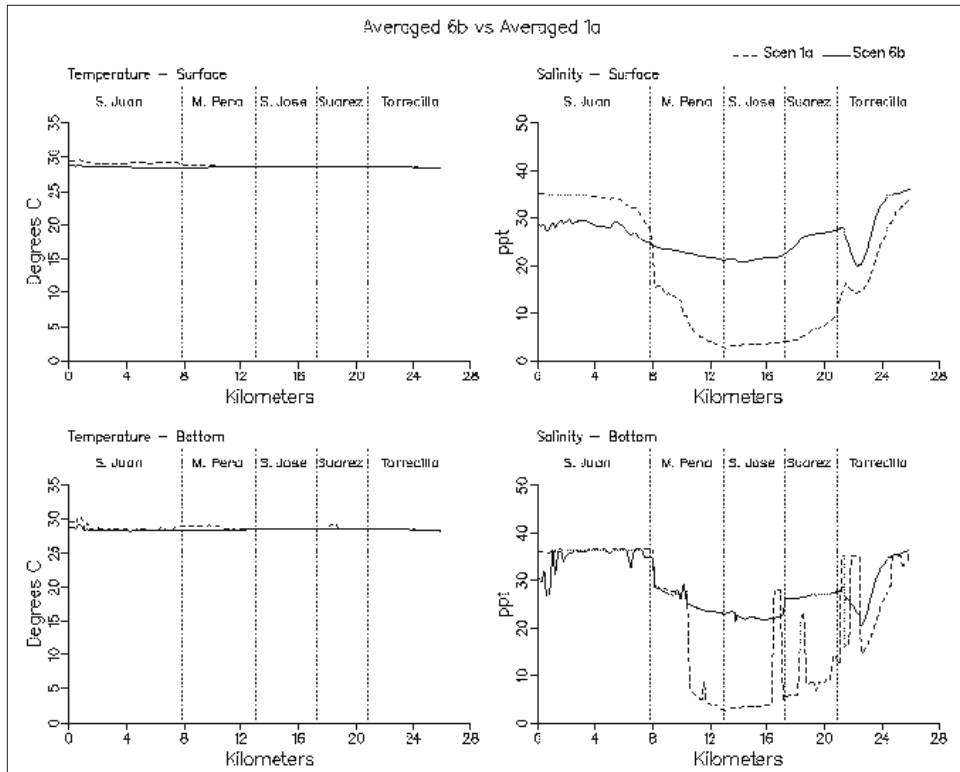


Figure 8-45. Simulation averaged transect plots comparing Scenario 6b with Scenario 1a (Sheet 1 of 11)

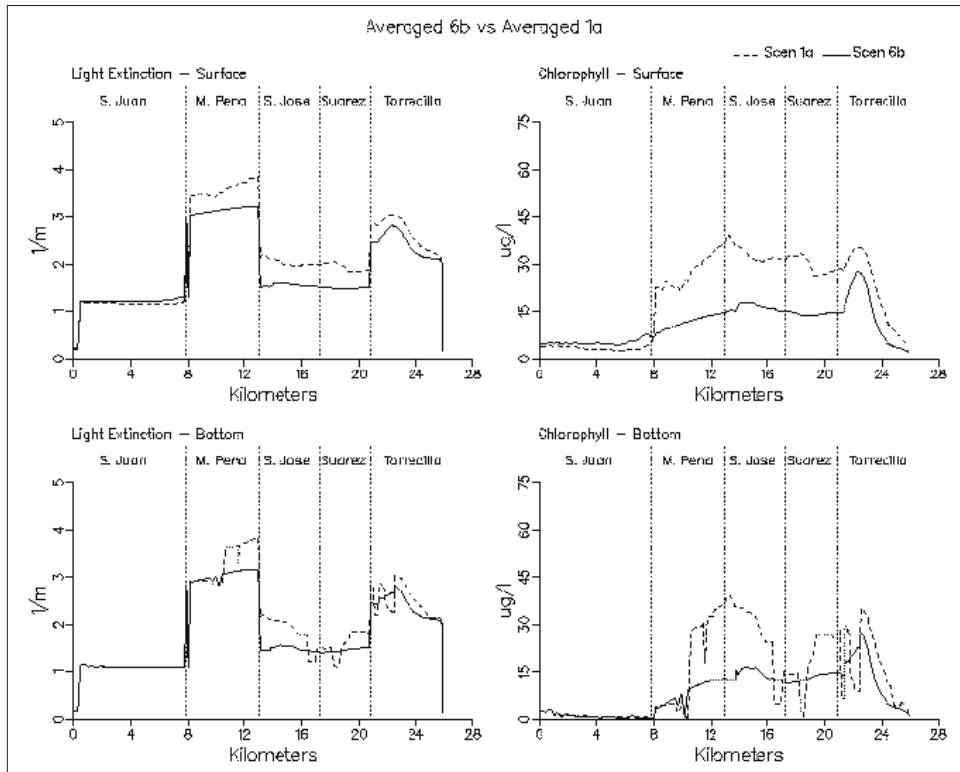


Figure 8-45. (Sheet 2 of 11)

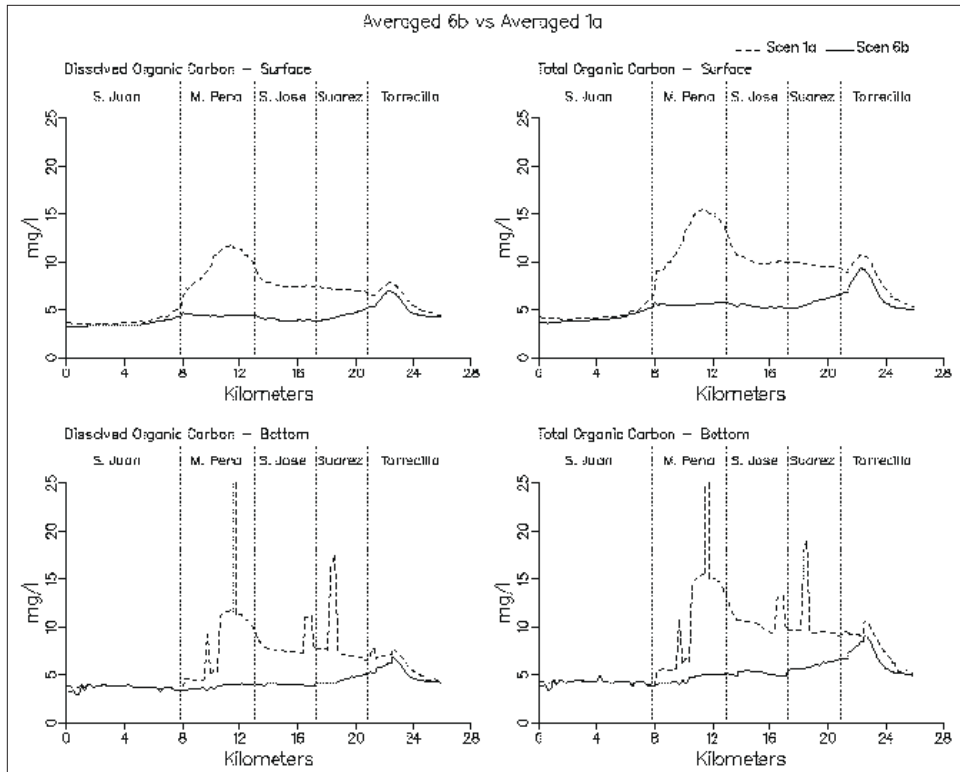


Figure 8-45. (Sheet 3 of 11)

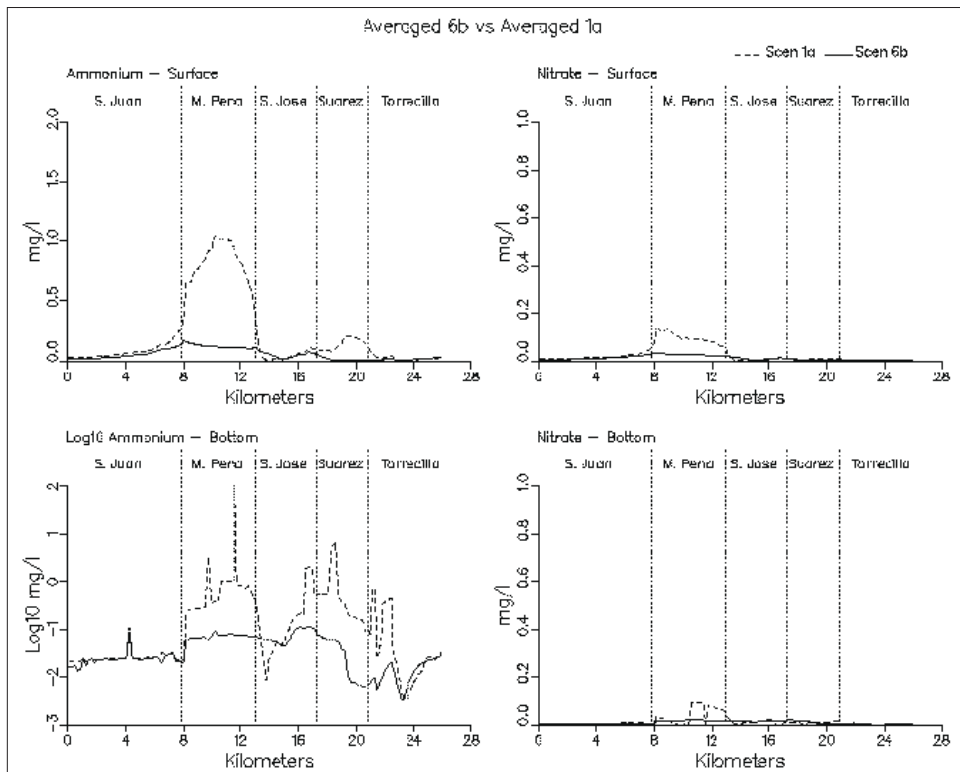


Figure 8-45. (Sheet 4 of 11)

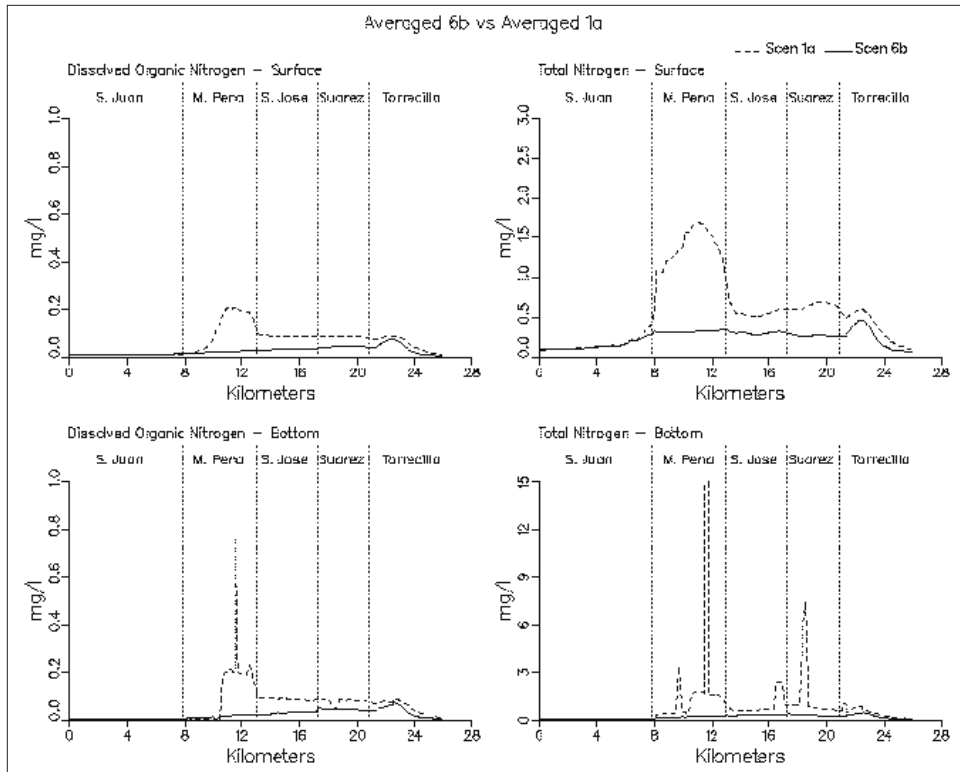


Figure 8-45. (Sheet 5 of 11)

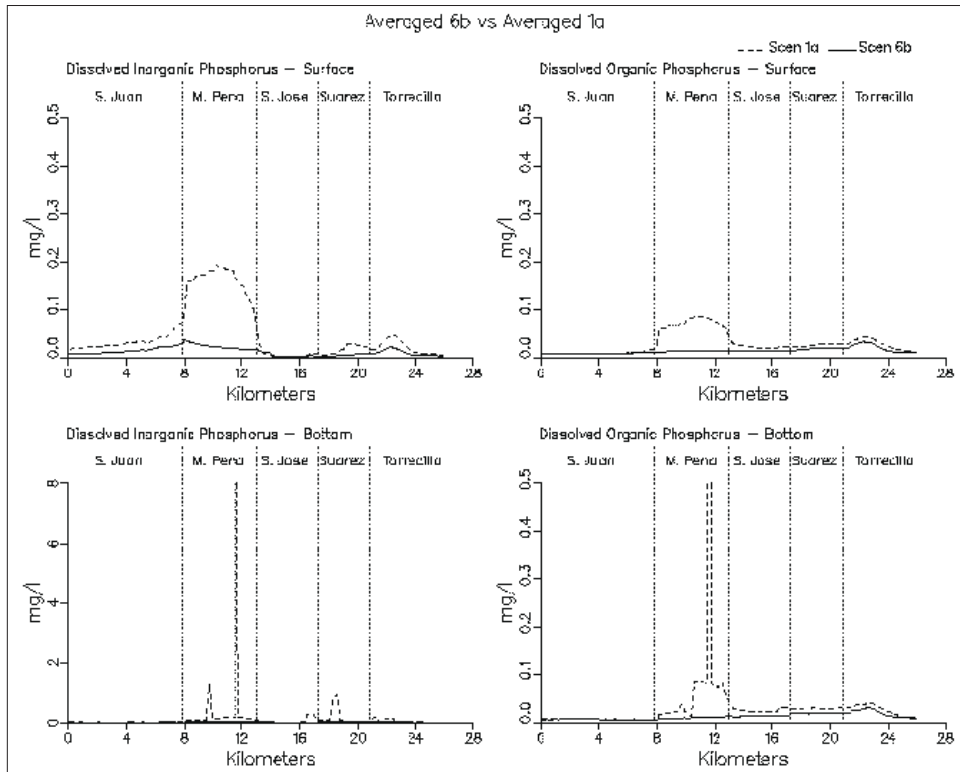


Figure 8-45. (Sheet 6 of 11)

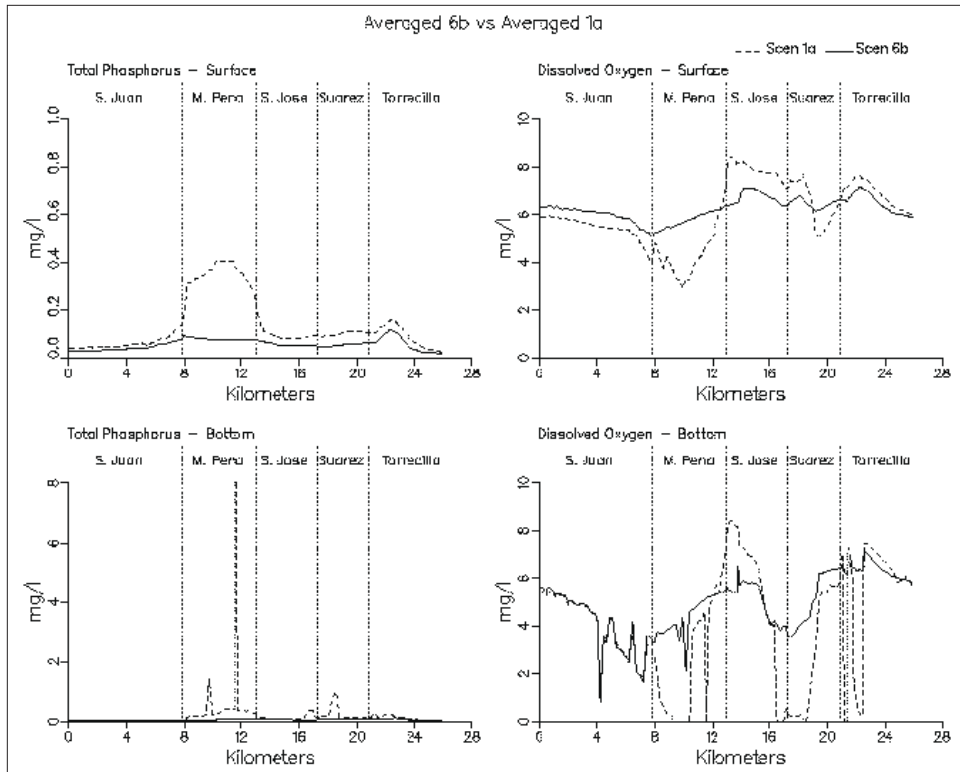


Figure 8-45. (Sheet 7 of 11)

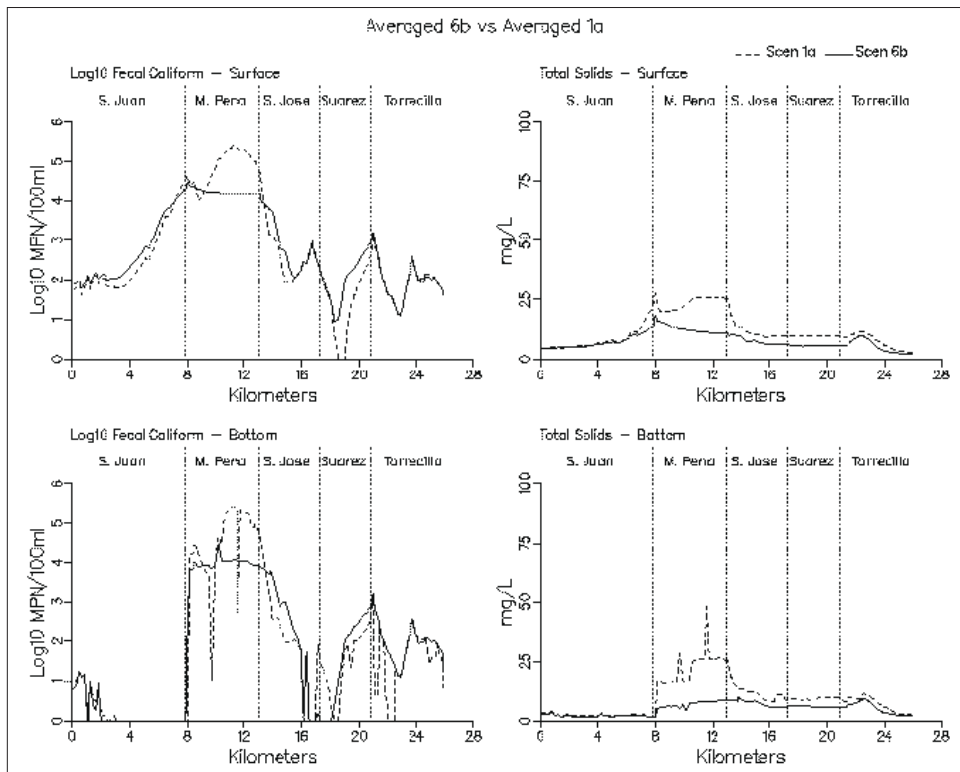


Figure 8-45. (Sheet 8 of 11)

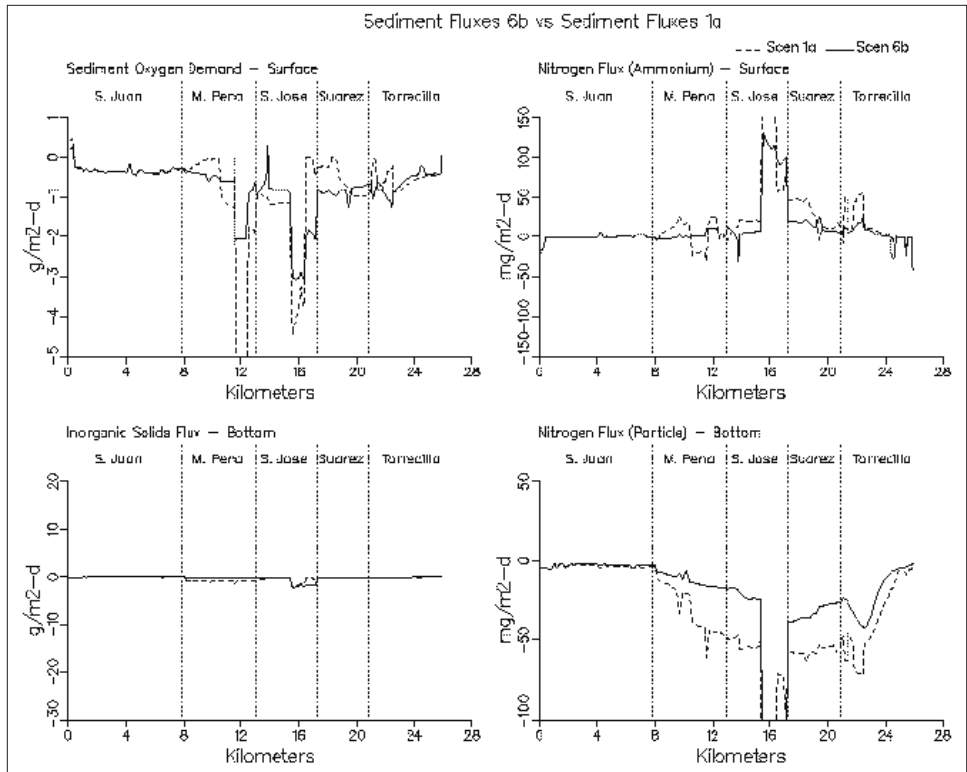


Figure 8-45. (Sheet 9 of 11)

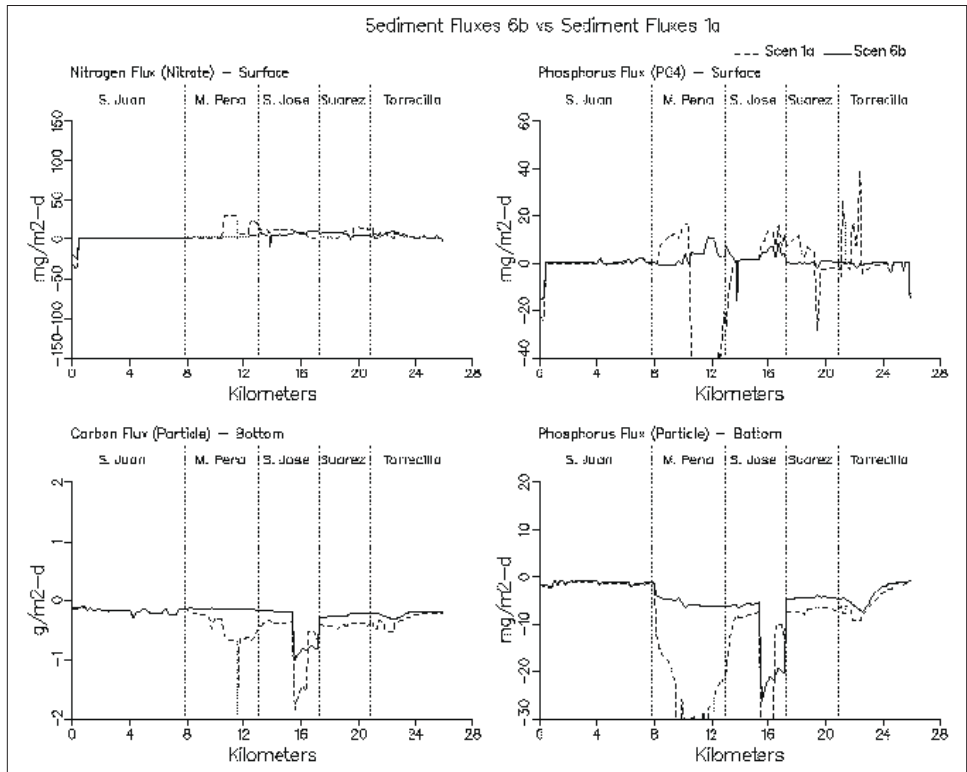


Figure 8-45. (Sheet 10 of 11)

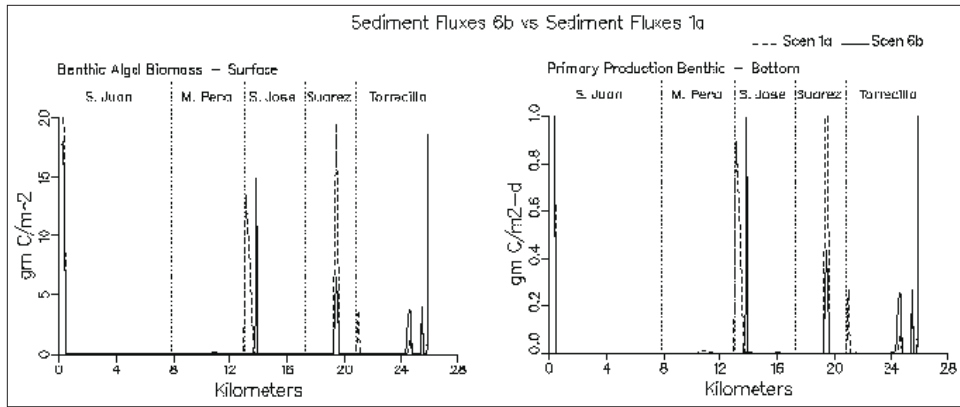


Figure 8-45. (Sheet 11 of 11)

9 Conclusions and Recommendations

A three-dimensional, coupled, hydrodynamic and water quality model of the SJBE system was calibrated using field observations for the summer of 1995. Overall, given the complexity of this system with the multiple ocean inlets, connecting channels, and lagoons, the calibrated model reproduces the observations reasonably well.

Following adjustments and calibration, the model was applied for scenarios to evaluate the effectiveness of various alternatives to increase flushing and reduce loadings for improving water quality. The impacts of each management alternative that was simulated are summarized in Table 9-1 in terms of fluxes of material from one region of the system to another over the scenario simulation duration. As an alternative for comparison, Appendix B contains a summary of the volume-weighted, scenario-average constituent concentrations and the percent change from the base (1a) concentration for all scenarios so that one can easily compare how each alternative affects water quality in an average sense.

All of the alternatives offer some benefits for improving water quality. However, improvements in some areas of the SJBE system can result in degradation to other areas. For example, Scenario 1c provides much improvement to Caño Martín Peña and Laguna San José, but at the expense of flushing more carbon, nitrogen, and phosphorus into San Juan Bay.

Clearly, alternatives were simulated that provide dramatic improvements to water quality. However, the improvements come with costs, including construction costs as well as changes in habitat. For example, it is possible to improve water quality through increased flushing (e.g., Scenarios 1b, 1c, and 3), but this will increase the salinity of Laguna San José and could result in loss of mangrove habitat. Stakeholders must first decide if altering the salinity of Laguna San José is acceptable in terms of habitat and how much mangrove loss is acceptable.

There is not an unequivocally best alternative for improving water quality since a *best* alternative will involve trade-offs, such as water-quality improvement in one area versus degradation in another, costs, habitat

**Table 9-1.
Summary of Impacts for Each Management Scenario**

Scenario	Flux from Laguna San José to Caño Martín Peña				Flux from Laguna San José to Canal Suárez				Laguna San José Primary Production	San Juan Bay Primary Production
	Flow, m ³ /s	C, kg/d	N, kg/d	P, kg/d	Flow, m ³ /s	C, kg/d	N, kg/d	P, kg/d	As C, kg/day	As C, kg/day
1a	0.5	454	8	2	1.98	1631	138	20	6093	3586
1b	1.45	1311	54	9	1.08	769	71	10	5825	4065
1c	3.05	3530	187	15	-0.4	-166	-5	-2	5860	5300
2	0.5	329	8.8	2	1.98	1060	18	13	1584	2264
3	0.1	-35	-38	-9	2.5	2261	178	23	6450	3060
4	2.55	2415	141	32	-0.2	-73	-2	-1	6675	4957
5a	0.5	513	27	6	1.98	1563	130	19	5741	3263
5b	0.5	369	10	1	1.98	1240	110	15	4541	3347
6a	3.05	2558	161	15	-0.4	-175	-7	-3	3973	4574
6b	3.05	2650	167	15	-0.4	-190	-7	-2	3470	3968

Note: C, N, and P fluxes are rounded off to near whole number

considerations, and other considerations. Even though trade-offs can be assessed to find the optimal solution, politics will eventually enter the decision process and can affect the final selection. However, if one studies the table in Appendix B and does not consider other factors, such as habitat considerations, it is clear that alternative 6b provides the best overall water quality, especially the best DO conditions.

In order to find the preferred alternative for water quality improvement, it is recommended that the stakeholders first specify the bounds of acceptable results in terms of water quality standards, construction/remediation costs, habitat, etc. For example, the stakeholders may decide that it is acceptable to degrade water quality slightly in San Juan Bay as long as water quality standards are satisfied. The stakeholders may decide that it is acceptable to increase the salinity of Laguna San José, thus favoring flushing alternatives involving enlargement of Caño Martín Peña. Conversely, the stakeholders may decide that the preference is to hold steady or even decrease the salinity of Laguna San José. In this case, alternative 4 (i.e., tide gate and removal of bridge constriction in Canal Suárez) may be preferred. Alternative 1c may result in more mangrove loss along Caño Martín Peña than alternative 1b, a consequence to consider.

Assuming that an increase in the salinity of Laguna San José is acceptable and ignoring mangrove losses, a combination of alternatives 1c, 2, and loading reductions seems intuitively appropriate. It is possible that material removed from Caño Martín Peña could be placed in the dredged borrow pits, thus solving two problems while providing added water quality benefits. Additionally, it seems logical that channel improvements in Caño Martín Peña would be accomplished concurrently with removal of un-sewered, untreated wastes in that area. The combination scenario, e.g., dredging of Caño Martín Peña, filling borrow pits, and removal of un-sewered loads (with the inclusion of the pumping station loads removed), was simulated with Scenario 6b which provided the most improvement in water quality. Based upon this logic and the degree of water-quality improvement, one would have to conclude that alternative 6b is preferred.

However, upon review of the results of Scenario 5b, the relatively minor benefits in water quality gained by removal of the Baldeorioty de Castro Pump Station loads may not warrant the cost of this additional waste treatment. Therefore, a preferred alternative may be 6b with the Baldeorioty de Castro Pump Station loads included.

10 References

- American Society of Civil Engineers. (1961). "Effect of water temperature on stream reaeration," *Journal of the Sanitary Engineering Division* 87(SA6), 59-71.
- Ammerman, J., and Azam, F. (1985). "Bacterial 5'-nucleodase in aquatic ecosystems: a novel mechanism of phosphorus regeneration," *Science* 227, 1338-40.
- Bird, D., and Kalff, J. (1984). "Empirical relationships between bacterial abundance and chlorophyll concentration in fresh and marine waters," *Canadian Journal of Fisheries and Aquatic Science* 41, 1015-23.
- Bloss, S., Lehfelddt, R., and Patterson, J. C. (1988). "Modeling turbulent transport in stratified estuary," *Journal of Hydraulic Engineering, Am. Soc. Civil Eng.* 114(9), 1113-33.
- Boni, L., Carpena, E., Wynne, D., and Reti, M. (1989). "Alkaline phosphatase activity in *Protogonyaulax Tamarensis*," *Journal of Plankton Research* 11, 879-85.
- Cerco, C. F. (1995a). "Simulation of long-term trends in Chesapeake Bay eutrophication," *J. Environ. Eng., Am. Soc. Civil Eng.* 121(4), 298-310.
- Cerco, C. F. (1995b). "Response of Chesapeake Bay to nutrient load reductions," *J. Environ. Eng., Am. Soc. Civil Eng.* 121(8), 549-57.
- Cerco, C. F., and Bunch, B. (1997). "Passaic River tunnel diversion model study, report 5, water quality modeling," Technical Report HL-96-2, U.S. Army Engineer Waterways Experiment Station, Vicksburg, MS.
- Cerco, C. F., and Cole, T. (1993). "Three-dimensional eutrophication model of Chesapeake Bay," *J. Environ. Eng., Am. Soc. Civil Eng.* 119(6), 1006-25.
- Cerco, C. F., and Cole, T. M. (1994). "Three-dimensional eutrophication model of Chesapeake Bay," Technical Report EL-94-4, U.S. Army Engineer Waterways Experiment Station, Vicksburg, MS.

- Cerco, C. F., and Cole, T. M. (1995). "User's guide to the CE-QUAL-ICM three-dimensional eutrophication model," Technical Report EL-95-15, U.S. Army Engineer Waterways Experiment Station, Vicksburg, MS.
- Cerco, C., and Seitzinger, S. (1997). "Measured and modeled effects of benthic algae on eutrophication in Indian River-Rehoboth Bay, Delaware," *Estuaries* 20(1), 231-48.
- Cerco, C. F., Bunch, B., Cialone, M. A., and Wang, H. (1994). "Hydrodynamic and eutrophication model study of Indian River and Rehoboth bay, Delaware," Technical Report EL-94-5, U.S. Army Engineer Waterways Experiment Station, Vicksburg, MS.
- Cerco, C. F., Bunch B., and Letter, J. (1999). "Impact of flood-diversion tunnel on Newark Bay and adjacent waters," *J. Environ. Eng., Am. Soc. Civil Eng.* 125(4), 328-38.
- Chrost, R., and Overbeck, J. (1987). "Kinetics of alkaline phosphatase activity and phosphorus availability for phytoplankton and bacterioplankton in Lake Plubsee (north German eutrophic lake)," *Microbial Ecology* 13, 229-48.
- Cole, J., Findlay, S., and Pace, M. (1988). "Bacterial production in fresh and saltwater ecosystems: a cross-system overview," *Marine Ecology Progress Series* 43, 1-10.
- DiToro, D. (1980). "Applicability of cellular equilibrium and Monod theory to phytoplankton growth kinetics," *Ecological Modelling* 8, 201-18.
- DiToro, D., and Fitzpatrick, J. (1993). "Chesapeake Bay sediment flux model," Contract Report EL-93-2, U.S. Army Engineer Waterways Experiment Station, Vicksburg, MS.
- Droop, M. (1973). "Some thoughts on nutrient limitation in algae," *Journal of Phycology* 9, 264-72.
- Edinger, J., Brady, D., and Geyer, J. (1974). "Heat exchange and transport in the environment," Report 14, Department of Geography and Environmental Engineering, Johns Hopkins University, Baltimore, MD.
- Ellis, S. R., and Gómez-Gómez, F. (1976). "Hydrologic Characteristics of Lagoons at San Juan, Puerto Rico, During a January 1974 Tidal Cycle," U.S. Geological Survey, WRI-38-75.
- Fagerburg, T. L. (1998). "San Juan Bay Estuary study: hydrodynamic field data collection," Miscellaneous Paper CHL-98-3, U.S. Army Engineer Waterways Experiment Station, Vicksburg, MS.

- Garratt, J. R. (1977). "Review of drag coefficients over oceans and continents," *Monthly Weather Review* 105, 915-29.
- Genet, L., Smith, D., and Sonnen, M. (1974). "Computer program documentation for the dynamic estuary model," U.S. Environmental Protection Agency, Systems Development Branch, Washington, DC.
- Gómez-Gómez, F., Quinones, F., and Ellis, S. (1983). "Hydrologic characteristics of lagoon at San Juan, Puerto Rico, during an October 1974 tidal cycle," U.S. Geological Survey Water Resources Investigations Open File Report 82-8349, San Juan, PR.
- Hall, R. W., and Dortch, M. S. (1994). "New York Bight study, development and application of a eutrophication/general water quality model," Technical Report CERC-94-4, Report 2, U.S. Army Engineer Waterways Experiment Station, Vicksburg, MS.
- HydroQual. (1987). "A steady-state coupled hydrodynamic/water quality model of the eutrophication and anoxia process in Chesapeake Bay," Final Report, HydroQual Inc., Mahwah, NJ.
- Johnson, B. H. (1980). "VAHM - a vertically averaged hydrodynamic model using boundary-fitted coordinates," Miscellaneous Paper HL-80-3, U.S. Army Engineer Waterways Experiment Station, Vicksburg, MS.
- Johnson, B. H., Heath, R. E., Hsieh, B. B., Kim, K. W., and Butler, H. L. (1991). "Development and verification of a three-dimensional numerical hydrodynamic, salinity, and temperature model of Chesapeake Bay," Technical Report HL-91-7, U.S. Army Engineer Waterways Experiment Station, Vicksburg, MS.
- Johnson, B. H., Kim K. W., Heath, R. E., Hsieh, B. B., and Butler, H. L. (1993). "Validation of three-dimensional hydrodynamic model of Chesapeake Bay," *J. of Hyd. Eng., Am. Soc. Civil Eng.* 119(1), 2-20.
- Kennedy, R. H., Hains, J. J., Boyd, W. A., Lemons, J., Herrmann F., Honnell, D., Howell, P., Way, C., Fernandez, F., Miller-Way, T., and Twilley, R. R. (1996). "San Juan Bay and Estuary study: water quality data collection," Miscellaneous Paper EL-96-9, U.S. Army Engineer Waterways Experiment Station, Vicksburg, MS.
- Leonard, B. (1979). "A stable and accurate convection modelling procedure based on quadratic upstream interpolation," *Computer Methods in Applied Mechanics and Engineering* 19, 59-98.
- Mark, D. J., Scheffner, N. W., Butler, H. L., Bunch, B. W., and Dortch, M. S. (1993). "Hydrodynamic and water quality modeling of lower Green Bay, Wisconsin," Technical Report CERC-93-16, U.S. Army Engineer Waterways Experiment Station, Vicksburg, MS.

- Matavulj, M., and Flint, K. (1987). "A model for acid and alkaline phosphatase activity in a small pond," *Microbial Ecology* 13, 141-58.
- Metcalf & Eddy., Inc. (1979). "*Wastewater engineering: treatment/disposal/reuse*. McGraw Hill Book Company, New York, NY.
- Mississippi Department of Environmental Quality, Mississippi Soil and Water Conservation Commission, USDA Soil Conservation Service (1994). "Planning and design manual for the control of erosion, sediment, & stormwater," Mississippi Department of Environmental Quality, Jackson, MS.
- Monod, J. (1949). "The growth of bacterial cultures," *Annual Review of Microbiology* 3, 371-94.
- Morel, F. (1983). *Principles of aquatic chemistry*, John Wiley and Sons, New York, NY, 150.
- O'Connor, D. (1983). "Wind effects on gas-liquid transfer coefficients," *Journal of the Environmental Engineering Division* 190, 731-52.
- O'Connor, D., and Dobbins, W. (1958). "Mechanisms of reaeration in natural streams," *Transactions of the American Society of Civil Engineers* 123, 641-66.
- Odum, E. (1971). *Fundamentals of ecology*, 3rd ed., W. B. Saunders, Philadelphia, PA, pp 106-7.
- Parsons, T., Takahashi, M., and Hargrave, B. (1984). *Biological oceanographic processes*. 3rd ed., Pergamon Press, Oxford.
- Redfield, A., Ketchum, B., and Richards, F. (1966). "The influence of organisms on the composition of sea-water." *The Sea Volume II*. Interscience Publishers, New York, 26-48.
- Rodi, W. (1980). "Turbulence models and their application in hydraulics: a state of the art review," *IAHR*, Delft, The Netherlands.
- Sheng, Y. P. (1986). "A three-dimensional mathematical model of coastal, estuarine and lake currents using boundary-fitted grid," Report No. 585, A.R.A.P. Group of Titan Research and Technology, Princeton, NJ.
- Stumm, W., and Morgan, J. (1981). *Aquatic chemistry*. 2nd ed., Wiley Interscience, New York.
- Tchobanoglous, G., and Schroeder, E. (1987). *Water quality*. Addison Wesley, Reading, MA.

- Thomann, R., and Fitzpatrick, J. (1982). "Calibration and verification of a mathematical model of the eutrophication of the Potomac Estuary," HydroQual Inc., Mahwah, NJ.
- Tuffey, T., Hunter, J., and Matulewich, V. (1974). "Zones of nitrification," *Water Resources Bulletin* 10, 555-64.
- U.S. Environmental Protection Agency. (1993). "National Estuary Program: bringing our estuaries new life," Technical Report EPA-842-F-93-002, Office of Wetlands, Oceans, and Watersheds, Washington, DC.
- Wen, C., Kao, J., Wang, L., and Liaw, C. (1984). "Effect of salinity on reaeration coefficient of receiving waters," *Water Science and Technology* 16, 139-54.
- Westerlink, J. J., Luettich, R. A., Baptista, A. M., Scheffner, N. W., and Farrar, P. (1992). "Tide and storm surge predictions using a finite element model," *Journal of Hydraulic Engineering, Am. Soc. Civil Eng.*, 118, 1373-90.
- Westrich, J., and Berner, R. (1984). "The role of sedimentary organic matter in bacterial sulfate reduction: the G model tested," *Limnology and Oceanography* 29, 236-49.
- Wezernak, C., and Gannon, J. (1968). "Evaluation of nitrification in streams," *Journal of the Sanitary Engineering Division* 94(SA5), 883-95.

Appendix A

Transformed Horizontal Momentum Diffusion Terms

X - Horizontal Diffusion

$$\begin{aligned}
 &= \frac{Y_\eta}{J^2} \left(\frac{A_h G_{22}}{J} \left[(X_\xi H \bar{u})_\xi + (X_\eta H \bar{v})_\xi \right] \right)_\xi \\
 &+ \frac{Y_\eta}{J^2} \left(\frac{A_h G_{11}}{J} \left[(X_\xi H \bar{u})_\eta + (X_\eta H \bar{v})_\eta \right] \right)_\eta \\
 &- \frac{X_\eta}{J^2} \left(\frac{A_h G_{11}}{J} \left[(Y_\xi H \bar{u})_\eta + (Y_\eta H \bar{v})_\eta \right] \right)_\eta \\
 &- \frac{Y_\eta}{J^2} \left(\frac{A_h G_{12}}{J} \left[(X_\xi H \bar{u})_\eta + (X_\eta H \bar{v})_\eta \right] \right)_\xi \\
 &- \frac{Y_\eta}{J^2} \left(\frac{A_h G_{12}}{J} \left[(X_\xi H \bar{u})_\xi + (X_\eta H \bar{v})_\xi \right] \right)_\eta \\
 &+ \frac{X_\eta}{J^2} \left(\frac{A_h G_{12}}{J} \left[(Y_\xi H \bar{u})_\eta + (Y_\eta H \bar{v})_\eta \right] \right)_\xi \\
 &+ \frac{X_\eta}{J^2} \left(\frac{A_h G_{12}}{J} \left[(Y_\xi H \bar{u})_\xi + (Y_\eta H \bar{v})_\xi \right] \right)_\eta
 \end{aligned}$$

Y - Horizontal Diffusion

$$\begin{aligned}
&= \frac{X_\xi}{J^2} \left(\frac{A_h G_{11}}{J} \left[(Y_\eta H\bar{v})_\eta + (Y_\xi H\bar{u})_\eta \right] \right)_\eta \\
&- \frac{Y_\xi}{J^2} \left(\frac{A_h G_{11}}{J} \left[(X_\eta H\bar{v})_\eta + (X_\xi H\bar{u})_\eta \right] \right)_\eta \\
&+ \frac{X_\xi}{J^2} \left(\frac{A_h G_{22}}{J} \left[(Y_\eta H\bar{v})_\xi + (Y_\xi H\bar{u})_\xi \right] \right)_\xi \\
&- \frac{Y_\xi}{J^2} \left(\frac{A_h G_{22}}{J} \left[(X_\eta H\bar{v})_\xi + (X_\xi H\bar{u})_\xi \right] \right)_\xi \\
&- \frac{X_\xi}{J^2} \left(\frac{A_h G_{12}}{J} \left[(Y_\eta H\bar{v})_\eta + (Y_\xi H\bar{u})_\eta \right] \right)_\xi \\
&- \frac{X_\xi}{J^2} \left(\frac{A_h G_{12}}{J} \left[(Y_\eta H\bar{v})_\xi + (Y_\xi H\bar{u})_\xi \right] \right)_\eta \\
&+ \frac{Y_\xi}{J^2} \left(\frac{A_h G_{12}}{J} \left[(X_\eta H\bar{v})_\eta + (X_\xi H\bar{u})_\eta \right] \right)_\xi \\
&+ \frac{Y_\xi}{J^2} \left(\frac{A_h G_{12}}{J} \left[(X_\eta H\bar{v})_\xi + (X_\xi H\bar{u})_\xi \right] \right)_\eta
\end{aligned}$$

Replacing $H\bar{u}$ and $H\bar{v}$ with \bar{U} and \bar{V} , respectively, the same expressions apply in the external mode equations.

Appendix B

Scenario Average Concentrations and Percent Change from Base Condition

Surface Salinity (PPT)											
Region	SC 1a	SC 1b	%	SC 1c	%	SC 2	%	SC 3	%	SC 4	%
San Juan Bay Cano Martin Pena	33.7 20.7	33.4 19.5	-1 -6	33.0 27.5	-2 33	26.0 18.2	-23 -12	33.9 23.8	1 15	32.8 16.9	-3 -19
Laguna San Jose Canal Suarez	3.2 5.5	6.0 10.0	90 81	22.7 27.3	619 396	0.5 1.8	-86 -67	7.7 12.4	144 126	5.2 26.0	65 373
Laguna La Torrecilla Laguna de Pinones	18.6 13.8	22.1 17.5	19 26	26.2 22.1	41 59	16.1 6.6	-14 -52	19.5 13.2	5 -5	26.2 22.4	41 61

Note: "SC" denotes Scenario.

Surface Salinity (PPT)									
Region	SC 1a	SC 5a	%	SC 5b	%	SC 6a	%	SC 6b	%
San Juan Bay Cano Martin Pena	33.7 20.7	33.7 20.7	0 0	33.7 20.7	0 0	33.0 27.5	-2 33	26.4 24.9	-22 20
Laguna San Jose Canal Suarez	3.2 5.5	3.2 5.5	0 0	3.2 5.5	0 0	22.7 27.3	619 396	19.9 25.8	529 369
Laguna La Torrecilla Laguna de Pinones	18.6 13.8	18.6 13.8	0 0	18.6 13.8	0 0	26.2 22.1	41 59	25.6 16.5	38 19

**Surface
Chlorophyll ($\mu\text{g/L}$)**

Region	SC 1a	SC 1b	%	SC 1c	%	SC 2	%	SC 3	%	SC 4	%
San Juan Bay Cano Martin Pena	3.95 13.53	4.78 16.76	21 24	7.44 11.66	88 -14	2.50 4.44	-37 -67	3.27 9.41	-17 -30	6.13 18.80	55 39
Laguna San Jose Canal Suarez	32.30 31.31	29.86 27.51	-8 -12	25.26 16.13	-22 -48	8.50 6.82	-74 -78	33.99 30.37	5 -3	34.00 13.53	5 -57
Laguna La Torrecilla Laguna de Pinones	26.90 38.26	17.70 19.78	-34 -48	18.22 33.79	-32 -12	17.49 32.62	-35 -15	26.18 38.55	-3 1	18.39 33.78	-32 -12

**Surface
Chlorophyll ($\mu\text{g/L}$)**

Region	SC 1a	SC 5a	%	SC 5b	%	SC 6a	%	SC 6b	%
San Juan Bay Cano Martin Pena	3.95 13.53	3.63 12.19	-8 -10	3.67 11.31	-7 -16	6.10 8.65	54 -36	5.42 8.06	37 -40
Laguna San Jose Canal Suarez	32.30 31.31	30.28 29.86	-6 -5	22.99 25.73	-29 -18	15.74 13.76	-51 -56	14.90 13.98	-54 -55
Laguna La Torrecilla Laguna de Pinones	26.90 38.26	26.34 37.98	-2 -1	24.95 37.27	-7 -3	18.15 33.75	-33 -12	18.48 33.62	-31 -12

**Surface
Total Nitrogen (mg/L)**

Region	SC 1a	SC 1b	%	SC 1c	%	SC 2	%	SC 3	%	SC 4	%
San Juan Bay Cano Martin Pena	0.1443 0.8100	0.1458 0.6238	1 -23	0.1640 0.3496	14 -57	0.1250 0.6967	-13 -14	0.1366 0.7645	-5 -6	0.1668 0.6863	16 -15
Laguna San Jose Canal Suarez	0.5809 0.6267	0.5553 0.5238	-4 -16	0.4568 0.2985	-21 -52	0.1789 0.1268	-69 -80	0.6085 0.5607	5 -11	0.6019 0.2694	4 -57
Laguna La Torrecilla Laguna de Pinones	0.4828 0.6610	0.3290 0.3585	-32 -46	0.3432 0.5881	-29 -11	0.3260 0.5854	-32 -11	0.4758 0.6680	-1 1	0.3466 0.5883	-28 -11

**Surface
Total Nitrogen (mg/L)**

Region	SC 1a	SC 5a	%	SC 5b	%	SC 6a	%	SC 6b	%
San Juan Bay Cano Martin Pena	0.1443 0.8100	0.1321 0.4756	-9 -41	0.1393 0.6800	-4 -16	0.1445 0.2883	0 -64	0.1315 0.2863	-9 -65
Laguna San Jose Canal Suarez	0.5809 0.6267	0.5453 0.5923	-6 -5	0.4296 0.5102	-26 -19	0.2945 0.2537	-49 -60	0.2947 0.2568	-49 -59
Laguna La Torrecilla Laguna de Pinones	0.4828 0.6610	0.4731 0.6563	-2 -1	0.4487 0.6446	-7 -2	0.3420 0.5875	-29 -11	0.3420 0.5986	-29 -9

**Surface
Total Phosphorus (mg/L)**

Region	SC 1a	SC 1b	%	SC 1c	%	SC 2	%	SC 3	%	SC 4	%
San Juan Bay Cano Martin Pena	0.0594 0.2270	0.0587 0.1677	-1 -26	0.0585 0.0943	-1 -58	0.0415 0.2190	-30 -4	0.0574 0.2304	-3 2	0.0639 0.1778	8 -22
Laguna San Jose Canal Suarez	0.0989 0.0949	0.0918 0.0798	-7 -16	0.0919 0.0748	-7 -21	0.0998 0.0790	1 -17	0.1055 0.0884	7 -7	0.1140 0.0804	15 -15
Laguna La Torrecilla Laguna de Pinones	0.1239 0.1034	0.0944 0.0728	-24 -30	0.1063 0.0934	-14 -10	0.0943 0.0788	-24 -24	0.1157 0.0974	-7 -6	0.1066 0.0929	-14 -10

**Surface
Total Phosphorus (mg/L)**

Region	SC 1a	SC 5a	%	SC 5b	%	SC 6a	%	SC 6b	%
San Juan Bay Cano Martin Pena	0.0594 0.2270	0.0568 0.1610	-4 -29	0.0592 0.2232	0 -2	0.0546 0.0830	-8 -63	0.0382 0.0765	-36 -66
Laguna San Jose Canal Suarez	0.0989 0.0949	0.0939 0.0907	-5 -4	0.0696 0.0770	-30 -19	0.0601 0.0674	-39 -29	0.0541 0.0496	-45 -48
Laguna La Torrecilla Laguna de Pinones	0.1239 0.1034	0.1227 0.1029	-1 0	0.1184 0.1009	-4 -2	0.1061 0.0932	-14 -10	0.0916 0.0811	-26 -22

**Surface
Fecal Coliform (MPN/ml)**

Region	SC 1a	SC 1b	%	SC 1c	%	SC 2	%	SC 3	%	SC 4	%
San Juan Bay Cano Martin Pena	1748.2 62863.0	1784.4 54475.0	2 -13	1810.6 32547.0	4 -48	1903.2 64263.0	9 2	1732.3 61782.0	-1 -2	1830.9 61210.0	5 -3
Laguna San Jose Canal Suarez	6534.3 41.4	6762.1 59.5	3 44	6981.6 114.3	7 176	6471.7 74.4	-1 80	7025.5 457.8	8 1005	5170.6 130.8	-21 216
Laguna La Torrecilla Laguna de Pinones	2235.9 745.9	2235.8 747.2	0 0	2243.0 749.6	0 0	2229.0 743.8	0 0	2093.5 743.8	-6 0	2259.2 750.0	1 1

**Surface
Fecal Coliform (MPN/ml)**

Region	SC 1a	SC 5a	%	SC 5b	%	SC 6a	%	SC 6b	%
San Juan Bay Cano Martin Pena	1748.2 62863.0	1730.9 53056.0	-1 -16	1748.2 62862.0	0 0	1718.4 30888.0	-2 -51	1839.3 31832.0	5 -49
Laguna San Jose Canal Suarez	6534.3 41.4	6478.3 41.4	-1 0	4088.6 41.4	-37 0	4196.6 114.0	-36 175	4287.9 129.5	-34 213
Laguna La Torrecilla Laguna de Pinones	2235.9 745.9	2235.9 745.9	0 0	2235.9 745.9	0 0	2243.0 749.6	0 0	2243.1 748.4	0 0

**Water Column
Dissolved Oxygen (mg/L)**

Region	SC 1a	SC 1b	%	SC 1c	%	SC 2	%	SC 3	%	SC 4	%
San Juan Bay Cano Martin Pena	4.2 2.8	4.2 3.0	-1 8	4.1 4.0	-2 42	4.8 3.2	15 14	4.2 2.9	1 3	4.1 3.0	-3 7
Laguna San Jose Canal Suarez	5.3 2.8	5.3 3.3	1 21	5.4 4.3	1 55	7.6 5.1	44 86	5.3 4.8	1 75	5.1 4.8	-5 74
Laguna La Torrecilla Laguna de Pinones	4.4 7.3	4.6 7.2	5 -2	4.5 6.9	2 -5	6.7 7.6	50 4	4.3 7.3	-3 0	4.5 6.9	3 -5

**Water Column
Dissolved Oxygen (mg/L)**

Region	SC 1a	SC 5a	%	SC 5b	%	SC 6a	%	SC 6b	%
San Juan Bay Cano Martin Pena	4.2 2.8	4.2 2.8	0 2	4.2 2.8	0 0	4.1 4.0	-2 43	4.7 4.4	12 59
Laguna San Jose Canal Suarez	5.3 2.8	5.3 2.8	0 1	5.4 3.0	2 10	5.4 4.3	2 57	6.1 5.8	15 109
Laguna La Torrecilla Laguna de Pinones	4.4 7.3	4.4 7.3	0 0	4.5 7.3	1 0	4.5 6.9	2 -5	6.2 7.1	41 -2

**Water Column
Bottom Dissolved Oxygen (mg/L)**

Region	SC 1a	SC 1b	%	SC 1c	%	SC 2	%	SC 3	%	SC 4	%
San Juan Bay Cano Martin Pena	4.0 2.3	3.9 2.5	-2 8	3.9 3.7	-3 62	4.4 2.6	12 13	4.0 2.3	1 1	3.8 2.5	-4 8
Laguna San Jose Canal Suarez	5.0 1.4	5.1 1.8	0 23	5.0 2.5	0 76	7.5 2.6	48 83	5.0 3.9	0 171	4.7 3.0	-7 109
Laguna La Torrecilla Laguna de Pinones	5.2 7.3	5.3 7.2	2 -2	5.1 6.9	-2 -5	6.4 7.6	22 4	5.1 7.3	-2 0	5.1 6.9	-2 -5

**Water Column
Bottom Dissolved Oxygen (mg/L)**

Region	SC 1a	SC 5a	%	SC 5b	%	SC 6a	%	SC 6b	%
San Juan Bay Cano Martin Pena	4.0 2.3	3.9 2.4	0 2	3.9 2.3	0 0	3.9 3.8	-3 63	4.3 4.2	9 83
Laguna San Jose Canal Suarez	5.0 1.4	5.1 1.5	0 1	5.1 1.6	2 11	5.1 2.6	1 79	5.4 4.6	8 224
Laguna La Torrecilla Laguna de Pinones	5.2 7.3	5.2 7.3	0 0	5.3 7.3	0 0	5.1 6.9	-2 -5	5.9 7.1	13 -2

Water Column Salinity (PPT)

Region	SC 1a	SC 1b	%	SC 1c	%	SC 2	%	SC 3	%	SC 4	%
San Juan Bay Cano Martin Pena	35.9 30.2	35.9 29.7	0 -2	35.7 31.5	-1 4	29.9 27.0	-17 -11	35.9 31.0	0 3	35.7 28.1	0 -7
Laguna San Jose Canal Suarez	7.2 9.6	9.6 13.6	34 42	24.1 27.6	235 188	0.5 2.1	-93 -78	11.2 14.9	55 55	9.0 27.6	25 188
Laguna La Torrecilla Laguna de Pinones	23.7 13.8	26.1 17.5	10 26	29.0 22.1	23 59	15.3 6.6	-35 -52	24.2 13.2	2 -5	29.1 22.4	23 61

Water Column Salinity (PPT)

Region	SC 1a	SC 5a	%	SC 5b	%	SC 6a	%	SC 6b	%
San Juan Bay Cano Martin Pena	35.9 30.2	35.9 30.2	0 0	35.9 30.2	0 0	35.7 31.5	-1 4	30.6 28.6	-15 -5
Laguna San Jose Canal Suarez	7.2 9.6	7.2 9.6	0 0	7.2 9.6	0 0	24.1 27.6	235 188	20.4 26.0	184 171
Laguna La Torrecilla Laguna de Pinones	23.7 13.8	23.7 13.8	0 0	23.7 13.8	0 0	29.0 22.1	23 59	24.8 16.5	5 19

Water Column Chlorophyll ($\mu\text{g/L}$)

Region	SC 1a	SC 1b	%	SC 1c	%	SC 2	%	SC 3	%	SC 4	%
San Juan Bay Cano Martin Pena	3.95 13.53	4.78 16.76	21 24	7.44 11.66	88 -14	2.50 4.44	-37 -67	3.27 9.41	-17 -30	6.13 18.80	55 39
Laguna San Jose Canal Suarez	32.30 31.31	29.86 27.51	-8 -12	25.26 16.13	-22 -48	8.50 6.82	-74 -78	33.99 30.37	5 -3	34.00 13.53	5 -57
Laguna La Torrecilla Laguna de Pinones	26.90 38.26	17.70 19.78	-34 -48	18.22 33.79	-32 -12	17.49 32.62	-35 -15	26.18 38.55	-3 1	18.39 33.78	-32 -12

Water Column Chlorophyll ($\mu\text{g/L}$)

Region	SC 1a	SC 5a	%	SC 5b	%	SC 6a	%	SC 6b	%
San Juan Bay Cano Martin Pena	3.95 13.53	3.63 12.19	-8 -10	3.67 11.31	-7 -16	6.10 8.65	54 -36	5.42 8.06	37 -40
Laguna San Jose Canal Suarez	32.30 31.31	30.28 29.86	-6 -5	22.99 25.73	-29 -18	15.74 13.76	-51 -56	14.90 13.98	-54 -55
Laguna La Torrecilla Laguna de Pinones	26.90 38.26	26.34 37.98	-2 -1	24.95 37.27	-7 -3	18.15 33.75	-33 -12	18.48 33.62	-31 -12

**Water Column
Total Nitrogen (mg/L)**

Region	SC 1a	SC 1b	%	SC 1c	%	SC 2	%	SC 3	%	SC 4	%
San Juan Bay Cano Martin Pena	0.0753 0.6112	0.0728 0.3230	-3 -47	0.0843 0.2262	12 -63	0.0591 0.5754	-21 -6	0.0727 0.3382	-3 -45	0.0815 0.3875	8 -37
Laguna San Jose Canal Suarez	0.9073 2.0877	0.7942 1.7914	-12 -14	0.5038 0.7041	-44 -66	0.1964 0.1433	-78 -93	0.8004 0.5963	-12 -71	1.0316 0.2971	14 -86
Laguna La Torrecilla Laguna de Pinones	0.6469 0.6610	0.3869 0.3585	-40 -46	0.4045 0.5881	-37 -11	0.3787 0.5854	-41 -11	0.6861 0.6680	6 1	0.4076 0.5883	-37 -11

**Water Column
Total Nitrogen (mg/L)**

Region	SC 1a	SC 5a	%	SC 5b	%	SC 6a	%	SC 6b	%
San Juan Bay Cano Martin Pena	0.0753 0.6112	0.0709 0.2822	-6 -54	0.0731 0.4977	-3 -19	0.0763 0.1879	1 -69	0.0634 0.1828	-16 -70
Laguna San Jose Canal Suarez	0.9073 2.0877	0.8577 2.0222	-5 -3	0.6790 1.8416	-25 -12	0.3250 0.6421	-64 -69	0.2985 0.2791	-67 -87
Laguna La Torrecilla Laguna de Pinones	0.6469 0.6610	0.6340 0.6563	-2 -1	0.6009 0.6446	-7 -2	0.4028 0.5875	-38 -11	0.3991 0.5986	-38 -9

**Water Column
Total Phosphorus (mg/L)**

Region	SC 1a	SC 1b	%	SC 1c	%	SC 2	%	SC 3	%	SC 4	%
San Juan Bay Cano Martin Pena	0.0383 0.1609	0.0370 0.1154	-3 -28	0.0375 0.0677	-2 -58	0.0241 0.1501	-37 -7	0.0375 0.1324	-2 -18	0.0396 0.1320	3 -18
Laguna San Jose Canal Suarez	0.1396 0.2856	0.1219 0.2551	-13 -11	0.0936 0.1481	-33 -48	0.1001 0.0841	-28 -71	0.1271 0.0955	-9 -67	0.1654 0.0892	18 -69
Laguna La Torrecilla Laguna de Pinones	0.1690 0.1034	0.1119 0.0728	-34 -30	0.1205 0.0934	-29 -10	0.1051 0.0788	-38 -24	0.1759 0.0974	4 -6	0.1194 0.0929	-29 -10

**Water Column
Total Phosphorus (mg/L)**

Region	SC 1a	SC 5a	%	SC 5b	%	SC 6a	%	SC 6b	%
San Juan Bay Cano Martin Pena	0.0383 0.1609	0.0373 0.1203	-2 -25	0.0381 0.1598	0 -1	0.0361 0.0606	-6 -62	0.0230 0.0528	-40 -67
Laguna San Jose Canal Suarez	0.1396 0.2856	0.1341 0.2806	-4 -2	0.1057 0.2622	-24 -8	0.0625 0.1407	-55 -51	0.0538 0.0513	-61 -82
Laguna La Torrecilla Laguna de Pinones	0.1690 0.1034	0.1675 0.1029	-1 0	0.1622 0.1009	-4 -2	0.1202 0.0932	-29 -10	0.1046 0.0811	-38 -22

**Water Column
Fecal Coliform (MPN/ml)**

Region	SC 1a	SC 1b	%	SC 1c	%	SC 2	%	SC 3	%	SC 4	%
San Juan Bay Cano Martin Pena	265.4 25974.0	270.4 25409.0	2 -2	335.4 19081.0	26 -27	292.1 26954.0	10 4	264.9 25689.0	0 -1	272.5 26534.0	3 2
Laguna San Jose Canal Suarez	2994.6 3.6	3086.6 13.8	3 281	3488.0 47.7	16 1219	4061.0 31.7	36 775	3281.5 283.1	10 7723	2562.1 28.9	-14 700
Laguna La Torrecilla Laguna de Pinones	1071.0 745.9	1071.4 747.2	0 0	1080.3 749.6	1 0	1781.6 743.8	66 0	1011.0 743.8	-6 0	1086.1 750.0	1 1

**Water Column
Fecal Coliform (MPN/ml)**

Region	SC 1a	SC 5a	%	SC 5b	%	SC 6a	%	SC 6b	%
San Juan Bay Cano Martin Pena	265.4 25974.0	264.4 22905.0	0 -12	265.4 25974.0	0 0	319.8 17729.0	21 -32	345.6 18320.0	30 -29
Laguna San Jose Canal Suarez	2994.6 3.6	2969.6 3.6	-1 0	1808.7 3.6	-40 0	2065.2 47.6	-31 1214	2827.9 79.1	-6 2084
Laguna La Torrecilla Laguna de Pinones	1071.0 745.9	1071.0 745.9	0 0	1071.0 745.9	0 0	1080.3 749.6	1 0	1792.2 748.4	67 0

REPORT DOCUMENTATION PAGE

Form Approved
OMB No. 0704-0188

Public reporting burden for this collection of information is estimated to average 1 hour per response, including the time for reviewing instructions, searching existing data sources, gathering and maintaining the data needed, and completing and reviewing the collection of information. Send comments regarding this burden estimate or any other aspect of this collection of information, including suggestions for reducing this burden, to Washington Headquarters Services, Directorate for Information Operations and Reports, 1215 Jefferson Davis Highway, Suite 1204, Arlington, VA 22202-4302, and to the Office of Management and Budget, Paperwork Reduction Project (0704-0188), Washington, DC 20503.

1. AGENCY USE ONLY (Leave blank)	2. REPORT DATE April 2000	3. REPORT TYPE AND DATES COVERED Final report	
4. TITLE AND SUBTITLE Hydrodynamic and Water Quality Model Study of San Juan Bay Estuary		5. FUNDING NUMBERS	
6. AUTHOR(S) Barry W. Bunch, Carl F. Cerco, Mark S. Dortch, Billy H. Johnson, Keu W. Kim			
7. PERFORMING ORGANIZATION NAME(S) AND ADDRESS(ES) U.S. Army Engineer Research and Development Center 3909 Halls Ferry Road, Vicksburg, MS 39180-6199		8. PERFORMING ORGANIZATION REPORT NUMBER ERDC TR-00-1	
9. SPONSORING/MONITORING AGENCY NAME(S) AND ADDRESS(ES) U.S. Army Engineer District, Jacksonville P.O. Box 4970 Jacksonville, FL 32232-0019		10. SPONSORING/MONITORING AGENCY REPORT NUMBER	
11. SUPPLEMENTARY NOTES			
12a. DISTRIBUTION/AVAILABILITY STATEMENT Approved for public release; distribution is unlimited.		12b. DISTRIBUTION CODE	
13. ABSTRACT (Maximum 200 words) This report describes a three-dimensional hydrodynamic and water quality model study of the San Juan Bay and Estuaries system conducted to evaluate the effectiveness of various management alternatives for improving water quality. Alternatives included methods to increase flushing, reduce pollutant loadings, and combinations of the two. The CH3D-WES hydrodynamic model and the CE-QUAL-ICM water quality model were employed in the study. The models were indirectly coupled and were adjusted and calibrated against data collected during the summer of 1995. Analysis of various management scenarios revealed that a combination of widening and deepening of Cano Martin Peña, filling of dredged submerged borrow pits, and removal of un-sewered loads in Cano Martin Peña provided the greatest water quality benefits.			
14. SUBJECT TERMS Estuary Flushing Hydrodynamic		15. NUMBER OF PAGES 298	
Loadings Model San Juan Bay		16. PRICE CODE	
17. SECURITY CLASSIFICATION OF REPORT UNCLASSIFIED		18. SECURITY CLASSIFICATION OF THIS PAGE UNCLASSIFIED	19. SECURITY CLASSIFICATION OF ABSTRACT
20. LIMITATION OF ABSTRACT			

Destroy this report when no longer needed. Do not return it to the originator.

Appendix A3

Development of the Benthic Index for the San Juan Bay Estuary System (PBS&J 2009a)

Table of Contents

1.0	Background	1
2.0	Methods	4
2.1.	Data Management.....	4
2.2.	Calculating the Index.....	5
2.3.	GIS Data	6
3.0	Results	7
3.1.	Benthic Index Scores	7
4.0	Discussion	22
4.1.	Prior Characterization Efforts	22
4.2.	Benthic Index Scores	22
5.0	Value And Use Of The Benthic Index And Other Findings	25
6.0	Literature Cited.....	26

List of Figures:

Figure 1	Location of Major Features in the San Juan Bay Estuary Program Study Area (from SJBEP 2000).....	1
Figure 2	Locations and Benthic Index Scores for stations located in San Juan Bay. Values are color-coded as to their Benthic Index Scores.....	8
Figure 3	Locations and Benthic Index Scores for stations located in Condado Lagoon. Values are color-coded as to their Benthic Index Scores.....	9
Figure 4	Locations and Benthic Index Scores for stations located in San José Lagoon. Values are color-coded as to their Benthic Index Scores.....	10
Figure 5	Locations and Benthic Index Scores for stations located in Torrecilla Lagoon. Values are color-coded as to their Benthic Index Scores.....	11
Figure 6	Locations and Benthic Index Scores for stations located in Piñones Lagoon. Values are color-coded as to their benthic Index Scores.....	12
Figure 7	Locations of benthic sampling stations and bathymetry. Bathymetry data from SJBEP [2000].....	16
Figure 8	Benthic Index scores across different depth categories.....	19
Figure 9	Benthic Index scores vs. distance from the Atlantic Ocean.....	20
Figure 10	Benthic Index scores for stations less than and greater than 5,000 meters from the Atlantic Ocean.....	21

List of Tables:

Table 1	Benthic Stations at Which There Were Location Issues.....	4
Table 2	Benthic Index Scores for Individual Waterbodies.....	7
Table 3	Summary of Benthic Index Scores, water depth (feet) and distance to the Atlantic Ocean (m) for each benthic sampling stations.....	18
Table 4	Comparison of scores produced using Water Quality Index and Benthic Index techniques.....	24

1.0 Background

The San Juan Bay estuarine complex (SJBE) includes San Juan Bay, Condado Lagoon, San José Lagoon, Los Corozos Lagoon, La Torrecilla Lagoon, and Piñones Lagoon. Also included are the Martín Peña Canal, which connects San Juan Bay and San José Lagoon, the San Antonio Canal, which connects San Juan Bay and Condado Lagoon, and the Suárez Canal, which connects San José Lagoon and Torrecilla Lagoon (see figure 1).



Figure 1
Location of Major Features in the San Juan Bay Estuary Program
Study Area (from SJBEP 2000)

Impacts to water and sediment quality include not only the high population density in some portions of the watershed, but also the very high density of automobiles used by the population. The density (vehicles per mile of paved road) in the San Juan Bay Estuary watershed is nearly three times the US mainland average (SJBEP 2000). Population densities were lowest in the region surrounding Piñones Lagoon, and highest in the regions surrounding Condado Lagoon (SJBEP 2000). The high level of automobile use in the watershed suggests that contaminants associated with such use (i.e., greases, PAHs, etc.) would also be elevated in the bay's sediments.

Water quality, and the quality of bottom sediments in the San Juan Bay system are impacted by point and non-point pollution, impacts to circulation from channel dredging and filling (especially adjacent to the Martín Peña Canal), erosion from upland areas of the watershed, and resuspension of bottom sediments (SJBEP 2000).

In recognition of these and other threats to the health of the SJBE, the Governor of Puerto Rico nominated the SJBE system for the U.S. Environmental Protection Agency's National Estuary Program in 1992. The goals of the SJBEP are the following:

- Establish a comprehensive water quality policy.
- Develop an administrative and regulatory framework for the SJBEP.
- Optimize the social, economic and recreational benefits of the estuary.
- Prevent further degradation, and improve water quality to ensure healthy terrestrial and aquatic systems and social well-being.
- Minimize health risks associated with bodily contact and the consumption of fish and shellfish.

These goals are to be accomplished via undertaking a series of actions meant to allow the SJBEP to meet specific measurable objectives:

- Identification of the major stressors to the system, and their relative importance.
- Develop action plans to remediate these stressors.
- Conserve and enhance the natural resources of the SJBEP system.
- Promote public awareness and address major concerns of various stakeholders.
- Develop a hydrologic model sufficient to determine appropriate mechanisms to improve circulation and guide future development.

In its early stages, the SJBEP completed a series of studies designed to collect baseline information, establish appropriate indicators of ecosystem health, and enable the analysis of such information to be used to assess progress toward achievement of program goals (Otero 2002).

This project was designed to provide the SJBEP with a regionally-appropriate benthic index for the SJBE. This index can then be used as an indicator of the environmental condition of the estuary. This indicator can be used to compare and contrast segments of the San Juan Bay Estuary system against each other, and also to track the health of the benthic communities over time both on a localized level (e.g., Torrecilla Lagoon) or a regional level (e.g., San Juan Bay Estuary as a whole).

A benthic index can be useful for summarizing complex information in a way that allows for review and assessment by technical staff without specific technical expertise in benthic ecology, and can also be a valuable tool for public education. According to EPA (2008) "Indicators can be a cost-effective, accurate alternative to monitoring the individual components of a system."

The EPA (2008) suggests that a suite of different indicators, such as the following, can be useful: 1) a water quality index, 2) a sediment quality index, 3) a benthic index, 4) a coastal habitat index, and 5) a fish tissue contaminants index. For a benthic index, the topic of this effort, EPA (2008) recommends it contain information on benthic community diversity, the presence or absence of pollution-tolerant taxa, and the presence or absence of pollution-sensitive taxa.

Benthic communities, and benthic indexes, can be a useful tool to track degradation and/or improvements in watershed-level pollutant loading, as they “integrate” water and sediment quality conditions on a longer timescale than a single point in time sample in a collection bottle.

With this information as background, we have developed a benthic index for the San Juan Bay Estuary, using the below-described approach.

2.0 Methods

2.1. Data Management

Benthic sampling data were provided by SJBEP in the form of Appendices C-E from Rivera (2005). These data were arranged into a single data table and data describing the family classification for each taxon were added based on a review of data via the Integrated Taxonomic Information System (ITIS, www.itis.gov). Location data for GIS maps were provided in Appendix J from Rivera (2005). These data were reviewed, and when the stated location (i.e. San Juan Bay, Condado Lagoon, etc.) did not agree with the provided coordinates these samples were removed from the maps. However some samples were still used in calculating descriptive statistics. The described location of a sample rather than provided coordinates was used to assign the station location for those stations where such a discrepancy occurred (Table 1).

Table 1
Benthic Stations at Which There Were Location Issues

STATION	COMMENT
BA-401	Is identified as being in a channel, however it's GIS position puts it squarely in San Juan Bay, index score of 1.78 seems to be more representative of the channels than San Juan Bay, use data for analysis of channels
JM-M001	Station is identified as being in a channel, it is located near the mouth of a drainage channel to SJL , this sample is within SJL proper and will be used in the SJL analyses
S1	Station is identified as being in SJB, however the GPS coordinates place it on land, the data from this station will be used for SJB analyses
S19	Station is identified as being in San José Lagoon (SJL), however the GPS coordinates place it in SJB, the Index Score would be the highest score in SJL, and would fit in very well in SJB, because of the uncertainty associated with the sample location it will not be included in the analyses
S29C	Station is identified as being in SJL, however the GPS coordinates place it on the Atlantic shoreline near CL, data from this sample will be included in the analyses for SJL
S4	Station is identified as "Atlantic", GPS coordinates place the sample in Torrecilla Lagoon (TL), there were no other TL samples from the Coastal 2000 study, so it is very likely that this sample actually occurred in TL, data from this sample will be included in the analyses
S43	Station is identified as being in Condado Lagoon (CL), however the GPS coordinates place it in SJB proper the Index Score of 2.85 appears to fit with either CL or SJB, because of the uncertainty associated with the sample location it will not be included in the analyses
S5	Station is identified as being in SJB, however the GPS coordinates place it in SJL, the index score of 3.33 does not fit in with the SJL samples surrounding it, because of the uncertainty associated with the location of this sample it will not be used in the analyses
SF-M001	Station is identified as being in a channel, it is located at the mouth of a small bay within SJB (see sample SJB_B004), this sample is within SJB proper and will be used in the SJB analyses
SJB_B004	Sample is in a small bay within SJB that is not representative of the general condition of SJB, Index score of 0.0 will be used in SJB calculations, but the site difference needed to be described

2.2. Calculating the Index

All calculations were performed using Statistical Analysis Software (SAS). For all analyses the family taxonomic level was utilized. The total abundance of each family of organisms was calculated for each sample. The initial component of the index is Shannon Diversity scores. These scores integrate taxonomic richness, abundance, and evenness of distribution into a single calculated number. The equation for Shannon Diversity is:

$$H = - \sum_{i=1}^S (P_i * \ln P_i)$$

Where:

H= Shannon Diversity Index Score

P_i= Proportion of sample comprised of family i

S = Number of families in the sample

Based on recommendations found in the literature additional components were added to create the benthic index score. Adjustments were made so that the score would increase due to the presence of members of the families Aoridae and Ampeliscidae, which are generally pollution-sensitive organisms (Lee et al 2005, Weston 1996, Traunspurger and Drews 1996). The score also decreases due to the presence of members of the families Capitellidae and Tubificidae, which are regarded as pollution-tolerant, or indicative of disturbed benthic habitat (Paul et al 2001, Pinto et al. 2009). These components were added to the index equation in an iterative manner until the results matched a scale deemed appropriate. The resultant San Juan Bay benthic index equation is as follows:

$$B = H - P_{Cap}^2 - P_{Tub}^2 + P_{Aor}^{0.5} + P_{Amp}^{0.5} + 1$$

Where:

B = Benthic Index Score

H = Shannon Diversity Score

P_{cap} = Proportion of the sample in the family Capitellidae

P_{Tub} = Proportion of the sample in the family Tubificidae

P_{Aor} = Proportion of the sample in the family Aoridae

P_{Amp} = Proportion of the sample in the family Ampeliscidae

This equation was then applied to the provided benthic data and scores were generated based on those data. The results were reviewed with the ArcGIS software utilizing data for substrate type and depth to further explain the benthic index scores.

2.3. GIS Data

The SAV and bathymetry data were geo-referenced from the San Juan Bay Estuary Program Management Plan. The SAV data were then converted from raster data to vector features. All features corresponding to Non-Dredge SAV were selected and quantified. Bathymetry data was digitized and quantified.

In addition the shortest feasible non-landward route from each sample point to the Atlantic Ocean was measured in ArcGIS. An identity function was performed on the benthic stations, bathymetry, and habitat data for each station used in the Benthic Index.

3.0 Results

3.1. Benthic Index Scores

Mean benthic index scores ranged from 0 in the Suarez Canal to 2.74 in Torrecilla Lagoon. Torrecilla Lagoon, Condado Lagoon, and San Juan Bay were found to have higher mean benthic habitat scores than San José Lagoon and Piñones Lagoon (Table 2). Individual sample scores ranged from a minimum of 0.00 (in all waterbodies except Condado Lagoon and Torrecilla Lagoon) to a maximum of 4.13 in San Juan Bay.

Table 2
Benthic Index Scores for Individual Waterbodies

Waterbody	Mean	Standard Deviation	Maximum	Median	Minimum	Number of Observations
San Juan Bay	2.74	0.80	4.13	2.86	1.45	15
Condado Lagoon	2.62	1.09	4.01	3.04	1.00	7
San José Lagoon	1.14	1.03	2.24	1.63	0.00	12
Torrecilla Lagoon	3.07	0.42	3.41	3.21	2.35	5
Piñones Lagoon	1.01	0.88	2.14	0.95	0.00	4
San Antonio Canal	3.09		3.09	3.09	3.09	1
Martín Peña Canal	1.00		1.00	1.00	1.00	1
Suárez Canal	0.00	0.00	0.00	0.00	0.00	2
Other Channel Sites	1.48	0.20	1.63	1.56	1.26	3

These data were tested for differences, if any, between waterbodies for those systems with at least four samples. Benthic Index Scores were found to be normally distributed and homoscedastic for each waterbody, therefore ANOVA and Fischer's Least Significant Difference (LSD) multiple comparison test were used to compare scores for waterbodies with at least four samples. ANOVA indicated that significant ($p < 0.01$) differences existed for scores. Fischer's LSD test indicated that two groups existed, concerning Benthic Index scores; Piñones Lagoon and San José Lagoon were not different from each other, but they were different from San Juan Bay, Condado Lagoon, and Torrecilla Lagoon (which were also not different from each other).

Figures 2 to 9 illustrate the spatial distribution of benthic index scores for San Juan Bay, Condado Lagoon, San José Lagoon, Torrecilla Lagoon, Piñones Lagoon, San Antonio Canal, Martín Peña Canal, and Suárez Canal, respectively.



Figure 2
Locations and Benthic Index Scores for Stations Located in San Juan Bay
Values are Color-Coded as to their Benthic Index Scores



Figure 3
Locations and Benthic Index Scores for Stations Located in Condado Lagoon
Values are Color-coded as to their Benthic Index Scores



Figure 4
Locations and Benthic Index Scores for Stations located in San José Lagoon
Values are Color-coded as to their Benthic Index Scores

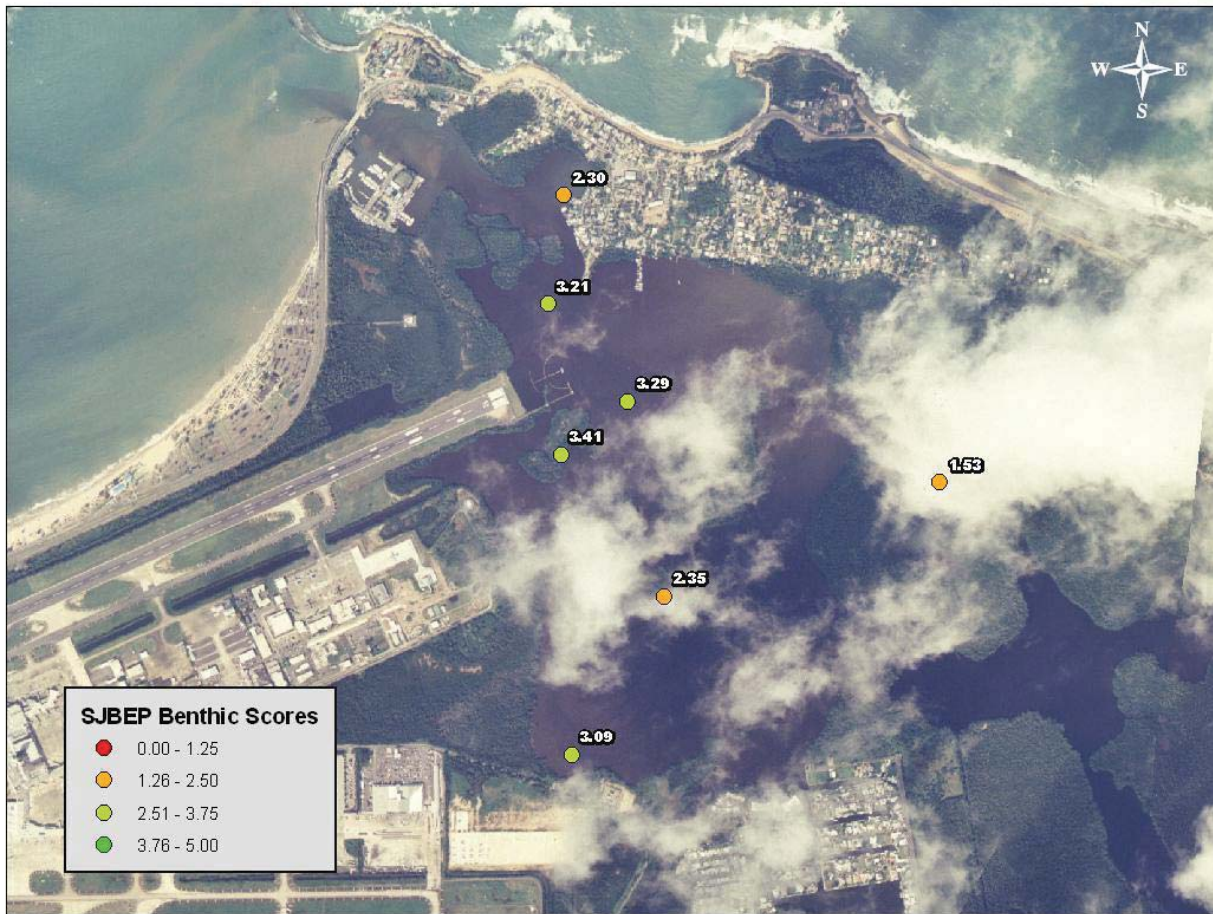


Figure 5
Locations and Benthic Index Scores for Stations located in Torrecilla Lagoon
Values are Color-coded as to their Benthic Index Scores

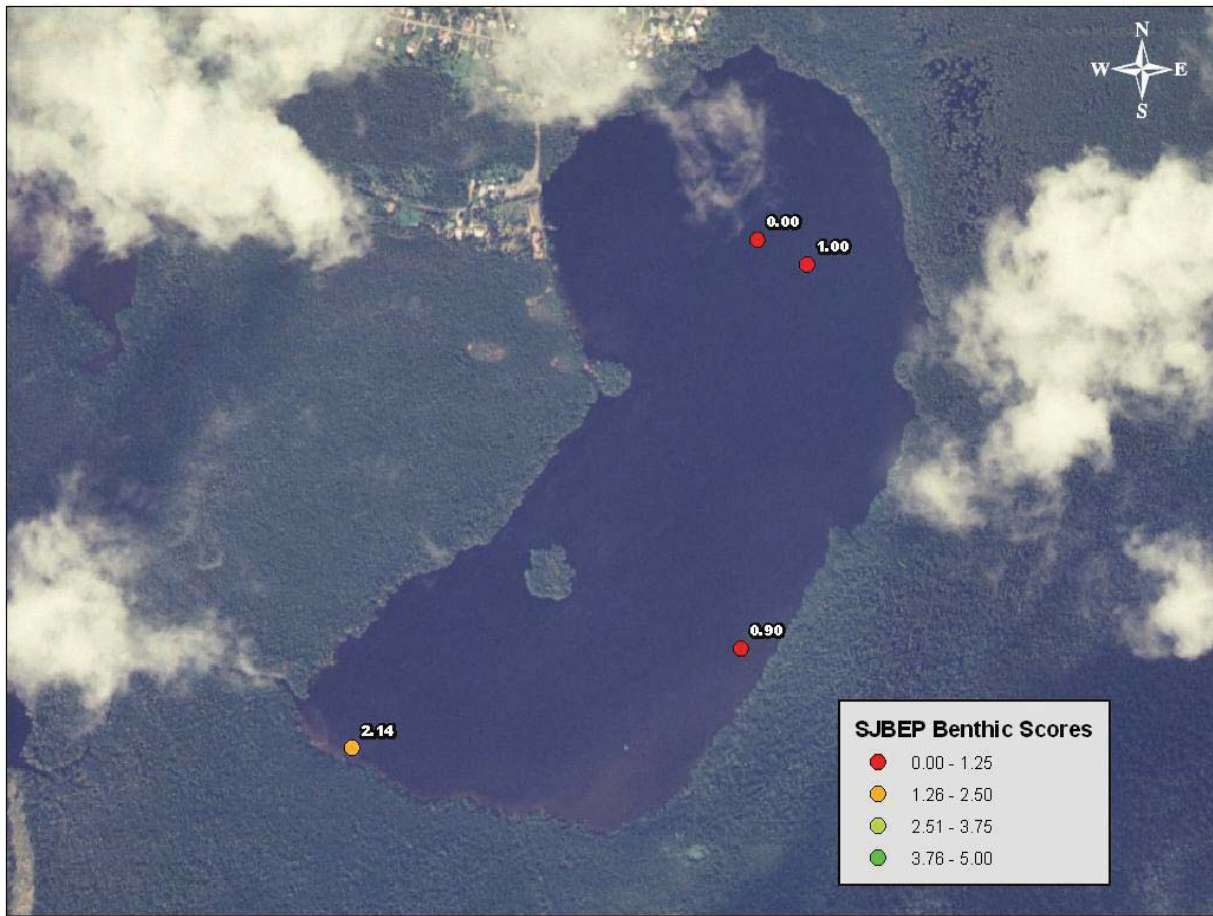


Figure 6
Locations and Benthic Index Scores for Stations located in Piñones Lagoon
Values are Color-coded as to their Benthic Index Scores

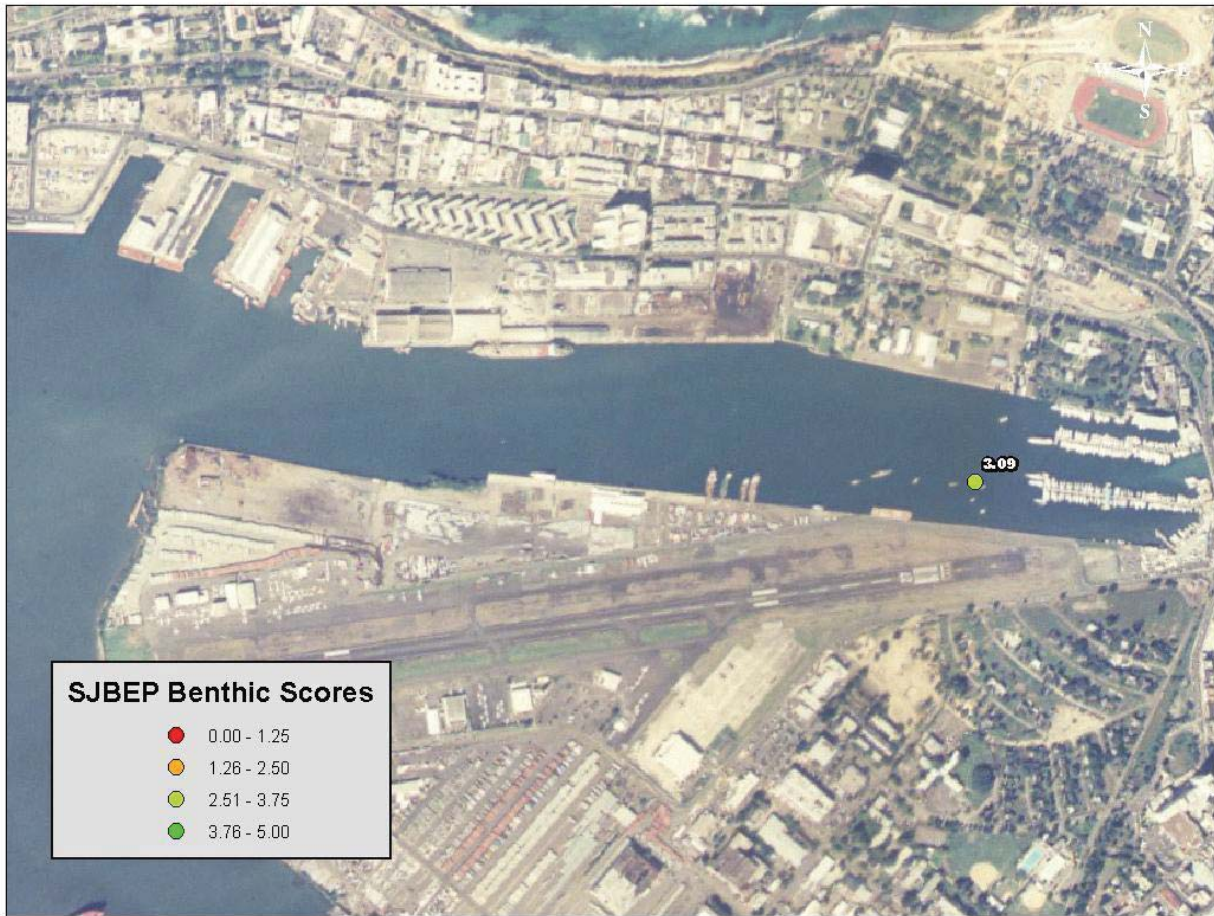


Figure 7
Locations and Benthic Index Scores for stations located in San Antonio Canal. Values are color-coded as to their benthic Index Scores.

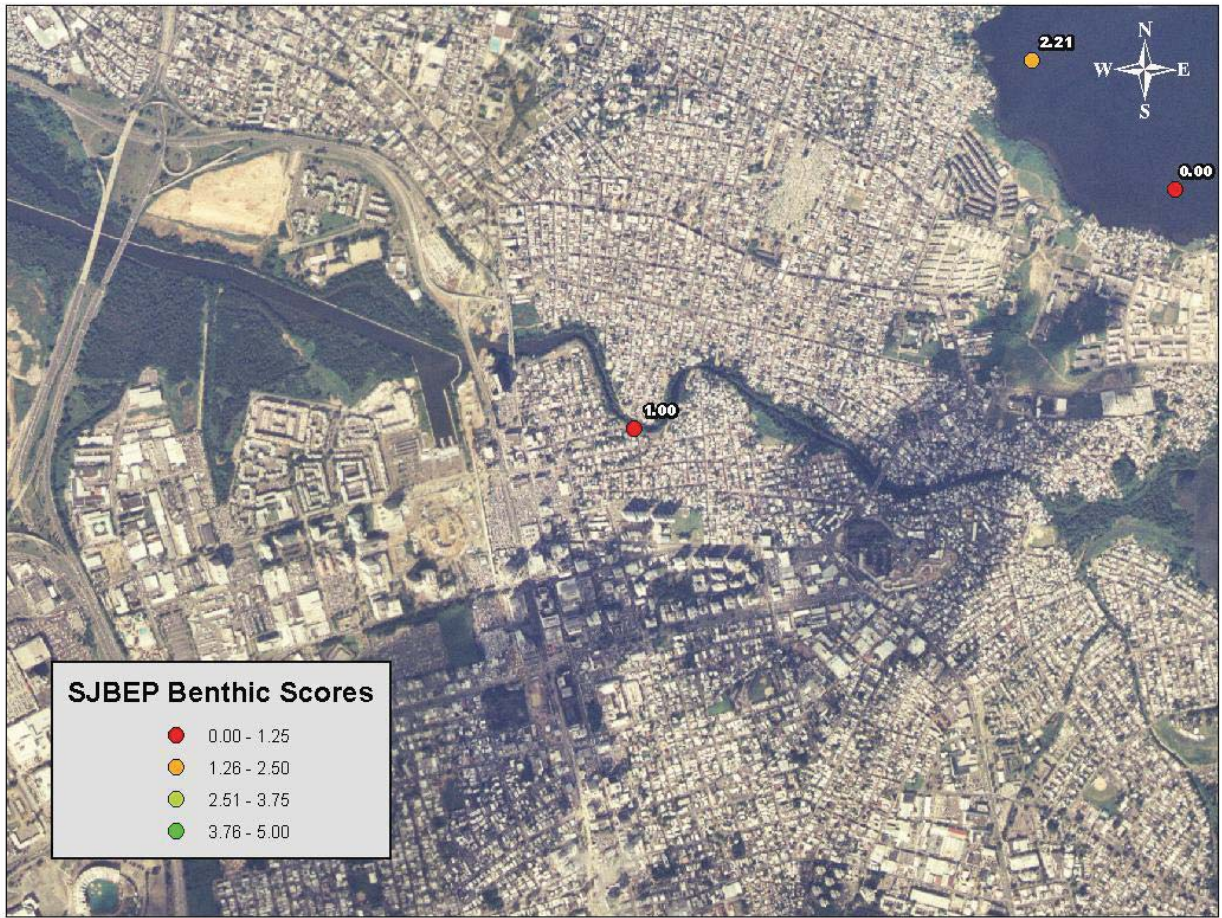


Figure 8
Locations and Benthic Index Scores for stations located in Martín Peña Canal. Values are color-coded as to their benthic Index Scores.

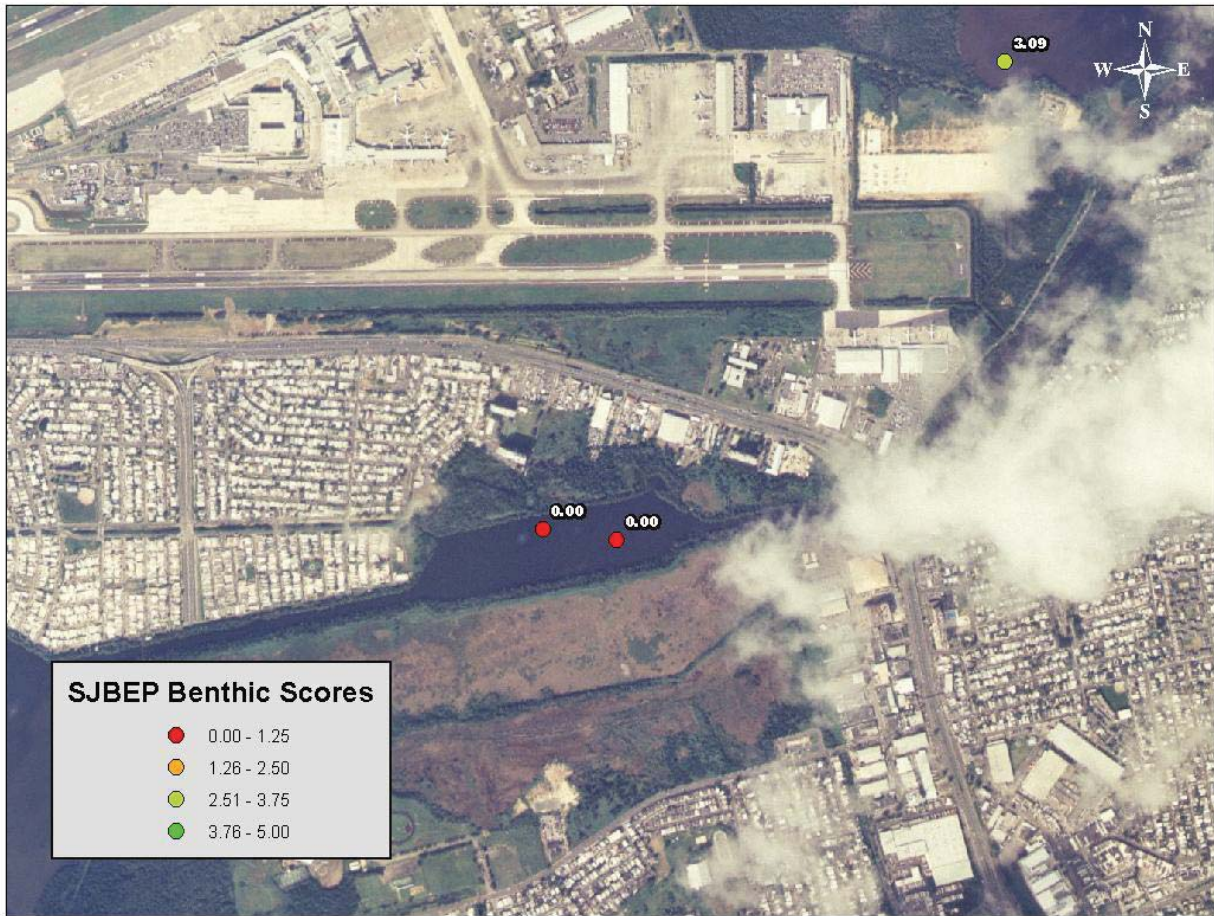


Figure 9
Locations and Benthic Index Scores for stations located in Suárez Canal. Values are color-coded as to their benthic Index Scores.

Additional data sets were analyzed to aid in the interpretation of the Benthic Index Scores. Using a bathymetry layer derived from the bathymetry map shown in SJBEP (2000), station locations were displayed on top the bathymetric contours derived from the map (Figure 10).

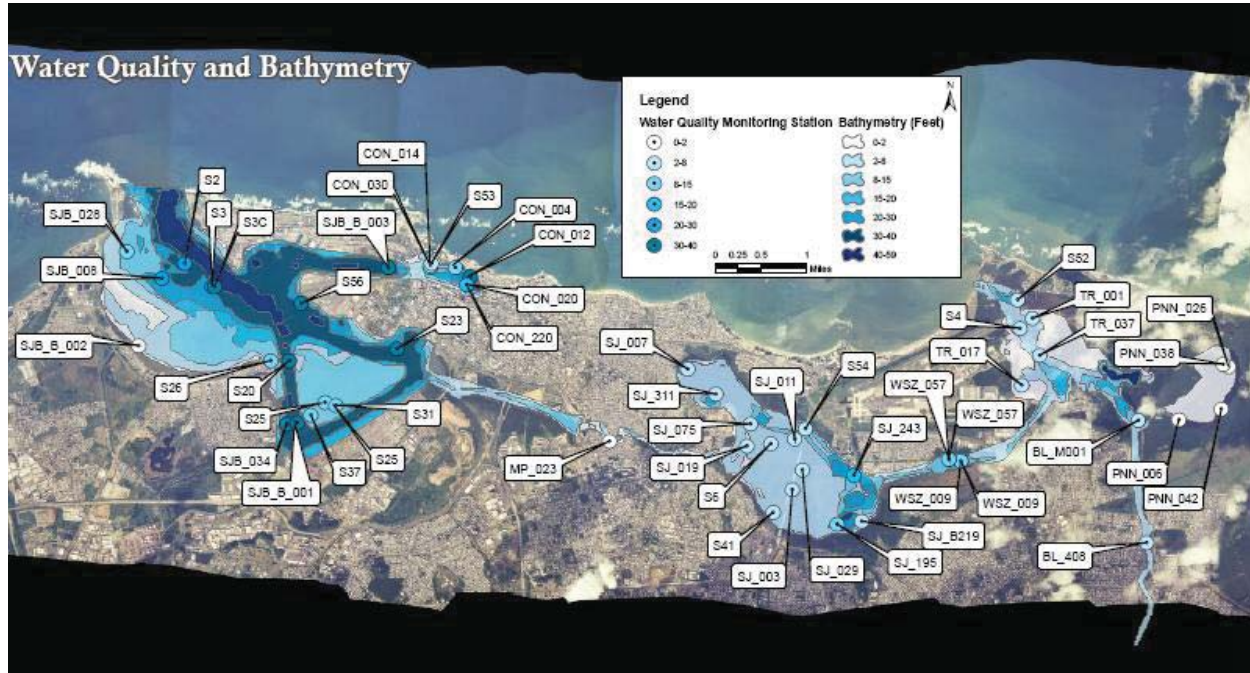


Figure 10
Locations of Benthic sampling Stations and Bathymetry
Bathymetry Data from SJBEP [2000]

Bathymetry within San Juan Bay itself is deeper along the northern boundary of the bay, especially near the opening to the Atlantic Ocean. There is a well-defined shipping channel in the southeastern portion of the bay, forming a triangle with a shallow shelf interior to the dredged channels. Within San Juan Bay, benthic sampling stations were located in both shallow water (0 to 2 feet), deep water (30 to 40 feet) and in all depth categories between these two extremes.

In Condado Lagoon, some of the sampling sites in the eastern part of the lagoon are located in dredged areas more than 20 feet in depth. Benthic sampling sites in the western part of Condado Lagoon are in shallower, non-dredged areas.

The bathymetry in San José Lagoon shows deeper dredged areas in the far eastern portions, with a mostly natural and shallow (2 to 8 feet) bottom. Two of the three benthic sampling sites in the easternmost part of San José Lagoon appear to be located in areas that have been dredged in the past.

In Torrecilla Lagoon, the irregular and angular boundaries of some of the bathymetry layer boundaries suggest significant dredging activities. Most of the benthic sampling sites in Torrecilla Lagoon appear to be located in areas that might be influenced by prior dredging.

The bathymetry data for Piñones Lagoon indicates no significant dredging activity, as the entirety of the lagoon appears to be uniformly shallow, with depths no deeper than 8 feet. Based on bathymetry data, Piñones Lagoon appears to have the least impact from dredging of any portion of the San Juan Bay system.

In addition to the existing bathymetry data, GIS was used to calculate the distance between benthic sampling sites and the nearest connection to the Atlantic Ocean. For each location, GIS was used to estimate the shortest practical distance between that location and the Atlantic; all routes were restricted to open water only, without crossing any land features. Flushing of San José Lagoon occurs almost entirely via the Suárez Canal, rather than the Martín Peña Canal. Therefore locations in San José Lagoon were measured based on an eastward connection to the Atlantic Ocean via Suárez canal.

Table 3 summarizes data for each station for Benthic Index Scores, water depth, and distance from that station to the Atlantic Ocean. These data were used for further analyses, described below.

Table 3
Summary of Benthic Index Scores, Water Depth (feet) and Distance to the Atlantic Ocean (m) for each Benthic Sampling Station

STATION	CODE	LONGITUDE	LATITUDE	BENTHIC INDEX SCORE	BATHYMETRY (ft)	Distance to Atlantic Ocean (m)
BL_M001	Channel	-65.96714	18.43283	1.26	8-Feb	4,097
BL_408	Channel	-65.96613	18.41338	1.56	8-Feb	6,248
S6	Channel	-66.02825	18.43009	1.63	8-Feb	8,097
S53	Condado Lagoon	-66.08413	18.45953	4.01	8-Feb	414
CON_030	Condado Lagoon	-66.08436	18.45916	3.04	15-Aug	452
CON_014	Condado Lagoon	-66.08436	18.45887	2.95	15-Aug	489
CON_004	Condado Lagoon	-66.08021	18.45889	1	15-Aug	690
CON_220	Condado Lagoon	-66.07837	18.4561	3.05	15-20	1,000
CON_012	Condado Lagoon	-66.07771	18.45734	1.24	30-40	1,014
CON_020	Condado Lagoon	-66.07814	18.45602	3.05	15-20	1,015
MP_023	Martin Pena Canal	-66.05505	18.43089	1	0-2	9,260
PNN_006	Pinones Lagoon	-65.96048	18.43277	2.14	0-2	4,906
PNN_042	Pinones Lagoon	-65.95335	18.43439	0.9	0-2	5,553
PNN_038	Pinones Lagoon	-65.95292	18.44151	0	0-2	5,948
PNN_026	Pinones Lagoon	-65.95203	18.44107	1	0-2	5,982
SJB_B_003	San Antonio Canal	-66.09133	18.45902	3.09	30-40	1,070
SJ_243	San Jose Lagoon	-66.0146	18.42487	0	15-20	6,364
SJ_B219	San Jose Lagoon	-66.01338	18.41753	0	8-Feb	7,064
SJ_195	San Jose Lagoon	-66.01749	18.41716	0	15-Aug	7,223
SJ_029	San Jose Lagoon	-66.02305	18.42589	2.24	8-Feb	7,522
SJ_003	San Jose Lagoon	-66.02484	18.42278	0	8-Feb	7,652
S54	San Jose Lagoon	-66.02249	18.43233	1.68	8-Feb	7,760
SJ_011	San Jose Lagoon	-66.02423	18.43075	2.13	8-Feb	7,780
S41	San Jose Lagoon	-66.02804	18.41918	1.69	8-Feb	8,026
SJ_019	San Jose Lagoon	-66.03222	18.42975	2.12	8-Feb	8,561
SJ_075	San Jose Lagoon	-66.03161	18.43332	1.58	8-Feb	8,679
SJ_311	San Jose Lagoon	-66.03724	18.43807	0	8-Feb	9,359
SJ_007	San Jose Lagoon	-66.04186	18.44217	2.21	8-Feb	10,127
SJB_028	San Juan Bay	-66.13472	18.46227	2.93	15-Aug	1,112
S2	San Juan Bay	-66.12514	18.46016	3	20-30	1,230
SJB_008	San Juan Bay	-66.12894	18.45788	2.27	20-30	1,420
S3	San Juan Bay	-66.12065	18.45645	2.86	20-30	1,802

S3C	San Juan Bay	-66.12025	18.45645	4.13	30-40	1,808
SJB_B_002	San Juan Bay	-66.13293	18.44726	3.04	0-2	2,922
S56	San Juan Bay	-66.10585	18.45357	2.25	30-40	3,115
S26	San Juan Bay	-66.11105	18.44456	4.1	15-Aug	3,445
S20	San Juan Bay	-66.10799	18.44453	2.68	30-40	3,631
S25	San Juan Bay	-66.10218	18.4378	2.5	15-Aug	4,584
SJB_034	San Juan Bay	-66.1086	18.43446	1.69	30-40	4,644
S37	San Juan Bay	-66.10463	18.4358	3.43	15-Aug	4,647
SJB_B_001	San Juan Bay	-66.10691	18.4346	3.03	30-40	4,664
S31	San Juan Bay	-66.10042	18.43726	1.45	15-Aug	4,743
S23	San Juan Bay	-66.09015	18.4461	1.69	30-40	5,102
WSZ_009	Suarez Canal	-65.9968	18.42689	0	20-30	4,642
WSZ_057	Suarez Canal	-65.99873	18.42719	0	20-30	4,936
S52	Torrecilla Bay	-65.98691	18.45223	3.21	8-Feb	887
TR_001	Torrecilla Bay	-65.98446	18.44926	3.29	8-Feb	1,323
S4	Torrecilla Bay	-65.98658	18.4477	3.41	8-Feb	1,475
TR_037	Torrecilla Bay	-65.98341	18.44341	2.35	8-Feb	2,004
TR_017	Torrecilla Bay	-65.9864	18.43869	3.09	8-Feb	2,587

These data were then used to test for the effects, if any, of water depth and distance from the Atlantic Ocean as potential influences on Benthic Index scores for the entire SJBE system combined (Figures 11 and 12, respectively).

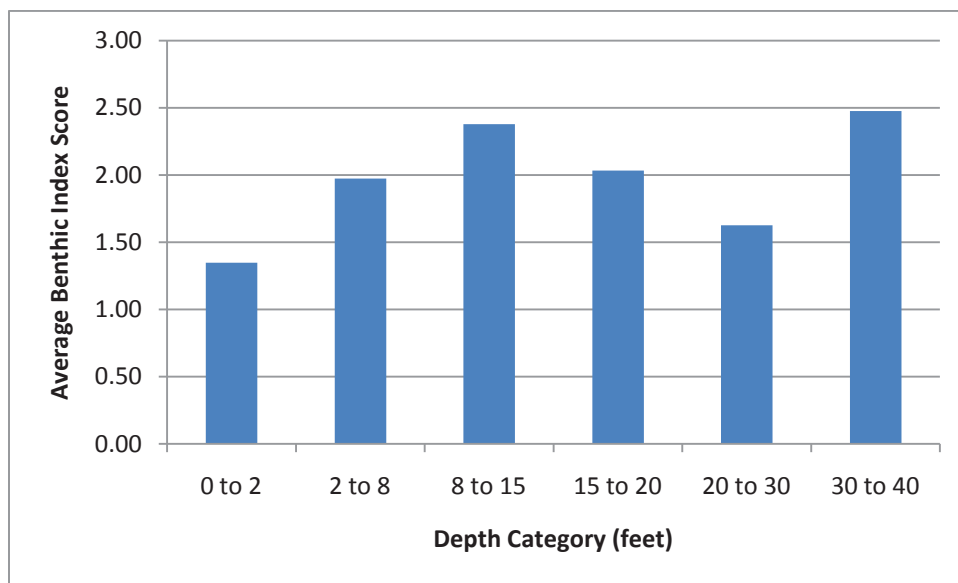


Figure 11
Benthic Index Scores across Different Depth Categories

When categorized for depth, Benthic Index scores were normally distributed and homoscedastic. ANOVA found no significant difference in Benthic Index scores between different depth categories ($p = 0.514$). As an additional assessment, the non-parametric Kruskal-Wallis test was employed, and it also found no affect of depth on Benthic Index scores ($p = 0.482$).

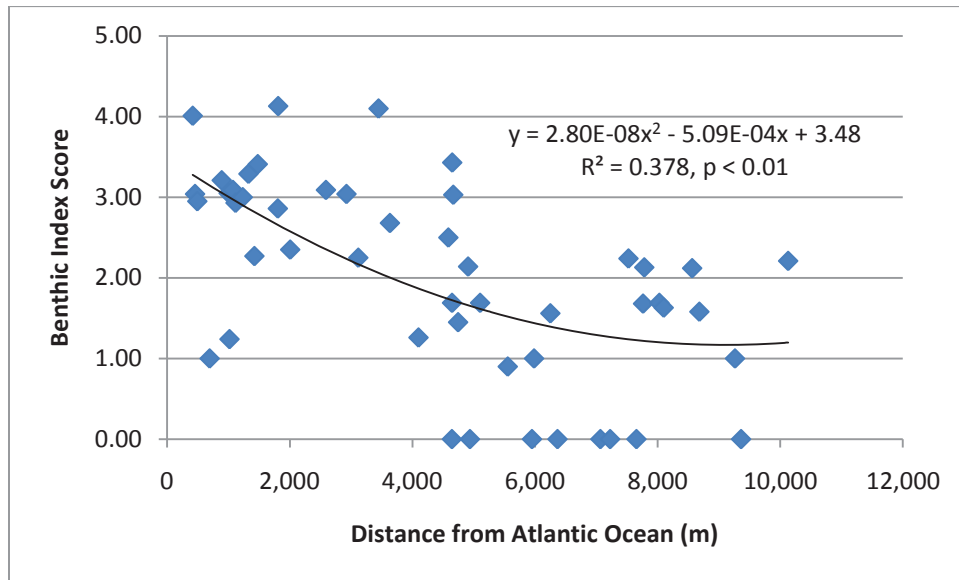


Figure 12
Benthic Index Scores vs. Distance from the Atlantic Ocean

Results shown in Figure 12 show a relationship wherein increasing distance from the Atlantic Ocean, an inverse proxy for the rate of flushing, is associated with a general pattern of decreasing Benthic Index scores. These data were found to be normally distributed and homoscedastic, and the polynomial equation relating Benthic Index scores to distance from the Atlantic was significant at $p < 0.01$. As an additional assessment, the non-parametric Spearman's Rho test was employed, which also found a statistically significant relationship between the ranked values of these two factors ($p < 0.01$).

When examining the distance vs. Benthic Index scores plot, it appeared as if the data more or less represented two groups of data, scores for stations less than 5,000 meters from the Atlantic Ocean, and scores for stations at greater distances. Figure 13 shows the results when data are segregated into these two groups.

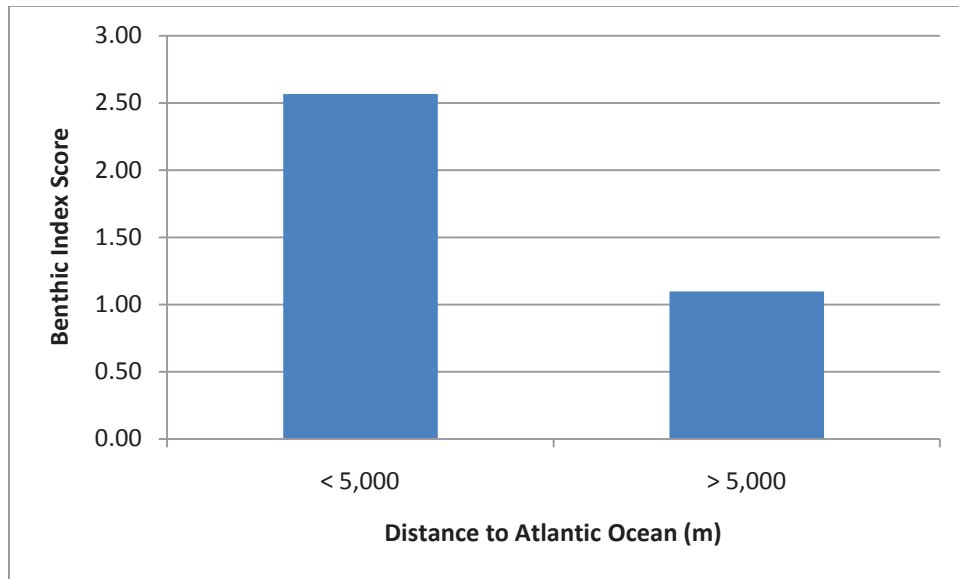


Figure 13
Benthic Index Scores for Stations Less Than and Greater Than 5,000 meters from the Atlantic Ocean

When grouped in this manner, the data are not normally distributed. The non-parametric Mann-Whitney U-test indicated that Benthic Index scores for stations less than 5,000 meters from the Atlantic Ocean were significantly higher ($p < 0.05$) than for stations greater than 5,000 meters from the Atlantic. However, waterbodies such as San José Lagoon and Piñones Lagoon may have underlying features such as toxicity of sediments, frequency of disturbance, etc., that could be equally if not more important influences on Benthic Index scores than flushing rates. Caution is required when interpreting these results as suggesting distance from the Atlantic Ocean (with distance acting as an inverse surrogate for flushing) is the dominant influence on the health of benthic communities.

4.0 Discussion

4.1. Prior Characterization Efforts

The sediments within the San Juan Bay Estuary System have been previously characterized by Webb and Gomez-Gomez (1998) and Webb et al. (1998). These reports summarized results of sediment contamination levels and sedimentation rates from six sites throughout the SJBEP study area. Sediment dating techniques were used to compare contamination levels between the time periods of 1925 to 1949, 1950 to 1974, and 1975 to 1995.

For the earliest (deepest) sediments analyzed, levels of lead, mercury, and arsenic in sediment were similar to values from streams in undisturbed portions of the watershed. These results indicate contamination was minimal in the time period prior to 1950 (Webb and Gomez-Gomez, 1998; Webb et al., 1998).

After 1950, levels of PCBs (used in electrical transformers, etc.), lead (from leaded gasoline and paints) and mercury increased in the sediments. Agricultural chemicals such as dieldrin and DDT also increased post-1950. Results also indicate recent declines in levels of dieldrin and DDT, as well as a decline in levels of arsenic throughout the San Juan Bay Estuary (Webb and Gomez-Gomez, 1998; Webb et al., 1998). Declines in lead and DDT are expected to occur as a result of relatively recent (mid-1980s) phase-out of leaded gasoline and bans on DDT, but sediments do not yet show such a pattern.

Sedimentation rates appear to be nearly two orders of magnitude higher in the Martín Peña Canal than in other locations, suggesting that location is a probable “hot spot” for the accumulation of toxins in bottom sediments, a finding not at all in conflict with expectations (SJBEP 2000).

In addition to the potential impacts to benthic communities from toxins in sediments, benthic communities can also be stressed via fluctuations in salinity regimes (Montague and Ley, 1993, Fleischer and Zettler, 2008) and depressed levels of dissolved oxygen and other stressors (Dauer et al. 2000, Llanso et al. 2002).

In the San Juan Bay Estuary, Webb and Gomez-Gomez (1998) and Webb et al. (1998) showed evidence of declining levels of phosphorus within the waters of the bay itself, possibly related to upgrades in levels of wastewater treatment. As a whole, trends in sediment contaminant levels and water quality are suggestive of a situation where the San Juan Bay system may be degraded, but it also may be improving over time – albeit perhaps not at an equal rate in all locations.

4.2. Benthic Index Scores

The Benthic Index created for San Juan Bay can be used to compare the waterbodies of the SJBE against each other, as well as tracking waterbodies over time. Comparing waterbodies against each other, San Juan Bay, Condado Lagoon and the Torrecilla Lagoon all had median Benthic Index scores close to (San Juan Bay) or higher than (Condado Lagoon and Torrecilla Lagoon) a value of three. As a whole, these three systems appear to have the healthiest benthic

communities, with greater species diversity, a lower percentage of pollution tolerant species, and a higher percentage of pollution intolerant species than other locations.

San José Lagoon and the various Channel locations (including the Martín Peña Canal) had median Benthic Index scores of 1.69 and 1.35, respectively. These data show that overall species diversity and the percentages of pollution intolerant organisms are lower in San José Lagoon and the various Channel locations than in San Juan Bay, and much lower than Condado Lagoon and Torrecilla Lagoon.

Based on median values, the lowest Benthic Index score of any waterbody was found in Piñones Lagoon (1.00). However, when comparing mean values, the Channel locations had slightly worse Benthic Index scores than Piñones Lagoon (1.18 and 1.21, respectively). The difference in order found when using mean vs. median values suggests that an appropriate classification scheme might be constructed as follows:

- Healthiest benthic communities: Torrecilla Lagoon and Condado Lagoon
- Healthy benthic communities: San Juan Bay
- Moderately healthy to stressed benthic communities: San José Lagoon
- Stressed benthic communities: Canal locations and Piñones Lagoon

The low scores in Piñones Lagoon should be interpreted considering the possibility that such a condition might be somewhat or entirely appropriate for that particular location. While Benthic Index scores were much higher in Condado Lagoon than in Piñones Lagoon, population density within the watershed of Condado Lagoon is much higher than in the region surrounding Piñones Lagoon (SJBEP 2000).

When comparing these Benthic Index scores to a previously constructed Water Quality Index (as summarized in the “Tarjeta de Calificaciones” produced by the SJBEP) both similarities and differences in the “health” of various components of the San Juan Bay Estuary were found. The Water Quality Index was based on the parameters of dissolved oxygen, turbidity, fecal coliform bacteria, and pH, and was developed in consideration of the number of contaminants that exceeded appropriate water quality standards, the frequency at which contaminants exceeded those standards, and the amount by which exceedances were above relevant standards. The index was developed using data from fourteen water quality stations in total. In San Juan Bay proper, there were three open water stations. San José Lagoon had two stations, Torrecilla Lagoon had two stations, Piñones Lagoon had one station, and no stations were located within Condado Lagoon. In comparison, there is a larger number and wider geographical spread of sampling locations for the Benthic Index scores.

The Water Quality Index ranked San Juan Bay and Piñones Lagoon as having a score of “B”, with San José Lagoon and Torrecilla Lagoon with ranks of “C”. The Suárez Canal was given a grade of “D” and the Martín Peña Canal was ranked as an “F”. To allow a comparison of findings between these two indices, median Benthic Index scores between 3.76 and 5 were given a rank of “A”, values between 2.51 and 3.75 were given a rank of “B”, 1.26 to 2.50 was given a “C”, and scores below 1.26 were given a score of “D/F”. Table 4 compares the relative scores for each main waterbody using the Water Quality Index and the Benthic Index.

Table 4
Comparison of Scores Produced using Water Quality Index
and Benthic Index Techniques

Waterbody	Water Quality Index Classification	Benthic Index Classification
San Juan Bay	B	B
Condado Lagoon	N/A	B
San José Lagoon	C	C
Torrecilla Lagoon	C	B
Piñones Lagoon	B	D/F
Suárez Canal	D	D/F
Martín Peña Canal	F	D/F

Both the Water Quality Index and the Benthic Index characterized San Juan Bay as a “B”. While individual sample locations had higher or lower scores, typical conditions indicate this waterbody has better than average water quality and benthic health, compared to the San Juan Bay Estuary system as a whole. While Condado Lagoon was not graded by the Water Quality Index, its Benthic Index score of a “B” was the same as in San Juan Bay. San José Lagoon was ranked as a “C” for both indices, indicating concurrence on this system’s reduced ecological health. For Torrecilla Lagoon, the Benthic Index score of “B” was higher than its Water Quality Index score of “C”.

The Suárez Canal was graded as a “D” for water quality, which matches its grade of “D/F” on the Benthic Index score. And the Martín Peña Canal’s Water Quality Index score of “F” was matched with a Benthic Index score of “D/F”.

The greatest discrepancy between Water Quality Index scores and Benthic Index scores was found in Piñones Lagoon; the Water Quality Index score of “B” is matched with a Benthic Index score of “D/F”.

The Water Quality and Benthic Index scores both indicate that the least healthy waterbodies in the San Juan Bay Estuary are the Martín Peña and Suárez Canals. Both systems had the lowest possible scores for both indicators of ecosystem health.

In contrast, Piñones Lagoon had a relatively good Water Quality Index score, but a much lower Benthic Index score. Rather than suggesting Piñones Lagoon is “polluted”, the benthic community in this system might be that of a natural condition that makes it inappropriate to compare it to other portions of the San Juan Bay Estuary. If water quality in Piñones Lagoon does in fact represent a healthy ecosystem (as would be expected based on its low population density) then a depauperate benthic community might be representative of a natural condition. Conversely, it could be that factors other than population density alone could be stressing the benthic communities in Piñones Lagoon without being manifested in those parameters used to construct the Water Quality Index.

5.0 Value and Use of the Benthic Index and Other Findings

The Benthic Index developed here is a tool that can be used to report on the status and trends (if any) of the health of the San Juan Bay Estuary and its individual component waterbodies. The technique is consistent with the wider body of literature on how such indices should be constructed, and it is consistent with guidance provided by EPA (2008) on the requirements of a benthic index.

This index can be used to grade portions of the San Juan Bay Estuary in a way that is technically sound, yet also able to be interpreted by non-technical stakeholders and the public and policy makers as well.

While researching topics related to water and sediment quality in San Juan Bay, we discovered a discrepancy in seagrass acreage estimates that may be of interest to the San Juan Bay Estuary Program. If the San Juan Bay Estuary system is improving over the past few years, as is indicated by results from Webb and Gomez-Gomez (1998) and Webb et al. (1998), then one of the bio-indicators that might be useful to track is the acreage of seagrass meadows throughout the system. Seagrass coverage has been previously found to correlate with spatial and temporal trends in water quality in Sarasota Bay, Florida (Tomasko et al. 1996), Lemon Bay, Florida (Tomasko et al. 2001), and Tampa Bay, Florida (Johansson 1995). Due to their proven relationships with water quality, seagrass coverage has been monitored as an indicator of ecosystem health in various locations in Southwest Florida for many years (Tomasko et al. 2005).

In the San Juan Bay Estuary, there does not appear to be a consistent approach to seagrass mapping and/or monitoring, even though one of the earliest papers relating seagrass distribution to water quality was conducted in Puerto Rico (Vicente and Riviera 1982). Also, some of the highest Benthic Index scores found in the San Juan Bay Estuary system were found in areas that appear to be associated with seagrass meadows.

Perhaps due to the differing techniques used, seagrass acreage estimates for the entirety of the San Juan Bay estuary range from 65 acres (listed as 26.5 hectares in SJBEP 2000) to 92 acres (derived from GIS data created by NOAA's Biogeography Program) to 375 acres (Riviera 2005). As seagrass coverage was previously shown to be sensitive to water quality in Puerto Rico (Vicente and Riviera 1982), and as seagrass coverage has been used a bio-indicator of system health in many locations, the finding that the San Juan Bay Estuary system may be recovering due to actions taken to reduce past pollutant impacts (Webb and Gomez-Gomez 1998, and Webb et al. 1998) highlights the need to have a consistent and repeatable program in place to track seagrass acreage over time. These results, in combination with the Water Quality Index and this Benthic Index, could be useful tools for determining the status and trends of overall ecological health throughout the San Juan Bay Estuary.

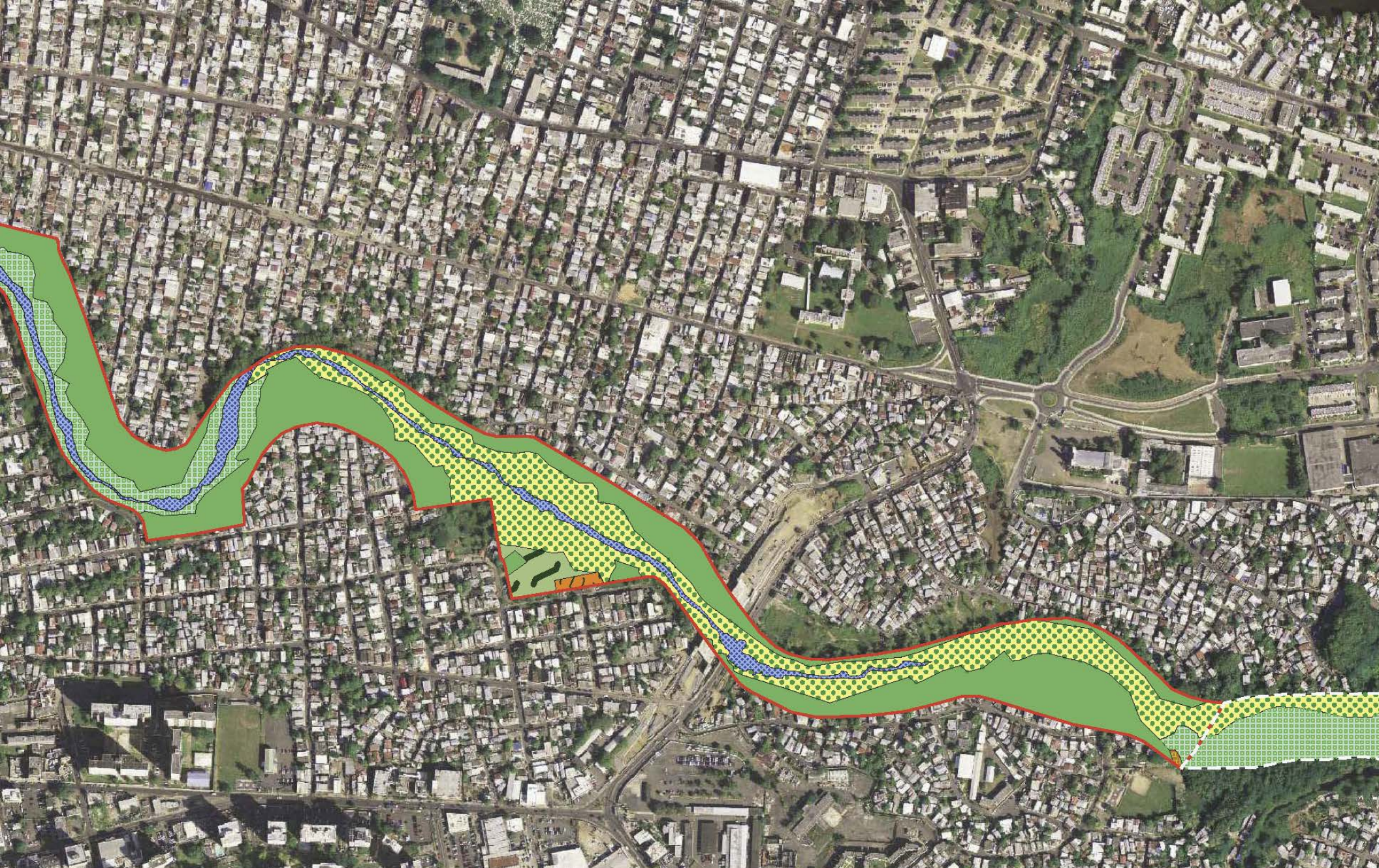
6.0 Literature Cited

- Dauer, D.M., J. A. Ranasinghe, and S. B. Weisberg. 2000. Relationships between benthic community condition, water quality, sediment quality, nutrient loads, and land use patterns in Chesapeake Bay. *Estuaries* 23: 80-96.
- EPA. 2008. *Indicator Development for Estuaries*. United States Environmental Protection Agency. Washington, D.C. 138 pp.
- Fleischer, D. and M.L. Zettler. 2008. An adjustment of benthic ecological quality assessment to effects of salinity. *Marine Pollution Bulletin*. 58: 351-357.
- Johansson, J.O.R. 1991. Long-term trends in nitrogen loading, water quality and biological indicators in Hillsborough Bay, Florida. In: Treat, S.F., Clark, P.A. (Eds), Proceedings, Tampa Bay Area Scientific Information Symposium 2. Tampa Bay Regional Planning Council, St. Petersburg, Florida, pp. 157-176.
- Llansó, R.J., L.C. Scott, J.L. Hyland, D.M. Dauer, D.E. Russell, and F.W. Kutz. 2002. An estuarine benthic index of biotic integrity for the mid-Atlantic region of the United States. II. Index development. *Estuaries* 25:1231-1242.
- Lee J. S., K. T. Lee, G. S. Park. 2005. Acute toxicity of heavy metals, tributyltin, ammonia, and polycyclic aromatic hydrocarbons to benthic amphipod *Grandidierella japonica*. *Ocean Science Journal*. 40, 2, 61-66.
- Montague, C. L., and J.A. Ley. 1993. A possible effect of salinity fluctuation on abundance of benthic vegetation and associated fauna in northeastern Florida Bay. *Estuaries* 16:703–717.
- Otero E. 2002. Environmental Indicators on the San Juan Bay Estuary (EISJBE). Draft Document 5-8-02.
- Paul J. F., K. J. Scott, D. E. Campbell, J. E. Gentile, C. S. Strobel, R. M. Valente, S. B. Weisberg, A. F. Holland, J. A. Ranasinghe. 2001. Developing and applying a benthic index of estuarine condition for the Virginian Biogeographic Province. *Ecological Indicators* 1, 83-99.
- Pinto R., J. Patricio, A. Baeta, B. D. Fath, J. M. Neto, J. C., Marques. 2009. Review and evaluation of estuarine biotic indices to assess benthic condition. *Ecological Indicators* 9, 1-25.
- Rivera J.A. 2005. Finding of the Benthic Assessment of the San Juan Bay Estuary, Puerto Rico. Final Report. NOAA-EPA Interagency Agreement #DW 1394 1778-01. 83 pp.
- SJBEP 2000. Plan Integral de Manejo y Conservacion para el Estuario de la Bahía de San Juan. San Juan, Puerto Rico. 433 pp.

- Tomasko D.A., C.A. Corbett, H.S. Greening, G.E. Raulerson. 2005. Spatial and temporal variation in seagrass coverage in Southwest Florida: assessing the relative effects of anthropogenic nutrient load reductions and rainfall in four contiguous estuaries. *Marine Pollution Bulletin* 50, 797-805.
- Tomasko D.A., C.J. Dawes, M.O. Hall. 1996. The effects of anthropogenic nutrient enrichment on turtle grass (*Thalassia testudinum*) in Sarasota Bay, Florida. *Estuaries* 19, 448-456.
- Tomasko D.A., D.L. Bristol, J.A. Ott. 2001. Assessment of present and future nitrogen loads, water quality, and seagrass (*Thalassia testudinum*) depth distribution in Lemon Bay, Florida. *Estuaries* 24, 926-938.
- Traunspurger W., C. Drews. 1996. Toxicity analysis of freshwater and marine sediments with meio- and macrobenthic organisms: a review. *Hydrobiologia* 328, 215-261.
- Vicente V.P. and J.A. Riviera. 1982. Depth limits of the seagrass *Thalassia testudinum* (Konig) in Jobos and Guayanilla Bays, Puerto Rico. *Caribbean Journal of Science* 17, 73-79.
- Webb R.M.T. and F. Gomez-Gomez. 1998. Synoptic Survey of Water Quality and Bottom Sediments, San Juan Estuary System, Puerto Rico, December 1994-July 1995. Prepared in cooperation with the PR Environmental Quality Board and U.S. Environmental Protection Agency for the San Juan Bay Estuary Program WRIR 97-4144. 69 pp.
- Weston D. P. 1996. Further development of a chronic *Ampelisca abdita* bioassay as an indicator of sediment toxicity. *A special study of the San Francisco Estuary Regional Monitoring Program*

Appendix A4

Mapped Habitat and Caño Martín Peña Channel Configurations



T BOUNDARY
 BOUNDARY
 WETLANDS—MANGROVE
 R
 WETLANDS

EXISTING WETLAND AREAS					
DESCRIPTION	WESTERN END CMP (ACRES)	LIMIT OF PUBLIC DOMAIN CMP (ACRES)	EASTERN END CMP (ACRES)	TOTAL (ACRES)	
ESTUARINE FORESTED WETLANDS—MANGROVE	0.35	7.39	7.79	15.53	
ESTUARINE OPEN WATER	1.71	5.69	0	7.40	
MANAGED GREEN AREA	0	0.31	0	0.31	
PALUSTRINE EMERGENT WETLANDS	0	0.06	0	0.06	



PROPOSED 75' CHANNEL AREAS

	DESCRIPTION	WESTERN END CMP (ACRES)	LIMIT OF PUBLIC DOMAIN CMP (ACRES)	EASTERN END CMP (ACRES)	TOTAL (ACRES)
BOUNDARY	ESTUARINE FORESTED WETLANDS-MANGROVE	0	0.82	0	0.82
BOUNDARY	MANAGED GREEN AREA	0	0.30	0	0.30
WETLANDS	PALUSTRINE EMERGENT WETLANDS	0	0.03	0	0.03
WETLANDS-MANGROVE	PALUSTRINE FORESTED WETLANDS-MANGROVE	0	6.28	1.51	7.79
	SECONDARY FOREST	0	1.17	0	1.17



PROPOSED 100' CHANNEL AREAS

T BOUNDARY
 BOUNDARY
 WETLANDS—MANGROVE
 WETLANDS
 WETLANDS—MANGROVE

DESCRIPTION	WESTERN END CMP (ACRES)	LIMIT OF PUBLIC DOMAIN CMP (ACRES)	EASTERN END CMP (ACRES)	TOTAL (ACRES)
ESTUARINE FORESTED WETLANDS—MANGROVE	0	0.82	0	0.82
MANAGED GREEN AREA	0	0.30	0	0.30
PALUSTRINE EMERGENT WETLANDS	0	0.03	0	0.03
PALUSTRINE FORESTED WETLANDS—MANGROVE	0	5.64	1.03	6.67
SECONDARY FOREST	0	1.17	0	1.17



PROPOSED 125' CHANNEL AREAS

BOUNDARY
BOUNDARY
WETLANDS—MANGROVE
WETLANDS
WETLANDS—MANGROVE

DESCRIPTION	WESTERN END CMP (ACRES)	LIMIT OF PUBLIC DOMAIN CMP (ACRES)	EASTERN END CMP (ACRES)	TOTAL (ACRES)
ESTUARINE FORESTED WETLANDS—MANGROVE	0	0.82	0	0.82
MANAGED GREEN AREA	0	0.30	0	0.30
PALUSTRINE EMERGENT WETLANDS	0	0.03	0	0.03
PALUSTRINE FORESTED WETLANDS—MANGROVE	0	5.01	0.18	5.19
SECONDARY FOREST	0	1.17	0	1.17

Appendix B
Real Estate Plan

**FINAL
REAL ESTATE PLAN
CAÑO MARTÍN PEÑA
ECOSYSTEM RESTORATION PROJECT
SAN JUAN, PUERTO RICO**

Prepared for:



Corporación del Proyecto ENLACE del Caño Martín Peña
Apartado Postal 41308
San Juan, Puerto Rico 00940-1308

February 2016

Contents

	Page
List of Exhibits.....	iv
List of Figures.....	iv
List of Tables.....	iv
Acronyms and Abbreviations.....	v
1. STATEMENT OF PURPOSE.....	1
2. PROJECT AUTHORIZATION.....	1
3. PROJECT LOCATION.....	1
4. PROJECT DESCRIPTION.....	2
5. REAL ESTATE REQUIREMENTS.....	3
6. ESTATES TO BE ACQUIRED.....	5
7. NAVIGATIONAL SERVITUDE.....	6
8. FEDERALLY OWNED LAND.....	6
9. NON-FEDERALLY OWNED LAND.....	6
10. NON-FEDERAL OPERATION/MAINTENANCE RESPONSIBILITIES.....	6
11. NON-FEDERAL AUTHORITY TO PARTICIPATE IN THE PROJECT.....	6
12. ATTITUDE OF OWNERS.....	7
13. MINERALS.....	7
14. HAZARDOUS, TOXIC AND RADIOACTIVE WASTES (HTRW).....	8
15. INDUCED FLOODING.....	8
16. RELOCATIONS ASSISTANCE (PL 91-646).....	8
17. RELOCATIONS, ALTERATIONS, VACATIONS AND ABANDONMENTS (UTILITIES, STRUCTURES AND FACILITIES, CEMETERIES AND TOWNS).....	9
18. STANDING TIMBER AND VEGETATIVE COVER.....	10
19. RECREATION RESOURCES.....	10
20. CULTURAL RESOURCES.....	10
21. OUTSTANDING RIGHTS.....	11
22. MITIGATION.....	11
23. ACQUISITION/ADMINISTRATIVE COSTS.....	12
24. SUMMARY OF PROJECT REAL ESTATE COSTS.....	13
25. REAL ESTATE ACQUISITION SCHEDULE.....	14
26. REAL ESTATE CHART OF ACCOUNTS.....	15

List of Exhibits

- Exhibit A: Figures
- Exhibit B: Assessment of Non-Federal Sponsor’s Real Estate Acquisition Capability
- Exhibit C: Memorandum of Agreement between ENLACE and USACE
- Exhibit D: Caño Martín Peña Ecosystem Restoration Project LERRDs Relocation of the 115kW Power Transmission Line
- Exhibit E: Caño Martín Peña Ecosystem Restoration Project LERRDs Relocation of the Rexach Trunk Sewer and Borinquen Water Transmission Line

List of Figures (Exhibit A)

	Page
Figure A-1. Caño Martín Peña Ecosystem Restoration Project Area Map & San José Lagoon Pits 1 and 2	1
Figure A-2. Caño Martín Peña Ecosystem Restoration Project Demolition Areas Map	2
Figure A-3. Caño Martín Peña Ecosystem Restoration Project Humacao Regional Landfill Map & Potential Sediment Disposal Yauco, Peñuelas and Ponce Landfills Map	3
Figure A-4. Mangrove Restoration Area Map	4
Figure A-5. <i>Ciudad Deportiva Roberto Clemente</i> Staging Area Map	5
Figure A-6. Recreation Access Parks Map	6
Figure A-7. <i>Piedritas Stadium</i> Staging Area Map	7
Figure A-8. Caño Martín Peña Aerial Photo (1936).....	8
Figure A-9. Relocations, Alterations, Vacations and Abandonments Areas Map (utilities, structures and facilities, cemeteries and towns).....	9

List of Tables

Table 1	Summary of Project Real Estate Costs (LERRDs)	13
Table 2	Summary of Completed Project Real Estate Costs (Waived)	14
Table 3	Summary of Project Demolition Costs (Work-In-Kind)	14
Table 4	Real Estate Lands & Damages	15
Table 5	Relocations	16
Table 6	Demolitions	16

Acronyms and Abbreviations

CAD	Contained Aquatic Disposal
CDRC	Ciudad Deportiva Roberto Clemente
CMP	Caño Martín Peña
CMP-ERP	Caño Martín Peña Ecosystem Restoration Project
CMP-CLT	Caño Martín Peña Community Land Trust
DNER	Puerto Rico Department of Natural and Environmental Resources
DSS	Decent, Safe and Sanitary
EIS	Environmental Impact Statement
ENLACE	Corporación del Proyecto ENLACE del Caño Martín Peña
G-8	Group of the Eight Communities bordering the Caño Martín Peña
HTRW	Hazardous, Toxic and Radioactive Waste
MCACES	Micro-Computer Aided Cost Engineering System
MTZ	Maritime-Terrestrial Zone
NEP	USEPA's National Estuary Program
NER	National Ecosystem Restoration Plan
OMRR&R	Operations, Maintenance, Repair, Rehabilitation & Replacement
PL	Public Law
PPA	Project Partnership Agreement
PR	Puerto Rico
PREPA	Puerto Rico Electric Power Authority
REP	Real Estate Plan
SJL	San José Lagoon
URA	Uniform Relocation Assistance and Real Estate Acquisition Act
U.S.	United States of America
USACE	U.S. Corps of Engineers
USEPA	U.S. Environmental Protection Agency
WRDA	Water Resources Development Act of 2007

This page intentionally left blank.

1. STATEMENT OF PURPOSE

The purpose of this Real Estate Plan (REP) is to present the overall plan describing the minimum real estate requirements for the construction, operation, maintenance, repair and rehabilitation of the proposed Project. It is Appendix B to the *Caño Martín Peña Ecosystem Restoration Project (CMP-ERP) Feasibility Report* dated December 2015.

2. PROJECT AUTHORIZATION

The Water Resources Development Act of 2007 (WRDA 2007, United States Public Law 110-114, 121 Stat. 1048) was enacted and provided for the conservation and development of water and related resources, and authorized the Secretary of the Army to carry out various projects for improvements to rivers and harbors of the United States and for other purposes. In particular, Section 5127 of WRDA 2007 states the following:

Section 5127. Cano Martin Pena, San Juan, Puerto Rico.

The Secretary shall review a report prepared by the non-Federal interest concerning flood protection and environmental restoration for Caño Martín Peña, San Juan, Puerto Rico, and, if the Secretary determines that the report meets the evaluation and design standards of the Corps of Engineers and that the project is feasible, the Secretary may carry out the project at a total cost of \$150,000,000.

On October 27, 2008, the Director of Civil Works issued an implementation guidance memorandum for Section 5127 of the WRDA 2007, which established that the feasibility report “will follow the requirements set forth in Appendix H of ER 1105-2-100 for projects authorized without a report and be submitted for approval by the Assistant Secretary of the Army (Civil Works).” This Feasibility Report is submitted in accordance with the guidance memorandum, and the Memorandum of Agreement executed on June 26, 2012, between the United States Corps of Engineers (USACE) and the Caño Martín Peña ENLACE Project Corporation (ENLACE), the non-Federal sponsor for report revision.

3. PROJECT LOCATION

The location of the CMP-ERP is within the Municipalities of San Juan and Carolina, Puerto Rico (see **Figure A-1**). More specifically, the CMP-ERP will be located in the eastern part of the Caño Martín Peña (CMP). In addition, it will extend to the *Ciudad Deportiva Roberto Clemente* (CDRC) in Carolina, P.R. Most of the CMP-ERP lies within the flood zone AE and the public domain lands associated with the Maritime-Terrestrial Zone (MTZ) of the CMP District (see **Figure A-2**), with the exception of the Humacao Regional Landfill and CDRC staging area. The public domain lands of the CMP District (encompassing the CMP and its associated conservation strip) were

established by Puerto Rico Law No. 489 of 2004, known as the *Comprehensive Development of the Cano Martín Peña Special Planning District Act*, as amended (hereinafter, PR Law 489-2004); are property of the people of Puerto Rico and administered by the Department of Natural and Environmental Resources (DNER).

The CMP-ERP is located within a residential area that has the highest population density on the Island, having over twenty six thousand (26,000) persons per square mile. The urban environment in which the CMP-ERP is being developed is in the heart of the city of San Juan, which highly increases the real estate costs associated with the plan. **Figure A-3** depicts the CMP and adjacent development in 1936.

4. PROJECT DESCRIPTION

The purpose of the CMP-ERP is to re-establish the tidal connection between the San José Lagoon (SJL) and the San Juan Bay, and thus, the eastern and western sections of the San Juan Bay Estuary, the only tropical estuary that is included in the United States Environmental Protection Agency (USEPA) National Estuary Program (NEP). The CMP-ERP consists of the dredging of approximately 2.2 miles of the eastern half of the CMP, starting from the SJL towards the west, in the vicinity of the Luis Muñoz Rivera Avenue Bridge. The CMP-ERP would improve dissolved oxygen levels and salinity stratification, increase biodiversity by restoring or enhancing, among others, fish habitat and benthic conditions, and overall health of the San Juan Bay Estuary System. The CMP-ERP is also critical for the revitalization of eight impoverished communities settled along the Martín Peña tidal channel, and restoration of this system will significantly improve human health and safety in the area. Recreational navigation will also be reestablished in the area, allowing for increased public and commercial use of the entire estuary.

The National Ecosystem Restoration Plan (NER) consists of dredging approximately 2.2 miles of the eastern half of the CMP to a width of 100 feet and a depth of 10 feet, with slight variations in channel width and depth at the four (4) bridges to the west, the Barbosa Bridge to the east, and at the terminus of the CMP with the SJL. The walls of the CMP-ERP Channel would be constructed with vertical concrete-capped steel sheet piles with hydrologic connections to the surrounding lands. The sill depth of the window would be set at mean low water so that tidal exchanges are facilitated to the mangrove beds. Rip rap would be placed at the four bridges. At the terminus of the CMP-ERP Channel with the SJL, an extended channel would be dredged east into the SJL (over a distance of approximately 4,300 feet) as a hydraulic transition from the CMP. This extended channel would transition from the 10-foot-deep CMP-ERP Channel to the 6-foot-deep areas of SJL. The extended channel would maintain the CMP-ERP Channel's 100-foot width but replace its steel sheet pile walls with a trapezoidal configuration with 5-foot to 1-foot earthen side slopes. The NER includes the following management measures:

- a. One-hundred-foot-wide, ten-foot-deep rectangular channel with concrete-capped steel sheet pile walls (with the variations in channel width and depth for the Barbosa Avenue Bridge and terminus of the CMP with the SJL as described in Section 5.2.1.1 of this report);
- b. Solid waste debris would be transported by barge to a staging area for subsequent landfill disposal. Sediments would be transported by barge for disposal at the SJ1 and SJ2 Contained Aquatic Disposal (CAD) in the SJL pits;
- c. A weir at the western end of the project area for mitigating water flows into the adjacent waterways and to protect the structural integrity of the four bridges; and
- d. Restoration of the disturbed mangrove by grading the site and planting with native vegetation. After dredging and construction of mangrove planting beds, the CMP would consist of 25.57 acres of open water and 34.48 acres of mangrove wetland

5. REAL ESTATE REQUIREMENTS

The Project Area is comprised of 68.47 acres associated with the CMP (56.97 acres in the eastern CMP, 2.06 in the western portion of CMP Project channel, and 9.44 acres of the extended channel into SJL), and 8 acres associated with staging areas (6 acres at the CDRC and 2 acres at Las Piedritas). Lands will be required for the CMP-ERP as follows:

- a. **Channel Restoration** – The CMP-ERP falls within the public domain lands associated with the maritime terrestrial zone of the MTZ-CMP, and an extended channel (transition area) into the SJL (see **Figure A-2**). These public domain lands are administered by the Commonwealth of Puerto Rico, acting through the Department of Natural and Environmental Resources (DNER); thus, they will not need to be acquired. As per PR Law 489-2004 and as requested by the Puerto Rico Department of Housing, the Department of Justice of Puerto Rico established, through Opinion No. 11-131-A, the criteria to recognize the validity of land titles previously issued on the MTZ-CMP. Based on experience, ENLACE estimates that approximately 5% of the acquisitions within the MTZ-CMP will include the acquisition of legally recognized land titles in fee simple. Of the 96 acquisitions already conducted in the MTZ-CMP, 5 involved the acquisition of privately owned land titles. The average value of the land titles already acquired is \$14,573.75.
- b. **Mangrove Restoration** (34.48 acres within the Project Channel footprint) – The width of the mangrove planting area would extend from the channel wall to the limit of the Public Domain Lands associated with the MTZ-CMP. Since these are property of the Commonwealth of Puerto Rico, the non-Federal sponsor would not be responsible for any land acquisitions (see **Figure A-4**).

- c. **Temporary Work Area (6 acres)** – A 6-acre staging area would be located at the CDRC on the southeast shore of the SJL. Of these 6 acres, 5 acres are upland habitat and 1 acre is mangrove fringe. The CDRC staging area includes a dock for loading/unloading the dredged material to be transported to the landfill (see **Figure A-5**). The 5 upland acres are within a previously disturbed 35-acre parcel. After all solid waste has been disposed in the upland landfill, the 5 acre CDRC staging area would be restored with native upland vegetation, and the 1 acre of mangrove fringe would be restored with mangroves. This land belongs to CDRC; however, no lands need to be acquired by the non-Federal sponsor. ENLACE has already initiated the dialogue with the CDRC's Board of Directors to request the right to use the area and incorporate the Project in their future development plans' timeline.
- d. **Temporary Work Area (2 acres)** – A staging area will be located in a vacant lot owned by the CMP Community Land Trust, currently known as the "Piedritas Stadium" (see **Figure A-6**), to be used during construction of the weir and cofferdam in the western CMP. ENLACE has initiated dialogue with the Caño Martín Peña Community Land Trust (CMP-CLT)'s Land Administration Coordinator to request the right to use the area and incorporate the Project in their future development plan's timeline.
- e. **Solid Waste Disposal Areas** – Solid waste debris resulting from housing and construction would be transported from Project's site to the CDRC staging area. Subsequently, the solid waste debris would be transported from the CDRC staging area to the Humacao Regional Landfill, which is owned by the Local government and is located at approximately 32 miles from the project site. The CMP-ERP would use a local landfill going to the transfer station of the Municipality of San Juan, as such; no additional permits are required. Slurry from the dredged channel would be pumped into dump scows, which would be transported to and deposited in the SJ1/2, which will be used as CAD sites. Solid waste and sediment generated from the construction of the weir would be temporarily placed at the Las Piedritas staging area (see **Figure A-7**) and trucked to the Humacao landfill. The transportation routes and the SJL are property of the Commonwealth of Puerto Rico; therefore no lands need to be acquired. In addition, the non-Federal sponsor has identified at least three other potential landfills located in: Yauco, Peñuelas and Ponce (see **Figure A-8**).
- f. **Recreation Areas (5 acres)** – There are no formal areas where CMP District and Cantera Peninsula residents may access the Project Channel for fishing, bird watching, or other activities except at the three bridges which cross the channel. Fishing and navigation for recreational purposes are highly impaired and unsafe. The linear nature of the Project allows for the placement of recreational features along the length of the CMP. There will be three types of recreation access areas: (a) recreation access parks, (b) recreation parks with a trail to the CMP, (c) and recreation parks without a trail. In addition, there will be a linear park extension along the southern bank of the Project Channel. The land associated with the recreation areas is already owned by the

Commonwealth of Puerto Rico, through the Department of Natural and Environmental Resources (DNER), thus they will not need to be acquired (see **Figure A-7**).

- g. **Road Access** – Road access would be over public roads and highways. No lands would need to be acquired by the non-Federal sponsor.
- h. **Operation and Management** – After construction is completed, operation and management of the channel would be done within the public domain lands associated with the MTZ-CMP. At this time, it appears that no additional lands would need to be acquired by the non-Federal sponsor.

6. ESTATES TO BE ACQUIRED

a. Standard Estates

No Standard Estates would be acquired for this project.

b. Non-Standard Estates

No Non-Standard Estates would be acquired for this project.

Temporary Work Area Easement – A staging area would be located at the CDRC. This land belongs to the CDRC and would be provided by the non-Federal sponsor. A temporary easement and right-of-way in, on, over and across (the land described in Schedule A) (Tracts Nos. 063-000-005-07); for a period not to exceed five years would be acquired by the Commonwealth of Puerto Rico for this Project. The Commonwealth of Puerto Rico has the means to acquire the permits needed to use CDRC. As a governmental entity, ENLACE would be able to use the same permits for CDRC during project construction. ENLACE would share the right to use permit with the USACE for and during project construction.

Temporary Work Area Easement – A staging area would be located at a vacant lot currently known as the “Piedritas Stadium”. This land belongs to the CMP –CLT and would be provided by ENLACE. A temporary easement and right-of-way in, on, over and across (the land described in Schedule A) (Tracts No. 063-001-552-07); for a period not to exceed three years would be acquired by the Commonwealth of Puerto Rico for this Project. The Commonwealth of Puerto Rico has the means to acquire the permits needed to use the Piedritas Stadium. As a governmental entity, ENLACE would be able to use the same permits for Piedritas Stadium during project construction. ENLACE would share the right to use permit with the USACE for and during project construction.

7. NAVIGATIONAL SERVITUDE

Although the lands required for the project will not be provided through an exercise of the navigation servitude, they remain subject to the navigation servitude.

8. FEDERALLY OWNED LAND

There are no federally owned lands within the Project limits.

9. NON-FEDERALLY OWNED LAND

PR Law 489 creates a new delimitation establishing the public domain lands associated with the MTZ-CMP, which are property of the people of Puerto Rico and administered by the DNER. The Project Channel lies only within the limits of these public domain lands associated with the MTZ-CMP. Consistent with PR Law 489, ENLACE does not own any lands within the public domain limits where the Project Footprint is located.

As per the dispositions of PR Law 489 and the regulations for the public domain lands, ENLACE would have access to the lands within the Project Footprint for construction and will provide said access to the USACE.

10. NON-FEDERAL OPERATION/MAINTENANCE RESPONSIBILITIES

Operations, Maintenance, Repair, Rehabilitation & Replacement (OMRR&R) will be the responsibility of the DNER. The non-Federal sponsor shall provide, if necessary, all lands, easements, and rights-of-way. The USACE will develop an O&M manual detailing expected OMRR&R requirements and periodically inspect the Project to ensure that DNER is implementing the identified procedures. In addition, the Government of Puerto Rico is and will be conducting all the necessary alterations and/or relocations of facilities and utilities located within the Project's Footprint, the cost of these alterations and relocations are included in the Project's costs and are disaggregated in the Micro-Computer Aided Cost Engineering System (MCACES).

11. NON-FEDERAL AUTHORITY TO PARTICIPATE IN THE PROJECT

The non-Federal sponsors, ENLACE and the DNER, derived their authority to participate in the CMP-ERP from PR Law 489 and Puerto Rico Law No. 23 of 1972, as amended, respectively.

12. ATTITUDE OF OWNERS

Many residents affected by the present conditions of the CMP support the proposed restoration of the CMP since it represents an improvement in the quality of urban life. Hundreds of meetings have been held with local residents to gather data necessary for the investigation, assessment, and evaluation of alternatives to ensure that the CMP-ERP counts with the active participation and approval of the CMP bordering communities. A "no action" alternative would not be acceptable to many residents of the Project area, the environmental community, or to the government of Puerto Rico. All landowners impacted by the proposed project have been involved in the planning process and have indicated strong support for the Project. In addition, the G-8, Inc., a nonprofit organization that represents leaders of twelve grassroots organizations based in the eight communities that border the CMP, have expressed their support to the CMP-ERP and has established as their mission to promote the interest and involvement of residents in the decision-making process and in the implementation of the CMP Comprehensive Development Plan, in order to ensure the permanence of their communities.

ENLACE is also incorporating a new replacement housing alternative under the Caño Martín Peña Community Land Trust (CMP-CLT). The CMP-CLT is a pioneering entity in Puerto Rico, created to guarantee affordable housing, resolve land tenure issues, and reinvest any future increase in land value in the community. The CMP-CLT is a critical instrument for the implementation of the CMP Comprehensive Development District Plan, as it prevents gentrification and ensures that the current residents benefit directly from investment in infrastructure, urban reform, and environmental restoration.

The ultimate implementation and operation of the CMP-CLT is expected to provide an additional source of affordable housing for relocation purposes. This mechanism enacted by ENLACE have eliminated the displacement of residents as an alternative to conduct the Project and have been essential to ensure the willing support of the community members.

13. MINERALS

All minerals discovered in Puerto Rico are the property of the people of Puerto Rico and the Government of Puerto Rico is their steward. The right to mine and exploit mineral deposits and all laws and regulations regarding this industry are overseen by DNER and the Mining Commission, assigned to the Governor's Office.

There are no known minerals of value in the Project Area.

14. HAZARDOUS, TOXIC AND RADIOACTIVE WASTES (HTRW)

Based on the Project Area's condition there is no evidence of Recognized Environmental Conditions (RECs) in connection with the CMP. Possible exceptions to the aforementioned statement are the nondescript solid waste content (e.g., substances remaining within bottles), discarded appliances, and equipment that are evident at the ground surface. Although there is evidence of historical REC supporting either past or ongoing contamination to the Study Area (in accordance with ASTM E1527-05), the potential for Hazardous, Toxic and Radioactive Waste (HTRWs) within the CMP Project Area appears to be minimal. The solid waste found within the Study Area may include C&D and HW materials, and whether they contain Actionable Hazardous Substances (Section 7.2.1.2 of the Feasibility Report) will be determined in accordance with a sampling plan to be agreed by the parties.

15. INDUCED FLOODING

Tidal amplitude within the CMP and San José Lagoon would increase as a result of construction of the channel. The lagoon's tide range is expected to increase 1.28 feet after construction, which would equate to a 0.64-foot increase in average monthly water levels. The water surface rise may affect extremely low-lying structures around San José Lagoon and Los Corozos Lagoon. Preliminary analysis indicates that there are four areas adjacent to San José Lagoon and Los Corozos Lagoon where approximately 18 urban structures may be affected from the restoration of tidal activity upon completion of the CMP-ERP. In addition, storm sewers from the airport, at the north of the Suarez Canal, outfall into the SJL. The airport has been present for decades and presumably operating prior to the filling of the CMP. The airport is higher than its outfalls and thus may be able to build up a hydraulic head in its conduit to offset these monthly events. Nevertheless, a storm water management investigation will be conducted to determine any potential impact to the effectiveness of the airport's existing storm water sewers with the completion of the CMP-ERP.

Additional hydraulic and hydrologic (H&H) modeling and analyses are needed to confirm the potential for induced flooding as a result of the implementation of the CMP-ERP. This additional technical investigation would be completed before the conclusion of preconstruction engineering and design (PED).

16. RELOCATIONS ASSISTANCE (PL 91-646)

Approximately, 393 total acquisitions and 394 total relocations would occur as part of the federal project. Of these, 96 structure acquisitions have already been carried out or are in process, and an estimated 297 structures with 217 eligible resident owners and 115 tenants remain to be relocated as a consequence of the CMP-ERP. Currently there is no estimate for the number of businesses within the project footprint. In accordance with the Uniform Relocation

Assistance and Real Property Acquisition Policies Act of 1970 (URA), as amended (42 U.S.C. 9601 et seq.), relocation assistance will be provided to persons and businesses, if any, displaced as a result of the project. In order to qualify as a “displaced person” under the URA, the person must be a lawful occupant. The non-Federal sponsor will determine on a case by case basis whether an occupant of the Project Area is a lawful occupant, as per the criteria established under applicable Puerto Rico State law. The nature and amount of assistance provided to displaced persons will be determined in accordance with the URA and the lead agency implementing regulations at 49 CFR Part 24.

ENLACE has been advised about and acknowledges the risk of proceeding with acquisitions and relocations in advance of Project Authorization and a Project Partnership Agreement (PPA). The \$5,712,669 cost associated with the 96 completed structure acquisitions and the 62 completed relocations are being waived by ENLACE from the Total Project Cost; however, despite the waiving of these costs, the completed structure acquisitions and completed relocations are still considered a part of the Federal project.

17. RELOCATIONS, ALTERATIONS, VACATIONS AND ABANDONMENTS (UTILITIES, STRUCTURES AND FACILITIES, CEMETERIES AND TOWNS)

The entire known infrastructure affected by the CMP-ERP falls within the public domain lands associated with the MTZ-CMP. Alterations and relocations will be responsibility of the non-Federal sponsor, following the detailed list of infrastructure affected by the CMP-ERP (see **Figure A-9**):

- Relocation of the Rexach Trunk Sewer Siphon, CIP 1-66-5104: The project, with a total estimated cost of \$5,987,788, consists in lowering the depth of the existing trunk sewer by installing a siphon so that it does not conflict with the proposed depth of the NER after completion of the CMP-ERP. The Puerto Rico Aqueduct and Sewer Authority (PRASA) have scheduled the bidding process to start in the second half of 2016.
- Relocation of the Borinquen Water Transmission Line, CIP 1-66-7005: The project, with a total estimated cost of \$3,191,211, consists in lowering the depth of the existing potable water force main so that it does not conflict with the proposed depth of the NER after completion of the CMP-ERP. PRASA has scheduled construction to start in late 2016.
- Line Segment Improvement for 115kV Power Transmission Line – 38900: The height of the existing 115-kV Power Transmission Line, that runs from a substation near the Tren Urbano guiderail on the western end of the Project Channel, east via Rexach Avenue and then south to the canal and SJL, was increased with reference to ground level, not less that 50ft, above Caño Martín Peña in order to allow the implementation of the CMP-ERP. The project, with a total cost of \$269,733.00, started on October 23, 2014, and was completed by the Puerto Rico Electric Power Authority (PREPA) on December 23, 2014.
- Construction of the CMP-ERP requires demolition of tertiary roadways adjacent to the canal, which would occur during project construction.

- Construction of the CMP-ERP requires the capping of several tertiary drinking water lines, which would occur prior to dredging activities associated with the project.
- Demolition of 393 structures and associated infrastructure, which would be completed prior to construction.

These structures would be demolished and their utility services rerouted or terminated; debris and existing surface streets within the Project's limits would be removed, as listed above. Any existing raw sewage discharges and/or uncontrolled storm water runoff from the area will be stopped prior to commencing dredging activities. No bridge relocations or alterations are being considered as part of the CMP-ERP. No towns or cemeteries would be relocated as result of the CMP-ERP.

18. STANDING TIMBER AND VEGETATIVE COVER

Currently the CMP is mostly covered by approximately 33 acres of mangrove wetland. As a result of the CMP-ERP, both the north and south sides of the Project Channel would be graded to allow the creation of 34 acres of habitat for mangrove planting and a future forested wetland. The planting bed would be graded from the channel margin to, in most cases, the upland side of the Project limit.

Initial control of invasive species would be provided during construction of the mangrove planting beds. Visual surveys would be conducted and removal of identified invasive vegetation would be accomplished by physical removal or through the use of herbicide, as applicable. Over the life of the CMP-ERP, monitoring for invasive species establishments would be included as part of the monitoring plan, and additional physical removal or herbicide application would be utilized, as necessary. The CMP-ERP would be designed to provide optimal conditions for native vegetation, reducing the probability for establishment and spread of invasive species. As such, no costs have been estimated for future control efforts.

19. RECREATION RESOURCES

The CMP-ERP would include nine recreation access parks, six recreation parks with a trail to the CMP, six recreation parks without a trail, and a linear park extension along the southern bank in the Project Channel that would terminate in the Parada 27 community (see **Figure A-7**). The recreational features fall within the public domain lands associated with the MTZ-CMP; therefore, no land acquisition is required.

20. CULTURAL RESOURCES

At present, no previously recorded sub-aquatic prehistoric cultural resources have been identified in the area, and there is no historic evidence of smaller marine vessels encountered

in the CMP; however, the investigations conducted in the area have been limited due to restricted access and pollution in the CMP Channel. The possibility of encountering submerged cultural remains still exists and is considered to be high. There is also a probability of encountering cultural remains from the old bridges constructed in the area, as well as remains from fishing corrals and middens resulting from the first squatter settlements in the early twentieth century.

The Martín Peña Bridge is located above the CMP in the 8 km of the Ponce de Leon Avenue and is regarded as one of the most important historic structures in the CMP District. Built in 1939, the Martín Peña Bridge is the last of several bridges which were located in the same area and that constituted the main crossing between Hato Rey and Santurce since the 1500s. This location is also the site of one of the key battles that led to the defeat of the British invasion of San Juan of 1797, led by Admiral Ralph Abercromby. Community efforts to preserve the Martín Peña Bridge led to the enactment of Puerto Rico Law No. 110 of 2007, which declares the Martín Peña Bridge as a Historical Monument of Puerto Rico. In 2008, the Martín Peña Bridge was listed on the United States National Register of Historic Places. The Martín Peña Bridge will be photo-documented as part of the Project.

A Field Archeologist will be employed full-time to monitor construction activities conducted near the Martín Peña Bridge, as well as the dredged materials during the dredging process. The Field Archeologist will be aided by a Supervising Archeologist who will be employed part-time. The Field Archeologist will be present on the materials barge where the screening of the dredged materials will be conducted; if multiple dredges are operating simultaneously, at least one Archaeologist per dredge will be required. Cultural resources monitoring would be conducted as each clamshell bucket of material is laid onto the barge. Additional information on *Cultural Resources* can be found in Section 3.15 of the EIS.

21. OUTSTANDING RIGHTS

There are no known outstanding rights in the Project Area.

22. MITIGATION

Construction mitigation entails noise and vibration mitigation efforts. Temporary noise curtains would be installed to the north and south of the dredging operations. Dredging and construction operations would be limited to 12 hours a day, no dredging or construction activities will be conducted on Sundays. Noise levels in areas adjoining construction sites will be monitored with appropriate portable and/or stationary equipment to ensure the levels are under the maximum allowed. If the maximum allowed is exceeded, the response will be to stop work; conduct noise producing operations during daylight hours; and/or review procedures to determine means and methods that are more effective to reduce noise levels.

Four stationary vibration monitoring devices will be installed along the border between the working area and the adjoining structures, both north and south of the CMP. In addition, a photo-survey of the exterior of existing structures facing and adjoining the work would be prepared to document pre-construction condition. Visual observation of existing structures in areas adjoining construction sites would be conducted for visible damage. If excessive levels of vibration occur, the response would be to stop work; avoid using equipment near adjoining structures that produces heavy vibrations; and/or review procedures to determine means and methods that are more effective to reduce vibration levels. Alternative sheet pile installation methods such as “press-in” pile drivers or other drivers that produce less vibration may be used, if available and feasible. Potential temporary relocations are incorporated as part of the Cost Risk Analysis that determined the 15 percent contingency for Relocations (families).

23. ACQUISITION/ADMINISTRATIVE COSTS

The estimate of the Federal real estate acquisition/administrative cost is \$1,687,250. This figure includes Project REP, review, monitoring, land acquisition, and transportation costs. The non-Federal sponsor will receive credit towards its share of future real estate acquisition/administrative project costs incurred for certification. Non-Federal acquisition/administrative costs are estimated to be \$3,802,751, of which \$334,138 will be waived as these administrative costs were associated with the 96 completed structure acquisitions and 62 completed relocations.

24. SUMMARY OF PROJECT REAL ESTATE COSTS

The following cost figures are subject to change prior to construction. Table 1 summarizes the LERRDs associated with the CMP-ERP, which would be contained in Folders 01 Lands and Damages and 02 Relocations. Table 2 summarizes the costs for completed structure acquisitions and relocations that are being waived by the non-Federal sponsor, and cannot be applied to the cost share. Table 3 summarizes the creditable and non-creditable costs from associated demolitions of structure acquisitions. Demolitions are not LERRDs, but rather Work-In-Kind, and creditable demolition costs will be contained in the Folder 09 Channel and Canal folder of the MCACES.

Table 1. Summary of Project Real Estate Costs (LERRDs)

Type	Cost
Federal	
Lands and Damages (Structures, Relocation, Administrative Costs)	
Labor (DS-RE) (146 hrs.)	\$14,000
Labor (Appraisal) (\$1,750 x 393 app. Reports)	\$687,750
Labor (RE-A) (\$2,500 x 393 credit packages)	\$982,500
Transportation	\$3,000
Total Federal Cost	\$1,687,250¹
Local	
Lands and Damages (Structures, Relocation, Administrative Costs)	
Real Estate Acquisition (CDRC staging area)	\$126,000
Real Estate Adm. Costs (CDRC staging area)	\$50,000
Structure Acquisitions (280 structures @\$50,000 per structure)	\$14,000,000
Structure Acquisition (17 structures @ \$50,000 per structure – Cantera)	\$850,000
Relocations (200 owner occupants@ \$81,510 per occupant)	\$16,302,000
Relocations (115 tenant occupants @ \$7,200 per occupant)	\$977,500
Relocations (17 owner occupants @ \$81,510 per occupant)	\$1,385,670
Administrative for 280 structures (e.g., appraisals, attny costs, mapping)	\$3,326,153
Administrative for 17 structures (e.g., appraisals, attny costs, mapping) @ \$8,380 per structure) - Cantera	\$142,460
Total Local Lands and Damages Cost	\$38,847,033
Relocations (Utilities)	
115 kW Transmission Line (completed)	\$269,773
Borinquen Water Transmission Line	\$3,191,211
Rexach Trunk Sewer	\$5,987,788
Total Local Utility Relocations Cost	\$9,448,732

Total Local Real Estate Costs (LERRDs)	\$48,295,765
Total Local Real Estate Estimated Cost (with contingency)²	\$57,353,812
Total Local Real Estate Project First Cost (with PED and CM)	\$59,111,969
Total Local Real Estate Fully Funded Cost	\$59,853,979

¹ Federal administrative costs (LERRDs) would be cost shared 65/35 between the USACE and the non-Federal sponsor.

² Contingency for Lands and Damages is 15 percent, while contingency for Relocations (utilities) is 35.2 percent

Table 2. Summary of Completed Project Real Estate Costs (Waived)

Type	Cost
Local	
Lands and Damages (Structures, Relocation, Administrative Costs)	
Structure Acquisitions (96 structures completed)	\$2,575,371
Relocations (39 owner occupants completed)	\$2,656,119
Relocations (23 tenant occupants completed)	\$147,070
Administrative for 96 structures (completed)	\$334,138
Total Local Cost (Waived)	\$5,712,699

Table 3. Summary of Project Demolition Costs (Work-In-Kind)

Type	Cost
Local	
Demolitions	
Structure Demolitions (280 structures @ \$9,025)	\$2,527,000
Structure Demolitions (17 structures @ \$6,859 per structure) - Cantera)	\$154,425
Total Local Cost (Creditable)	\$2,681,425
Structure Demolitions (96 structures completed)	\$664,108 ²
Total Local Cost (Not-Creditable)	\$664,108

¹ Any future demolitions associated with the CMP-ERP would be creditable prior to the signing of a PPA so long as ENLACE and the USACE sign an agreement that would make the sponsor's Work-In-Kind demolition efforts creditable.

² Demolition costs associated with the 96 completed structure acquisitions are not creditable and cannot be used for the sponsor's cost share for the CMP-ERP because there was no Work-In-Kind agreement in place between ENLACE and the USACE at the time of their demolition.

25. REAL ESTATE ACQUISITION SCHEDULE

Ninety six structure acquisitions and sixty two relocations have already been completed. For the remaining acquisitions and relocations, the acquisition process will be an aggressive one that would encompass 297 structures with 217 eligible resident owners and 115 tenants to be relocated utilizing PL 91-646 criteria. ENLACE will carry out 75 relocations in the first year, 75 in the second year and 130 in the third year, prior to start of construction. The non-Federal sponsor will acquire the necessary permits and rights for the establishment of the temporary work area.

26. REAL ESTATE CHART OF ACCOUNTS

Table 4. Real Estate Lands & Damages

LANDS & DAMAGES

RELOCATION AND CONDEMNATION EXPENSES – FEDERAL	
Relocation and Moving Cost – By Federal Government	Cost (\$)
Relocation and Moving Cost (Federal) for Administrative Expenses	
Administrative Cost for Relocation and Moving – Appraisal Review by USACE	687,750
Administrative Cost for Relocation and Moving – Relocation Review by USACE	982,500
Transportation (Per USACE)	3,000
Real Estate Administrative Labor Expense (Per ENLACE)	14,000
STRUCTURE ACQUISITION - LOCAL	
Structure Acquisition – By Local Sponsor	
Structure Acquisition Cost (By ENLACE)	16,575,372 ¹
Structure Acquisition Cost (Cantera)	850,000
RELOCATION AND CONDEMNATION EXPENSES – LOCAL	
Relocation and Moving Cost – By Local Sponsor	
Relocation and Moving Cost (By Local Sponsor) Paid to Eligible Occupying Owner	
Relocation and Moving Expense, Per Occupying Owner (ENLACE)	18,958,119 ²
Relocation and Moving Expense, Per Occupying Tenant (ENLACE)	1,124,570 ³
Relocation and Moving Expense, Per Occupying Owner (Cantera)	1,385,670
Relocation and Moving Cost (By Local Sponsor) for Administrative Expenses	
Administrative Cost for Relocation and Moving – Appraisal Expense	527,520 ⁴
Administrative Cost for Relocation and Moving – Relocation Expense	1,190,000 ⁴
Administrative Cost for Relocation and Moving – Condemnation Expense	222,000 ⁴
Administrative Cost for Relocation and Moving (Cantera)	142,460
REAL ESTATE ACQUISITION AND ADMINISTRATIVE COST	
Real Estate Temporary Operation Cost	
Temporary Operations and Land Use Cost	
Parking Area Land Use Fee	126,000
Project Planning (from real Estate Division Operations)	50,000

¹ Includes the (waived) completed structure acquisitions cost of \$2,575,372

² Includes the (waived) completed owner occupant relocations cost of \$2,656,119

³ Includes the (waived) completed tenant occupied relocation cost of \$147,070

⁴ Includes the (waived) completed administrative costs of \$334,138

Table 5. Relocations

RELOCATIONS

UTILITY RELOCATIONS	
Utility Relocations Rexach Sewer Line	Cost (\$)
Rexach Sewer Line Replacement & Relocation	5,987,788
Borinquen Water Main	
Borinquen Water Main Relocation	3,191,211
115-kV Transmission Line	
Power Line Relocation, 115 kV	269,733

Table 6. Demolitions

DEMOLITIONS

Demolitions	
ENLACE	Cost (\$)
Structure Demolition Cost (By ENLACE)¹	3,191,108
Cantera	
Structure Demolition Cost (Cantera)	154,425

¹ Includes the non-creditable Work-In-Kind demolition cost of \$664,108

Exhibit A

Figures

Figure A-3. Caño Martín Peña Ecosystem Restoration Project Humacao Regional Landfill Map & Potential Sediment Disposal Yauco, Peñuelas and Ponce Landfills Map



Figure A-4. Mangrove Restoration Area Map

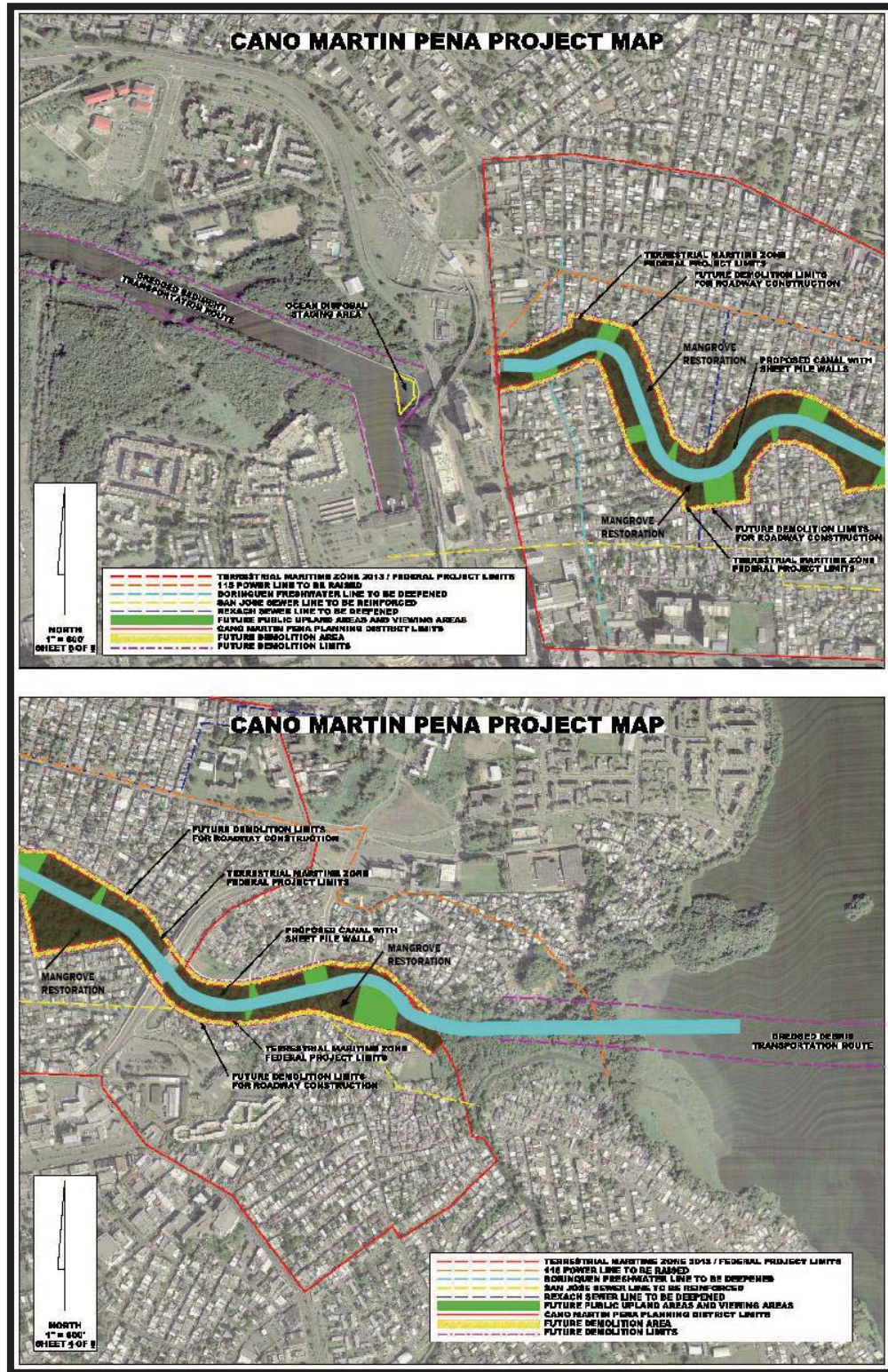


Figure A-5. Ciudad Deportiva Roberto Clemente Staging Area Map

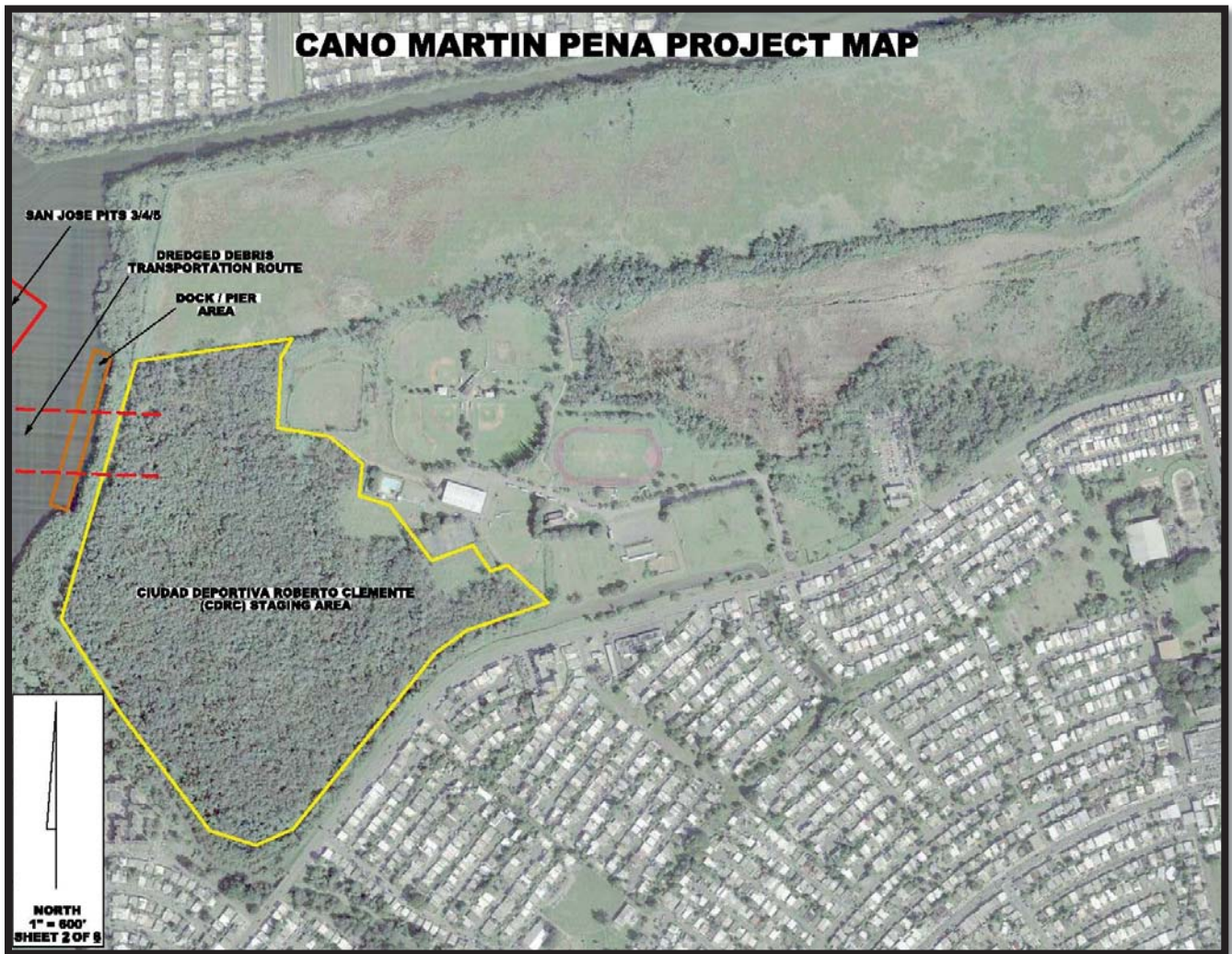


Figure A-6. Recreation Access Parks Map

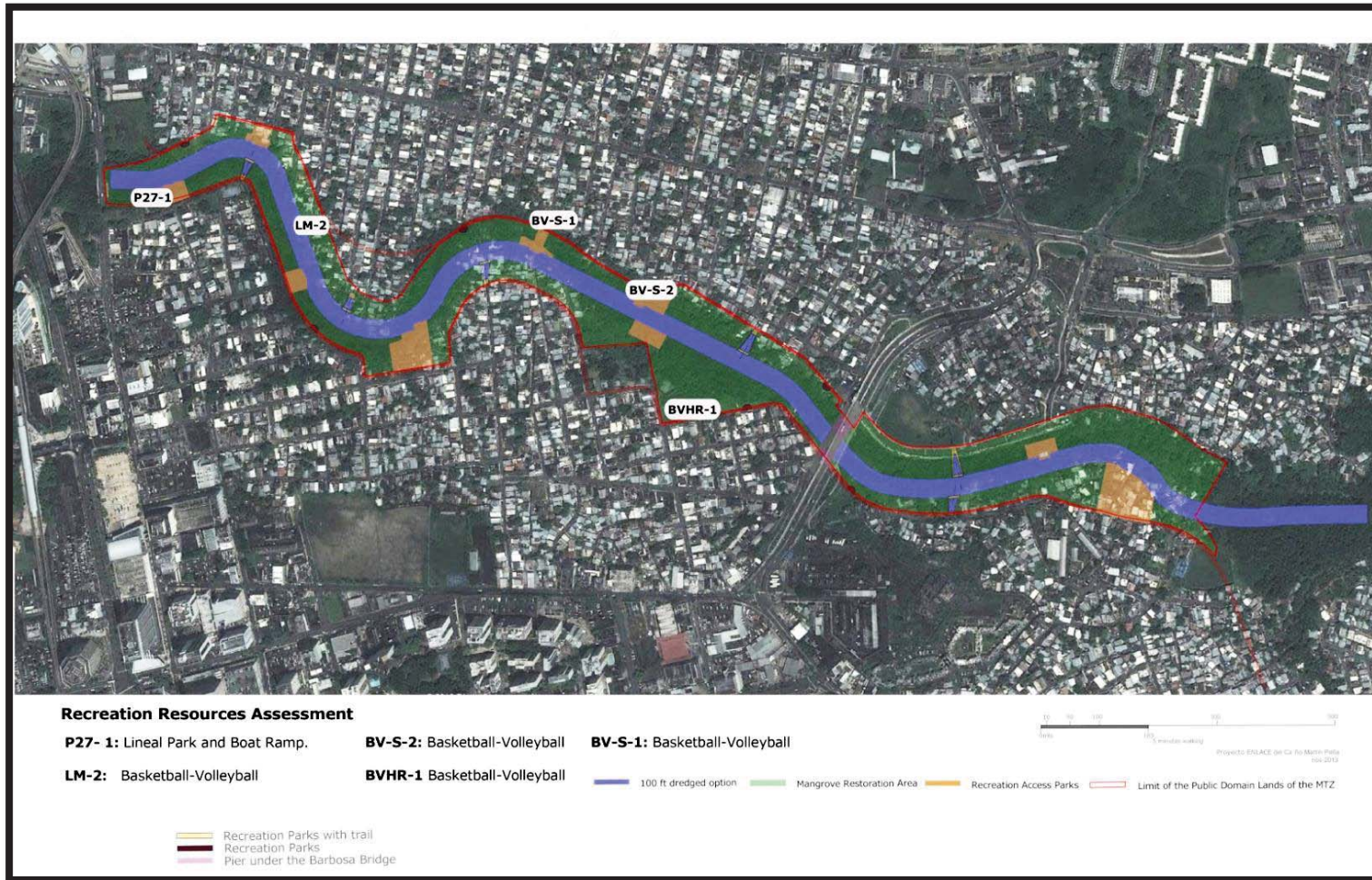


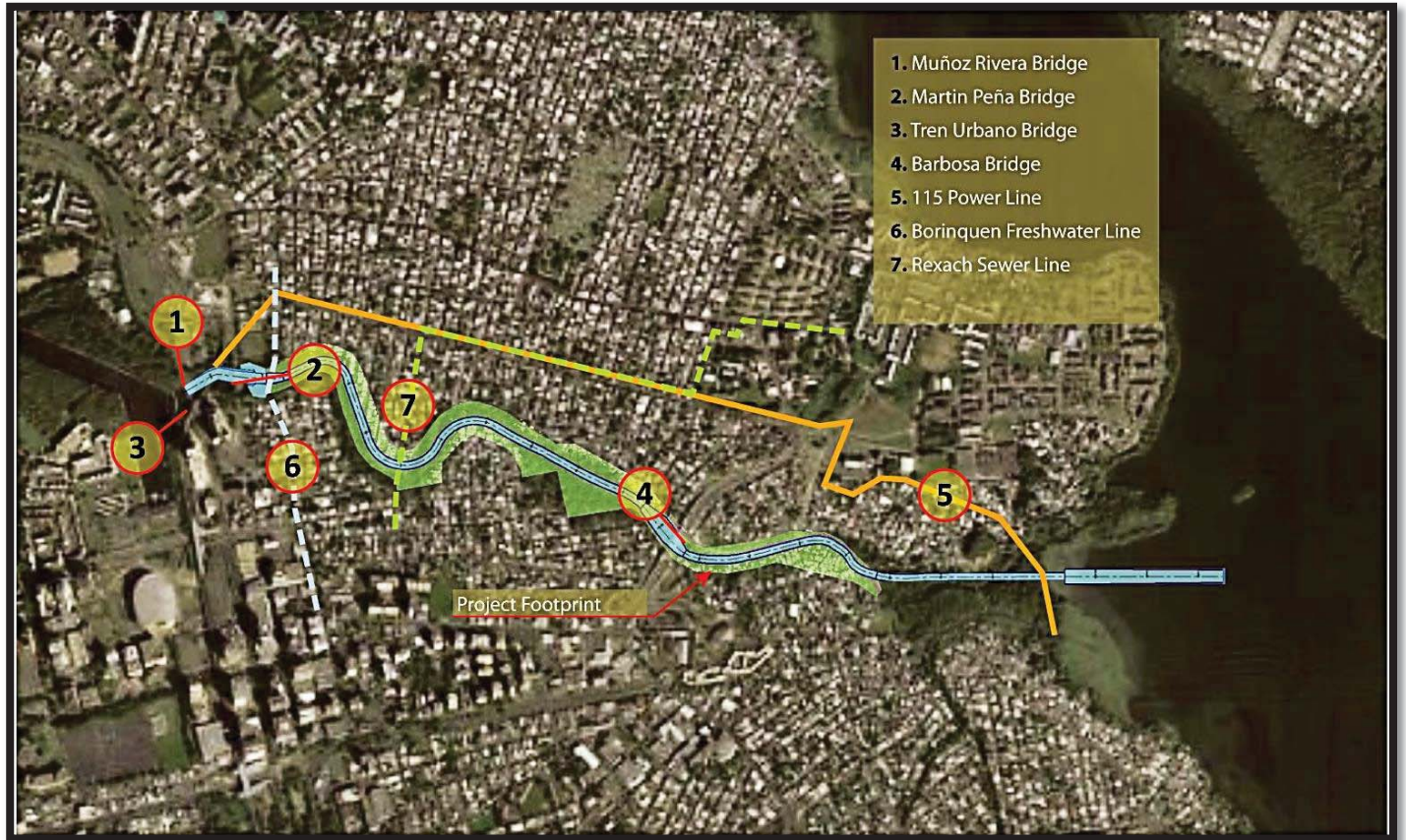
Figure A-7. *Piedritas Stadium Staging Area Map*



Figure A-8. Caño Martín Peña Aerial Photo (1936)



Figure A-9. Relocations, Alterations, Vacations and Abandonments Areas Map
(utilities, structures and facilities, cemeteries and towns)



This page intentionally left blank.

Exhibit B

**Assessment of Non-Federal Sponsor's
Real Estate Acquisition Capability
Corporación del Proyecto ENLACE del Caño Martín Peña**

**EXHIBIT B – Assessment of Non-Federal Sponsor's
Real Estate Acquisition Capability
Corporación del Proyecto ENLACE del Caño Martín Peña**

**PROJECT:
Caño Martín Peña Ecosystem Restoration Project**

I. LEGAL AUTHORITY:

- a. Does the sponsor have legal authority to acquire and hold title of real property for project purposes? **YES**
- b. Does the sponsor have the power of eminent domain for this project? **YES**
- c. Does the sponsor have "quick-take" authority for this project? **YES**
- d. Are any of the lands/interests in land required for the Project located outside the non-Federal sponsor's political boundary? **NO**
- e. Are any of the lands/interests in land required for the project owned by an entity whose property the sponsor cannot condemn? **NO**

II. HUMAN RESOURCE REQUIREMENTS:

- a. Will the sponsor's in-house staff require technical training to become familiar with the real estate requirements of Federal projects including U.S. Public Law 91-646, as amended? **NO**
- b. If the answer to IIa. is "yes," has a reasonable plan been developed to provide such training? **N/A**
- c. Does the sponsor's in-house staff have sufficient real estate acquisition experience to meet its responsibilities for the project? **YES**
- d. Is the sponsor's projected in-house staffing level sufficient considering its other work load, if any, and the project schedule? **YES**
- e. Can the sponsor obtain contractor support, if required in a timely fashion? **YES**
- f. Will the sponsor likely request United States Corps of Engineers (USACE) assistance in acquiring real estate? **NO**

III. OTHER PROJECT VARIABLES:

- a. Will the sponsor's staff be located within reasonable proximity to the project site? **YES**

-
- b. Has the non-Federal sponsor approved the project/real estate schedule/milestones?
YES

IV. OVERALL ASSESSMENT:

- a. Has the sponsor performed satisfactorily on other USACE projects? **N/A**
- b. With regard to the project, the sponsor is anticipated to be: **HIGHLY CAPABLE**

V. COORDINATION:

- a. Has this assessment been coordinated with the sponsor? **YES**
- b. Does the sponsor concur with this assessment? **YES**

Date: _____

Prepared by:

Realty Specialist
Real Estate Division
Jacksonville District

Reviewed by:

Hansler A. Bealyer
Chief
Acquisition Branch
Real Estate Division
Jacksonville District

Reviewed and approved by:

Audrey C. Ormerod
Chief
Real Estate Division
Jacksonville District

Exhibit C


**Memorandum of Agreement
Between ENLACE and USACE**

MEMORANDUM OF AGREEMENT
BETWEEN
THE DEPARTMENT OF THE ARMY
AND
CORPORACIÓN DEL PROYECTO ENLACE DEL CAÑO MARTÍN PEÑA
FOR THE REVIEW OF THE
FEASIBILITY REPORT AND ENVIRONMENTAL IMPACT STATEMENT
FOR THE
CAÑO MARTÍN PEÑA, ECOSYSTEM RESTORATION PROJECT

This MEMORANDUM OF AGREEMENT (hereinafter the "MOA") is entered into this 26th day of June, 2012, by and between the Department of the Army (hereinafter the "Government"), represented by the U.S. Army Engineer, Jacksonville District (hereinafter the "District Engineer"), and the Corporación del Proyecto ENLACE del Caño Martín Peña (hereinafter the "Contributor"), represented by its Executive Director.

WITNESSETH, THAT:

WHEREAS, Section 5127 of the Water Resources Development Act of 2007, Public Law 110-114, directs the Secretary of the Army to review a report prepared by the non-Federal interest concerning flood protection and environmental restoration for Caño Martín Peña, San Juan, Puerto Rico (hereinafter "report"), and, if the Secretary of the Army determines that the report meets the evaluation and design standards of the Corps of Engineers and that the project is feasible, the Secretary may carry out the project at a total cost of \$150,000,000;

 WHEREAS, the Contributor considers it to be in its own interest to contribute funds voluntarily (hereinafter the "Contributed Funds") to be used by the Government for the review of the report, entitled "Feasibility Report and Environmental Impact Statement for the Caño Martín Peña Ecosystem Restoration Project," to be completed by the Contributor in July 2012 (hereinafter "Review"); and

WHEREAS, the Government is authorized pursuant to 33 U.S.C. 701h to accept Contributed Funds to be used for the Review.

NOW, THEREFORE, the Government and Contributor agree as follows:

1. The Contributor shall provide to the Government Contributed Funds for all costs associated with the Review. While the Government will endeavor to limit costs associated with the Review under this MOA to the current estimate of \$300,000, the Contributor understands that the actual costs for the Review may exceed the amount of the estimate due to claims or other unforeseen circumstances.

2. Within seven (7) calendar days of execution of this MOA, the Contributor shall provide to the Government the sum of \$300,000, which is the current estimated cost of the

Review. Within thirty (30) calendar days of written notification by the Government that additional funds are needed to fund costs of the Review, the Contributor shall provide such additional funds.

3. The Contributor currently has \$300,000 allocated and available to fund the Review, as well as an additional \$50,000 in reserve to fund potential cost overages.

a. Nothing in this MOA shall constitute, nor be deemed to constitute, an obligation of future appropriations by the Government of the Commonwealth of Puerto Rico, where creating such obligation would be inconsistent with Law 230 of July 23, 1974, known as the Accounting Law of the Government of Puerto Rico (3 L.P.R.A. § 283, et seq., as amended).

b. The Contributor intends to fulfill its obligation under this MOA. In the event that the costs of the Review will exceed \$350,000, the Government will notify the Contributor of the additional funds needed to fund costs of the Review. The Contributor shall include in its budget request or otherwise propose appropriations of these funds and shall use all reasonable and lawful means to secure these funds. The Contributor reasonably believes that funds in amounts sufficient to fulfill these obligations lawfully can and will be appropriated and made available for this purpose. In the event funds are not appropriated in amounts sufficient to fulfill these obligations, the Contributor shall use its best efforts to satisfy any requirements for Contributed Funds under this MOA from any other source of funds legally available for this purpose.

4. The Contributor shall provide the Contributed Funds to the Government by delivering a check payable to "FAO, USAED Jacksonville" to the District Engineer; or verifying to the satisfaction of the Government that such funds have been deposited in an escrow or other account acceptable to the Government, with interest accruing to the Contributor; or presenting the Government with an irrevocable letter of credit acceptable to the Government for such funds; or providing an Electronic Funds Transfer of such funds in accordance with procedures established by the Government.

5. The Government shall provide the Contributor with quarterly accountings of obligations of the Contributed Funds for the Review. The first such accounting shall be provided within thirty (30) calendar days after the final day of the first complete Government fiscal year quarter following receipt of the Contributed Funds, and subsequent accountings shall be provided within thirty (30) calendar days after the final day of each succeeding quarter until the Government concludes the Review. Upon conclusion of the Review and resolution of all relevant claims and appeals, the Government shall conduct a final accounting of the costs of such work and furnish the Contributor with written notice of the results of such final accounting. Such final accounting shall in no way limit the Contributor's responsibility to pay for all costs associated with the Review, including contract claims or any other liability that may become known after the final accounting.

6. Should the final accounting show that the costs of the Review exceed the amount provided by the Contributor, the Contributor shall provide the additional required funding in

accordance with paragraph 4 of this MOA within sixty (60) calendar days of written notice of the final accounting. Should the final accounting show that the costs of the Review is less than the amount provided by the Contributor, the Government shall refund the excess to the Contributor within sixty (60) calendar days of the written notice of the final accounting.

7. No credit or repayment is authorized, nor shall be provided, for any Contributed Funds obligated by the Government.

8. Nothing herein shall constitute, represent, or imply any commitment to budget or appropriate funds for the Project in the future; and nothing herein shall represent, or give rise to, obligations of the United States.

9. Before any party to this MOA may bring suit in any court concerning an issue relating to this MOA, such party must first seek in good faith to resolve the issue through negotiation or other forms of nonbinding alternative dispute resolution mutually acceptable to the parties.

10. In the exercise of their respective rights and obligations under this MOA, the Contributor and the Government agree to comply with all applicable Federal and State laws and regulations, including, but not limited to, Section 601 of the Civil Rights Act of 1964, Public Law 88-352 (42 U.S.C. 2000d), and Department of Defense Directive 5500.11 issued pursuant thereto, as well as Army Regulation 600-7, entitled "Nondiscrimination on the Basis of Handicap in Programs and Activities Assisted or Conducted by the Department of the Army."

11. In the exercise of their respective rights and obligations under this MOA, the Government and the Contributor each act in an independent capacity, and neither is to be considered the officer, agent, or employee of the other.

12. Notices.

a. Any notice, request, demand, or other communication required or permitted to be given under this MOA shall be deemed to have been duly given if in writing and either delivered personally or mailed by first-class, registered, or certified mail, as follows:

If to the Contributor:

Executive Director
Corporación del Proyecto
ENLACE del Caño Martín Peña
PO Box 41308
San Juan, PR 00940-1308

If to the Government:

District Engineer
Jacksonville District
U.S. Army Corps of Engineers
P.O. Box 4970
Jacksonville, Florida 32232-0019

b. A party may change the address to which such communications are to be directed by giving written notice to the other party in the manner provided in this paragraph.

c. Any notice, request, demand, or other communication made pursuant to this paragraph shall be deemed to have been received by the addressee at the earlier of such time as it is actually received or seven (7) calendar days after it is mailed.

13. To the extent permitted by the laws governing each party, the parties agree to maintain the confidentiality of exchanged information when requested to do so by the providing party.

14. This MOA may be modified or amended only by written, mutual agreement of the parties.

IN WITNESS WHEREOF, the parties have executed this MOA as of the day, month, and year first above written.

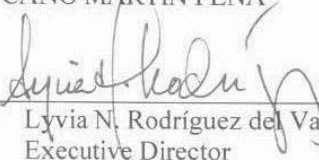
THE DEPARTMENT OF THE ARMY

CORPORACIÓN DEL PROYECTO ENLACE
DEL CAÑO MARTÍN PEÑA

BY: _____


Alfred A. Pantano, Jr.
Colonel, U.S. Army
District Commander

BY: _____


Lyvia N. Rodríguez del Valle
Executive Director

DATE: 26 June 2012

DATE: June 25, 2012

CERTIFICATE OF AUTHORITY

I, Myriam González Torres, do hereby certify that I am the legal officer for this agreement for the CORPORACIÓN DEL PROYECTO ENLACE DEL CAÑO MARTÍN PEÑA, that the CORPORACIÓN DEL PROYECTO ENLACE DEL CAÑO MARTÍN PEÑA is a legally constituted public body with full authority and legal capability to perform the terms of the Agreement between the Department of the Army and the CORPORACIÓN DEL PROYECTO ENLACE DEL CAÑO MARTÍN PEÑA, and to pay damages in accordance with the terms of this Agreement, if necessary, in the event of the failure to perform and that the persons who have executed this Agreement on behalf of the CORPORACIÓN DEL PROYECTO ENLACE DEL CAÑO MARTÍN PEÑA have acted within their statutory authority.

IN WITNESS WHEREOF, I have made and executed this certification this 25th day of June 2012.

Myriam González Torres
Myriam González Torres, Attorney for
Corporación del Proyecto ENLACE del Caño Martín Peña

CERTIFICATION REGARDING LOBBYING

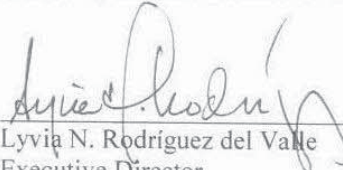
The undersigned certifies, to the best of his or her knowledge and belief that:

(1) No Federal appropriated funds have been paid or will be paid, by or on behalf of the undersigned, to any person for influencing or attempting to influence an officer or employee of any agency, a Member of Congress, an officer or employee of Congress, or an employee of a Member of Congress in connection with the awarding of any Federal contract, the making of any Federal grant, the making of any Federal loan, the entering into of any cooperative agreement, and the extension, continuation, renewal, amendment, or modification of any Federal contract, grant, loan, or cooperative agreement.

(2) If any funds other than Federal appropriated funds have been paid or will be paid to any person for influencing or attempting to influence an officer or employee of any agency, a Member of Congress, an officer or employee of Congress, or an employee of a Member of Congress in connection with this Federal contract, grant, loan, or cooperative agreement, the undersigned shall complete and submit Standard Form-LLL, "Disclosure Form to Report Lobbying," in accordance with its instructions.

(3) The undersigned shall require that the language of this certification be included in the award documents for all sub-awards at all tiers (including subcontracts, sub-grants, and contracts under grants, loans, and cooperative agreements) and that all sub-recipients shall certify and disclose accordingly.

This certification is a material representation of fact upon which reliance was placed when this transaction was made or entered into. Submission of this certification is a prerequisite for making or entering into this transaction imposed by 31 U.S.C. 1352. Any person who fails to file the required certification shall be subject to a civil penalty of not less than \$10,000 and not more than \$100,000 for each such failure.


Lyvia N. Rodriguez del Valle
Executive Director

DATE: June 25, 2012

Exhibit D

**Caño Martín Peña Ecosystem Restoration Project
LERRDs Relocation of the
115-kW Power Transmission Line**



COMMONWEALTH OF PUERTO RICO
Puerto Rico Electric Power Authority

Javier A. Quintana Méndez, P.E.
Executive Director

December 4th, 2015

Lyvia N. Rodríguez Del Valle
Executive Director
Corporación del Proyecto ENLACE
del Caño Martín Peña
P.O. Box 41308
San Juan, PR 00940-1308

**CAÑO MARTÍN PEÑA ECOSYSTEM RESTORATION PROJECT LEERDs
RELOCATION OF THE 115KW POWER TRANSMISSION LINE**

Dear Ms. Rodríguez Del Valle:

As the non-Federal sponsor of the Caño Martin Peña Ecosystem Restoration Project (CMP-ERP), the *Corporación del Proyecto ENLACE del Caño Martín Peña* (ENLACE) must provide a cost share. The cost share will be provided in a combination of in-kind services, cash contribution and lands, easements, rights-of-way, relocations and disposal areas (LERRDs). ENLACE must also provide a Self-Certification of Financial Capability, certifying that it has the financial capability to satisfy its financial obligations, including its cost share requirements. The following is in support of ENLACE's Self-Certification.

I hereby certify that the Puerto Rico Electric Power Authority (PREPA) invested a total of \$269,733 to improve the 115kV Power Transmission Line, which is part of the LEERDs for the CMP-ERP, and that the information provided in this letter is correct. The funding source for such investment is PREPA's Capital Improvement Program (CIP). As requested by the U.S. Army Corps of Engineers, below is a description of the nature, timing of performance, and value of this project:

J.A. Quintana

1. 115kV Power Transmission Line Improvement
 - a. Nature of the Contribution: Line Segment Improvement for 115kV Power Transmission Line – 38900.
 - b. Schedule: October 23, 2014 to December 23, 2014.

G.P.O. BOX 364287 SAN JUAN, PUERTO RICO 00936-4287 PHONE: (787) 521-4666 FAX: (787) 521-4665

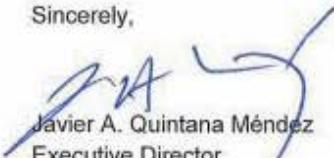
"We are an equal opportunity employer and do not discriminate on the basis of race, color, gender, age, national or social origin, social status, political ideas or affiliation, religion; for being or perceived to be victim of domestic violence, sexual aggression or harassment, regardless of marital status, sexual orientation, gender identity or immigration status; for physical or mental disability or veteran status or for genetic information."

Lyvia N. Rodríguez Del Valle
Page 2
December 4, 2014

- c. Scope of Work: Increase Power Cables (115kV) height with reference to ground level, not less than 50ft. above Caño Martin Peña in order to allow the U.S. Army Corps of Engineers to dredge the Caño.
- d. Value of the contribution: \$269,733.00.

For additional information please contact engineer Carlos J. Laureano Rivera, Head of Electrical Distribution Division, at claureano8008@aepr.com or (787) 521-6552.

Sincerely,



Javier A. Quintana Méndez
Executive Director

38900 LINE COST BREAK DOWN

ITEM	EXPENSE	COMMENTS
PURCHASE ORDER FOR POLE STRUCTURE BASES	\$ 60,000.00	
CHANGE ORDER (CAGE STEEL BARS MODIFICATION)	\$ 3,500.00	
2 POLES TYPE C (97 feet), Boundle Circuit	\$ 158,790.00	Two poles
MISCELLANEUS MATERIALS FOR CONSTRUCTION	\$ 5,000.00	
WORK FORCE LABOR (HUMAN RESOURCES, TRANSPORTATION, PER DIEM, OVERHE	\$ 42,443.00	
TOTAL	\$ 269,733.00	

Exhibit E

**Caño Martín Peña Ecosystem Restoration Project
LERRDs Relocation of the Relocation of the Rexach
Trunk Sewer and Borinquen Water Transmission Line**



Commonwealth of Puerto Rico
Puerto Rico Aqueduct and Sewer Authority
 - Infrastructure Area -

ESTADO LIBRE ASOCIADO DE PUERTO RICO

Project : **RELOCATION OF THE BORINQUEN POTABLE WATER TRANSMISSION PIPELINE AT CAÑO MARTIN PEÑA SAN JUAN, PUERTO RICO**

- BASE PROPOSAL -

CIP Number: 1-66-7005 Funds: PRASA

Cost Estimate

Item	Quantity	Unit	Description	Unit Price	\$ Total
A. TRANSMISSION PIPELINE					
<u>42" DIA Ductile Iron Piline & Appurtenances</u>					
1	3870	CM	Trench Excavation	60.00	232,200.00
2	1982	CM	Backfill (A-2-4)	60.00	118,920.00
3	782	CM	Backfill with existing material	60.00	46,920.00
4	943	CM	Trench Material Disposal	30.00	28,290.00
5	128	CM	3/4" Clean Crushed Rock for Bedding	50.00	6,400.00
6	1600	SM	Temporary Sheet Piling	400.00	640,000.00
7	540	SM	Permanent Sheet Piling	400.00	216,000.00
8	60.72	LM	42" diameter DI Pipe Class 250 out of CMP	600.00	36,432.00
9	61.33	LM	42" diameter DI Pipe Class 250 on CMP	600.00	36,798.00
10	8	EA	45 Deg. Elbow 42" diameter DI Pipe	5,000.00	40,000.00
11	2	EA	36"-42" diameter Reducer	8,000.00	16,000.00
12	2	EA	4" diameter Gate Valves	1,500.00	3,000.00
13	2	EA	42" Butterfly Valves, Pipes and Appurtenances	30,000.00	60,000.00
14	2	EA	Air Release Valves	4,000.00	8,000.00

Cost Estimate

Item	Quantity	Unit	Description	Unit Price	\$ Total
15	622	CY	Concrete Protection For Pipe	500.00	311,000.00
16	125	CY	Concrete Manholes	600.00	75,000.00
17	2	EA	36"x36" Access door	3,200.00	6,400.00
18	2	EA	28"x55" Access door	3,600.00	7,200.00
19	1	LS	Miscellaneous Materials and Fittings	25,000.00	25,000.00
20	1	LS	Asphalt and Base for repair of San José & Argentina Streets	10,000.00	10,000.00
21	2	EA	PRASA'S fees related to connection to Existing 36-inch pipeline valves	30,000.00	60,000.00
				Subtotal Item A:	\$ 1,983,560.00
B. PLAYGROUND AND GAZEBO WORKS					
22	27.6	LM	Chain Link Fence Removal (6')	20.00	552.00
23	26.13	LM	New Chain Link Fence (6')	90.00	2,351.70
24	16.35	LM	Existing Concrete and Galvanize Steel Fence Removal	30.00	490.50
25	16.35	LM	New Concrete and Galvanize Steel Fence	200.00	3,270.00
26	1	LS	Play ground equipment removal, storage and re-installation	4,000.00	4,000.00
27	3	LS	Benches removal, storage and re-installation	500.00	1,500.00
28	3	EA	Poles and luminaries removal, storage and re-installation	800.00	2,400.00
29	323	SF	Gazebo Demolition and Reconstruction	30.00	9,690.00
				Subtotal Item B:	\$ 24,254.20

Cost Estimate

Item	Quantity	Unit	Description	Unit Price	\$ Total
C. LEVEE SYSTEM					
30	912	CM	A-2-4 and A-5 Fill Material	40.00	36,480.00
31	276	CM	Gabion Matress	300.00	82,800.00
Subtotal Item C:					\$ 119,280.00
D. GENERAL					
32	4	MTH	Dewatering System	35,000.00	140,000.00
33	1	LS	Reforestation and Mitigation Plan	50,000.00	50,000.00
34	4	MTH	MOT Plan	3,000.00	12,000.00
35	1	LS	Furnish and Installation of Project Sign	1,500.00	1,500.00
36	1	LS	PRASA Field Office Inspection including Maintenance	20,000.00	20,000.00
Subtotal Item D:					\$ 223,500.00
SUB- TOTAL PROJECT COST					\$ 2,350,594.20

Cost Estimate

Item	Quantity	Unit	Description	Unit Price	\$ Total
------	----------	------	-------------	------------	----------

SUB-TOTAL PROJECT COST					\$ 2,350,594.20
-------------------------------	--	--	--	--	------------------------

			General Administrative Project Costs	12.0%	282,071.80
			Sub total		\$ 2,632,666.00
			Overhead & Profit	15.0%	394,900.00
			Sub total		\$ 3,027,566.00
			Construction Tax	5.5%	166,516.00
1.a			Sub total		\$ 3,194,082.00

2 - UNIT PRICE BASIS ITEM

a.	80	CM	Rock excavation as per section 02A015 of the Standard Technical Specification.	100.00	\$ 8,000.00
----	----	----	--	--------	-------------

CONSTRUCTION COST FOR PRASA PARTICIPATION - \$ 3,202,082.00
 (1.a + 2.a)

ESTIMATED CONSTRUCTION COST - BASE PROPOSAL - \$ 3,202,082.00





**Commonwealth of Puerto Rico
Puerto Rico Aqueduct and Sewer Authority
- Infrastructure Area -**

Project : **RELOCATION OF THE BORINQUEN POTABLE WATER
TRANSMISSION PIPELINE AT CAÑO MARTIN PEÑA
SAN JUAN, PUERTO RICO**

- BASE PROPOSAL WITH ALTERNATIVE I -

CIP Number: 1-66-7005 Funds: PRASA

Cost Estimate

Item	Quantity	Unit	Description	Unit Price	\$ Total
A. TRANSMISSION PIPELINE					
<u>42" DIA PCCP Transmission Line & Appurtenances</u>					
1	3870	CM	Trench Excavation	60.00	232,200.00
2	1982	CM	Backfill (A-2-4)	60.00	118,920.00
3	782	CM	Backfill with existing material	60.00	46,920.00
4	943	CM	Trench Material Disposal	30.00	28,290.00
5	128	CM	3/4" Clean Crushed Rock for Bedding	50.00	6,400.00
6	1600	SM	Temporary Sheet Piling	400.00	640,000.00
7	540	SM	Permanent Sheet Piling	400.00	216,000.00
8	60.72	LM	42" diameter PCCP AWWA C301 out of CMP	1,480.00	89,865.60
9	61.33	LM	42" diameter PCCP AWWA C301 on CMP	1,480.00	90,768.40
10	8	EA	45 Deg. Elbow 42" diameter PCCP AWWA C301 Pipe	9,600.00	76,800.00
11	2	EA	36"-42" diameter PCCP AWWA C301 Reducer	16,000.00	32,000.00
12	2		4" diameter Gate Valves	1,500.00	3,000.00
13	2	EA	42" Butterfly Valves, Pipes and Appurtenances	30,000.00	60,000.00

Cost Estimate

Item	Quantity	Unit	Description	Unit Price	\$ Total
14	2	EA	Air Release Valves	4,000.00	8,000.00
15	622	CY	Concrete Protection For Pipe	500.00	311,000.00
16	125	CY	Concrete Manholes	600.00	75,000.00
17	2		36"x36" Access door	3,200.00	6,400.00
18	2		28"x55" Access door	3,600.00	7,200.00
19	1	LS	Miscellaneous Materials and Fittings	25,000.00	25,000.00
20	1	LS	Asphalt and Base for repair of San José & Argentina Streets	10,000.00	10,000.00
21	2	EA	PRASA'S fees related to connection to Existing 36-inch pipeline valves	30,000.00	60,000.00
				Subtotal Item A:	\$ 2,143,764.00
B. PLAYGROUND AND GAZEBO WORKS					
22	27.6	LM	Chain Link Fence Removal (6')	20.00	552.00
23	26.13	LM	New Chain Link Fence (6')	90.00	2,351.70
24	16.35	LM	Existing Concrete and Galvanize Steel Fence Removal	30.00	490.50
25	16.35	LM	New Concrete and Galvanize Steel Fence	200.00	3,270.00
26	1	LS	Play ground equipment removal, storage and re-installation	4,000.00	4,000.00
27	3	LS	Benches removal, storage and re-installation	500.00	1,500.00
28	3	EA	Poles and luminaries removal, storage and re-installation	800.00	2,400.00
29	323	SF	Gazebo Demolition and Reconstruction	30.00	9,690.00
				Subtotal Item B:	\$ 24,254.20

Cost Estimate

Item	Quantity	Unit	Description	Unit Price	\$ Total
C. LEVEE SYSTEM					
30	912	CM	A-2-4 and A-5 Fill Material	40.00	36,480.00
31	276	CM	Gabion Matress	300.00	82,800.00
Subtotal Item C:					\$ 119,280.00
D. GENERAL					
32	4	MTH	Dewatering System	35,000.00	140,000.00
33	1	LS	Reforestation and Mitigation Plan	50,000.00	50,000.00
34	4	MTH	MOT Plan	3,000.00	12,000.00
35	1	LS	Furnish and Installation of Project Sign	1,500.00	1,500.00
36	1	LS	PRASA Field Office Inspection including Maintenance	20,000.00	20,000.00
Subtotal Item D:					\$ 223,500.00
SUB- TOTAL PROJECT COST					\$ 2,510,798.20

Cost Estimate

Item	Quantity	Unit	Description	Unit Price	\$ Total
------	----------	------	-------------	------------	----------

SUB-TOTAL PROJECT COST					\$ 2,510,798.20
-------------------------------	--	--	--	--	------------------------

			General Administrative Project Costs	12.0%	301,296.80
			Sub total		\$ 2,812,095.00
			Overhead & Profit	15.0%	421,814.00
			Sub total		\$ 3,233,909.00
			Construction Tax	5.5%	177,865.00
1.a			Sub total		\$ 3,411,774.00

2 - UNIT PRICE BASIS ITEM

a.	80	CM	Rock excavation as per section 02A015 of the Standard Technical Specification.	100.00	\$ 8,000.00
----	----	----	--	--------	-------------

CONSTRUCTION COST FOR PRASA PARTICIPATION - **\$ 3,419,774.00**
 (1.a + 2.a)

ESTIMATED CONSTRUCTION COST - BASE PROPOSAL WITH ALTERNATIVE I - \$ 3,419,774.00



RELOCATION OF THE BORINQUEN POTABLE WATER
TRANSMISSION PIPELINE AT CAÑO MARTIN PEÑA
SAN JUAN, PUERTO RICO



CIP Number: 1-66-7005 Funds: PRASA

Cost Estimate

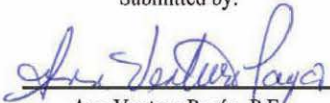
PROJECT CONSTRUCTION COST

ESTIMATED CONSTRUCTION COST - BASE PROPOSAL -	\$ 3,202,082.00
ESTIMATED CONSTRUCTION COST - BASE PROPOSAL WITH ALTERNATIVE I -	\$ 3,419,774.00


Estimated Construction Cost - Base Proposal	\$ 3,202,082.00
--	------------------------

Construction Cost for PRASA Participation	\$ 3,202,082.00
Contingencies	\$ 320,208.00
Survey and Design	\$ 188,922.00
Engineering Services During Construction	\$ 37,784.00
Construction Management and Inspection	\$ 160,104.00
General and Adm. Expenses	\$ 586,365.00
Estimated Total Project Cost	\$ 4,495,465.00

Submitted by:


Ann Ventura Payán, P.E.
Specifications and Estimate Section

Approved by:


José J. Rivera, P.E.
Auxiliary Director for Engineering

Prepared:
June 2, 2015





Commonwealth of Puerto Rico
 Puerto Rico Aqueduct and Sewer Authority
 Specifications and Estimates Section

Project: **RELOCATION OF REXACH TRUNK SEWER AT CAÑO MARTÍN
 PEÑA
 SAN JUAN, PUERTO RICO**

CIP No. 1-66-5104

Funds: PRASA

Cost Estimate

Item	Quantity	Unit	Description	Unit Price	\$ Total
A. GRAVITY SEWER LINE					
48" DIA Gravity Trunk Sewer					
1	343	LM	Furnishing and installation of 48" DIA gravity RCP pipe with PVC lining	931.58	319,531.94
2		LM	Unclassified Trench Excavator for 48" DIA Trunk Sewer including backfill		
	124		4.00 - 5.00 M	1,595.04	197,784.96
	219		5.00 - 6.00 M	738.36	161,700.84
3			Precast MH 2.44M including excavation, backfill		
	2	EA	4.00 - 5.00 M	16,045.28	32,090.56
	4	EA	5.01 - 6.00 M	31,535.60	126,142.40
4			<u>For demolition and reposition of asphalt pavement as follows:</u>		
a	1	LS	Cutting and demolition of existing pavement and base within trench	15,324.72	15,324.72
b	160	CM	Reposition of 6" thick gravel subbase site improvements and base within trench	39.90	6,384.00
c	78	CM	Reposition of 4" Macadam base	22.22	1,733.16
d	178	Ton	Wearing course (S-1) within trench limits	175.00	31,150.00
5	1	LS	Reconstruction of sidewalks and gutters	25,000.00	25,000.00
6	1	LS	Intercepting existing 48" and 66" Sanitary Trunk Sewers	70,000.00	70,000.00
7	882	CM	Additional excavation for bedding material	3.28	2,892.96

Item	Quantity	Unit	Description	Unit Price	\$ Total
8	1	EA	Watertight Manhole Cover	791.00	791.00
9	131	CY	Furnishing casting concrete protection	242.95	31,826.45
10	35	LM	Repairs to existing pipe lines	1430.50	50,067.50
11	15	EA	For demolition of existing structures	5161.37	77,420.55
8" DIA Gravity Trunk Sewer					
12	320	LM	Furnishing and installation of 8" PVC SDR 35 sewer pipe	125.35	40,112.00
13	320	LM	Pipe Marking, Detection tape	1.71	547.20
14	6	EA	Deep fittings 8" DIA 2.01- 3.00 M	4,890.45	29,342.70
15	8	EA	Intercepting existing sanitary sewer	3,000.00	24,000.00
<u>Water supply isolation valves during construction:</u>					
16	3	EA	4" Gate Valve	4,239.00	12,717.00
Storm Sewers					
17			Replacing Existing Storm Sewer		
a	1	LS	Excavation for 12" and 24" DIA RCP Pipe 2.01 - 3.00 M	8,283.00	8,283.00
b	1	LS	Manhole or Catch Basin Installing 2.01 - 3.00 M	58,315.00	58,315.00
c	62	LM	Furnishing and installation of 12" DIA PVC	495.00	30,690.00
d	20	CM	Concrete protection	392.00	7,840.00
e	2	EA	Reinforce concrete for Head wall	4,500.00	9,000.00
Sub-Total A					\$ 1,370,687.94
B. INVERTED SIPHON					
Siphon Inlet/Outlet					
INLET No. 2					
18			Excavation at Inlet No. 2		
a	1	LS	Excavation at Inlet No. 2	18,113.00	18,113.00
b	1	LS	18" SOG at Inlet No. 2	17,571.00	17,571.00
c	1	LS	18" walls at Inlet No. 2	60,178.00	60,178.00

Item	Quantity	Unit	Description	Unit Price	\$ Total
d	1	LS	Elevated slab at Inlet No. 2	18,157.00	18,157.00
e	4	EA	36" watertight MH covers	1,100.00	4,400.00
f	1	LS	Grating and Railing	3,245.00	3,245.00
g	3	EA	36" Sluice Gates	12,250.00	36,750.00
OULET No. 3					
19 a	1	LS	Excavation at Outlet No. 3	18,113.00	18,113.00
b	1	LS	18" SOC at Outlet No. 3	17,571.00	17,571.00
c	1	LS	18" walls at Outlet No. 3	60,178.00	60,178.00
d	1	LS	Elevated slab at Outlet No. 3	18,157.00	18,157.00
e	4	EA	36" watertight MH covers	1,100.00	4,400.00
f	1	LS	Grating and Railing	3,245.00	3,245.00
g	3	EA	36" Sluice Gates	12,250.00	36,750.00
Siphon (115 meters of length)					
20	345	LM	Furnishing and Installation of 36" Pipe Class 350 with Procto 401	1,654.34	570,747.30
21	1	LS	Furnishing and installing sheet piling in place, cofferdams	404,907.00	404,907.00
22	1	LS	Concrete Encasement	124,302.00	124,302.00
23	1	LS	Construction of embankment to reach site	275,000.00	275,000.00
24	6	EA	Repair to existing lines	5,000.00	30,000.00
25	5	EA	Light Pole Repairs	1,500.00	7,500.00
26	1	LS	Remove existing 48" Trunk Sewer at Cato Martín Peña	63,000.00	63,000.00
Sub-Total B					\$ 1,792,284.30

Item	Quantity	Unit	Description	Unit Price	\$ Total
C. GENERAL					
27	14	Mo	Dewatering activities during construction	35,000.00	490,000.00
28	1	LS	Existing pipe cleaning and obstruction removals	150,000.00	150,000.00
29	14	Mo	Environmental Mitigation during Construction	25,000.00	350,000.00
30	14	Mo	Local Traffic Flow Modifications during construction	20,000.00	280,000.00
Sub-Total C					\$ 1,270,000.00
SUB- TOTAL PROJECT COST					\$ 4,432,972.24

SUB- TOTAL PROJECT COST		\$4,432,972.24
General Conditions	10.0%	443,297.00
Sub total		4,876,269.24
Overhead	10.0%	487,627.00
Profit	8.0%	390,102.00
Sub total		5,753,998.24
Construction Tax	7.5%	431,550.00
Sub total		6,185,548.24
1.a - BASE BID (LUMP SUM PRICE)		\$6,185,548.24

2 - ALLOWANCES

Consist of the payment of the monetary compensation as mitigation for the tree removal and trimming as authorized by the "OGPE". Contractor Shall perform the payment as indicated in "OGPE" letter include in A.10 - "Endorsements". Tree Inventory Plan included in A.10 - "Endorsements".

\$ 4,200.00

3 - UNIT PRICE BASIS ITEM

a	120	CM	Rock excavation as per section 02A015 of the Standard Technical Specification.	130.00	\$ 15,600.00
---	-----	----	--	--------	--------------

Item	Quantity	Unit	Description	Unit Price	\$ Total
b	260	Ton	Wearing course asphalt pavement for repavement of streets, municipal and state roads.	190.00	\$ 49,400.00
e		EA	4' Dia. Sewer service connection including excavation, backfilling, demolition and replacement of pavement.		\$ -
d		EA	6' Dia. Sewer service connection including excavation, backfilling, demolition and replacement of pavement.		\$ -

CONSTRUCTION COST FOR PRASA PARTICIPATION

(1.a + 2.a + 3.a + 3.b + 3.c + 3.d)

\$6,254,838.24**NET CONSTRUCTION COST**

(1.a + 2.a + 3.a + 3.b + 3.c + 3.d)

\$6,254,838.24

RELOCATION OF REXACH TRUNK SEWER AT CAÑO
MARTÍN PEÑA
SAN JUAN, PUERTO RICO

CEP No. 1-66-5104 Funds: PRASA



Cost Estimate

Net Construction Cost	\$ 6,254,838.24
<hr/>	
Construction Cost for PRASA Participation	\$ 6,254,838.24
Contingencies	\$ 938,226.00
Survey and Design	\$ 292,500.00
Architect or Engineering Services During Construction	\$ -
Construction Management and Inspection	\$ 312,742.00
Land and /or Right of Way Acquisition	\$ -
General and Adm. Expenses	\$ 1,559,661.00
Estimated Total Project Cost	\$ 9,357,967.24

Submitted by:

Eng. Ann Ventura Payán
Specifications and Estimate Section

Approved by:

Eng. José J. Rivera, PE
Auxiliary Director for Engineering



Prepared: Evelio Agustin, PE
February 19, 2014
EAL



Appendix C

Recreation Resources Assessment and Recreation Plan

FINAL
FEDERAL RECREATION PLAN AND
RECREATION RESOURCE ASSESSMENT
CAÑO MARTÍN PEÑA
ECOSYSTEM RESTORATION PROJECT
SAN JUAN, PUERTO RICO

Prepared for:



Corporación del Proyecto ENLACE del Caño Martín Peña
Apartado Postal 41308
San Juan, Puerto Rico 00940-1308

February 2016

Contents

	Page
List of Figures	iv
List of Tables	iv
1.0 INTRODUCTION.....	1-1
1.1 ECOSYSTEM RESTORATION PROJECT STUDY AUTHORITY	1-1
1.2 ECOSYSTEM RESTORATION PROJECT DESCRIPTION	1-1
1.3 LOCAL COOPERATION	1-2
2.0 FEDERAL RECREATION PLAN DEVELOPMENT	2-1
2.1 RECREATION PLAN CONSTRAINTS	2-1
2.2 RECREATION PLAN PURPOSE	2-1
2.3 RECREATION PLAN FEATURES	2-1
2.4 RECREATION PLAN ACCESS AREAS.....	2-2
2.4.1 Linear Park	2-3
2.4.2 Recreation Access Park	2-4
2.4.3 Recreation Park	2-4
2.4.4 Proposed Non-Federal Recreation Features	2-7
2.5 POTENTIAL LOCATION OF RECREATIONAL AREAS	2-7
2.6 PROPOSED FEDERAL RECREATION PLAN	2-7
3.0 RECREATION RESOURCE ASSESSMENT.....	3-1
3.1 EXISTING CONDITIONS.....	3-1
3.1.1 Recreational Opportunities.....	3-1
3.1.2 Population Projections	3-1
3.1.3 Recreational Needs Identified by SCORP	3-5
3.2 RECREATION BENEFIT	3-5
3.2.1 National Economic Development Benefit.....	3-5
3.2.2 Assigning Points for General Recreation.....	3-6
3.2.3 Conversion of Points to Dollar Value.....	3-9
3.2.4 Most Likely Recreation Participation User Day Projection Scenario	3-10
3.3 ECONOMIC JUSTIFICATION OF RECREATION PLAN.....	3-12
3.3.1 Recreation Facilities Cost Estimate.....	3-13
3.3.2 Recreation Facilities Benefits.....	3-13
3.3.3 Sensitivity Analysis.....	3-14
4.0 CONCLUSION.....	4-1
5.0 REFERENCES	5-1

List of Figures

	Page
Figure 1. Caño Martín Peña Ecosystem Restoration Project Area Map.....	1-3
Figure 2. Sample Designs for Recreational Access Areas	2-3
Figure 3. Sample Design of Recreation Access Park	2-5
Figure 4. Sample Design of Recreation Parks (With and Without Trail).....	2-6
Figure 5. Potential Federal Recreation Plan Access Areas (yellow dots).....	2-8
Figure 6. Proposed Federal Recreation Plan.....	2-9
Figure 7. Proposed Federal Recreation Plan and Viewsheds.....	2-10
Figure 8. Existing Recreation.....	3-4

List of Tables

Table 1. Existing Recreation Facilities.....	3-2
Table 2. Study Area Population through 2025 (1,000).....	3-3
Table 3. Guidelines for Assigning Points for General Recreation	3-8
Table 4. Conversion of Points to Dollar Values.....	3-9
Table 5. Most Likely Recreation Participation User Day Projection Scenario	3-12
Table 6. Recreation Facilities Cost Estimate.....	3-13
Table 7. Summary of Recreation Costs and Benefits	3-14
Table 8. Sensitivity Analysis.....	3-14

Acronyms and Abbreviations

CDLUP	Comprehensive Development and Land Use Plan
CDRC	Ciudad Deportiva Roberto Clemente
CM	Construction Management
CMP	Caño Martín Peña
CMP-ERP	Caño Martín Peña Ecosystem Restoration Project
CPI	Consumer Price Index
CVM	Contingent valuation method
EGM	USACE Economic Guidance Memorandum
ER	Engineering Regulation
FRP	Federal Recreation Plan
FY	Fiscal year
NED	National Economic Development
PED	Preconstruction Engineering and Design
PR SCORP	Puerto Rico State Comprehensive Outdoor Recreation Plan
SJBE	San Juan Bay Estuary
TCM	Travel cost method
UDV	Unit day value
USEPA	U.S. Environmental Protection Agency

This page intentionally left blank.

1.0 INTRODUCTION

The Caño Martín Peña (CMP) is an approximately 4-mile-long waterway, which connects the San Juan Bay and San José Lagoon, in metropolitan San Juan, Puerto Rico. It is part of the San Juan Bay Estuary (SJBE), the only tropical estuary that is included in the U.S. Environmental Protection Agency (EPA) National Estuary Program. The total drainage area of the CMP is about 4 square miles (2,500 acres). The eastern 2.2-mile-long segment of the CMP (Project Channel) and its adjacent areas, including the San José Lagoon, are the focus of this restoration project.

Historically, the CMP waterway had an average width of at least 200 feet and 6 to 8 feet in depth. The CMP provided tidal exchange between the San Juan Bay and San José Lagoon; however, since the 1920s, the channel and its wetlands began to be modified as a result of development in the area. The wetlands adjacent to the San Juan Bay and along the CMP were used as a disposal site for material dredged from the San Juan Harbor Project, affecting or eliminating more than 80 percent of the original mangrove acreage found in this area of the SJBE. In addition, as a result of the decay of the sugar cane industry, among other factors, massive migration from rural Puerto Rico to San Juan led to squatter settlements in areas along the CMP. Today, there are eight communities located to the north and south of the eastern segment of the CMP. The population is estimated to total 26,000 inhabitants. Approximately 350 families still live within the construction footprint.

1.1 ECOSYSTEM RESTORATION PROJECT STUDY AUTHORITY

The 110th Congress enacted Public Law 110-114, known as the Water Resources Development Act of 2007 in which Section 5127 directed that:

The Secretary shall review a report prepared by the non-Federal interest concerning flood protection and environmental restoration for Cano Martin Pena, San Juan, Puerto Rico, and, if the Secretary determines that the report meets the evaluation and design standards of the Corps of Engineers and that the project is feasible, the Secretary may carry out the project at a total cost of \$150,000,000.

1.2 ECOSYSTEM RESTORATION PROJECT DESCRIPTION

The CMP's ability to convey flows has been almost completely blocked as a result of siltation, accumulation of sediment and solid waste and the encroachment of housing and other structures. The CMP ecosystem restoration project (CMP-ERP) proposes to dredge the eastern segment of the canal to restore the CMP and its adjacent areas and to increase tidal flushing of the San José Lagoon in order to achieve environmental restoration and, as ancillary benefits, reduce flooding. In addition, the CMP-ERP will promote recreation and tourism with minimal negative impact on the ecosystem and the adjacent communities. The "Project Area," which mostly lays out the construction footprint, has been defined as the Project Channel, where dredging would take place,

the adjacent delimitation of the public domain lands within the MTZ-CMP where relocations are scheduled to occur. Also included in the Project Area is the 2-acre dredged material staging area adjacent to the Martín Peña bridge (Las Piedritas), the 6-acre dredged material staging area within the 35-acre Ciudad Deportiva Roberto Clemente (CDRC) site, the boating routes from the eastern limit of the CMP to the CDRC and the nearby San José Lagoon pits, and the five pits in San José Lagoon (Figure 1).

1.3 LOCAL COOPERATION

The Caño Martín Peña ENLACE Project Corporation, hereinafter referred to as ENLACE, and the Commonwealth of Puerto Rico, acting through the Department of Natural and Environmental Resources (DNER), are the non-Federal sponsors for the ecosystem restoration project. The Caño Martín Peña Special Planning District (Planning District) is interested in the completion of the project to improve environmental conditions along the CMP and provide opportunities for recreation to assist with the completion of the Comprehensive Development and Land Use Plan (CDLUP). The Planning District has requested that the Corps pursue recreation development opportunities in conjunction with the ecosystem restoration project. The local sponsors understand and accept the following constraints:

- The total recreation plan cost cannot exceed 10 percent of the Federal cost for the ecosystem recreation project.
- The recreation plan cannot reduce the environmental benefits of the ecosystem restoration project.
- Any additional recreation features not authorized for 50/50 cost share will be 100 percent non-Federal cost.
- The cost of any betterments to the proposed Federal Recreation Plan will be 100 percent non-Federal cost.
- The cost of operation and maintenance of the Federal Recreation Plan will be 100 percent non-Federal cost.
- The proposed recreation plan will not require purchase of additional project lands.

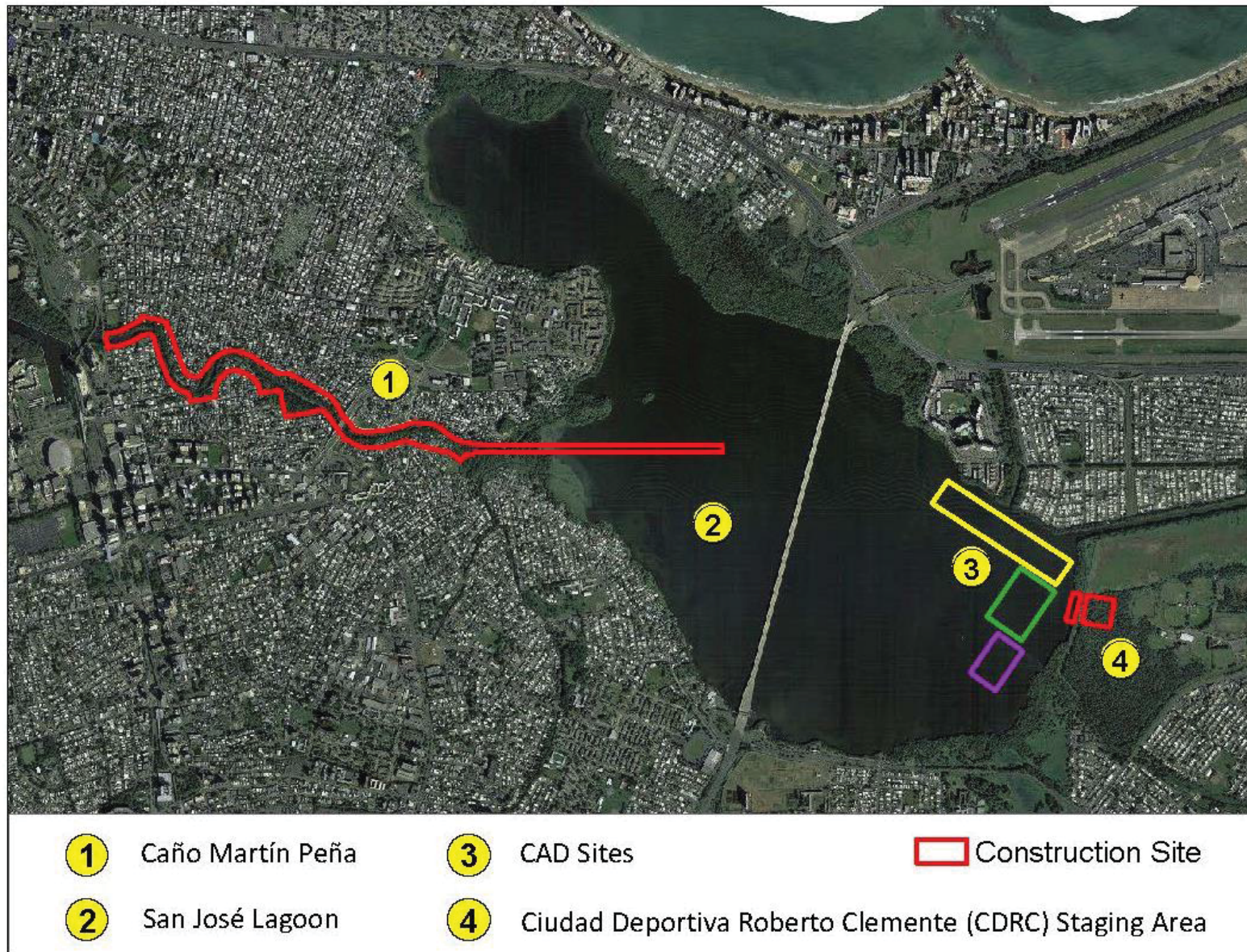


Figure 1. Caño Martín Peña Ecosystem Restoration Project Area Map

This page intentionally left blank.

2.0 FEDERAL RECREATION PLAN DEVELOPMENT

The design of the Federal Recreation Plan is largely influenced by the CDLUP for the Planning District and the Commonwealth of Puerto Rico State Comprehensive Outdoor Recreation Plan (PR SCORP). After reviewing the CDLUP, PR SCORP, existing data, and other related documentation, the project team developed a list of recreational features and identified potential areas for recreational use. The proposed Federal Recreation Plan is directed by the importance of balancing the needs of the community with protecting the restored areas and the function of the CMP. Based on existing studies, gap analysis, community input, and project constraints, a recreation resource assessment was completed to support the justification of the proposed Federal Recreation Plan.

2.1 RECREATION PLAN CONSTRAINTS

The following constraints were identified for the development of the Federal Recreation Plan.

1. No proposed recreational features will increase flooding in the CMP project area.
2. Recreational uses and facilities shall be compatible with the purpose of the ecosystem restoration project.
3. Proposed recreational features shall be compliant with the Corps and Federal Government regulations and design standards.

2.2 RECREATION PLAN PURPOSE

The recreational plan is considered an important component of the ecosystem restoration plan as it helps serve to alleviate the historic primary cause of ecosystem degradation in the area. The linear nature of the project area provides for water related recreational use. The goal of the Federal Recreation Plan would be to provide access, connectivity, and additional recreational facilities within the project limits.

2.3 RECREATION PLAN FEATURES

The CDLUP and State Comprehensive Recreational Opportunity Plan are the foundation of recreational features selected for the project. The recreation features and final recreation measures that are identified in the Federal Recreation Plan were developed and selected through an intensive public participation and feedback process from the population in the surrounding communities. Over 700 public activities were conducted to promote effective participatory planning, decision making, and implementation over a 2-year period leading up to the initiation of the Feasibility Report.

Recreational features have been refined to ensure that they are in compliance with Exhibit E-3 of ER 1105-2-100, and thus allowable for use in the Federal Recreation Plan (FRP). The following is a list of the recreational features identified as acceptable for the FRP.

- Trails
- Walks
- Steps/ramps
- Footbridges
- Picnic tables
- Trash receptacles
- Benches
- Entrance/Directional Marker
- Instructional signs
- Interpretive markers
- Gates
- Guardrails
- Lighting
- Handrails
- Walls

2.4 RECREATION PLAN ACCESS AREAS

The linear nature of the project allows for the placement of recreational features along the length of the CMP to maximize the benefit of the local community and reduce the impacts to the restored ecosystem. The project team, using the list of potential recreational features listed in Exhibit E-3 of ER 1105-2-100, identified 3 types of recreation access areas. The 3 types allow for major recreational use in some areas and median use in others. Two types would be adjacent to the proposed “Paseo” (a roadway that would parallel the CMP), whose construction is not a part of this federal ecosystem restoration project. This approach allows for large uninterrupted areas of restoration with major recreation areas that have access to the water, and median use areas along the smaller neighborhoods while connecting to the Paseo along the CMP (Figure 2). Recreation areas are designed to discourage improper use and facilitate educational programs to increase environmental stewardship of the restored ecosystem.

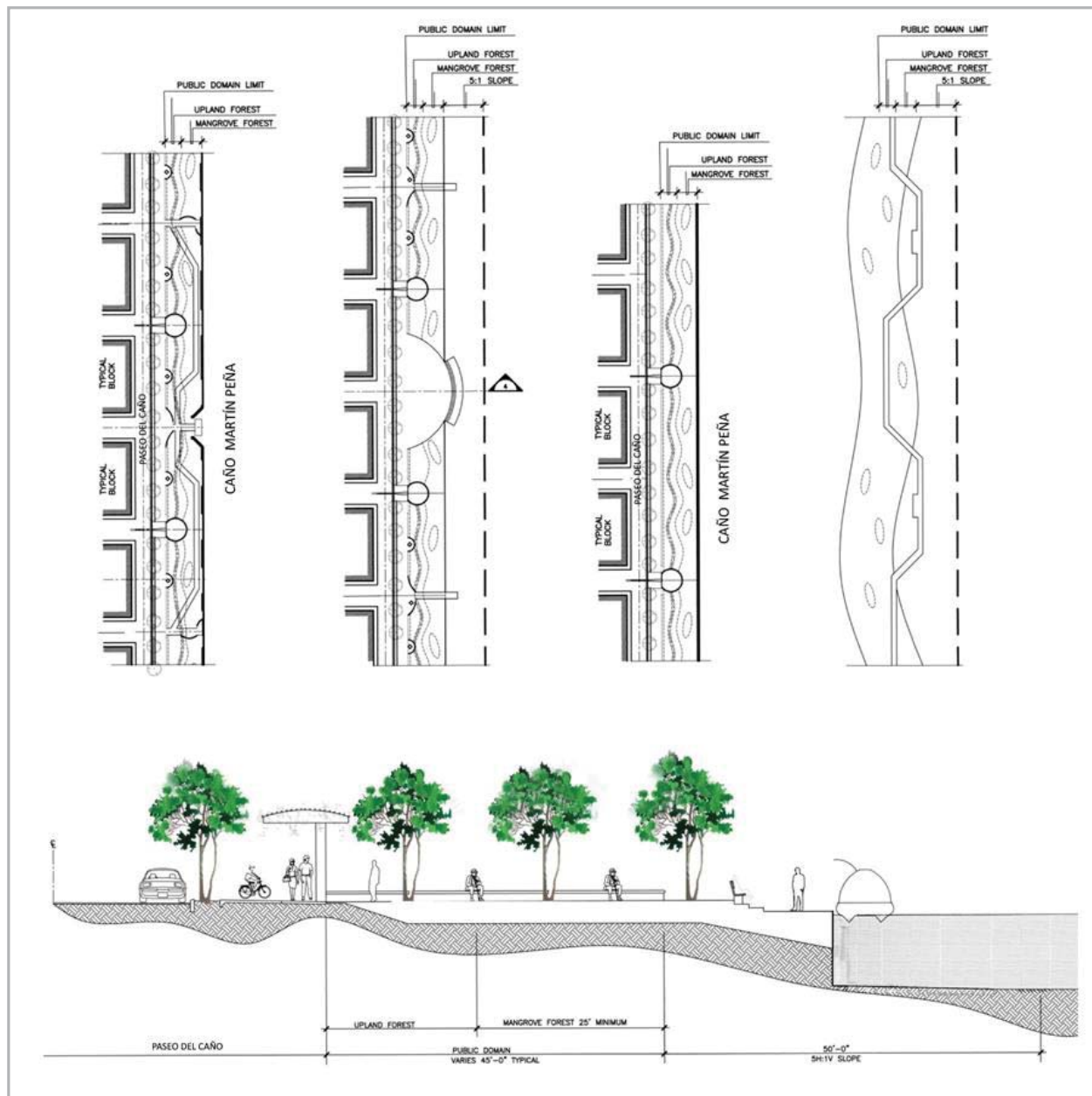


Figure 2. Sample Designs for Recreational Access Areas

2.4.1 Linear Park

This recreation area would consist of a trail, walk, and/or footbridge that extends the existing linear park located to the west of the Project Channel. The extended linear park trail would be constructed over the sheet pile bulk head in the channel (with the mangrove fringe between the linear park trail and the Paseo), and would be located on the southern side of the CMP, extending past the four western bridges in the project area and terminating at the first recreation access area in the Parada 27 community. In the vicinity of the western bridges, where the sheet pile wall is replaced with a

riprap edge, the trail would be constructed on piles. If possible, benches may be placed in strategic locations to provide rest and or observation areas. The area would have entrance, instructional, and interpretive signs to educate the public on the CMP-ERP, proper use of the recreational area, and informative facts about the restored ecosystem. A gate and fence, or wall, would be placed along the CMP for safety and to discourage the disposal of materials into the CMP. Guardrails, handrails, steps, ramps, and lighting would be used as appropriate to maintain a safe and accessible recreation area. The linear park would fall within the navigational servitude.

2.4.2 Recreation Access Park

This type of recreational area would have open access to the restored CMP and would be scaled to accommodate more than 100 persons for passive recreation (Figure 3). The nine recreation access parks would provide visual openings through mangrove forest to the CMP, providing a strong community connection at these strategic locations. Each would be located strategically at the intersection of the Paseo del Cano walkway and an important community transportation artery. They would include picnic tables and benches to encourage educational gatherings and nature enthusiasts to enjoy the restored ecosystem. Each recreation access park would have an entrance sign, instructional signs and interpretive signs to educate the public on the CMP-ERP, proper use of the recreational area, and educational facts about the restored ecosystem. A gate and fence, or wall, would be placed along the CMP for safety and to discourage the disposal of materials into the CMP. Guardrails, handrails, steps, ramps, and lighting would be used, as appropriate, to maintain a safe and accessible recreation area. The recreation access parks would provide for navigation access to the CMP.

2.4.3 Recreation Park

This type of recreational area would be smaller in scale than the proposed recreational access park, and would be scaled to accommodate less than 100 persons for passive recreation. With the natural mangrove forest serving as a backdrop, the twelve recreation parks would be strategically located along the Paseo del Cano walkway corridor to serve immediately adjacent blocks. In six of the recreation parks, a trail would be built through the forest to allow access to the CMP (Figure 4). The recreation parks would include benches to create an outdoor classroom and be strategically positioned to enhance nature watching. They would have an entrance sign, instructional signs and interpretive signs to educate the public on the CMP-ERP, proper use of the recreational area, and educational facts about the restored ecosystem. A gate and fence, or wall, would be placed along the recreation parks and CMP where applicable for safety and to discourage the disposal of materials into the CMP. Guardrails, handrails, steps, ramps, and lighting would be used as appropriate to maintain a safe and accessible recreation area.

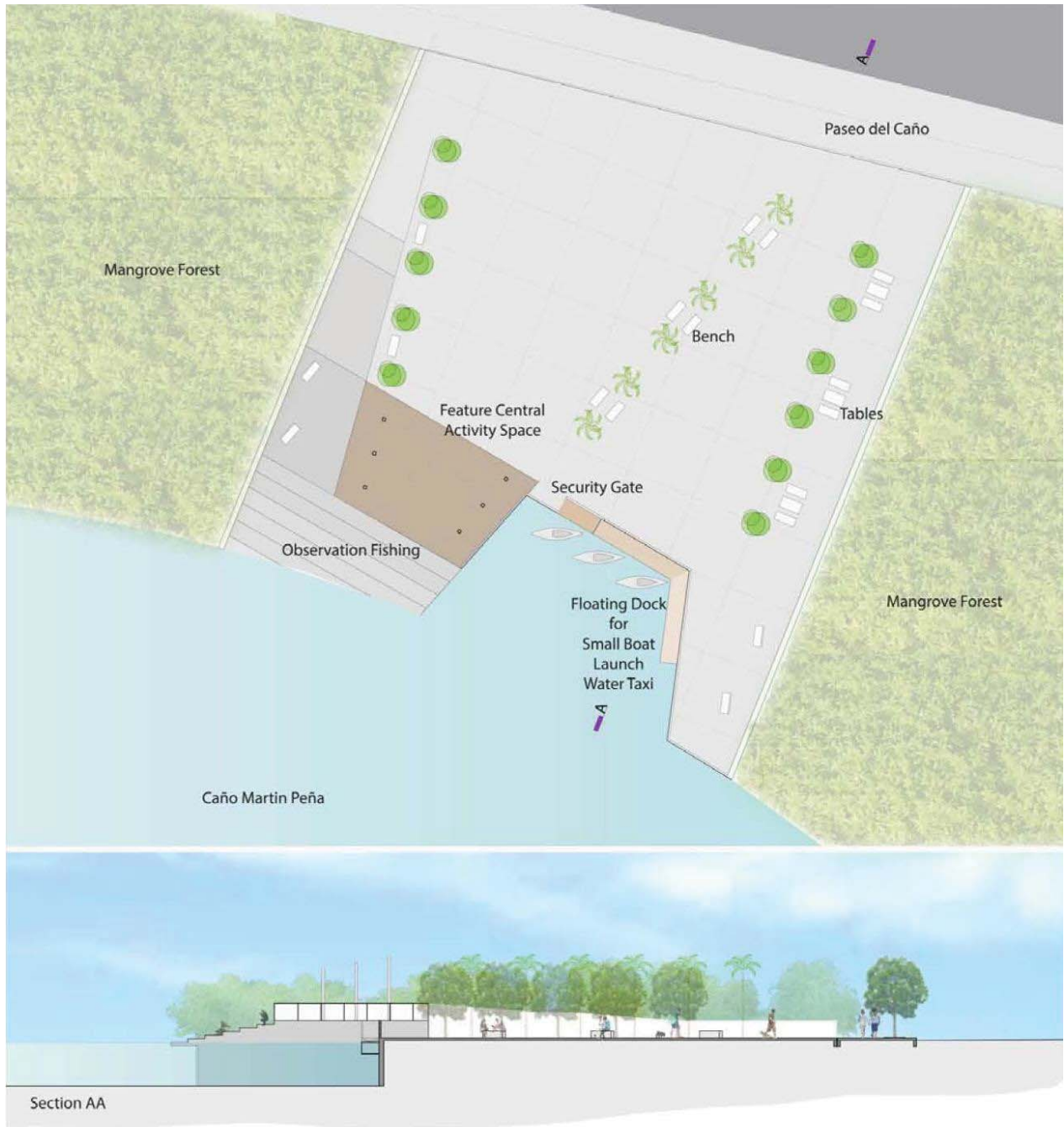


Figure 3. Sample Design of Recreation Access Park

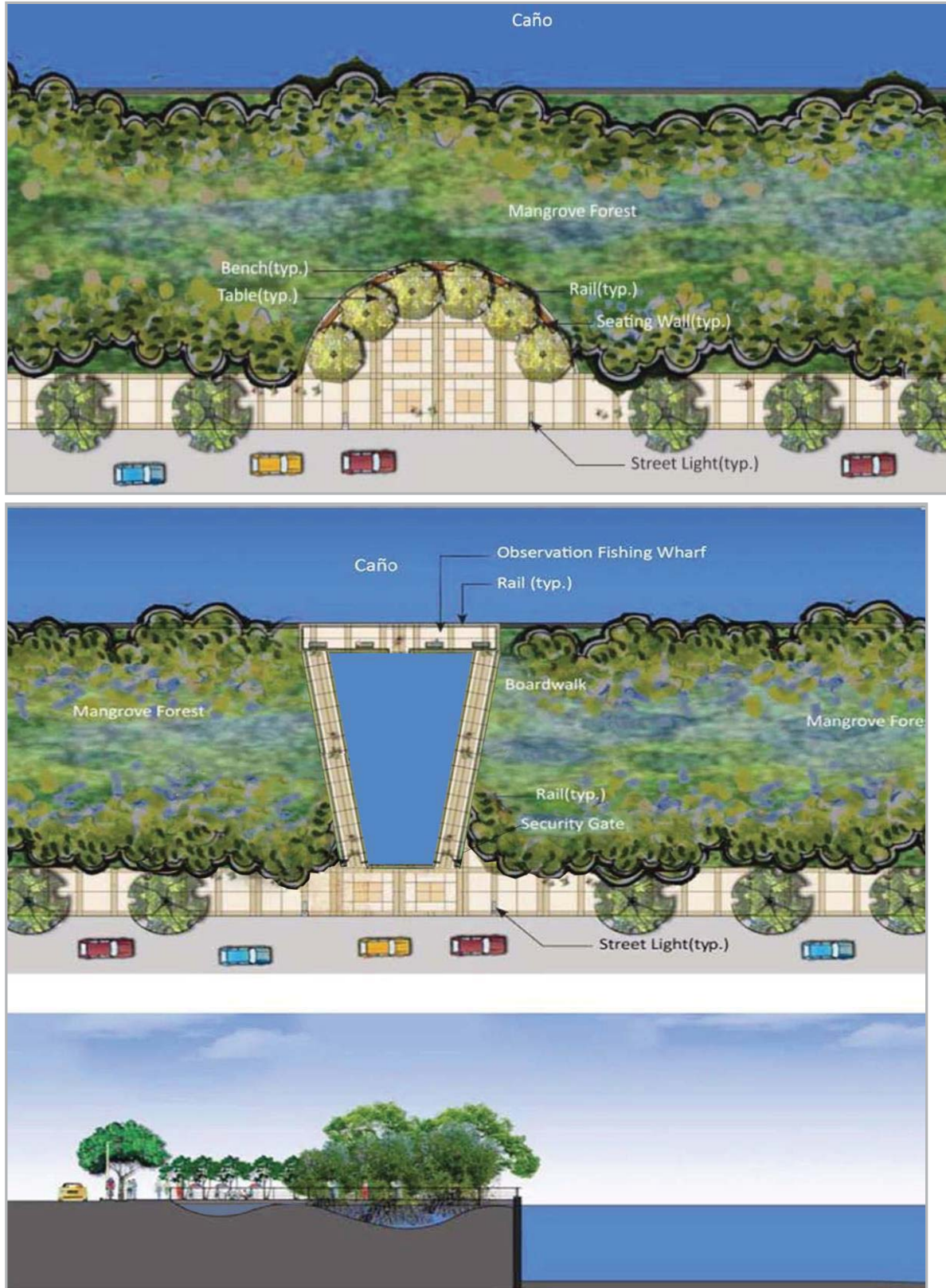


Figure 4. Sample Design of Recreation Parks (With and Without Trail)

2.4.4 Proposed Non-Federal Recreation Features

The non-Federal sponsor, ENLACE, will continue to work with the local community to implement the CDLUP. As part of the CDLUP, ENLACE proposes to include improvements to the aesthetic appearance and include additional opportunities in the Federal Recreation Plan areas. ENLACE will continue to refine the improvements and additional opportunities with the community in a timely manner to incorporate them into the construction of the Federal Recreation Plan at 100 percent non-Federal cost. ENLACE is currently considering the addition of betterments to the lights, including figures or statues, and incorporating exercise stations, fishing, and kayak or canoeing opportunities. Navigation access would be provided through the Federal recreation access parks.

2.5 POTENTIAL LOCATION OF RECREATIONAL AREAS

The locations of the recreational areas were strategically identified along the CMP to serve the local communities and minimize impact on the restored ecosystem. In Figure 5, twenty-two potential areas have been identified for recreational use within the project limits. The three types of recreational areas would be interspersed to provide a variety of opportunities for each of the local communities.

2.6 PROPOSED FEDERAL RECREATION PLAN

The proposed Federal Recreation Plan consists of a combination of the recreation features outlined in Section 2.3 on approximately 5 acres. The recreation features would be organized in each of the three types of recreation areas, as outlined in Section 2.4, to maximize recreational opportunities. The Federal Recreation Plan would include nine recreation access parks, six recreation parks with a trail to the CMP, six recreation parks without a trail, and a linear park extension along the southern bank in the Project Channel that terminates in the Parada 27 community (Figure 6). The major and minor viewsheds that are associated with the CMP and their relation to the proposed Federal Recreation Plan are illustrated in Figure 7. The Cano Martín Peña recreation measure as presented is only one scale. Other measures/plans/scales were identified and considered in 700 plus public meeting activities to promote effective participatory planning, decision making, and implementation during the 2-year period leading up to the Feasibility Report.

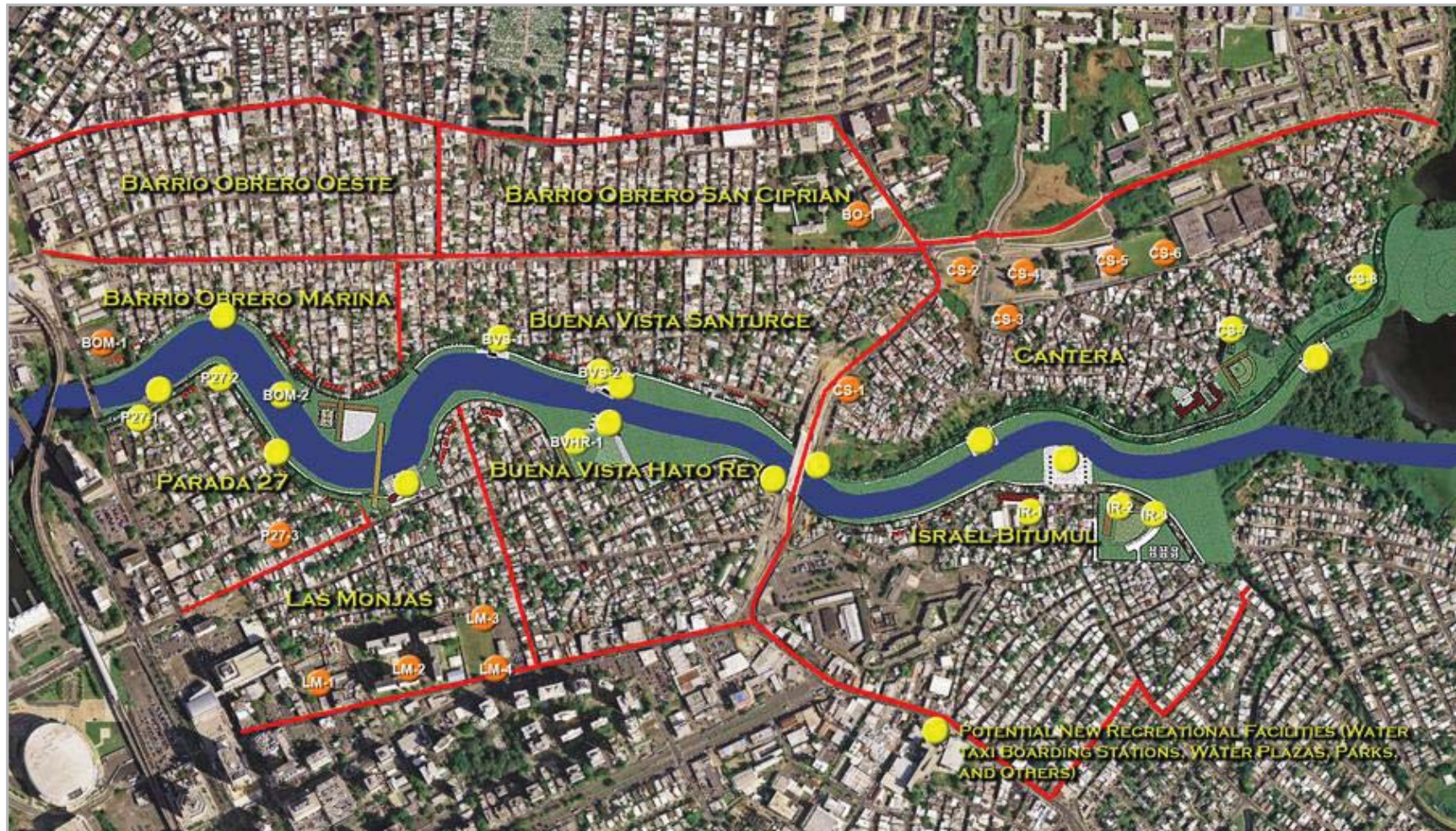


Figure 5. Potential Federal Recreation Plan Access Areas (yellow dots)

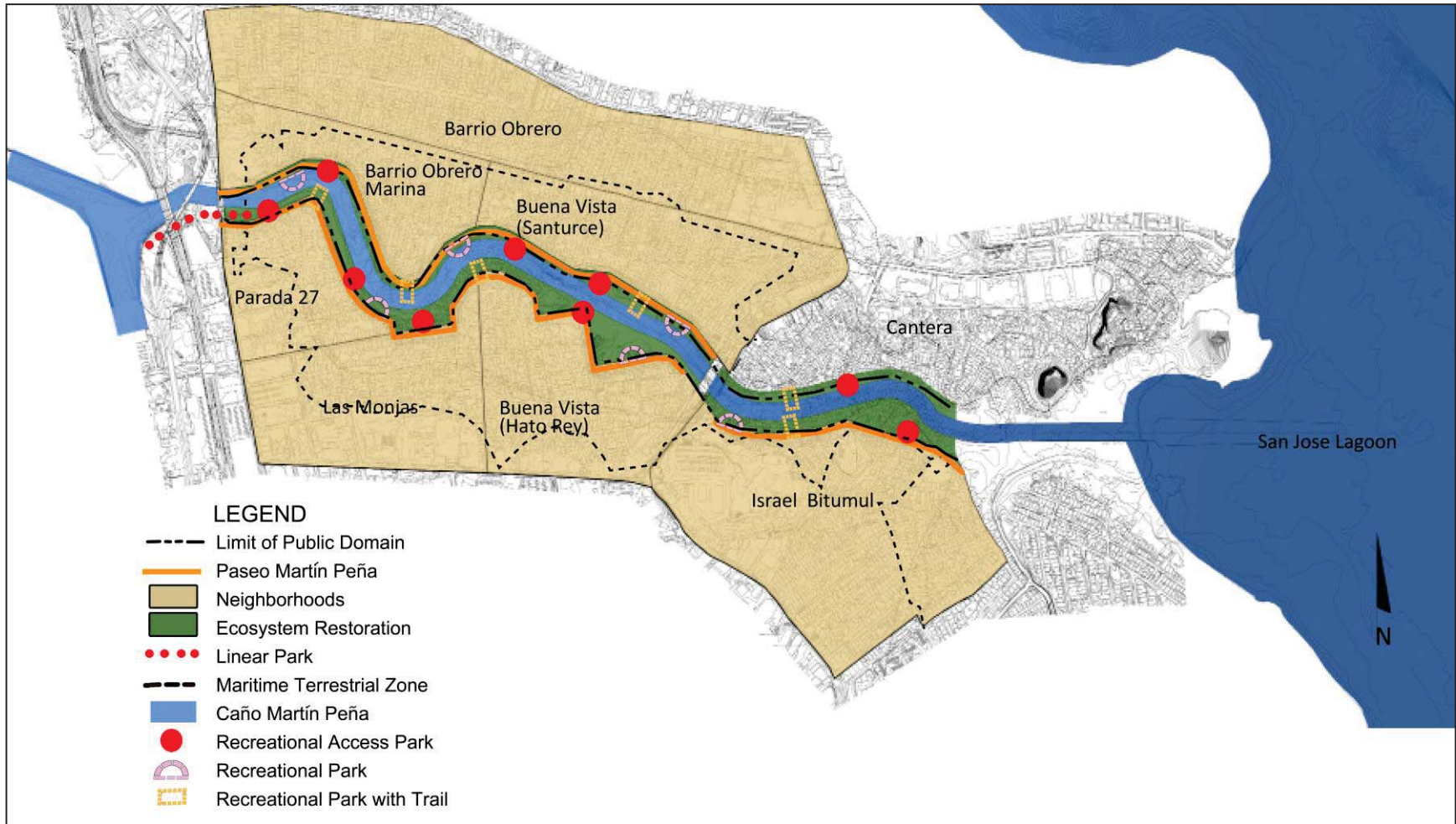


Figure 6. Proposed Federal Recreation Plan

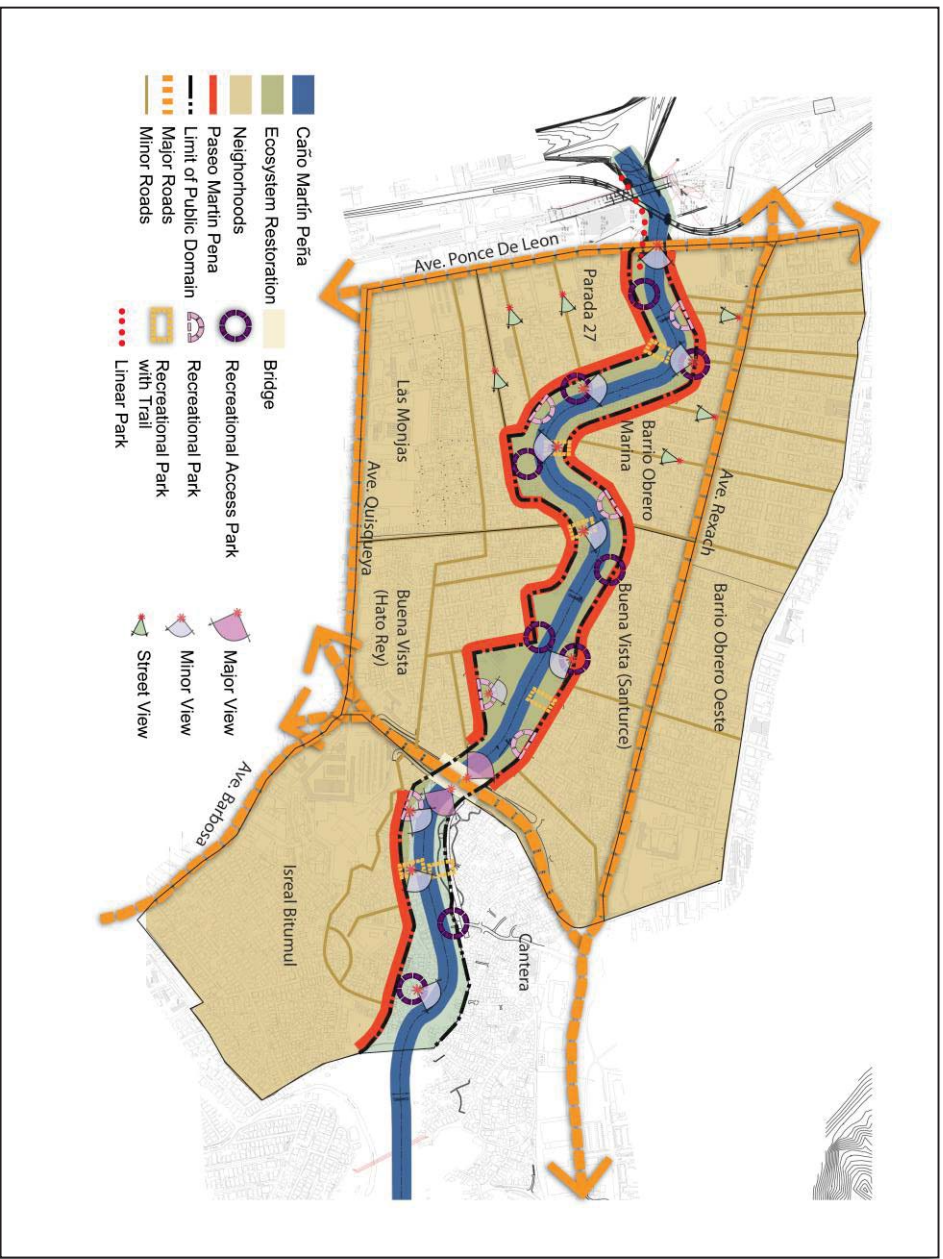


Figure 7. Proposed Federal Recreation Plan and Viewsheds.

3.0 RECREATION RESOURCE ASSESSMENT

The recreation resource assessment will analyze existing recreational data, costs, and anticipated National Economic Development (NED) benefits to determine whether the proposed Federal Recreation Plan is justified as a component of the ecosystem restoration plan.

3.1 EXISTING CONDITIONS

The most recent recreational data was gathered to establish the current state and need for additional recreational opportunities in the ecosystem restoration project area.

3.1.1 Recreational Opportunities

An inventory of existing recreation facilities is summarized in Table 1 and shown on Figure 8. Of these existing recreation facilities, four basketball/volleyball courts and a small impromptu dock are located within the project footprint.

There are no water-related recreation features currently within the Project Area, and as a result, there is no current or historic visitation information available for the types of proposed water-related recreational facilities. The existing land-related basketball/volleyball courts within the Project Area would be removed under the No Action Alternative because they are in the public domain boundary. They will be replaced on a one-to-one usage basis and located outside the public domain using 100 percent non-Federal funds, and undertaken as part of the CDLUP. Their relocation is not associated with the CMP-ERP.

3.1.2 Population Projections

The population density of Puerto Rico and the San Juan Metropolitan Area demands an increase in urban recreational spaces. Population projections are presented in Table 2, which shows the projected study area population and United States population growth through 2025.

Table 1. Existing Recreation Facilities

NEIGHBORHOOD	KEY	TYPE OF FACILITY	LOCATION
NORTH AREA			
BARRIO OBRERO SAN CIPRIAN	BO-1	BASKETBALL-VOLLEYBALL	ALBERT EINSTEIN SCHOOL
BARRIO OBRERO MARINA	BOM-1	BASKETBALL-VOLLEYBALL	SANTIAGO IGLESIAS PANTIN ELEMENTARY SCHOOL
	BOM-2	BASKETBALL-VOLLEYBALL	CALLE 10 SUR
BUENA VISTA SANTURCE	BVS-1	BASKETBALL-VOLLEYBALL	CALLE EL FARO
	BVS-2	BASKETBALL-VOLLEYBALL	CALLE WILLIAM
CANTERA	CS-1	BASKETBALL-VOLLEYBALL	AVE BARBOSA & CALLE SAN MIGUEL
	CS-2	BASEBALL	COLEGIO SAN JUAN BOSCO
	CS-3	SPORT CENTER	COLEGIO SAN JUAN BOSCO
	CS-4	SPORT CENTER	CALLE CONSTITUCION
	CS-5	BASKETBALL-VOLLEYBALL	CALLE LOS PADRES
	CS-6	FOOTBALL	COLEGIO SAN JUAN BOSCO
	CS-7	RECREATION ASSOCIATION	CALLE SANTA ELENA
	CS-8	MAKESHIFT DOCK	
	CS-9	LAGUNERA ASSOCIATION	AVE A
SOUTH AREA			
PARADA 27	P27-1	LINEAR PARK AND BOAT RAMP	CALLE SAN JOSE
	P27-2	BASKETBALL-VOLLEYBALL	CALLE SAN JOSE esq BUENOS AIRES
	P27-3	MULTI-USE COURT	CALLE SANTIAGO IGLESIAS
LAS MONJAS	LM-1	BASKETBALL-VOLLEYBALL	EMILIO del TORO SCHOOL CALLE CHILE, CALLE URUGUAY
	LM-2	BASKETBALL-VOLLEYBALL	LAS GLADIOLAS CONDOMINIUM CALLE QUISQUEYA, CALLE CHILE
	LM-3	BASKETBALL-VOLLEYBALL	CALLE QUISQUEYA
	LM-4	BASEBALL	CALLE DOLORES
BUENA VISTA			
HATO REY	BVHR-1	BASKETBALL-VOLLEYBALL	CALLE 3 esq CALLE G
ISRAEL-BITUMUL	IB-1	BASKETBALL-VOLLEYBALL	JUANITA GARCIA PERAZA SCHOOL AVE GAUTIER, CALLE ROBLEDO
	IB-2	BASKETBALL-VOLLEYBALL	CALLE ALCANIZ
	IB-3	BASEBALL	CALLE ALCANIZ

Table 1, cont'd

SUMMARY	TYPE OF FACILITY	QUANTITY
NORTH AREA		
	BASKETBALL-VOLLEYBALL	7
	HALF COURT BASKETBALL	
	BASEBALL	1
	SPORT CENTER	2
	FOOTBALL	1
	RECREATION ASSOCIATION	11
	MAKESHIFT DOCK	1
	LAGUNERA ASSOCIATION	1
	MULTI-USE COURT	
	LINEAR PARK	
SOUTH AREA		
	BASKETBALL-VOLLEYBALL	8
	HALF COURT BASKETBALL	
	BASEBALL	2
	SPORT CENTER	
	FOOTBALL	
	RECREATION ASSOCIATION	
	MAKESHIFT DOCK	
	LAGUNERA ASSOCIATION	
	MULTI-USE COURT	1
	LINEAR PARK	1

Recreation Facilities Inventory, Corporación del Proyecto ENLACE del Caño Martín Peña and field validation.

Table 2. Study Area Population through 2025 (1,000)

	2010	2015	2020	2025
San Juan Totals	428	423	416	412
Puerto Rico	4,022	4,096	4,149	4,177
San Juan percent of Puerto Rico Population	10.6%	10.3%	10.0%	9.9%
United States	308,936	322,371	335,805	349,694
San Juan percent of United States Population	0.14%	0.13%	0.12%	0.12%
Puerto Rico growth rate		1.02%	1.02%	0.67%
U.S. growth rate		1.04%	1.04%	1.04%

Source: Puerto Rico Planning Board, Economic and Social Planning Program, Census Bureau.
Prepared December 2005, BEBR Projections for United States.

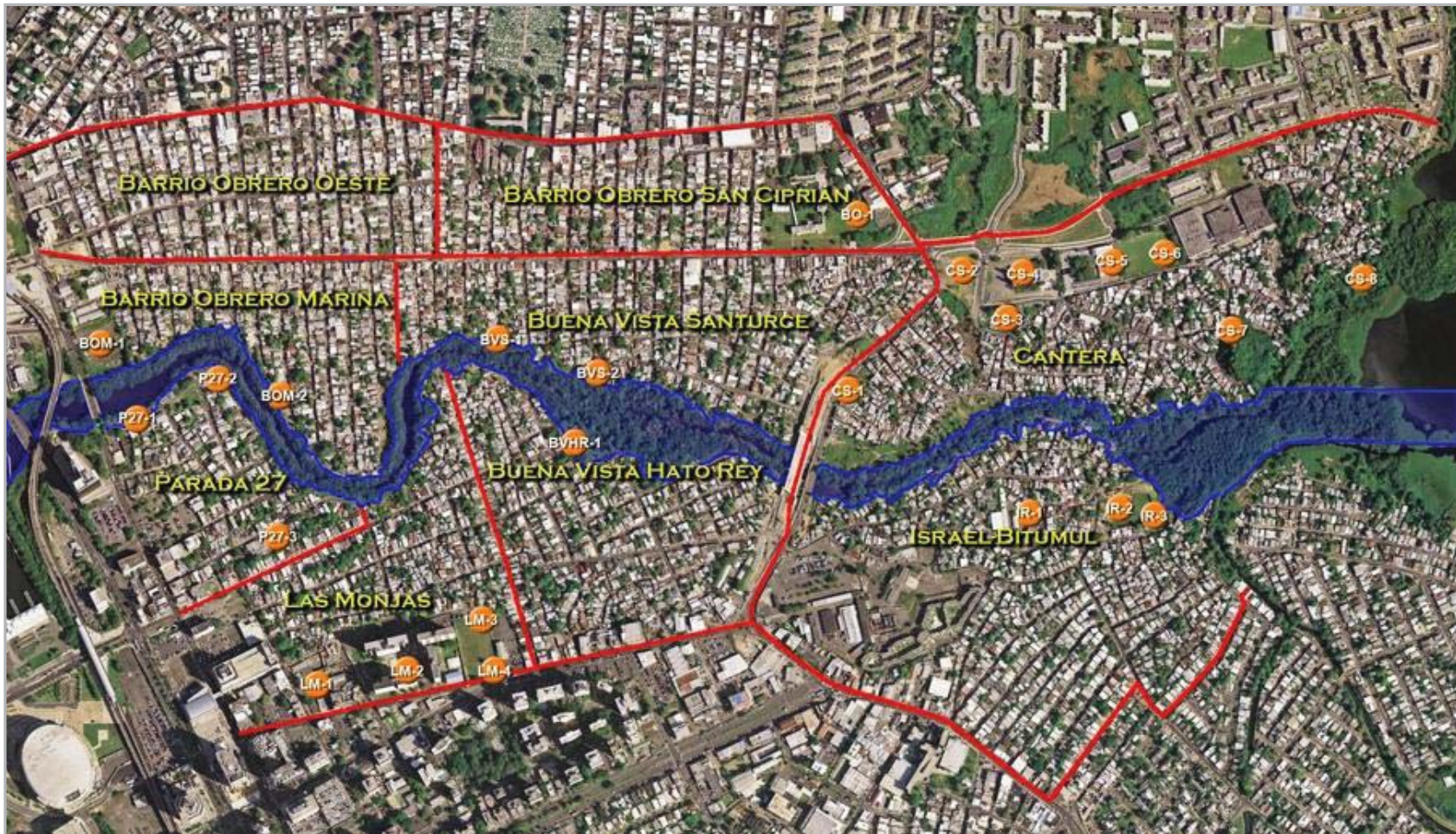


Figure 8. Existing Recreation

3.1.3 Recreational Needs Identified by SCORP

One of the key elements in the SCORP was the identification of population needs and preferences related to outdoor recreation. Those needs, which determine the demand for outdoor recreational services, were found through a general population survey complemented by focus groups. The participants in the SCORP were asked about outdoor recreation facilities that they thought are needed in Puerto Rico. Among those mentioned were facilities associated with the enjoyment of nature and the enhancement of physical and emotional health. This coincided with the opinions of the general population, as captured by the survey. Among the facilities most frequently mentioned were: walking trails, bike trails and parks with trees and vegetation. Also, participants frequently mentioned their desire for restored and revitalized urban centers. Recreation trends show increased usage of existing facilities and a latent need for new facilities. With ensuing development in the project area, and the high population density in the San Juan Metropolitan Area, there would be extensive use of the proposed recreation facilities.

3.2 RECREATION BENEFIT

3.2.1 National Economic Development Benefit

The National Economic Development (NED) benefit evaluation procedures contained in ER 1105-2-100 (April 22, 2000), Appendix E, Section VII, include three methods of evaluating the beneficial and adverse NED effects of project recreation: travel cost method (TCM), contingent valuation method (CVM), and unit day value (UDV) method.

The basic premise of the travel cost method (TCM) is that per capita use of a recreation site will decrease as out-of-pocket and time costs of traveling to the site increase, other variables being constant. TCM consists of deriving a demand curve by using the variable costs of travel and the value of time as proxies for price. The TCM was not used because a large portion of the recreation users live in the surrounding areas and the poverty rate in the surrounding areas is over 50 percent.

The contingent valuation method (CVM) estimates NED benefits by directly asking individual households their willingness to pay for changes in recreation opportunities at a given site. The CVM was not used due to the impoverished nature of the surrounding communities expected to heavily use the recreation facilities. It is not perceived the subject population would be able to accurately define their willingness to pay or a willingness to pay that reflects the value of the recreation opportunities.

The arguments for employing the user day approach is based on two foundations: (1) Infeasibility for the technical reasons mentioned above; and, (2) formulation or plan selection was not materially affected by willingness to pay value or by expected visitation. (ER 1105-2-100 22 Apr 2000 E-50. NED Benefit Evaluation Procedure, Paragraph (4) (a)) Plan selection was based on

feedback received from the population in the surrounding communities in over 700 public meetings conducted to promote effective participatory planning, decision making, and implementation over a 2-year period leading up to the Feasibility Report.

The unit day value method was selected for estimating recreation benefits associated with the creation of the CMP-ERP. When the unit day value method is used for economic evaluations, planners select a specific value from the range of values provided annually. Application of the selected value to estimate annual use over the project life, in the context of the with- and without-project framework of analysis, provides the estimate of recreation benefits.

As per ER 1105-2-100 Appendix E, Paragraph E-50 b.(4), when the Unit Day Approach is to be used annual usage cannot exceed 750,000 users. Therefore, even though expected usage was estimated at more than 750,000, the number of users used in the calculation of recreation benefits was held at 750,000.

The without-project condition analysis has no recreation value because, without the CMP-ERP, there would be no public access to the CMP. The with-project condition is the expected value of the recreational activity based on the unit day value method.

3.2.2 Assigning Points for General Recreation

The value of a day of general recreation at the restored CMP was determined using the guidelines for General Recreation in USACE Economic Guidance Memorandum (EGM) 13-03 (Table 3). EGM 13-03 provides judgment factor evaluations to assign points to the five criteria that determine the value of the expected general recreation experience. Point values for the general recreation experience provided by the proposed recreation features were determined after conducting site visits and coordinating with local agencies. Point values for the judgment were selected for each of the five criteria of: (1) recreation experience; (2) availability of opportunity; (3) carrying capacity; (4) accessibility; and (5) environmental quality based on the degree that the CMP-ERP would fulfill the judgment factor requirements.

- A point value rating of 14 out of a maximum of 30 was selected for the general recreation criteria. The point value of 14 was selected because the proposed facilities would provide several general activities and one high quality value activity in the densely populated Planning District and the San Juan metropolitan area. The CMP-ERP's proposed recreation resources would provide an area specific, unique recreation opportunity afforded by the project setting and the CMP. The site offers solitude and panoramic views in a growing metropolitan area, and would provide specific recreation amenities for densely populated District. The linear nature of the project provides recreational uses for each of the eight communities in the Planning District and for many users from outside the Planning District. The multi-use recreational areas provide panoramic view sheds at the recreational access parks and recreation parks. One high quality value activity would be the visual openings

through the Mangrove Forest to the CMP that currently are nonexistent. The high quality value activity would be further enhanced if a trail were built through the forest to allow access to the CMP.

- The score for the availability of opportunity criteria is low at 6 out of 18 possible because of the current local recreation facilities near the project area within the proposed recreation resource location. At the high end of the scale are those recreational facilities that are a geographical rarity; these are sites for which there is no close substitute within two hours. There is insufficient access to water-oriented activities in the San Juan metropolitan area but limited access to mangrove forests. With the exception of visual contact with mangrove forests, alternative facilities exist that provide availability of opportunity for all other recreation activity classifications; however, the proposed recreation facilities would provide availability of opportunity to meet Puerto Rico SCORP-identified needs associated with the enjoyment of nature and the enhancement of physical and emotional health. In addition, the walking trails, bike trails, and parks with trees and vegetation offered by the proposed recreation facilities would provide opportunities to meet other needs frequently mentioned in the Puerto Rico SCORP.
- The CMP-ERP's recreation resources carrying capacity criteria point value is relatively high at 10 out of a maximum of 14 because the proposed recreation facilities provide optimum amenities to conduct general recreation activity at site potential. The general recreation values are based on the optimum use of the site potential, without overuse of the proposed recreation resources. Good water resources, and access to them for environmental observation purposes comprise a large part of the projected recreation resources use. According to the Puerto Rico SCORP, most of the people were engaged in outdoor recreational activities throughout the 12 months of the year due to a climate that is tropical marine and mild with little seasonal temperature variations. Therefore, use of the recreation facilities is projected to occur throughout the 12 months of the calendar year.
- The accessibility criteria point value is 16 out a possible 18 because there is good access, high standard roads to site, including public transportation. In addition, the proposed facilities would provide good access within site, compliant upon the availability of local highways, roads and streets in good condition that would provide access to these amenities.
- The environmental quality criteria rating is 13 out of a maximum of 20 based on the existing aesthetic values of the CMP-ERP recreation resource facilities and the ease of correcting any limiting aesthetic factors. The limiting aesthetic factors that currently exist would be eliminated by the CMP-ERP. The proposed site would possess panoramic views with no factors lowering environmental quality. The views through the Mangrove Forest to the CMP provided by the proposed recreation access parks, recreation parks, and the linear park that connects them merit the criteria rating of 13.

The points for the five criteria used for assigning points for general recreation total to 59 points.

Table 3. Guidelines for Assigning Points for General Recreation

Criteria	Judgment factors				
Recreation experience ¹ Total Points: 30	Two general activities ²	Several general activities	Several general activities: one high quality value activity ³	Several general activities; more than one high quality high activity	Numerous high quality value activities; some general activities
Point Value: 14	0–4	5–10	11–16	17–23	24–30
Availability of opportunity ⁴ Total Points: 18	Several within 1-hour travel time; a few within 30 minutes travel time	Several within 1-hour travel time; none within 30 minutes travel time	One or two within 1-hour travel time; none within 45 minutes travel time	None within 1-hour travel time	None within 2-hour travel time
Point Value: 6	0–3	4–6	7–10	11–14	15–18
Carrying capacity ⁵ Total Points: 14	Minimum facility for development for public health and safety	Basic facility to conduct activity(ies)	Adequate facilities to conduct without deterioration of the resource or activity experience	Optimum facilities to conduct activity at site potential	Ultimate facilities to achieve intent of selected alternative
Point Value: 10	0–2	3–5	6–8	9–11	12–14
Accessibility Total Points: 18	Limited access by any means to site or within site	Fair access, poor quality roads to site; limited access within site	Fair access, fair road to site; fair access, good roads within site	Good access, good roads to site; fair access, good roads within site	Good access, high standard road to site; good access within site
Point Value: 16	0–3	4–6	7–10	11–14	15–18
Environmental quality Total Points: 20	Low esthetic factors ⁶ that significantly lower quality ⁷	Average esthetic quality; factors exist that lower quality to minor degree	Above average esthetic quality; any limiting factors can be reasonably rectified	High esthetic quality; no factors exist that lower quality	Outstanding esthetic quality; no factors exist that lower quality
Point Value: 13	0–2	3–6	7–10	11–15	16–20
Total Point Value					59

Source: Economics Guidance Memorandum, 09-03, Unit Day Values for Recreation, Fiscal Year 2009.

1. Value for water-oriented activities should be adjusted if significant seasonal water level changes occur.
2. General activities include those that are common to the region and that are usually of normal quality. This includes picnicking, camping, hiking, riding, cycling, and fishing and hunting of normal quality.
3. High quality value activities include those that are not common to the region and/or Nation, and that are usually of high quality.
4. Likelihood of success at fishing and hunting.
5. Value should be adjusted for overuse.
6. Major esthetic qualities to be considered include geology and topography, water, and vegetation.
7. Factors to be considered to lowering quality include air and water pollution, pests, poor climate, and unsightly adjacent areas.

3.2.3 Conversion of Points to Dollar Value

The point values assigned in Table 4 were converted to dollar values based on the EGM 15-03, Unit Day Values for Recreation, 2015, which is based on ER 1105-2-100. Values provided for FY 2015 may be used to convert points to a UDV dollar amount if the point assignment method is used. The table was adjusted from Table K-31, *Federal Register* Vol. 44, No. 242, p. 72962, December 14, 1979, and the subsequent Table VIII-3-1 “Conversion of Points to Dollar Values,” Economic and Environmental Principles and Guidelines for Water and Related Land Resources Implementation Studies, March 10, 1983, using the Consumer Price Index (CPI) factors published by the Bureau of Labor Statistics. The CPI basis of Table VIII-3-1 from Principles and Guidelines is July 1, 1982 (CPI value = 97.5). The FY 2015 CPI basis is September, 2014 (CPI value = 238.031).

Table 4 displays the point value conversion of a unit day value in fiscal year 2015 (FY15) to dollars. The 59 total points from Table 3 falls between the General Recreation Point values for 50 points and 60 points. The General Recreation Dollar Value for 50 points is \$8.30 and for 60 points is \$9.03. The difference between \$8.30 and \$9.03 is \$0.73. The 59 total points represents 90 percent of the \$0.73 difference. Therefore, 90 percent of the \$0.73 was added to \$8.30 to produce the UDV of \$8.96 for the 59 General Recreation Point Value.

Table 4. Conversion of Points to Dollar Values

General Recreation Point Values	General Recreation Dollar Values
0	\$3.91
10	\$4.64
20	\$5.13
30	\$5.86
40	\$7.32
50	\$8.30
60	\$9.03
70	\$9.52
80	\$10.50
90	\$11.23
100	\$11.72

Source: Economic Guidance Memorandum, 15-03, Unit Day Values for Recreation for Fiscal Year 2015.

3.2.4 Most Likely Recreation Participation User Day Projection Scenario

The PR SCORP does not provide recreation user-day guidelines for resource based outdoor recreation activities. The capacity method is an alternative method of estimating use according to USACE Economic Guidance Memorandum (EGM), 15-03, Unit Day Values for Recreation for Fiscal Year 2015:

“The capacity procedure involves the estimation of annual recreation use under without-project and with-project conditions through the determination of resource or facility capacities (taking into consideration instantaneous rates of use, turnover rates, and weekly and seasonal patterns of use). Seasonal use patterns are dependent on climate and culture and probably account for the greatest variation in use estimates derived through this method. In general, annual use of outdoor recreation areas, particularly in rural locations and in areas with pronounced seasonal variation, is usually about 50 times the design load, which is the number of visitors to a recreation area or site on an average summer Sunday. In very inaccessible areas and in those known for more restricted seasonal use, the multiplier would be less; in urban settings or in areas with less pronounced seasonal use patterns, the multiplier would be greater. In any case, the actual estimation of use involves an analytical procedure using instantaneous capacities, daily turnover rates, and weekly and seasonal use patterns as specific data inputs.

Because the capacity method does not involve the estimation of site-specific demand, its use is valid only when it has been otherwise determined that sufficient demand exists in the market area of project alternatives to accommodate the calculated capacity. Its greatest potential is therefore in urban settings where sufficient demand obviously exists. Additionally, its use should be limited to small projects with (1) a facility orientation (as opposed to a resource attraction), and (2) restricted market areas that would tend to make the use of alternative use estimating procedures less useful or efficient.”

The guidance provided in EGM 15-03 to estimate reasonable user rate projections requires determination of resource or facility capacities and assumes that adequate demand exists. As mentioned in EGM 15-03, use is valid if it is determined that sufficient demand exists in the market area of project alternatives to accommodate the calculated capacity. Therefore, its greatest potential lies in urban settings, where sufficient demand exists due to the especially densely populated conditions of the CMP neighboring communities. The PR SCORP determined that sufficient demand exists in the market area for facilities associated with the enjoyment of nature and the enhancement of physical and emotional health. Among the facilities most frequently mentioned were: walking trails, bike trails and parks with trees and vegetation. The PR SCORP also reported that sufficient demand exists for restored and revitalized urban centers. The recreation facilities proposed for the CMP-ERP would address these needs.

The recreation plan has a linear park, nine recreation access parks, and 12 recreation parks (6 with 1,000 square feet of trail and 6 without trails). The facility capacity of the recreation parks is designed to accommodate less than 100 individuals. The recreation access parks are designed for more than 100 individuals participating in passive recreation. In this densely populated urban setting with no pronounced seasonal use patterns, the multiplier is estimated as the instantaneous capacity. The estimation of use involves an analytical procedure using instantaneous capacities, daily turnover rates, and weekly and seasonal use patterns as specific data inputs. Instantaneous capacity was estimated as the design capacity of the recreation facilities. The instantaneous capacity is the expected number of users and it is estimated at 90 for the recreation parks with trails, 80 for each of the recreation parks without trails, 110 for each of the recreation access areas, and 50 for the linear park. The 90 users for the recreation park with trail are 10 percent less than the 100 users, and the 80 users for the recreation park without trail are 20 percent less. The 110 users for the recreation access park are 10 percent more than 100. The 50 users of the linear park are based on 2 users per 60 feet of the 1,500-foot facility.

According to the PR SCORP, most of the people were engaged in outdoor recreational activities throughout the 12 months of the year due to a tropical marine climate, which is mild with little seasonal temperature variations. Therefore, 365 user days were selected as the number of days available annually for outdoor recreation for this analysis. With weekends accounting for 104 user days, and with 19 Public and National Holidays in Puerto Rico, a total of 123 days would be available for peak use. The remaining 242 user days for the rest of year are identified as off peak use days. Daily turnover rates were estimated to be two per day for peak use days and one per day for off peak use days. The number of units provided times the daily turnover rate times the peak use days or off peak use days provides the projected expected user days shown in Table 5.

The EGM for Unit Day Value states that the application of the selected value to estimated annual use over the project life, in the context of the with- and without-project framework of analysis, provides the estimate of recreation benefits. The starting point of the evaluation is the value in the without-project condition. This report estimates that all the without-project values for all criteria equals zero, because under without-project conditions the area is not suitable for recreational activities. The next step was the point evaluation of the with-project recreation facilities. The difference in points between the without-project and with-project conditions is the basis for the benefits.

Table 5. Most Likely Recreation Participation User Day Projection Scenario

Activity	Units Provided	Daily Turnover Rates	Capacity Guidelines	User Occasions	Project Expected Users
Recreation Access Parks	9	2/day weekends and holidays	110	123	243,540
Recreation Access Parks	9	1/day weekdays	110	242	239,580
Recreation Parks	6	2/day weekends and holidays	80	123	118,080
Recreation Parks	6	1/day weekdays	80	242	116,160
Recreation Parks with trail	6	2/day weekends and holidays	90	123	132,840
Recreation Parks with trail	6	1/day weekdays	90	242	130,680
Linear Park	6	2/day weekends and holidays	50	123	73,800
Linear Park	6	1/day weekdays	50	242	72,600
General Recreation Total					1,127,280¹

3.3 ECONOMIC JUSTIFICATION OF RECREATION PLAN

The justification of incurring additional costs for recreation features is derived by utilizing a benefit to cost ratio. The tangible economic justification of the proposed project can be found by comparing the equivalent average annual costs with the estimated equivalent average annual benefits, which would be realized over the period of analysis. The federally mandated project evaluation interest rate of 3.125 percent, an economic period of analysis of 50 years and current prices were used to evaluate economic feasibility (FY16 rate is 3.125%, per EGM #16-01). ER 1105-2-100 provides economic evaluation procedures to be used in all federal water resources planning studies. The ER guidelines were used in preparing this benefit to cost analysis.

¹ Capped at 750,000 (ER 1105-2-100 Appendix E, Paragraph E-50 b.(4), when the Unit Day Approach is to be used annual usage cannot exceed 750,000 users).

3.3.1 Recreation Facilities Cost Estimate

Only cost shared items were included in the recreation cost. The cost of clearing and grubbing, grading and land form are for the restoration project and the proposed recreation facilities take up only 0.1 percent of the ecosystem restoration area. The costs of the recreation facility components (not including associated CM and PED) are: nine Recreation Access Parks \$3,105,897, six Recreation Parks without trail \$533,481, six Recreation Parks with trail \$1,110,431, the Linear Park \$4,451,393, and Mobilization and Demobilization \$611,798, for a total cost of \$9,813,000 (Table 6).

Table 6. Recreation Facilities Cost Estimate

Recreation Facilities	Cost
Recreation Access Area (9)	\$3,105,897
Recreation Park (6)	\$533,481
Recreation Park w/trail (6)	\$1,110,431
Linear Park (1,500 linear feet)	\$4,451,393
Mobilization and Demobilization	\$611,798
Total Cost	\$9,813,000

The proposed recreation facilities project cost is \$9,813,000. Preconstruction Engineering and Design (PED) is estimated at 9 percent and Construction Management (CM) is estimated at 6 percent, for a total of ~15 percent for PED and CM, or \$1,472,000, bringing the total recreation first cost to \$11,285,000. Interest during construction was calculated to be \$153,300, bringing the total recreation fully funded investment to \$11,438,300 (Table 7). The Federal share of the project first cost of the recreation facilities is 50 percent of \$11,285,000 or \$5,642,000. This represents 4.3 percent of the non-recreation Federal share of the project first cost of \$131,866,000 and is in compliance with the 10 percent maximum of the non-recreation total Federal cost share of the project.

3.3.2 Recreation Facilities Benefits

The annual benefits were calculated by multiplying the User Day Value of \$8.96 by the user day projection scenario capped at 750,000 per year. The average annual benefit of the proposed recreation facilities is \$6,720,000. The benefit-to-cost ratio of 6.8 to 1 was calculated by dividing the average annual benefits of \$6,720,000 by the total annual costs of \$986,600. Net annual benefits are \$5,733,400 (average annual benefits \$6,720,000 minus total annual costs \$986,600).

Table 7. Summary of Recreation Costs and Benefits

Recreation Construction Costs	\$9,813,000
PED & CM (~15%)	\$1,472,000
Total Recreation Construction First Cost	\$11,285,000
Construction Duration	27 months
Interest During Construction Costs	\$153,300
Total Recreation Fully Funded Investment	\$11,438,300
Period of Analysis	50 years
Annualized Cost	\$396,600
OMRR&R	\$590,000
Total Annual Costs	\$986,600
Annual Benefits	
User Day Value	\$8.96
Average Daily Use	2,055
Annual Use	750,000
Average Annual Benefit	\$6,720,000

3.3.3 Sensitivity Analysis

A sensitivity analysis was performed to determine what the impacts would be if actual benefits fell far short of the expected benefits and to provide additional justification for the proposed recreation features (Table 8). This sensitivity analysis suggests there would be ample benefits to conservatively justify the construction of the proposed recreation facilities for the CMP-ERP. If annual use was only 25 percent of capacity, the number of annual users would be 187,500 and annual benefits would be \$1,675,520 (187,500 annual users multiplied by the \$8.96 User Day Value). Dividing the annual benefits of \$1,675,520 by the total annual costs of \$986,600 produces a benefit to cost ratio of 1.7 to 1. Net annual benefits would be the annual benefits \$1,675,520 minus the total annual costs of \$986,600, or \$688,920.

Table 8. Sensitivity Analysis

Scenario	Annual Users	Daily Users	Annual Benefit
Most Likely	750,000	2,055	\$6,720,000
Worst Case	187,500	514	\$1,675,520

As a result of economically driven and car oriented urban development, the metropolitan area of Puerto Rico lacks an efficient integration of public recreational spaces as well as an effective infrastructure of public transportation. The SJBE and CMP provide an excellent opportunity for alternate modes of transportation to develop in the municipality of San Juan as well as the development of recreational outlets such as the areas described in section 2.4. The implementation of recreational areas along the CMP could provide a forum where some of the community's economic needs would be met by the local tourism, inversely fueled by these recreation areas and parks, in addition to providing leisure space for the community. The impact of the recreation access parks, linear park and recreation parks would fill a need for environment-oriented urban parks in the city. These much-needed public urban recreation spaces would be visited by many urban dwellers looking for nature related activities in the heart of the municipality.

The Federal Recreation Plan for the CMP-ERP would consist of a linear park along a portion of the CMP, nine recreation access parks, six recreation parks with a trail to the CMP, and 6 recreation parks without a trail. The linear park would extend an existing linear park that is currently located at the western project limit. The trail would be constructed over the sheet pile bulkhead. If possible, benches may be placed in strategic locations to provide rest and/or observation areas. The recreation access parks would provide open access to the CMP. They would include picnic tables and benches to encourage educational gatherings and nature enthusiast to enjoy the restored ecosystem. The recreation parks would be smaller in scale than the proposed recreational access park. The recreation parks would not have direct access to the CMP, except in those locations where a trail would be built to connect to the CMP, and would include strategically positioned benches to enhance nature watching and create an outdoor classroom. In each of the recreational areas, there would be an entrance sign, instructional signs and interpretive signs to educate the public on the ecosystem restoration project, proper use of the recreational area, and educational facts about the restored ecosystem. A gate and fence, or wall, would be placed along the recreation area and CMP where applicable for safety, and to discourage the disposal of materials into the CMP. Guardrails, handrails, steps, ramps, and lighting would be used as appropriate to maintain a safe and accessible recreation area.

The Federal Recreation Plan is considered an essential component of the ecosystem restoration plan as it provides for a significant increase in recreational opportunities along the CMP, as well as helping alleviate the historic primary cause of ecosystem degradation in the area. The proposed recreational features are compatible with the ecosystem outputs for which the project is designed. They are compatible with the ecosystem restoration purpose by providing an appropriate interface within the urban environment and the aquatic environment. The features are appropriate in scale and have no impacts to the ecosystem restoration benefits that justify the CMP-ERP. The acreage necessary for the recreation features does not result in a loss of mangroves as the existing acreage

of wetlands would be replaced with a net increase of higher-functioning wetlands in the CMP, even with the 5 acres reserved for recreational features. In addition, the tidal connectivity for mangroves would still occur through the water, and the fish and wildlife that inhabit the mangroves would still be able to connect to other mangrove areas along the CMP through this water connection.

The recreational features are incrementally justified. The individual recreation elements are similar to each other and would thus provide a similar level of benefits. The combined recreational features have a benefit-to-cost ratio of 6.8 to 1 and appropriately cost-shared 50 percent non-Federal and 50 percent Federal. The total recreation facilities first cost is \$11,285,000 (includes facilities cost, PED, and CM costs) and the Federal share is \$5,642,000, or 4.3 percent of the estimated non-recreation Federal cost share of \$131,866,000 for the ecosystem restoration project. The 4.3 percent is in compliance with the requirement of not exceeding 10 percent of the non-recreation Federal project cost. The non-Federal sponsor, DNER, would be 100 percent responsible for operation and maintenance of recreation features.

The linear nature of the project area provides recreational uses for all eight neighboring communities; careful placement of these measures throughout the project area is also intended to protect the investment in ecosystem restoration by facilitating appropriate uses of the project area after the CMP-ERP is constructed. This approach facilitates the creation of larger, uninterrupted restored ecosystems, allows for easy access for project maintenance, and discourages improper and unmanaged uses of the area. It also aids educational programs in increasing the environmental stewardship of this urban wetland. For example, improved and formalized access to the CMP and the resulting community engagement would facilitate strict enforcement of trash-dumping regulations and incentivize local conservation, thus avoiding future degradation in the process.

Provision of recreational access infrastructure has been demonstrated to foster community connection to the restored ecosystem and build and maintain a positive connection to their local landscapes (Golet et al., 2006; Ulrika Åberg & Tapsell, 2013). Additionally, increases in recreational activities such as wildlife viewing, hunting, and fishing often translate to increases in support for conservation actions (Ulrika Åberg & Tapsell, 2013). These activities provide the basis for new and existing community-based enterprises to flourish (e.g., Excursiones Eco, Bici-Caño).

5.0 REFERENCES

- Bureau of Economic and Business Research (BEBR), UF, Bureau of Economic and Business Research, Warrington College of Business. Florida Statistical Abstract 2004 38 (2004).
- Commonwealth of Puerto Rico Planning Board, Economic and Social Planning Program, Census Bureau. Prepared December 2005.
- Commonwealth of Puerto Rico State Comprehensive Outdoor Recreation Plan, 2008–2013.
- Comprehensive Development and Land Use Plan for the Caño Martín Peña Special Planning District, PRHTA, adopted by the PRPB, March 2006.
- Ecosystem Restoration – Supporting Policy Information Engineer Pamphlet (EP) No. 1165-2-502, Washington, D.C. (SEP 1999).
- E. Ulrika Åberg, Sue Tapsell, Revisiting the River Skerne: The long-term social benefits of river rehabilitation, *Landscape and Urban Planning*, Volume 113, May 2013, Pages 94-103, ISSN 0169-2046, <http://dx.doi.org/10.1016/j.landurbplan.2013.01.009>. (<http://www.science-direct.com/science/article/pii/S0169204613000169>)
- Golet, G.H., Roberts, M.D., Larsen, E.W., Luster, R.A., Unger, R., Potts, G., Werner, G., and White, G.G. 2006. Assessing Societal Impacts When Planning Restoration of Large Alluvial Rivers: A Case Study of the Sacramento River Project, California. *Environmental management*, Vol. 37, Num. 6, pp. 862-879.
- South Florida Water Management District (SFWMD). A8 Website, C-111 SC Project, <https://my.sfwmd.gov/>.
- U.S. Army Corps of Engineers (USACE). 1998. Civil Works, Policy Division (CECW-AG), Policy Guidance Letter (PGL) No. 59, Recreation Development at Ecosystem Restoration Projects. Memo.
- . 1999. ER 1165-2-501 Civil Works Ecosystem Restoration Policy.
- . 2000. Regulation ER 1105-2-100 Planning Guidance Notebook, Appendix E – Civil Works Programs, Section V – Ecosystem Restoration, April 22, 2000.
- . 2014. Civil Works, Water Resources Policies and Authorities (CECW-A), Economic Guidance Memorandum (EGM) 13-03, Unit Day Values for Recreation for Fiscal Year 2013.
- U.S. Department of Interior (DOI: 10.1007/s00267-004-0167-x). n.d. Environmental Assessment Assessing Societal Impacts When Planning Restoration of Large Alluvial Rivers: A Case Study of the Sacramento River Project, California. Gregory H. Golet, Michael D. Roberts, Ryan A. Luster, Gregg Werner.

This page intentionally left blank.